Preliminary version

SUPPLEMENT

TO

THE FINAL REPORT ON THE CAPSIZING ON 28 SEPTEMBER 1994 IN THE BALTIC SEA OF THE RO-RO PASSENGER VESSEL MV ESTONIA

Part II

The Joint Accident Investigation Commission
of
Estonia, Finland and Sweden

Preliminary version

SUPPLEMENT

TO

THE FINAL REPORT ON THE CAPSIZING ON 28 SEPTEMBER 1994 IN THE BALTIC SEA OF THE RO-RO PASSENGER VESSEL MV ESTONIA

Part II

The Joint Accident Investigation Commission
of
Estonia, Finland and Sweden

Preface

The Joint Accident Investigation Commission publishes in this Supplement the most important documents used in Commission's work. Large appendices of some research reports have been edited, but a list of appendices has been included.

This publication is a preliminary version. The final version will be published soon in one volume. Some documents will be added which due to editorial reasons had to be left out from this preliminary version.

CONTENTS

PART I

		Hand-written strength calculations for the VIKING SALLY-ESTONIA's bow visor locks.
205	ENG	Extracts from Bureau Veritas Rules and Regulations for the construction and classification of Steel Vessels 1977. Paris.
206	ENG	Bureau Veritas Note Documentaire BM2. Paris 5.4.1976.
207	GER	Extrakt von Germanischer Lloyd Vorschriften für Klassifikation und Bau von stählernen Seeschiffen. Ausgabe 1978. Band 1. Hamburg.
		Extracts from Germanischer Lloyd Regulations for the classification and building of Steel Vessels. Version 1978. Part 1. Hamburg
208	ENG	Extracts from Lloyd's Register of Shipping Rules and Regulations for the Construction and Classification of Steel Ships 1976. London.
209	SWE	Correspondence between Von Tell and the Finnish Maritime Administration about approval of the visor design in general.
210	ENG	Von Tell telex to Bureau Veritas 18.3.1980 about visor attachment design loads and stresses.
211	ENG	Extracts from notes made by the Bureau Veritas surveyor on the visor assembly drawing 590/1103 rex 6.
212	SWE	M/S ESTONIA & M/S MARE BALTICUM - Utredning beträffande placering av kollisionsskott/förlig ramp. Nordström & Thulin. Stockholm 1994.
		M/S ESTONIA & M/S MARE BALTICUM - Investigation on placing of collision bulkhead/bow ramp. Nordström & Thulin. Stockholm 1994.
213	FIN	Letter 20.4.1977 from the Finnish Maritime Administration to the Wärtsilä Turku Shipyard on the approval of the bow ramp as an upper extension of the collision bulkhead in MV TURELLA.
214	SWE	Correspondence between the Swedish Maritime Administration and

		the Götaverken Öresund Shipyard 8.1.1979 on the application of the SOLAS regulations for an upper extension of the collision bulkhead in two passenger ferries for the Gotland traffic.
215	SWE	Correspondence between the Swedish Maritime Administration and the Stena Line 20.3 - 26.3.1981 concerning MV KRON-PRINSESSAN VICTORIA.

Ship documents

216	ENG	*Lehtola Kari*: VIKING SALLY - ESTONIA. SOLAS Passenger Ship Certificates and Inspection Certificates. Working paper 31.3.1996
217	ENG	Selection of MV ESTONIA's certificates valid at the time of the accident.
218	ENG	MV ESTONIA's classification certificates of 12.1.1993 for machinery and hull.
220	ENG	Extracts from the Trim and Stability booklet of MV WASA KING. Ship Consulting Ltd Oy. Turku 20.1.1991

Surveys

221	FIN SWE	Section 45 of the Commercial Vessel Degree no. 23/1920. 12.12.1920.
222	SWE	Decision of the Finnish Maritime Administration 1921 to approve certain classification societies for carrying out hull surveys.
223	ENG	Protocol of MV ESTONIA's exercise Port State Control in Tallinn 27.9.1994.
224	ENG	List of surveys carried out by Bureau Veritas on VIKING SALLY - ESTONIA.

Ship operation

225	ENG	VIKING SALLY - SILJA STAR - WASA KING. Dockings and recorded damages to the bow 1981 - 1993. Memorandum 16.8.1995/FIN.

226	ENG	Extracts from M/S ESTONIA Safety Manual.
228	ENG	Safety round on board MV ESTONIA of the AB seaman on watch.
229	ENG	Arrival times of MV ESTONIAand some other passenger ferries at the entrance of Stockholm Archipelago and in Stockholm 3.2.1993 - 26.9.1994. Extract from the log book at the Stockholm Pilot Station.
230	ENG	List of maintenance and repair works on MV ESTONIA. April 1993 - August 1994. Nordström & Thulin AB. Stockholm.
231	SWE	Extracts from docking specification and quotation 25.9.1992 for Wasa Line re MV WASA KING's docking 1993.

3 CREW

4 VOYAGE CONDITIONS

Weather

401	ENG	Weather Conditions on the Northern Baltic at September 28, 1994. Estonian Meteorological and Hydrological Institute. Tallinn 1995.
402	ENG	*Komulainen Marja-Leena*: The Baltic Sea Storm on 28.9.1994. An investigation into the weather situation which developed in the northern Baltic at the time of the accident to m/s Estonia. Helsinki 1994.
403	ENG	The m/s ESTONIA accident. Weather conditions on September 27 th and 28th 1994. Swedish Meteorological and Hydrological Institute. Norrköping 1995.

Wave conditions

405	ENG	*Kahma Kimmo - Pettersson Heidi - Myrberg Kai - Jokinen Hannu*: Estimated Wave Conditions and Currents during the last Voyage of M/S Estonia. Finnish Institute of Marine Research. Helsinki 1996.

406 FIN Merkitsevän aallonkorkeuden todennäköisyydet M/V ESTONIAn käyttämillä reiteillä. Merentutkimuslaitos. Helsinki 11.4.1997.

Significant wave height probabilities on the routes operated by MV ESTONIA. Finnish Institute of Marine Research. Helsinki 11.4.1997.

407 ENG *Kahma Kimmo - Pettersson Heidi*: Wave Height - Wave Period Distribution from the Northern Baltic Proper. Finnish Institute of Marine Research. Helsinki 1996.

Seakeeping

408 ENG *Karppinen Tuomo - Rintala Sakari - Rantanen Antti*: MV ESTONIA Accident Investigation. Numerical predictions of wave loads on the bow visor. Technical Report VALC106. VTT Manufacturing Technology. Espoo 1995.

409 ENG *Huss Mikael*: Wave loads on visor attachments. MV ESTONIA Accident Investigation. Internal report 1995 - 1997.

410 ENG *Trägårdh Peter*: Model test with M/S ESTONIA. Sea loads on bow visor and yawing behaviour due to heel. SSPA Maritime Consulting. Report 7524. Gothenburg 1995.

411 ENG *Sundell Tom*: MV ESTONIA Accident Investigation. Forces acting on the bow visor due to stationary flow. Technical Report VALC55. VTT Manufacturing Technology. Espoo 1995.

412 ENG *Karppinen Tuomo - Rantanen Antti*: MV ESTONIA Accident Investigation. Numerical predictions of wave-induced motions. Technical Report VALC53. VTT Manufacturing Technology. Espoo 1995.

413 ENG *Karppinen Tuomo*: MV ESTONIA Accident Investigation. Effect of speed on the visor loads. Working paper 29.10.1996.

PART II

5 OTHER INVESTIGATIONS

General observations after the accident

501 FIN M/S Estonian hylyn ympäristöstä laadittujen merenpohjakarttojen selitys. Merivoimien Tutkimuslaitos. Helsinki 28.3.1995.

502 SWE Rapport angående de tekniska och legala förutsättningarna att återfinna och omhänderta omkomna från färjan Estonia. Sjöfartsverket. 1994.

Report concerning technical and legal conditions to find and take care of victims from the ferry Estonia. Swedish Maritime Administration.

503 ENG *Rockwater A/S*: Condition Survey of the Vessel "Estonia" for the Swedish National Maritime Administration. Survey Report.

The vessel

504 ENG *Karppinen Tuomo - Rantanen Antti*: MV Estonia Accident Investigation. Stability calculations. Technical Report VALC177. VTT Manufacturing Technology. Espoo 1996.

505 ENG *Karppinen Tuomo - Rintala Sakari*: MV Estonia Accident Investigation. Stability calculations with water on the tank deck. Research Report VAL313-7331. VTT Manufacturing Technology. Espoo 1997.

506 ENG *Ingerma A. - Strizhak V.*: The Strength Studies for the Locking Devices of the Bow Visor of M/V ESTONIA. Estonian Maritime Academy & Tallinn Technical University. Tallinn 1997.

507 ENG *Metsaveer Jaan*: MV ESTONIA Accident Investigation. Calculation of Load-Carrying Capacity of the Bow Visor Locks. Tallinn Technical University. Tallinn 1996.

508 ENG *Katajamäki Kai*: MV Estonia Accident Investigation. Strenght investigation of the visor side locking device, numerical

calculations. Technical report VALC-246. VTT Manufacturing Technology. Espoo 1996.

509 ENG *Häkkä-Rönnholm Eeva*: Investigation of paint systems from MV Estonia Visor Bottom Lock. Research Report No. RTE57243/96. VTT Building Technology. Espoo 1996.

510 ENG *Ingerma A. - Strizhak V.*: An Analysis of the Reasons of the Failure of the Locking Devices of MV Estonia. Estonian Maritime Academy. Tallinn Technical University. Tallinn 1996.

511 ENG *Rahka Klaus*: MV Estonia. Visor Damage and Visor Attachment Strenght Investigations at VTT. Report VALB243. VTT Manufacturing Technology. Espoo 1997.

512 ENG *Airaksinen Jukka*: MV ESTONIA. Accident Investigation. Strength Investication of the Visor Hinge, Numerical Calculations. Technical Report VALC312. VTT Manufacturing Technology. Espoo 1997.

513 FIN *Kleimola Matti*: Laskelmat ESTONIAn keulavisiirin lukituslaitteiden kuormituksista. Espoo 1997.

Kleimola Matti: Calculations of the loadings on MV ESTONIA's bow visor locking devices. Espoo 1997

514 FIN *Kleimola Matti*: Laskelmat ESTONIAn keulavisiirin lukituslaitteiden kuormituksista (2. raportti). Espoo 1997.

Kleimola Matti: Calculations of the loadings on MV ESTONIA's bow visor locking devices. 2nd Report. Espoo 1997.

515 ENG *Niemi Erkki*: Upper Bound Estimation on the Ultimate Load Capacity of the Atlantic Lock. Lappeenranta University of Technology. Lappeenranta 1997.

516 ENG *Nilsson Fred - Öberg Hans*: Strength and failure assessments of parts from MV ESTONIA. Royal Institute of Technology. Stockholm 1996.

517 ENG *Pettersson Kjell - Söderholm P-O - Lange Nils*: Metallographic and fractographic examinations of samples from MV Estonia. Royal Institute of Technology. Stockholm 1995.

518 ENG *Pettersson Kjell - Söderholm P-O*: Notes from metallographic and fractographic examinations of samples from MV Estonia. Royal Institute of Technology. Stockholm 1996.

519 ENG *Öberg Hans*: Investigation of deformations and related loads, applied to the lug of the visor bottom lock of MV ESTONIA. Royal Institute of Technology. Stockholm 1996.

520 ENG MS ESTONIA Bow Visor. Inspection Report of PS-side Hydr. Lifting Cylinder. MacGREGOR (FIN) Oy. Piikkiö 1995.

Ship operations

521 ENG *Larjo Kari*: ESTONIA's shedule, ETA-PILOT and NaviSailor 2100. 15.10.1996.

522 ENG *Huss Mikael*: Simulation of the capsize. MV ESTONIA Accident Investigation. Internal report 1995 - 1997.

523 ENG *Rintala Sakari - Karppinen Tuomo*: MV ESTONIA Accident Investigation. Numerical predictions of the water inflow to the car deck. Technical Report VALC174. VTT Manufacturing Technology. Espoo 1996.

Operating history

524 ENG *Wermelin Hans*: M/S Estonia, a ship emanating from The Baltic Phenomenon. An historical overwiev made by *ADC Support AB*. Stockholm 1995.

Damages to bow of other vessels

525 ENG *Laur Uno*: Report. Damage to bow visor locking devices of passenger car ferry "DIANA II" in January, 1993, and preliminary conclusion i.r.o. the loss of the bow visor of m.v. "ESTONIA" on September 28th, 1994. Tallinn 1994.

526 ENG *Lehtola Kari*: Damage to the Bow of the SILJA EUROPA at the Time of the Accident Involving the ESTONIA 28.9.1994.

6 EVACUATION AND RESCUE

602 FIN Suuronnettomuuden pelastussuunnitelma Saaristomeren meripelastusalueella. 18.6.1991.

Rescue Plan for Major Maritime Accident in the Archipelago Sea Maritime SRR. 18.6.1991.

603 SWE *ARCC Arlanda*: Bakgrund avtal enl Räddningstjänstlagen, larmtider och erfarenheter.

604 ENG *Penttilä Antti - Ranta Helena*: Medicolegal Examination and Identification of Victims of M/S Estonia Mass Disaster. Department of Forensic Medicine, University of Helsinki - The Finnish DVI Team - Ministry of Justice. Helsinki 1996.

SUPPLEMENT No. 501

M/S Estonian hylyn ympäristöstä laadittujen merenpohjakarttojen selitys.

Merivoimien Tutkimuslaitos.

Helsinki 28.3.1995.

MERIVOIMIEN TUTKIMUSLAITOS
Tutkimus- ja kehittämisosasto
Helsinki

SELOSTE

28.3.1995

m/s ESTONIAN HYLYN YMPÄRISTÖSTÄ LAADITTUJEN MERENPOHJAKARTTOJEN SELITYS

1. YLEISTÄ

m/s ESTONIAn hylyn ympäristöstä on laadittu seuraavat kartat:
syvyyskartta 1: 5 000, käyräväli 2 m
syvyyskartta 1:10 000, käyräväli 2 m
merenpohjan kerrostumat 1: 5 000
merenpohjan kerrostumat 1:10 000
merenpohjan kerrostumat 1:20 000
saven paksuus 1:1500
saven paksuus: tulkitut poikkiprofiilit

Kartat on laadittu akustisesta aineistosta, joka kerättiin m/s ESTONIAn keulavisiirin etsinnän yhteydessä 5.- 18.10.1994. Etsintäaluksena toimi SMMV:n VL TURSAS. Paikanmääritys tehtiin DGPS:llä ja Syledikselläa. Luotaimina käytettiin Klein 595 digital side scan sonaria (viistokaikuluotainta) (100/500 kHz), Furuno FE-881 kaikuluotainta (28 kHz) sekä Tursaksen omaa Simrad-kaikuluotainta (33/210 kHz). Kaikuprofiilista saatiin veden syvyys ja tulkittiin pohjan kerrostumat. Viistokaikuluotaimen sonogrammista, joka on akustinen varjokuva merenpohjasta sivusuunnassa, eli eräänlainen "ilmavalokuva", tulkittiin kohteet, pinnan kivisyys ja laatu akustisen heijastuvuuden perusteella. Viistokaikuluotaimen data talletettiin luotausten yhteydessä myöhempää analyysiä varten.

Aineiston koko käsittää n. 156 linjakilometriä viistokaikuprofiilia sekä n. 160 km kaikuprofiilia. Koko aineisto oli kerätty analogisessa muodossa, joten sen jälkikäsittely digitaalisessa muodossa oli aikaa vievää. Merivoimien monikeilaisen kaikuluotainjärjestelmän käyttö olisi säästänyt huomattavasti myös jälkikäsittelyaikaa.

Aineisto käsiteltiin merivoimien tutkimuslaitoksella Helsingissä. Käsittelyn on tehnyt FT Jouko Nuorteva osin virka- osin vapaa-ajalla. Käsittelyyn on osallistunut myös mittauksissa koko ajan mukana ollut tutkimusassistentti Antti Ratia virka-ajallaan. Yhteensä aineiston käsittelyyn on kulunut lähes 400 tuntia aikaa.

2. KARTTOJEN LAADINTA

Ajoreitit

Paikannuksessa alus käytti DGPS:ää ja viistokaikuluotaimeen paikannus tehtiin Syledikselllä 30 sekunnin välein aluksen ajaessa ennalta määrättyjä suoria linjoja pitkin. Syledikseen

ja DGPS:n eron havaittiin olevan korkeintaan vain muutamia metrejä paikasta riippuen. Koska ajoreittipiirturia ei saatu kytkettyä Tursaksen navigointijärjestelmään, jouduttiin jälkikäteen ennen karttojen laatimista määrittämään ajoreitit koordinaattitulostusten mukaan. Tämä tehtiin lukemalla viisto-kaikuluotaimen sonogrammeilta 30 s:n välein tulostunut x-y -koordinaatti (yhteensä n. 3300 pistettä) manuaalisesti mitta-kaavassa 1:5000, jonka jälkeen reitit voitiin piirtää.

Maalajikerrostumien tulkinta

Merenpohjan maalajitulkinta tehtiin ajoreittipohjalle tulkitsemalla akustiset profiilit. Tulkinta perustuu fysikaaliseen ja geologiseen tietouteen, joka aikaisemmin on varmistettu mm. pohjavalokuvauksella ja näytteenotolla. Tässä tapauksessa yhtään pohjanäytettä ei ole otettu ja seismisen luotauskaluston puute haittasi lähinnä saven paksuuksien mittausta sekä moreeni/hiekkamuodostumien erottamista toisistaan. Käsityksen mukaan tutkitulla alueella ei kuitenkaan sijainnut yhtään hiekkamuodostumaa.

Tulkinnassa erotettiin seuraavat pohjatyypit:
kallio, moreeni, 'kova' savi ja 'pehmeä' savi sekä pintakerroksesta hiekka, kivet ja lohkareet. Usein maalajit vaihettuvat luonnossa toiseksi ilman jyrkkää rajaa, joten yhdessä tulkintatarkkuuden kanssa maalajirajojen paikkavirhe voi olla +/- 30 - 50 m.

Syvyyskarttojen laadinta

Syvyyskartat laadittiin lukemalla syvyysarvo kaikugrammilta n. 10-30 s:n välein ja korjaamalla se oletetulla äänen etenemisnopeudella vedessä (kaikugrammeissa äänen etenemisnopeutena oli käytetty 1500 m/s, tulkinnassa käytettiin 1430 m/s). Syvyyksien sama-arvokäyrät (2 m:n välein) piirrettiin manuaalisesti hyväksikäyttäen pohjan laadun tulkintaa.

Koska syvyyskarttojen laadinta perustui ajolinjojen välillä tulkintaan (kattavaa monikeilaista syvyysluotausta ei ollut), on joissain kalliopaikoissa mahdollista olla 2 - 3 m matalampiakin paikkoja. Pohjan muodot ovat kuitenkin kokemusten perusteella pääpiirteissään varsin luotettavia .

Suurin havaittu veden syvyys oli 121 m ja pienin 51 m.

3. POHJANLAATUKARTTOJEN SELITYKSET

Maalaji (väri)

kallio (punainen)

Kallio on paljastuneena pinnalla tai hyvin ohuen irtomaalajin peittämä. Laaja-alaisten kallioiden painanteissa voi olla savea enemmänkin, mutta sitä ei voitu tulkita tehtyihin karttoihin pienen pinta-alallisen koonsa vuoksi.

moreeni (oranssi)

Mannerjäätikön kerrostama aines, jonka koostumus vaihtelee betonimaisesta pohjamoreenista lähes savimaiseen ainekseen. Tulkintojen perusteella moreenia on vain paikoitellen ja suhteellisen ohuina (muutama metri) kerrostumina kallion päällä.

'kova' savi (harmaa)
Mannerjäätikön perääntymisen ja sulamisen aikana kerrostunut yleensä kerrallinen ja kerroksellinen savi tai siltti (ns. glasiaalisavi ja -siltti).
Rakenteeltaan se on useimmiten tiivistä ja kulutusta hyvin kestävää.

'pehmeä, savi (sininen)
Jääkauden jälkeen syntyneitä savi- ja liejusavikerrostumia (ns. postglasiaaliset savet). Nämä savet ovat rakenteeltaan edellisiä löyhempiä ja niiden kerrostuminen voi jatkua nykyisinkin, jolloin niiden pinta on hyvin 'upottavaa.' Tällaisia kohtia alueella on sinisellä merkittyjen alueiden keskiosissa. Sinisten alueiden reunaosissa voi - varsinkin pohjan syvyyserojen vahvasti muuttuessa - olla vallalla eroosio, jolloin pohjan kantavuus yleensä lisääntyy.

Pintamerkinnät

Hiekkaa ja kiviä
Pohjan pinnalle eroosion vaikutuksesta syntynyt ohut, usein korkeintaan muutamien senttimetrien paksuinen hiekkakerros, jossa varsinkin moreenialueilla voi olla kiviä. Tällaiset alueet ovat vaikeasti havaittavissa ja ne on merkitty karttoihin vain silloin kun ne on todettu. Moreenialueille ei tätä merkintää kuitenkaan ole useimmiten tehty. Savialueilla osa kivistä voi olla myös konkreetioita.

Lohkareita
Erilliset isot lohkareet on merkitty karttaan siltä osin kuin ne ovat olleet tulkittavissa. Moreenialueille ei näitä merkintöjä ole usein tehty sillä moreeni sinällään jo pitää sisällään myös lohkareita.

Hylystä pudonneita tavaroita
Tällä merkinnällä on kuvattu n. 500 m:n pituinen alue hylystä länsilounaaseen, jossa tulkinnan perusteella pohjan pinnalla on sinne kuulumatonta erikokoista kohdetta. Kaukaisin pudonneeksi tavaraksi tulkittu kohde on n. 1100 m hylystä länsilounaaseen. Kohteiden suuren määrän vuoksi ei jokaisen kohteen paikkaa ole laskettu vaan merkinnät lähinnä rajaavat kohteiden esiintymisalueen.

4. SAVEN PAKSUUSKARTAN SELITYS

Hylyn ympäristöstä tehtiin 500 m x 600 m:n alueelta saven paksuutta kuvaava kartta mittakaavassa 1:1500. Savikerrostumien paksuus mitattiin 28 kH:n kaikuprofiilista käyttäen äänen etenemisnopeutena 1500 m/s. Oranssilla on merkitty kalliopaljastumat, joiden pinnalla voi olla ohuelti moreenia. Harmaalla merkitty "glasiaalityyppinen" kova savi tai siltti on paljastuneena kallion päällä viitaten eroosiovoimiin. Saven paksuudesta ei ole voitu tehdä samanarvokäyriä riittämättömän luotausmäärän vuoksi, mutta saven paksuutta kuvaavat metrimäärät antavat kuitenkin hyvän kokonaiskuvan paksuudesta. Sinisellä värillä kuvattu alue on nuorempien "postglasiaalisavien" peittämä. Postglasiaalisavien alapintana on käytetty

kerrostumissa näkyvää akustista rajapintaa, joka on tulkittu Ancylus-sedimentiksi (syntynyt n. 7200 v sitten).

Kaikuluotainten riittämättömän penetraation vuoksi ei savien kokonaispaksuutta saatu mitatuksi postglasiaalisavien alla. On myös mahdollista, että näiden pehmeiden savien paksuus ylittää vielä kartassa olevat paksuudet. Kokemusten mukaan vastaavan tyyppisillä paikoilla lähialueilla saven kokonaispaksuus voi hyvin olla ainakin 50 - 70 m.

5. TULKITUT PROFIILIT -SELITYS

Hylyn ympäristöstä on tulkittu kaksi poikkiprofiilia mittakaavaan 1:2000 (A - B ja C - D). Havainnollisuuden vuoksi pystymittakaavaa on suurennettu nelinkertaisesti. Tällöin myös itse hylky piirtyy vääristyneenä, jollaiselta se useimmiten näyttää myös kaikugrammilla. Hylystä on piirretty tarkempi kuva myös oikeassa suhteessa. Akustiikan tulkinnan perusteella hylky näyttäisi olevan n. 110 - 115 astetta kallellaan oikealla kyljellään, perä kovalla savella ja keula pehmeällä savikolla.

6. KARTTOJEN TULOSTAMINEN

Pohjanlaatukartat on digitoitu ja osin myös tulostettu TOPOS-kartanpiirto-ohjelmalla (Timo Pekkonen Tmi, Helsinki). Tulostuksessa käytettiin Calcomp-kynäplotteria ja HP-Paintjet piirturia. Ohjelmiston testausvaiheen vuoksi on osa karttojen merkinnöistä ja tekstit jouduttu tekstaamaan manuaalisesti (ohjainhäiriöiden vuoksi).

Syvyyskartat on tehty manuaalisesti, myöhemmin osa niistä on myös digitoitu TOPOS-ohjelmalla.

7. AINEISTON SÄILYTTÄMINEN

Akustinen luotausaineisto säilytetään merivoimien tutkimuslaitoksessa Helsingissä. Suurin osa karttamateriaalista on digitaalisessa muodossa ja sitä voidaan tarvittaessa tulostaa.

Erikoistutkija
Filosofian tohtori

Jouko Nuorteva

SUPPLEMENT No. 502

Rapport angående de tekniska och legala förutsättningarna att återfinna och omhänderta omkomna från färjan Estonia.

Sjöfartsverket.

1994.

Report concerning technical and legal conditions to find and take care of victims from the ferry Estonia.

Swedish Maritime Administration.

1994.

SJÖFARTSVERKET

RAPPORT

angående de tekniska och legala förutsättningarna att återfinna och omhänderta omkomna från färjan Estonia.

Sjöfartsverket

1994-10-11

1.2 Kort om färjan Estonia m m

De här nedan antecknade kortfattade uppgifterna lämnas för att förståelsen av fortsättningen av rapporten skall underlättas.

Fartyget ligger på havsbotten på position N 59 23,9 O 21 42,2. Denna position är utanför Finlands territorialhav men i den finländska ekonomiska zonen. Fartyget utgör inget hinder för sjöfarten.

Fartyget ligger vält på ena sidan. När denna rapport skrivs är de enda undersökningar av fartyget som gjorts den videofilmning som gjorts på begäran om haverikommissionen. På de bilder av fartyget som tagits fram syns inga skador på skrovet med undantag för att bogvisiret är borta och att rampen är skadad. Vissa fönsterrutor är sönderslagna. Vid de filmningar som genomförts har inte observerats några kroppar utanför fartyget.

Rederiet har uppgivit att Estonia vid förlisningen beräknas ha haft ca 160 ton fueloil och 42 ton diesel ombord. Lasten bestod av långtradare och personbilar. Såvitt har kunnat utrönas finns inget farligt gods ombord.

Vid de sammanträffanden, som förevarit mellan Sjöfartsverket och dem som nämnts ovan, har frågan om var de omkomna troligen befinner sig diskuterats. Den samstämmiga uppfattningen var därvid att det övervägande flertalet befinner sig i fartyget. Skälet till detta är att det finns uppgifter från personer, som räddats, om att relativt få människor befann sig på båtdäck innan fartyget sjönk. De som då inte befann sig där fanns inne i fartyget. Detta leder vidare till den troliga slutsatsen att jämförelsevis få omkomna ligger på havsbotten i närheten av fartyget. Att ha någon uppfattning om hur många i absoluta tal som finns i fartyget och utanför fartyget är dock inte möjligt.

Om man avser att återfinna och omhänderta de omkomna kan detta när det gäller dem i fartyget i princip ske antingen genom lyft av fartyget eller dykning i det på havsbotten. Detta är i och för sig en självklarhet. De, som ligger på havsbotten, måste eftersökas på annat sätt. Att alla omkomna slutligen skulle kunna återfinnas förefaller mycket osannolikt; ett antal skulle under alla omständigheter inte kunna återfinnas och omhändertas.

2. Legala förutsättningar

En behandling av de legala förutsättningarna för att återfinna och omhänderta omkomna från färjan Estonia leder till beröring med ett flertal rättsområden. Flera av dessa har dock inte några egentliga beröringspunkter med de frågor som skall behandlas. För att undanröja vissa oklarheter behandlas dessa dock här inledningsvis.

2.1 Ägare och redare

Det finns inga folkrättsliga eller i nu förevarande fall relevanta nationella regelverk som föreskriver en skyldighet för fartygets ägare eller redare att återfinna och omhänderta omkomna från ett sjunket fartyg.

2.2 Vissa försäkringar

Färjan Estonia var försäkrad. Det fanns dels en kaskoförsäkring, dels en P & I försäkring. Här bortses från eventuella försäkringar av lasten.

En kaskoförsäkring är en beloppsmässigt begränsad försäkring. Försäkringsbeloppet motsvarar i princip fartygets värde. Om en totalförlust av ett fartyg uppkommer, betalas en totalförlustersättning motsvarande det försäkrade värdet ut till försäkringshavaren. Svenska kaskoförsäkringsvillkor och - såvitt är bekant för Sjöfartsverket - även andra länders villkor innebär att äganderätten till ett fartyg, som är en totalförlust, efter utbetalningen av försäkringsersättningen övergår till försäkringsgivaren om denne inte avstår från denna rätt. Ett sådant avstående sker, såväl i Sverige som internationellt, i det ofta förekommande fallet att bärgningskostnaderna förväntas överstiga vrakets värde i bärgat skick. - Kaskoförsäkringsgivarens enda skyldighet efter en totalförlust är således att till försäkringshavaren betala ut det försäkringsbelopp försäkringsavtalet föreskriver.

Det som nu sagts är en beskrivning av hur det normalt förhåller sig. Eftersom olyckan inträffade för så kort tid sedan kan man utgå från att försäkringstagaren och -givaren ännu inte hunnit reglera sina mellanhavanden.

En P & I försäkring är en ansvarsförsäkring. Den är avsedd att täcka det rättsliga ansvar försäkringshavaren, d v s fartygsägaren/redaren, kan ådra sig. Eftersom något ansvar för dessa att återfinna och omhänderta omkomna inte finns är P & I försäkringen utan betydelse i detta sammanhang.

2.3 Vissa konventioner

När fartyget sjönk innehöll det - som tidigare sagts - uppskattningsvis 200 ton olja. Det innehöll med stor sannolikhet inte något farligt gods.

Det finns tre konventioner, som ratificerats i varje fall av Finland och Sverige, som ger stater möjlighet att ingripa mot fartyg från vilka olja släpps ut eller från vilka ett hot om utsläpp av olja föreligger. Konventionerna har lett till nationell finsk och svensk lagstiftning.

De nämnda konventionerna är 1969 års ingreppskonvention, MARPOL 73/78 och Helsingforskonventionen. De två sistnämnda är när det gäller olja likalydande. Konventionerna kan inte användas mot fartygsägaren/redaren för att tvinga honom att ta bort fartyget - och därmed i praktiken omhänderta vissa omkomna - av flera skäl, som här inte närmare skall behandlas. Om mot Sjöfartsverkets förmodan ett åläggande att förhindra oljeutsläpp skulle utfärdas mot redaren/ägaren skulle oljan kunna avlägsnas med annan teknik än att lyfta fartyget. Om ett åläggande skulle utfärdas täcks kostnaderna för åtgärderna av P & I försäkringen.

2.4 Statens skyldigheter

Det finns inga internationella eller i detta sammanhang relevanta nationella regelverk som föreskriver någon rättslig skyldighet för någon berörd stat att återfinna och omhänderta omkomna från en fartygsolycka sedan sjöräddningsinsatserna avslutats.

2.5 Bärgning

I sjörättsliga sammanhang är bärgning - enkelt uttryckt - åtgärder för att rädda ekonomiska värden som vidtas med ett förolyckat fartyg och/eller dess last och som ersätts genom att bärgaren får bärgarlön. Ordet bärgning används i dagligt tal också för att beskriva en viss typ av åtgärder, t ex att lyfta fartygsvrak och liknande, men dessa åtgärder faller inte alltid helt in under det sjörättsliga begreppet bärgning främst därför att incitamentet att vidta dem inte är ekonomiskt. Här bortses från den distinktionen av skäl som framgår nedan.

Inledningsvis sades att ett av de sätt man kan omhänderta ett stort antal av de omkomna är att lyfta fartyget, att bärga det. Man kan utgå från att ingen privat intressent kommer att göra det. Frågan är då om en eller flera stater gemensamt kan göra det.

Om fartygsägaren/redaren inte motsätter sig en bärgning uppstår inga rättsliga problem. Om fartygsägaren/redaren skulle motsätta sig en bärgning är det Sjöfartsverkets uppfattning att bärgningen lagligen kan genomföras ändå. Skälet till denna uppfattning är att de sjörättsliga bärgningsreglerna inte ger ägaren till ett förolyckat fartyg rätt att förbjuda genomförandet av en bärgning. Om han uttalar ett befogat förbud har detta endast betydelse för beräkningen av bärgarlön. Ett befogat förbud har således principiellt inte att göra med bärgarens rätt att bärga.

Det ovan beskrivna rättsliga förhållandet måste anses vara internationellt vedertaget.

För fullständighetens skull bör här nämnas att Sjöfartsverket inte frågat fartygsägaren/redaren om hans inställning i frågan.Det bör slutligen också sägas att om Estonia skulle lyftas är resultatet juridiskt att betrakta som en bärgning även om fartygets ekonomiska värde inte varit drivkraften. Den som ombesörjt lyftet har rätt till bärgarlön, som begränsas till det bärgades värde.

2.6 Finländsk lagstiftning

Vid kontakt med finska myndigheter har konstaterats att - som tidigare nämnts - fartyget ligger i Finlands ekonomiska zon. Ett förbud har utfärdats enligt lagen om undersökning av storolyckor. Avsikten med förbudet är - såvitt Sjöfartsverket förstått - att förhindra att någon vidtar åtgärder med fartyget, som hindrar eller försämrar förutsättningarna för en olycksutredning.

Finländsk lagstiftning innehåller i övrigt - såvitt kunnat utrönas - inte några rättsliga hinder för åtgärder för att återfinna och omhänderta omkomna från Estonia.

2.7 Slutsatser

Det finns inga legala skyldigheter för någon och inte heller några legala hinder, med undantag för det nämnda, temporära förbudet enligt den finska lagen om undersökning av storolyckor, mot ett omhändertagande av omkomna från Estonia. Det finns inte några legala hinder mot att lyfta fartyget även om en privaträttslig intressent skulle motsätta sig detta; det finns inte någon anledning att tro att någon skulle göra detta.

Bland de legala förutsättningarna för att återfinna och omhänderta omkomna kommer inte att behandlas det som följer

av regler för det mellanstatliga umgänget. Sjöfartsverket gör inte heller folkrättsliga överväganden som kan aktualiseras av att medborgare i andra stater än Estland, Finland och Sverige befann sig ombord i fartyget.

3. Tekniska förutsättningar

Som tidigare nämnts finns omkomna från Estonia utanför och i fartyget. Det har tidigare också sagts att det med all sannolikhet förhåller sig så att det övervägande antalet omkomna befinner sig i fartyget eftersom - såvitt kunnat utrönas vid samtal med företrädare för Haverikommissionen - vittnen uppgivit att endast en mindre mängd människor befann sig på båtdäck när fartyget höll på att sjunka. Detta innebär att ett försök att återfinna och omhänderta omkomna förutsätter åtgärder såväl med fartyget som i området utanför fartyget.

Sjöfartsverket kommer nedan att kortfattat redovisa de tekniska förutsättningarna för eftersökande och omhändertagande av omkomna utanför och i fartyget. Först kommer att redovisas de tekniska förutsättningarna för sökande efter och omhändertagande av omkomna utanför fartyget. Därefter kommer förutsättningarna för omhändertagandet av omkomna i fartyget att redovisas. Innan den senare redovisningen lämnas skall dock först redovisas vissa förhållanden, som kan ha betydelse för bedömningen.

3.1 Omkomna utanför fartyget

Vrakets position motsvarar ett läge ca 30 nautiska mil sydväst om finska Utö. Det är öppet hav och helt oskyddat för väder och vind. De människor som omkommit utanför fartyget har antingen redan hämtats under sjöräddningsfasen eller sjunkit i havet. De, som inte återfunnits och inte finns i fartyget, kan flyta upp till ytan, flyta i vattnet eller ligga på botten.

För att återfinna och omhänderta dem som flyter upp måste en avpatrullering av ett lämpligt vattenområde ske under viss tid. Hur stort området bör vara kan Sjöfartsverket inte uttala sig om. Det måste bestämmas med utnyttjande bl a av

oceanografisk expertis. Ett sådant arbete kan utföras av en eller flera kustbevakningsorganisationer eller liknande.

Dem som flyter i vattnet är det förmodligen omöjligt att återfinna om de inte flyter upp eller sjunker till botten.

De omkomna som ligger på havsbotten kan ligga utspridda på ett stort område. Det har inte gått att utreda vilka bottenströmmar, som finns i området. Enligt uppgift kan det emellertid antas att det kan förekomma kortvariga strömmar, som kan vara jämförelsevis starka, i skiftande riktningar. Med hänsyn till att en människokropp i vatten är mycket lätt, kan de omkomna ha flyttats långa sträckor från fartyget.

Det bör dessutom beaktas att ett okänt antal människor kan ha lämnat fartyget innan detta sjönk och ha förts av vind och vågor från fartyget innan de sjönk.

Det bör här nämnas att vid kontakt med rättsmedicinsk expertis har Sjöfartsverket fått beskedet att det inte är möjligt att ange vad som faktiskt händer med en drunknad människas kropp i vattnet. Beroende på de lokala förhållandena kan den flyta upp, flyta i vattnet eller sjunka till botten.

För att söka omkomna på havsbotten finns flera tekniker. Man kan använda ROV (Remotely Operated Vehicles) för att visuellt söka av havsbotten. Att använda enbart denna teknik skulle vara tidsödande och sannolikt inte ge ett godtagbart resultat.

Man kan också söka efter omkomna på havsbotten genom att använda side scanning sonars. Det är en teknik, som har använts för detta ändamål på andra platser. Det kan ifrågasättas hur pass tillförlitlig den är. Människokroppens täthet är så liten att det inte är säkert att man säkert kan identifiera vad som är en misstänkt människokropp.

Sonarteknik måste följas upp med en ROV undersökning för att säkerställa vad det är man har funnit.

En tredje teknik är att scanna havsbotten med hjälp av laserteknik. Den information man då får fram kan bearbetas digitalt och ge närmast fotografiliknande återgivningar av havsbotten.

Oavsett vilken teknik man skulle använda finns möjligheten att med i det närmaste meternoggrannhet fastställa positionen för det man funnit. Omhändertagandet, som måste ske med ROV, kan därför genomföras med god säkerhet. Orsaken till att man måste genomföra omhändertagande med ROV är att djupen på de platser man finner omkomna sannolikt skulle variera så mycket att man av dykeritekniska orsaker skulle tvingas avstå från att använda dykare.

Tidsåtgången för en avsökning av havsbotten är självfallet beroende av hur stort område man väljer att söka i. Man kan uppskatta tidsåtgången till mellan ett par veckor och en månad.

En genomsökning av havsbotten kan behandlas som en uppgift helt skild från sökande och omhändertagande av omkomna i fartyget.

3.2 Omkomna i fartyget

3.2.1 Fartyget och dess läge

Estonia är ett 155,40 meter långt och 24,20 meter brett fartyg. Hon har tio däck. På sex av dessa finns passagerar- och besättningsinredning. Fartygets vikt i vattnet kan sannolikt uppskattas till strax under 10 000 ton.

Fartyget ligger i en sluttning på havsbotten. Det har medfört att fartygets akter ligger ca tio meter djupare än fören. Vattendjupet på platsen är ca 70 meter. Fartyget synes ha

sjunkit med aktern först. Vissa omständigheter tyder på att aktern stått på botten under en tid när fartyget sjönk medan fören fortfarande befunnit sig över vattenytan. Haverikommissionen kommer att behandla detta i sin slutliga rapport men här har gjorts antagandet att fartyget sjunkit på detta sätt. Det kan ha en betydelse, som verket återkommer till nedan.

Fartyget ligger på sin ena sida. Slagsidan uppgår till omkring 115 grader. Enkelt uttryckt innebär det att fartyget ligger närmare upp och ned än på rätt köl. Vid filmning av fartyget har förutom det saknade bogvisiret och den skadade bogrampen inte kunnat iakttas några skador på skrovet. Vissa fönster i fartyget är krossade. Det säger sig självt att det varit omöjligt att observera den del av fartyget, som ligger mot botten.

3.2.2 Fartygets inre

Det har ännu inte varit möjligt att gå in i fartyget. Erfarenhetsmässigt kan man utgå från att fartygets inredning är mycket förstörd. Möbler, mattor, innertak och mellanväggar ligger sannolikt rasade överallt. Detta har åstadkommits av fartygets rörelser när det sjunkit men det är inte osannolikt att förstörelsen delvis åstadkommits av inträngande vatten i samband med att fartyget sjönk. Det är känt att vattnet på vissa platser i ett sjunkande fartyg kan komma in med mycket stor kraft. Så har troligen skett i Estonia med tanke på det sätt hon sjunkit på.

Det är inte möjligt att ha någon säker uppfattning om var de omkomna befinner sig ombord. Det är sannolikt så att de finns på alla de däck, som haft passagerar- och besättningsutrymmen. Någon möjlighet att idag avgöra om de flesta befinner sig i publika utrymmen eller i hytter finns inte.

Ett arbete att ta ut omkomna från fartyget skulle medföra behov av att röja sig fram genom förstörelsen ombord för att kunna finna de omkomna. Detta är ett riskfyllt arbete oavsett om det sker under vatten eller över.

3.2.3 Dykning

Några allmänna ord bör här sägas om dykning. Oavsett vilken teknik man skulle använda för att omhänderta omkomna i fartyget - genom enbart dykning i fartyget eller genom lyft av fartyget - måste en omfattande dykinsats göras. För den typ av dykning det är fråga om finns inga statliga resurser i Estland, Finland eller Sverige.

Det djup fartyget ligger på medför att den dykteknik som måste användas är s k mättnadsdykning. Den innebär att ett dyklag i en tryckkammare utsätts för ett tryck som motsvarar det som råder på det djup dykaren skall arbeta. Dykaren hålls därefter under tryck under något mindre än en månad. Han transporteras från det fartyg i vilket hans trycksatta bostadsutrymme finns till arbetsplatsen i en dykarklocka. När han lämnar denna är han försedd med en s k navelsträng, genom vilken gasledning för andningsgas, varmvatten för uppvärmning av hans dräkt, kommunikationledningar m m går. Navelsträngen, som enligt norska regler får vara 29 meter lång och enligt brittiska 75 meter lång, begränsar självfallet dykarens aktionsradie. Dykaren förflyttar sig simmande. Han är således betydligt rörligare än en traditionell tungdykare men mindre rörlig än en traditionell lättdykare, som man använder på mindre djup.

Varje dykeriarbete i omedelbar närhet av, på eller i fartyget är mycket riskfyllt. Frånsett den allmänt förekommande risken att dykaren fastnar kan hans navelsträng skadas, dykaren skadas av löskommande räddningsflottar, skadade dörrar, glas, olja m m. Varje dykeriföretag på fartyget måste således föregås av ett omfattande förberedande inspektions- och säkerhetsarbete.

De dykeriföretag, som skulle kunna användas för arbeten på eller i Estonia, är samtliga offshoreföretag. Arbeten av den typ det här kan vara fråga om är självfallet - utom när det gäller arbeten utanför fartyget - inte det de normalt sysslar med. Några av de företag, som är kända för Sjöfartsverket har emellertid erfarenhet av att omhänderta katastrofoffer.

Den typ av undervattensarbete det här skulle vara fråga om skulle vara en kombination av arbete med ROV och dykare. De ROVs som utvecklats för offshorebruk är utomordentligt sofistikerade arbetsredskap.

3.2.4 Omhändertagande av omkomna i fartyget under vattnet

Det är enligt Sjöfartsverkets uppfattning möjligt att återfinna och omhänderta en del av de omkomna, som finns i fartyget, genom att använda dykare. Det är troligt att man tämligen väl kan söka genom de fem översta däcken, där passagerar- och besättningsutrymmen finns. Dessa utrymmen består av publika utrymmen som restauranger, korridorer, trapphus och andra öppna utrymmen samt hytter. Det kan inte uteslutas att förhållandena är sådana på vissa platser att man förhindras från att göra en fullständig genomsökning. Om väggar mellan hytter kollapsat eller om förhållandena i övrigt blivit utomordentligt besvärliga kan det vara farligt för dykarnas säkerhet, även om delar av undersöknings- och röjningsarbetet görs med ROV, att göra en fullständig genomsökning.

På däcket under bildäck finns passagerarutrymmen. Dessa kommer att vara mycket svåra att söka igenom. Det är inte säkert att man kan komma åt dessa från bildäck utan man skulle vara tvungen att gå genom skrovet. Arbetet på detta däck skulle dessutom försvåras av att fartygets vattentäta indelning finns där. Man kan utgå från att samtliga vattentäta dörrar har slutits vilket påtagligt kommer att hindra dykarna.

Maskinutrymmet kan vara svårt att genomsöka. Bildäcket är sannolikt omöjligt att genomsöka. Detta beror på att lasten kommer att ligga förskjuten åt ena sidan. Visserligen finns ett längsgående skott genom bildäcket i hela dess längd men på ömse sidor om detta skott ligger lasten åt samma håll. För dykarna skulle det vara förenat med stor fara att försöka röja sig fram genom lasten.

Sjöfartsverket kan inte uppskatta hur stor andel av de omkomna ombord som skulle kunna omhändertas genom en dykeriinsats. När verket konsulterat dykeri- och bärgningsteknisk expertis har mycket olika uppfattningar framkommit.

Ett särskilt dykeritekniskt problem som möjligen kan uppkomma är att de högsta och lägsta punkterna på fartyget befinner sig ca 35 meter från varandra i höjdled. Detta kan vara för mycket med hänsyn till det tryck dykarna är satta under. Problemet är möjligt att tekniskt lösa.

En genomsökning av fartyget med hjälp av dykare skulle ta mellan två och fyra månader. För genomsökning av fartyget och omhändertagande av omkomna skulle behövas ett eller två särskilda dykerifartyg eller -plattformar. Arbetet kan i princip utföras utan att hänsyn behöver tas till väderförhållandena. Arbetet kan dock inte utföras om isen lägger sig.

3.2.5 Omhändertagande av omkomna genom lyft av fartyget

Om man lyfter fartyget från den plats där hon ligger följer naturligtvis allt som finns ombord med. Med hänsyn till det djup fartyget ligger på och hennes storlek är detta en från tekniska utgångspunkter utomordentligt krävande uppgift. Djupet utgör i sig inget hinder men gör att arbetet kommer att ta längre tid och vara svårare.

Sjöfartsverket har under den tid som gått från det att verket fick Regeringens uppdrag att utreda förutsättningarna fått ett antal förslag om hur man bör förfara vid en bärgning av fartyget. Dessa förslag, som i vissa fall avser användning av inte beprövad teknik, har inte utvärderats före ingivandet av denna rapport. Det verket värderat är den beprövade teknik, som finns för denna typ av lyft. Det finns ingen anledning att vid en utredning av de förutsättningar uppdraget avser gå utöver denna om den kan leda till det eftersträvade resultatet.

Som tidigare sagts ligger fartyget på havsbotten med 115 graders slagsida och med aktern ca 10 meter djupare än fören. Det är inte möjligt att lyfta fartyget när hon ligger så. Ett lyft av fartyget måste föregås av att hon rätas upp så att hon står på rätt köl.

Innan fartyget kan rätas upp måste ett omfattande och tidsödande förberedelsearbete genomföras. Med hänsyn till fartygets stora vikt måste mycket stora krafter användas när hon skall vändas och lyftas. För att dessa krafter skall kunna appliceras på fartyget måste fästpunkter och förstärkningsarbeten på fartyget utföras. Detta arbete kan bedrivas tämligen väderoberoende men inte oberoende av förekomsten av is.

Ett lyft av fartyget måste ske i två omgångar på grund av det stora djup hon ligger på. Målet för ett lyft bör inte vara att fartyget efter det att hon kommit upp till ytan skall flyta. Fartyget har efter det att hon fått slagsida förlorat sin stabilitet och sjunkit. Hon kan inte med säkerhet återges stabilitet förrän bildäcket rensats. Ett lyft måste därför sannolikt avslutas med att fartyget sätts på en pråm.

Det finns kranfartyg och annan sådan utrustning som har mycket stor lyftkraft. För att genomföra ett lyft av Estonia som är ett stort föremål skulle behöva användas ett antal kranar och lyftpråmar. Skälet till att ett antal lyftredskap

måste användas är att lyftpunkterna på Estonia måste vara utspridda. Man kan inte samla tyngden från alla dessa till en eller två punkter ovan vattnet.

Enligt Sjöfartsverkets uppfattning är det möjligt att med beprövad teknik lyfta fartyget.Det arbete som skulle erfordras för ett lyft av Estonia skulle emellertid vara mycket tidsödande. Enligt Sjöfartsverkets uppfattning kan man utgå från att det inte kan vara klart förrän i juni-augusti 1995.

När fartyget lyfts ovan ytan måste det sökas igenom. När genomsökningen och omhändertagandet av de omkomna avslutats måste fartyget skrotas eller sänkas på stort djup.

Det finns - såvitt är känt för Sjöfartsverket - endast en handfull företag i världen som har kompetens att genomföra ett lyft av Estonia. Huruvida de alla har den erforderliga utrustningen är inte känt.

3.2.6 Statens ansvar

För fullständighetens skull bör här nämnas att om staten ensam eller i förening med andra stater låter vidta åtgärder för att omhänderta omkomna från Estonia kan det inträffa att staten ådrar sig ansvar i ett eller annat avseende. Denna fråga förbigås här.

4. Sammanfattning

Sammanfattningsvis konstaterar Sjöfartsverket följande.

Det finns inga legala hinder mot och heller ingen legal skyldighet för någon att eftersöka och omhänderta omkomna efter en fartygsolycka.

Alla omkomna kommer inte, oberoende av vilka arbetsmetoder eller tekniker man använder, att kunna återfinnas.

Det är inte känt hur många omkomna som finns i respektive utanför fartyget.

Eftersökning och omhändertagande av omkomna utanför fartyget kan göras med användning av olika tekniker. Bestämning av det område som bör genomsökas måste göras med hjälp av oceanografisk expertis. Resultatet av en genomsökning kommer att vara osäkert men de omkomna som återfinns kommer att kunna omhändertas.

Eftersökning och omhändertagande av omkomna i fartyget kan ske genom dykare/ROV eller lyft av fartyget. Om en genomsökning och omhändertagande av omkomna sker med användning av dykare/ROV kommer man inte att kunna återfinna och omhänderta samtliga omkomna ombord. Hur många som inte skulle kunna återfinnas och omhändertas är omöjligt att ange. Om fartyget lyfts, vilket förutsätter ett långvarigt och tekniskt komplicerat arbete, är det med stor sannolikhet möjligt att finna och omhänderta samtliga de omkomna, som finns ombord.

SUPPLEMENT No. 503

Rockwater A/S:

Condition Survey of the Vessel "Estonia" for the Swedish National Maritime Administration.

Survey Report.

SJÖFARTSVERKET

ROCKWATER A/S
CONDITION SURVEY OF THE VESSEL "ESTONIA"
FOR THE
SWEDISH NATIONAL MARITIME ADMINISTRATION

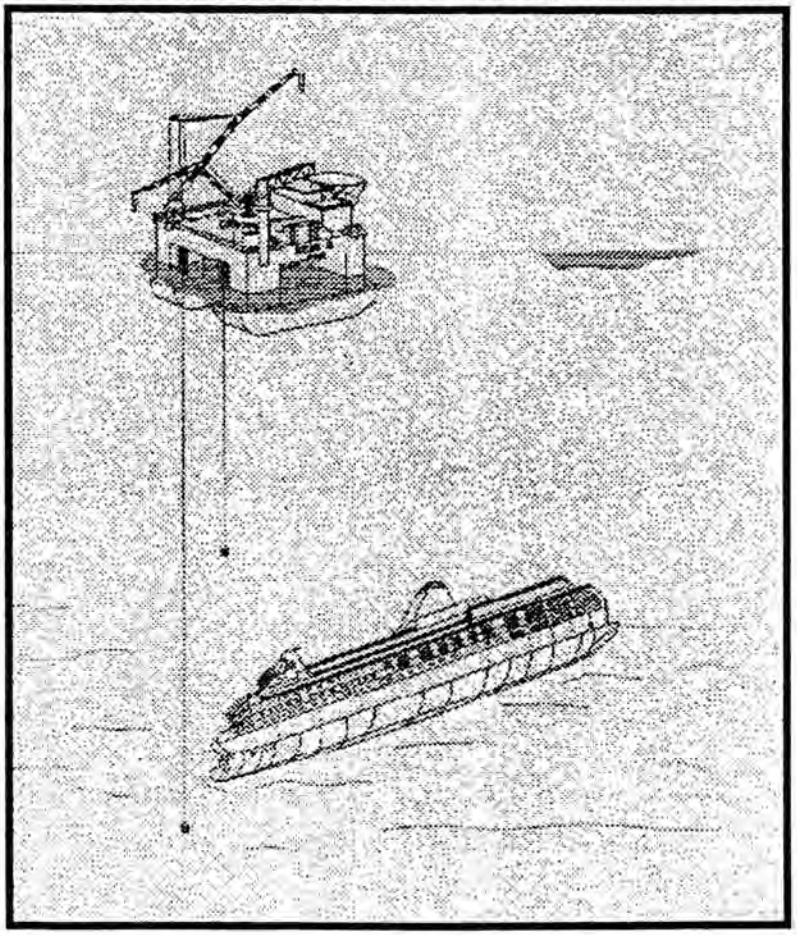

Survey Report

TABLE OF CONTENTS

1.0 INTRODUCTION

Rockwater A/S were contracted by the Swedish National Maritime Administration (NMA) to perform a condition survey of the stricken ferry "Estonia" in the Baltic Sea.

The purpose of the survey was to provide information to assist the Swedish Government in their consideration of any further action in respect of the Estonia after the tragic sinking of the vessel in September 1994. In order to ensure that the survey provided sufficient information to assist the Swedish Government in their consideration of all possibilities, Rockwater and Smit Tak established a consortium to make best use of the combined experience of both companies in the disciplines of deep water survey, saturation diving inspection and salvage operations. All disciplines were represented in all phases of the work from the initial planning to the issue of this report.

By necessity, the operation was a fast track project. The NMA were to report verbally to the Swedish Government on the 7th of December 1994 with a written report on the 12th. The contract was awarded on the 24th of November. The schedule for the work is presented in Section 3.0.

This report, together with the video tapes (19 in number), copies of the dive plans and marked-up drawings handed over to the Representatives of the NMA and the Swedish Police onboard, constitute the final report for the survey work.

This report comprises not only the results of the survey, but a description of the means by which those results were obtained in order to assist the Swedish Government in their consideration of the form of any future intervention in respect of the Estonia.

2.0 TECHNICAL SOLUTION

2.1 General

The condition survey of the ferry Estonia was performed generally in accordance with the as tendered work scope as follows:

- Approximate geological sea bed survey over a 4km^2 block around the Estonia
- Vibrocore sea bed sampling in the immediate vicinity of the Estonia
- Saturation diver inspection of the inside of selected areas within the Estonia
- ROV survey of the hull and superstructure of the Estonia (including a mudline survey)
- Diver and ROV investigation of the bow visor area and bridge of the Estonia

The marine spread utilised for the work comprised the semi-submersible vessel "Rockwater Semi 1" from which all diving, ROV and sea bed sampling work was performed; and the "Sira Supporter" which was used to perform the approximate geological sea bed survey.

The operation was overseen and directed by Representatives of the NMA, the Swedish Police and the Swedish Accident Investigation Authorities. During the mobilisation and prior to the commencement of the survey work, the objectives of the survey were discussed onboard the vessel and certain areas of the Estonia were targeted for inspection by the saturation divers. A dive plan was established for each deck of the vessel comprising a scope of work, drawings indicating the planned point of entry and the target area and a checklist for the findings of the survey.

The conditions on site required that the dive plans serve as a basis for the work with supplementary instructions being issued by the Representatives of the Swedish Authorities throughout the operation.

Both ROV and diving operations were continuously recorded on VHS video cassettes.

2.2 Safety & Risk Analysis

The offshore operation was conducted in accordance with standard Rockwater procedures which provide a framework for the safe performance of all aspects of the work, including diving.

During the mobilisation and prior to commencement of the offshore operation, a crude risk analysis was performed generally in accordance with Rockwater procedures. The purpose of the analysis was to identify any activities entailed in the Estonia works which were outwith Rockwater's normal operations together with any associated risks.

The analysis took the form of a meeting, attended by representatives of all disciplines involved in the operation, at which the planned steps in the operation were discussed and the associated risks identified.

Having identified the risks, the assembled team then identified actions to be undertaken in order to reduce or eliminate the risks. These items were summarised in the following table which was made known to the crew and displayed in dive control throughout the duration of the work.

Discussion of the hazards and risks actually encountered in the performance of the work is incorporated in the survey results in Section 4.0 of this report.

2.3 Humane Issues & Confidentiality

The tragic circumstances under which the Estonia sank and the number of victims involved in the disaster represented a huge public relations challenge to the Authorities and a threat to the sensibilities of the relatives of the victims and to the offshore work force, particularly the divers.

Rockwater were acutely aware of the risks both in terms of the release of unauthorised information or material to the public and the risk of trauma to those required to view or handle victims of the disaster.

2.3.1 Confidentiality

All communications to and from the vessel were controlled by the OIM and the Project Superintendent and were between the vessel, the company's offices and the Authorities. Several calls were received by the vessel from personnel seeking information regarding the operation though no information was released.

Prior to arriving on location, all personnel onboard the vessel were required to sign a statement of confidentiality. These statements were retained.

All video materials for the recording of the survey work were controlled throughout the operation. The video cassettes of the survey work (19 in number) were handed over to the NMA Representative at demobilisation. The remaining video cassettes (used as a method of continuous monitoring for safety purposes) have been removed from the vessel and will be retained in safe storage at Rockwater's Stavanger office for a period of 1 week after the divers have completed their decompression. The tapes will then be destroyed.

Note: The Representatives of the Swedish Police made their own edited tape of the survey work during the course of the operation and will be responsible for the control of this tape.

This report shall be issued directly to the NMA only and the survey findings shall not be divulged to any other than those directly involved in the works.

2.3.2 Welfare Of The Offshore Work force

The offshore team chosen to perform the condition survey of the Estonia included a large proportion who had undertaken similar work in the past. This included the divers, diving supervisory personnel and project engineers.

Prior to travelling offshore, the divers were screened to ensure that each diver was suitable for the work and that their personal circumstances were unlikely to add to the trauma derived from contact with the victims of the disaster.

During the mobilisation, the entire offshore team were briefed as to what they could expect in terms of the conditions at the site and their emotional reactions to the work. The briefing was given by a qualified Psychologist with considerable experience of similar work.

Throughout the diving section of the survey, contact with victims of the disaster was frequent though due consideration was given to the divers and contact was kept to a minimum. Manual handling of the bodies of the victims was occasionally required in order to gain access to targeted areas. The divers were able to gently move bodies within the vessel in order to clear access without causing any further deterioration in the condition of the bodies.

Whilst the work undertaken by the diving team inside the vessel was unpleasant and memorable, the problems associated with this work were not insurmountable and, at the time of writing, no psychological problems had been reported. Rockwater will continue to monitor those involved.

2.4 Approximate Geological Sea bed Survey

The geological sea bed survey was performed from the vessel "Sira Supporter" in tandem with the diving and ROV operations conducted from the Rockwater Semi 1.

The methodology and results are presented in a separate report. (See Section 4.2).

2.5 ROV Mudline Survey

The mudline survey was undertaken by the UFO 350c ROV deployed from Semi 1. The survey comprised a video survey and bathimetry at intervals along the length of the Estonia. The results are presented in Section 4.5.

2.6 Saturation Diving Internal Survey

The conditions actually encountered on site vindicated the choice of divers as the primary means of intervention inside the vessel. It is quite clear from the operation that ROV or ADS alone would have failed to gain access.

The diving operation was conducted from the Rockwater Semi 1 using the vessel's twin bell saturation diving system. Storage depths varied through the operation from 42 metres to 65 metres.

The agreed diving work scope was achieved in 9 bell runs.

The diving operation was carried out with three man bell runs and divers working inside the vessel were wet tended at all times from the point of entry.

Dive plans were developed for each deck which indicated the point of entry and the area of that deck which was to be surveyed. The dive plan also contained a check list which was completed by the Project Engineer in dive control as the work progressed. Due to the conditions on site, the plans were used as a basis only and actual points of entry and areas surveyed varied as a result of safety considerations and accessibility due to debris.

Whilst many of the ports and windows on the Estonia had been opened, broken or removed during the sinking, providing unimpeded access to some areas of the vessel, it was necessary to force entry at a number of locations. Two means of forced entry were utilised as follows:

Breaking Through Windows

The windows aft on Decks 4, 5 and 6 (E, F and G respectively) were large enough to allow safe access for divers to enter the vessel when broken. This was achieved by hammering a large marlin spike into the corner of the selected window in order to shatter the glass. The glass could then be removed using a hammer. Care was taken to remove fragments of glass from the frame in order to preserve the diver's umbilicals.

Oxy-Arc Cutting

Access to Deck 4 (C-Deck), amidships and to the Tween Deck required hatches to be cut using oxy-arc equipment (Broco rods). In addition, the forward windows on Decks 4, 5 and 6 (E, F and G respectively) had to be smashed and extended by oxy-arc cutting to allow diver access.

Resealing Access Points

In instances where there was a risk that buoyant material inside the vessel may be lost through access points made by the divers, the access points were resealed once the survey work at that location had been completed. Due to the attitude of the vessel, the accesses could be sealed using oversized plates or grills held in position by gravity only. Beams were welded to the backs of the plates in order to ensure that they did not slide off the hatches.

Generally, access to the vessel from the port side presented no problems for divers though, due to the attitude of the vessel , the starboard side was, for the most part inaccessible due to debris.

Conditions inside the vessel were intrinsically hazardous to the diver and constant vigilance was required in respect of the possibility of entrapment due to poor visibility and falling debris.

The operation was performed safely and with no incidents reported in association with the diving work. Divers accessed as far as it was safe to do so and did not remove debris in order to gain further access. Due to the unpleasant nature of the work inside the vessel, duration's spent in the vessel were kept short.

Details of the points of access, the extent of the areas surveyed and the location of victims are contained in Section 4.0.

2.7 Vibrocore Sea bed Sampling

A total of 6 bore holes were made at pre-determined locations to the north and south of the vessel. The results are presented in a saperate report. (See Section 4.3.)

The Vibrocore equipment was deployed using the vessel crane and no problems were encountered in connection with this element of the survey.

2.8 Investigation Of The Bow And Bridge

Under the direction of the Representatives of the Swedish Accident Investigation Authorities, divers carried out a survey of the bow of the vessel, paying particular attention to the points of attachment of the bow visor and car loading ramp. Certain attachments were recovered to surface and handed over to the Authorities onboard. In addition, the bulbous bow was inspected both by ROV and Diver.

Also under the direction of the Authorities, divers accessed the Bridge of the vessel and retrieved a number of navigational aids, a man-overboard beacon and the hydrostatic release mechanism for one of the vessel's EPIRB beacons. The bodies of 3 of the victims of the disaster were found on the Bridge.

As agreed with the Representatives of the Authorities onboard, no reporting is made of the results of this investigation work though the performance of the work is recorded on the video cassettes which have already been delivered to the client.

3.0 SCHEDULE

The following schedule reflects the sequence of events and the time frame within which the survey was performed:

ID	Task Name	21 Nov	Mon 28 Nov	Mon 05 Dec	Mon
		T F S S	M T W T F S S	M T W T F S S	M T W
1	*CONTRACT AWARD*	24/11			
2	Mobilisation to Offshore Sweden				
3	Vessel Transit to Worksite				
4	Arrive on Location		21:55 01.12.94		
5	Locate Vessel Estonia		07:57 02.12.94		
6	Commence Diving Operations		08:46 02.12.94		
7	Diver Inspection			Commence 22:10 04.12.94	
8	ROV Survey Work			Commence 22:10 04.12.94	
9	Vibrocore Seabed Sampling				
10	Geological Survey				
11	Vessel Transit to Offshore Sweden		22:20 04.12.94	05:00 06.12.94	
12	Demob. of Personnel			06/12	
13	Survey Vessel Depart Field			18:45 04.12.94	
14	Production of Final Report				
15	Submission of Final Report				12/12

4.0 SURVEY RESULTS

The means by which the following results were obtained are described in Section 2.0 of this report.

4.1 Location Of The Vessel

The original co-ordinates for the location of the Estonia provided by the Finnish Authorities were found to be incorrect after visual and sonar surveys carried out by ROV had failed to find the vessel.

The Sira Supporter then undertook a survey of the area using the ORE Side scan Sonar Towfish, running survey lines to the east and west of the original location. The operator onboard the Sira Supporter identified a hard sonar target and calculated the offset distance by reviewing the images recorded on the Thermal Linescan Recorder and the lay-back of the Towfish.

Original Location:	Latitude:	59°23'54.60"
	Longitude:	21°42'10.20"
As-Found Location:	Latitude:	59°22'56.13"
	Longitude:	21°41'00.98"
Offset Distance:	2112 metres	
Bearing:	211.1°	

The position was derived by UDI-Wimpol Seastar Differential GPS with an accuracy of 5 metres. This was confirmed by repeating the process on a different sonar line.

The Semi 1 moved to the new location and confirmed the target as the wreck of the Estonia using the ROV.

4.2 Approximate Geological Sea bed Survey

The geological sea bed survey was performed over a 4 km^2 block centred on the location of the Estonia.

The whole area surveyed is crossed by a series of generally east/west valleys which have cut into the underlying stiff clays. The valleys are generally less than 30 metres deep, but 2 in the southern side of the site are much deeper. The infilling of these valleys comprises well laminated, very soft silts and clays. These 2 deep valleys contain gas, biogenic in origin which is within 2 to 3 metres of the sea bed.

The bathymetry is quite complex and varies considerably from line to line and along lines. Some of the valleys, particularly those towards the eastern side of the site are divided by high ridges of outcropping clays up to 50 metres high.

The weather deteriorated towards the end of the survey scope and prevented us from removing the relevant personnel from the Sira Supporter, they ultimately disembarked in Aberdeen some five days later. As a direct result of this the preparation of the Geological input was delayed. In order to allow us to satisfy our Clients requirements with regard to the delivery of this report, the details of the methodology and results of the Geological survey will be presented under a separate cover.

4.3 Vibrocore Sea bed Sampling

A total of 6 bore holes were made at pre-determined locations to the north and south of the vessel. The results will be presented under a separate cover (see note above.)

4.4 Saturation Diver Inspection Of Selected Areas

The survey work inside the vessel was controlled by work packs developed onboard during the mobilisation and was essentially broken down by deck. The results are also presented by deck. The progress of the diver inside the vessel and the ports through which the diver was able to look into the vessel are recorded in the fold-out plans in this section and are marked in green. The location of victims found by the diver are marked in pink. Other items are numbered and marked in yellow.

4.4.1 General Summary

Access to any part of the port side of the vessel is possible by the means described in Section 2.6 with the exception of the shopping area amidships on Deck 5 (D-Deck) where the collapse of the partitions which formed the main shopping area and the accumulation of debris against these partitions prevent all but the most limited access to the whole area.

In general, access to most of the starboard side of the vessel was not possible within the scope of this survey and would require a protracted programme of debris removal at each point of entry in order to make the area safe for divers with the ship in its current attitude.

Visibility within the vessel was variable but tended to deteriorate as the divers entered the vessel due to the re-suspension of silt caused by the movement of the divers.

Although a light covering of silt was found throughout the vessel, the overall volume of silt which had penetrated the accessible sections of the vessel was not significant.

Despite initial safety concerns regarding floating debris, the soft furnishings, clothing, sales goods and personal effects did not present a danger to the divers but were an inconvenience when accessing cabins and enclosed spaces generally.

Internal doors, especially those to cabins, were predominantly locked or jammed. Where necessary, they were forced with a crow bar and were easily opened. Once forced, many of the doors fell from their hinges. In the case of those cabins where the doors opened to starboard, debris lying on the door made safe access impossible. Some of the doors from the main stairwell amidships to companionways aft were locked electronically and were not forced.

The bodies of a total of 125 of the victims of the Estonia disaster were individually sighted by the divers during the course of the internal survey though certain areas, especially the port side forward stairwell and the central stairwell, undoubtedly contain many more.

With the exception of those bodies found on the bridge and some of those found in the central stairwell on level 5, the bodies were intact and firm with the sex of the victim being easily identifiable. The bodies on the bridge were more badly decomposed though were also intact. Some of the bodies on Deck 5 at the central stairwell were bloated and buoyant; the remainder were effectively neutral. Many of the bodies exhibited evidence of crush injuries.

4.4.2 Deck 8 (G-Deck)

Refer to attached fold-out plan of Deck 8.

Video references:	RW/SEMI 1/EST/D/001	0:00 to 2:50
	RW/SEMI 1/EST/R/001	1:44 to 1:53

Prior to entry, the divers inspected through the ports to each of the port side cabins at the aft end of Deck 8. Poor visibility inside revealed little detail.

Access was made to Deck 8 only once, through the port side door on the aft bulkhead, at the stairs (the door itself was missing). The diver followed the aft and port side bulkheads around the periphery of the officer's day room to access cabins 835 to 843.

The stern/port quarter of the vessel sustained structural damage of the upper levels of the superstructure during the sinking and the targeted cabins had been all but destroyed. The partitions between the cabins had collapsed, as had the partitions which formed the toilets in each cabin. Plumbing, wiring and the fixtures had spilled from the cabins and into the now collapsed companionway running forward.

The diver reached the end of his umbilical adjacent to cabin 837 which was more intact than those cabins further aft.

No victims were found in the surveyed section of Deck 8.

The following features were noted by the diver and are marked up on the attached drawing:

#1. All liferafts and lifeboats on the port side were missing, presumably released during the sinking.

#2. Door 848 and the surrounding bulkhead were found to be intact.

#3. The window to cabin 835 was found to be open, as was the window furthest to port on the aft bulkhead. The remainder were intact and closed.

#4. The aft bulkhead and deck head to Deck 8 were buckled in the area of the port side external aft stairs.

#5. The deck itself appeared buckled adjacent to cabin 841.

4.4.3 Deck 7 (F-Deck)

Refer to attached fold-out plan of Deck 7.
Video references: RW/SEMI 1/EST/D/002 0:00 to 1:42

The divers viewed the amidships port side cabins 747 to 757 from outside the vessel through the ports. Visibility was limited and the view partially obscured by floating debris however, a total of 12 victims were seen in these cabins as indicated on the attached drawing in cabins 748, 749, 750 and 757.

The diver then entered the vessel as planned through the amidships saloon doors 739C to the main stairwell area. The diver attempted to gain access to the aft port side companionway through door 738A (ref. item #1 below). Failing to gain access to the companionway, the diver surveyed the stairwell. The port side stairwell was relatively clear of debris and was accessible. The starboard stairwell was only accessible near the centre line of the vessel as the starboard side of the stairs were blocked by collapsed deck head linings and debris. A further victim was found in the starboard stairwell.

The bulkheads themselves in the stairwells were intact.

Visibility in the stairwells was fair, up to 2 metres.

The diver was able to access the aft companionway on the starboard side of the vessel through door 738B as far as cabin 760. Access was made to cabin 758 which was found to be intact with all main partitions in place.

The following features were noted by the diver and are marked up on the attached drawing:

#1. Door 738A fitted with an electronic lock. The door was locked and the diver was unable to access using a crowbar.

#2. Cabins 747 to 751 were viewed from the outside of the vessel through the ports. Though the main partitions were intact, the deck head linings and fixtures had collapsed in most of the cabins obscuring the view. Visibility within the cabins was generally poor.

#3. The windows to cabins 752, 754 and 757 were open and/or broken.

#4. The identification of a victim in cabin 749 is suspect due to poor visibility.

#5. Doors 746 to the lift shaft in the starboard companionway were missing.

#6. The combined door frame for cabins 759 and 760 had collapsed into the companionway.

4.4.4 Deck 6 (E-Deck)

Refer to attached fold-out plan of Deck 6.

Video references:	RW/SEMI 1/EST/D/002	1:53 to 2:36
	RW/SEMI 1/EST/D/003	0:00 to 1:22
	RW/SEMI 1/EST/D/017	0:00 to 3:01
	RW/SEMI 1/EST/D/018	0:00 to 1:24
	RW/SEMI 1/EST/D/019	0:00 to 1:42

A total of 4 entries were made to Deck 6 as indicated in the attached plan. All were effected by entering through windows though, due to the small size of the windows to forward on this deck, the window port had to be extended by means of oxy-arc cutting.

In the large public dance bar area amidships, a total of 11 victims were found. The starboard side of this area was not accessed due to the accumulation of debris and it would seem likely that considerably more victims would be found among the debris.

In the port side forward companionway, a further 8 victims were found. The cabins in this part of the vessel were intact and access was made to cabins 6118, 6124, 6130, 6132, 6134 and 6230. Almost all cabins in this area were locked though those accessed were all empty.

The inner glass door to the port side forward stairwell (601) had broken from its mountings (as was the case on Deck 5) and blocked the forward transverse companionway adjacent to the door to cabin 6229.

The lack of furnishings in the lounge at the stern stairwell on the port side made it difficult for the diver to move around with the vessel in its current attitude though the accessed areas contained a further 8 victims.

The following features were noted by the diver and are marked up on the attached drawing:

#1. Many of the hard furnishings throughout the dance bar area were bolted to the deck.

#2. The bar/pantry itself was not accessible due to the accumulation of debris. The recovery of cash boxes or tills would require the removal of a considerable volume of furniture debris.

#3. The window to cabin 617 was open/broken.

#4. The entire starboard stairwell was blocked by debris. The deck head linings had collapsed.

#5. The 4 victims identified adjacent to the men's WC in the port side lounge were surrounded by debris and it is suspected that more victims are present beneath the debris.

#6. It is suspected that access to the port side forward stairwell was blocked by the number of victims present in the stairwell behind door 601.

4.4.5 Deck 5 (D-Deck)

Refer to attached fold-out plan of Deck 5.

Video references:	RW/SEMI 1/EST/D/003	1:22 to 3:03
	RW/SEMI 1/EST/D/004	0:00 to 2:31
	RW/SEMI 1/EST/D/016	0:00 to 2:11
	RW/SEMI 1/EST/D/018	1:24 to 2:21

A total of 5 entries were made to Deck 5 as marked on the attached plan, all were through existing access via windows or doors though, due to the small size of the windows to forward on this deck, the window port had to be extended by means of oxy-arc cutting.

In the large public shopping area amidships, access was severely impeded by the collapse of the display arrangements and by the accumulation of sales goods. The bodies of 2 victims were identified in the very limited area which was accessible with a third being seen through one of the port side windows during the course of the work.

In the port side cabin area to forward, access was through cabin 5129 into the companionway. A total of 8 victims were found in the accessible length of this companionway.

Cabins 5119 to 5135 were intact though access was largely impeded by locked doors, debris or the bodies of victims. Only cabins 5129 and 5131 were accessed.

As on Deck 6, the glass door (503) to the port side forward stairwell had been removed and was blocking the forward transverse companionway and trapping 2 bodies. The stairwell on this level was accessible through the second of the doors at 503 and it was found to be congested with a minimum of 6 bodies.

The starboard forward stairwell was accessed through door 501 to the companionway beyond. Surprisingly, this area was found to be clear of victims though access along the companionway was blocked due to the collapse of the companionway deck head linings.

Access was made to the stern cafeteria through door 578 on the port side. Once again, the accumulation of debris to starboard made safe access impossible and only the port side was inspected. The bodies of 2 victims were discovered in this limited area though it would seem likely that more would be found amongst the debris to starboard.

Two further victims were identified in the hall containing the stern stairwell on the port side though, once again, only a limited area of the hall was accessible.

The following features were noted by the diver and are marked up on the attached drawing:

#1. The deck head linings to the companionway on the port side running forward from the amidships stairwell had collapsed at door 506 refusing access to the diver.

#2. Cabin 523 had collapsed.

#3. Port side stern doors 578 were missing.

#4. Forward starboard door 501 was open.

#5. The stern of the vessel was partly buried denying access to the stern starboard side doors.

#6. Virtually the entire deck head linings in the port side stern hall containing the stairwell had collapsed allowing very little access for diver survey.

#7. The doors 510A and 510B from the shopping area to the main stairwell could not be identified by the diver due to accumulation of debris.

#8. The glass door (503) to the port side forward stairwell had been removed and was blocking the forward transverse companionway and trapping 2 bodies.

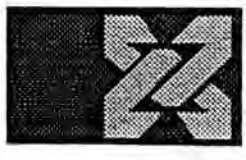

4.4.6 Deck 4 (C-Deck)

Refer to attached fold-out plan of Deck 4.

Video references:	RW/SEMI 1/EST/D/005	0.00 to 3:02
	RW/SEMI 1/EST/D/006	0:00 to 2:25
	RW/SEMI 1/EST/D/007	0:00 to 2:58
	RW/SEMI 1/EST/D/008	0:00 to 2:46

Two entry points were made to Deck 4, one through the gangway hatch amidships on the port side, the other through the window of cabin 4121 on the port forward quarter. Both entries required the use of oxy-arc cutting taking approximately 90 minutes each.

The stairwell area to amidships was relatively clear of major debris but many victims were located in this area. The diver counted 35 bodies in the stairwell area (indicated on the attached drawing by the large pink rectangle). Access aft through door 499 to the stern port side cabins was blocked by bodies as was access forward through door 422. More victims blocked the access to the data room through door 436.

One victim was seen through the window of the office (cabin 434) and a further victim was seen through the windows of the bar area towards the stern on the port side.

The diver was able to gain access through door 445 to the companionway leading aft along the centre line of the vessel though access to cabins 4501 to 4503 was blocked by debris.

The ports to all cabins on the port side were inspected and the cabins appeared to be intact though visibility was poor and partially obscured by floating debris. The bodies of 2 victims were seen in cabin 4131 and 1 in 4129.

Access through cabin 4121 to the companionway revealed a further 4 victims, 3 of which were clustered around the door 402 preventing access to the stairwell in the port forward quarter. Access was made to cabin 4126 where a further 2 bodies were found.

Access to most of the cabins was not made as the doors were mostly locked, jammed or held closed by debris.

Companionway door 419 was jammed preventing further access along the companionway.

4.4.7 Tween Deck

Refer to attached fold-out plan of the Tween Deck.

Video references:		
	RW/SEMI 1/EST/D/009	0.00 to 3:00
	RW/SEMI 1/EST/D/010	0:00 to 2:42
	RW/SEMI 1/EST/D/011	0:00 to 3:00
	RW/SEMI 1/EST/D/012	0:00 to 2:16
	RW/SEMI 1/EST/D/013	0:00 to 0:16

After metrology on the hull to identify the points of entry, 2 access hatches were made at the Tween Deck. The first access was made through cabin 1086, having miscalculated in the metrology and having missed the adjacent companionway. The second access was measured from the first and was in the correct position, bringing the divers into the Tween Deck in the companionway adjacent to cabin 1012.

Both access hatches were made with the use of oxy-arc cutting through the hull. Once the steel hull was breached, the internal lagging and panelling was removed easily with a crowbar though this activity was time consuming. A ram suspended on the crane of the Semi 1 was used to speed the process up.

Once access had been achieved, visibility on this deck was good, up to 3 metres.

Most cabins surveyed on the Tween Deck were intact, the exceptions being cabins 1005 and 1006 amidships.

Cabins 1078 to 1086 to forward were all empty and appeared not to have been used on the night of the disaster. Cabins 1005 to 1012 were used and a total of 4 victims were found in these cabins. Two further victims were found in the aft companionway.

Access along the companionways towards the centre line of the vessel was clear though debris obstructed the divers in their attempts to access the main passages running fore and aft along the centre line of the vessel. Doors 114, 121 and 128A in the water-tight bulkheads on this Deck were not accessible. Door 107 was inspected and found to be closed. Access to the spiral staircase 110 was not possible due to accumulated debris.

4.5 ROV Survey Of The Hull & Superstructure (including mudline survey)

Video references:	RW/SEMI 1/EST/R/001	0:00 to 1:53
	RW/SPRINT/94/ESTONIA/001	0:00 to 2:55

The ROV survey of the hull and superstructure was undertaken by the Sprint vehicle whilst the mudline survey was performed by the UFO 350c. The survey was directed by personnel from Smit Tak and the results are the presented in the following report.

5.0 CONCLUSIONS

Rockwater's brief in performing the condition survey of the ferry "Estonia" was to provide information to assist the Swedish Government in their consideration of any further action in respect of the stricken vessel and/or in the handling of the bodies of the victims of this tragic event.

The 3 day survey comprising geological survey, sea bed sampling, ROV inspection and diver intervention into the vessel has enabled the Rockwater and Smit Tak personnel, and the onboard Representatives of the various Authorities to gain a clear understanding of the condition of the vessel itself, the surrounding environment and the conditions which prevail inside the vessel.

Ultimately, the Authorities charged with bringing the Estonia affair to a satisfactory conclusion are faced with many difficult decisions and it would be inappropriate for Rockwater/Smit Tak to advise on the course of action to be followed. The following points however are the conclusions drawn from the survey work after due consideration of the results of the survey by the combined expertise of Rockwater and Smit Tak. This information may indicate the options available from a purely operational view.

5.1 Salvageability Of The Vessel

The Estonia is salvageable though the consideration of a salvage operation is complicated by the considerations with respect to the handling of the bodies of victims of the disaster. The issues are discussed in part 6 of the Smit Tak report contained in Section 4.5 of this document.

5.2 Internal Intervention

It is quite clear from the experience gained during the survey work that the use of divers is the only means by which useful work can be undertaken inside the vessel. The chaotic nature of the furnishings and fittings would simply not allow an ROV to operate, with fouling being a constant problem. The width of the access points, companionways, internal doors etc. would preclude the use of any ADS currently available.

The survey work demonstrated that the recovery of individual targeted items was only possible within the bridge and not in the public areas due to the chaotic arrangement of debris. The recovery of targeted valuables to reduce the risk of plunder is not practical with the vessel in its current attitude.

The ROVs proved to be quite capable of accessing all parts of the exterior of the hull and superstructure and their sonar and bathymetric equipment proved useful in establishing the location and attitude of the vessel.

5.3 Condition & Location Of Victims

All of the victims found during the survey were inside the vessel.

Although not all areas of the vessel were surveyed internally, those areas to which access was achieved could be considered a representative sample. The relatively small proportion of victims actually pinpointed by the divers (some 125 bodies) would suggest that the remainder would be concentrated in those areas of the vessel which were not accessed, namely, the starboard side.

It was established during the survey that most loose items accumulated on the starboard side when the vessel overturned and sank and it would be reasonable to assume that the bodies of many of the victims would have been carried with the debris to the starboard side.

Any efforts to recover these trapped bodies would have to involve the methodical removal of debris from the point of entry to the full extent of the incursion in order to maintain diver safety. This would not be a quick process and would be hampered by poor visibility as the silt inside the vessel was disturbed by the actions of the divers.

At the time of the survey, the condition of the bodies of the victims was, in general, surprisingly good though some showed obvious signs that deterioration had commenced. It would be reasonable to assume that, once deterioration becomes widespread, the process will accelerate.

The condition of the bodies at the time of the survey would allow them to be handled and recovered in the traditional manner though this condition will not be maintained indefinitely. Any recovery of the vessel to surface would further accelerate the deterioration and the logistics of such an operation would need to be carefully considered.

With the vessel in its current attitude, the same means of intervention used to perform the survey work could be utilised to recover a significant percentage of the victims in a relatively short operation by targeting those areas which are accessible and which are known to contain large numbers of bodies. The efficiency of any such recovery operation would decrease with time and the optimum cut-off would have to be established as the work progressed.

SUPPLEMENT No. 504

Karppinen Tuomo - Rantanen Antti:

MV Estonia Accident Investigation. Stability calculations.

Technical Report VALC177.

VTT Manufacturing Technology. Espoo 1996.

MV ESTONIA ACCIDENT INVESTIGATION

Stability calculations

CONFIDENTIAL

TECHNICAL REPORT VALC177

Tuomo Karppinen & Antti Rantanen

Espoo, May 1996

VTT MANUFACTURING TECHNOLOGY
Tekniikantie 12, Espoo, P.O.Box 1705
FIN–02044 VTT, Finland
Tel. + 358 0 4561, Fax + 358 0 455 0619, Telex 122972 vttha fi

Projekti/työ - Project identification	Sivuja - Pages	Päiväys - Date	Raportin nro - Report No.
	22	21.05.1996	VALC177

Otsikko ja tekijä - Title and author

MV ESTONIA ACCIDENT INVESTIGATION
Stability calculations

Tuomo Karppinen & Antti Rantanen

Päivitys raporttiin nro - Update to report no.	Hyväksynyt - Approved by
VALC110	

Julkisuus - Availability statement — Määräpäivä - Until date

[] B (Julkinen - Public) [x] C (Luottamuksellinen - Confidential) [] C (Salainen - Secret)

Abstrakti, sisällysluettelo, tms. - Abstract, list of contents etc.

Abstract

The static and dynamic stability of MV Estonia were calculated. The current most accurate estimates of the real loading condition in the night of accident was used in the calculations. This report replaces the technical report no. VALC110 released in December 1995 with the same title. Some additions and amendments have been made to the previous version.

In the calculation case where the side of the ship effectively contributes to the righting moment, the static heel angles were 23, 39 and 49 degrees when there was respectively 1000, 2000 and 3000 tons of water on the cardeck. When the side above the 4th deck is not included in the calculations, the ship capsizes with more than 2000 tons of water on the cardeck. The lower corner of the bow ramp descended gradually near the calm water level. When there was about 2000 tons of water on the cardeck, the freeboard at the ramp corner was 0.4 m. As more water flooded in the freeboard remained almost constant until the amount of water was about 3500 ton after which the ramp corner began to sink reaching finally the calm water level.

The effect of cargo shifting on static and dynamic stability was investigated. The static heel angles in the case of cargo not shifted were about 0, 10 and 20 degrees when there was 0, 400 and 1000 ton water on cardeck. In the case of cargo shifted an unrealistically large displacement, the corresponding heel angles were about 10, 20 and 30 degrees.

The vessel was built to satisfy the two compartment stability regulations according to the 1974 Solas Convention. The stability was checked also according to the alternative regulations of IMO Resolution A.265 on subdivision and stability of passenger ships. Neither the metacentric height nor subdivision index of MV Estonia meet the requirements of A.265.

TABLE OF CONTENTS

VTT VALMISTUSTEKNIIKKA
Laiva- ja konetekniikka

VTT MANUFACTURING TECHNOLOGY
Maritime and Mechanical Engineering

P.O. Box 1705
FIN-02044 VTT
FINLAND

Tel.int.+358 0 4561
Telefax +358 0 455 0619
Telex 122972 vtiha sf

1 INTRODUCTION

The static and dynamic stability of MV Estonia have been calculated using the current most accurate estimates of the real loading condition in the night of accident. This report replaces the technical report no. VALC110 released in December 1995 with the same title. Some additions and amendments have been made to the previous version.

The calculations of static righting arm h_ϕ or GZ and dynamic stability in terms of area below the static stability curve were carried out for cases with different amounts of water on the cardeck. The static and dynamic heel angles are presented as functions of water weight on cardeck. The calculations were first made assuming that the side above the 4th deck (roof of the cardeck) is included i.e. the whole hull volume above the 4th deck is effective and contributes to righting moment. The same calculations were then made for the case in which the side above the 4th deck is not included representing situation where water can freely flow inside the hull above the 4th deck. The static heel angle, draught and trim were calculated also for the case where the hull side between 4th and 6th decks at the aft part of the ship was not included. This corresponds an assumed condition that the large restaurant windows on decks 4 and 5 broke as they sank under the water being the first openings besides the ramp through which water flooded inside the superstructure.

Also the effect of cargo shifting on the cardeck was investigated. The static and dynamic stability were compared to the case where the cargo was assumed not shifted. The calculations were made with the amount of water on cardeck as parameter. The side above the 4th deck was not included in these calculations.

The damage analysis was accomplished for MV Estonia. The static stability was calculated for cases where water tight hull volume above the cardeck gradually decreases as the ship heels and more water flows inside through openings. Also the freeboard of some critical openings was calculated as function of water weight on the cardeck.

The vessel was built to satisfy the two compartment stability regulations according to the 1974 Solas Convention. The imaginary damage in the 1974 SOLAS regulations is limited to the compartments under the cardeck. The kind of damage which occurred to MV Estonia where water enters the cardeck is not taken into account in these regulations. The stability was also checked according to the IMO Resolution A.265. The overall GM-requirement in accordance with regulation 5 and the subdivision index of regulation 6 were calculated according to the A.265 regulations on subdivision and stability of passenger ships.

2 COMPUTATION METHOD

The program package NAPA was used in the stability calculations and damage analysis. NAPA (the Naval Architectural Package) is a computer-aided engineering system used in the basic design work for a ship project and in naval architectural calculations. The package comprises the definition of hull form, superstructures, bulkheads, decks and compartments. Besides stability and damage analysis NAPA can be used when calculating hydrostatics, tank volumes, capacities, loading conditions, inclining test results etc.

The NAPA program package is used world wide by shipyards, consultants, navies etc. In Finland, NAPA has been a long time the standard method by which the shipyards have made hydrostatic calculations.

The hull form of MV Estonia was defined in the NAPA program already before the accident for a new stability booklet. This hull form definition has been used in the stability calculations which were actually made by Mr Junnila at Ship Consulting Ltd. in Turku. Mr Junnila had also made the former valid stability booklet of the vessel dating from 20 January 1991. The stability booklet was made after an inclination test made 11 January 1991 at Masa Yards in Turku. The present stability calculations are based on the results of the same inclination tests.

The report containing the damage stability calculations according to the IMO MSC/Circ. 574 was also made by Mr. Junnila at Ship Consulting Ltd. in July 1994. These calculations are part of the IMO Resolution MSC. 26(60) which came into force at 1. October 1994.

3 LOADING CONDITION

The main particulars of MV ESTONIA are presented in Table 3.1. The lines drawing is shown in Figure 3.1. The lines drawing does not show the ducktail attached to the transom which, however, is included in the stability calculations.

Table 3.1 Main particulars of MV Estonia.

	Symbol	Dimension	Actual values	Actual values without visor	Preliminary values
Length over all	L_{oa}	m	155.4	150.7	155.4
Waterline length	L_{wl}	m	144.8	144.8	144.8
Length btw. perp.	L_{pp}	m	137.4	137.4	137.4
Beam mld, A deck	B	m	24.2	24.2	24.2
Waterline beam	B_{wl}	m	23.6	23.6	23.6
Draught mean	T	m	5.389	5.356	5.500
Draught at aft. perp.	T_a	m	5.607	5.665	5.750
Draught at forw. perp.	T_f	m	5.172	5.047	5.250
Trim, positive by stern		m	0.435	0.618	0.500
Displacement	∇	m^3	11931	11872	12243
Volume of whole hull		m^3	74730	-	74730
Length of cardeck		m	136.0	136.0	136.0
Breadth of cardeck		m	24.20	24.20	24.20
Volume of cardeck		m^3	18543	18543	18543
Longitudinal CG from aft. perp.	LCG	m	63.85	63.48	63.70
Vertical CG from keel	KG	m	10.62	10.62	10.50
Transverse metacentric height	GM_T	m	1.17	1.26	1.28

The calculations of static and dynamic stability for the case with side above the 4th deck is not included as well as the investigation of cargo shifting effects were carried out in such an early stage that only the preliminary estimates of main particulars were available. In all the other cases, the actual values were used. They are also estimates but based on more accurate information of vessel's loading condition. The difference between the actual and the preliminary loading conditions has some effects on the results mainly due to the change of transverse metacentric height GM_T.

4 RESULTS

4.1 Definitions

Static stability is expressed in terms of static righting arm h_ϕ or GZ as a function of heel angle. The righting arm is defined as the horizontal distance from the centre of gravity G to the vertical line through the centre of buoyancy B. The definitions are shown in Figure 4.1. The static stability is often illustrated as a curve of righting arm vs. heel angle. A typical static stability curve is presented in Figure 4.2. The heel angle at which the curve first intersects the horizontal axis represents equilibrium position when the righting and heeling moments are equal. This angle is referred as static heel angle.

Dynamic stability is the integral of static stability i.e. the area under the righting arm curve. This integral is denoted as e_ϕ and it is expressed as a function of heel angle. It is proportional to the work needed to heel the ship to a certain angle. The heel angle at which the dynamic stability curve intersects the horizontal axis (dynamic heel angle) represents the angle to which the ship heels from equilibrium position after a sudden heeling moment. At that heel angle the work done by heeling moment equals the work done by righting moment. The roll damping is assumed to have no effect on the dynamic heel angle though in reality some damping exist.

4.2 Static and dynamic stability (side included)

The static and dynamic stability for the case with side above the 4th deck included were calculated with 0, 200, 400, 600, 1000, 1400, 2000, 3000 and 4000 tons of water on cardeck. The draught and trim of the ship and the water level on the cardeck assuming neither heel nor trim angle, are shown in Figure 4.3 as functions of water amount on the cardeck. The effect of cargo on water level was not taken into account. Draught is defined at midships as in Figure 4.1. Trim is the difference of draughts at after and fore perpendiculars. In Figure 4.4 the static (solid line) and dynamic heel angles are shown as functions of water amount on cardeck. The actual values of ship main particulars excluding the visor were used. The h_ϕ and e_ϕ values as functions of heel angle are shown in Figures 4.5 and 4.6, respectively. The static heel angle and the inflooded water for four cases is visualised in Figure 4.7 corresponding 1000, 2000, 3000 and 4000 ton water on cardeck. The frames drawn in each case are #6, #80.5 and #156 with x-coordinates of 3.6, 69.0 and 134.8 m from AP, respectively. These drawings as well as the h_ϕ and e_ϕ values were calculated using the actual values with the visor but the influence of the visor on the results is insignificant.

4.3 Static and dynamic stability (side not included)

The stability for the case with side above the 4th deck not included was calculated with 0, 200, 400, 600, 1000, 1400 and 2000 tons of water on cardeck. The h_ϕ and e_ϕ values as functions of heel angle are presented in Figures 4.8 and 4.9, respectively. The static and dynamic heel angles as functions of water amount on cardeck are shown in Figure 4.10 where the last dynamic heel angle corresponding to 1350 ton water is interpolated using the adjacent values. The preliminary values of ship main particulars were used.

Assuming that some of the large windows on the 4th and 5th deck broke being the first openings through which the water flooded on these decks, a damage case where a large space between the 4th and 6th deck in the aft part of the ship was excluded from the watertight hull volume was also analysed. On the 4th deck, the hull volume from the aft bulkhead to the cabin department, i.e. to the frame no. 44, was disregarded. On the 5th deck, the disregarded space extended from the aft bulkhead to the frame V just aft from the main stairway. The static heel angle in the case when these spaces do not contribute any more to the stability is shown in Figure 4.4 (dotted line). The draught and trim compared to the

intact hull case are shown in Figure 4.11. These calculations were done using the actual values of ship main particulars but without the visor.

4.4 Effect of cargo shifting

The h_ϕ and e_ϕ values for the case where the cargo on the cardeck was assumed to be shifted were calculated in cases with 0, 400 and 1000 tons water on the cardeck. The side above the cardeck was not included in the righting moment calculations. The weight of cargo in both sides of the cardeck was 300 tons. The transverse locations of the centre of gravity for shifted cargo were conservatively estimated as 11.0 m on starboard side and -3.0 m on port side measured from ship centreline. These values are somewhat conservative because in reality the cargo could not move that much. It has been estimated that during the MV Estonia accident the cargo was able to move only about 1 m sideways. The static and dynamic heel angles are shown in Figure 4.12. The h_ϕ and e_ϕ values together with the corresponding results of unshifted case are presented as functions of heel angle in Figures 4.13 and 4.14, respectively. The preliminary values of ship main particulars were used.

4.5 Damage analysis

The freeboard from the calm water level to selected openings through which the progressive flooding may have started was predicted for different amounts of water on the cardeck. The openings considered were the door to foredeck from 5th deck aft, large side windows aft on 4th and 5th deck, a weathertight door to foredeck and the lower corner of the ramp opening. In addition, there were ventilation fans on the 4th deck along the front bulkhead, under the weathertight door. Similar fans were near to the side on the 4th deck aft. Water had access to the cardeck through these fans if they were not closed which is probable. A summary of the critical openings is given in Table 4.1.

Table 4.1 Critical openings.

Opening	Deck/Height from baseline (m)	Dist. from after perp. (m)	Transv. dist. from CL (m)	Area (m^2)	Number on SB side
Door to cafeteria aft	5th/16.2	2.4	9.7	3	1
Large side windows aft	4th/13.8	3.6	12.1	0.9	15
Large side window aft	5th/16.7	3.6	12.1	0.9	37
Door to foredeck	5th/16.2	123.6	8.4	1.5	1
Ramp opening (corner)	3rd/7.65	134.8	2.75	30	1
Fans to CD on aft deck	4th/14.2	-3.6	10.9	0.8	4
Fans to CD on fore deck	4th/14.2	124.3	10.9	0.8	4

The calculated freeboard values at the first five openings as functions of water on cardeck are drawn in Figure 4.15. It shows that the first openings which go under the calm water level are the side windows on the 4th deck. This occurs when there is about 2000 tons of water on the cardeck and the heel angle is about 40 degrees. At this stage, the lowest corner of the ramp opening is about 0.4 m above the calm water surface and it remains slightly above the water level until there is over 5000 tons of water on the cardeck.

Though it is impossible to predict how the flooding of the vessel hull and the superstructure developed, some simplified flooding cases have been analysed. The h_ϕ and e_ϕ values as functions of heel angle for different damage stages are presented in Figures 4.16 and 4.17, respectively. The static stability was calculated for cases where watertight hull volume above the cardeck gradually decreases as the ship heels and more water flows inside through openings. The notation of first damage stage 'cardeck out' in the figures means that water can flood in to the cardeck through the lower corner of the opened bow

ramp. The second stage 'cardeck & decks 5-6 out' means that water can flow in also to the 5th deck through the openings on that deck with the result that the hull volume between decks 5 and 6 does not contribute any more to the righting moment. In the next stage 'cardeck & decks 4-6 out' water has flowed down also between decks 4 and 5. After this stage openings on the upper decks gradually remain under the water level representing the last three damage stages. The actual values of ship main particulars including the visor have been used.

The allowed trim/draught combinations with regard to three stability criteria of 1974 Solas Convention have also been calculated. The criteria which the ship has to meet in the final flooded condition are:

- minimum GM = 0.05 m
- maximum heel angle = 12 degrees
- marginline not submerged

The allowed and not allowed trim/draught combinations for MV Estonia are shown in Figure 4.18. In Figure 4.19 the equilibrium floating position of the ship is shown for the case when the cardeck and decks between 4-6 are out. The cross-section is at the longitudinal coordinate x=79.4 m from the after perpendicular.

4.6 Stability check according to IMO Resolution A.265

The results of stability check according to IMO Resolution A.265 are presented in NAPA output format in Tables 4.2 and 4.3. The former table shows the minimum required intact GM in the final stage of flooding for the draughts of 5.02, 5.28 and 5.42 m and stern trim of 0.6 m in accordance with regulation 5 of A.265.

Regulation 5 states that in the final stage of flooding there shall be a positive metacentric height GM_T, calculated by the constant displacement method and for the ship in upright condition, of at least

$$GM_T = 0.003\frac{B_2^2(N_1+N_2)}{\Delta F_1} \quad \text{or}$$

$$GM_T = 0.015\frac{B_2}{F_1} \quad \text{or}$$

$GM_T = 0.05$ m whichever is greater,

where B_2 = is the extreme moulded breadth of the ship at midlength at the relevant bulkhead deck.
Δ = displacement of the ship in the undamaged condition.
F_1 = the effective mean damaged freeboard as defined in the regulation 1 of A.265.
N_1 = number of persons for whom life-boats are provided
N_2 = number of persons (including officers and crew) that the ship is permitted to carry in excess of N_1.

In two compartment flooding the heel angle shall not exceed 12 degrees either.

The table shows also the summary of calculation for regulation 6 using the minimum required intact GM values and thus attained subdivision index A and the required subdivision index R. The attained subdivision index A in regulation 6 is calculated as:

$$A = \sum aps$$

where 'a' accounts for the probability of damage as related to the position of the compartment in the ship's length
'p' evaluates the effect of the variation in longitudinal extent of damage on the probability that only the compartment or group of compartments under consideration may be flooded
's' evaluates the effect of freeboard, stability and heel in the final flooded condition for the compartment or group of compartments under consideration.

The required subdivision index R is determined as:

$$R = 1 - \frac{1000}{4L_s + N + 1500}$$

where L_s = subdivision length of ship = 143.158 m
$N = N_1 + 2N_2 = 3308$

The value of N which gives the required index equal to the attained one is also presented in the table.

The latter table shows the attained subdivision index calculated using minimum intact GM of 1.0, 1.3 and 1.6 m for the corresponding draughts expressed above. These GM values represent typical cases for the draughts in question. The actual values of ship main particulars were used.

The damage stability calculations were made in 1994 according to the IMO MSC/Circ. 574 which is a simplified method based upon resolution A.265. It is a calculation procedure to assess the survivability characteristics of existing Ro-Ro passenger ships. The following intact loading condition has been used in this investigation: mean moulded draught 5.55 m, trim 0.5 m by stern and GM 1.544 m. Cross-flooding has been assumed between fresh water tank 4A and 4B as well as heeling tanks 13 and 14. The filling of heeling tanks is about 50%. The side casings after and forward on deck A have been assumed weathertight.

The attained subdivision index A = 0.6531 when GM = 1.544 m. The required subdivision index $A_{max} = 0.6873$. Ro-Ro passenger ships constructed before 1 July 1997 shall comply with regulation 8, as amended by resolution MSC. 12(56), not later than the date of first periodical survey after the date of compliance which depends on the ratio A/A_{max}. In the case of MV Estonia the ratio A/A_{max} was 0.9502. For the ships having the ratio 0.95 or more but less than 0.975 the date of compliance is 1 October 2004.

5. DISCUSSION

Both the static and dynamic heel angles for the case of side included are larger than those for the case of sides not included when there is less than 2000 tons of water on the cardeck. This ambiguous result is a consequence of the fact that the actual transverse metacentric height used in the case of side included was smaller than the preliminary assumption used in the calculations for the other case. When the amount of water on the cardeck increases and the heel angle grows over 40 degrees, the effect of intact hull side is emphasised. The static righting arm increases when the ship heels to the maximum calculation angle of 90 degrees. The dynamic heel angle remains under 90 degrees even in the worst calculation case when there is 4000 tons of water on the cardeck. If the effect of side is not included, the ship capsizes when the amount of water on the cardeck is more than 2000 tons.

In the case of side not included the static righting arm starts to decrease right after the heel angle of 40 degrees and becomes rapidly negative. The dynamic heel angle cannot even be calculated when the amount of water on the cardeck is more than about 1350 tons.

The steady heel angle due to the ship's turn back to the opposite heading was not significant. If a steady turning circle diameter of $3L_{pp}$ and speed of 15 kn are assumed the heel angle was about 3 degrees when there was 400 - 1000 tons of water on the cardeck. Using speed of 10 kn the corresponding heel angle was about 1.5 degrees. The effect of roll damping fins which were active at the time of the accident, has been neglected in this simplified consideration.

With the heel angles of nearly 90 degrees the ship had not much dynamic stability left. Because the ship did not turn upside down, it could not have rolled much in the final stage of flooding but the situation must have been quite static.

The static heel angles in the case of cargo not shifted were about 0, 10 and 20 degrees when there was 0, 400 and 1000 tons of water on the cardeck. In the case of cargo shifted, the corresponding heel angles were about 10, 20 and 30 degrees. The cargo shifting reduces the static righting arm about 0.4 m in the heel angle range of 0 - 40 degrees. The distance of cargo shifting was, however, unrealistically large in the calculations.

A ship does not have to satisfy both the 1974 Solas regulations and A.265 Resolution but if the ship satisfy the A.265 regulations, the collision bulkhead need not to be extended weathertight to the deck next above the relevant bulkhead deck. The damage stability of a ship is considered sufficient according to the IMO Resolution A.265 if the metacentric height of the ship in damaged condition meets the requirements of regulation 5 and the attained subdivision index according to the regulation 6 is not less than the required subdivision index.

MV Estonia satisfies the damage stability criteria of 1974 Solas Convention but the damage stability cannot be considered sufficient with regard to the regulations in the resolution A.265. The actual GM was less than 1.3 m whereas the required GM should have been more than 2 m for the draught in question. Moreover, if the GM had been sufficient, the attained subdivision index would in any case have been too small. The required index was 0.8141 when the attained one was only 0.7090. This attained value would, however, have been sufficient if N ($=N_1 + 2N_2$) had been less than 1364.

6. CONCLUSIONS

The final situation before the ship sank was probably quite static without significant roll motion because the ship did not turn upside down though it had not much dynamic stability left.

The relatively small water amount of 1000 tons on the cardeck caused the static heel angle of about 20 degrees. The ramp corner remained above the calm water level until there was about 5000 tons of water on the cardeck. The progressive flooding started earlier probably on the 4th deck through the windows broken by the water pressure.

An unrealistically large cargo shift would increase the heel angle by about 10 degrees.

ACKNOWLEDGEMENTS

Special thanks to Mr Veli-Matti Junnila from Ship Consulting Ltd. and Associate Professor Jerzy Matusiak from the Technical University of Helsinki for proof-reading and valuable comments on this report.

Table 4.2 Results of stability check according to the IMO Resolution A.265. Subdivision index calculated using actual minimum intact GM values according to the regulation 5 of A.265.

```
Overall GM-requirement in accordance with regulation 5
------------------------------------------------------


  Initial condition     Minimum
    Draught   Trim      intact GM

    5.020   -0.600      1.465
    5.280   -0.600      2.447
    5.420   -0.600     32.315


Summary of a-calculation for Regulation 6
=========================================

 1-compartment groups sum a*p= 0.2782      sum a*p*s= 0.2782
 2-compartment groups sum a*p= 0.4091      sum a*p*s= 0.3792
 3-compartment groups sum a*p= 0.2248      sum a*p*s= 0.0516
 4-compartment groups sum a*p= 0.0808      sum a*p*s= 0.0000
-----------------------------------------------------------

Attained subdivision index A =                      0.7090
Required subdivision index R calc. for N= 3308      0.8141
Attained index A = 0.7090 corresponds to
required index R for N= 1364
```

Table 4.3 Results of stability check according to the IMO Resolution A.265. Subdivision index calculated using typical intact GM values for the respective draughts.

```
Overall GM-requirement in accordance with regulation 5
------------------------------------------------------


  Initial condition     Minimum
    Draught   Trim      intact GM

    5.020   -0.600      1.000
    5.280   -0.600      1.300
    5.420   -0.600      1.600


Summary of a-calculation for Regulation 6
=========================================

 1-compartment groups sum a*p= 0.2782      sum a*p*s= 0.2782
 2-compartment groups sum a*p= 0.4091      sum a*p*s= 0.2683
 3-compartment groups sum a*p= 0.2248      sum a*p*s= 0.0328
 4-compartment groups sum a*p= 0.0808      sum a*p*s= 0.0000
-----------------------------------------------------------

Attained subdivision index A =                      0.5793
Required subdivision index R calc. for N= 3308      0.8141
Attained index A = 0.5793 corresponds to
required index R for N=  304
```

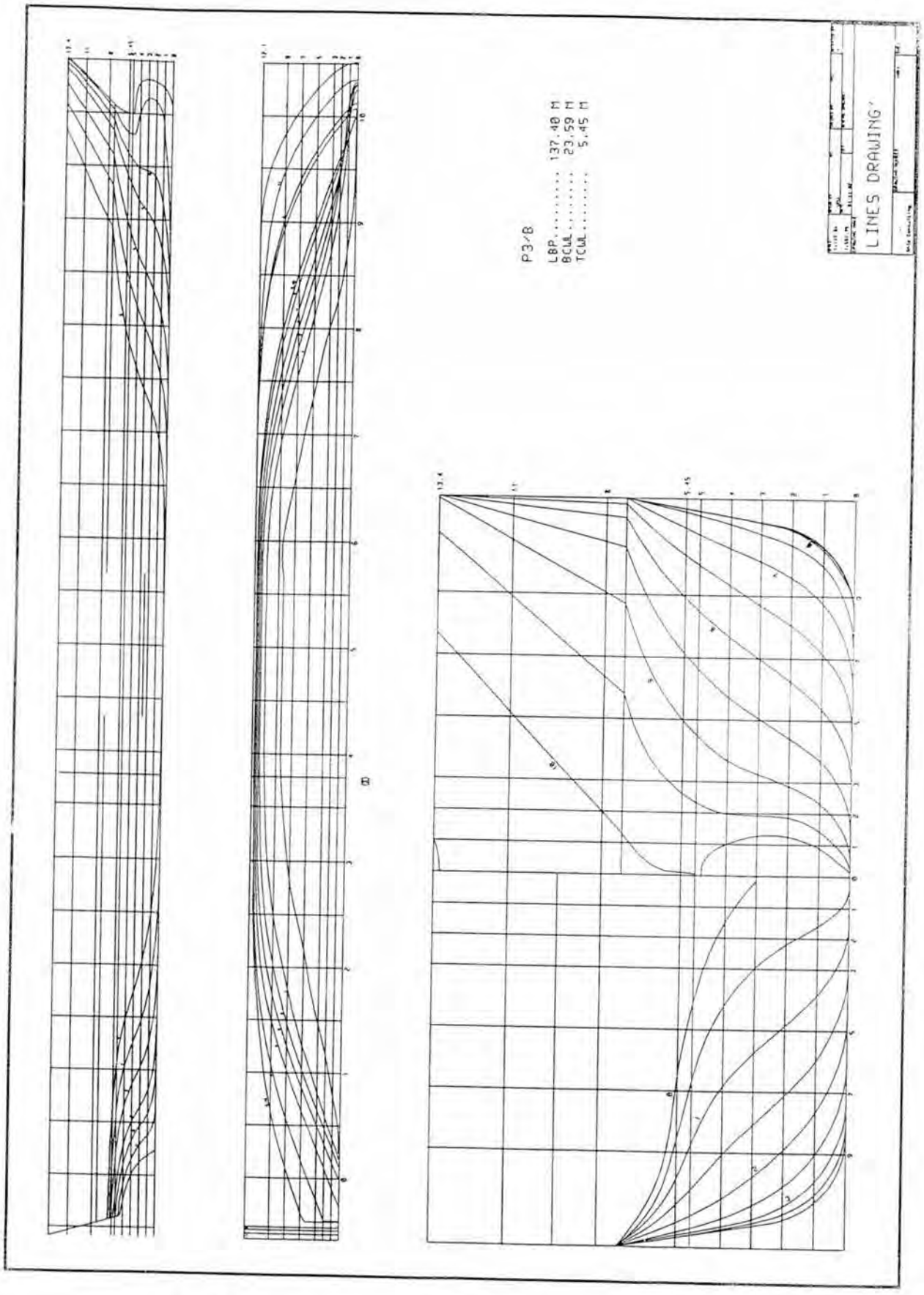

Figure 3.1 Lines drawing of MV Estonia.

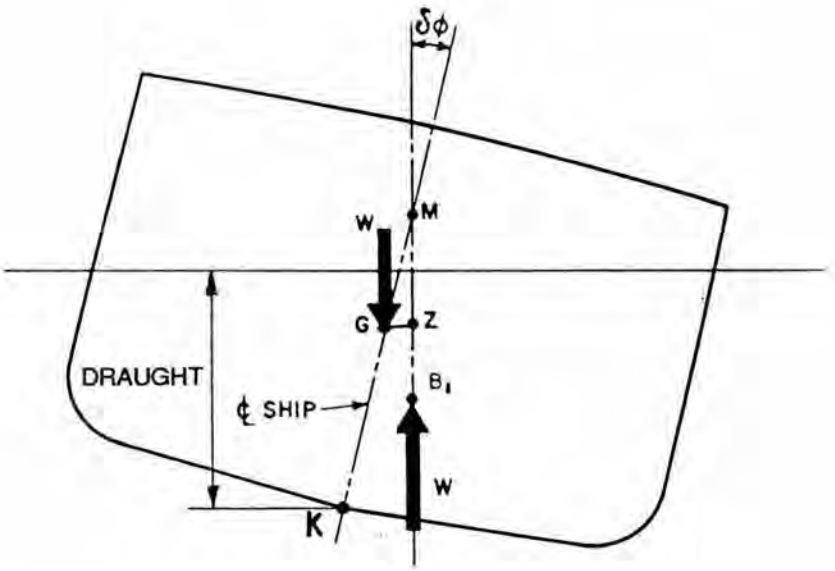

Figure 4.1 Definition of symbols.

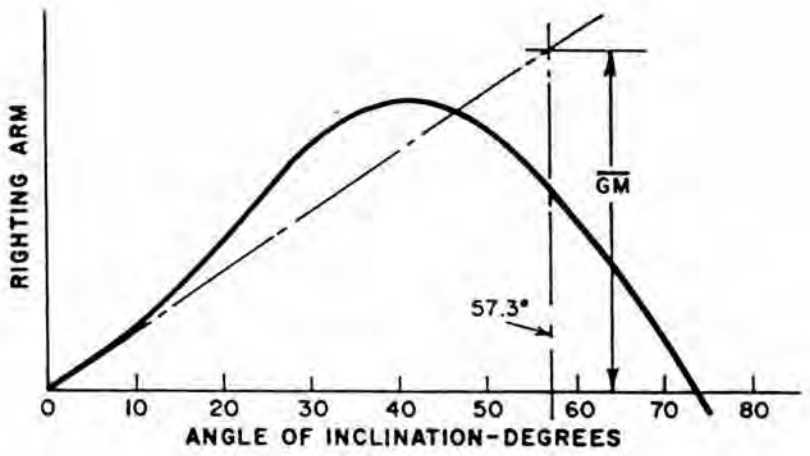

Figure 4.2 Typical righting arm (GZ) curve.

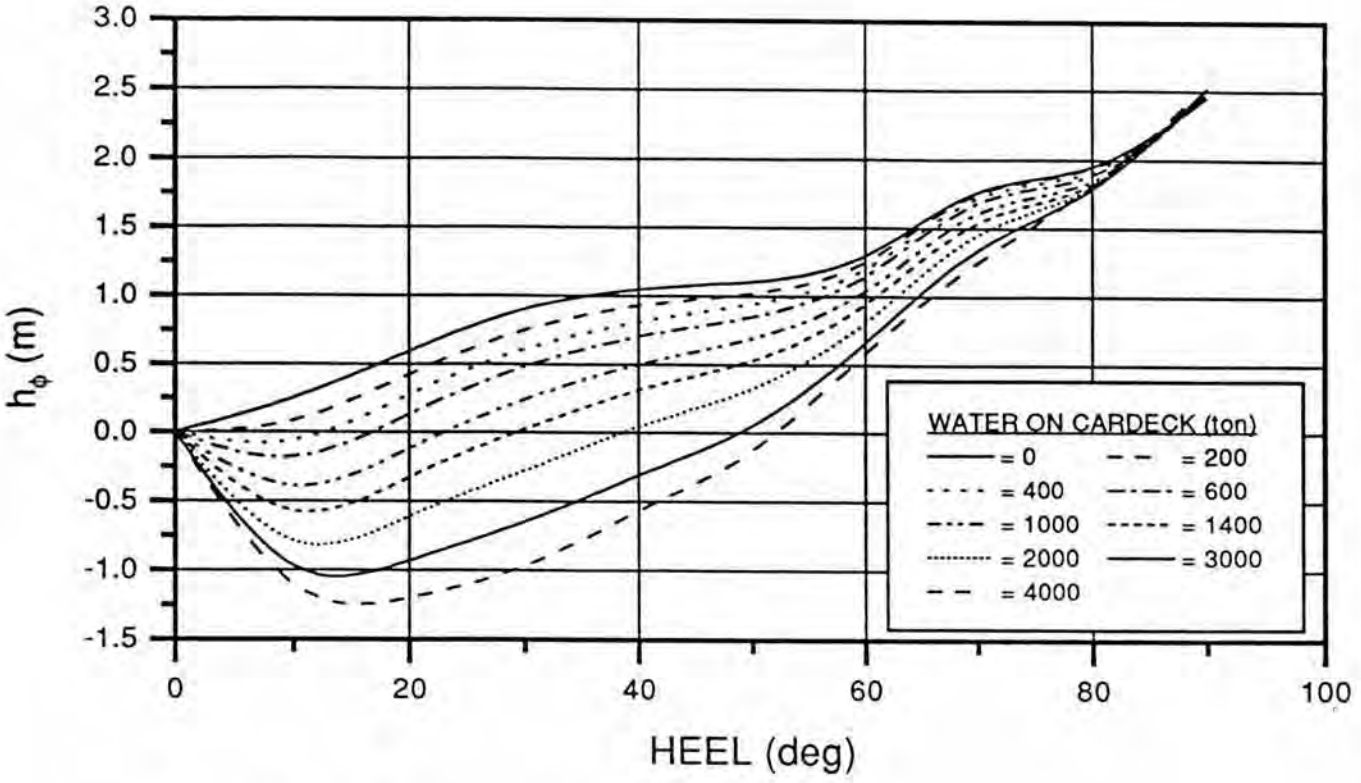

Figure 4.5 Static stability curves, side included.

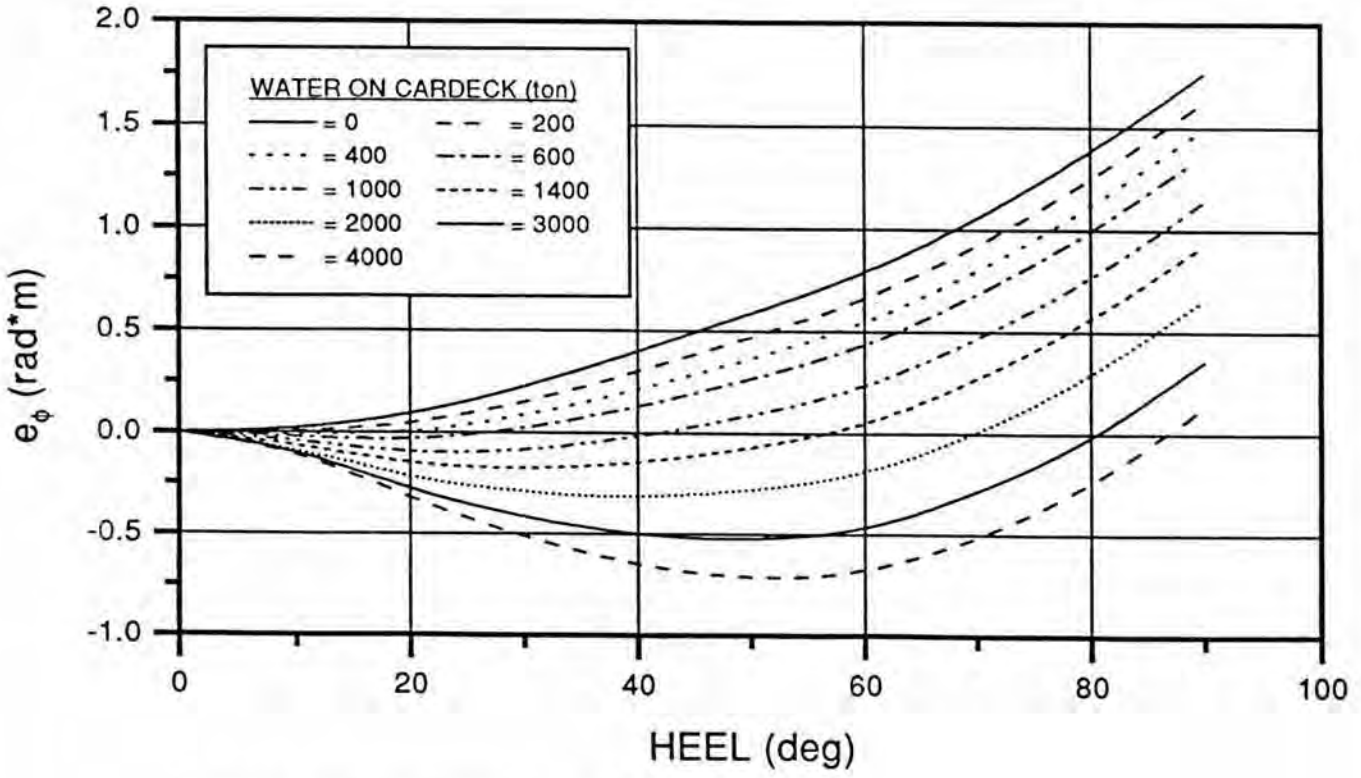

Figure 4.6 Dynamic stability curves, side included.

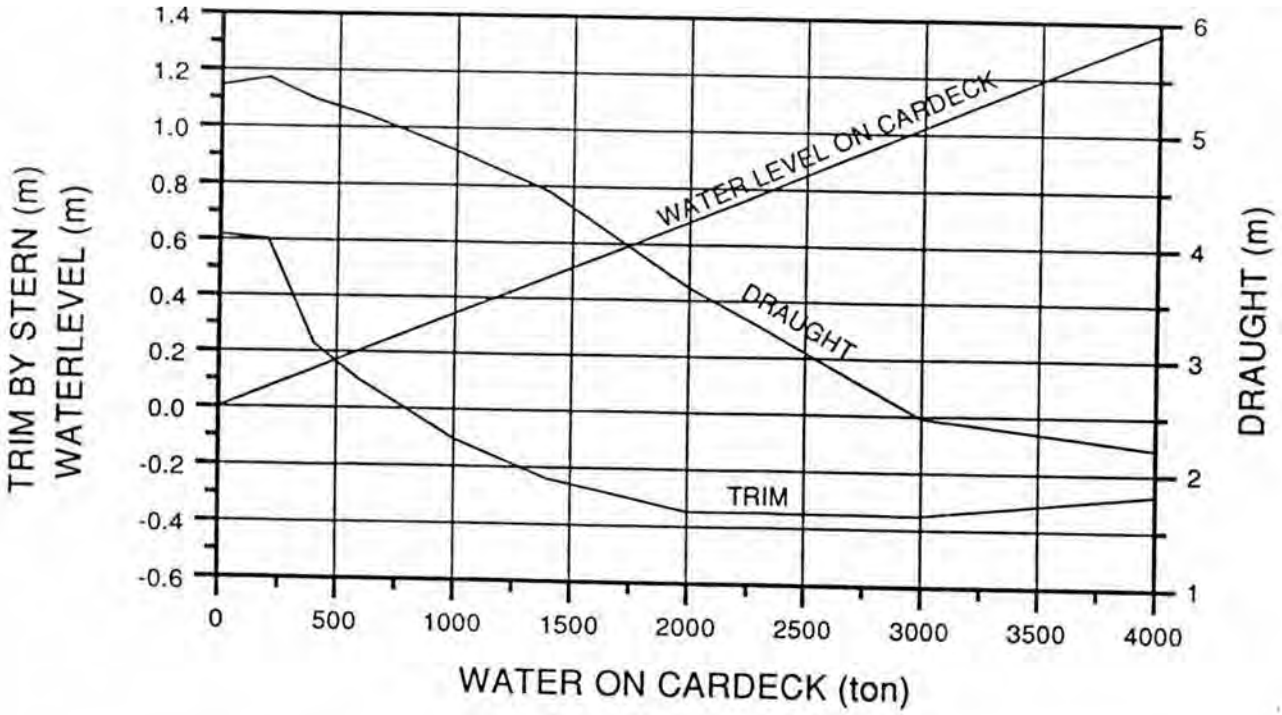

Figure 4.3 The water level on the cardeck, draught and trim as functions of water amount on the cardeck, side included.

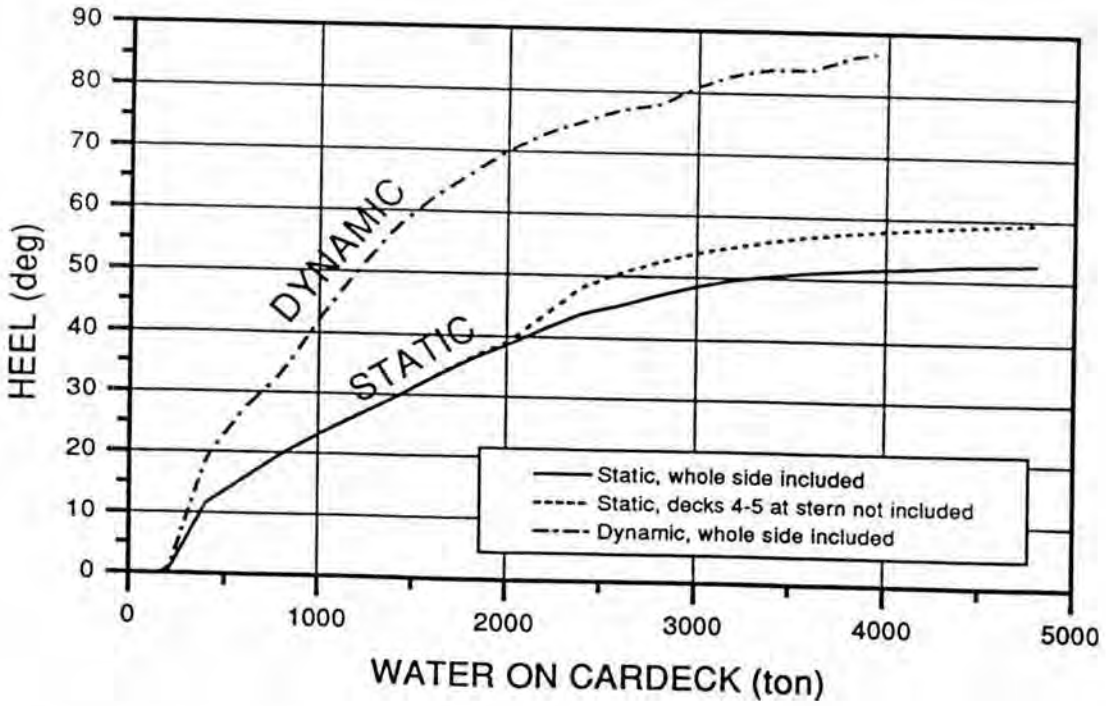

Figure 4.4 Static and dynamic heel angles.

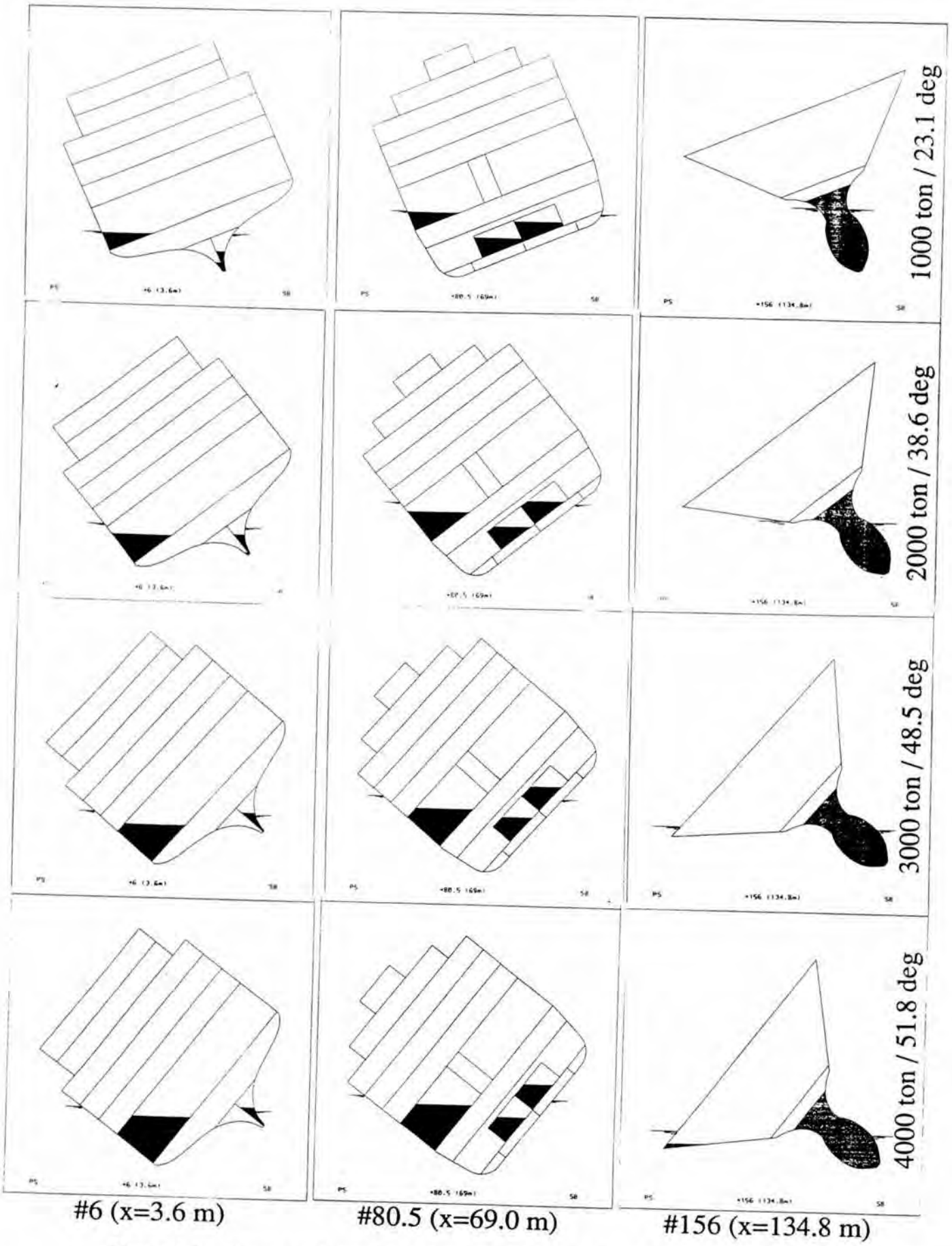

Figure 4.7 Cross-sections at frames #6, #80.5 and #156. The amount of inflooded water 1000, 2000, 3000 and 4000 ton.

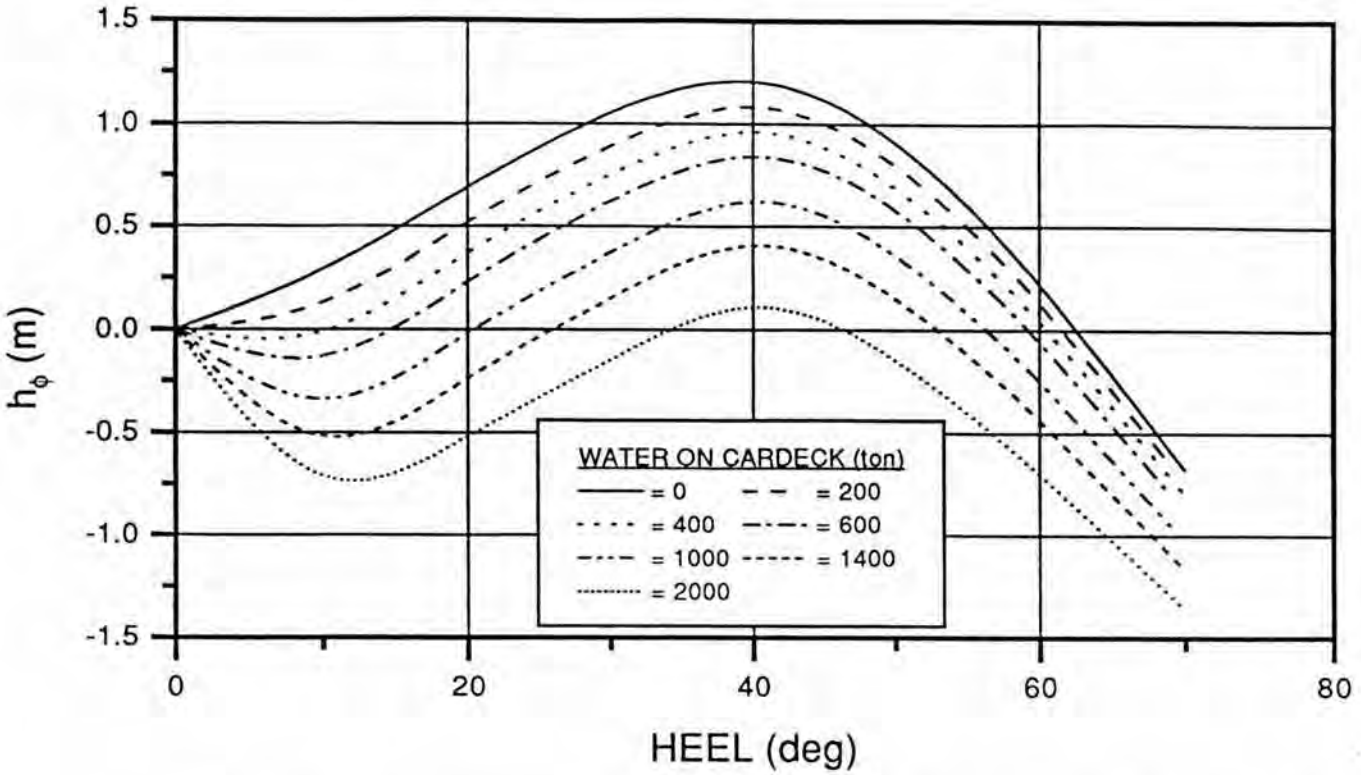

Figure 4.8 Static stability curves. Side above 4th deck not included, preliminary load condition.

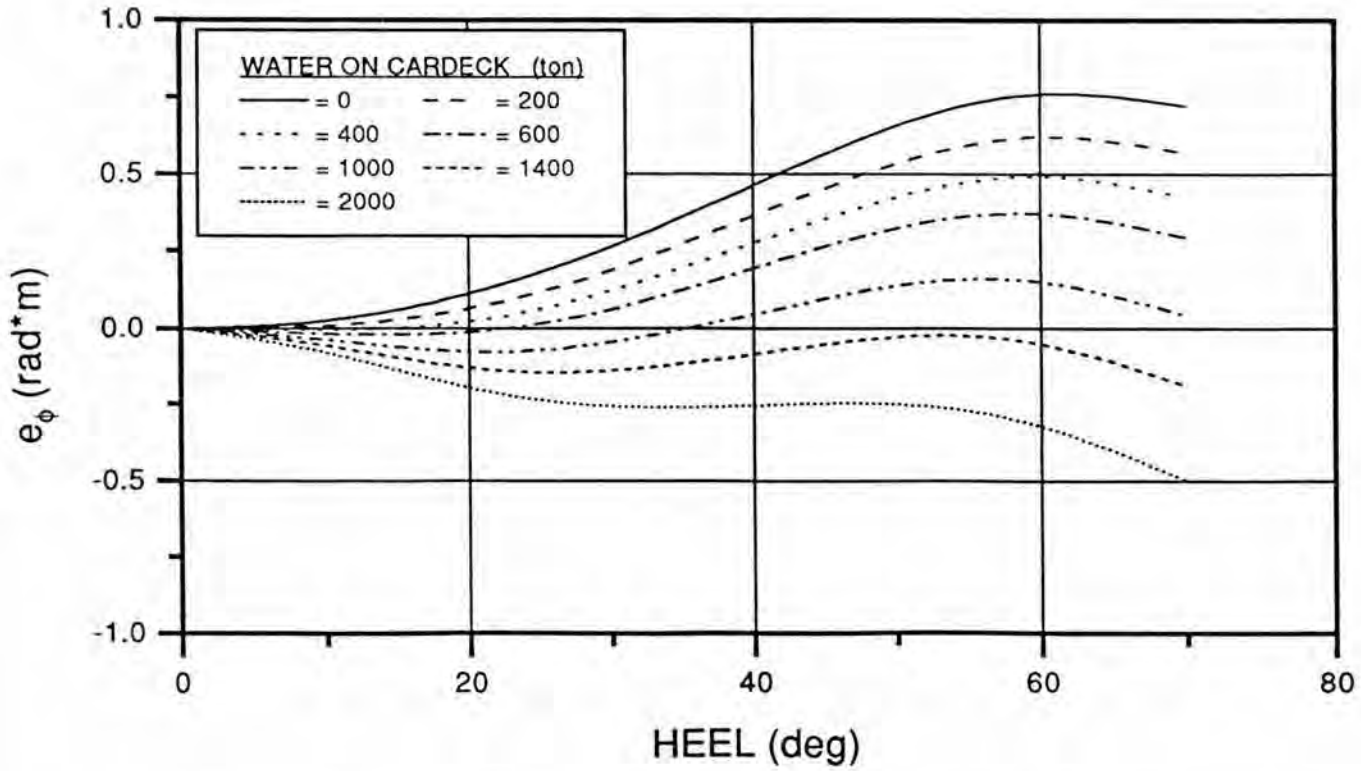

Figure 4.9 Dynamic stability curves. Side above 4th deck not included, preliminary load condition.

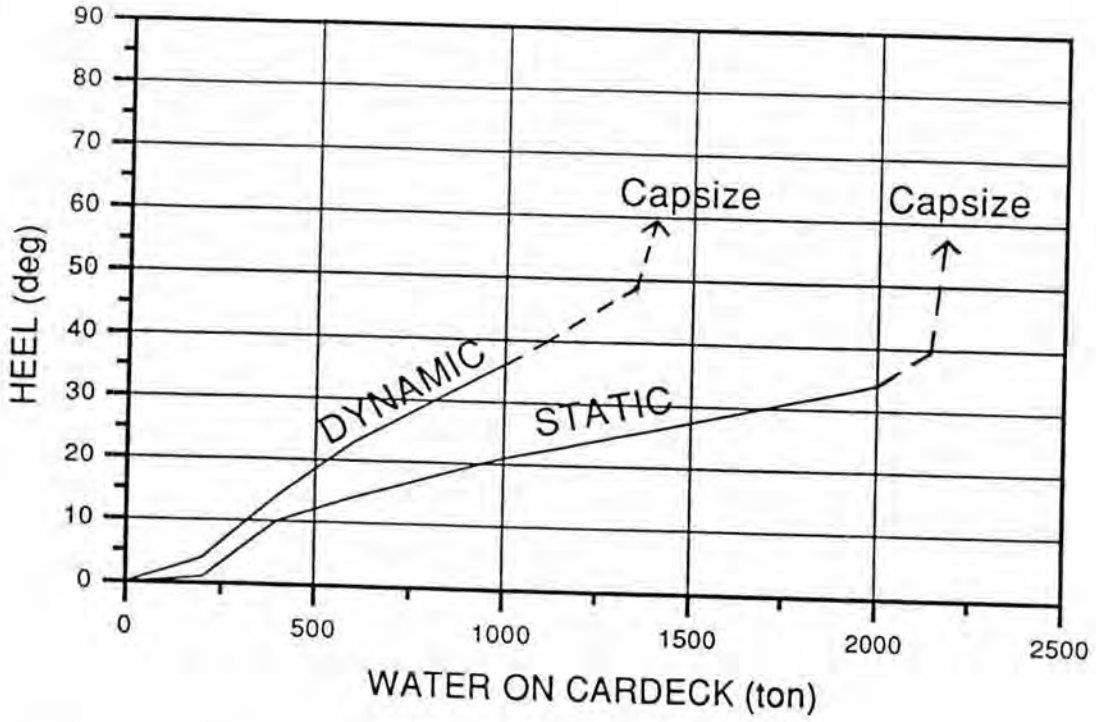

Figure 4.10 Static and dynamic heel angles. Side above 4th deck not included, preliminary load condition.

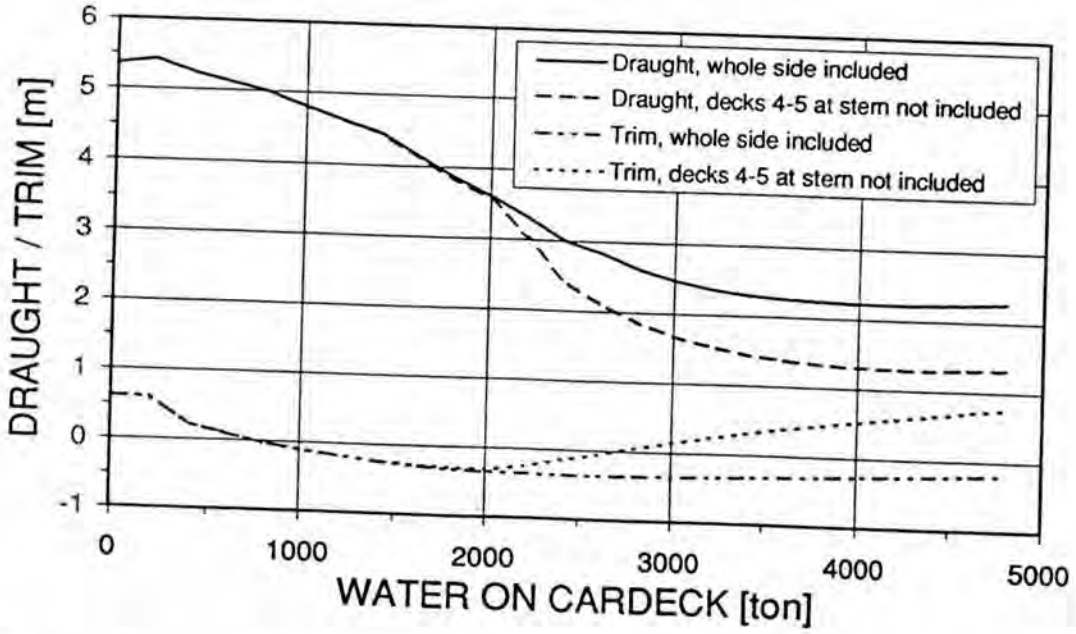

Figure 4.11 Draught and trim, whole side included and decks 4-5 at stern not included, actual load condition without the visor.

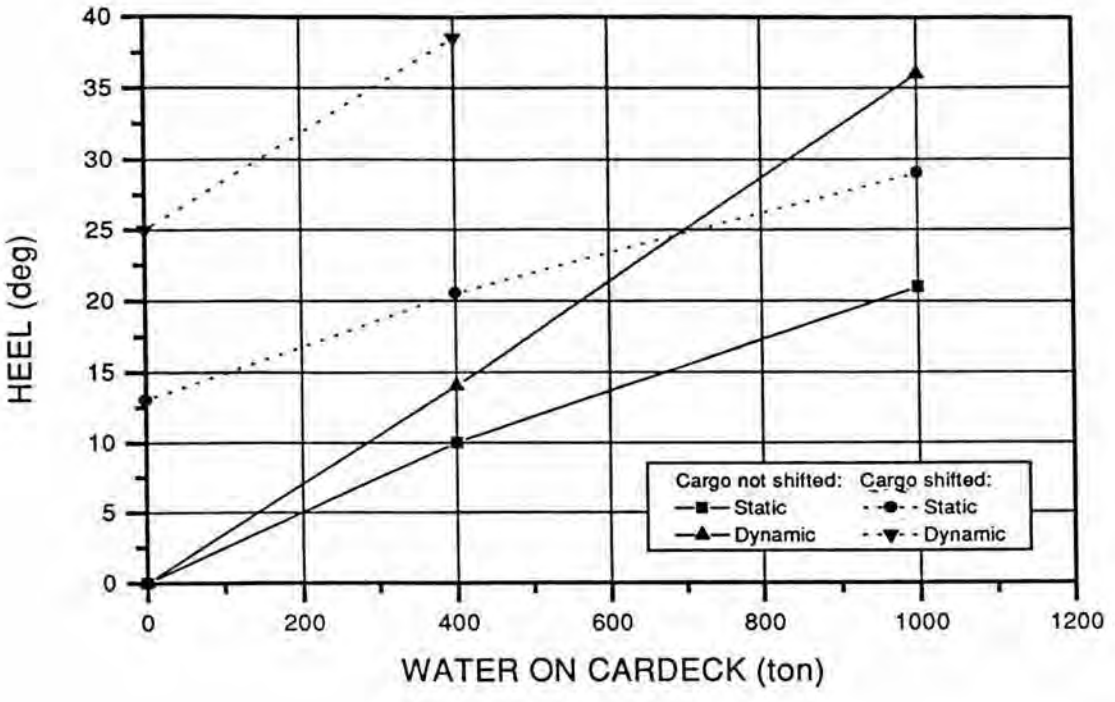

Figure 4.12 Static and dynamic heel angles, effect of cargo shift, side above 4th deck not included.

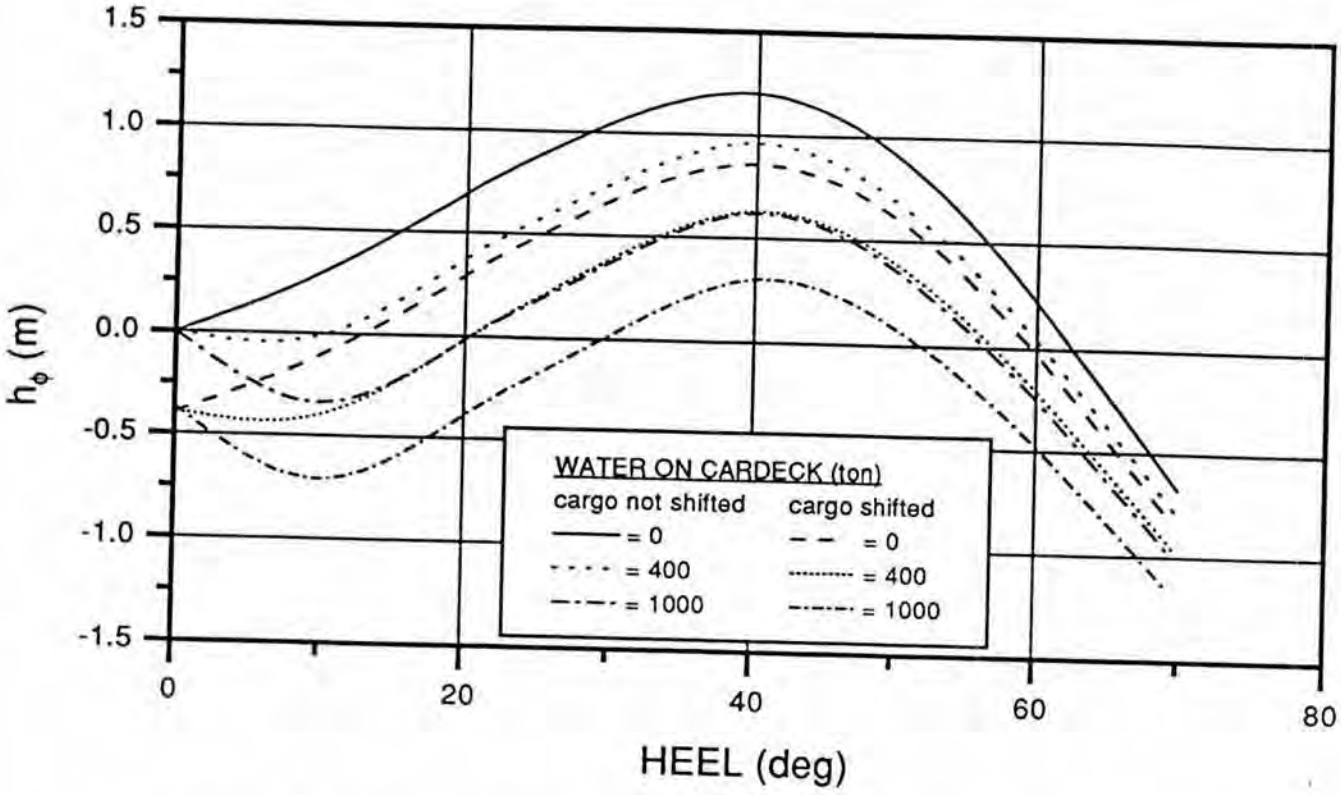

Figure 4.13 Static stability curves, effect of cargo shift. Side above 4th deck not included, preliminary load condition.

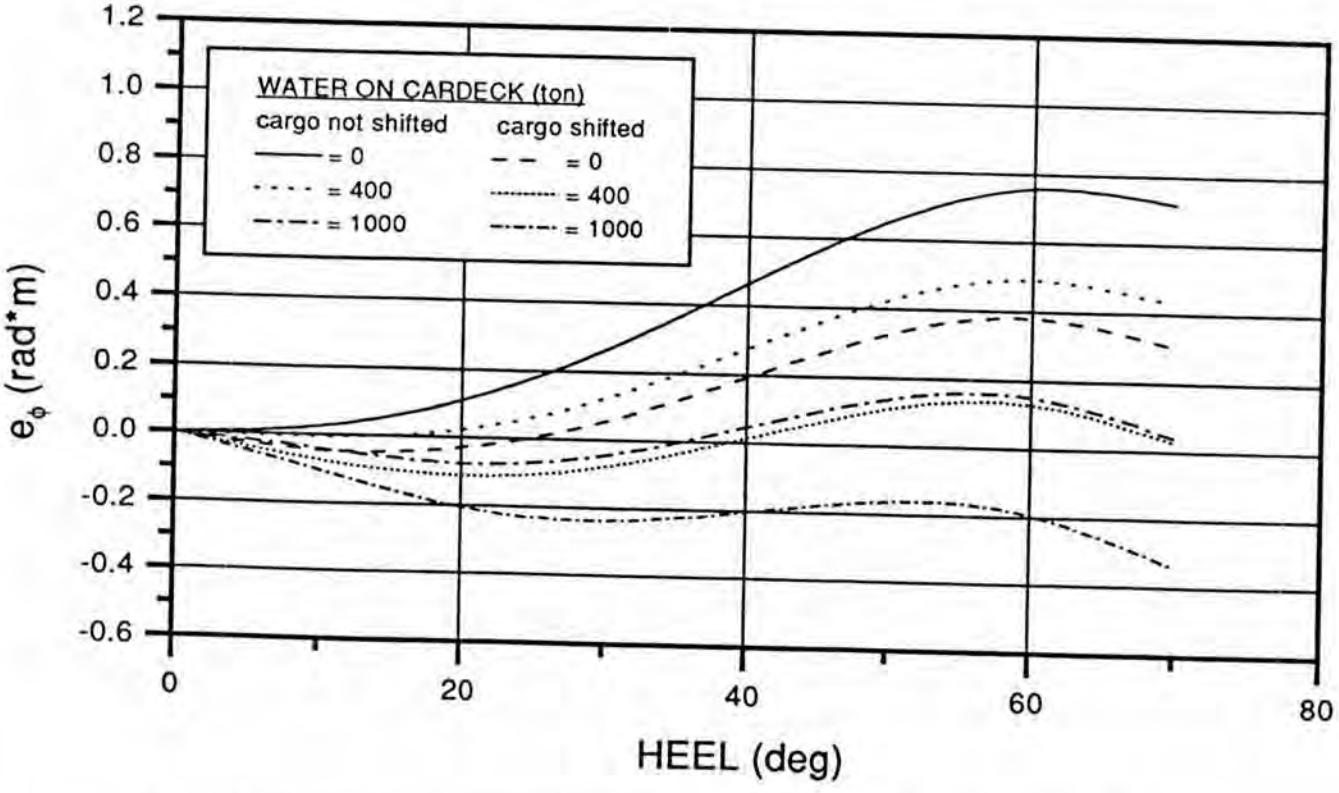

Figure 4.14 Dynamic stability curves, effect of cargo shift. Side above 4th deck not included, preliminary load condition.

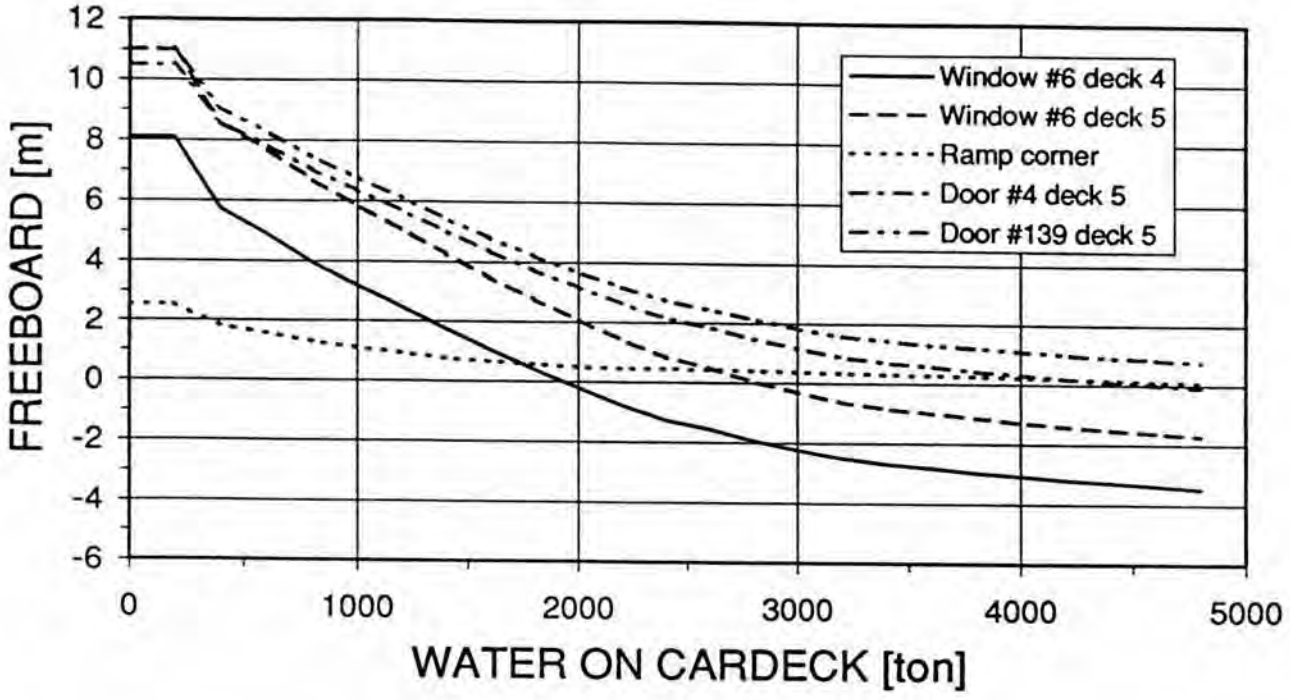

Figure 4.15 Freeboard to some critical openings.

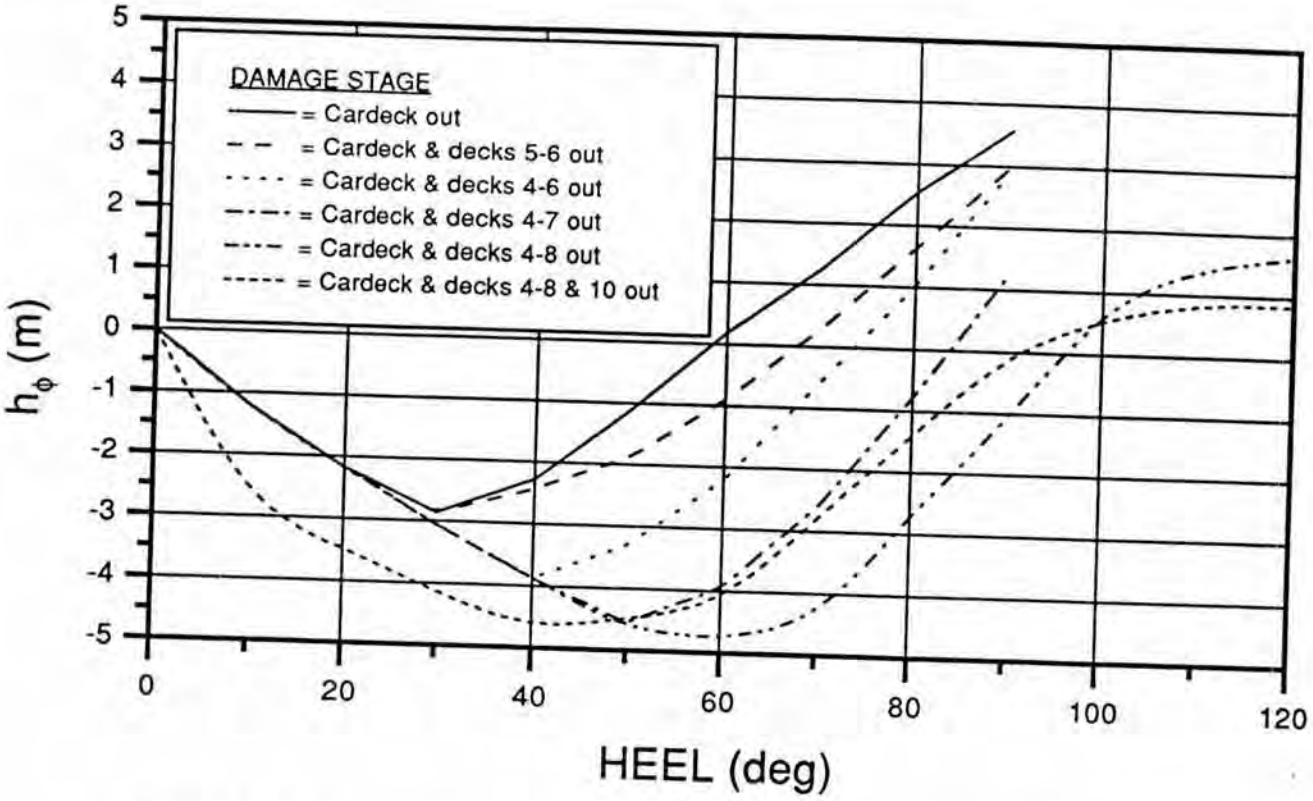

Figure 4.16 Static stability curves, effect of damage stage, 3200 ton water on cardeck.

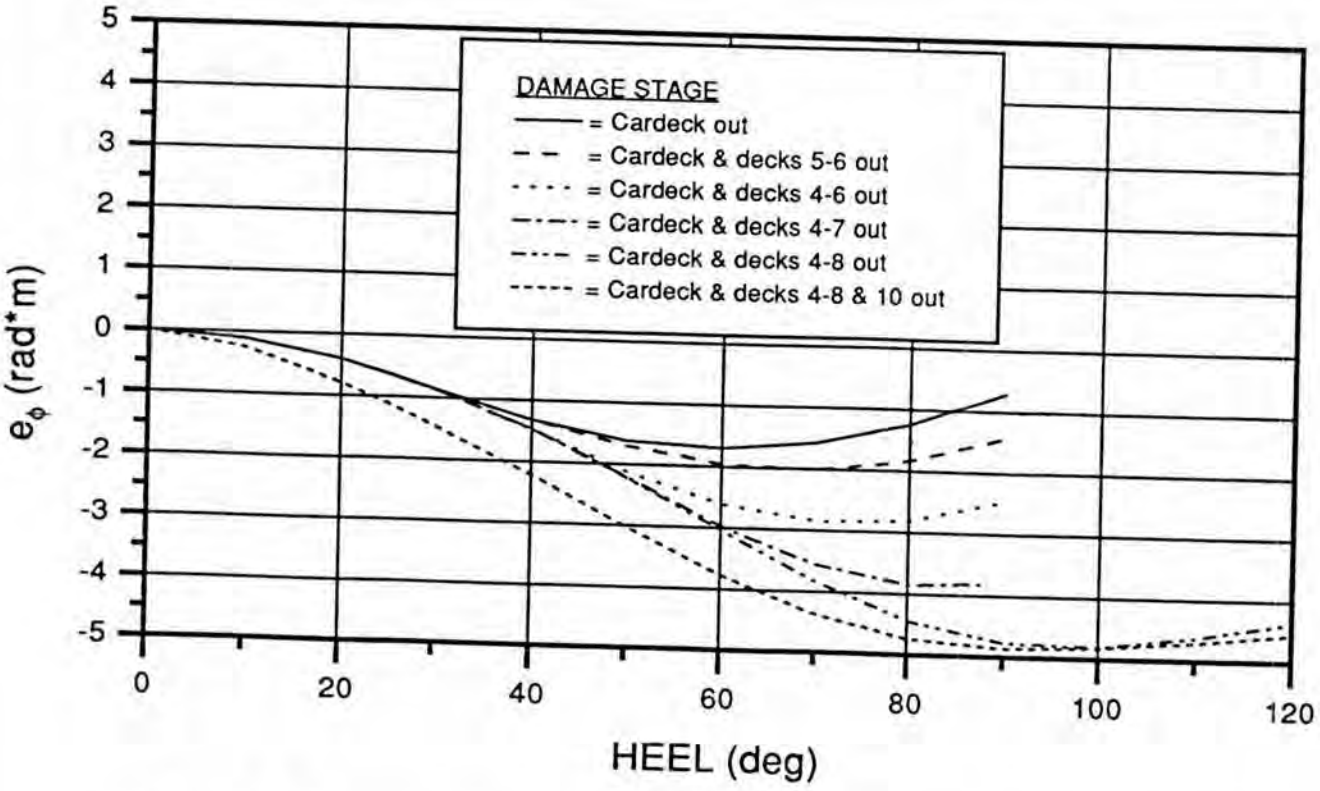

Figure 4.17 Dynamic stability curves, effect of damage stage, 3200 ton water on cardeck.

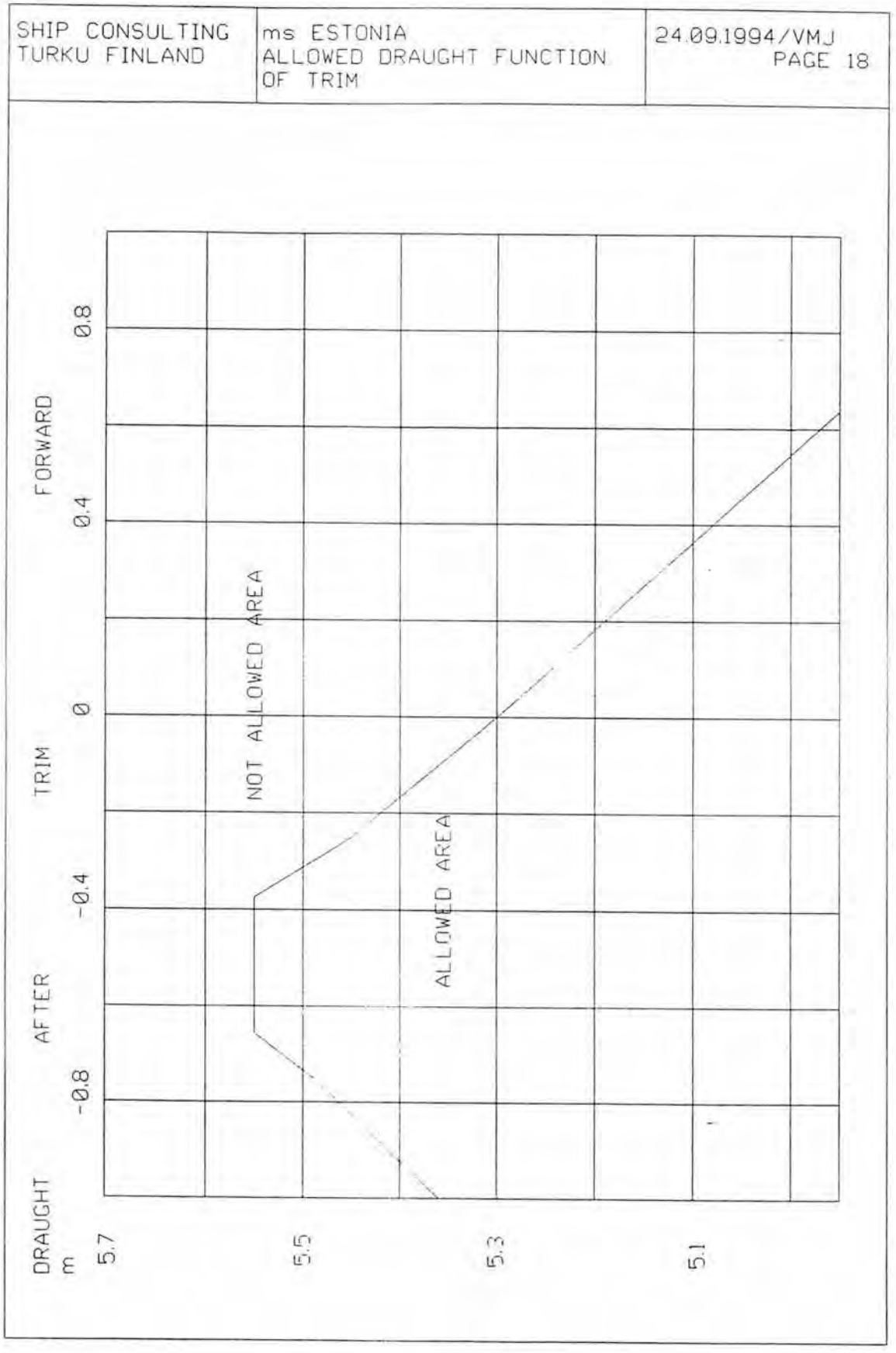

Figure 4.18 The allowed and not allowed trim/draught combinations for MV Estonia.

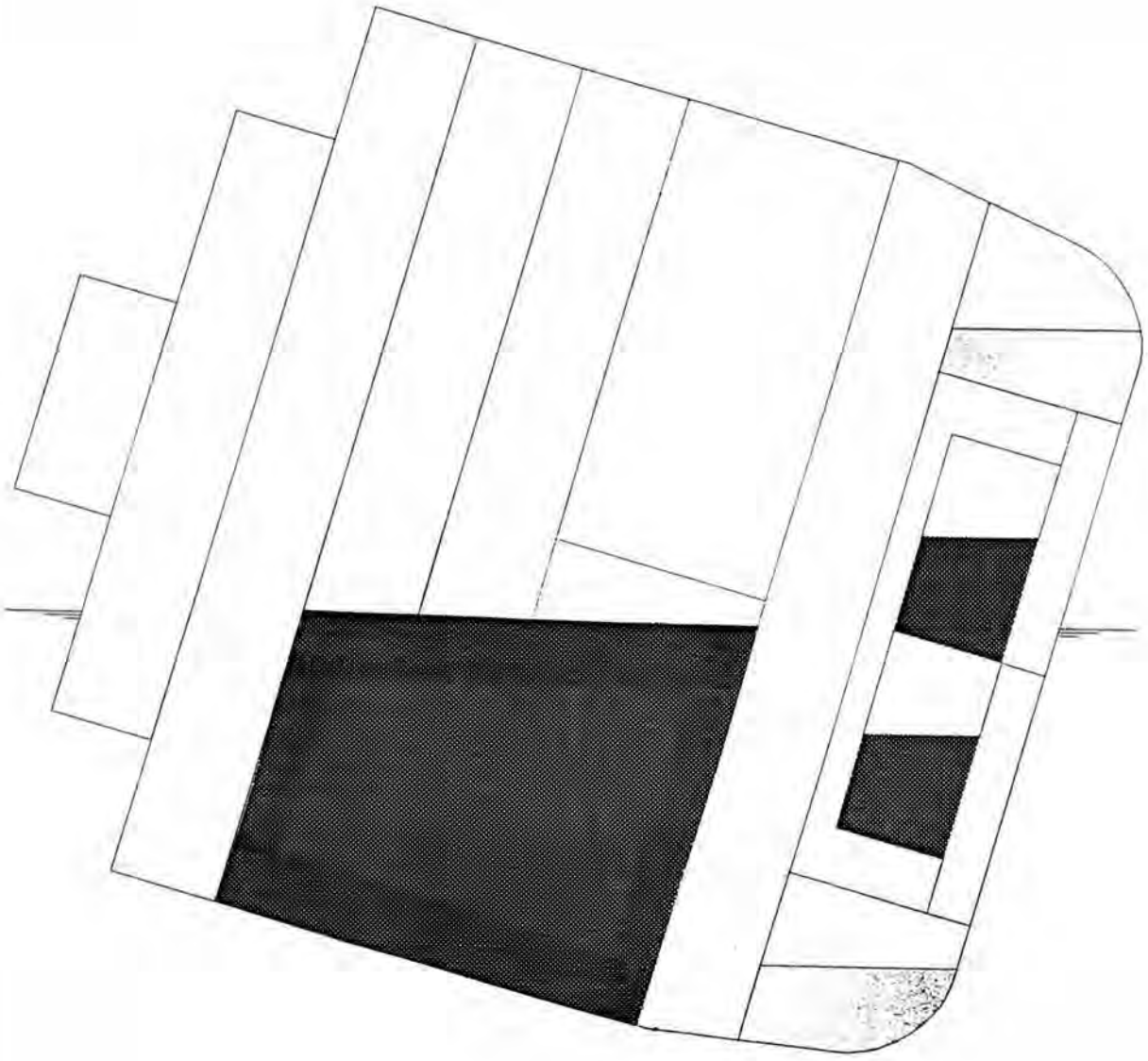

Figure 4.19 The equilibrium floating position of the ship for the case when the cardeck and decks between 4-6 are out. The cross-section is at the longitudinal coordinate x=79.4 m from the after perpendicular.

SUPPLEMENT No. 505

Karppinen Tuomo - Rintala Sakari:

MV Estonia Accident Investigation. Stability calculations with water on the tank deck.

Research Report VAL313-7331.

VTT Manufacturing Technology.

Espoo 1997.

MV ESTONIA ACCIDENT INVESTIGATION

Stability calculations with water on the tank deck

Research Report VAL313-7331

Espoo, Finland
27 November, 1997

Title	
Stability calculations with water on the tank deck	
Client/sponsor of project and order Oikeusministeriö	Research Report No. VAL313-7331
Project MV ESTONIA ACCIDENT INVESTIGATION	Project No. VAL4354
Author(s) Tuomo Karppinen & Sakari Rintala	No. of pages/appendices 37
Keywords Stability	

Summary

The stability of MV ESTONIA has been estimated using the current most accurate estimates of the actual loading condition on the accident night and assuming that different amounts of water flooded three compartments on the tank deck. These compartments located in the fore part of the ship between frames #85 and #120. The volume of water flooded into the tank deck varied from 0 ton to 1300 ton.

The free water surface thus arising on the tank deck reduces the stability of the ship. The mass of water in the three compartments on the tank deck did, however, not make the initial transverse stability negative. Since the stability was in all the cases positive, the vessel would have been floating upright without the action of any outside inclining moments. The list angle due to the wind heeling moment would have been increased due to the significant reduction of the transverse metacentric height.

Date Espoo 27.11.1997

Matti K. Hakala	Sakari Rintala	TiK.
Research Manager	Research Scientist	Checked

Distribution:
Client, 1 copy
VTT Manufacturing Technology/VAL3, 3 copies

VTT Manufacturing Technology
Maritime and Mechanical Engineering
P.O. Box 1705
FIN-02044 VTT, Finland

Phone: +358 9 4561
Telefax: +358 9 455 0619, +358 9 456 5888
E-mail: Sakari.Rintala@vtt.fi
WWW: http://www.vtt.fi/manu/

Table of contents

1 Introduction

The transverse stability of MV ESTONIA has been estimated using the current most accurate estimates of the actual loading condition on the accident night and assuming that different amounts of water flooded three compartments on the tank deck. These compartments located in the fore part of the ship between frames # 85 and # 120. Amount of water flooded into the tank deck varied from 0 ton to 1300 tons.

2 Computation method

The program package NAPA was used in the stability calculations. NAPA (The Naval Architectural Package) is a computer-aided engineering system used in the basic design work for a ship project and in naval architectural calculations. The package comprises the definition of hull form, superstructures, bulkheads, decks and compartments. Besides stability and damage analysis, NAPA can be used when calculating hydrostatics, tank volumes, capacities, loading conditions, inclining test results etc.

The NAPA program package is used world wide by shipyards, consultants, navies etc. In Finland, NAPA has been a long time the standard method by which the shipyards have made hydrostatic calculations.

The hull form definition of MV ESTONIA introduced by the report VALC177 has been used in the stability calculations which were actually made at Ship Consulting Ltd.

3 Loading conditions

MV ESTONIA's main particulars and the loading condition departure from Tallin are presented in Table 3.1.

Table 3.1. MV ESTONIA's main particulars and departure loading condition.

	Symbol	Dimension	Actual values
Length over all	Loa	m	155.4
Waterline length	Lwl	m	144.8
Length btw. perp.	Lpp	m	137.4
Beam mld, A-deck	B	m	24.2
Waterline beam	Bwl	m	23.6
Draught mean	T	m	5.355
Draught at forw. perp	Tf	m	5.118
Draught at aft perp.	Ta	m	5.593
Trim, positive by bow		m	-0.475
Displacement	∇	m^3	11961

In the stability calculations the change of the transverse metacentric height GM_T was investigated when different volumes of water flooded three compartments on the tank deck. These compartments were separated from each other by transverse watertight bulkheads. The locations of the compartments are shown in Table 3.2.

Table 3.2. Locations of the compartments on the tank deck.

Name of the compartment	Frames of the compartment	Distances from AP m	Volume of the compartment [m^3]
T410	#110-#120	101.8-109.8	491
T510	#98 -#110	92.2-101.8	709
T610	#85- #98	81.8-92.8	782

Altogether eight combinations of the loading conditions were studied by changing the volume of water on the tank between 0 and 1300 tons.

4 Results and discussion

The results of the calculations are shown in Figs 4.1.a-4.8.d and a summary of the results is presented in Table 4.1.

Table 4.1. Summary of the stability calculations.

Loading cond.	Water [ton] T410	Water [ton] T510	Water [ton] T610	Water on the tank deck [ton]	Displ. [ton]	Draught [m]	Trim [m]	GM_r [m]
K0	0	0	0	0	11961	5.355	-0.475	1.15
K1	0	0	100	100	12061	5.398	-0.369	0.51
K2	0	0	200	200	12161	5.440	-0.264	0.60
K3	0	100	200	300	12261	5.485	-0.122	0.22
K4	0	200	300	500	12461	5.571	0.122	0.23
K5	100	250	350	700	12661	5.658	0.414	0.11
K6	200	350	450	1000	12961	5.785	0.814	0.14
K7	300	450	550	1300	13261	5.909	1.265	0.20

Because the doors on the tank deck had quite high doorsteps (about 1 m), water would not have been able to spread from a compartment to another immediately. The free surface of water on the tank deck would have reduced the stability of the vessel. In practice the mass of water in the three compartments on the tank deck would, however, not have been able to make the stability (the transverse metacentric height) negative. Due to the positive stability in all the cases considered the vessel would not have attained a permanent list. Since the stability would have been reduced by the free water surface, the inclining angle of the vessel due to wind forces would have somewhat increased. The free water surface would have had a remarkable effect on the rolling motion of the vessel.

LOADING CONDITION K.0, DEP. FROM TALLIN, heeling tanks unsym

L O A D I N G C O M P O N E N T S

Name		Max. weight	Mass	Center of gravity cgx	cgy	cgz	Free s. moment
HEAVY FUEL OIL, RHO= 0.900							
T10	DEEP TANK 10	171.1	97.2	74.20	2.75	2.03	146.7
T11	DEEP TANK 11	171.1	97.2	74.20	-2.75	2.03	146.7
T36	DAY TANK 36	23.1	22.5	36.23	9.28	2.76	9.1
T38	SETTLING TAN.	28.9	18.0	32.35	8.96	2.36	7.3
Total of HEAVY FUEL OIL		394.3	234.9	67.36	1.58	2.13	309.9
DIESEL OIL, RHO= 0.860							
T18	DB TANK 18	61.1	27.5	58.20	3.50	0.22	250.5
T20	DB TANK 20	17.8	8.6	59.81	8.31	0.30	15.0
T41	DAY TANK 41	12.8	8.6	31.04	-8.91	2.48	3.3
Total of DIESEL OIL		91.7	44.7	53.28	2.04	0.67	268.9
FRESH WATER, RHO= 1.000							
T4A	FW TANK 4 A	72.2	69.0	114.24	4.23	2.83	54.5
T4B	FW TANK 4 B	72.2	69.0	114.24	-4.23	2.83	54.5
T5	FW TANK 5	146.5	145.0	113.61	0.00	2.68	0.0
T56	FW TANK 56	148.3	45.0	9.93	1.35	1.18	40.9
T57	FW TANK 57	148.3	45.0	9.93	-1.35	1.18	40.9
T17	CIRCUL TANK .	19.7	18.0	58.24	-9.00	0.55	13.6
T22	COOLING WATE.	2.9	2.0	55.40	8.90	0.43	1.6
T29	COOLING WATE.	16.6	15.0	45.85	-8.68	0.61	11.4
Total of FRESH WATER		626.6	408.0	85.74	-0.67	2.22	217.3
BALLAST WATER, RHO= 1.025							
T1	FORE PEAK TA.	178.9	175.8	134.08	0.00	4.02	0.0
T14	HEELING TANK.	185.1	185.0	77.54	8.87	2.63	0.0
Total of BALLAST WATER		364.0	360.8	105.09	4.55	3.31	0.0
PAS							
(PAS)	PASSENGERS &.	0.0	110.0	71.50	0.00	16.40	0.0
TRA							
(TRA)	TRAILERS 34 .	0.0	970.0	70.00	-2.00	9.50	0.0
CREW							
(CREW)	CREW	0.0	20.0	60.00	0.00	22.00	0.0
PRO							
(PRO)	PROVISION & .	0.0	80.0	46.00	0.00	10.00	0.0

Displacement (rho=1.01)	11961.4	63.80	-0.01	10.65	796.0

F L O A T I N G P O S I T I O N

Draught moulded	5.355	m	KM	11.87 m
Trim	-0.475	m	KG	10.65 m
TA	5.593	m	GM0	1.22 m
TF	5.118	m	GMCORR	-0.07 m
Trimming moment	-12664	tonm	GM	1.15 m

HEEL degree	MS m	HPHI m	EPHI rad*m	FSMOM tm	DGZ m
0.0	-0.004	0.00	0.000	0.0	0.000
10.0	0.040	0.24	0.019	125.2	0.010
20.0	0.185	0.58	0.091	212.5	0.018
30.0	0.314	0.90	0.223	307.4	0.026
40.0	0.282	1.03	0.394	375.8	0.031
50.0	0.183	1.08	0.578	406.1	0.034
60.0	0.246	1.27	0.779	406.5	0.034
70.0	0.625	1.74	1.042	389.1	0.033
80.0	0.759	1.93	1.362	354.1	0.030
90.0	1.237	2.43	1.739	306.0	0.026
100.0	1.895	3.08	2.217	249.0	0.021
110.0	2.807	3.94	2.829	187.1	0.016
120.0	3.389	4.43	3.565	123.3	0.010

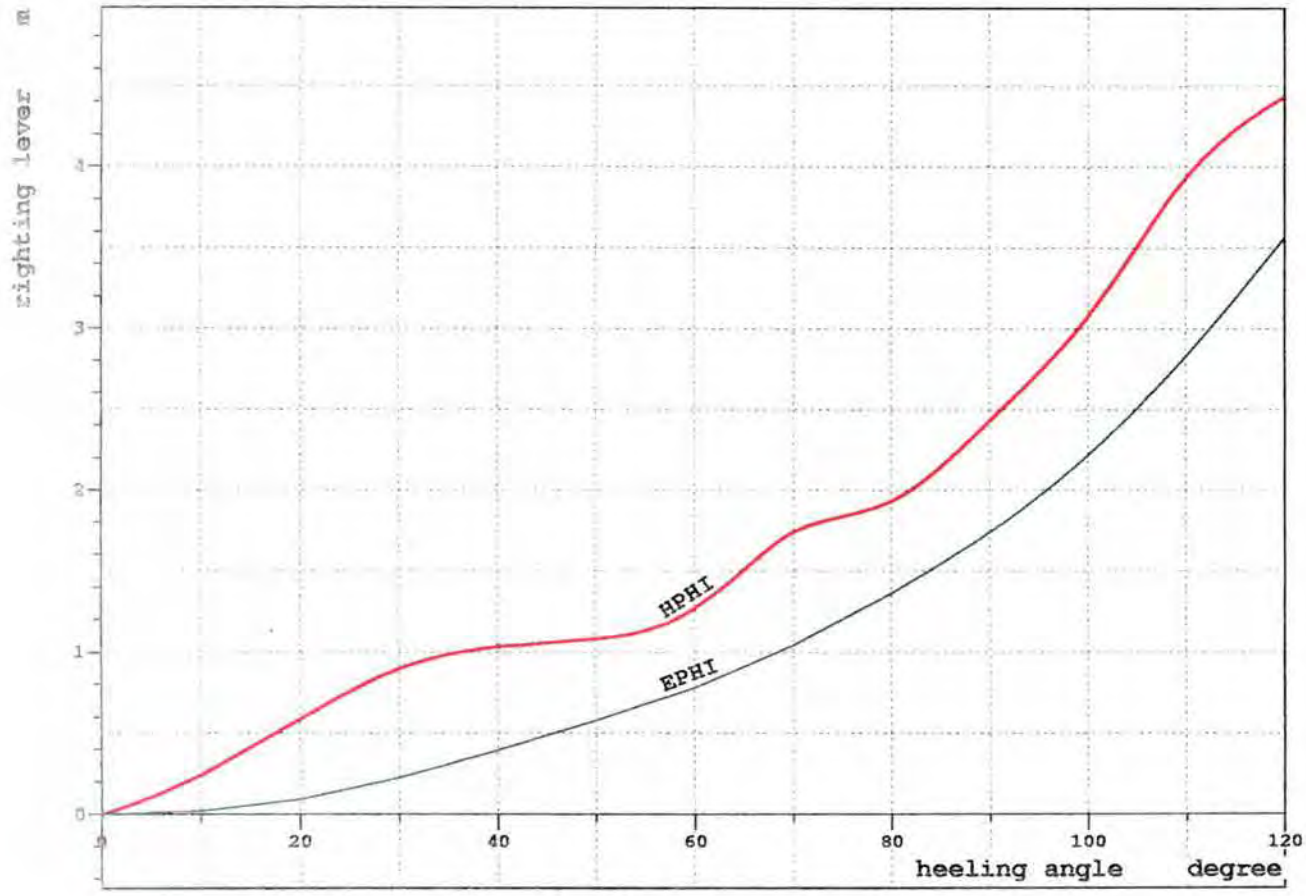
righting lever m
0
1
2
3
4
0
20
40
60
80
100
120
heeling angle degree
HPHI
EPHI

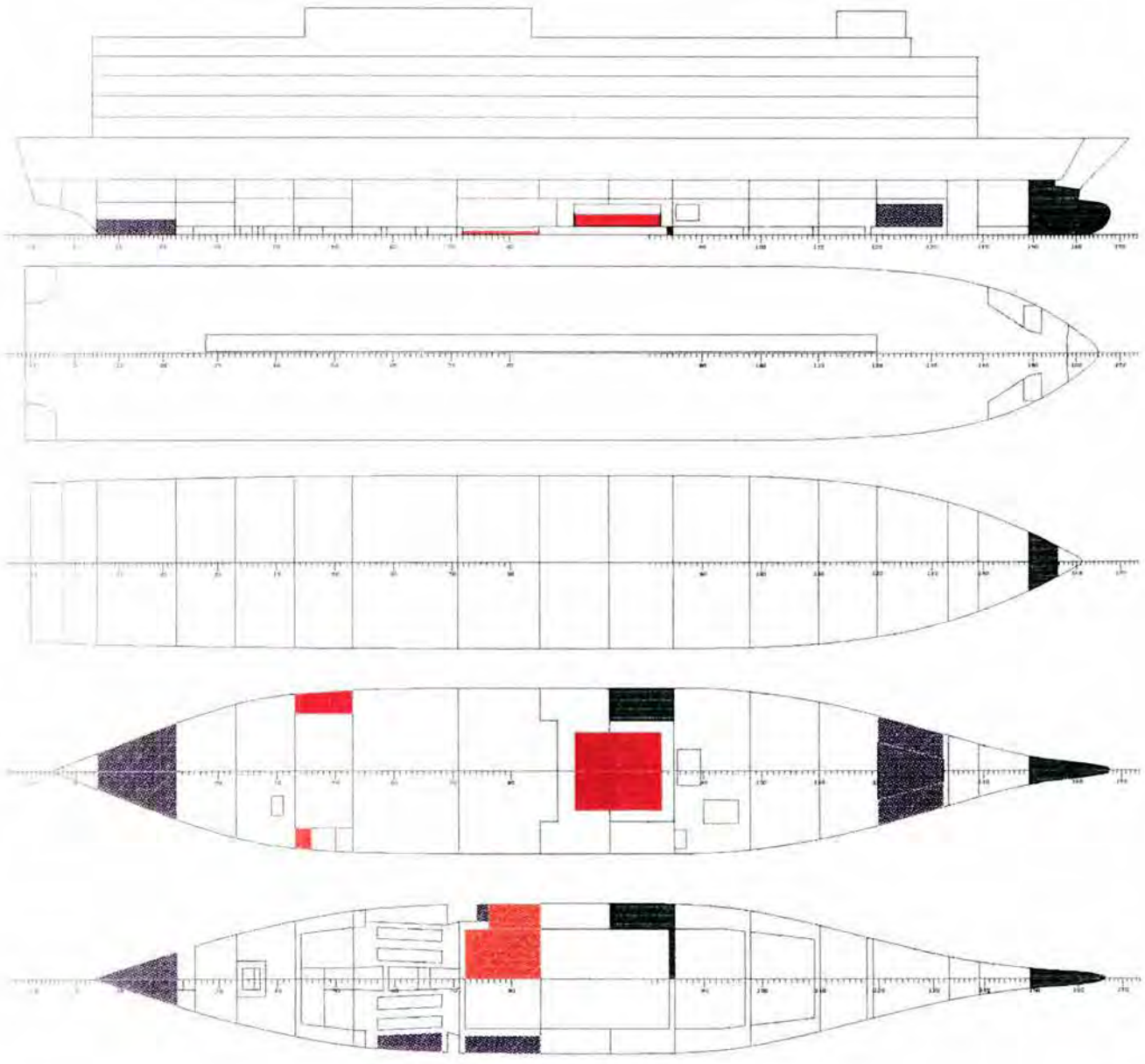

LOADING CONDITION K.1, DEP. FROM TALLIN, heeling tanks unsym

L O A D I N G C O M P O N E N T S

Name		Max. weight	Mass	Center of gravity cgx	cgy	cgz	Free s. moment
HEAVY FUEL OIL, RHO= 0.900							
T10	DEEP TANK 10	171.1	97.2	74.20	2.75	2.03	146.7
T11	DEEP TANK 11	171.1	97.2	74.20	-2.75	2.03	146.7
T36	DAY TANK 36	23.1	22.5	36.23	9.28	2.76	9.1
T38	SETTLING TAN.	28.9	18.0	32.35	8.96	2.36	7.3
Total of HEAVY FUEL OIL		394.3	234.9	67.36	1.58	2.13	309.9
DIESEL OIL, RHO= 0.860							
T18	DB TANK 18	61.1	27.5	58.20	3.50	0.22	250.5
T20	DB TANK 20	17.8	8.6	59.81	8.31	0.30	15.0
T41	DAY TANK 41	12.8	8.6	31.04	-8.91	2.48	3.3
Total of DIESEL OIL		91.7	44.7	53.28	2.04	0.67	268.9
FRESH WATER, RHO= 1.000							
T4A	FW TANK 4 A	72.2	69.0	114.24	4.23	2.83	54.5
T4B	FW TANK 4 B	72.2	69.0	114.24	-4.23	2.83	54.5
T5	FW TANK 5	146.5	145.0	113.61	0.00	2.68	0.0
T56	FW TANK 56	148.3	45.0	9.93	1.35	1.18	40.9
T57	FW TANK 57	148.3	45.0	9.93	-1.35	1.18	40.9
T17	CIRCUL TANK .	19.7	18.0	58.24	-9.00	0.55	13.6
T22	COOLING WATE.	2.9	2.0	55.40	8.90	0.43	1.6
T29	COOLING WATE.	16.6	15.0	45.85	-8.68	0.61	11.4
Total of FRESH WATER		626.6	408.0	85.74	-0.67	2.22	217.3
BALLAST WATER, RHO= 1.025							
T1	FORE PEAK TA.	178.9	175.8	134.08	0.00	4.02	0.0
T14	HEELING TANK.	185.1	185.0	77.54	8.87	2.63	0.0
Total of BALLAST WATER		364.0	360.8	105.09	4.55	3.31	0.0
BALLAST WATER, RHO= 1.010							
T610		789.4	100.0	86.93	0.00	1.43	8258.5
PAS							
(PAS)	PASSENGERS &.	0.0	110.0	71.50	0.00	16.40	0.0
TRA							
(TRA)	TRAILERS 34 .	0.0	970.0	70.00	-2.00	9.50	0.0
CREW							
(CREW)	CREW	0.0	20.0	60.00	0.00	22.00	0.0

Name	Max. weight	Mass	Center of gravity cgx	cgy	cgz	Free s. moment
PRO						
(PRO) PROVISION & .	0.0	80.0	46.00	0.00	10.00	0.0
Deadweight		2328.4	77.49	-0.05	6.46	9054.5
Lightweight		9733.0	60.76	0.00	11.56	
Displacement (rho=1.01)		12061.4	63.99	-0.01	10.57	9054.5

F L O A T I N G P O S I T I O N

Draught moulded	5.398	m	KM	11.84 m
Trim	-0.369	m	KG	10.57 m
TA	5.582	m	GM0	1.26 m
TF	5.213	m	GMCORR	-0.75 m
Trimming moment	-9860	tonm	GM	0.51 m

HEEL degree	MS m	HPHI m	EPHI rad*m	FSMOM tm	DGZ m
0.0	-0.004	0.00	0.000	0.0	0.000
10.0	0.042	0.19	0.014	833.8	0.069
20.0	0.188	0.54	0.077	1027.4	0.085
30.0	0.321	0.86	0.200	1144.2	0.095
40.0	0.300	1.01	0.366	1179.3	0.098
50.0	0.209	1.08	0.549	1132.1	0.094
60.0	0.282	1.29	0.751	1024.7	0.085
70.0	0.664	1.78	1.020	876.9	0.073
80.0	0.792	1.98	1.348	694.7	0.058
90.0	1.270	2.49	1.734	488.2	0.040
100.0	1.922	3.14	2.224	267.1	0.022
110.0	2.828	4.01	2.849	41.5	0.003
120.0	3.407	4.52	3.599	-179.7	-0.015

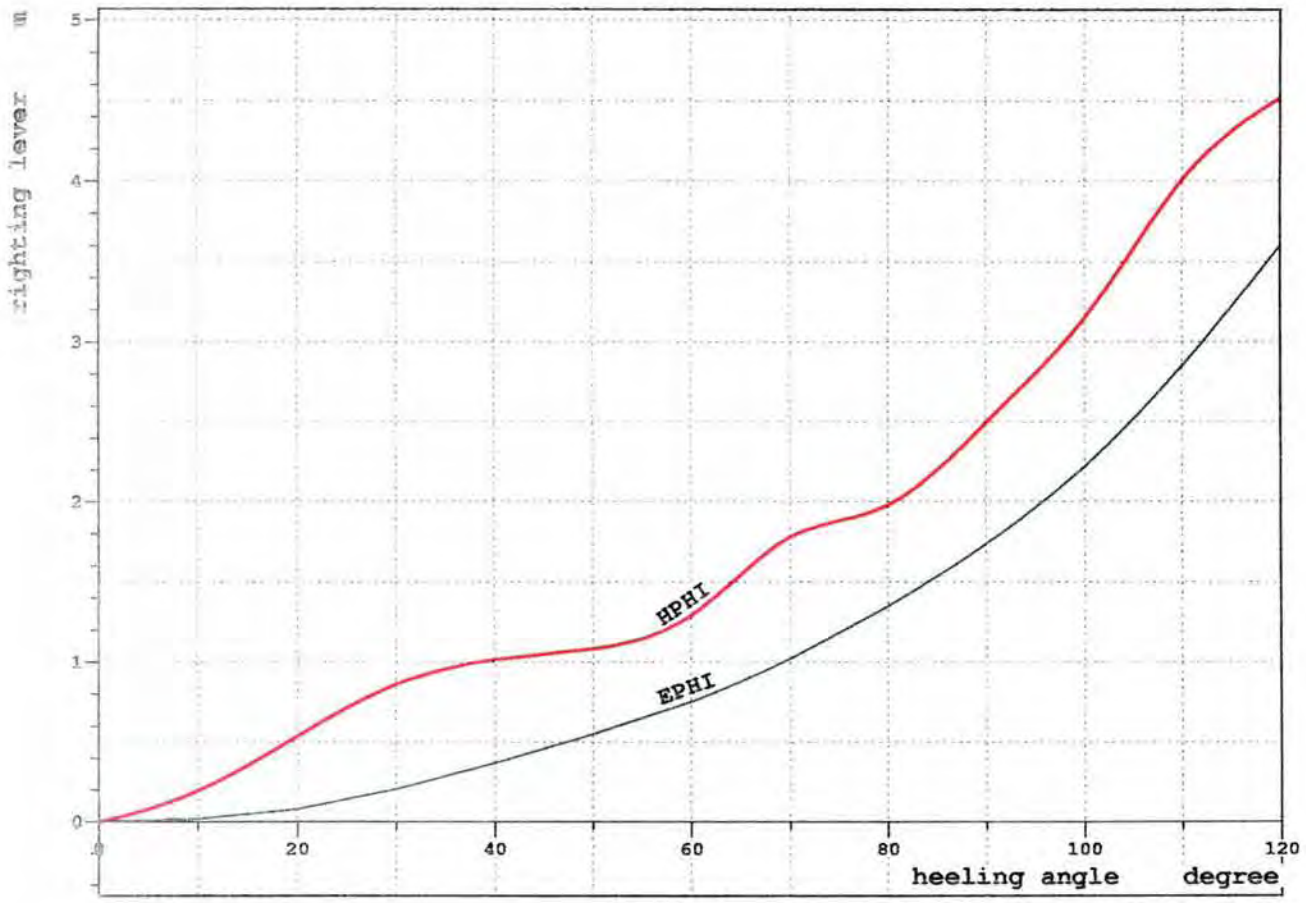
righting lever m
5
4
3
2
1
0
20
40
60
80
100
120
HPHI
EPHI
heeling angle degree

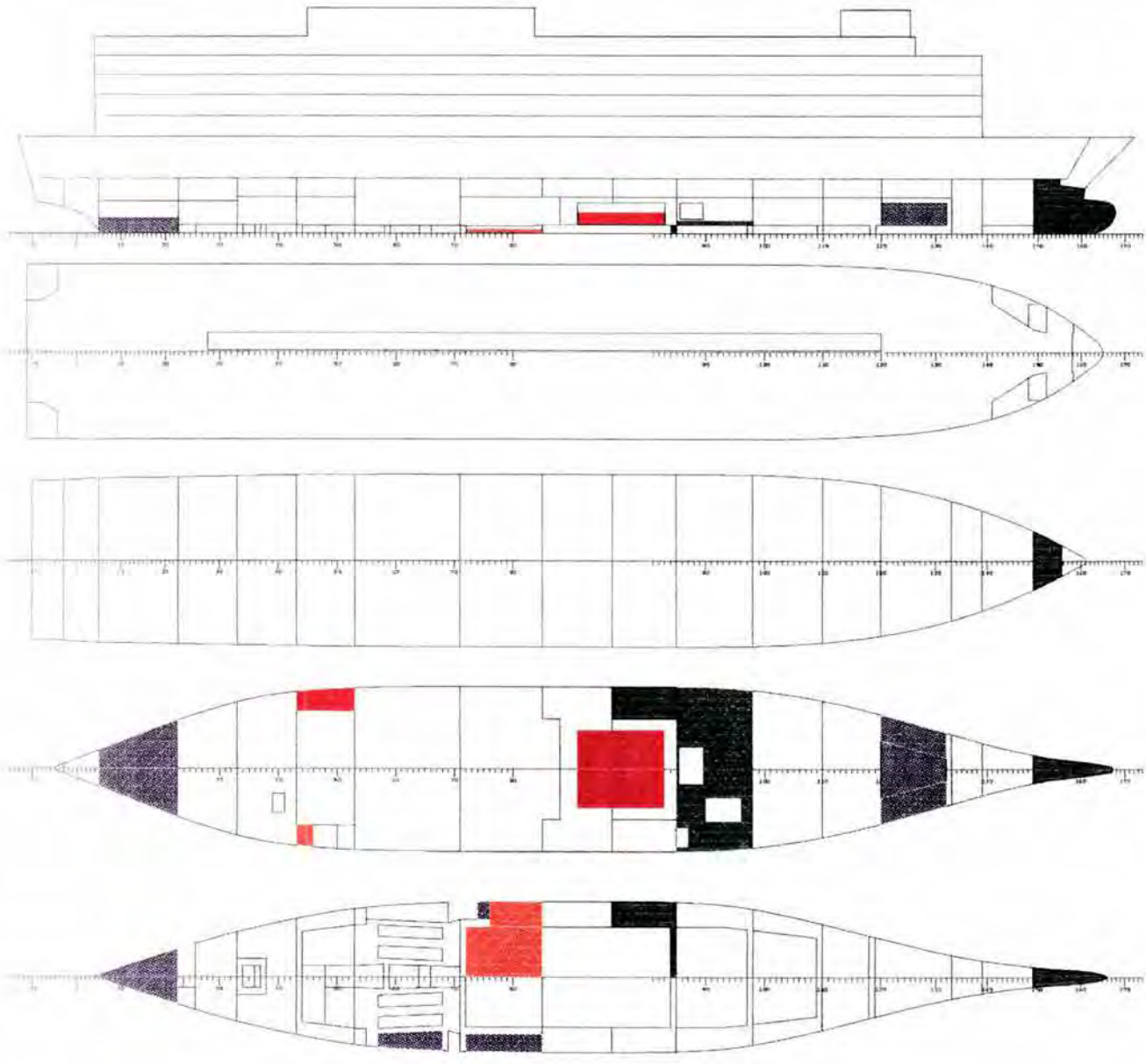

LOADING CONDITION K.2, DEP. FROM TALLIN, heeling tanks unsym

L O A D I N G C O M P O N E N T S

Name		Max. weight	Mass	Center of gravity cgx	cgy	cgz	Free s. moment
HEAVY FUEL OIL, RHO= 0.900							
T10	DEEP TANK 10	171.1	97.2	74.20	2.75	2.03	146.7
T11	DEEP TANK 11	171.1	97.2	74.20	-2.75	2.03	146.7
T36	DAY TANK 36	23.1	22.5	36.23	9.28	2.76	9.1
T38	SETTLING TAN.	28.9	18.0	32.35	8.96	2.36	7.3
Total of HEAVY FUEL OIL		394.3	234.9	67.36	1.58	2.13	309.9
DIESEL OIL, RHO= 0.860							
T18	DB TANK 18	61.1	27.5	58.20	3.50	0.22	250.5
T20	DB TANK 20	17.8	8.6	59.81	8.31	0.30	15.0
T41	DAY TANK 41	12.8	8.6	31.04	-8.91	2.48	3.3
Total of DIESEL OIL		91.7	44.7	53.28	2.04	0.67	268.9
FRESH WATER, RHO= 1.000							
T4A	FW TANK 4 A	72.2	69.0	114.24	4.23	2.83	54.5
T4B	FW TANK 4 B	72.2	69.0	114.24	-4.23	2.83	54.5
T5	FW TANK 5	146.5	145.0	113.61	0.00	2.68	0.0
T56	FW TANK 56	148.3	45.0	9.93	1.35	1.18	40.9
T57	FW TANK 57	148.3	45.0	9.93	-1.35	1.18	40.9
T17	CIRCUL TANK .	19.7	18.0	58.24	-9.00	0.55	13.6
T22	COOLING WATE.	2.9	2.0	55.40	8.90	0.43	1.6
T29	COOLING WATE.	16.6	15.0	45.85	-8.68	0.61	11.4
Total of FRESH WATER		626.6	408.0	85.74	-0.67	2.22	217.3
BALLAST WATER, RHO= 1.025							
T1	FORE PEAK TA.	178.9	175.8	134.08	0.00	4.02	0.0
T14	HEELING TANK.	185.1	185.0	77.54	8.87	2.63	0.0
Total of BALLAST WATER		364.0	360.8	105.09	4.55	3.31	0.0
BALLAST WATER, RHO= 1.010							
T610		789.4	200.0	86.98	0.12	1.66	7783.2
PAS							
(PAS)	PASSENGERS &.	0.0	110.0	71.50	0.00	16.40	0.0
TRA							
(TRA)	TRAILERS 34 .	0.0	970.0	70.00	-2.00	9.50	0.0
CREW							
(CREW)	CREW	0.0	20.0	60.00	0.00	22.00	0.0

Name	Max. weight	Mass	Center of gravity cgx	cgy	cgz	Free s. moment
PRO						
(PRO) PROVISION & .	0.0	80.0	46.00	0.00	10.00	0.0
Deadweight		2428.4	77.89	-0.04	6.27	8579.2
Lightweight		9733.0	60.76	0.00	11.56	
Displacement (rho=1.01)		12161.4	64.18	-0.01	10.50	8579.2

F L O A T I N G P O S I T I O N

Draught moulded	5.440	m	KM	11.81 m
Trim	-0.264	m	KG	10.50 m
TA	5.572	m	GM0	1.31 m
TF	5.308	m	GMCORR	-0.71 m
Trimming moment	-7060	tonm	GM	0.60 m

HEEL degree	MS m	HPHI m	EPHI rad*m	FSMOM tm	DGZ m
0.0	-0.002	0.00	0.000	0.0	0.000
10.0	0.046	0.17	0.012	1265.6	0.104
20.0	0.192	0.50	0.069	1698.4	0.140
30.0	0.330	0.83	0.187	1822.9	0.150
40.0	0.318	1.01	0.350	1804.0	0.148
50.0	0.235	1.10	0.533	1683.0	0.138
60.0	0.316	1.32	0.740	1485.6	0.122
70.0	0.702	1.83	1.016	1233.8	0.101
80.0	0.823	2.03	1.353	937.0	0.077
90.0	1.303	2.56	1.749	608.8	0.050
100.0	1.946	3.21	2.250	262.3	0.022
110.0	2.848	4.08	2.887	-88.7	-0.007
120.0	3.423	4.59	3.649	-431.4	-0.035

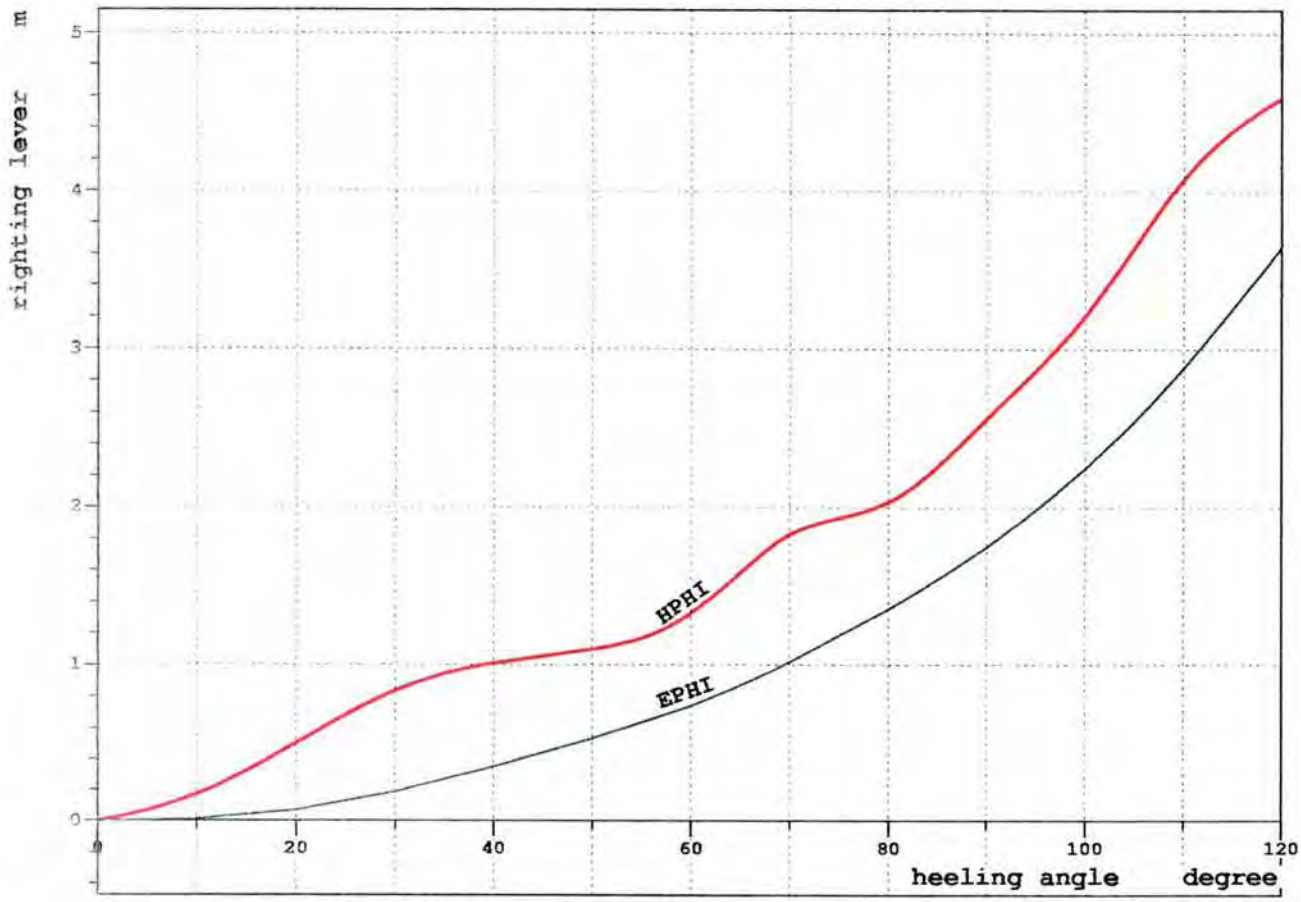
righting lever m
5
4
3
2
1
0
0
20
40
60
80
100
120
heeling angle degree
HPHI
EPHI

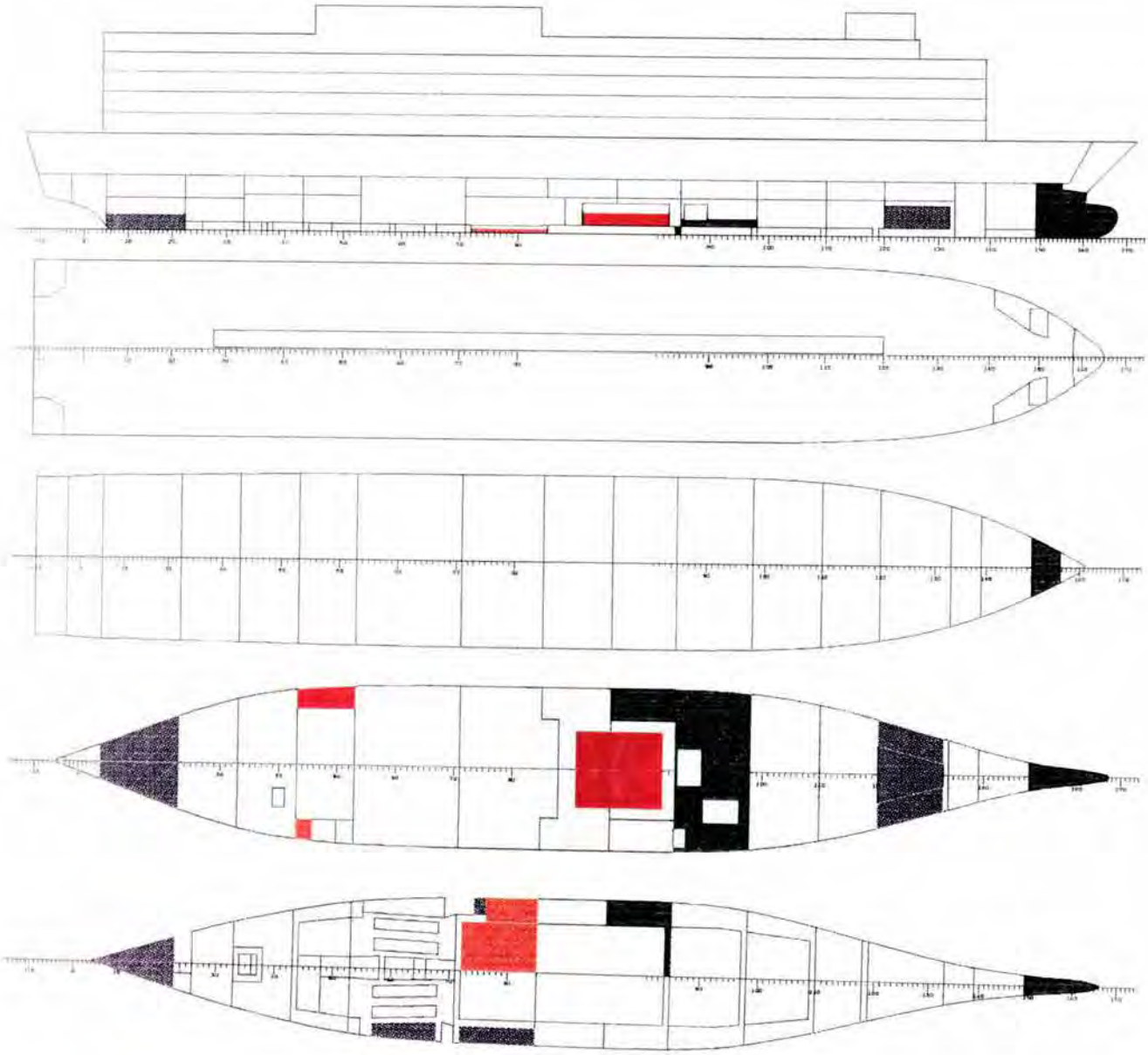

LOADING CONDITION K.3, DEP. FROM TALLIN, heeling tanks unsym

L O A D I N G C O M P O N E N T S

Name		Max. weight	Mass	Center of gravity cgx	cgy	cgz	Free s. moment
HEAVY FUEL OIL, RHO= 0.900							
T10	DEEP TANK 10	171.1	97.2	74.20	2.75	2.03	146.7
T11	DEEP TANK 11	171.1	97.2	74.20	-2.75	2.03	146.7
T36	DAY TANK 36	23.1	22.5	36.23	9.28	2.76	9.1
T38	SETTLING TAN.	28.9	18.0	32.35	8.96	2.36	7.3
Total of HEAVY FUEL OIL		394.3	234.9	67.36	1.58	2.13	309.9
DIESEL OIL, RHO= 0.860							
T18	DB TANK 18	61.1	27.5	58.20	3.50	0.22	250.5
T20	DB TANK 20	17.8	8.6	59.81	8.31	0.30	15.0
T41	DAY TANK 41	12.8	8.6	31.04	-8.91	2.48	3.3
Total of DIESEL OIL		91.7	44.7	53.28	2.04	0.67	268.9
FRESH WATER, RHO= 1.000							
T4A	FW TANK 4 A	72.2	69.0	114.24	4.23	2.83	54.5
T4B	FW TANK 4 B	72.2	69.0	114.24	-4.23	2.83	54.5
T5	FW TANK 5	146.5	145.0	113.61	0.00	2.68	0.0
T56	FW TANK 56	148.3	45.0	9.93	1.35	1.18	40.9
T57	FW TANK 57	148.3	45.0	9.93	-1.35	1.18	40.9
T17	CIRCUL TANK .	19.7	18.0	58.24	-9.00	0.55	13.6
T22	COOLING WATE.	2.9	2.0	55.40	8.90	0.43	1.6
T29	COOLING WATE.	16.6	15.0	45.85	-8.68	0.61	11.4
Total of FRESH WATER		626.6	408.0	85.74	-0.67	2.22	217.3
BALLAST WATER, RHO= 1.025							
T1	FORE PEAK TA.	178.9	175.8	134.08	0.00	4.02	0.0
T14	HEELING TANK.	185.1	185.0	77.54	8.87	2.63	0.0
Total of BALLAST WATER		364.0	360.8	105.09	4.55	3.31	0.0
BALLAST WATER, RHO= 1.010							
T510		716.2	100.0	96.82	0.00	1.49	5066.5
T610		789.4	200.0	86.98	0.12	1.66	7783.2
Total of BALLAST WATER		1505.6	300.0	90.26	0.08	1.61	12849.7
PAS							
(PAS)	PASSENGERS &.	0.0	110.0	71.50	0.00	16.40	0.0
TRA							
(TRA)	TRAILERS 34 .	0.0	970.0	70.00	-2.00	9.50	0.0
CREW							

Name		Max. weight	Mass	Center of gravity cgx	cgy	cgz	Free s. moment
PRO							
(PRO)	PROVISION & .	0.0	80.0	46.00	0.00	10.00	0.0
Deadweight			2528.4	78.64	-0.03	6.08	13645.7
Lightweight			9733.0	60.76	0.00	11.56	
Displacement (rho=1.01)			12261.4	64.45	-0.01	10.43	13645.7

F L O A T I N G P O S I T I O N

Draught moulded	5.485	m	KM	11.76 m
Trim	-0.122	m	KG	10.43 m
TA	5.546	m	GM0	1.33 m
TF	5.424	m	GMCORR	-1.11 m
Trimming moment	-3267	tonm	GM	0.22 m

HEEL degree	MS m	HPHI m	EPHI rad*m	FSMOM tm	DGZ m
0.0	-0.002	0.00	0.000	0.0	0.000
10.0	0.050	0.13	0.009	1850.5	0.151
20.0	0.200	0.46	0.058	2404.7	0.196
30.0	0.344	0.80	0.170	2567.9	0.209
40.0	0.344	0.99	0.328	2525.8	0.206
50.0	0.271	1.10	0.511	2340.1	0.191
60.0	0.364	1.35	0.720	2050.1	0.167
70.0	0.754	1.87	1.002	1684.9	0.137
80.0	0.870	2.08	1.347	1259.2	0.103
90.0	1.350	2.62	1.753	791.5	0.065
100.0	1.986	3.27	2.265	300.0	0.024
110.0	2.883	4.15	2.914	-196.4	-0.016
120.0	3.454	4.66	3.688	-679.6	-0.055

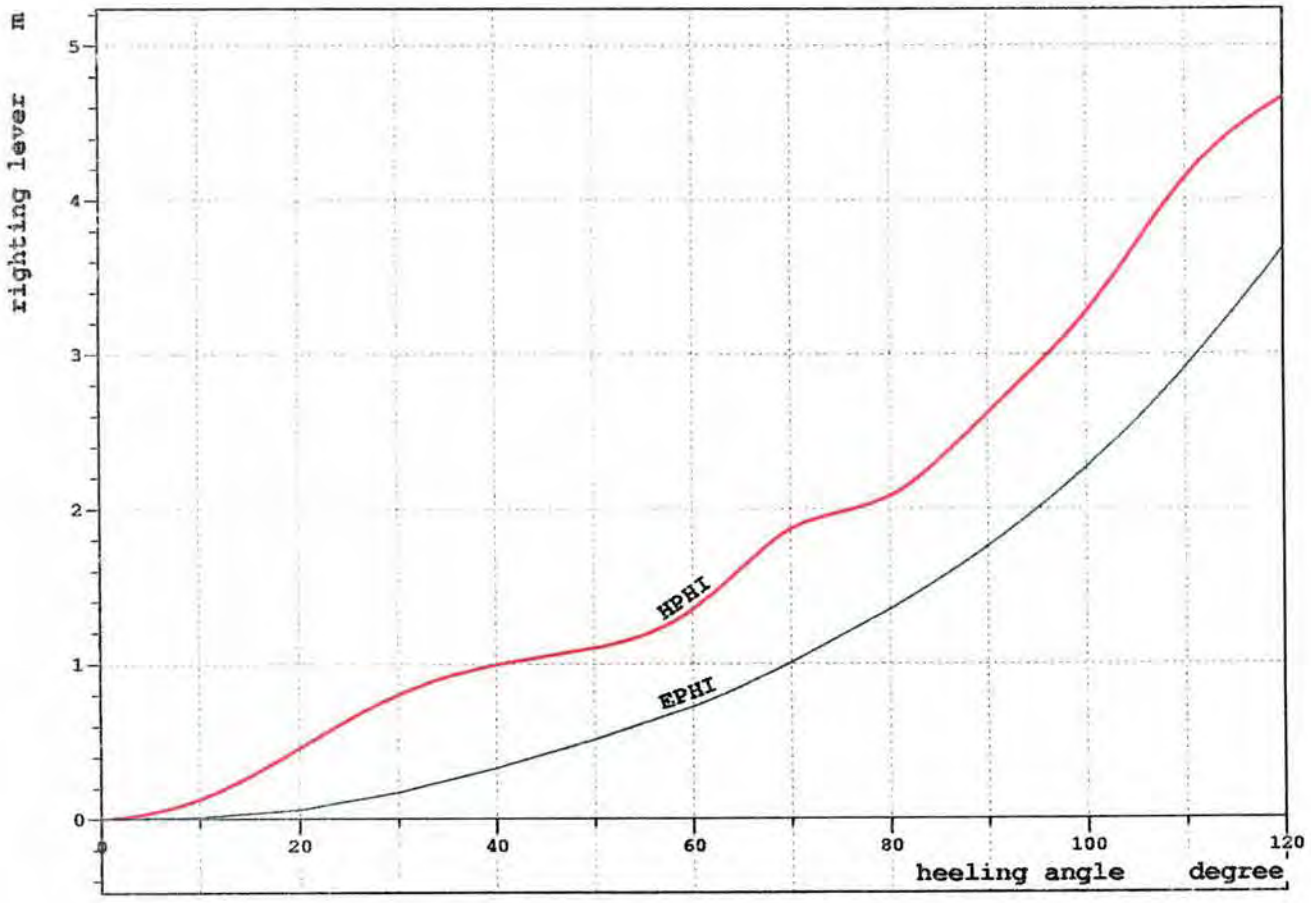
m
righting lever
5
4
3
2
1
0
0
20
40
60
80
100
120
HPHI
EPHI
heeling angle degree

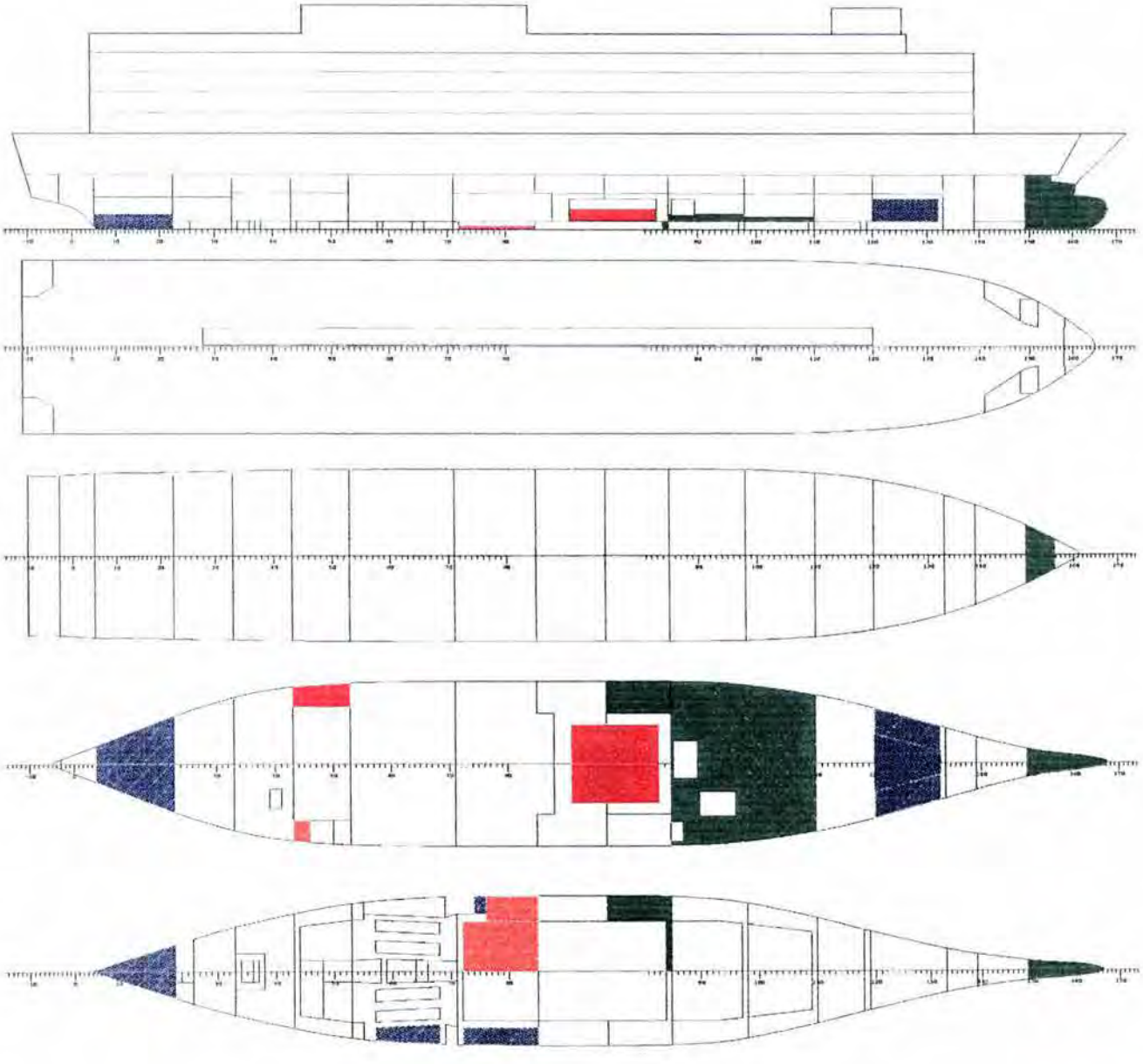

LOADING CONDITION K.4, DEP. FROM TALLIN, heeling tanks unsym

L O A D I N G C O M P O N E N T S

Name		Max. weight	Mass	Center of gravity cgx	cgy	cgz	Free s. moment
HEAVY FUEL OIL, RHO= 0.900							
T10	DEEP TANK 10	171.1	97.2	74.20	2.75	2.03	146.7
T11	DEEP TANK 11	171.1	97.2	74.20	-2.75	2.03	146.7
T36	DAY TANK 36	23.1	22.5	36.23	9.28	2.76	9.1
T38	SETTLING TAN.	28.9	18.0	32.35	8.96	2.36	7.3
Total of HEAVY FUEL OIL		394.3	234.9	67.36	1.58	2.13	309.9
DIESEL OIL, RHO= 0.860							
T18	DB TANK 18	61.1	27.5	58.20	3.50	0.22	250.5
T20	DB TANK 20	17.8	8.6	59.81	8.31	0.30	15.0
T41	DAY TANK 41	12.8	8.6	31.04	-8.91	2.48	3.3
Total of DIESEL OIL		91.7	44.7	53.28	2.04	0.67	268.9
FRESH WATER, RHO= 1.000							
T4A	FW TANK 4 A	72.2	69.0	114.24	4.23	2.83	54.5
T4B	FW TANK 4 B	72.2	69.0	114.24	-4.23	2.83	54.5
T5	FW TANK 5	146.5	145.0	113.61	0.00	2.68	0.0
T56	FW TANK 56	148.3	45.0	9.93	1.35	1.18	40.9
T57	FW TANK 57	148.3	45.0	9.93	-1.35	1.18	40.9
T17	CIRCUL TANK .	19.7	18.0	58.24	-9.00	0.55	13.6
T22	COOLING WATE.	2.9	2.0	55.40	8.90	0.43	1.6
T29	COOLING WATE.	16.6	15.0	45.85	-8.68	0.61	11.4
Total of FRESH WATER		626.6	408.0	85.74	-0.67	2.22	217.3
BALLAST WATER, RHO= 1.025							
T1	FORE PEAK TA.	178.9	175.8	134.08	0.00	4.02	0.0
T14	HEELING TANK.	185.1	185.0	77.54	8.87	2.63	0.0
Total of BALLAST WATER		364.0	360.8	105.09	4.55	3.31	0.0
BALLAST WATER, RHO= 1.010							
T510		716.2	200.0	96.83	0.00	1.78	5632.4
T610		789.4	300.0	87.05	0.29	1.91	8217.0
Total of BALLAST WATER		1505.6	500.0	90.96	0.18	1.86	13849.4
PAS							
(PAS)	PASSENGERS &.	0.0	110.0	71.50	0.00	16.40	0.0
TRA							
(TRA)	TRAILERS 34 .	0.0	970.0	70.00	-2.00	9.50	0.0
CREW							

Name	Max. weight	Mass	Center of gravity cgx	cgy	cgz	Free s. moment
PRO						
(PRO) PROVISION & .	0.0	80.0	46.00	0.00	10.00	0.0
Deadweight		2728.4	79.62	-0.01	5.80	14645.5
Lightweight		9733.0	60.76	0.00	11.56	
Displacement (rho=1.01)		12461.4	64.89	0.00	10.30	14645.5

F L O A T I N G P O S I T I O N

Draught moulded	5.571	m	KM	11.70 m
Trim	0.122	m	KG	10.30 m
TA	5.510	m	GM0	1.40 m
TF	5.631	m	GMCORR	-1.18 m
Trimming moment	3247	tonm	GM	0.23 m

HEEL degree	MS m	HPHI m	EPHI rad*m	FSMOM tm	DGZ m
0.0	-0.003	0.00	0.000	0.0	0.000
10.0	0.054	0.10	0.006	2449.7	0.197
20.0	0.204	0.41	0.048	3362.5	0.270
30.0	0.363	0.78	0.153	3508.9	0.282
40.0	0.384	1.01	0.312	3393.9	0.272
50.0	0.334	1.16	0.501	3109.0	0.249
60.0	0.443	1.44	0.723	2696.2	0.216
70.0	0.834	1.98	1.023	2188.3	0.176
80.0	0.939	2.19	1.386	1604.3	0.129
90.0	1.420	2.74	1.814	968.1	0.078
100.0	2.037	3.39	2.347	302.3	0.024
110.0	2.923	4.27	3.017	-369.3	-0.030
120.0	3.485	4.78	3.812	-1022.9	-0.082

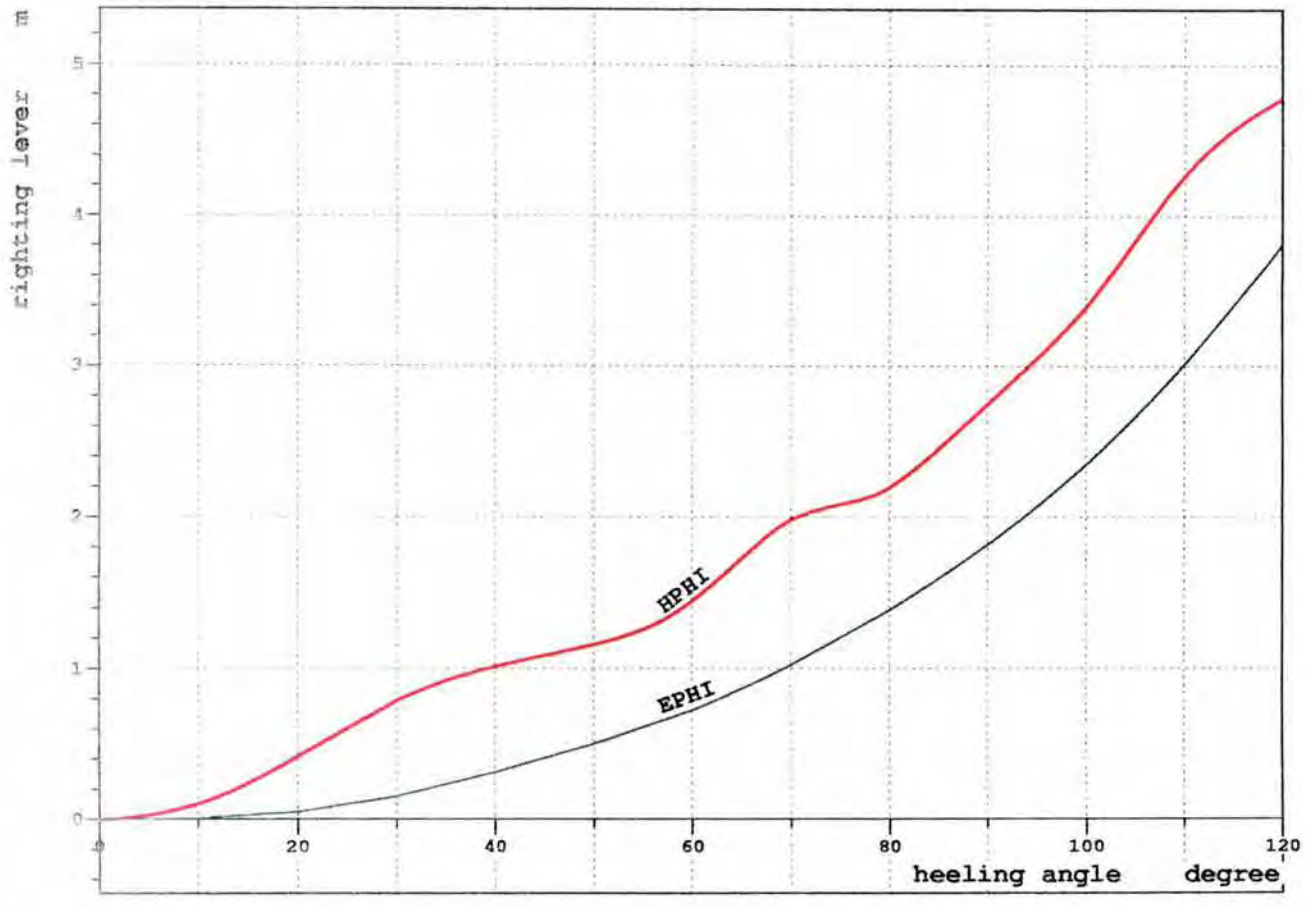
righting lever m
5
4
3
2
1
0
HPHI
EPHI
0
20
40
60
80
100
120
heeling angle degree

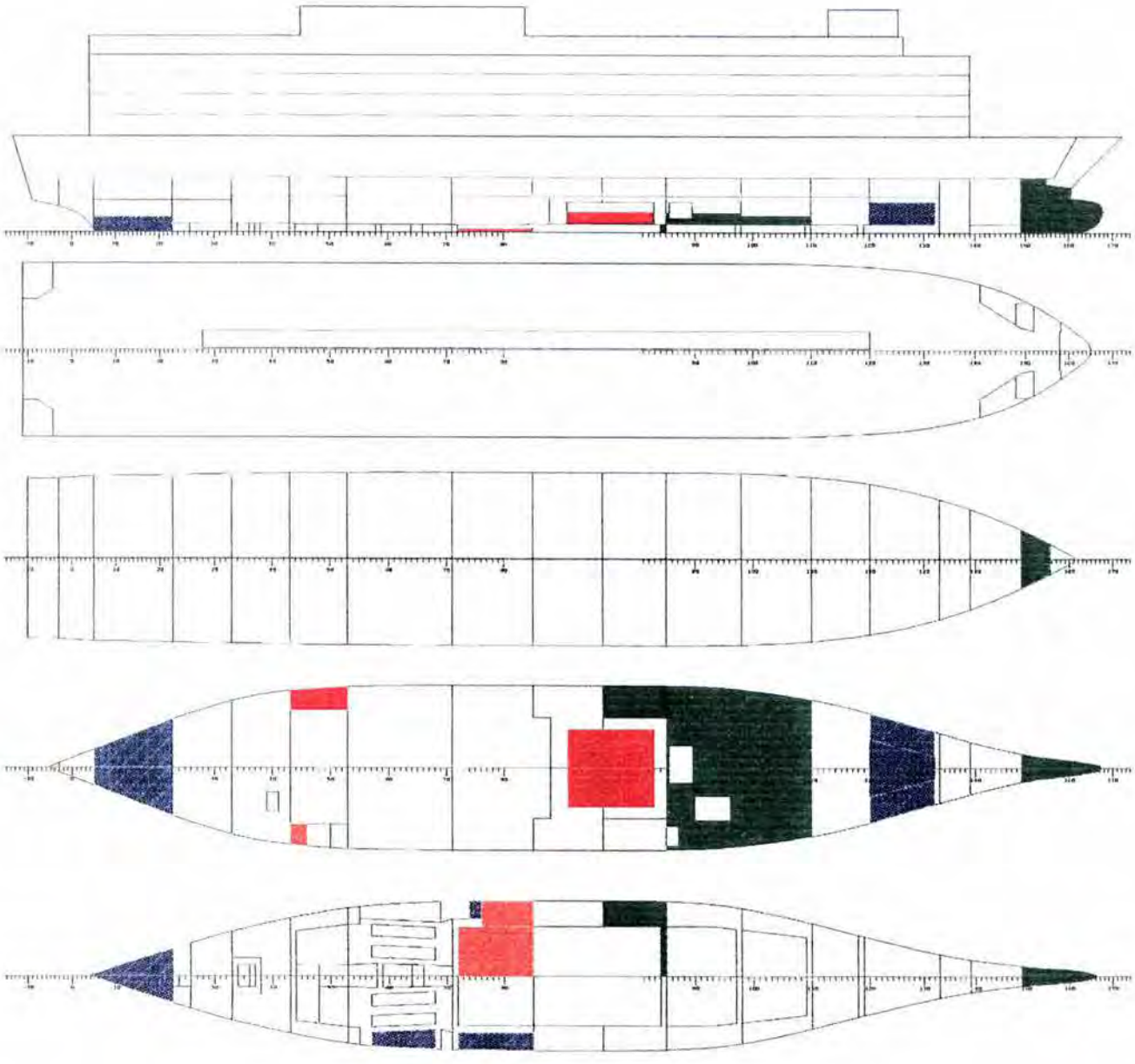

LOADING CONDITION K.5, DEP. FROM TALLIN, heeling tanks unsym

L O A D I N G C O M P O N E N T S

Name		Max. weight	Mass	Center of gravity cgx	cgy	cgz	Free s. moment
HEAVY FUEL OIL, RHO= 0.900							
T10	DEEP TANK 10	171.1	97.2	74.20	2.75	2.03	146.7
T11	DEEP TANK 11	171.1	97.2	74.20	-2.75	2.03	146.7
T36	DAY TANK 36	23.1	22.5	36.23	9.28	2.76	9.1
T38	SETTLING TAN.	28.9	18.0	32.35	8.96	2.36	7.3
Total of HEAVY FUEL OIL		394.3	234.9	67.36	1.58	2.13	309.9
DIESEL OIL, RHO= 0.860							
T18	DB TANK 18	61.1	27.5	58.20	3.50	0.22	250.5
T20	DB TANK 20	17.8	8.6	59.81	8.31	0.30	15.0
T41	DAY TANK 41	12.8	8.6	31.04	-8.91	2.48	3.3
Total of DIESEL OIL		91.7	44.7	53.28	2.04	0.67	268.9
FRESH WATER, RHO= 1.000							
T4A	FW TANK 4 A	72.2	69.0	114.24	4.23	2.83	54.5
T4B	FW TANK 4 B	72.2	69.0	114.24	-4.23	2.83	54.5
T5	FW TANK 5	146.5	145.0	113.61	0.00	2.68	0.0
T56	FW TANK 56	148.3	45.0	9.93	1.35	1.18	40.9
T57	FW TANK 57	148.3	45.0	9.93	-1.35	1.18	40.9
T17	CIRCUL TANK .	19.7	18.0	58.24	-9.00	0.55	13.6
T22	COOLING WATE.	2.9	2.0	55.40	8.90	0.43	1.6
T29	COOLING WATE.	16.6	15.0	45.85	-8.68	0.61	11.4
Total of FRESH WATER		626.6	408.0	85.74	-0.67	2.22	217.3
BALLAST WATER, RHO= 1.025							
T1	FORE PEAK TA.	178.9	175.8	134.08	0.00	4.02	0.0
T14	HEELING TANK.	185.1	185.0	77.54	8.87	2.63	0.0
Total of BALLAST WATER		364.0	360.8	105.09	4.55	3.31	0.0
BALLAST WATER, RHO= 1.010							
T410		495.9	100.0	105.89	0.00	1.52	2140.8
T510		716.2	250.0	96.83	0.00	1.92	5885.8
T610		789.4	350.0	87.07	0.34	2.04	8401.7
Total of BALLAST WATER		2001.5	700.0	93.25	0.17	1.92	16428.4
PAS							
(PAS)	PASSENGERS &.	0.0	110.0	71.50	0.00	16.40	0.0
TRA							
(TRA)	TRAILERS 34 .	0.0	970.0	70.00	-2.00	9.50	0.0

Name		Max. weight	Mass	Center of gravity cgx	cgy	cgz	Free s. moment
CREW							
(CREW)	CREW	0.0	20.0	60.00	0.00	22.00	0.0
PRO							
(PRO)	PROVISION & .	0.0	80.0	46.00	0.00	10.00	0.0
Deadweight			2928.4	80.94	0.00	5.54	17224.4
Lightweight			9733.0	60.76	0.00	11.56	
Displacement (rho=1.01)			12661.4	65.43	0.00	10.17	17224.4

F L O A T I N G P O S I T I O N

Draught moulded	5.658	m	KM	11.63 m
Trim	0.414	m	KG	10.17 m
TA	5.451	m	GM0	1.47 m
TF	5.865	m	GMCORR	-1.36 m
Trimming moment	11025	tonm	GM	0.11 m

HEEL degree	MS m	HPHI m	EPHI rad*m	FSMOM tm	DGZ m
0.0	-0.005	-0.01	0.000	0.0	0.000
10.0	0.056	0.08	0.004	2945.3	0.233
20.0	0.209	0.38	0.041	4152.7	0.328
30.0	0.378	0.77	0.141	4355.4	0.344
40.0	0.418	1.03	0.300	4212.9	0.333
50.0	0.384	1.20	0.495	3857.4	0.305
60.0	0.512	1.52	0.727	3344.1	0.264
70.0	0.908	2.07	1.042	2712.4	0.214
80.0	1.006	2.29	1.422	1986.8	0.157
90.0	1.487	2.86	1.870	1196.6	0.095
100.0	2.091	3.51	2.423	369.7	0.029
110.0	2.971	4.39	3.112	-464.8	-0.037
120.0	3.525	4.90	3.928	-1277.2	-0.101

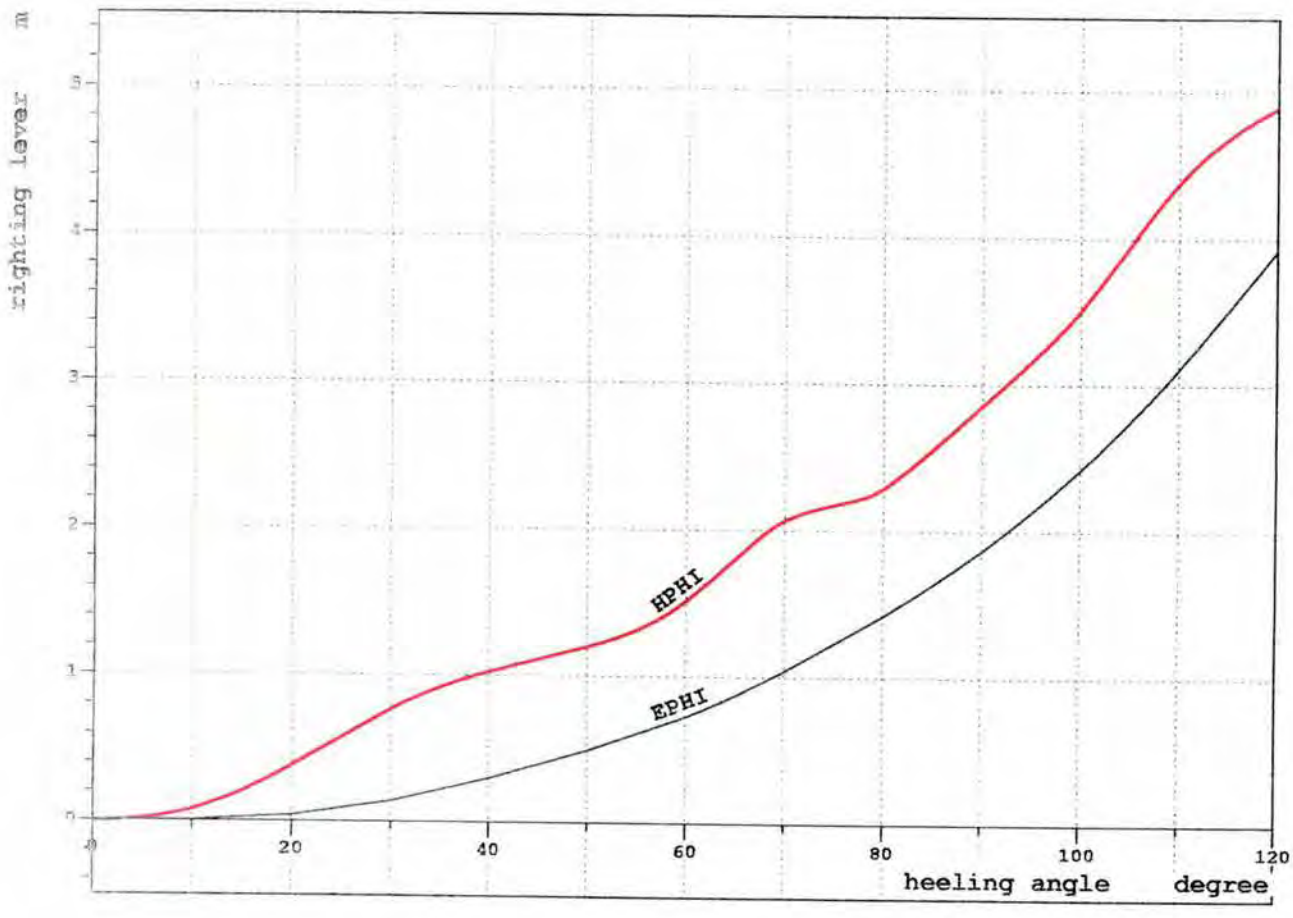
righting lever m
5
4
3
2
1
0
0
20
40
60
80
100
120
heeling angle degree
HPHI
EPHI

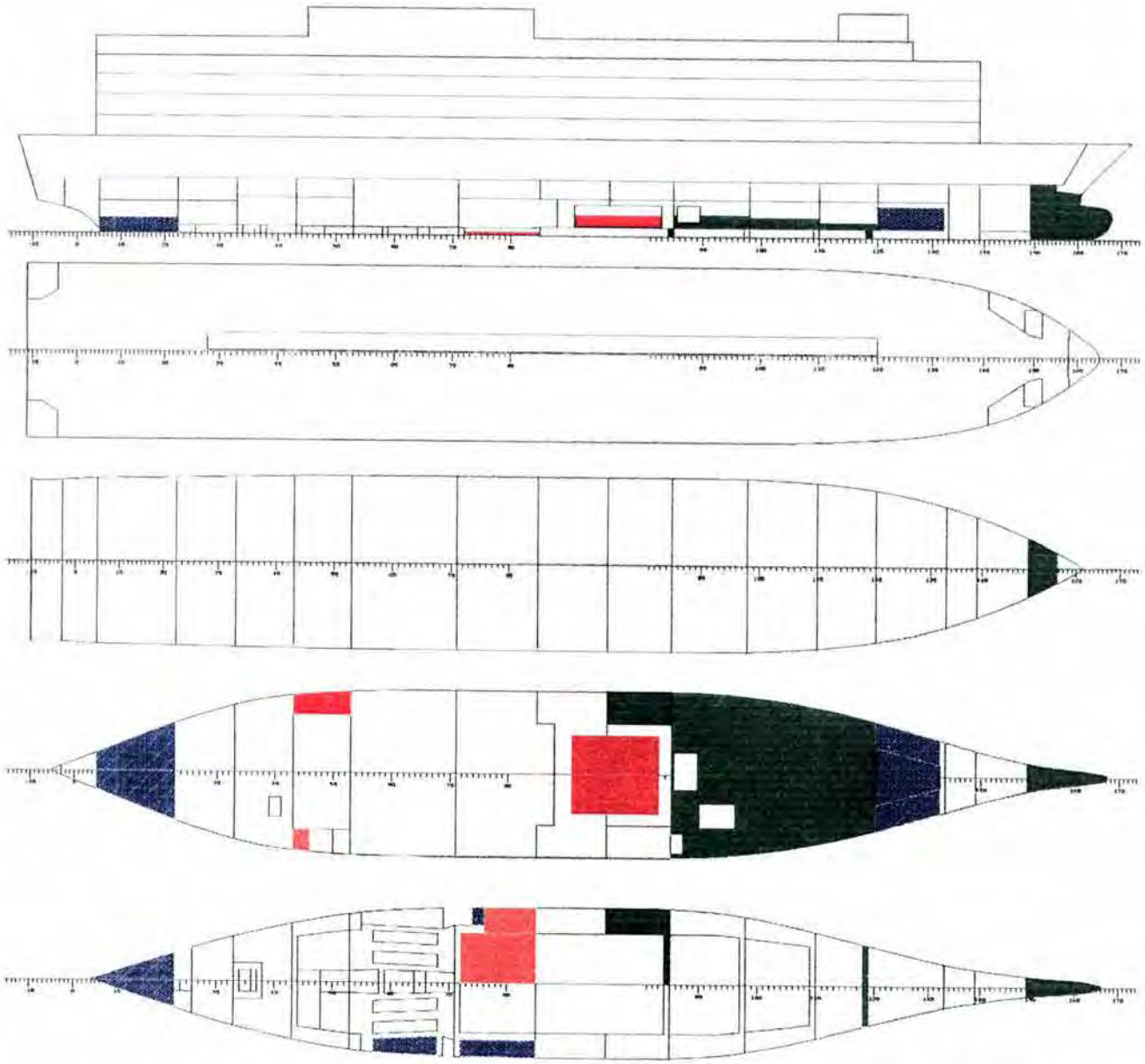

LOADING CONDITION K.6, DEP. FROM TALLIN, heeling tanks unsym

L O A D I N G C O M P O N E N T S

Name		Max. weight	Mass	Center of gravity cgx	cgy	cgz	Free s. moment
HEAVY FUEL OIL, RHO= 0.900							
T10	DEEP TANK 10	171.1	97.2	74.20	2.75	2.03	146.7
T11	DEEP TANK 11	171.1	97.2	74.20	-2.75	2.03	146.7
T36	DAY TANK 36	23.1	22.5	36.23	9.28	2.76	9.1
T38	SETTLING TAN.	28.9	18.0	32.35	8.96	2.36	7.3
Total of HEAVY FUEL OIL		394.3	234.9	67.36	1.58	2.13	309.9
DIESEL OIL, RHO= 0.860							
T18	DB TANK 18	61.1	27.5	58.20	3.50	0.22	250.5
T20	DB TANK 20	17.8	8.6	59.81	8.31	0.30	15.0
T41	DAY TANK 41	12.8	8.6	31.04	-8.91	2.48	3.3
Total of DIESEL OIL		91.7	44.7	53.28	2.04	0.67	268.9
FRESH WATER, RHO= 1.000							
T4A	FW TANK 4 A	72.2	69.0	114.24	4.23	2.83	54.5
T4B	FW TANK 4 B	72.2	69.0	114.24	-4.23	2.83	54.5
T5	FW TANK 5	146.5	145.0	113.61	0.00	2.68	0.0
T56	FW TANK 56	148.3	45.0	9.93	1.35	1.18	40.9
T57	FW TANK 57	148.3	45.0	9.93	-1.35	1.18	40.9
T17	CIRCUL TANK .	19.7	18.0	58.24	-9.00	0.55	13.6
T22	COOLING WATE.	2.9	2.0	55.40	8.90	0.43	1.6
T29	COOLING WATE.	16.6	15.0	45.85	-8.68	0.61	11.4
Total of FRESH WATER		626.6	408.0	85.74	-0.67	2.22	217.3
BALLAST WATER, RHO= 1.025							
T1	FORE PEAK TA.	178.9	175.8	134.08	0.00	4.02	0.0
T14	HEELING TANK.	185.1	185.0	77.54	8.87	2.63	0.0
Total of BALLAST WATER		364.0	360.8	105.09	4.55	3.31	0.0
BALLAST WATER, RHO= 1.010							
T410		495.9	200.0	105.76	0.00	1.97	2659.7
T510		716.2	350.0	96.84	0.00	2.19	6355.0
T610		789.4	450.0	87.10	0.40	2.29	8751.5
Total of BALLAST WATER		2001.5	1000.0	94.24	0.18	2.20	17766.2
PAS							
(PAS)	PASSENGERS &.	0.0	110.0	71.50	0.00	16.40	0.0
TRA							
(TRA)	TRAILERS 34 .	0.0	970.0	70.00	-2.00	9.50	0.0

Name		Max. weight	Mass	Center of gravity cgx	cgy	cgz	Free s. moment
CREW							
(CREW)	CREW	0.0	20.0	60.00	0.00	22.00	0.0
PRO							
(PRO)	PROVISION & .	0.0	80.0	46.00	0.00	10.00	0.0
Deadweight			3228.4	82.39	0.02	5.29	18562.3
Lightweight			9733.0	60.76	0.00	11.56	
Displacement (rho=1.01)			12961.4	66.15	0.01	10.00	18562.3

F L O A T I N G P O S I T I O N

Draught moulded	5.785	m	KM	11.57 m
Trim	0.814	m	KG	10.00 m
TA	5.378	m	GM0	1.58 m
TF	6.192	m	GMCORR	-1.43 m
Trimming moment	21727	tonm	GM	0.14 m

HEEL degree	MS m	HPHI m	EPHI rad*m	FSMOM tm	DGZ m
0.0	-0.010	-0.01	0.000	0.0	0.000
10.0	0.054	0.08	0.004	3191.4	0.246
20.0	0.203	0.39	0.042	4600.9	0.355
30.0	0.382	0.80	0.146	4782.3	0.369
40.0	0.445	1.10	0.314	4608.5	0.356
50.0	0.430	1.31	0.525	4206.2	0.325
60.0	0.582	1.67	0.780	3635.0	0.280
70.0	0.979	2.23	1.123	2936.5	0.227
80.0	1.071	2.46	1.531	2137.4	0.165
90.0	1.548	3.03	2.008	1269.3	0.098
100.0	2.136	3.66	2.590	362.5	0.028
110.0	3.007	4.53	3.305	-551.3	-0.043
120.0	3.552	5.03	4.145	-1439.7	-0.111

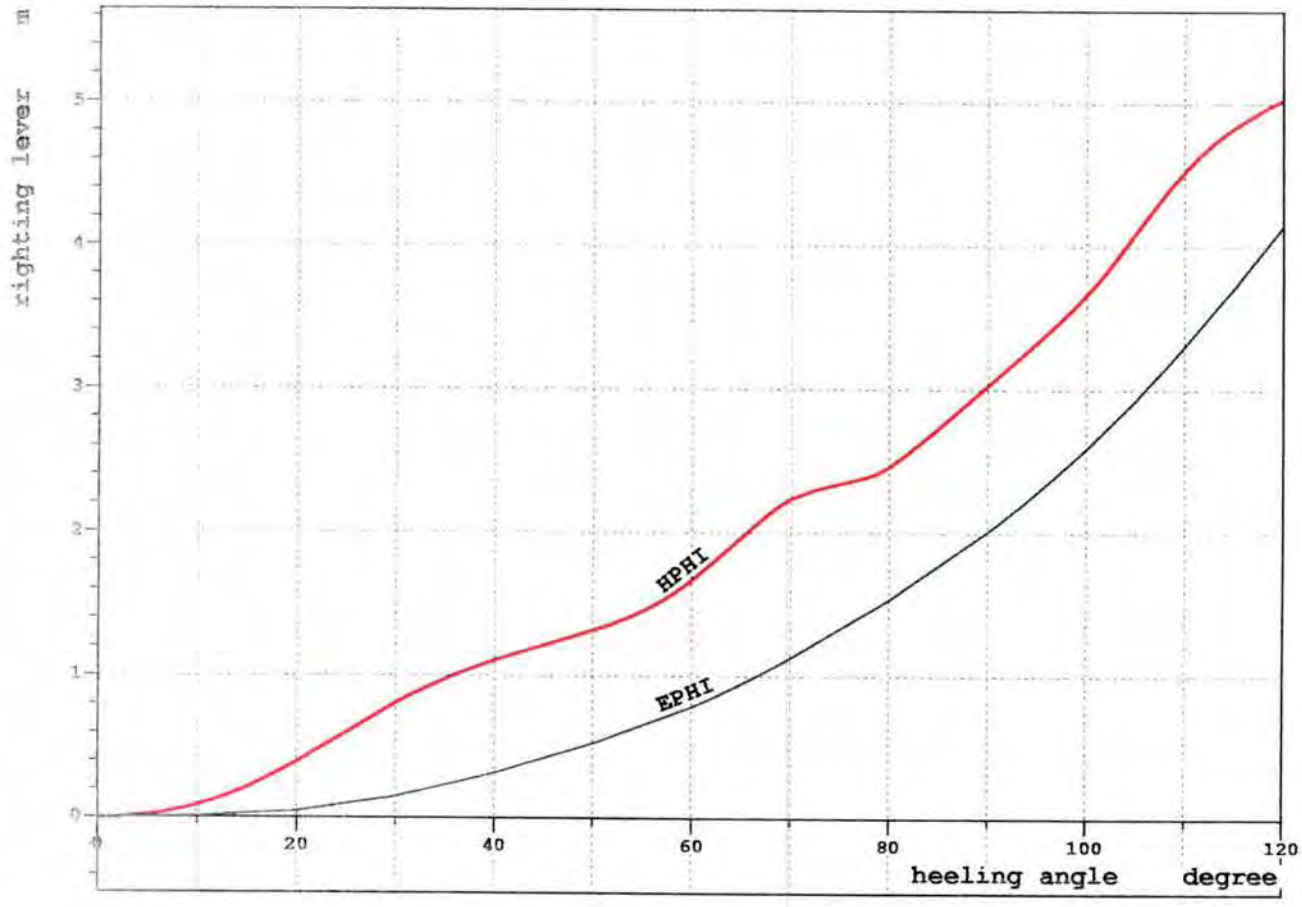
righting lever m
0
1
2
3
4
5
HPHI
EPHI
0
20
40
60
80
100
120
heeling angle degree

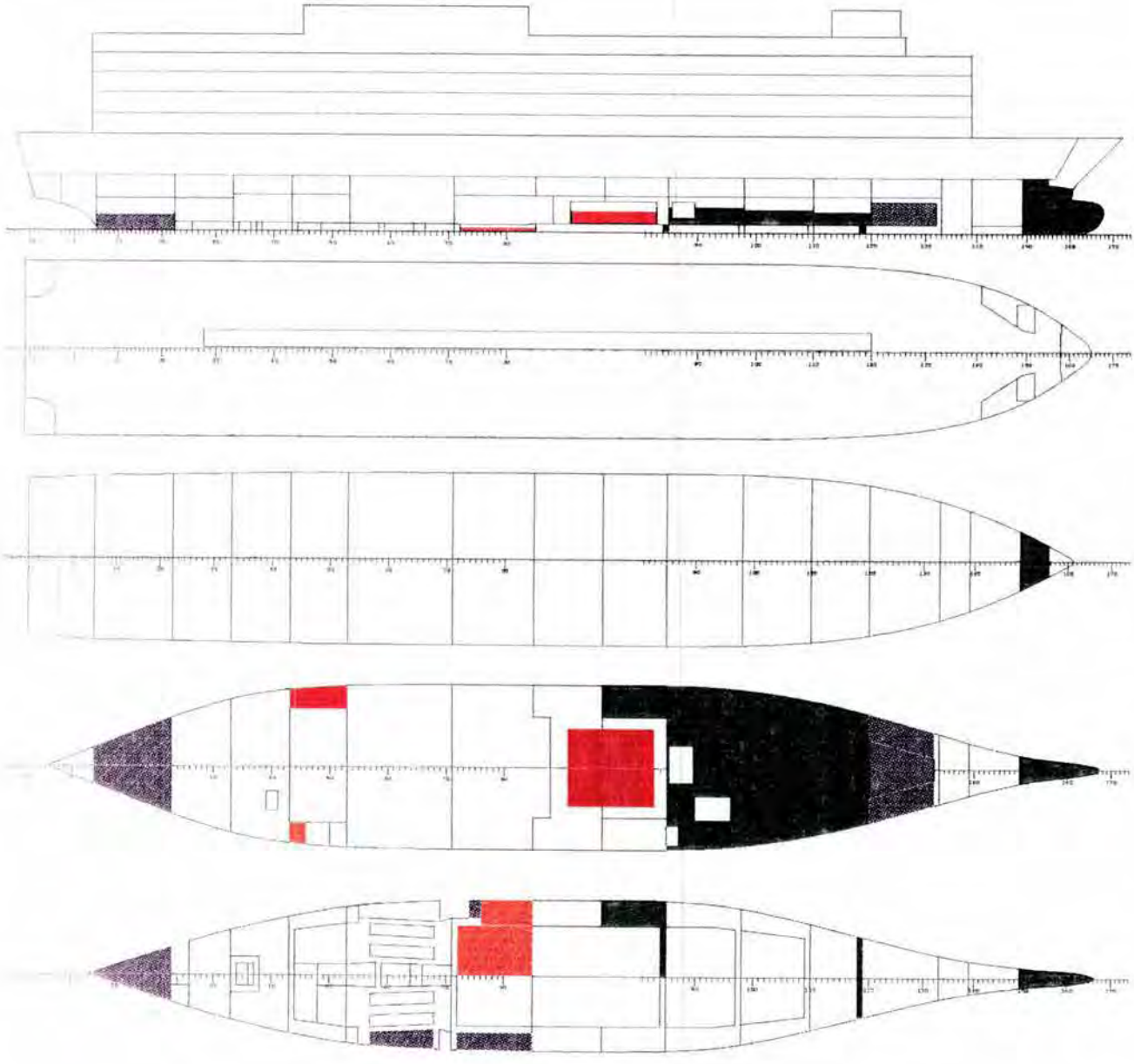

LOADING CONDITION K.7, DEP. FROM TALLIN, heeling tanks unsym

L O A D I N G C O M P O N E N T S

Name		Max. weight	Mass	Center of gravity cgx	cgy	cgz	Free s. moment
HEAVY FUEL OIL, RHO= 0.900							
T10	DEEP TANK 10	171.1	97.2	74.20	2.75	2.03	146.7
T11	DEEP TANK 11	171.1	97.2	74.20	-2.75	2.03	146.7
T36	DAY TANK 36	23.1	22.5	36.23	9.28	2.76	9.1
T38	SETTLING TAN.	28.9	18.0	32.35	8.96	2.36	7.3
Total of HEAVY FUEL OIL		394.3	234.9	67.36	1.58	2.13	309.9
DIESEL OIL, RHO= 0.860							
T18	DB TANK 18	61.1	27.5	58.20	3.50	0.22	250.5
T20	DB TANK 20	17.8	8.6	59.81	8.31	0.30	15.0
T41	DAY TANK 41	12.8	8.6	31.04	-8.91	2.48	3.3
Total of DIESEL OIL		91.7	44.7	53.28	2.04	0.67	268.9
FRESH WATER, RHO= 1.000							
T4A	FW TANK 4 A	72.2	69.0	114.24	4.23	2.83	54.5
T4B	FW TANK 4 B	72.2	69.0	114.24	-4.23	2.83	54.5
T5	FW TANK 5	146.5	145.0	113.61	0.00	2.68	0.0
T56	FW TANK 56	148.3	45.0	9.93	1.35	1.18	40.9
T57	FW TANK 57	148.3	45.0	9.93	-1.35	1.18	40.9
T17	CIRCUL TANK .	19.7	18.0	58.24	-9.00	0.55	13.6
T22	COOLING WATE.	2.9	2.0	55.40	8.90	0.43	1.6
T29	COOLING WATE.	16.6	15.0	45.85	-8.68	0.61	11.4
Total of FRESH WATER		626.6	408.0	85.74	-0.67	2.22	217.3
BALLAST WATER, RHO= 1.025							
T1	FORE PEAK TA.	178.9	175.8	134.08	0.00	4.02	0.0
T14	HEELING TANK.	185.1	185.0	77.54	8.87	2.63	0.0
Total of BALLAST WATER		364.0	360.8	105.09	4.55	3.31	0.0
BALLAST WATER, RHO= 1.010							
T410		495.9	300.0	105.72	0.00	2.39	3204.4
T510		716.2	450.0	96.85	0.00	2.46	6806.2
T610		789.4	550.0	87.12	0.44	2.55	9087.1
Total of BALLAST WATER		2001.5	1300.0	94.78	0.19	2.48	19097.7
PAS							
(PAS)	PASSENGERS &.	0.0	110.0	71.50	0.00	16.40	0.0
TRA							
(TRA)	TRAILERS 34 .	0.0	970.0	70.00	-2.00	9.50	0.0

Name		Max. weight	Mass	Center of gravity cgx	cgy	cgz	Free s. moment
CREW							
(CREW)	CREW	0.0	20.0	60.00	0.00	22.00	0.0
PRO							
(PRO)	PROVISION & .	0.0	80.0	46.00	0.00	10.00	0.0
Deadweight			3528.4	83.60	0.04	5.13	19893.7
Lightweight			9733.0	60.76	0.00	11.56	
Displacement (rho=1.01)			13261.4	66.84	0.01	9.85	19893.7

F L O A T I N G P O S I T I O N

Draught moulded	5.909	m	KM	11.54 m
Trim	1.205	m	KG	9.85 m
TA	5.306	m	GM0	1.70 m
TF	6.512	m	GMCORR	-1.50 m
Trimming moment	32395	tonm	GM	0.20 m

HEEL degree	MS m	HPHI m	EPHI rad*m	FSMOM tm	DGZ m
0.0	-0.014	-0.01	0.000	0.0	0.000
10.0	0.047	0.11	0.005	3127.1	0.236
20.0	0.189	0.46	0.051	4170.0	0.314
30.0	0.373	0.89	0.169	4353.5	0.328
40.0	0.453	1.23	0.356	4201.7	0.317
50.0	0.452	1.46	0.591	3840.4	0.290
60.0	0.624	1.84	0.875	3319.6	0.250
70.0	1.016	2.41	1.249	2681.5	0.202
80.0	1.107	2.63	1.688	1951.2	0.147
90.0	1.576	3.19	2.194	1157.9	0.087
100.0	2.151	3.80	2.802	329.4	0.025
110.0	3.013	4.65	3.539	-505.4	-0.038
120.0	3.552	5.12	4.398	-1320.3	-0.100

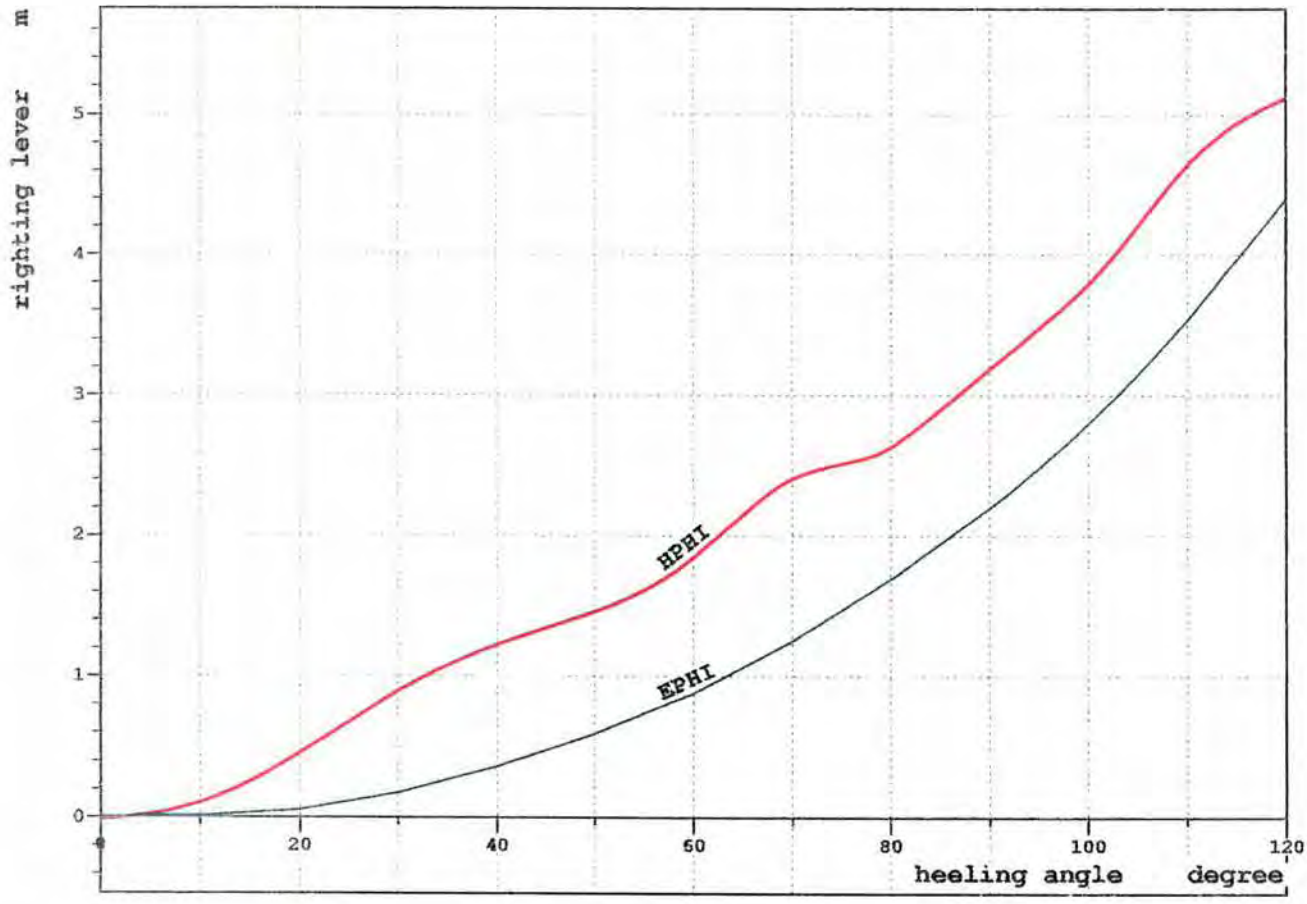
righting lever m
5
4
3
2
1
0
HPHI
EPHI
0
20
40
60
80
100
120
heeling angle degree

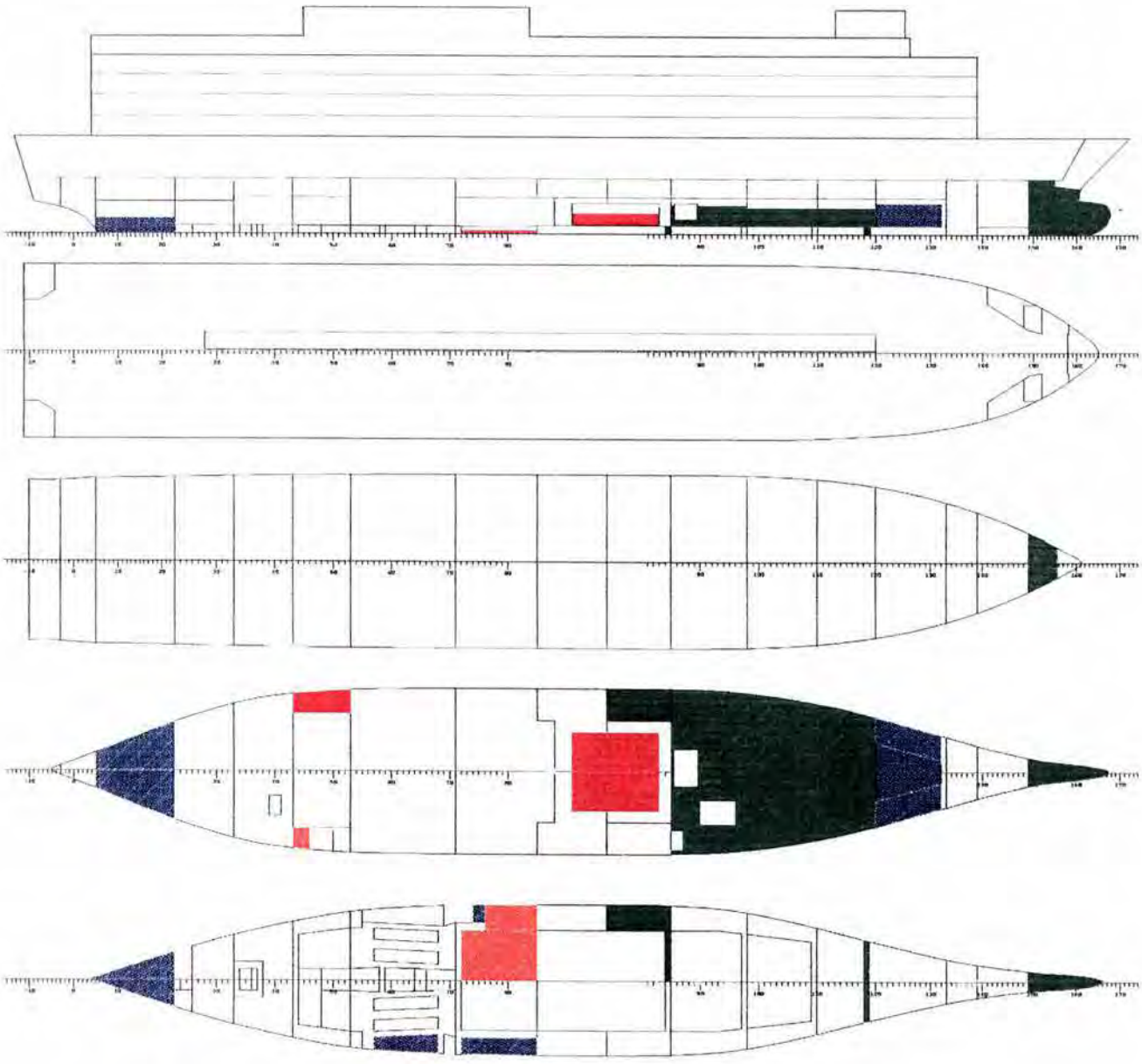

SUPPLEMENT No. 506

Metsaveer Jan: MV ESTONIA Accident Investigation. Calculation of Load-Carrying Capacity of the Bow Visor Locks.

Tallinn Technical University.

Tallinn 1996.

TALLINN TECHNICAL UNIVERSITY

MV ESTONIA ACCIDENT INVESTIGATION

CALCULATION OF LOAD-CARRYING CAPACITY OF THE BOW VISOR LOCKS

by

Jaan Metsaveer

Tallinn 1996

1. LOAD-CARRYING CAPACITY OF THE ATLANTIC LOCK

The Atlantic lock (bottom lock) consists of a locking bolt, guide bushing and support bushing. The lock was fixed to the vessel by three lugs. One lug attached to the visor was locked by the bolt (Figure 1).

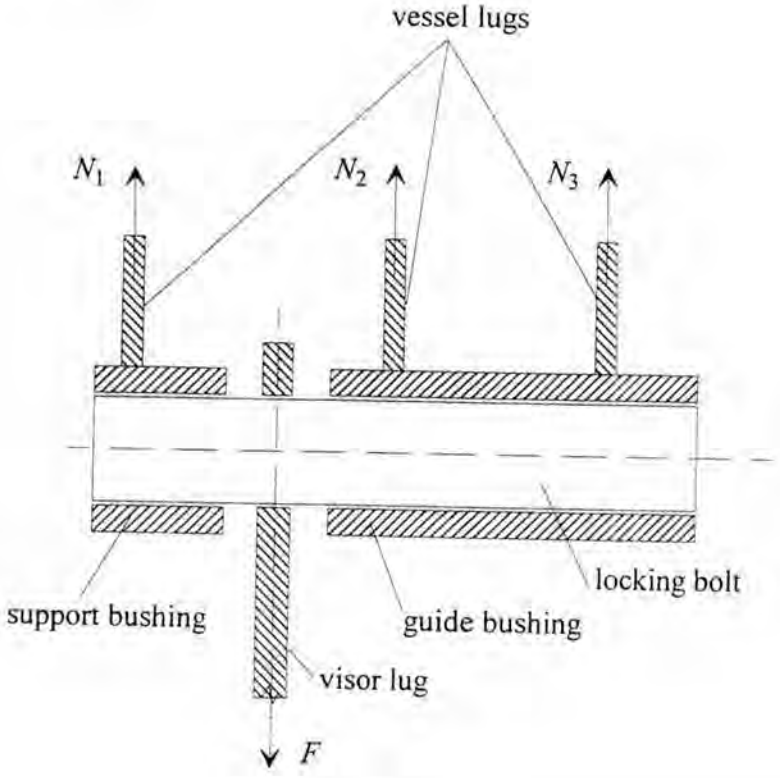

Figure 1.

On calculations we start with the following assumptions:

1. As the bottom lock was not manufactured in the vessel, but was mounted in finished shape, then we have reason to suppose that both bushings were sufficiently co-axial, i.e., well centered and all clearances with equal magnitude, and that all the three lugs which were fixed to the vessel started to carry loads simultaneously.

2. Damage observations showed that the locking bolt was not deformed significantly during the accident. Thus, we can consider the bolt as a rigid member, and only lugs as deformable.

3. Taking into account that the deformations of lugs can be quite large (20-25 mm), and that usually weld joints can not be deformed in such extent, we start from assumptions, that the limit value of one lug consists of the contributions of the weldings at ultimate strength and the contributions of the lug at yield stress.

A. Determination of the load-carrying capacity of one lug.

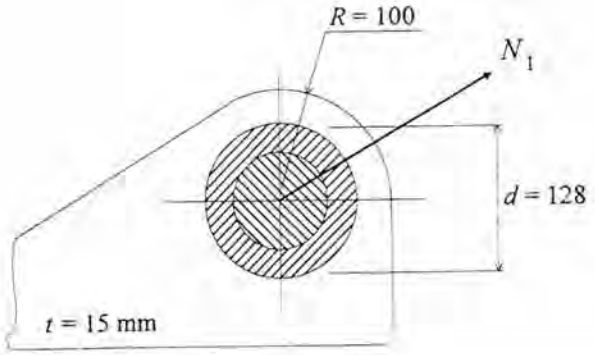

Figure 2.

Supposing that contribution of the lug N_1 is divided equally between the two halves of the lug (Figure 2), we get the contribution of the lug

$$N_{II} = 2A\sigma_y$$

where σ_y is the yield stress, and A is the failure area of one half of the loop. With σ_y=243 MPa and $A = 15 \cdot 36 = 540$ mm² we have the contribution of the lug

$$N_{II} = 0.26 \text{ MN}.$$

The contribution of the weldings between the bushing and lug consist of contributions of both side weldings in tension zone.

$$N_{Iw} = 2\tau_u 0.7k\pi d / 2$$

where τ_u=290 MPa is the ultimate shear strength of the weldments, k=3 mm is the side of weldings and d=128 mm is the diameter of the bushing. Therefore, the contribution of the weldings is

$$N_{Iw} = 0.24 \text{ MN}$$

and the total value of the load-carrying capacity of one lug is

$$N_I = 0.50 \text{ MN}$$

Investigations carried out in VTT show that the ultimate strength of the weldments were considerably higher than the ultimate strength of the plating. If we take that the ultimate strength of the weldments were two times higher than the ultimate strength of the plating, then we get

$$N_{Iw} = 0.48 \text{ MN}$$

and the total value of the load-carrying capacity of one lug is

$$N_I = 0.74 \text{ MN}$$

After the weldings are failed, the stress in lug grows up to the ultimate strength $\sigma_u = 417$MPa. The load-carrying capacity of one lug in this case is

$$N_I = 2A\sigma_u = 0.45 \text{ MPa}.$$

B. Load carrying capacity of the assembly of lock.

Forces acting on each lug can be determined using a computation scheme (Figure 3), in which bars 1 - 3 represent deformable lugs and the rigid beam represents the locking bolt.

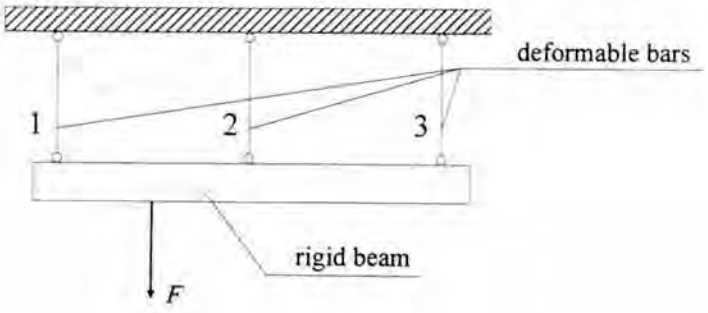

Figure 3.

By applying the force F, bars 1 - 3 will extend by quantities u_1, u_2, and u_3, and corresponding internal forces N_1, N_2, and N_3 will appear in these bars (Figure 4).

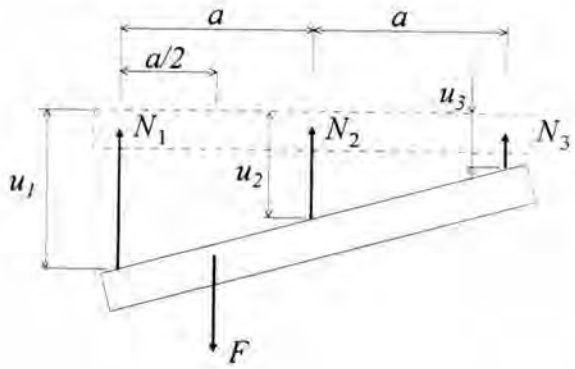

Figure 4.

Since the beam is rigid and the distance between forces N_1 and N_2 is equal to the distance between N_2 and N_3, then $u_1 - u_2 = u_2 - u_3$, and following this $N_1 - N_2 = N_2 - N_3$, or

$$N_1 - 2N_2 + N_3 = 0.$$

By adding here the equations of equilibrium,

$$N_1 + N_2 + N_3 = F,$$
$$N_2 a + N_3 2a - F\frac{a}{2} = 0,$$

we get a set of three equations, that has the following solution:

$$\mathrm{N_1} = \frac{7}{12}\mathrm{F}, \mathrm{N_2} = \frac{4}{12}\mathrm{F}, \mathrm{N_3} = \frac{1}{12}\mathrm{F}.$$

Thus we get $F = 1.71N_1$.

However, if the visor lug is not on equal distance from vessel lugs, but is closer to the separate support bushing (lug 1), then the force N_1 is even greater. In the extreme case, when the visor lug is against the support bushing, then the force holding the visor is $F = 1.53N_1$.

That kind of force distribution is valid, when the system behaves linearly. With the increase of force F the limit will be reached, from which the displacement u_1 and force N_1 will not increase proportionally. In the limit case, if the $\varepsilon - \sigma$ diagram is horizontal, only the displacement u_1 increases and the force N_1 remains constant. If the horizontal part of the $\varepsilon - \sigma$ diagram is long enough and the force F is applied at equal distance from neighboring lugs, then the displacement u_1 increases until the force N_2 reaches its limit that equals to force N_1. At the same time force N_3 decreases continuously and approaches to zero when force N_2 approaches to force N_1. In that case the force distribution is as shown in Figure 5.

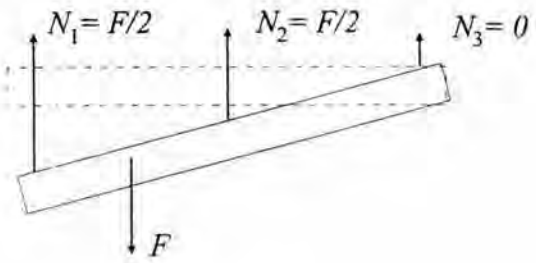

Figure 5.

It seems as the beam would have been turned over the application point of force N_3 $(u_3 = 0)$. If the visor lug is against the separate support bushing and the material of two fixing lugs is in plastic state, then $N_1 = 0.55F$ and $F = 1.83N_1$.

Thus, in case of actual $\varepsilon - \sigma$ diagram the most loaded lug is subjected to a force in the range of $N_1 = (0.65 \div 0.55)F$, and the force holding the visor is $F = (1.53 \div 1.83)N_1$.

Resulting from this in the case, if the ultimate strength of the weldments were equal to the ultimate strength of the plating, the load-carrying capacity of the atlantic lock is

F = 0.80 ... 0.90 MN.

and in the case, if the ultimate strength of the weldments were two times higher than the ultimate strength of the plating, is

F = 1.15 ... 1.35 MN.

and its moment about the axis of visor hinges $M = F \cdot l$, where the arm l=6.25 m, are respectively

M =5.0 ... 5.6 MNm, or

M =7.2 ... 8.4 MNm.

2. LOAD-CARRYING CAPACITY OF THE SIDE LOCK

The side locks are similar to the atlantic lock, but they are loaded in different directions and therefore the failure took place in another way. The visor lugs of both side locks have been torn out of the aft bulkhead of the visor, leaving rectangular holes in the bulkhead. The design of the visor lug and the aft bulkhead of the visor are presented in figure 6. The lug is welded to the plating of the bulkhead, which is reinforced by one horizontal and two vertical stringers. The failure surfaces of the side locking are shown in figure 7. Dimensions of the rectangular hole in the bulkhead plating are approximately 390 x 80 mm.

The calculations are started with the following assumptions:

1. In the bulkhead plating between the lug and vertical stringers there were shear stresses oriented both perpendicularly to the plate (vertical stringers) and along it. Because of very high stiffness of the visor lug, the first ones are taken to be linearly distributed along the failure surface. Shear stresses oriented along the plate are not very big and they are taken to be constant.

2. Because of the low bending stiffness of the bulkhead plating, the primary failure took place in the horizontal stringer. The maximum shear stress in bulkhead plating is taken to be $\alpha\tau_u$, where τ_u is the ultimate shear stress of plating material and α is the variable parameter.

3. Because of the very high longitudinal and very low transverse stiffness of the horizontal stringer only the in-plane forces of stringers are taken into account.

The load-carrying capacity of the horizontal stringer is

$$F_h = \sigma_u^h A,$$

where σ_u^h is the ultimate tensile strength of the material of the horizontal stringer, $\sigma_u^h = 476$ MPa, and A is the cross section area of the broken part of horizontal stringer, $A = 10 \cdot 80 = 800$ mm^2.

Thus we obtain

$$F_h = 0.38 \text{ MN}$$

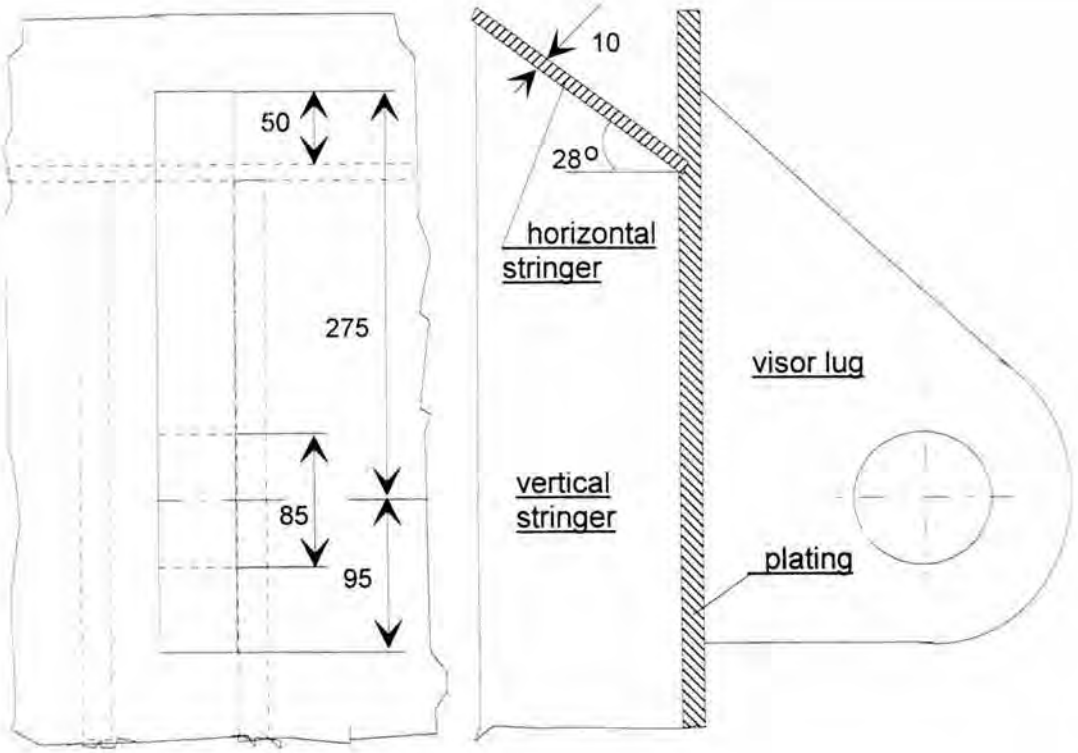

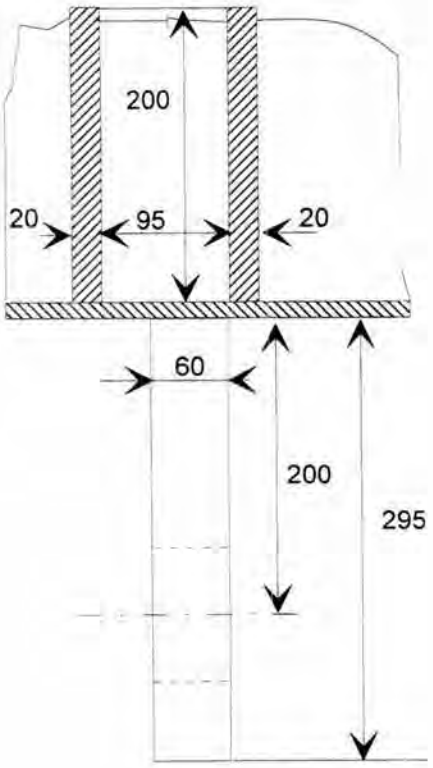

Figure 6. Design of the side locking

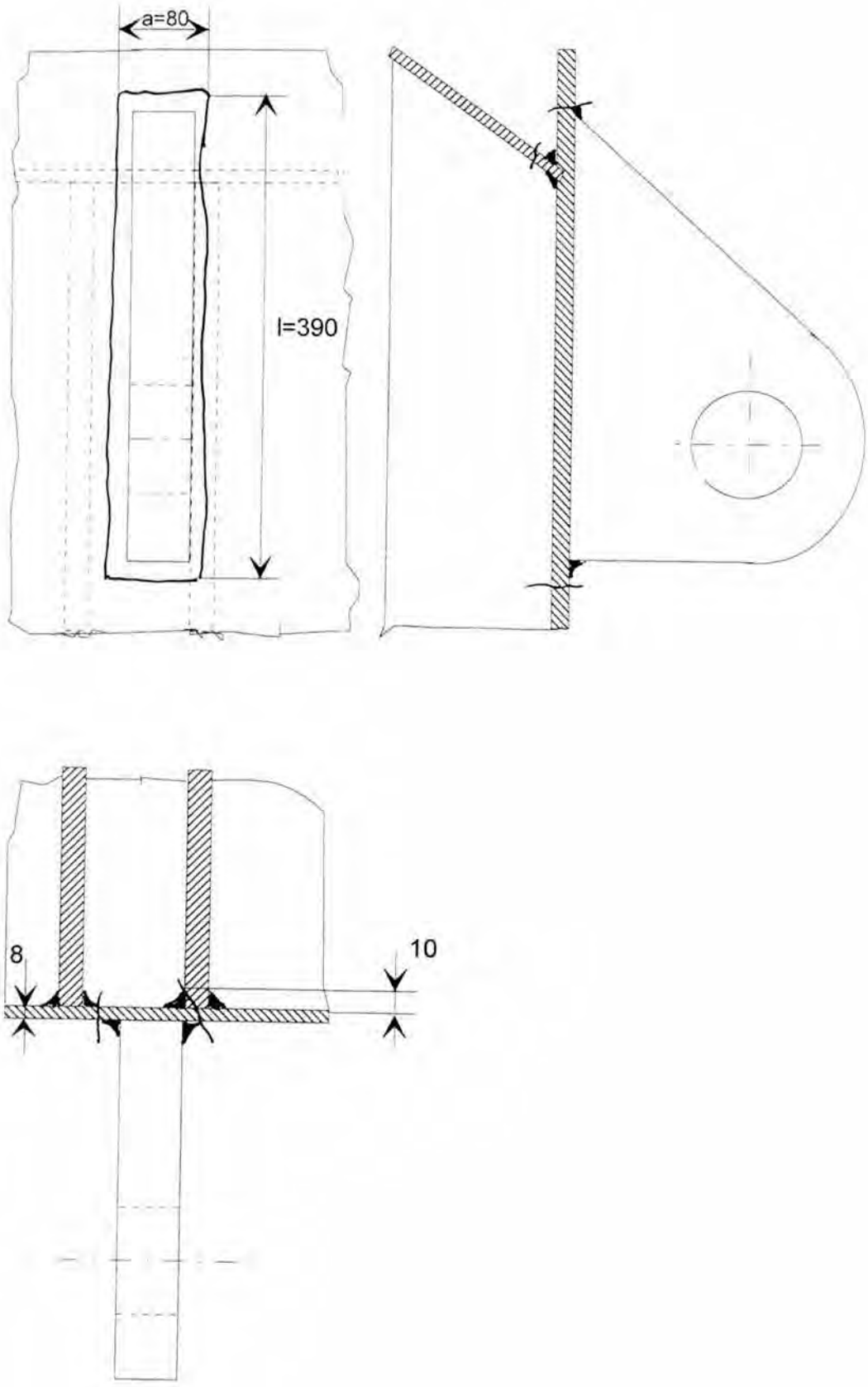

Figure 7. Failure surfaces of the side locking

The load-carrying capacity F of the side locking device can be determined from equilibrium equations of the lug, (see figure 8).

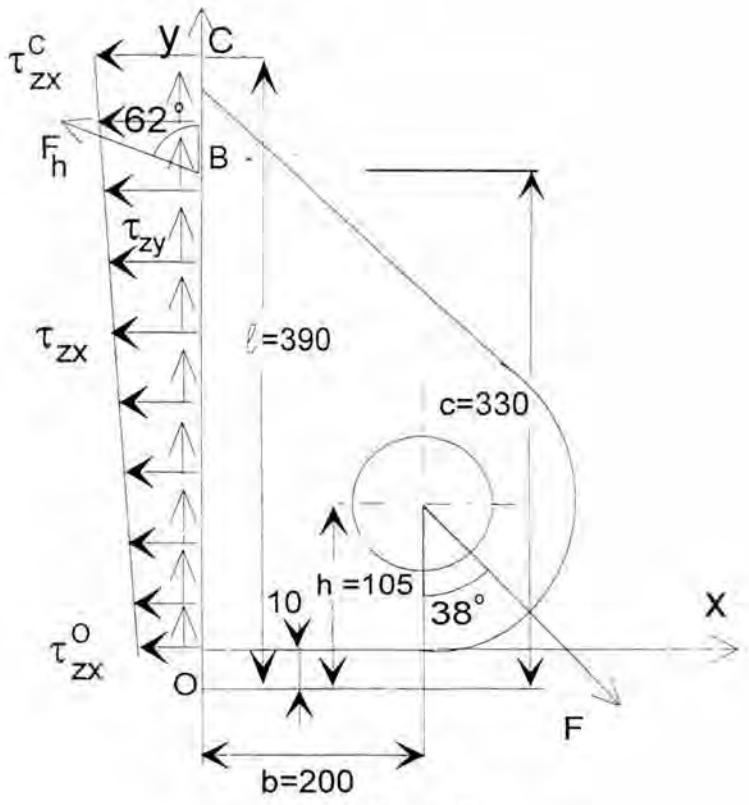

Figure 8.

$$\sum F_x = 0 \rightarrow F\sin 38^0 - F_h \sin 62^0 - \frac{1}{2}(\tau^0_{zx} + \tau^c_{zx})2\ell t_p - (\tau^0_{zx} + \tau^c_{zx})at_p - \frac{1}{2}(\tau^0_{zx} + \tau^B_{zx})ct_s = 0,$$

$$\sum F_y = 0 \rightarrow F_h \cos 62^0 - F\cos 38^0 + \tau_{zy}(2a + 2\ell)t_p + \tau_{zy}ct_s = 0,$$

$$\sum M_0 = 0 \rightarrow F_h \sin 62^0 c - F\sin 38^0 h - F\cos 38^0 b + 2\tau^0_{zx}t_p\ell\frac{\ell}{2} + 2\frac{1}{2}(\tau^C_{zx} - \tau^0_{zx})\ell t_p\frac{2\ell}{3} +$$

$$+\tau^C_{zx}at_p\ell + \tau^0_{zx}ct_s\frac{c}{2} + \frac{1}{2}(\tau^B_{zx} - \tau^0_{zx})ct_s\frac{2c}{3} = 0 \ldots\ldots \tau^B_{zx} = \tau^0_{zx} + \frac{\tau^C_{zx} - \tau^0_{zx}}{\ell}c$$

Here: τ_{zy} is a constant shear stress, $\tau^0_{zx}, \tau^B_{zx}, \tau^C_{zx}$ are values of linear shear stress in points 0, B and C respectively, dimensions ℓ, b, h are presented in Fig. 8, and further, t_p is the thickness of plating, $t_p = 8$ mm and t_s is the height of the broken part of the vertical stringer, $t_s = 10$ mm (Fig. 6), and a is the width of the rectangular failure hole in plating of the visor, a=80 mm (Fig. 7).

For getting the closed system of equations we use the strength condition in point C

$$\sqrt{(\tau^c_{zx})^2 + (\tau_{xy})^2} = \alpha\tau_u,$$

For shipbuilding steels, the ultimate shear strength assumed to be approximately 0.6 times ultimate tensile strength,

$$\tau_u = 0.6\,\sigma_u^p ,$$

where σ_u^p is the tensile ultimate strength of plating steel, $\sigma_u^p = 454$ MPa.
Thus we obtain

$$\tau_u = 272 \text{ MPa} .$$

From presented system of equations we can determine the load carrying capacity of the side locking device F, as the function of the parameter α.

α	0.1	0.2	0.3	0.4	0.5	0.6	0.7	0.8	0.9	1.0
F MN	0.55	0.69	0.83	0.97	1.10	1.23	1.36	1.49	1.62	1.75

For evaluation of the value of the parameter α we proceed from assumption that the horizontal stringer fails then, when the stress in plating grows up to yield stress. Then the parameter α is about 0.7 and the load-carrying capacity of the side lock without damages is

$$F = 1.35....1.40 \text{ MN}.$$

As the arm from the force F to the hinges axis equals a = 4.1 m, then the lifting moment is

$$M = Fa = 5.5...5.7 \text{ MNm}.$$

In these calculations we supposed that there were no cracks in structure and that the shear stresses are distributed linearly along the failure surface. By observations on the recovered bow visor we can not say with full certainty, whether the cracks in the structure existed or not. If there were cracks, then the load-carrying capacity of the side lock might have been considerably lower. As the side lock is statically undetermined complicate structure, it is difficult to say, which was the real distribution of the shear stresses and which was real value of the parameter α. The real distribution of the shear stresses before the failure may in fact have not been linear and the parameter α somewhat different. Consequently, the calculated load-carrying capacity is only the approximate value for this force. The real load carrying capacity of the side lock is probably lower.

For comparison we estimate also the load carrying capacity F of the weldments, assuming the side of the weldments k = 8 mm. For that we have three equilibrium equations of the lug in the form (see Fig. 9):

$$\sum F_x = 0 \rightarrow F\sin 38^0 - (\tau_{zx}^c + \tau_{zx}^0)0.7ka - (\tau_{zx}^c + \tau_{zx}^0)0.7kl = 0$$

$$\sum F_y = 0 \rightarrow 2\tau_{xy}(l+a)0.7k - F\cos 38^0 = 0$$

$$\sum M_0 = 0 \rightarrow \tau_{zx}^c 0.7kal + 2\left[\tau_{zx}^0 l^2/2 + (\tau_{zx}^c - \tau_{zx}^0)l^2/3\right]0.7k - F(b\cos 38^0 + h\sin 38^0) = 0.$$

The values of dimensions a, l, b, h are indicated on Fig. 9.

Adding the strength condition to failure in point C

$$\sqrt{(\tau_{zx}^c)^2 + (\tau_{zy})^2} = \tau_u.$$

we get the closed system of equations.

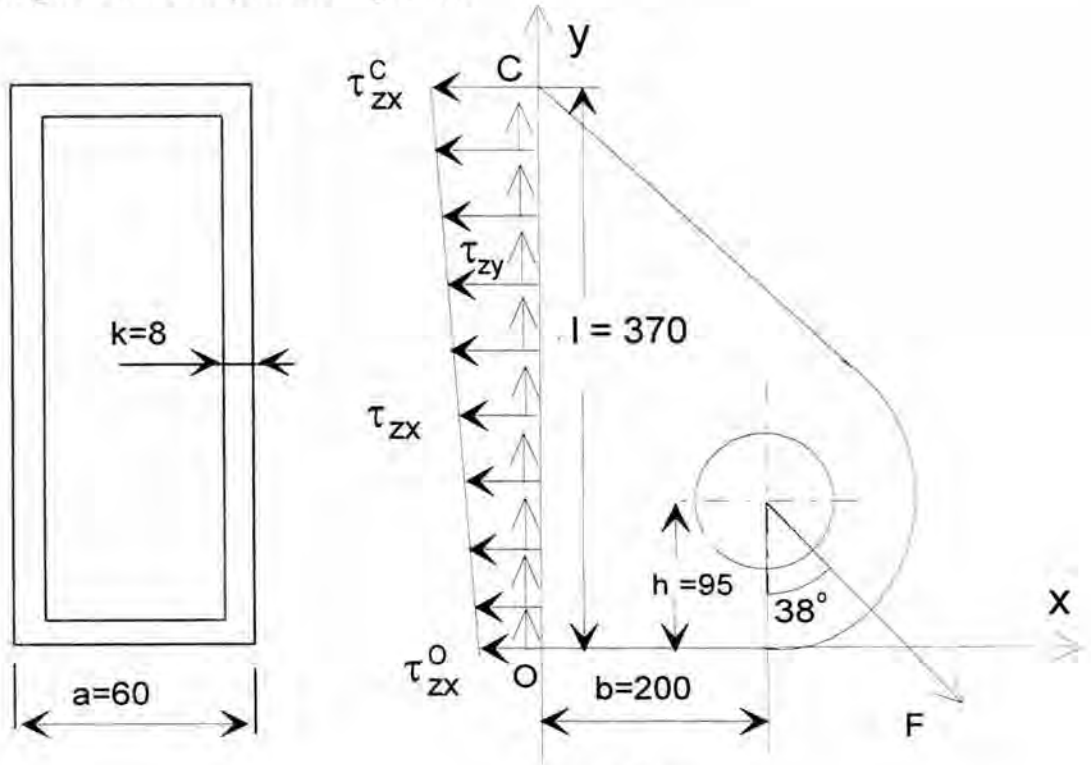

Figure 9.

Usually for weldments the value of the ultimate shear stress is assumed to be

$$\tau_u = (0.65...0.70)\sigma_u = (0.65...0.70)\cdot 454 = 295...318 \text{ MPa}$$

and the solution of the system of equations (for $\tau_u = 318$MPa) is:

F=0.741 MN; τ_{zx}^c =294 MPa; τ_{zx}^0 =-105 MPa; τ_{zy} =121 MPa.

Thus the load carrying capacity of the weldments of the side lock at k=8 mm is

F=0.7...0.75 MN.

The real ultimate strength of weldments may be considerably higher than the ultimate strength of plating. If the ultimate strength were two times higher, then the load carrying capacity of weldments would be 1.40 - 1.50 MN and if at the same time the side of weldments were a little bigger, then the load carrying capacity of weldments would be even higher. This may be the reason why the weldments really did not fail.

3. CALCULATION OF REACTIONS OF THE BOW VISOR LOCKING DEVICES.

A. Assumptions.

1. During the long life of the ship, the wear abolish differences of clearances in different locking devices and therefore all locking devices take the load simultaneously.

2. Reactions of the atlantic and side locks are directed parallel to ξ axes.

3. The displacement u between the visor and hull, caused by sea loads, are distributed linearly

$$u = u_0 + \varphi\eta - \gamma y$$

where the unknown quantities u_0, φ, γ are the displacement and the angles of rotation about axis y and η, respectively, and η, y are the coordinates (see figure 10).
4. All locking devices deform linearly, i.e.,

$$F_h = ku_h, \quad F_a = k_a u_a, \quad F_s = k_s u_s$$

where F_h, F_a, F_s are the reactions, u_h, u_a, u_s, the displacements and k, k_a, k_s the stiffness of the hinges, atlantic lock and side locks, respectively.

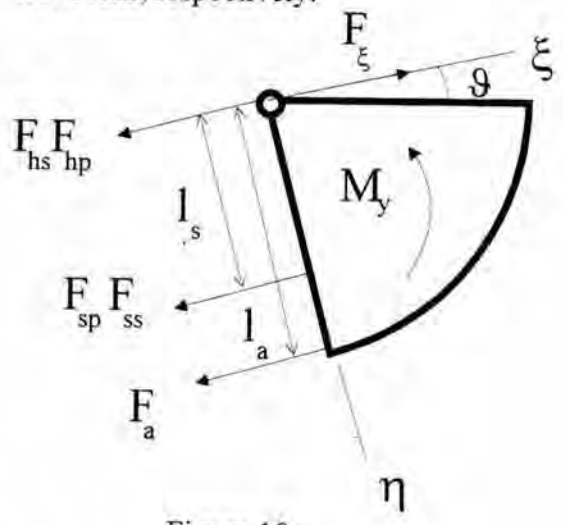

Figure 10.

B. Calculation formulae.

If we denote $\alpha = k_a / k$, $\beta = k_s / k$, then the displacements and reactions in hinges, side locks and atlantic lock will be the following:

a) in port side hinge:
$u_{hp} = u_0 + \gamma l; F_{hp} = ku_0 + k\gamma l;$

b) in starboard hinge:
$u_{hs} = u_0 - \gamma l; F_{hs} = ku_0 - k\gamma l;$

c)in port side lock:
$u_{sp} = u_0 + \gamma l + \varphi l_s;\ F_{sp} = \beta k u_0 + \beta k \gamma l + \beta k \varphi l_s;$

d) in starboard lock::
$u_{ss} = u_0 - \gamma l + \varphi l_s;\ F_{ss} = \beta k u_0 - \beta k \gamma l + \beta k \varphi l_s$

e) in atlantic lock:
$u_a = u_0 - \gamma y_a + \varphi l_a;\ F_a = \alpha k u_0 - \alpha k \gamma y_a + \alpha k \varphi l_a.$

Here 2l is the distance between the hinges and side locks, l = 3.40 m, the distances from hinge axis (y-axis) to atlantic and side locks are $l_a = 6.25$m, $l_s = 4.10$m, respectively, and the transverse distance to atlantic lock is y_a=0.4 m.
For finding three unknown parameters $ku_0, k\gamma, k\varphi$ we have three equations of the visor equilibrium :

$$F_{hp} + F_{hs} + F_{sp} + F_{ss} + F_a = F_\xi$$
$$F_{sp}l_s + F_{ss}l_s + F_a l_a = M_y^*.$$
$$F_{hp}l - F_{hs}l + F_{sp}l - F_{ss}l - F_a y_a = M_\eta$$

where,

$$F_\xi = F_x \cos\vartheta - (F_z + W)\sin\vartheta,$$
$$M_y^* = M_y - M_W$$
$$M_\eta = M_z \cos\vartheta + M_x \sin\vartheta$$

Here: $\vartheta = 15^0$ is the angle between axes x and ξ, quantities F_x, F_z, M_x, M_y, M_z are the sea load components and $W = 0.55$MN, $M_W = 2.0$MNm are the weight of the visor and its moment about y axis.

From this equations we get:

$$(2 + 2\beta + \alpha)ku_0 + (2\beta l_s + \alpha l_a)k\varphi - (\alpha y_a)k\gamma = F_\xi,$$
$$(2\beta l_s + \alpha l_a)ku_0 + (2\beta l^2{}_s + \alpha l^2{}_a)k\varphi - (\alpha y_a l_a)k\gamma = M_y^*,$$
$$-(\alpha y_a)ku_0 - (\alpha l_a y_a)k\varphi + \left[2(1+\beta)l^2 + \alpha y_a^2\right]k\gamma = M_\eta.$$

If the port side lock is failed then the equations take a from:

$$F_{hp} + F_{hs} + F_{ss} + F_a = F_\xi$$
$$F_{ss}l_s + F_a l_a = M_y^*$$
$$F_{hp}l - F_{hs}l - F_{ss}l - F_a y_a = M_\eta.$$

Thus for determination unknown parameters $ku_0, k\gamma, k\varphi$ we have three equations:

$$(2 + \alpha + \beta)ku_0 + (\alpha l_a + \beta l_s)k\varphi - (\beta l + \alpha y_a)k\gamma = F_\xi$$
$$(\alpha l_a + \beta l_s)ku_0 + (\alpha l_a^2 + \beta l_s^2)k\varphi - (\beta l l_s + \alpha y_a l_a)k\gamma = M_y^*$$
$$-(\beta l + \alpha y_a)ku_0 - (\beta l l_s + \alpha y_a l_a)k\varphi + \left[(2+\beta)l^2 + \alpha y_a^2\right]k\gamma = M_\eta$$

C. The results.
The calculated reactions of atlantic and side locks F_a, F_{sp}, F_{ss} and full reactions of hinges R_{hp}, R_{hs}, which are directed forward and down, are presented in Figure 11 and 12 as function of stiffness ratio k_s / k_a for five different stiffness ratio values k / k_a in two different combinations of sea loads. The results are presented in two cases: a) if all locking devices are in order (above);

$F_x = -6.3MN, F_z = -6.3MN, M_x = 7.4MNm, M_y = 20.0MNm, M_z = 2.5MNm.$

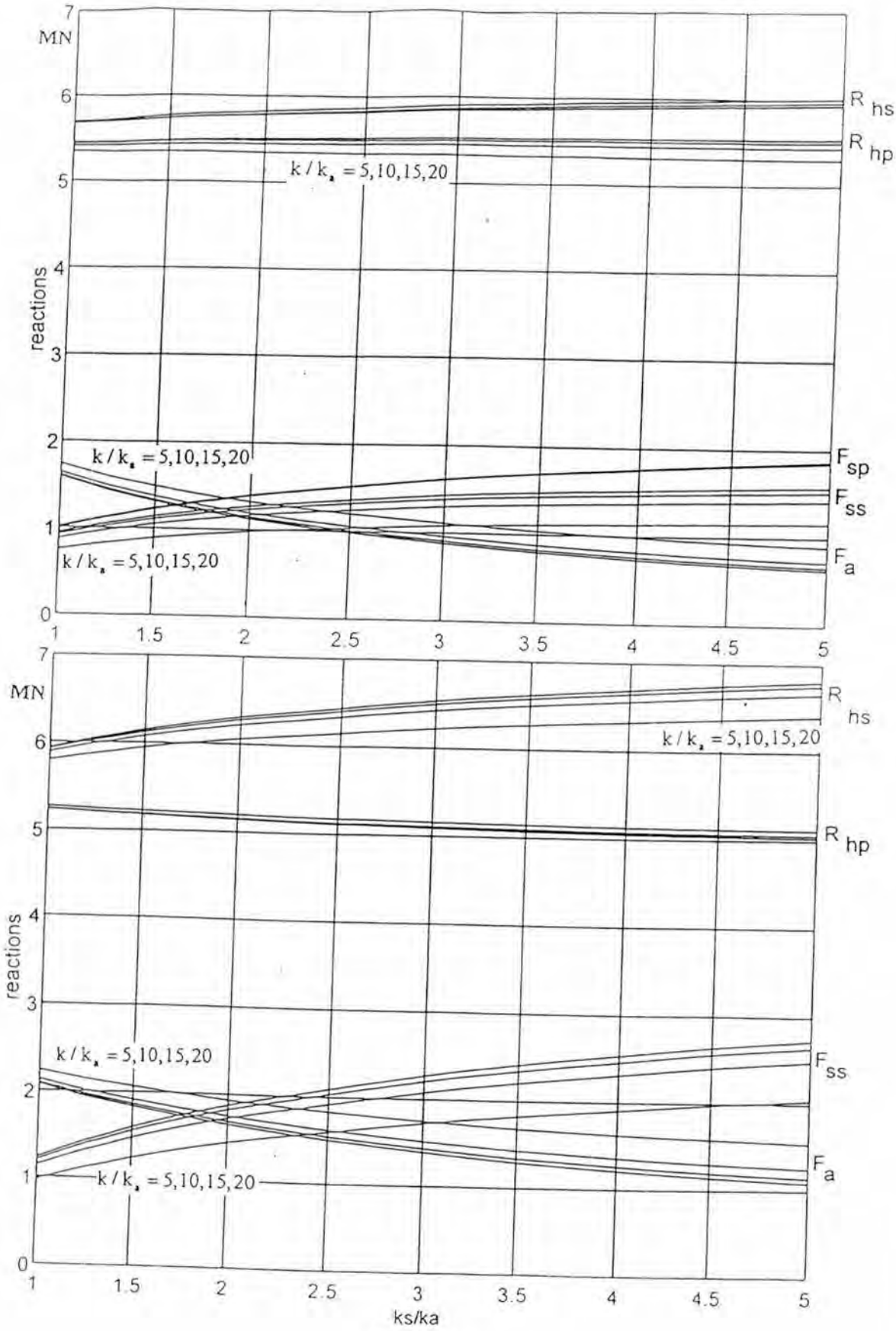

Figure 11.

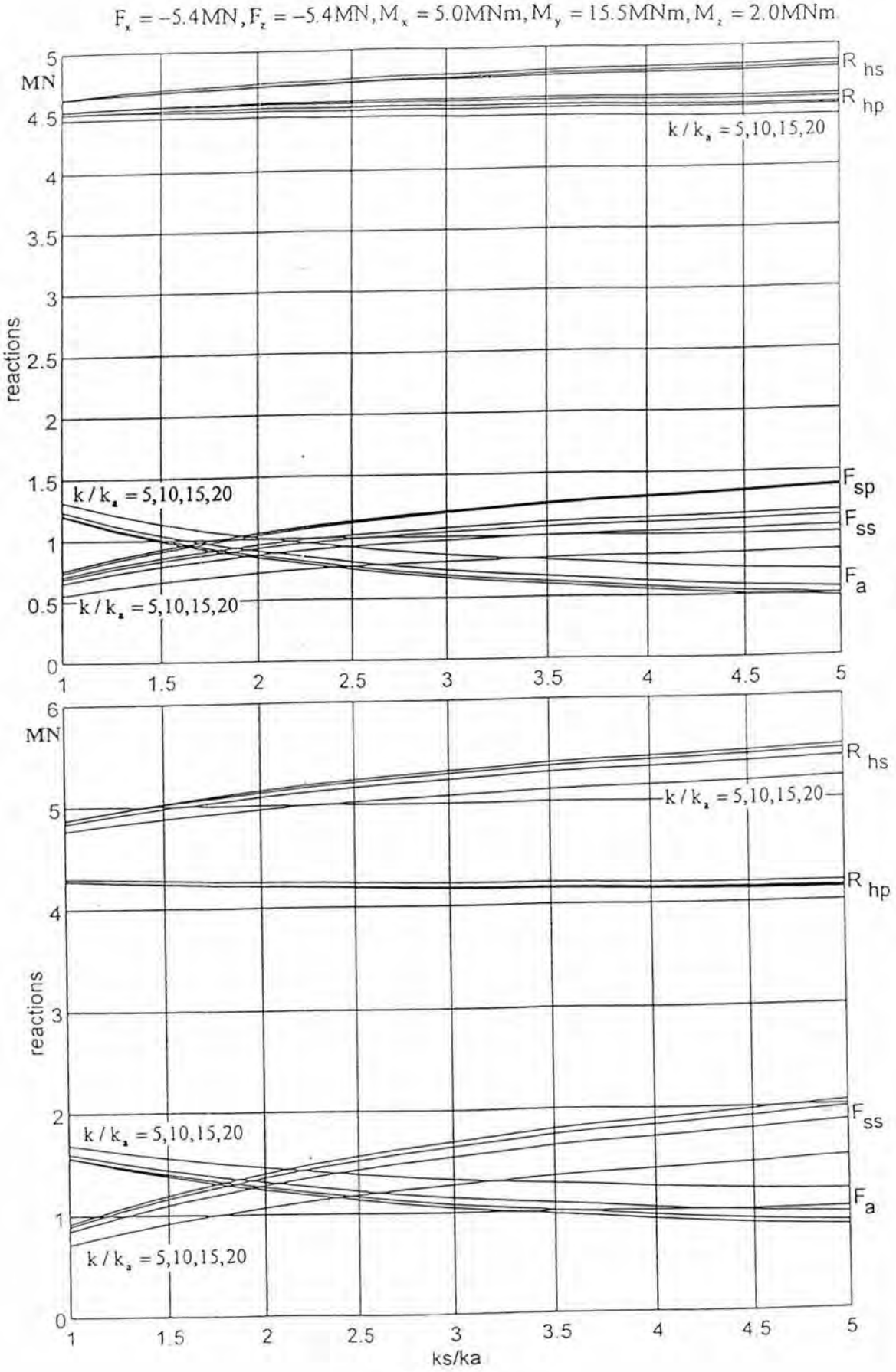
$F_x = -5.4MN, F_z = -5.4MN, M_x = 5.0MNm, M_y = 15.5MNm, M_z = 2.0MNm$
MN
reactions
R_{hs}
R_{hp}
$k/k_a = 5,10,15,20$
F_{sp}
F_{ss}
F_a
$k/k_a = 5,10,15,20$
$k/k_a = 5,10,15,20$
MN
reactions
R_{hs}
$k/k_a = 5,10,15,20$
R_{hp}
F_{ss}
$k/k_a = 5,10,15,20$
F_a
$k/k_a = 5,10,15,20$
ks/ka

Figure 12.

SUPPLEMENT No. 507

Ingerma A. - Strizhak V.: The Strength Studies for the Locking Devices of the Bow Visor of M/V ESTONIA.

Estonian Maritime Academy & Tallinn Technical University.

Tallinn 1997.

THE STRENGTH STUDIES FOR THE LOCKING DEVICES OF THE BOW VISOR OF MV ESTONIA

A.INGERMA
V.STRIZHAK

ESTONIAN MARITIME ACADEMY
TALLINN TECHNICAL UNIVERSITY

1997

CONTENTS

AN ANALYSIS OF THE CALCULATION METHODS OF THE LOAD CARRYING CAPACITY OF THE LOCKING DEVICES OF THE BOW VISOR OF MV ESTONIA

1. INTRODUCTION

In the fifteenth chapter of the Final Report of the Joint Accident Investigation Commission of MV ESTONIA the calculations by the experts M. Huss, K. Rahka and J. Metsaveer on the load carrying capacity and the breaking force of the locking devices of the bow visor have been presented.. The forces affecting the bow visor are viewed as static.

The objective of this study is to present the calculations of the safe load carrying capacity and the failure force of the locking devices from a mechanics engineer's/designer's point of view.

2. LOADS AFFECTING THE BOW VISOR

2.1 The nature of the loads

The loads affecting the bow visor are mostly caused by sea loads. Besides sea forces the locking devices of the bow visor are affected by the vibration of the ship's engine and by the rolling and pitching of the vessel at sea, even when the sea loads are not directly affecting the bow visor. Both the sea load and the other loads are cyclic by nature. The cyclic nature and magnitude of the sea forces is not directly determinable and the distribution shown on Fig. 1, straight line A [1] can be used in practice.

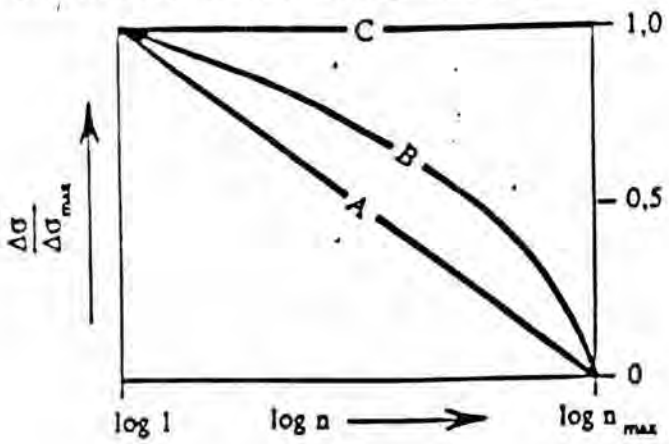

Fig. 1

where $\Delta\sigma$ — applied stress range (σ_{max}-σ_{min})
$\Delta\sigma_{max}$ — applied peak stress range within a stress range spectrum
n — the number of applied stress cycles

A: straight-line spectrum (typical stress range spectrum of seaway-induced stress ranges)

B: parabolic spectrum (approximated normal distribution of stress range $\Delta\sigma$);

C: rectangular spectrum (constant stress range within the whole spectrum; typical spectrum of engine- or propeller-excited stress range).

The theoretical calculations [3, 4] and model simulations [5] and the measurements of the pressure of sea forces on the bow visor [6] contribute to the statement that there exists alternating cyclic load from sea forces to the bow visor.

The study [4] presents a possible distribution of load on the bow visor of MV ESTONIA one hour before the accident.

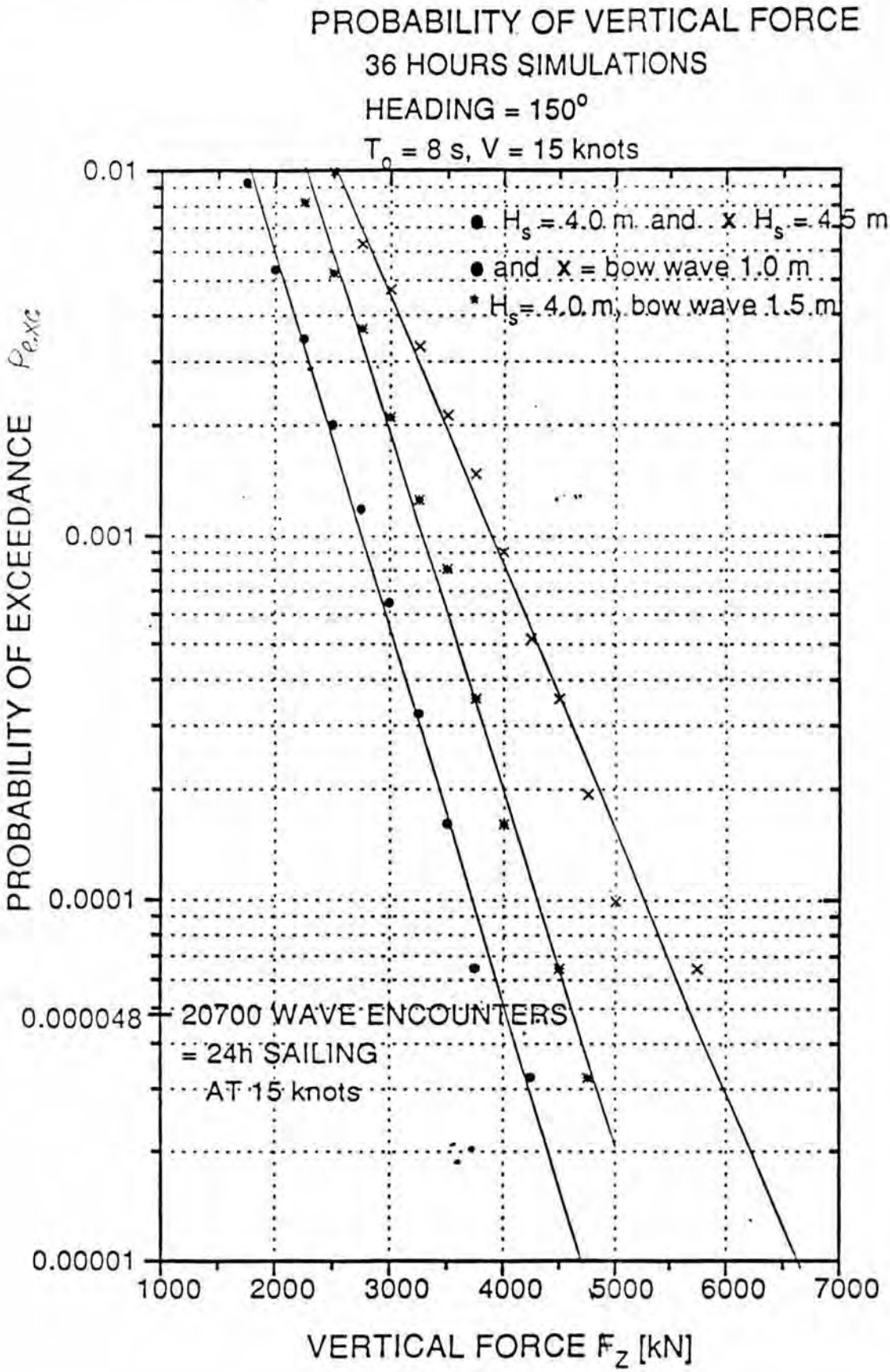

Fig. 5.8 Vertical wave loads on the visor in bow oblique seas with H_S = 4 m and 4.5 m.

VTT VALMISTUSTEKNIIKKA
Laiva- ja konetekniikka
VTT MANUFACTURING TECHNOLOGY
Maritime Technology
P.O. Box 1705
FIN-02044 VTT
FINLAND
Tel.int.+358 0 4561
Telefax +358 0 455 0619
Telex 122972 vtths sf

Fig. 2.A

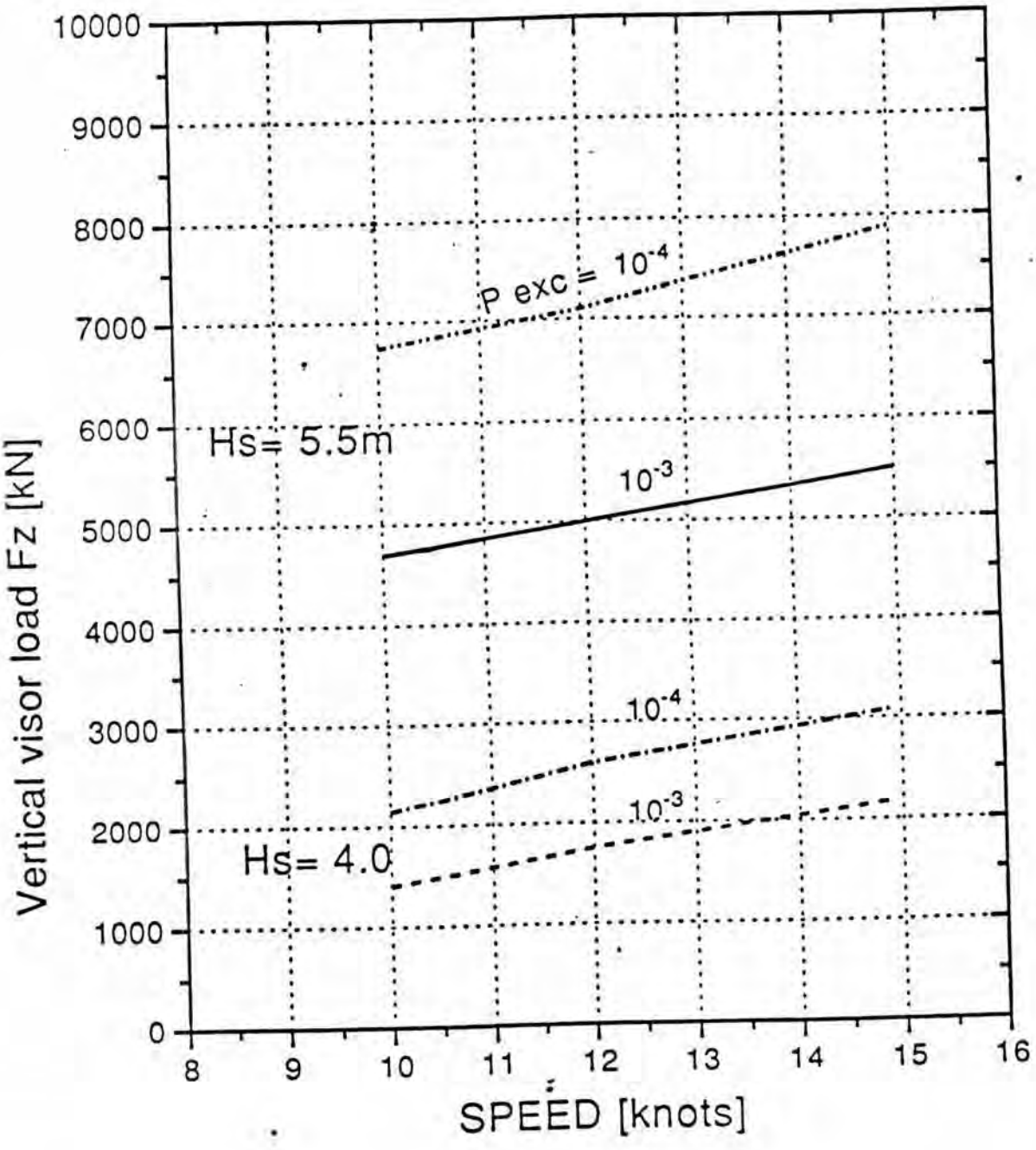

Fig. 5.9 The effect of wave height and speed on the loads of MV Estonia's visor in head seas.

Fig. 2 B

SSPA MODEL EXPERIMENTS

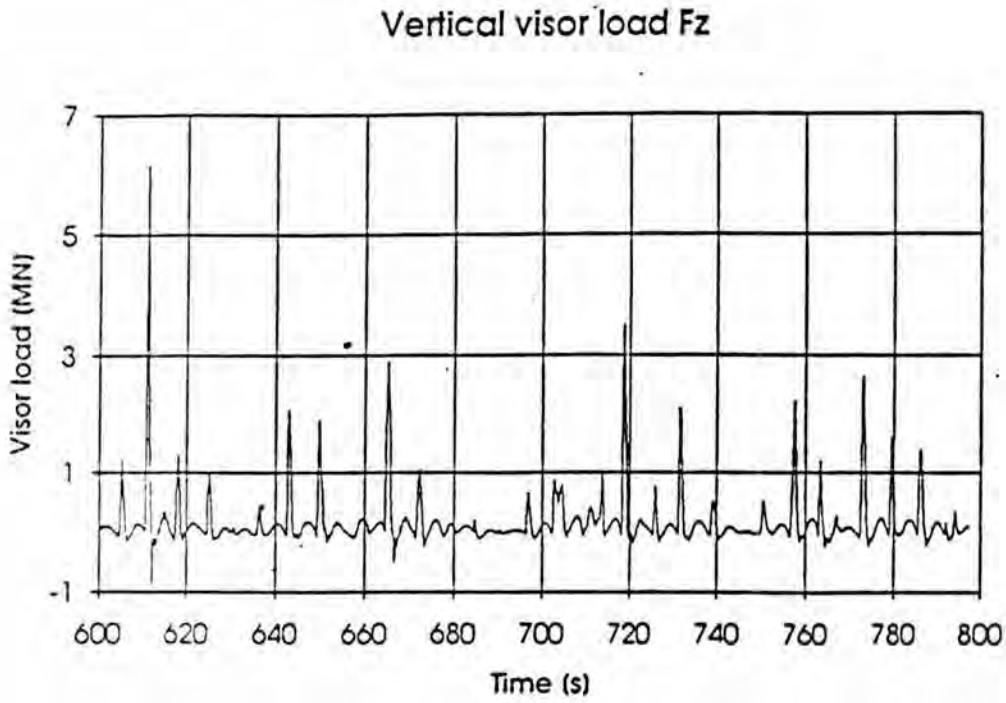

VTT SIMULATIONS

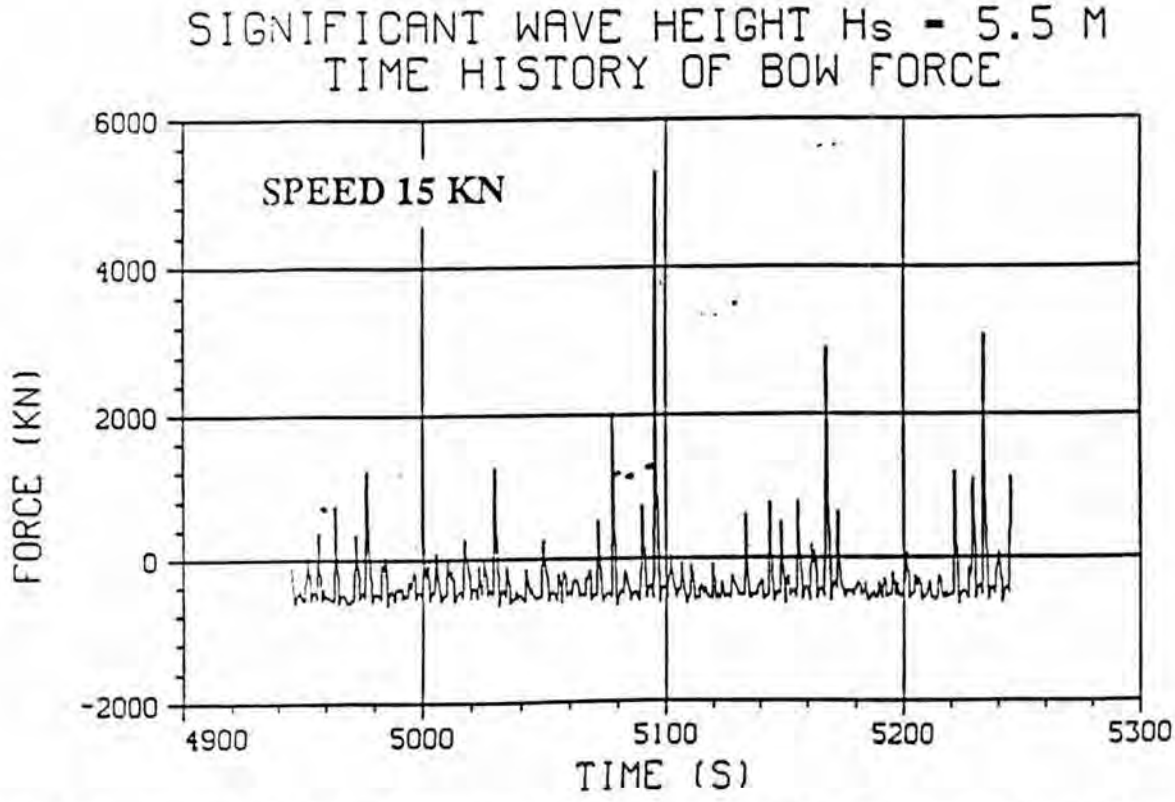

Fig. 5.10 Experimental (SSPA) and simulated records of visor loads in head seas, Hs = 5.5.

TURBO
TECHNIK
Reparatur-Werft Dassler KG

7

Inspection Report

Vessel: M/S "DIANA II"
Order-No.: 1.293-94
Port: Warnemünde
Date: 03.10.94
Subject: Bow hatch and car ramps

Inspection of bow hatch:

On deck side a crack test by "Dye-check" method was carried out on all welding areas of hatch hinge, therefore it was necessary to remove all paint etc., this cleaning was carried out by crew.

The result of crack test was good, no cracks visible.

On the hatch securing device for open position we found some welding seams on foundation of hydraulic lock bolts. This welding was possibly carried out in an emergency after damaging of bolts-foundation by collide of bolts in lock position with hatch securing eye pads.

As the second point of inspection we checked the three hatch securing-locking devices. We found them in the following condition:

The stb lockbolt shows about 20 mm clearance to the eye pad hole in fwd direction with good contact of bolt-eye pad in close position of hatch.

The portside lockbolt shows a clearance of about 40 mm to the eye pad hole in aft direction with the consequence that a movement of hatch is possible.

The center locking device is in the same condition as the port device with a clearance of about 35 mm in aft direction.

All three eye pads were welded on again, maybe after having been cut off by opening of hatch with hydraulic force by locked bolts.

As a third point we found three hydraulic cylinders with eyes welded on, two on fwd car ramp and one on port aft car ramp.

On the open portside aft car ramp it was possible to check the clearance of ramp hinge. We found most of the bolts with high clearance to the eye pads.

Comment:

On the whole we do not consider it save to run the vessel under this condition.

Wilhelmshaven, 05.10.94

TURBO-TECHNIK
REPARATUR - WERFT
Dassler KG

i.A.

M. Gronewold

Fig. 4

ESTONIA

SB visir Lösning
93 01 16 DIANA II

SB visir Lösning
93 01 16 DIANA II

Fig. 6

Fig 5

Bureau Veritas MARINE BRANCH

DETAILED REPORT OF SURVEY

Annex No B to Report No. HBG/93/7-A Page No 1 Total Pages 1

Register Number 35.V.002 Name of Ship "DIANA II" (one square only to be ticked off)

Cert. concerned PROV HULL X MACH AUT MS AB RMCI

Visa No endorsed 7 or survey of C.S. or O.S. items (continuation to AdE 2528).

Survey carried out from 16/01/93 to 17/01/93

REPORT OF SURVEY

On request by the Chief Engineer survey of the closing devices for the bow door carried out and following damages were found on the bow door.

The lug for SB lock plunges was lost.

The lug in center line (the "Atlantic lock") was bent and the weld cracked.

The lug for Port side lock plunges was bent and the weld cracked.

A minor crack at the hinge on SB side.

The girder in center line and two webs on SB side cracked.

Following repairs carried out:
The lug SB side renewed with a doubling plate on the back side.

The lug in center line faired and rewelded. The stay above the lug renewed.

The lug Port side faired and the crack chiselled and welded.

The crack at SB hinge chiselled and welded.

The cracks at the girder and the webs chiselled and welded.

Function test of the bow door carried out and found to be in order.

BUREAU VERITAS EXPERT. DE GÖTEBORG PARIS 1828 REGISTRE INTERNATIONAL

new name

Mar Balticum

Fig. 7

The significant wave height is 4 and 4.5 m and during the last hour the ship was affected by approximately 1000 waves and the possible occurrence frequency of the greatest vertical force was 1/1000 and the greatest vertical sea force has been estimated to be 5000 kN or less probably 6000 kN, as shown on Fig. 2 [4].

The theoretical calculations [4] and model simulations [5] are in agreement and have been presented on Fig. 3 [4].

In case of waves of lesser magnitude the forces affecting the bow visor are also smaller and directed towards the closing direction of the bow visor. Actually, however, the number of the affecting cycles is significantly greater.

The existence of the cyclic loads is confirmed by the inspection of the locking devices of MV DIANA II on 30. 10. 94 [7], i.e. one week after the accident of MV ESTONIA (Fig. 4).

During the inspection the following clearances were measured between the locking bolt and the eye.

The Atlantic lock — 35 mm, aft direction
stb side lock — 20 mm, fwd direction
portside side lock — 40 mm, aft direction

Such increases in clearances occur during operation **only due to alternating cyclic loads**.

The differences in the amounts and directions of the wear indicate that:

1. The distribution of loads on the locking devices is not uniform. The distribution of loads cannot be determined as the entire locking installation is not statically determined.
2. Some of the welds of the locking devices (being sensitive to cyclic loads) are subject to pressure and some to tension.

The wear of the eye in the aft direction indicates the effect of the sea forces in the direction of the opening of the bow visor and the expansion in the forward direction indicates the effect in the closing direction of the bow visor.

The existence of alternating cyclic load is also proven by the fact that the lug of the Atlantic lock of the bow visor of MV ESTONIA has hammered eyes on both sides (3.7 and 4.3 mm) in fwd direction. Hammered eyes can only be caused by a great number of impacts between the bolt and the lug (Fig. 5).

The existence of the alternating cyclic loads is also confirmed by the damages to the locking devices of MV DIANA II 16. 01. 93 (Figs. 6 and 7).

The lug of the stb side lock has been torn out of the plating of the bow visor and the portside lock was bent and the weld cracked. The photos

show a darkening of the paint at the upper edge of the left side lock, caused by corrosion. Corrosion occurs in the proximity of cracks. Consequently, there is a crack in the weld joint, which has been caused by cyclic load. As shown later, the upper edge of the side lock is under greater load and the first crack appears there.

The analogous failures of locking devices on RO-RO passenger ferries operating on the Baltic Sea indicate the existence of alternating cyclical loads and clearances between the locking bolts and the eyes. The clearances increase during operation accompanied by an increase in the lack of uniformity in the distribution of the loads, causing the failure of the lock. The incomplete lists include 8 marine accidents involving Finnish and Swedish RO-RO vessels (mainly passenger ferries) during the years 1973-1993 that were due to the damage to the locking devices of their bow visors. Four accidents occurred within a year after the construction. The conclusion to be drawn from this is that the locking system with clearances used in Scandinavia (one bottom lock/Atlantic lock and two side locks) is underdimensioned and poorly designed due to the clearances, sooner or later resulting in damage or maritime accident.

RO-RO ships built in the former USSR (years 1975 and later) have a clearance-free locking system — forced locking (a power screw and a nut). The total number of locking devices is 14, 10 of these bottom locks and 4 side locks. There have been no reports on the failure of these locking devices. The Estonian Shipping Company has 4 ships of this kind and they are operated for 20...22 years.

Conclusion.

1. The forces affecting the locking devices of the bow visor (sea forces, vibration and forces caused by the rolling and pitching of the vessel) are alternating and cyclic by nature.
2. These forces vary significantly both in extent and direction and cause different stresses (tension-pressure, bending, shear) in the components of the locking devices.
3. All the locking devices have components with weld joints which are especially sensitive to alternating cyclic loads.
4. **The cyclic nature of the loads calls for fatigue calculations when calculating the strength of the components of the locking devices.**
5. As the number of operative cycles and the magnitude of the operative forces are undeterminable, the strength calculations have to be performed for fatigue and the minimal allowable stresses should be used, providing for larger safety factors.

3. ALLOWABLE STRESSES

The main type of steel used in shipbuilding is St 37 — a mild carbon steel with good welding characteristics.
The main characteristics of this steel are the following:

ultimate stress $\sigma_u = 340 \div 470$ N/mm^2,
yield strength $\sigma_y = 235$ N/mm^2,
relative lengthening $A_s = 22\%$.

Allowable stresses are affected by the situation of the applied loads and should therefore be discussed separately.
The Bureau Veritas rules from 1977 [8] do not directly determine the allowable stresses of the attachments of the locking devices of the bow visor, but such stresses have been determined for the attachments of moving platforms.
As moving platforms, ramp and bow visor are all operating in difficult conditions, the allowable stresses valid for the attachments of the moving platforms can be used for the calculations for the attatchments of the locking devices of the bow visor.
The 1977 rules by Bureau Veritas set the minimum safety factor at 5.
The components of the locking devices must be based on direct calculations and the following allowable stresses must be used:

bending stresses $\sigma \le 85$ N/mm^2,
shear stresses $\tau \le 42$ N/mm^2,
combined stresses $\sigma_c = \sqrt{\sigma^2 + 3\tau^2} \le 112$ N/mm^2.

The 1987 and 1996 Bureau Veritas rules directly specify the following allowable stresses for the locking devices of the bow visor:

bending stresses $\sigma \le 120/k$ N/mm^2,
shear stresses $\tau \le 80/k$ N/mm^2,
combined stresses $\sigma_c = \sqrt{\sigma^2 + 3\tau^2} \le 150/k$ N/mm^2.

The material factor k is determined by the yield point of the steel and equals

σ_y	k
235	1
263	0.91
315	0.78
355	0.72
390	0.66

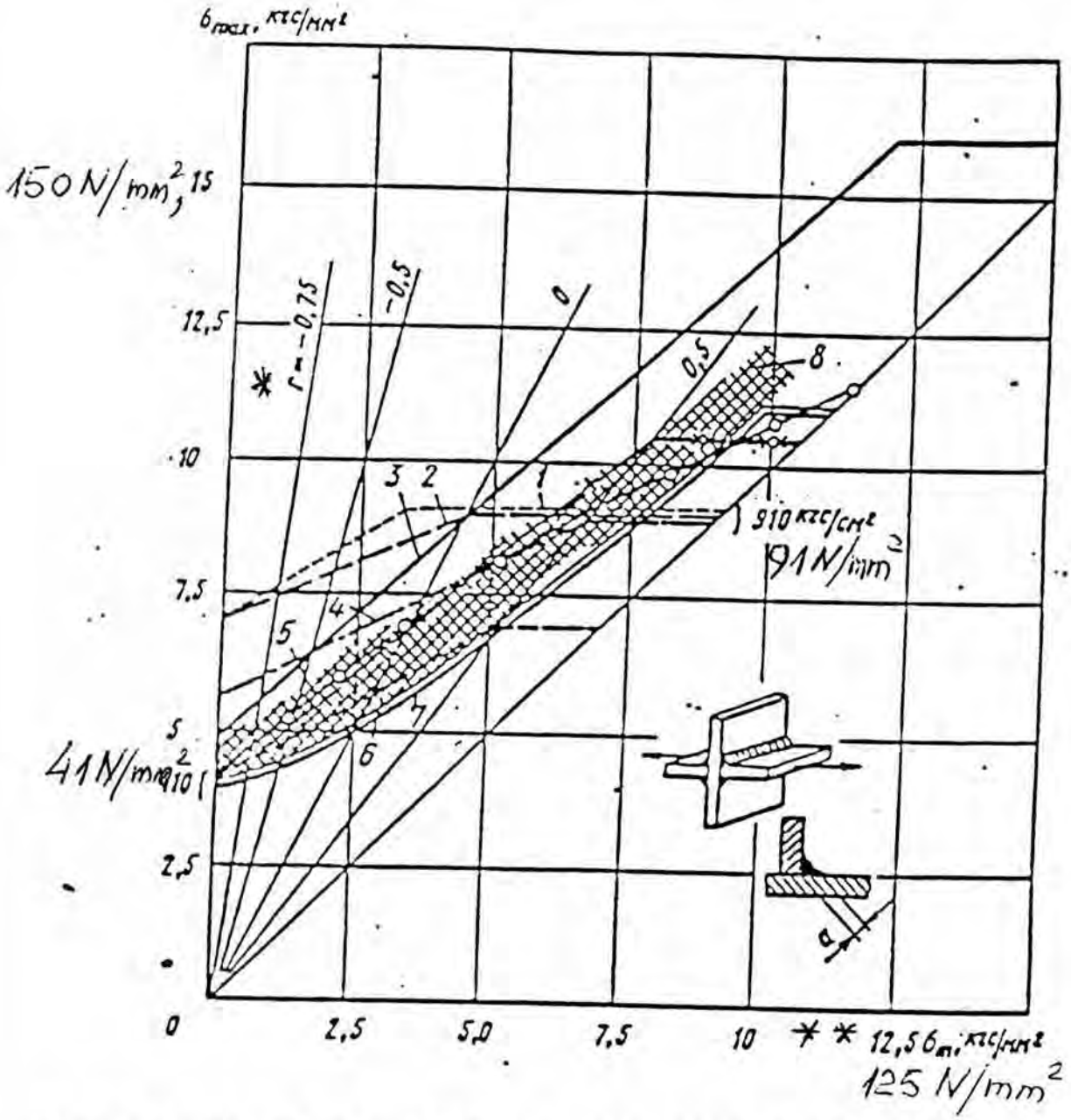

The permitted stress for unprocessesed T-weld joint of CT3 type steels (C~0,15) from different sources [10]

1. Poland
2. East Germany
3. West Germany
4. Czekhoslovakia
5. Austria
6. Switzerland
7. USSR
8. Fatigue limits

Fig. 8

* $r = \frac{\sigma_{min}}{\sigma_{max}}$

** $\sigma_m = \frac{\sigma_{max} + \sigma_{min}}{2}$

The latter allowable stresses are the same as stated by in the rules of the Germanischer Lloyd [1]. In the same source allowable stresses for statically loaded weld joints have been provided. For a steel with a yield point of $\sigma_y = 235$ N/mm^2 the allowable shear stress is $\tau \leq 115$ N/mm^2.

The allowable stresses for fillet(T) weld joints for Cm3 steel (C ~ 0.15%) according to various sources is τ=41÷91 N/mm^2 (Fig. 8 [9])

For alternating cyclic loads the allowable fatigue shear stresses for a fillet(T)-weld are in the range $\tau = 35 \div 50$ N/mm^2 [1].

As the shipbuilder has not determined the lifespan of the locking devices and the magnitudes, directions and working cycles of the loads affecting the locking devices are unknown, the only solution is to use the fatigue strength necessary to ensure the safe operation of the devices for the calculations.

Conclusions

1. The allowable stresses for weld joints according to different sources are in the range of $\tau = 35 \div 90$ N/mm^2.
2. The allowable stresses for bending (tension) are in the range $\sigma = 85 \div 120$ N/mm^2.
3. The fatigue strength calculations should be the basis for design.
4. **If the operational loads are greater than the fatigue limit, the breaking of the device is inevitable.**

4. THE CALCULATION OF THE LOAD CARRYING CAPACITY OF THE LOCKING DEVICES OF THE BOW VISOR

4.1. Introduction

The objective of this chapter is to calculate the load carrying capacities and the breaking forces of the locking devices of the bow visor. Methods of engineering calculations which are recognized world-wide are used in these calculations.
The bow visor was attached to the vessel with three locking devices and pivoted around two hinges on the deck for opening and closing the visor. Thus there are five attachment points which form a statically undeterminable system. Therefore it is impossible to directly calculate the

forces affecting the locking devices. In the calculations provided by the shipyard the general load of 5000 kN (500 tons) is distributed equally (1000 kN) over the five attachment points.
The drawings provided by shipyard and by the company designing the locking devices (von Tell) are assembly drawings and they lack the dimensions of the attachments to the bow visor and to the hull. The drawings lack symbols and characteristics for welds. Some examples of the drawings by the shipbuilder (Fig. 9) and by von Tell (Figs. 10, 11) have nevertheless been included.
The bow visor was secured by a bottom lock (the Atlantic lock) and two side locks. All the three lock are of similar bolt-bushing construction. To enable the pivoting of the bow visor, there were two hinges on the deck. The calculations of the load carrying capacities and breaking forces of the bottom lock, side lock and the hinges are presented below.

4.2 The strength calculation of the bottom lock

The bottom lock is shown in Fig. 12.
The bottom locking device consists of a locking bolt 5, movable horizontally in a transverse direction guided by a bolt housing 2. In its extended (closed) position the tip of the bolt is engaged in the support bushing 1. The bolt housing was fixed to the forepeak deck by two steel lugs (II and III) and the support bushing was secured with a third similar lug (I). A mating lug 3, which is between the bolt housing 2 and support bushing 1, is attached to the visor itself. When the visor is in a closed position, the extended bolt 5 engaged the mating lug 3 and the support bushing 1.
The bolt 5 was moved in the bushings 1 and 2 by a hydraulic actuator.
The lug of the bow visor 3 was secured to the transverse beams of the bottom structure of the bow visor.
The lug had a hole for the locking bolt with an original diameter of 85 mm. During the operation of the vessel the diameter of the hole increased and after the shipwreck the hole was oval, the dimensions being 90 by 105 mm.
There are no detailed drawings of the locking devices, some general dimensions have been presented on the assembly drawings by von Tell, the supplier of the locking devices.
All of the three lugs of the bolt housing and the support bushing of the bottom lock are broken. The lug of the bow visor did not fail but tore apart the lugs attached to the forepeak deck (I, II, III) and was then separated.

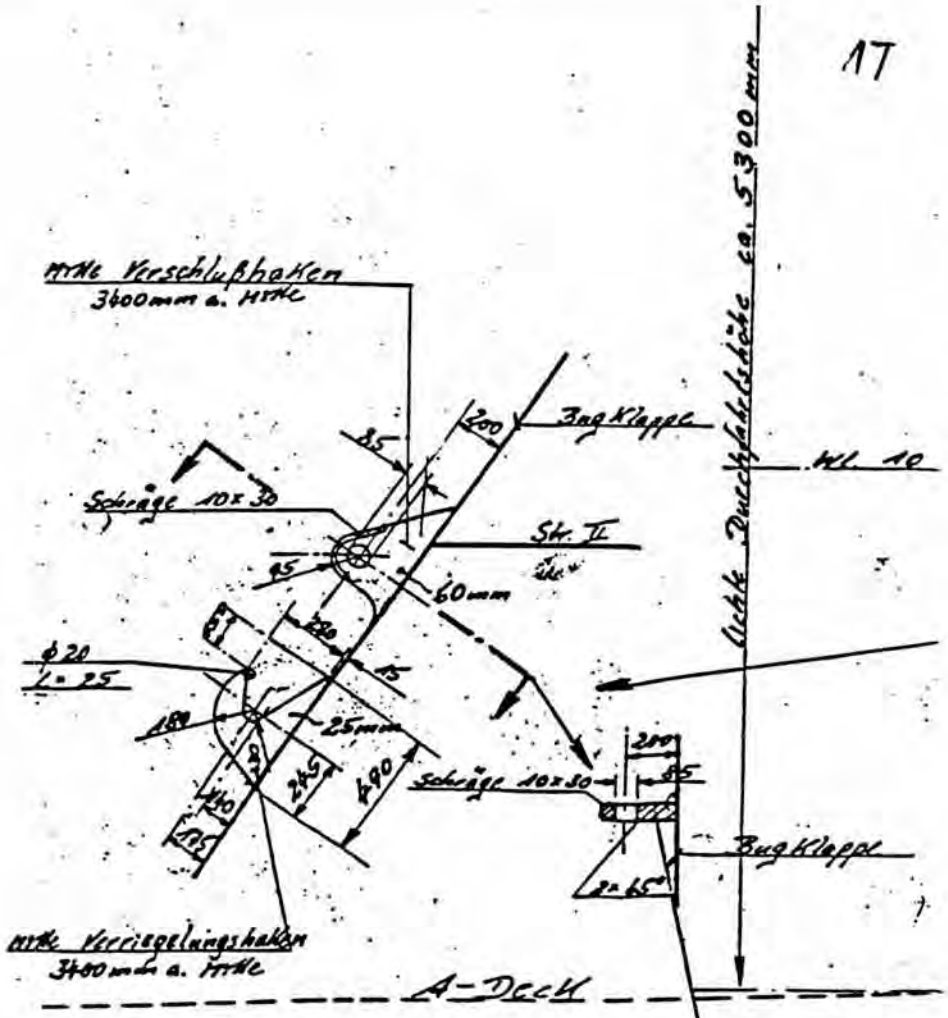
mittl. Verschlußhaken
3400mm a. mittl.
Bug Klappe
Schräge 10×30
St. II
60mm
Schräge 10×30
Bug Klappe
mittl. Verriegelungshaken
3400mm a. mittl.
A-Deck

Fig. 9

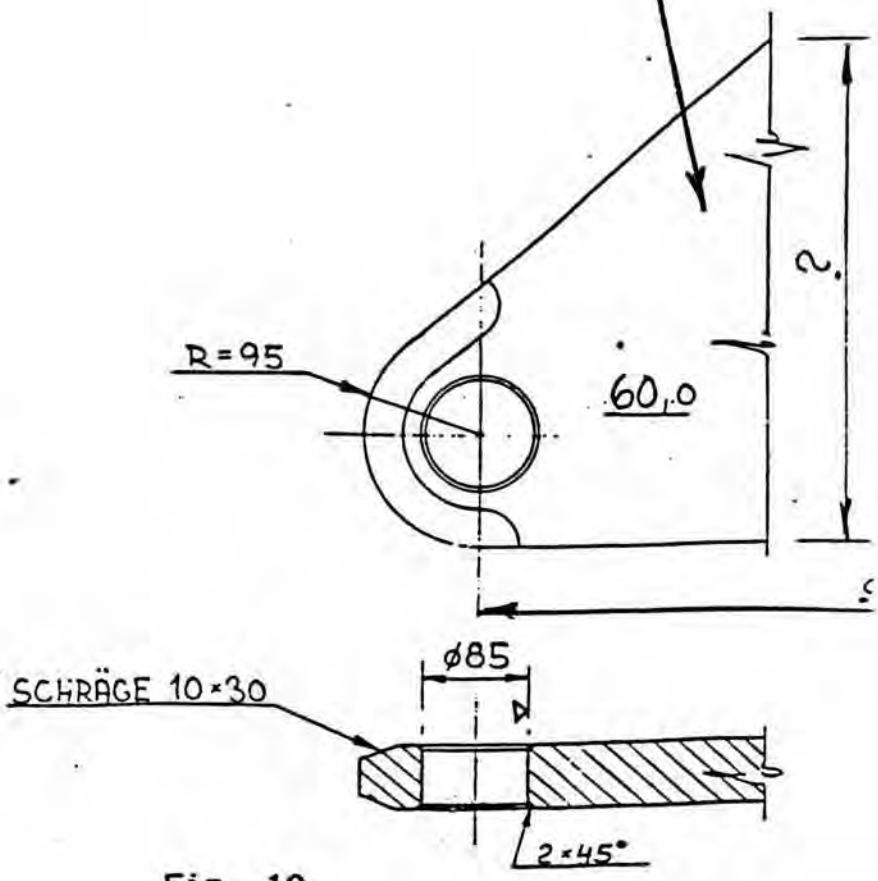
R=95
60,0
ø85
SCHRÄGE 10×30
2×45°

Fig. 10

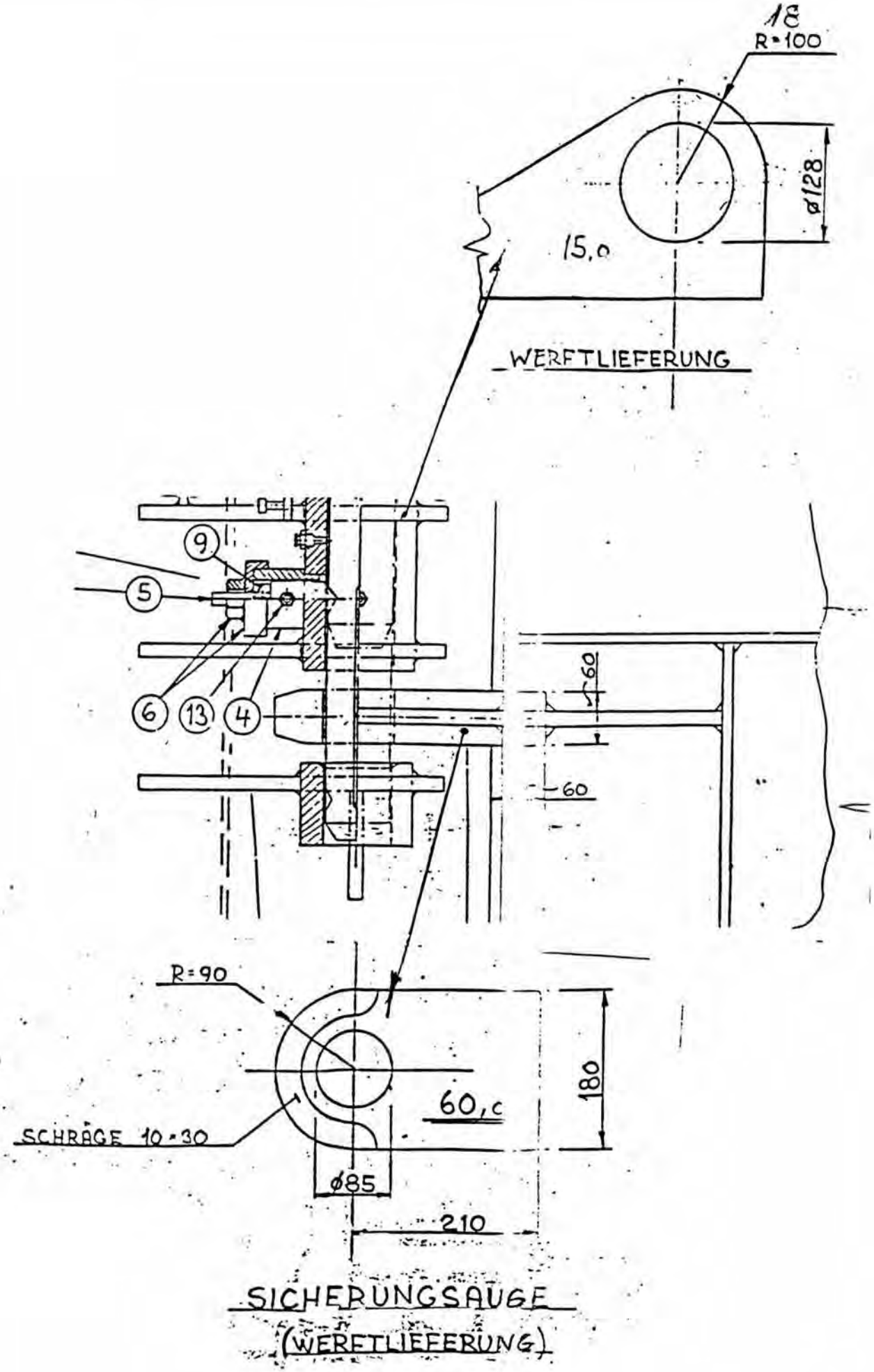
18
R=100
ø128
15,0
WERFTLIEFERUNG
9
5
6
13
4
60
60
R=90
60,0
180
SCHRÄGE 10-30
ø85
210
SICHERUNGSAUGE
(WERFTLIEFERUNG)

Fig. 11

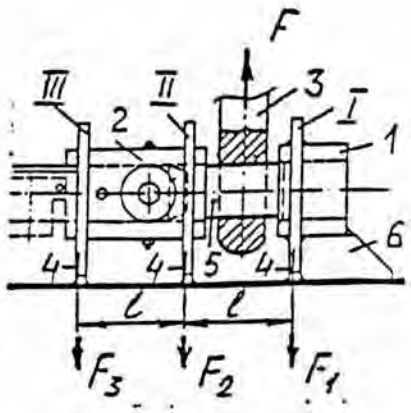

Fig. 12

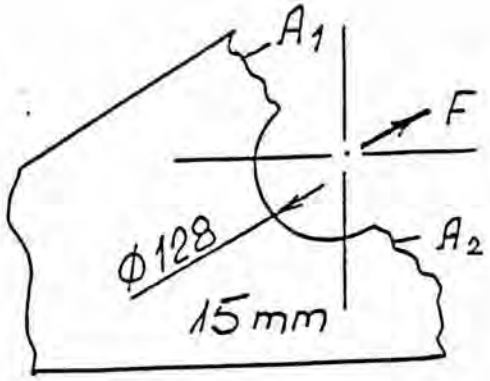

Fig. 13

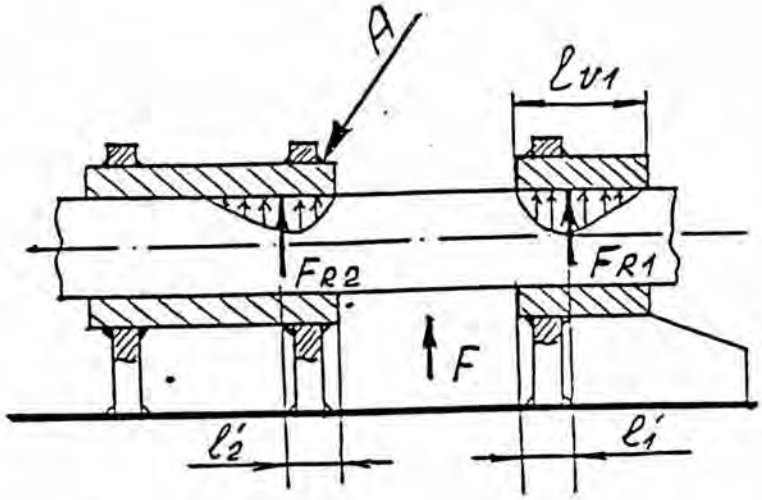

Fig. 14

The dimensions of the failed lugs are shown in Fig. 13.
The calculation scheme of the bottom lock is shown in Fig. 14.
The force F (Fig. 14) affecting the supports of the bolt 1 can be viewed as a shaft on a sleeve bearing [10].
F_{R1} and F_{R2} are the forces affecting the bushings.
The distance l_1' of the force F_{R1} can be derived from

$$l_1' = (0.25 \div 0.3) l_{v1} \le 0.5d$$

Provisionally we may assume that the reactive forces on both sides of the lug 3 are equal, resulting in:

$$F_{R1} = F_{R2} \quad \text{and} \quad F_1 = F_2 = F/2 \ .$$

In that case $F_3 = 0$.
The failure of the bottom lock can be viewed as the failure of the weld joints between the bushings and the lugs (Fig. 14 arrow A) and the failure of the lugs with surfaces A_1 and A_2.
The bottom lock fails in two stages. The reason for this is the fact that the bushing in the lug has a clearance relative to the lug and this causes the failure of the weld joints in the first stage. Subsequently the load is transferred from the bushing to the lugs and the lugs fail. As the failure takes place in two stages, the load carrying capacity of the bottom lock can not be considered equal to the sum of the failure loads of the weld joints and the lugs.

The first stage of the failure:

The strength calculations for the weld joints.
The weld joints are calculated for shear stresses, hence

$$\tau = \frac{F}{2} \cdot A \quad ; \quad F = \frac{2\tau}{A},$$

where A is the failure surface of the weld joint (Fig. 13). The leg of the weld joint k is approximately 3 mm [2], hence

$$A = 2\pi \cdot d_1 \cdot 0.7k = 2 \cdot 3.14 \cdot 128 \cdot 0.7 \cdot 3 = 1688.9\,\text{mm}^2$$

Let us determine the breaking force of the welds of the two lugs F_{wu}, when the ultimate stresses are $\tau_u = 0.6\sigma_u = 0.6 \cdot 400 = 240\,\text{N/mm}^2$, where

$$\sigma_u = 400\,\text{N/mm}^2.$$

$$F_{wu} = 2\tau_u \cdot A = 2 \cdot 240 \cdot 1688.9 = 810.672N = 810.67kN = 811\,kN$$

Now let us determine the calculational load carrying capacity F_{wp} of the weld joints if the allowable stresses are $\tau_p = 80\,\text{N/mm}^2$

$$F_{wp} = 2\tau_p \cdot A = 2 \cdot 80 \cdot 1688.9 = 270224N \approx 270\,kN$$

Let us calculate the calculational load carrying capacity of the weld joints F_{wp}, if the allowable stresses $\tau_p = 42\ \text{N/mm}^2$ (BV 1977 rules)

$$F_{wp} = 2\tau_p \cdot A = 2 \cdot 42 \cdot 1688.9 = 141867.6N = 14187kN \approx 142\ \text{kN}.$$

The calculational load carrying capacities F and the factor of underdimensioning K of the weld joints are presented in Table 1.

Table 1

τ, N/mm^2	F, kN	K = 1000 / F
42	142	7.1
80	270	3.7
240	811	1.23

The second stage of the failure:

Strength calculations for the lugs.

The lugs break with breaking surfaces A_1 and A_2 (Fig. 13).

Let us calculate the breaking surfaces, if the thickness of the lug was t = 15 mm.

$$A_1 = A_2 = (R - d_1 / 2) \cdot t = (100 - 128/2) \cdot 15 = 540\,\text{mm}^2$$

Thus the breaking surface of a lug is $A = A_1 + A_2$

$$A = 540 + 540 = 1080\ \text{mm}^2 .$$

Let us now calculate the breaking force to tension F_{Tu}, when the breaking stress to tension is σ_u = 400 N/mm^2 for two lugs if $F_{R1} = F_{R2}$, See Fig. 14.

$$F_{Tu} = 2 \cdot \sigma_u \cdot A = 2 \cdot 400 \cdot 1080 = 864000N = 864\ \text{kN}.$$

Let us determine the calculational load carrying capacity of the two lugs F_{Tp}, if the allowable stresses were σ_p = 120 N/mm^2

$$F_{Tp} = 2 \cdot \sigma_p \cdot A = 2 \cdot 120 \cdot 1080 = 259200N = 259.2kN \approx 260\ \text{kN}.$$

The calculational load carrying capacity of the lugs F_{Tp}, when allowable stresses σ_p = 85 N/mm^2 (BV 1977 rules)

$$F_{Tp} = 2 \cdot \sigma \cdot A = 2 \cdot 85 \cdot 1080 = 183600N = 183.6kN \approx 184\ \text{kN}.$$

The calculational load carrying capacities F and the factor of underdimensioning K of the lugs are presented in Table 2.

Table 2

τ, N/mm^2	F, kN	K = 1000 / F
85	184	5.5
120	260	3.8
400	864	1.1

Conclusions

1. It must be observed that failure of the bottom lock took place in two stages. First, the failure of the weld joints and secondly, the failure of the lugs.
2. The bottom lock is underdimensioned by a factor of 1.1 ÷ 5.5 at calculational loads of F = 1000 kN.

4.3 The strength calculations of the side lock

There are two side locks which consist of two lugs, mounted to the aft bulkhead of the bow visor and extended, when the visor was closed, into two holes in the front bulkhead of the hull, one at each side of the ramp opening. In the closed position hydraulically operated bolts engaged holes in the visor lugs (Fig. 15). The hydraulic bolt installations were similar to that of the bottom lock.

The side locks failed at the welding of the lugs and the aft plating of the bow visor. The weld leg was 8 mm long. The lug is welded to the plating as a fillet joint (T-joint) along a closed contour.

Such fillet joints are calculated for shear stress τ and are calculated for a plane at a 45° angle at the leg k of the weld, hence the width of the weld is 0.7k (Fig. 16).

As the side locks operate at alternating cyclic loads the nature of which cannot be determined, the strength calculations have to be performed using the minimal allowable stresses in the range of $\tau = 42 \div 80$ N/mm^2.

The scheme of the calculations is shown in Fig. 16. When calculating shear stresses at sign-changing loads, a 180 degree change in the direction of the force does not affect the stress state of the weld.

The force F_1 affecting the lug causes bending and section stress and the force F_2 causes tension-pressure stresses. Let us determine the stresses in the weld joint:

Tension-pressure	$\tau_1 = F_2/A$
Area	$A = 2(B+H)\ 0.7k$
Shear	$\tau_2 = F_1/A$
Bending	$\tau_3 = M\,y/I$
Bending moment	$M = F_1 L$
Inertia moment	$I = I_1 - I_2$

$$I_1 = (B+1.4k)(H+1.4k)^3/12$$

$$I_2 = BH^3/12$$

The distance of the weld in question from the axis

$$y = H/2+d$$

The arm of force F_1 L = 210 mm.

The calculational width d of weld joint

$$d = 0.7k = 0.7 \quad 8 = 5.6 \text{ mm}$$

The projections of force F

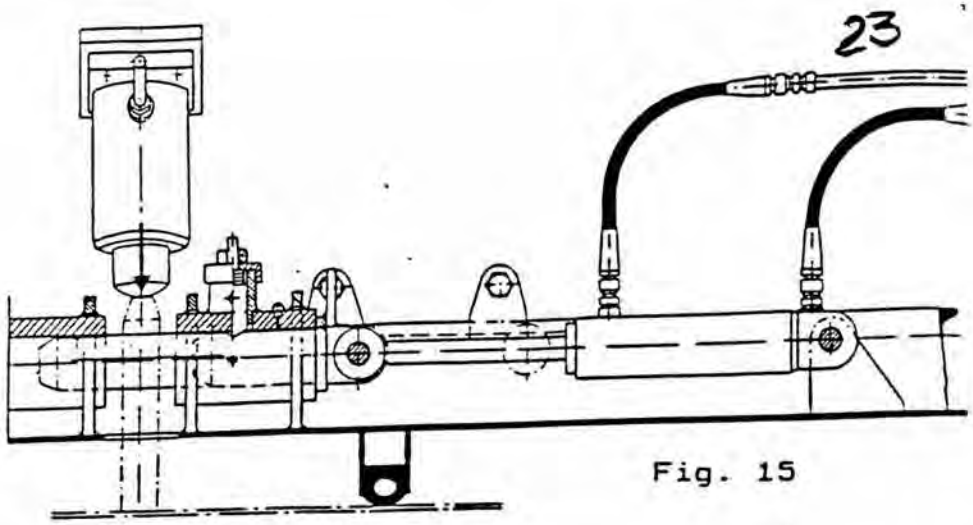

Fig. 15

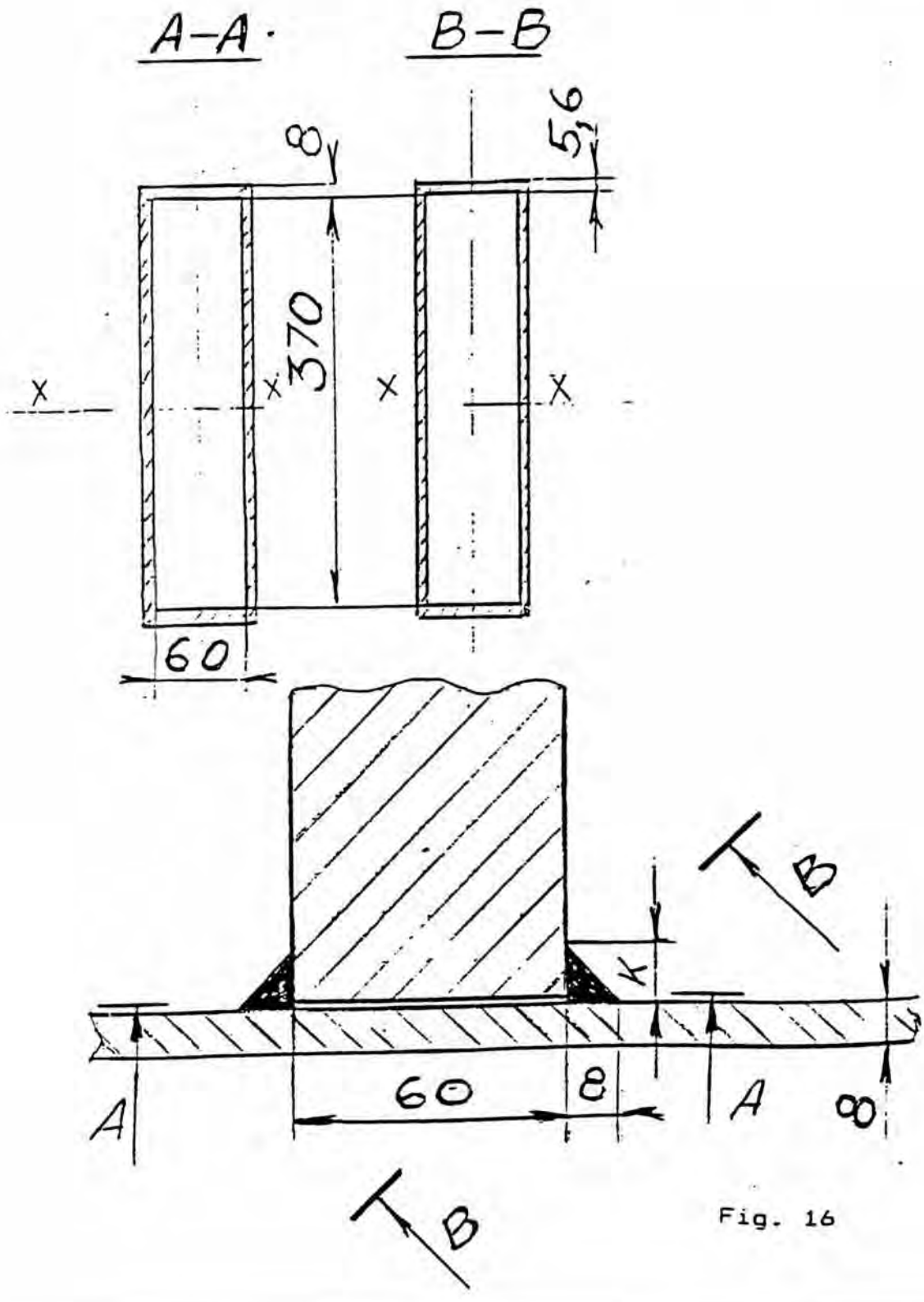

Fig. 16

SIDE LOCK

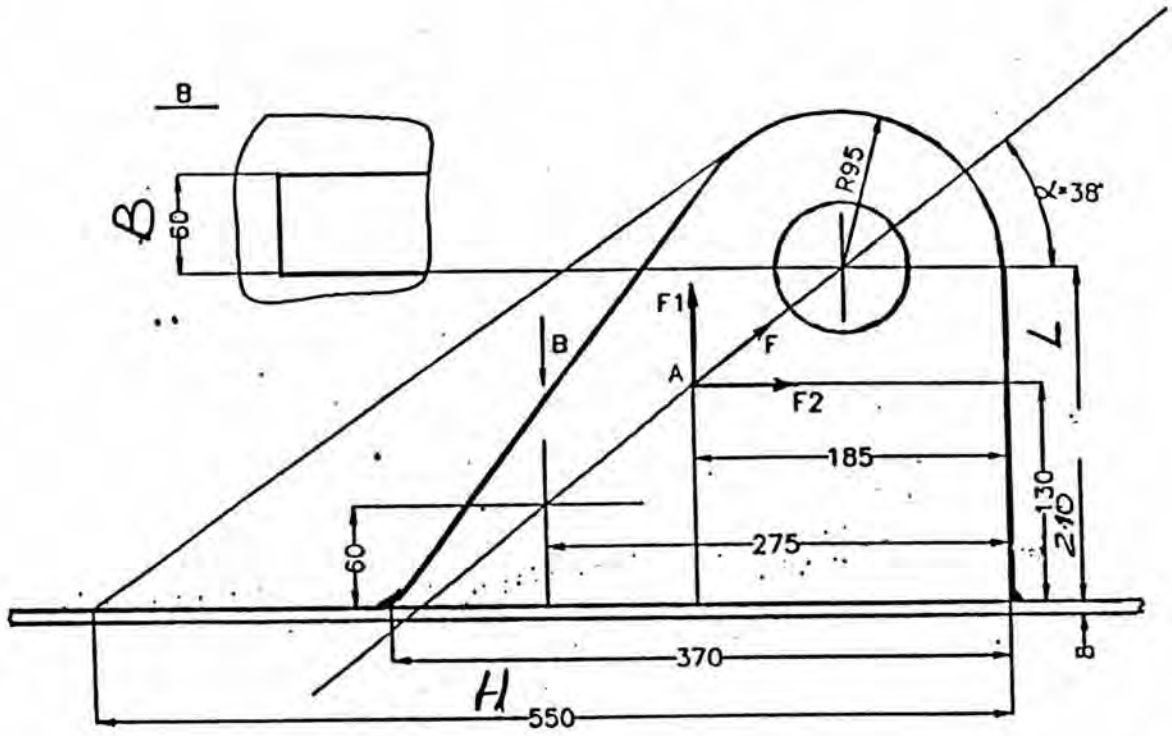

$$\tau_1 = F_1/A \; ; \quad \tau_2 = F_2/A \; ; \quad \tau_3 = F_2 L/W \; ; \quad \tau = \sqrt{(\tau_1 + \tau_3)^2 + \tau_2^2} \leq \tau_p$$

Fig. 16 A

```
REM     QBASIC A.INGERMA  20.01.97
     PI = 3.1416


  AL = 38 * PI / 180
           H = 370
k = 8
B = 60
LV = H / 2 - 95
L1 = LV * SIN(AL) / COS(AL)
LH = 210 - L1

        A = 2 * .7 * k * (B + H)
  I = ((B + 1.4 * k) * (H + 1.4 * k) ^ 3) / 12 - (B * H ^ 3) / 12
  W = I / (H / 2 + k)
  CONSTANT = ((SIN(AL) / A + COS(AL) * LH / W) ^ 2 + (COS(AL) / A) ^ 2)^
  FC = ps / CONSTANT
  PRINT "LH,L1,LV,=";  LH;  L1;  LV
  PRINT "CONSTANT=";  CONSTANT
  PRINT "FORCE CAPACITY TONS=";  FC / 10000
  LPRINT "CONSTANT=";  CONSTANT
    LPRINT "H=";  H
    LPRINT "LH,L1,LV,k,ALFA=";  LH;  L1;  LV;  k;  AL * 180 / PI
    LPRINT "PERMISSIBLE  STRESS MPa=";  ps
  LPRINT "FORCE CAPACITY TONS=";  FC / 10000
  LPRINT "STRESS  MPa "
  LPRINT "TENSION=";  FC * SIN(AL) / A
  LPRINT "BEND=";  FC * COS(AL) * LH / W
  LPRINT "SHEAR=";  FC * COS(AL) / A
   LPRINT "WELD LEG-K =";  k

  CONSTANT= 4.4105E-04
  H= 370
  LH,L1,LV,k,ALFA= 139.6841   70.31593   90   8   38
  PERMISSIBLE  STRESS MPa= 42
  FORCE CAPACITY TONS= 9.522729

  CONSTANT= 4.4105E-04
  H= 370
  LH,L1,LV,k,ALFA= 139.6841   70.31593   90   8   38
  PERMISSIBLE  STRESS MPa= 63.5
  FORCE CAPACITY TONS= 14.39746

  CONSTANT= 4.4105E-04
  H= 370
  LH,L1,LV,k,ALFA= 139.6841   70.31593   90   8   38
  PERMISSIBLE  STRESS MPa= 80
  FORCE CAPACITY TONS= 18.13853

  CONSTANT= 4.4105E-04
  H= 370
  LH,L1,LV,k,ALFA= 139.6841   70.31593   90   8   38
  PERMISSIBLE  STRESS MPa= 100
  FORCE CAPACITY TONS= 22.67316

  CONSTANT= 4.4105E-04
  H= 370
  LH,L1,LV,k,ALFA= 139.6841   70.31593   90   8   38
  PERMISSIBLE  STRESS MPa= 240
  FORCE CAPACITY TONS= 54.41559
```

Fig. 16 B

$$F_1 = F \cdot \cos\alpha = F \cdot \cos 38^\circ ,$$
$$F_2 = F \cdot \sin\alpha = F \cdot \sin 38^\circ .$$

Total stresses τ equal

$$\tau = \sqrt{(\tau_1 + \tau_3)^2 + \tau_2^2} \ .$$

By solving this equation we obtain the relationship between τ and F. A computer program was drawn up and the results are presented below in Table 3.

The allowable stresses are:

1. $\tau = 42$ N/mm^2 - Weld joints operating under alternating loads in practice.
2. $\tau = 63.5$ N/mm^2 - As presented by Swedish experts.
3. $\tau = 80$ N/mm^2 -The requirements of the majority of the classification societies.
4. $\tau = 240$ N/mm^2 - The ultimate strength of the steel St 37 to shear ($\tau_u = 0.6 \cdot \sigma_u$).

The load-carrying capacity of the side lock and the distribution of stresses in the weld joint is presented in Table 3.

Table 3

		Calculational shear stresses N/mm^2				
		42	63.5	80	100	240
Load-carrying capacity of the side lock kN		95.2	144.0	181	227	544
The stresses in the weld joints of the side lock N/mm^2	Tension and Pressure	12.2	18.4	23.2	29.0	69.6
	Bending	26.8	40.6	51.1	63.9	153.3
	Shear	15.6	23.6	29.7	37.1	89.0
The relation between the calculational load and the load carrying capacity K		10.5	6.9	5.5	4.4	1.8

The factor K shows the underdimensioning of the side lock.

SIDE LOCK

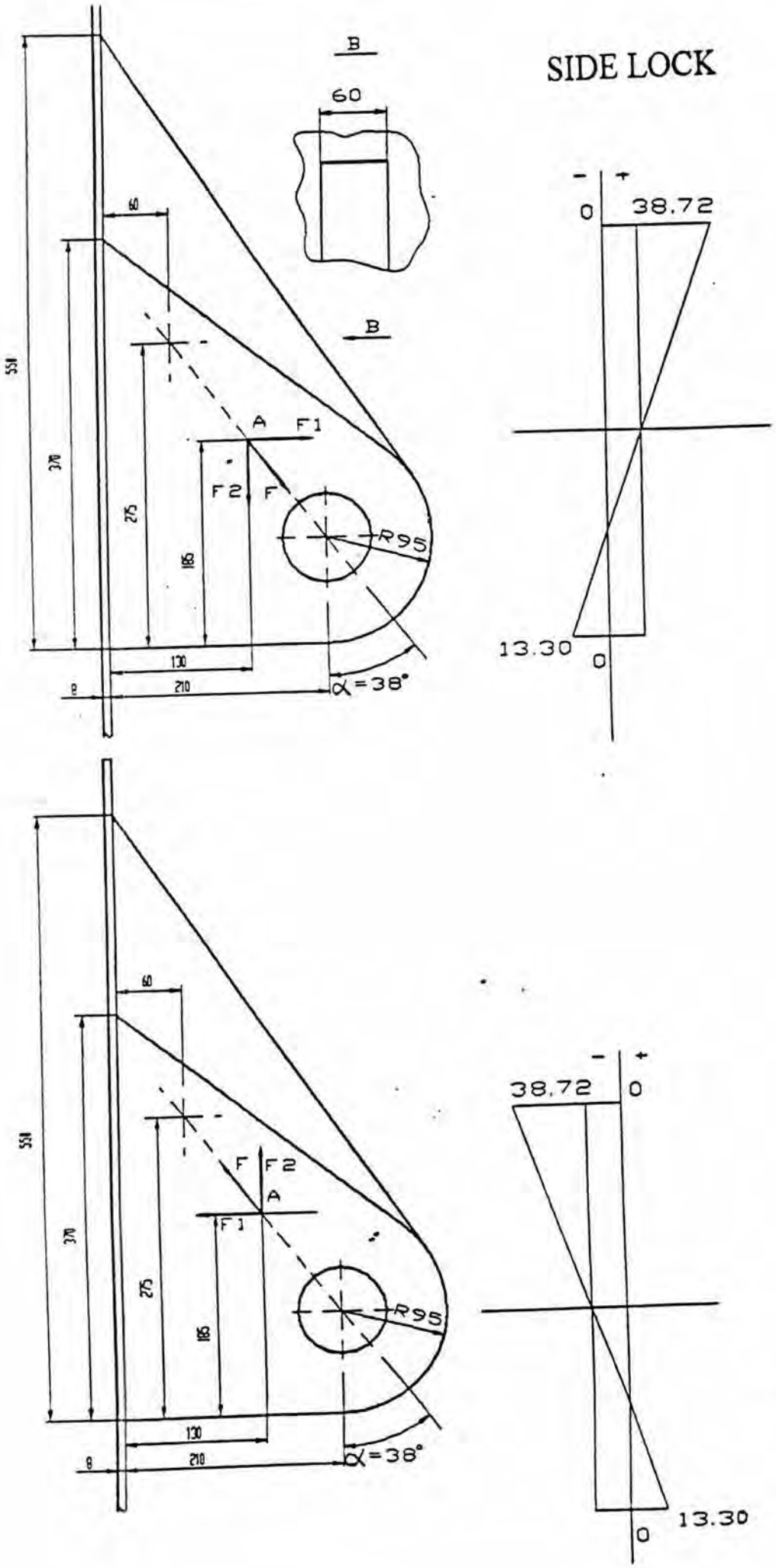

Fig.17

The larger construction is ROUND EYE PLATES from table 25 with nominal size 100 - permissible load 1000 kN.["Regulations for the Constructions and Survey of Lifting Appliances". 1992 Edition. Published by: Germanischer Lloyd.] The smaller construction is of a side lock of a visor of the MV ESTONIA. Both of the constructions are similar and have the same safety working (calculated) load capacity SWL=F=1000 kN (100 tons). I have made strength calculations on both of the constructions. SWL for a side lock of a visor of the MV ESTONIA is 4.6 times less than calculation for the construction of ROUND EYE PLATES by Germanischer Lloyd.

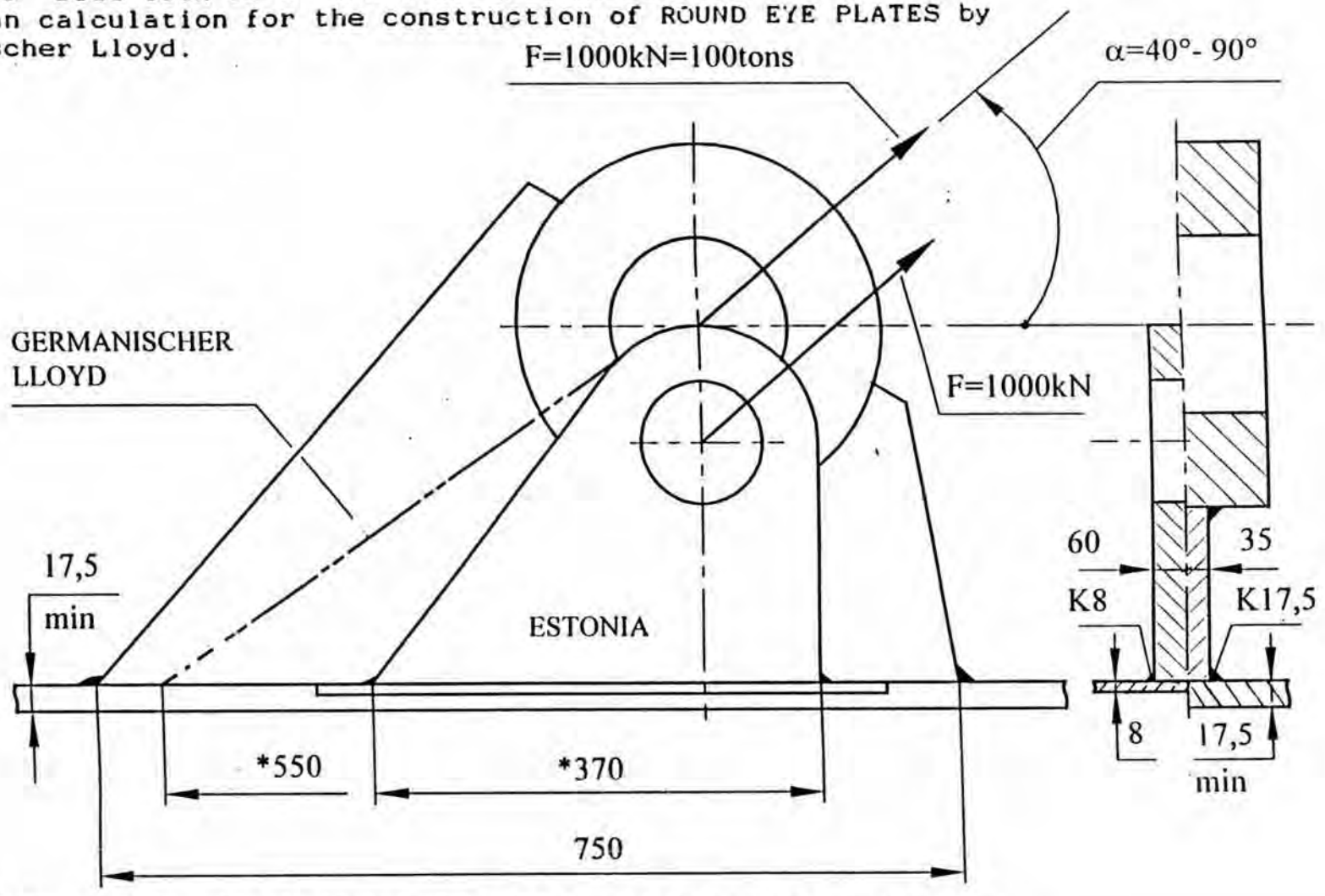

Fig. 8

* The actual dimension of a side lock of the M/V Estonia is 370, and the same dimension of the assembly drawing is 550

```
REM     QBASIC A.INGERMA  20.06.1996
     pi = 3.1416


AL = 90 * pi / 180

k = 17.5
 H = 750

B = 35
LV = H / 2 - 237
L1 = LV * SIN(AL) / COS(AL)
LH = 300 - L1


ps = 80
A = 2 * .7 * k * (B + H)
 I = ((B + 1.4 * k) * (H + 1.4 * k) ^ 3) / 12 - (B * H ^ 3) / 12
 W = I / (H / 2 + k)
 CONSTANT = ((SIN(AL) / A + COS(AL) * LH / W) ^ 2 + (COS(AL) / A) ^ 2)^
 FC = ps / CONSTANT
 PRINT "LH,L1,LV,="; LH; L1; LV
 PRINT "CONSTANT="; CONSTANT
 PRINT "FORCE CAPACITY TONS="; FC / 10000
 LPRINT "CONSTANT="; CONSTANT
   LPRINT "H="; H
   LPRINT "LH,L1,LV,k,ALFA="; LH; L1; LV; k; AL * 180 / pi
   LPRINT "PERMISSIBLE  STRESS MPa="; ps
 LPRINT "FORCE CAPACITY TONS="; FC / 10000


CONSTANT= 9.390068E-05
H= 750
LH,L1,LV,k,ALFA= 184.2039  115.7961  138  17.5  40
PERMISSIBLE  STRESS MPa= 80
FORCE CAPACITY TONS= 85.1964


CONSTANT= 9.390068E-05
H= 750
LH,L1,LV,k,ALFA= 184.2039  115.7961  138  17.5  40
PERMISSIBLE  STRESS MPa= 100
FORCE CAPACITY TONS= 106.4955

CONSTANT= 9.390068E-05
H= 750
LH,L1,LV,k,ALFA= 184.2039  115.7961  138  17.5  40
PERMISSIBLE  STRESS MPa= 95
FORCE CAPACITY TONS= 101.1707
```

Fig. 19

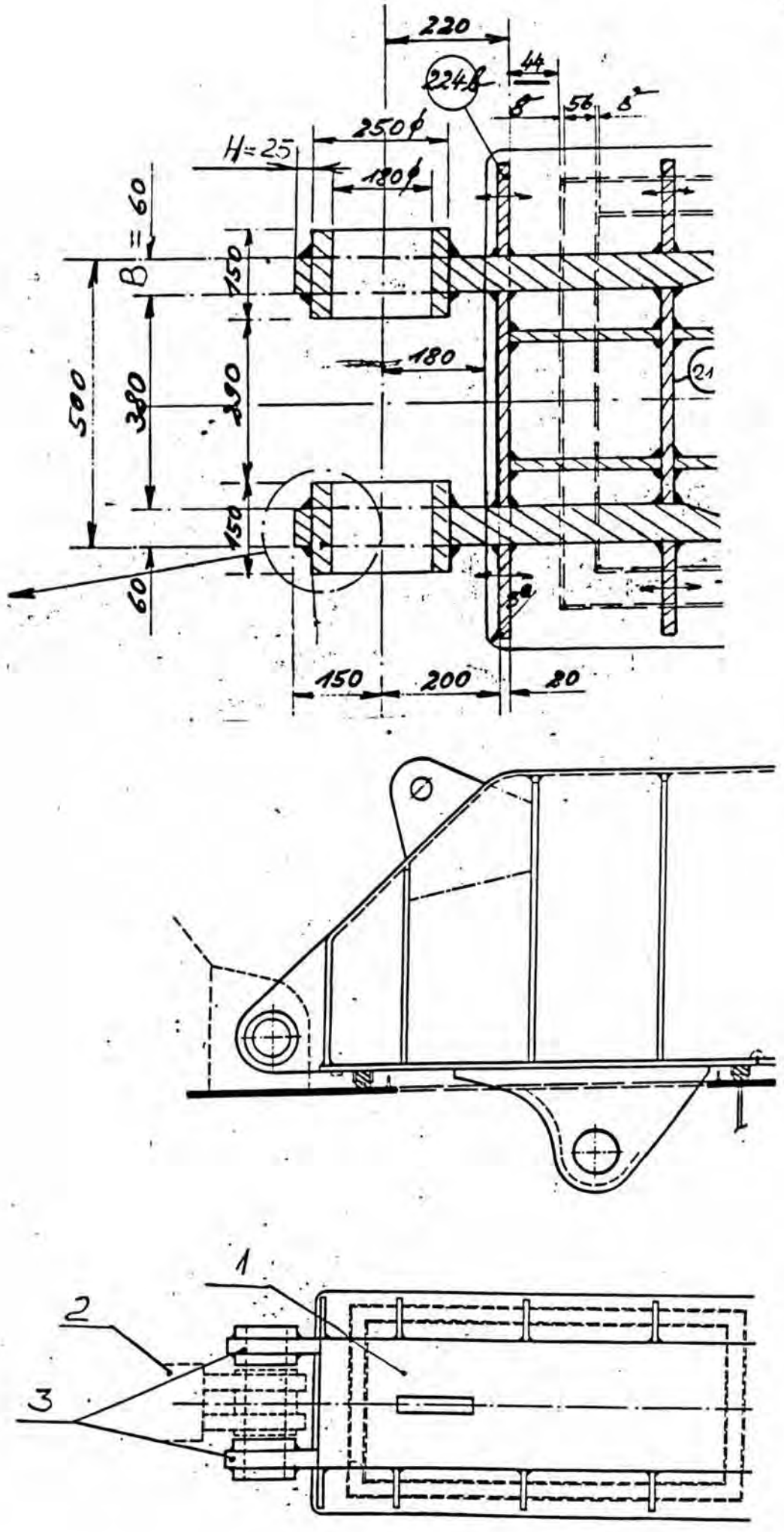
220
44
224 f
8
56
8
250 f
H=25
180 f
B=60
150
180
21
500
380
190
150
60
8
150
200
20
1
2
3

Fig. 20

Hence the side lock is underdimensioned by a factor of 10.5÷7.1 using calculational allowable stresses and by a factor of 1.8 using failure stresses. When conducting an analyses on the stress situation during tension (opening of the bow visor) and pressure (the closing direction of the bow visor) it becomes apparent that the upper edge of the lug is always under heavier load (Fig. 17). Hence the failure initiates at the upper edge. This is further confirmed by the damages to the side locks of DIANA II on Jan. 16th, 1993, Figs 5 and 6.

The underdimensioning of the side lock is also proven by the analogous construction presented in [11]. At the permissible load of 1000 kN (100 tons) of this round eye plate and at the similar calculational load carrying capacity of the side lock of MV ESTONIA the devices of MV ESTONIA have been underdimensioned by a factor of 4.6 at allowable shear stresses of $\tau = 95$ N/mm^2 and by a factor of 10.4 at allowable shear stresses of $\tau =$ 42 N/mm^2. This proves again that the side lock was underdimensioned by a factor of 4÷10.

Both constructions are shown in Fig. 18. The strength calculations for the lug are presented, which made it possible to derive the allowable stresses used at design (Fig. 19).

Conclusion.

1. The calculational load carrying capacity of the side locks by allowable stresses is 4÷10 times too small.
2. The calculational load carrying capacity according to breaking stresses is underdimensioned by a factor of 2.

4.4 Strength calculations of the hinges

4.4.1. The design and failure of the hinges

The two beams 1 on the deck of the visor extended about 3 meters aft of the aft edge of the visor deck (Fig. 20).

A heavy steel bushing was welded into a hole in each of the two side plates 3 of each beam. The bushings had a bore, carrying a bronze bushing. The deck part of the hinge consisted of two lugs 2 welded to the deck, carrying between them a steel housing.

The hinges fail in two stages. The reason is that the holes in the side plating are not mechanically (accurately) elaborated but are made by flame cutting. Hence the bushings welded into these holes have significant

clearances and thus the weld joint fails in the first stage due to fatigue. Consequently the load is distributed over to the lugs of the side plating (the second stage) and these break due to overloads at a small quantity of cycles. This is the final failure of the hinges. As the failure takes place in two stages, the sum of breaking loads of the weld and the lugs cannot be considered to be the total load carrying capacity of the hinges.

4.4.2 The strength calculations of the welds

The bushing is welded into the side plates with a diameter of 250 mm and the weld has a leg of 10 mm. Weld joints are calculated to shear stress τ.

$$\tau = \frac{F}{A} \quad ; \quad F = \tau \cdot A \ .$$

A - the failure surface of the weld joint, consisting of four circular welds.

$$A = 4 \cdot \pi d \cdot 0{,}7K = 4 \cdot \pi \cdot 250 \cdot 0.7 \cdot 10 = 21991 mm^2 \approx 22000 \ \text{mm}^2 \ .$$

Table 4 shows the calculational load carrying capacity and failure strengths (τ = 240 N/mm^2) of the weld joints of the hinges without any cracks. Actually the weld joints had cracks [2] and as the stress concentration factor of cracks is 3÷50 [12], the actual failure loads of the welds of the hinges could be 3÷50 times smaller. It can also be observed that weld joints without cracks are underdimensioned only at shear stresses of $\tau = 42$ N/mm^2

Table 4

τ , N/mm^2	F , kN	K=1000/F
42	923.6	1.08
63.5	1396.4	0.71
80	1759.3	0.57
100	2199.1	0.45
240	5277.8	0.018

4.4.3 Strength calculations of the lugs of the side plates

The failure surface of the lugs of the two support beams is calculated using the width and height of the legs(B = 60 mm, H = 25 mm).
One lug has two failure surfaces, hence

$$A = 2 \cdot 2 \cdot B \cdot H = 4 \cdot 60 \cdot 25 = 6000 \text{ mm}^2 .$$

The failure takes place at low-numbered cyclic loads and based on the analysis of the failure surfaces the following calculations can be considered to be static failure due to tension stresses. It should be kept in mind, however, that the hole in the side plating was made by flame cutting and the cut surface had many stress concentrators, which are in this case not taken into consideration.

The strength calculation to tension stresses is

$$\sigma = \frac{F}{A} \quad ; \quad F = \sigma \cdot A .$$

The calculational load carrying capacity using allowable stresses of $\sigma = 123$ N/mm^2 is

$$F = 120 \cdot 6000 = 720000 \text{ N} = 720 \text{ kN} .$$

The load carrying capacity at failure stresses of $\sigma = 400$ N/mm^2 equals

$$F = 400 \cdot 6000 = 2400000 \text{ N} = 2400 \text{ kN} .$$

Conclusions

1. The failure of the hinges takes place in two phases. First, the failure of the welds and then the failure of the lugs of the side plates.
2. As cracks formed in the hinge during operation, the actual failure strength can not be estimated to be over 2400 kN, more likely even less due to the stress concentrators in the holes in the side plates made by flame cutting.

5. GENERAL ASSESSMENT OF THE DESIGN AND MANUFACTURING OF THE LOCKING DEVICES.

If the locking devices had been properly designed, manufactured and inspected in accordance with current requirements, would the accident of MV Estonia have been likely to take place?

First, let us define the term "properly designed and manufactured".

1. The calculational loads of 1000 kN per locking device should have been taken into consideration by using a safety factor of at least 2.5(5.0).
2. All the locking devices should have been under equal loads simultaneously (clearance free locks), i.e. forced locking (a power screw and a nut)

Let us determine the resistance moments of the Atlantic lock and the side locks relative to the axis of the hinges in the opening direction of the bow visor. The maximum opening moment on the bow visor caused by the sea load has been estimated at Mm=29000÷35400 kNm by calculations and experimnents.

Which of the moments is greater — the resistance momentum or the sea load momentum? The answers are presented in Table 5.

Table 5

Name of the part	Arm from hinge axis, m	Calculational force Fa, kN	Moment from hinge axis Ma, kNm	Failure force Fp, kN	Moment from hinge axis Mp, kNm
The Atlantic lock	6.87	1000	6870	2500	17175
The side lock (2 pcs.)	4.45	2·1000	8900	2·2500	22250
Gravity of the bow visor	4.9	600	2940	600	2940
	Total	-	18710	-	42395

The calculational resistance moment or Safety Working Load (SWL) is Ma=18710 kNm, which is less then the opening moment caused by the sea load Mm=35400 kNm, which is in turn smaller than the combined resistance/failure momentum Mp=42395 kNm.

$$Ma=17450 < Mm=35400 < Mp=42395 \text{ kNm}$$

When designing as critical a component as the bow visor it is necessary and reasonable to use a safety factor of 5. In that case we get

$$Ma=17450 < Mm=35400 < Mp=78850 \text{ kNm}$$

Thus it can be stated with great probability that the Safety Working Load of 1000 kN is sufficient for locking devices. Thus, once more, the mistake was made in the engineering/manufacturing of the devices. It is not acceptable to use the fact that the design was a traditional one as an excuse. Every engineer/manufacturer is responsible for his work.

6. FINAL CONCLUSIONS

1. As the sea forces are varying in direction and magnitude during operation, the only proper method of calculation is to fatigue strength and only locking devices that are simultaneously and equally loaded should be used i.e. clearance free forced locking.
2. The allowable stresses must take into consideration the imprecise methods of determining the loads and maximum safety factors should be used in determining the allowable stresses.
3. As welded structures are especially sensitive to alternating loads, the allowable shear stresses should not be greater than $40 \div 60$ N/mm^2 for steels with ultimate stresses of up to 450 N/ mm^2. This value is currently used world-wide.
4. Explaining the underdimensioning of the locking devices with the fact that there were no Bureau Veritas rules for calculations and allowable stresses is no justification for the engineer.
5. The Atlantic lock and the side locks were underdimensioned and were the first to fail. Then the weld joints of the hinges and finally the lugs of the hinge side plates failed. As the Atlantic lock and the side locks were underdimensioned and the holes in the side plates of the hinges were imprecisely manufactured, not securing the maximum load carrying capacity, the failure of the locking devices was inevitable already at the stage of engineering.

Tallinn, April 10th, 1997

A. INGERMA

Head of the Chair of Port Management in Estonian Maritime Academy, Prof., Ph.D.

V. STRIZHAK

Professor of the Mechanical Engineering Institute of Tallinn Technical University, Ph.D.

SOURCES

1. Germanischer Lloyd. Rules for Classification and Construction. I-Ship Technology. Part 1 - seagoing Ship Chapter 1 - Hull Structures Germanischer Lloyd. Hamburg 1992.
2. ESTONIA FINAL REPORT (97.01.25)
3. T.Karppinen and others. Numerical predictions of wave-induced motions. Technical Report VALC53 VTT. Espoo, December 1995.
4. T.Karppinen and others. Numerical predictions of wave loads on the bow visor. Technical Report VALC106 VTT, Espoo, December 1995.
5. M.Huss. Wave impact loads on visor of MS ESTONIA. A quick summary of results from model tests at SSPA. 21.08.1995. Stockholm.
6. S.Liukkonen. The bow door wave pressure measurements of MS SILJA SYMPHONY. Technical Report VALC138 VTT, Espoo, December 1995.
7. INSPECTION REPORT. TURBOTECHNIK Wilhelmshaven, 05.10.1994.
8. Bureau Veritas. Rules and Regulations. Steel Vessels. 1977.
9. S.V.Serensen, V.P.Kogaev, R.M.Shneiderovitch. Load capacity and strength calculation of Machine parts. Guidance and reference textbook. Under editing S.V.Serensen. Moscow, "Mashinostroenie", 1975, pp. 488 (in Russian).
10. A.Blinov, K.Ljalin. Weld Constructions. Stroiizdat. Moskva 1990 (in Russian).
11. Regulations for the constructions and Survey of Lifting Appliances Germanischer Lloyd. Hamburg, 1992.
12. R.E.Peterson. Stress concentration factors. John. Wiley and Sons. N-Y, 1974.

SUPPLEMENT No. 508

Katajamäki Kai:

MV Estonia Accident Investigation. Strenght investigation of the visor side locking device, numerical calculations.

Technical report VALC-246.

VTT Manufacturing Technology.

Espoo 1996.

VTT MANUFACTURING TECHNOLOGY

CONFIDENTIAL

MV ESTONIA ACCIDENT INVESTIGATION

Strength investigation of the visor side locking device, numerical calculations

TECHNICAL REPORT
VALC-246

Kai Katajamäki

VTT MANUFACTURING TECHNOLOGY
PL 1705, 02044 VTT
Tel. +358-0-4561, Fax +358-0-455 0619

Projekti/työ - Project identification	Sivuja - Pages	Päiväys - Date	Raportin nro - Report No.
	17 + 38	27.06.96	VTT VALC-246

Otsikko ja tekijä - Title and author

MV ESTONIA ACCIDENT INVESTIGATION
Strength investigation of the visor side locking device, numerical calculations
Kai Katajamäki

Päivitys raporttiin nro - Update to report no.	Hyväksynyt - Approved by

Julkisuus - Availability statement — Määräpäivä - Until date

[] B (Julkinen - Public) [x] C (Luottamuksellinen - Confidential) [] C (Salainen - Secret)

Abstrakti, sisällysluettelo, tms. - Abstract, list of contents etc.

Abstract

The structural behaviour of the visor side locking device of MS Estonia was numerically examined. The loading was assumed to be caused by wave pressure distribution acting on the visor shell plating that generates an opening moment to the visor. Load-deflection behaviour was predicted and an estimate of the load carrying capacity of the structure was obtained.

Non-linear elasto-plastic as well as linear elastic analyses were conducted using finite element method (FEM). Both physical and geometrical non-linearities were taken into account in the analyses. A total of three different calculation models were prepared. Firstly, a model describing the undamaged original structure was prepared. Variation of the loading direction was conducted with this model. Secondly, a model with damaged horizontal stringer was prepared. In this model the welding between the stringer and the bulkhead below the lug at some distance was supposed to be detached. The background for this model was the high stress level that was induced into the horizontal stringer at loaded condition. It indicates that the stringer would eventually be teared apart from the bulkhead. Thirdly, a model describing the first experimental test was prepared. The object for this model was to measure the quality of the calculations with experimental results.

The estimated ultimate load for the side locking lug is 1.6 MN. At that load level the plastic deformations in horizontal stringer become so large that the stringer plating below the lug will be teared apart from the bulkhead. After the stringer is detached the load-carrying capacity will be lowered and according to calculations the ultimate load for the damaged structure is about 1.3 MN. If the plane at which the loading force is acting, is rotated towards the side plating, the calculated ultimate load will be lowered.

DISTRIBUTION

The Joint Accident Investigation Comission of Estonia, Finland and Sweden 15 pcs
VTT Manufacturing Technology 2 pcs

VTT VALMISTUSTEKNIIKKA
Laiva- ja konetekniikka

VTT MANUFACTURING TECHNOLOGY
Maritime and Mechanical Engineering

P.O. Box 1705
FIN-02044 VTT
FINLAND

Tel.int.+358 0 4561
Telefax +358 0 455 0619
Telex 122972 vttha sf

CONTENTS

1 INTRODUCTION

The aim of this study was to numerically examine the structural behaviour of the visor side locking device of MS Estonia. The loading was assumed to be caused by wave pressure distribution acting on the visor shell plating. This loading generates in turn an opening moment to the ship's visor [1].

The load-deflection behaviour of the side locking device was predicted and furthermore an estimate of the load carrying capacity of the structure was obtained.

Non-linear elasto-plastic as well as linear elastic analyses were conducted using finite element method (FEM). Both physical and geometrical non-linearities were taken into account in the analyses.

A total of three different calculation models were prepared. Firstly, a model describing the undamaged original structure was prepared. This model was applied to make predictions of the load-carrying capacity of the side locking device. Also variation of the loading direction was conducted with this model.

Secondly, a model with damaged horizontal stringer was prepared. In this model the welding between the stringer and the bulkhead below the lug at some distance was supposed to be damaged. The background for this model was the high stress level that was induced into the horizontal stringer at loaded condition. It indicates that the stringer would eventually be teared apart from the bulkhead plating under the lug. The numerical procedure used in this study is, however, formulated such that this kind of phenomena can not be modelled. So, with the second model the situation at which the stringer is damaged was simulated.

Thirdly, a model describing the first experimental test was prepared. The object for this model was to measure the quality of the calculations with experimental test results.

1.1 Structure and loading

The locking device consisted of a lug that was welded at the bulkhead plating of the visor. The plating below the lug was strengthened with two vertical stringers and a horizontal stringer. The lug was situated unsymmetrically with respect to the beams. The plate thicknesses of the primary structural members were as follows:

- bulkhead 8 mm,
- horizontal stringer 10 mm and
- vertical stringers 20 mm.

The arrangement of the lug in respect with the stringers is shown in Fig. 1. Fig. 2 shows the dimensions of the lug that were used in the calculations. The drawings prepared by the shipyard did not give clearly the dimensioning of the lug. To estimate the dimensions, manual measurements from the actual visor were made and it was found out that the height of the lug was about 380 mm and width about 60 mm.

The material was modelled with the following mechanical properties:

Young´s modulus: 207 GPa and
Poisson´s ratio: 0.29.

The yield stress and ultimate strength were taken from experimental tension test results (Appendix A) and they were found to be:

for the horizontal stringer:
yield stress: 332 MPa and
ultimate stress in uniaxial tension: 476 MPa,
other members excluding the lug and weld:
yield stress: 306 MPa and
ultimate stress in uniaxial tension: 454 MPa.

In the calculations elasto-plastic material model that uses the von Mises yield surface was used. The stress-strain curve consisting of three linear parts (Figs. 3a and b) was applied to describe the non-linear material behaviour. The material model makes the assumption that after 18 % strain the material is perfectly plastic which means that further straining does not induce higher stress in the material.

The lug as well as the welds were modelled to have pure linear-elastic material behaviour.

The force acting on the locking device was thought to be induced by the opening moment caused by the sea load to the visor. The direction of the loading is shown in Fig. 4.

The following element types were used in the FE-idealization: the lug and the weld were modelled with solid elements. The bulkhead plating, the horizontal stringer beneath the lug and the vertical stringers beneath the lug were modelled with shell elements.

1.2 Analysis programs

A computer aided design package, I-DEAS [2], was used as a pre- and post-processor. In addition, the linear elastic analyses were done with I-DEAS. The non-linear elasto-plastic cases were analyzed with commercial finite element package ABAQUS [3]. Also the post-processing software ABAQUS-POST [4] was used in post-processing the ABAQUS results. Following ABAQUS element types were used in non-linear analyses:

S8R: shell element (8-noded quadrilateral),
STRI65: shell element (6-noded triangle),
C3D20: solid element (20-noded brick),
C3D15: solid element (15-noded wedge) and
C3DD10: solid element (10-noded tetrahedra).

The solutions of the non-linear equilibrium equations were obtained by using so called modified RIKS method. This solution algorithm can handle unstable problems where the load or displacement may decrease as the solution evolves.

2 STRENGTH INVESTIGATION OF THE SIDE LOCK

2.1 Numerical models

The finite element discretization is shown in Figs. 5 and 6.

Characteristic sizes of the model were:

- number of elements 907,
- number of nodes 3019 and
- degrees of freedom 15963.

The FE-model extended up to the side plating in the horizontal direction and in the vertical direction two stringer spaces. The horizontal stringer as well as the vertical stringers below the lug were modelled. Moreover, local plate stiffeners attached to the bulkhead as well as to the horizontal stringer plating were modelled.

Fixed boundary conditions were used at the model edges as shown in Fig. 7.

The load was applied as nodal forces acting on the inner surface of the lug's attachment hole.

2.2 Results

In the analysis run displacement and also stress and strain state were calculated and stored at selected load increment steps. The solution procedure calculates the stresses and the strains at so called integration points which are located inside the elements. These integration point values were then extrapolated to element nodes and furthermore to the element mid-plane using element's shape functions. The extrapolation was done by the analysis program.

In the analysis five integration points through the element thickness were used.

Only the membrane values (i.e., values that are calculated at the element mid-plane) are considered.

2.2.1 Undamaged structure

The calculated results are shown in Appendix B and they consist of:

- load-displacement curve of one loaded point of the lug,
- structure's deformed shape at the last calculation step,
- von Mises stresses at the horizontal stringer,
- membrane stresses at the horizontal stringer,
- von Mises strains at the horizontal stringer,
- membrane strains at the horizontal stringer,
- von Mises stresses at the bulkhead,
- von Mises strains at the bulkhead,
- equivalent plastic strain at the horizontal stringer and
- equivalent plastic strain at the bulkhead.

The analysis-run consisted of a total of 74 load increments and was then terminated because the load increment was becoming very small. At that point the load level was 1.63 MN. The calculated load-deflection curve for one loaded point at the lug measured in the loading direction is shown in Appendix B. According to the curve the maximum displacement in the load's direction is about 3.5 mm. In the figure the curve is extrapolated linearly up to 5 mm's displacement and the load obtained at that point is about 1.9 MN. Due to the plastic deformation the stiffness of the structure is gradually decreasing. At the load level of 1.63 MN the stiffness is approximately 20 % of the structure's original stiffness. (Here the stiffness of the structure is defined as the tangent of the load-deflection curve.)

In Appendix B also the equivalent plastic strain at the horizontal stringer is shown. At the load level of 1.37 MN a narrow strip just below the lug has become plastic. As the loading increases, the plastic region increases also and finally at the load level of 1.63 MN another continuous plastic region below the lug is formed. It is interesting to note that at that load level the membrane stress distribution at the stringer also shows a continuous high stress region below the lug. This indicates that it is quite possible for the horizontal stringer material to be teared apart from the bulkhead plating by the lug.

By integrating the stress distributions in stringer and bulkhead the resulting forces acting in these members were calculated. They were found to be when the loading is about 1.6 MN:

- horizontal stringer: 0.56 MN
- bulkhead plating: 0.63 MN + 0.36 MN + 0.04 MN + 0.01 MN= 1.07 MN

2.2.2 Structure with damaged stringer

In this model the horizontal stringer was detached from the bulkhead plating between the vertical stringers (about 130 mm) and moreover the vertical stringers were detached from the bulkhead by a distance of 30 mm.

The calculated results are shown in Appendix C. The corresponding results as in Appendix B are shown.

The analysis-run consisted of a total of 69 load increments. At the last calculation point the load level was 0.94 MN. The calculated load-deflection curve for one loaded point at the lug measured in the loading direction is shown in Appendix C. According to the curve the maximum displacement in the load's direction is about 2.9 mm. In the figure the curve is extrapolated linearly up to 5 mm's displacement and the load obtained at that point is about 1.3 MN. At the load level of 0.94 MN the stiffness is approximately 37 % of the structure's original stiffness.

2.2.3 Variation of the loading direction

The effect of the loading direction was studied with two different load cases. As the loading was in the previously described case acting in a plane parallel with the ship's centre plane, now the loading was rotated towards the side plating to have angles of 30° and 60° between the loading plane and the ship's centre plane. The angle between the horizontal plane and the loading plane was however the same as in the previous case.

The calculated results for the two cases are shown in Appendix D.

The analysis-run consisted of a total of 50 load increments. At the last calculation point the load level was 1.26 MN when load was acting on 30° angle and only 0.43 MN when load was acting on 60°. The maximum displacement in the load's direction is about 14 mm and 16 mm respectively. The stiffness at the last calculation point is approximately 34 % when the loading direction is 30° and 28 % when the direction is 60° compared with the structure's original stiffness. A comparison with all the calculated load-deflection curves is shown in Fig. 8.

3 NUMERICAL CALCULATION OF THE TEST

3.1 Numerical model

The test structure consisted of two similar lugs. The finite element model of the analysed structure is shown in Appendix E Figs. 1 and 2. Due to symmetry only one half of the other lug was modelled.

Because the horizontal stringer would eventually buckle as the loading is increased, the modelling of the attachment of the stringer to the vertical bulkhead as well as to the side plate and also to the vertical stringers was important. In the calculation model the horizontal stringer was attached to the bulkhead all along its length. Moreover, the stringer was attached to the side plating in 87 mm's distance according to Fig. 2 in Appendix E.

By using shell elements in the modelling only the mid-plane of the vertical stringers were modelled. To make realistic aspect ratio for the horizontal stringer that would buckle, the thickness of the vertical stringer was taken into account by multi-point constraints (see Fig. 2, Appendix E). The equation for each slave node was of the form:

$$u_{ys} = u_{ym} + \Delta x \cdot \theta_{zm}, \text{ where}$$

u_{ys} and u_{ym} are the displacement components in y-axis direction of the slave and master nodes respectively, θ_{zm} is the rotation about z-axis of the master node and Δx is the distance between the slave and the master node.

Fixed boundary conditions at the model edges and symmetrical boundary conditions at the model symmetry plane were used, see Appendix E. Fig. 3.

Characteristic sizes of the model were:

- number of elements 763,
- number of nodes 2654,
- degrees of freedom 14349.

The analysis run consisted of 141 load increments.

In the analysis five integration points through the element thickness were used.

3.2 Results

In Appendix E Fig. 4 the measuring points with measuring directions are shown. Transducer S measured the displacement at the loaded point in the load's direction. S1 measured displacement at the plating at the upper edge of the lug. The direction was perpendicular to the plating. R1, R2, R3, R4, R6, R7, R8 and R9 were strain transducers and the were located at the bulkhead plating above the stringer. The measuring direction was the stringer's plane. R5 and R10 were also strain transducers. In the figure strain transducers R6, R7, R8 and R9 are not shown but they measured at the corresponding locations as the transducers R1, R2, R3, R4, respectively, but were located at the plating near the other lug.

In Appendix E Fig. 5 the calculated displacement at the loaded point in load's direction is compared with the measured data. It can be seen that calculation model was somewhat stiffer than the measuring set-up. In the calculations the vertical stringer buckled at about 810 kN's load. The buckled stringer is shown in Appendix E Fig. 12. After buckling the load required to increase the displacement was lower but as displacement increased the required loading was also increasing and the calculation terminated at the loading level of about 880 kN. The displacement of the loaded point at the buckling point was about 8 mm and at the final calculation point about 34 mm. Figure 13 in Appendix E shows the distribution of the equivalent plastic strain at the last calculation step.

In Appendix E Fig 6 the calculated and measured values for the displacement transducer S1 are shown. At that point the linear-elastic stiffness is the same for both cases but the measured structure shows earlier softening behaviour. At load around 790 kN the transducer reached it measuring range and was thereafter not active. The displacement was then about 20 mm. The calculated displacement reached about 43 mm.

In Appendix E Figs 7 and 8 the calculated strain near the weld above the horizontal stringer is compared with measured values of R1 ... R4 and in Figs 9 and 10 the same values are compared with measured values of R6 ... R9. In Fig. 11 the measured values of R5 and R10 are compared with the calculated values.

In the measurements it was found that at the load level of about 300 kN the strain transducers R5 and R10 showed small permanent deformation in the structure. Visually clear deformations were observed at around 600 kN. At load around 850 - 900 kN the structure finally collapsed.

4 CONCLUSIONS

The estimated ultimate load is about 1.6 MN. At that load level the plastic deformations in horizontal stringer become so big that the stringer plating below the lug will be teared apart from the bulkhead. After the stringer is teared apart the load-carrying capacity will be lowered and according to calculations the ultimate load for the damaged structure is about 1.3 MN.

In the case when the load vector does not lie in a plane parallel with ship's centre plane, the load required to cause excessive yielding to the structure is lowered dramatically. When the load vector is offset an angle of 30°, the estimated ultimate load is 1.3 MN and when the load vector is offset by an angle of 60°, the ultimate load is 0.43 MN. When considering these values, it should be kept in mind, that in the modelling the lug was free to move sideways. In reality the locking arrangement would create supporting forces that would restrain the sideways movement of the lug.

In the FE-modelling various idealizations were made. These idealizations came mainly from the analysis effectiveness requirements. Non-linear analysis is usually time consuming especially in the solution stage. Also the required disk storage space increases rapidly as the model size increases. For these reason's idealizations are inevitable. In this analysis the modelling practice where the bulkhead plating as well as the stringers are modelled with shell elements is based on two factors: firstly, the aim of this study was to calculate the force distribution in the structure ignoring very local effects. Secondly, as it became evident that membrane stress distribution in the horizontal stringer is the most important factor, the choice of shell elements seemed to be adequate.

To verify the applicability of the used modelling practice, experimental test was conducted. The calculated ultimate load was about 850 kN and measured ultimate load around 900 kN. The horizontal stringer buckled at around 800 kN. This kind of buckling was also detected in the test structure. On the other hand, it should be noted that buckling of the horizontal stringer was not detected in real visor structure.

The buckling phenomena in the test structure caused some special requirements to the corresponding calculation model. These were as follows: a) the welding to the side plating was critical and in the model the extent of this weld must be taken into account and b) the thickness effect of the vertical stringer showed some effect on the buckling load and was taken into account with constraint equations. These modelling practises were not applied in the calculation model of the ship's visor because no buckling occurred there.

The measured and calculated displacement-load curves agreed quite well. The calculation model was somewhat stiffer as was expected.

REFERENCES

1. Part-report covering technical issues on the capsizing on 28 September 1994 in the Baltic Sea of the ro-ro passenger vessel MV Estonia. The Joint Accident Investigation Commission of Estonia, Finland and Sweden.

2. I-DEAS (Integrated Design Engineering Analysis Software) Master Series 2.1. Structural Dynamics Research Corporation.

3. ABAQUS, Version 5.5, Hibbit, Karlsson & Sorensen, Inc.

4. ABAQUS-POST, Version 5.5, Hibbit, Karlsson & Sorensen, Inc.

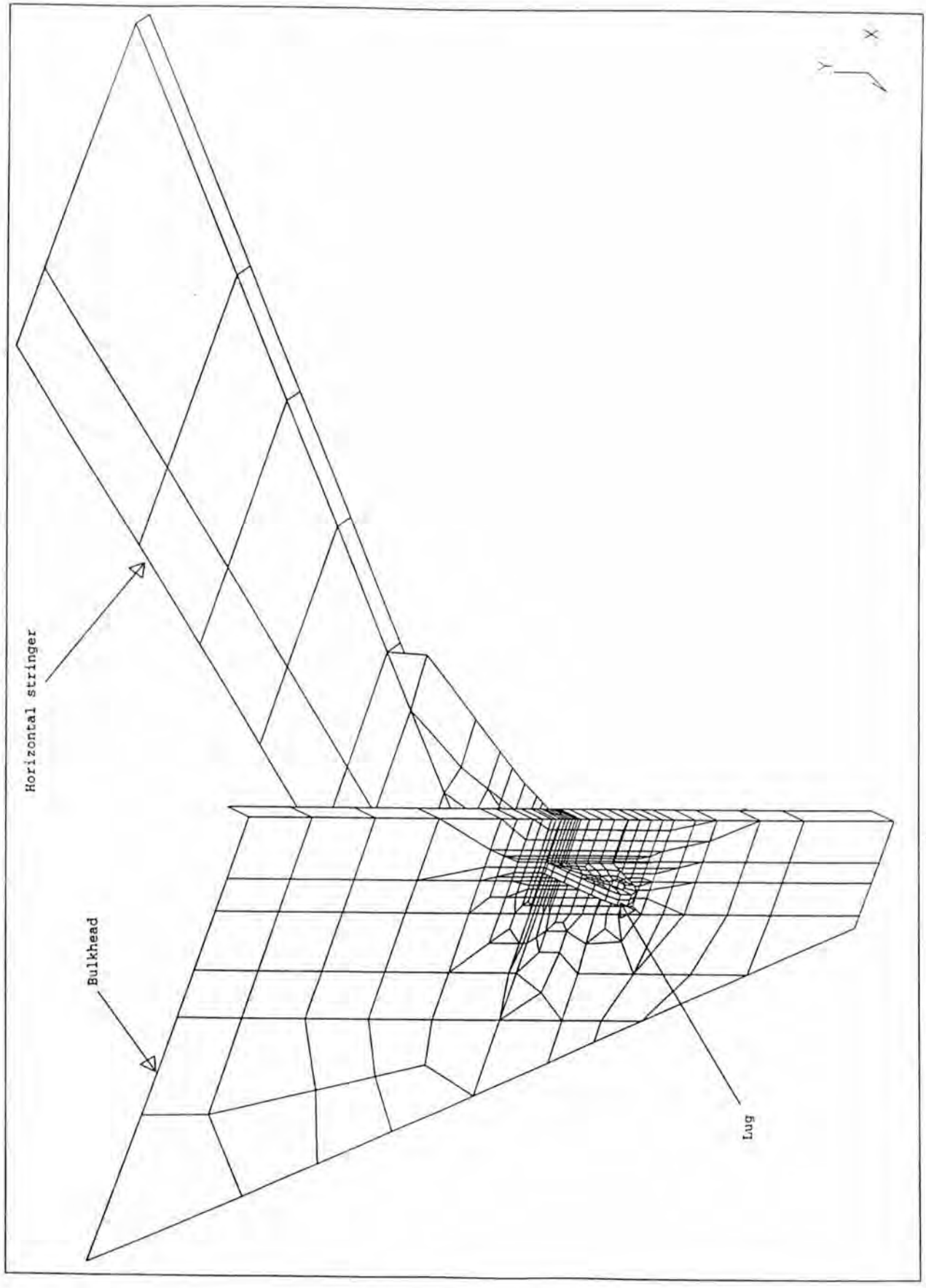

Figure 5. FE idealization

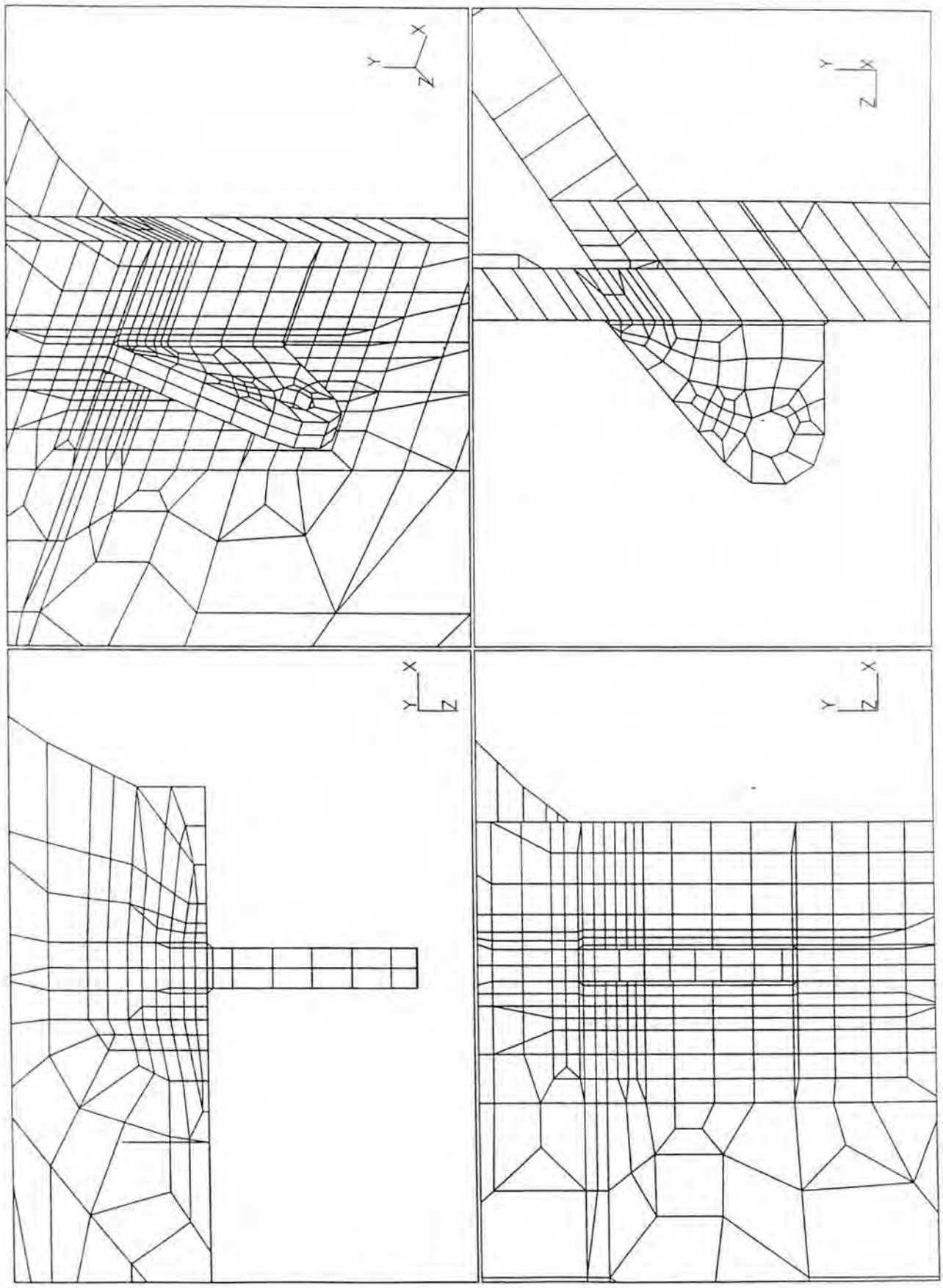

Figure 6. Finite element model of the side lock.

Figure 8. Calculated load-deflection curves.

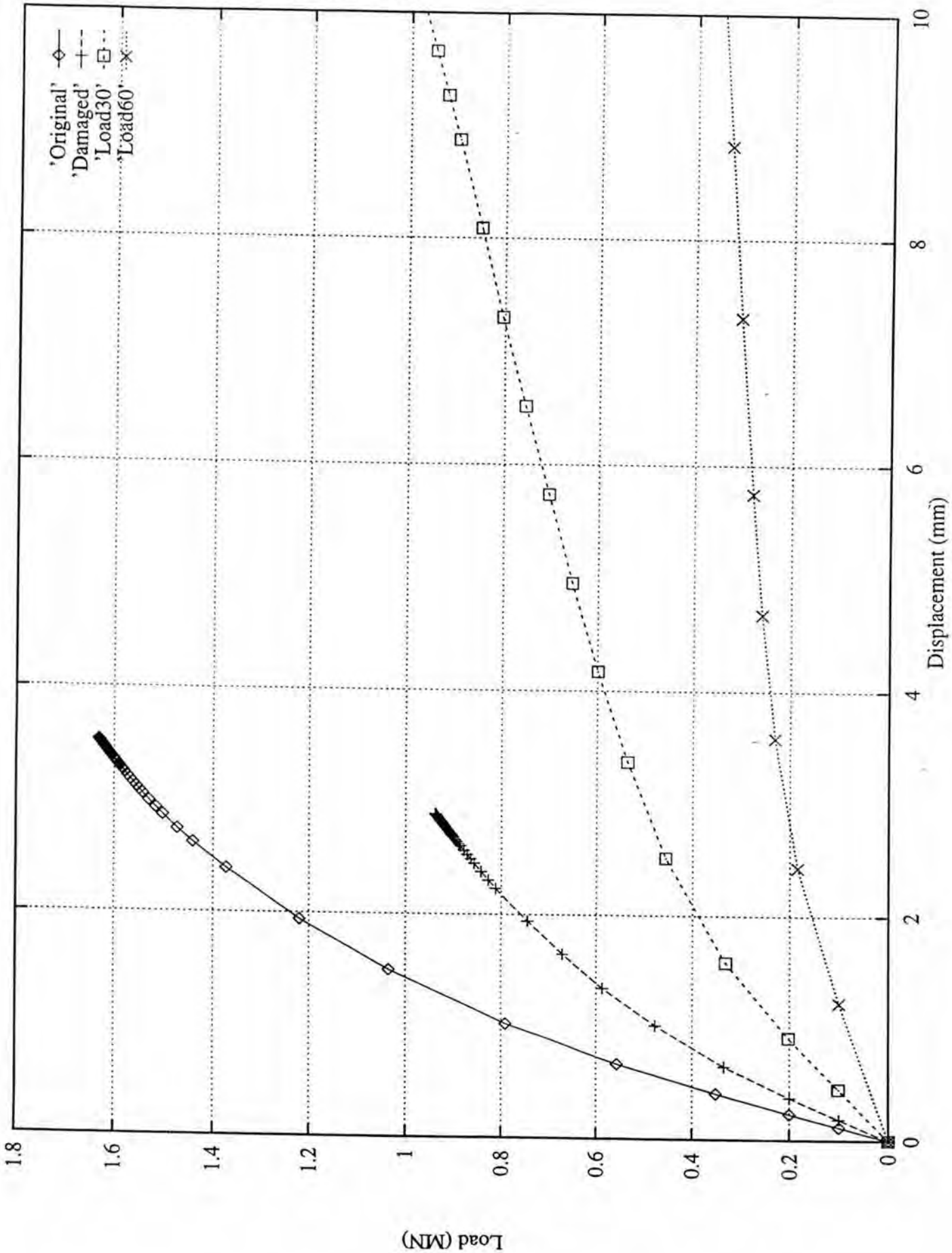

APPENDIX B
Deformed shape at 1.63 MN

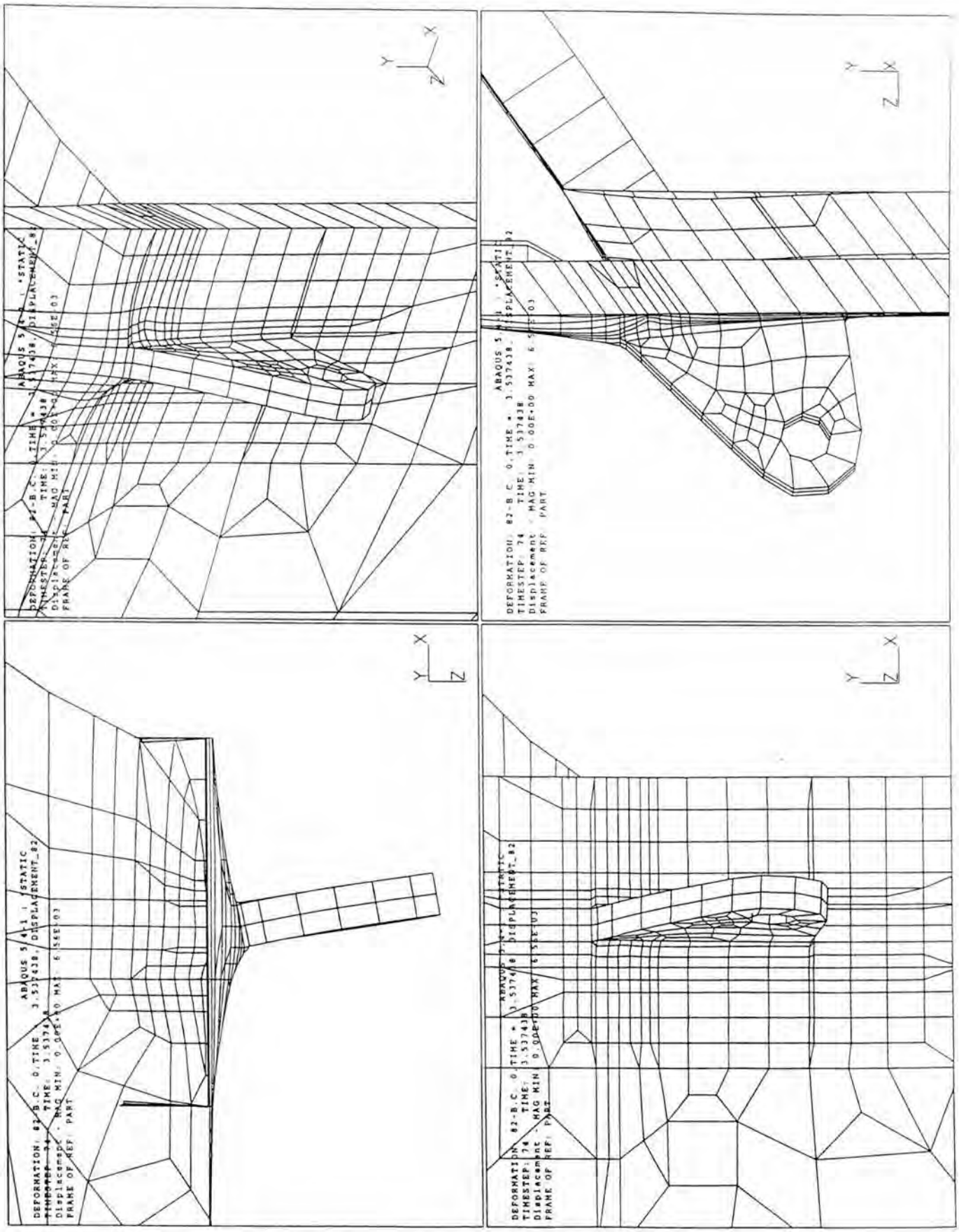

APPENDIX B
Equivalent plastic strain at the horizontal stringer with load values of 0.56, 1.37, 1.52 and 1.63 MN

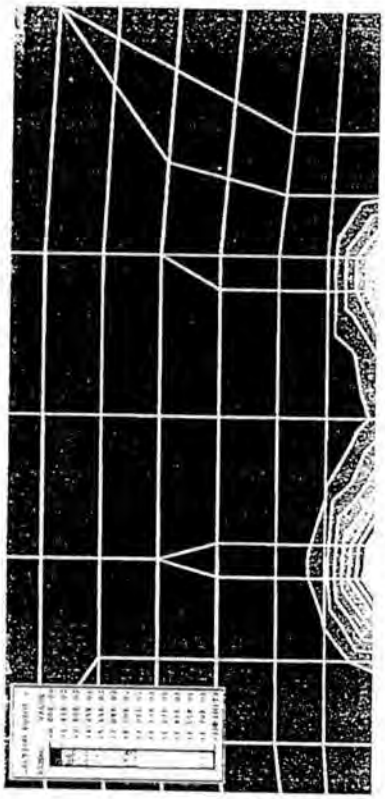

Load 1.37 MN

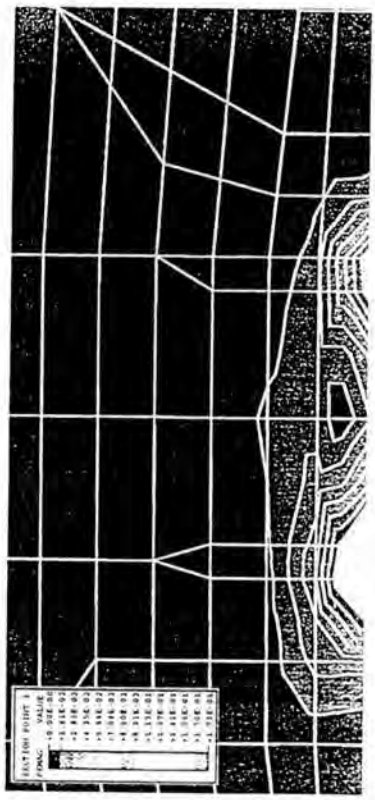

Load 1.63 MN

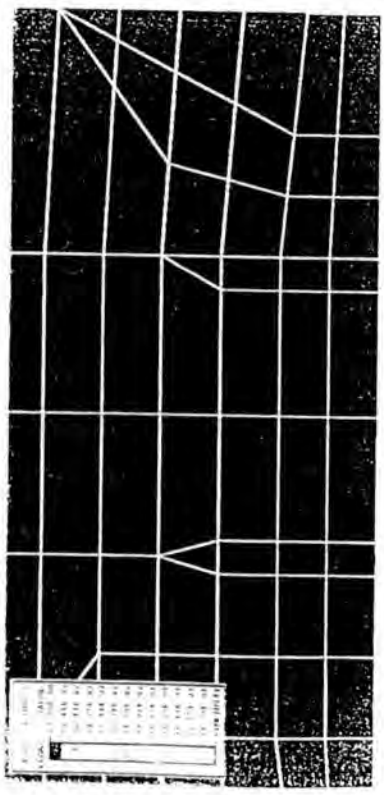

Load 0.56 MN

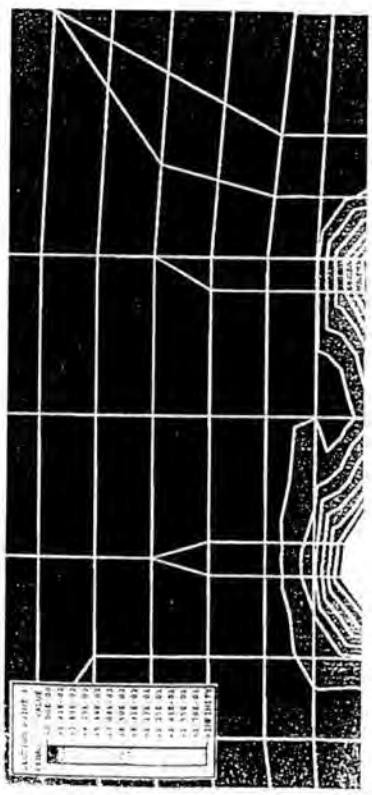

Load 1.52 MN

APPENDIX B

Equivalent plastic strain at the bulkhead with load values of 0.56, 1.37, 1.52 and 1.63 MN

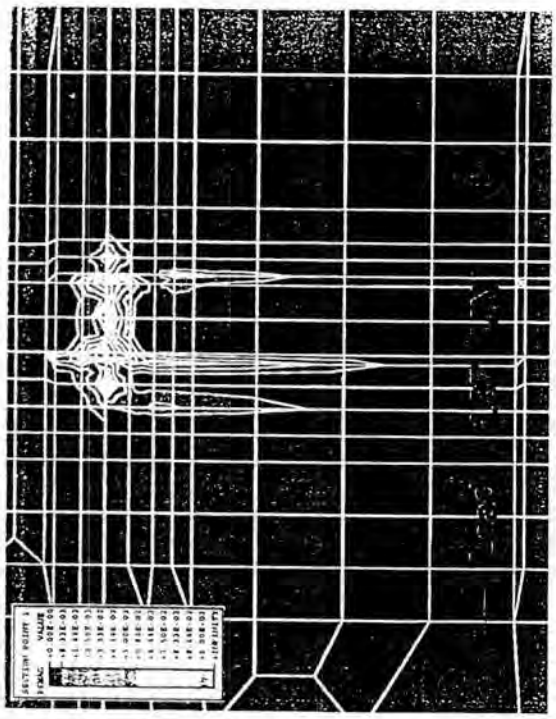

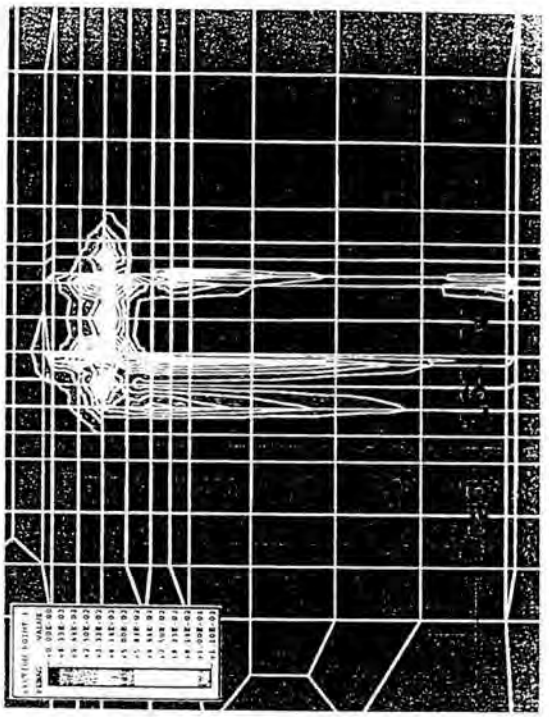

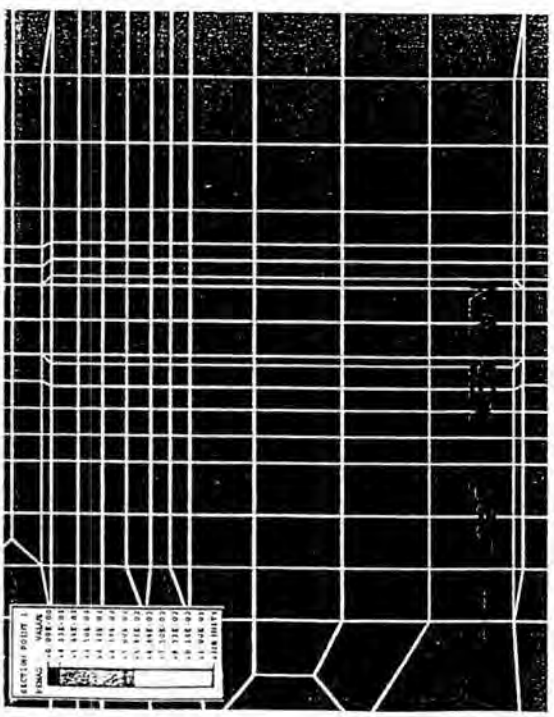

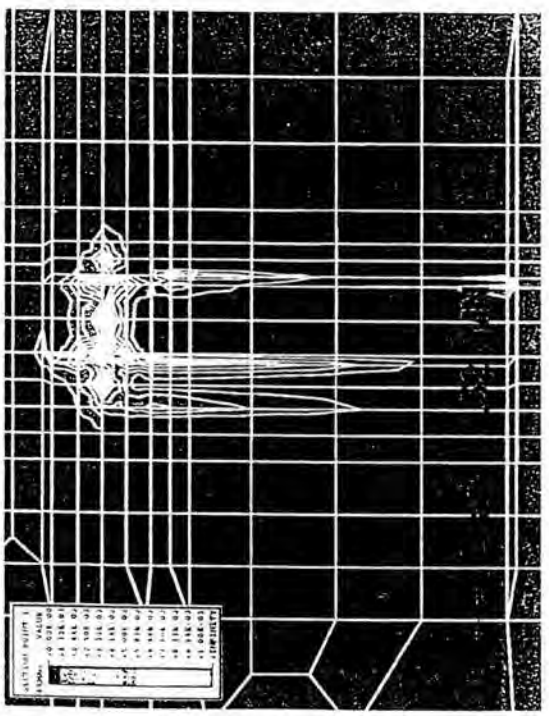

APPENDIX C
Equivalent plastic strain at the horiz. stringer (damaged) with load values of 0.48, 0.81, 0.87 and 0.94 MN

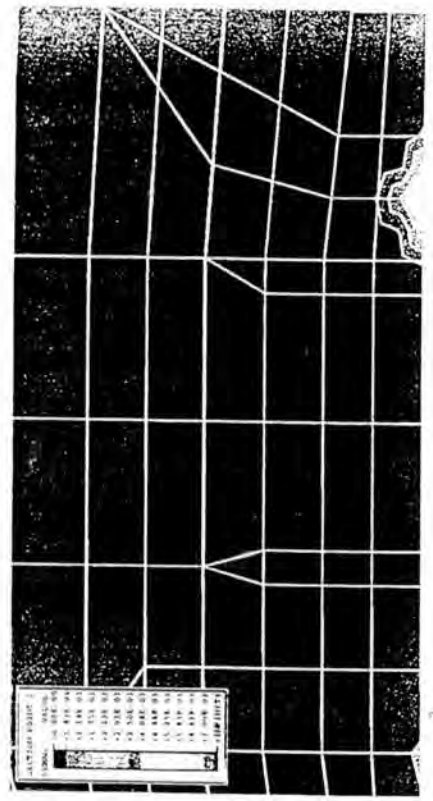

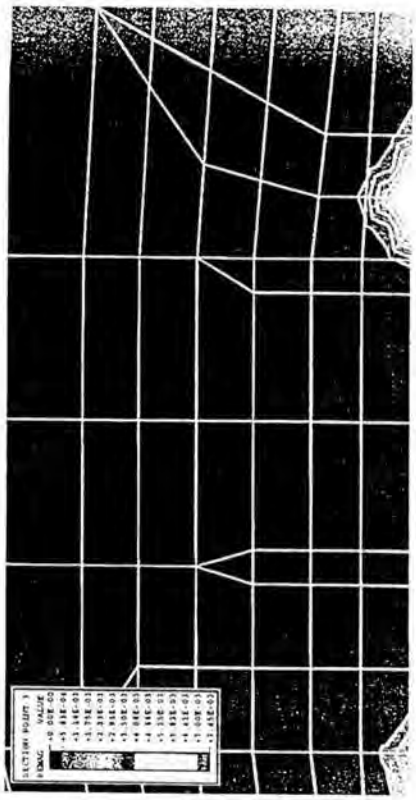

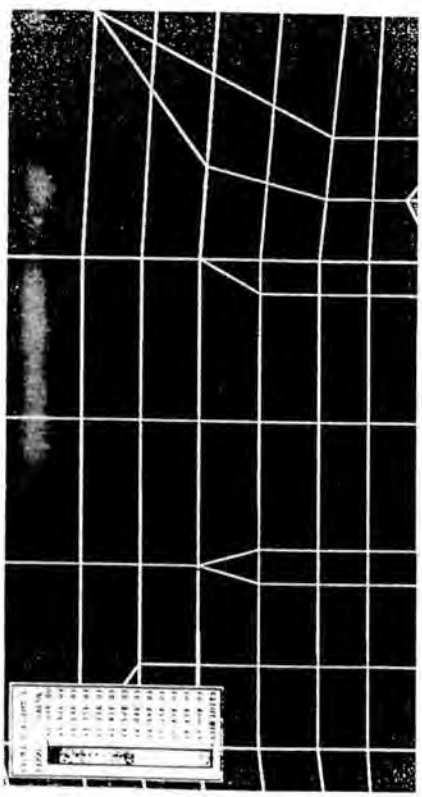

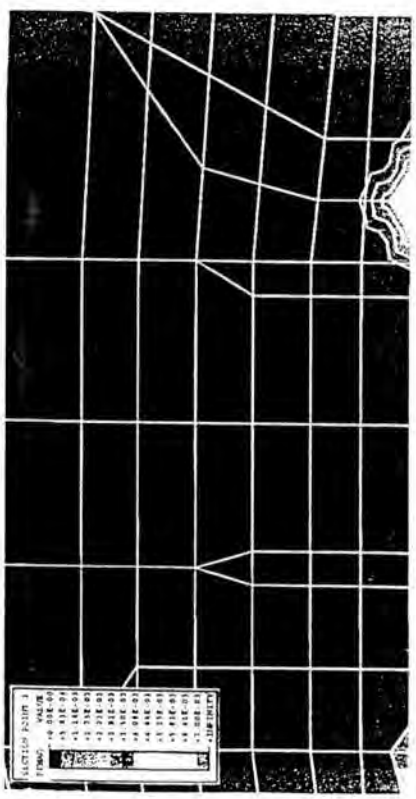

APPENDIX C

Equivalent plastic strain at the bulkhead with load values of 0.48, 0.81, 0.87 and 0.94 MN (damaged)

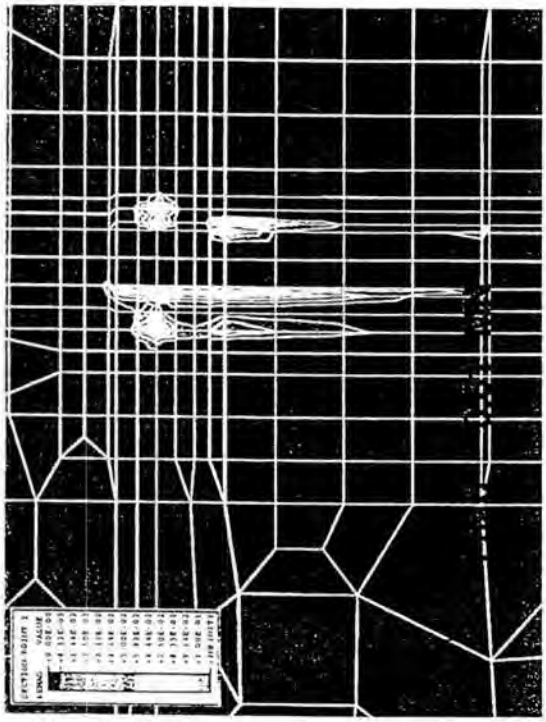

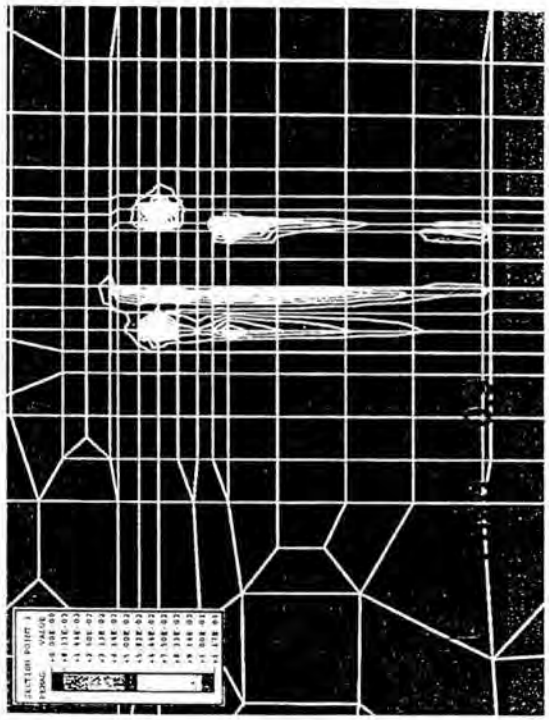

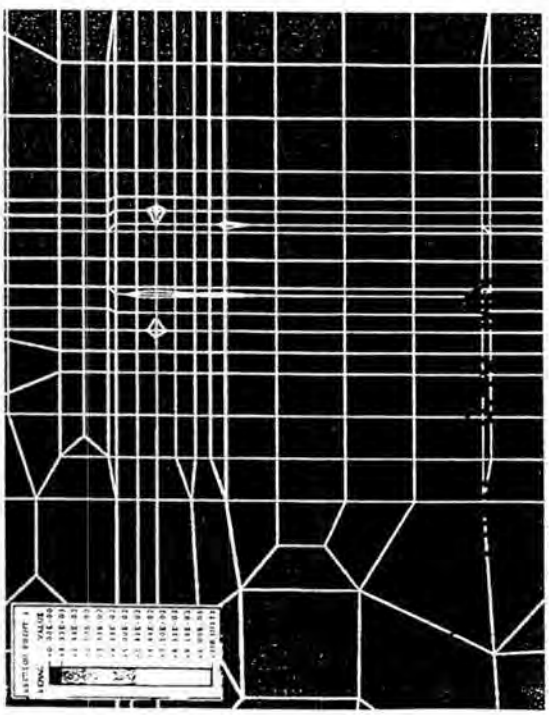

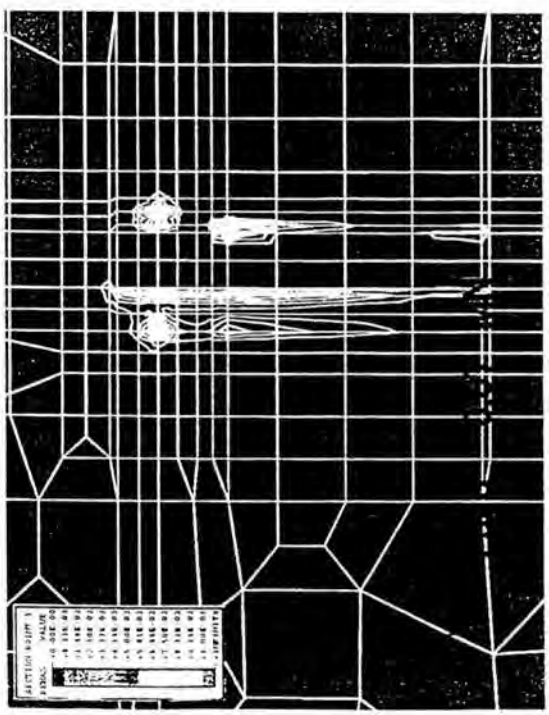

APPENDIX E

Fig. 8. Strain for points R2 and R4.

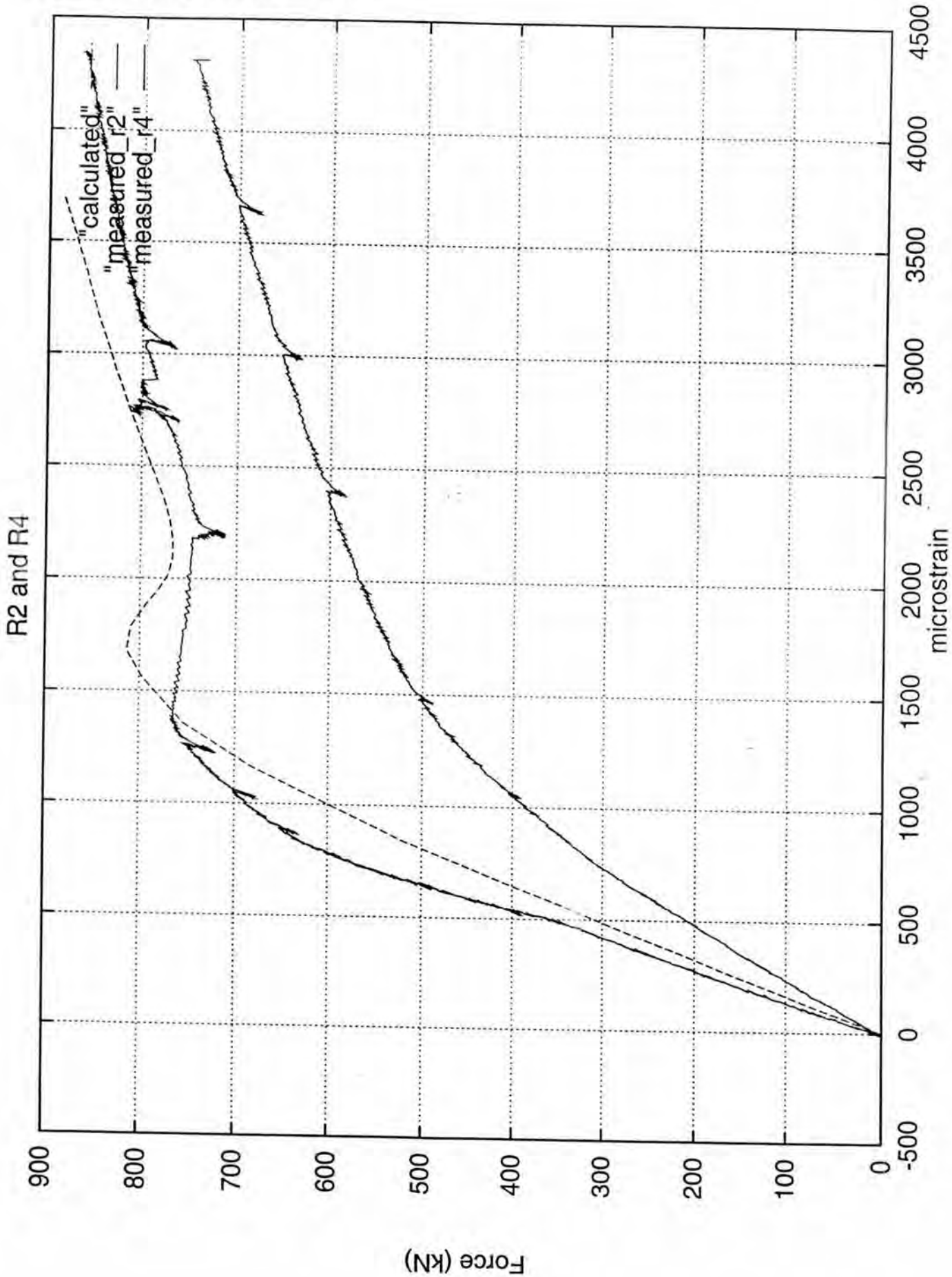

SUPPLEMENT No. 509

Häkkä-Rönnholm Eeva:

Investigation of paint systems from MV Estonia Visor Bottom Lock.

Research Report No. RTE57243/96.

VTT Building Technology.

Espoo 1996.

Requested by

The Joint Accident Investigation Commission of MV ESTONIA
Accident Investigation Board
P.O.Box 1
FIN 00131 Helsinki

Order

Chief Research Scientist Klaus Rahka, VTT, 4.12.1996

Contact person

Group Manager Eva Häkkä-Rönnholm
VTT Building Technology
P.O.Box 18011
02044 VTT
Tel. + 358 9 456 4930
Fax. + 358 9 456 7006

Task

Investigation of the paint systems from MV Estonia Visor Bottom Lock

Note: This report is a revised version of the research report RTE57243/96 dated 7.1.1997. In this revised version the layout of figures 1 and 4 has been changed, the locations of sampling have been pointed out and the views of the objects have been clarified.

Samples

Paint coatings from MV Estonia Visor Bottom Lock taken from:

- the Forepeak deck starboard lug (Royal Institute of Technology, KTH sample nr 4543) and

- the Visor lug (Royal Institute of Technology, KTH sample nr 4511)

The samples are presented in figures 1-5.

Paint sample taken from top face

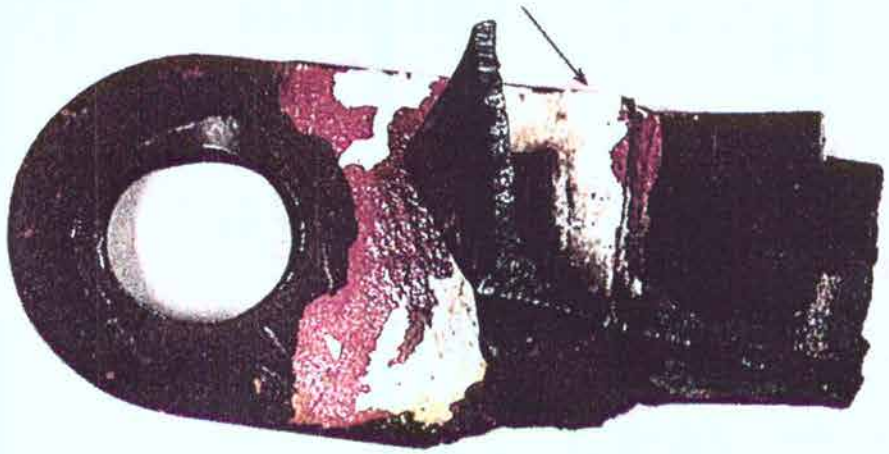

Figure 1. Visor lug, KTH sample nr 4511, view from starboard.

Figure 2. Visor lug, KTH sample nr 4511, bottom view.

Paint sample from top face

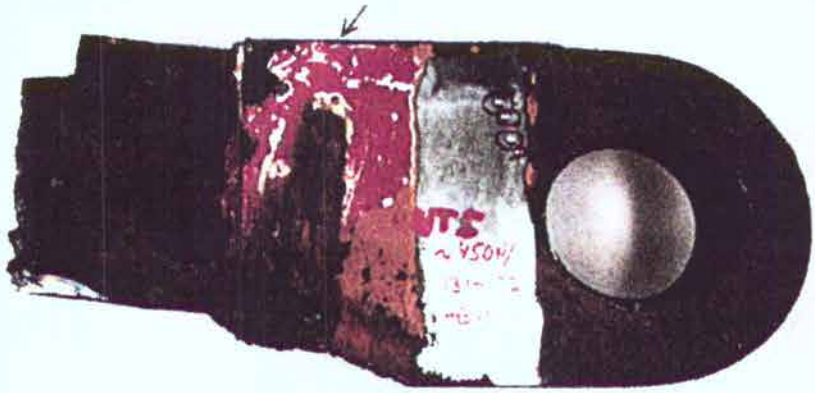

Figure 3. Visor lug, KTH sample nr 4511, view from port.

Paint sample 1

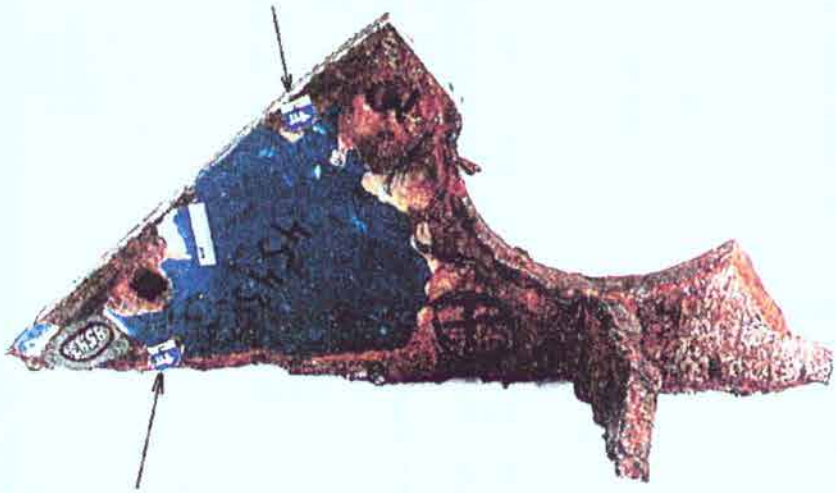

Paint sample 4

Figure 4. Forepeak deck starboard lug, KTH sample nr 4543, view from starboard.

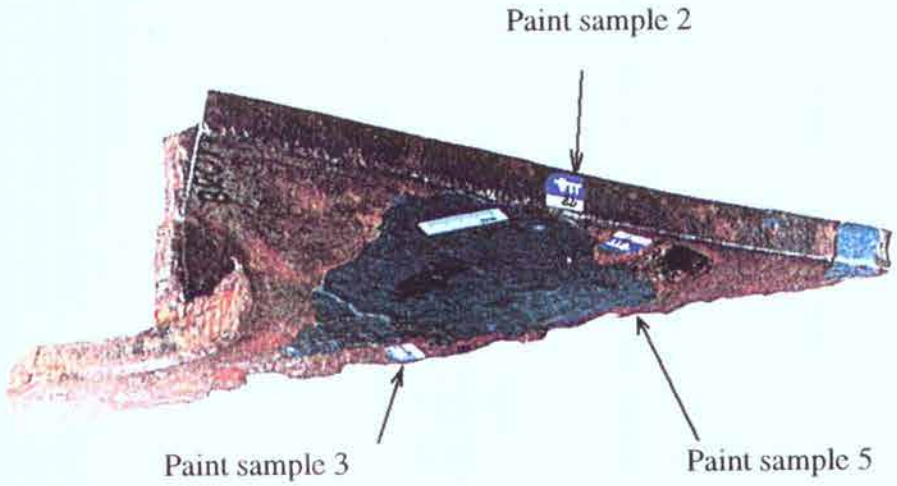

Figure 5. Forepeak deck starboard lug, KTH sample nr 4543, view from above aft port.

Performance of the task

Samples of paint coatings were taken at VTT from the surface of the Forepeak deck starboard lug and from the Visor lug. From the paint coatings cross section samples were prepared.

The cross sections were investigated by using stereomicroscope and Scanning Electron Microscope (SEM). The image of the cross section was prepared using the backscatter electron - technique (BSE). The BSE-image gives information of the composition of the sample: elements with small atomic weight show darker in the image and the higher the atomic weight, the lighter the appearance.

Analysis of the cross section was performed by using Energy Dispersive Spectrometry (EDS). The EDS-equipment was connected to the Scanning Electron Microscope. EDS gives qualitative and semi-quantitative analysis of the elements.

Research results

Forepeak deck starboard lug (KTH 4543)

The paint system consisted of several paint layers. Many of the layers were discontinuous. The shade of the partly flaked top paint of the coating system was blue. The underlying paint layer was of a slightly lighter shade of blue. White and red paint spots (splashes) were found on the surface. The white and red paint spots on the surface as well as cross sections of four pieces of paint sample from the Forepeak deck starboard lug were analysed.

- Forepeak deck starboard lug , paint sample 1

Six paint layers were found. The BSE-image of the cross section of the sample is given in figure 6 and the corresponding EDS-analyses of the paint layers are given in Appendix 1 in figures A1-1 to A1-6.

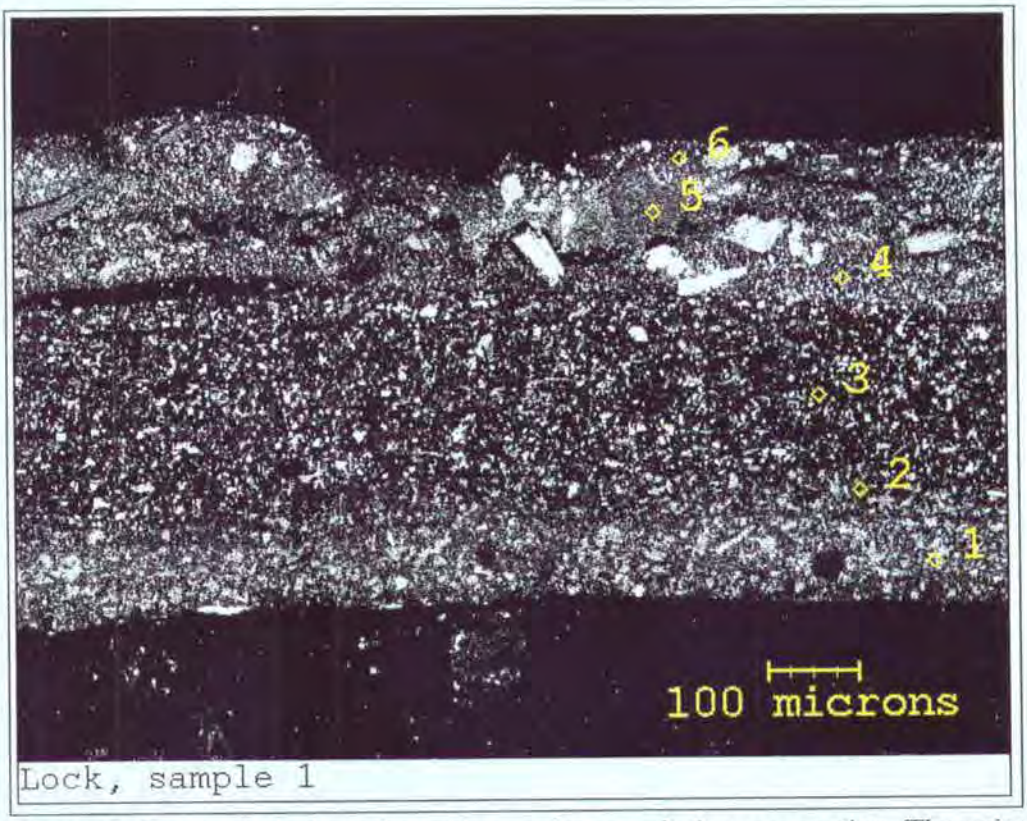

Figure 6. Forepeak deck starboard lug, paint sample 1, cross section. The paint layers and the analysis spots are numbered from 1 to 6.
Shades of the layers: 1-white; 2-grey; 3-blue; 4-red; 5-white; 6-blue

- Forepeak deck starboard lug, paint sample 2

Seven paint layers were found. The BSE-image of the cross section of the sample is given in figure 7 and the corresponding EDS-analyses of the paint layers are given in Appendix 2 in figures A2-1 to A2-7. According to the appearance and the results of the EDS-analysis the layers 4 and 5 seem to be identical.

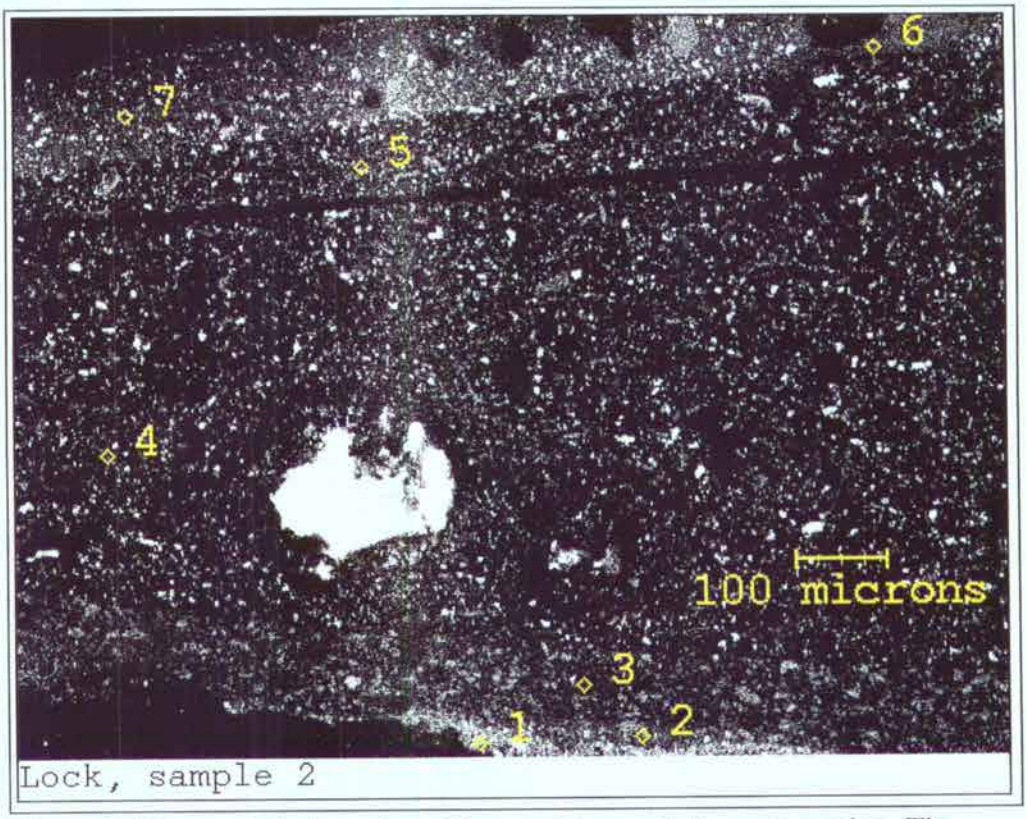

Figure 7. Forepeak deck starboard lug, paint sample 2, cross section. The layers and the analysis spots are numbered from 1 to 7.
Shades of the layers: 1-light brown; 2-white (discontinuous), 3-grey; 4- blue; 5-blue; 6-white (discontinuous); 7-blue. Black crevice between layers 4 and 5.

- Forepeak deck starboard lug, paint sample 3

Five paint layers were found. The BSE-image of the cross section of the sample is given in figure 8 and the corresponding EDS-analyses of the paint layers are given in Appendix 3.

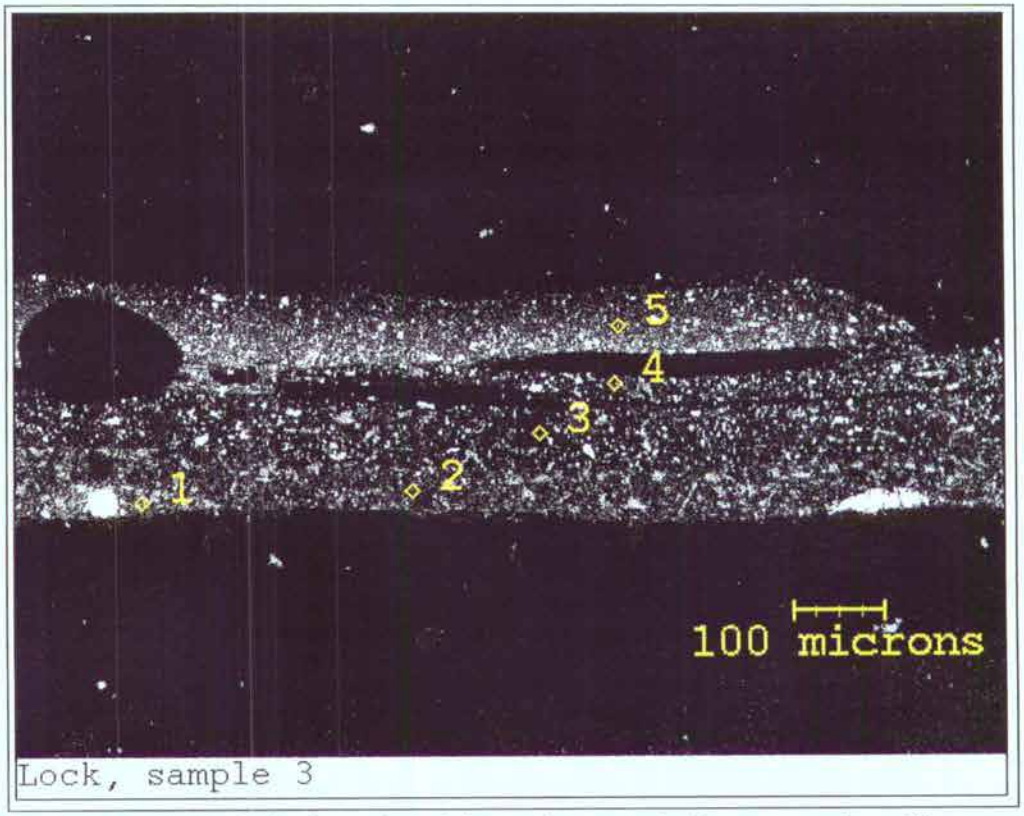

Figure 8. Forepeak deck starboard lug, paint sample 3, cross section. The layers and the analysis spots are numbered from 1 to 5.
Shades of the layers: 1-white (discontinuous), 2-grey; 3- blue; 4-blue; 5- blue.
Black crevice between the layers 3 and 4 as well as between layers 4 and 5.

- Forepeak deck starboard lug, paint sample 4

Four paint layers were found. The BSE-image of the cross section of the sample is given in figure 9 and the corresponding EDS-analyses of the paint layers are given in Appendix 4.

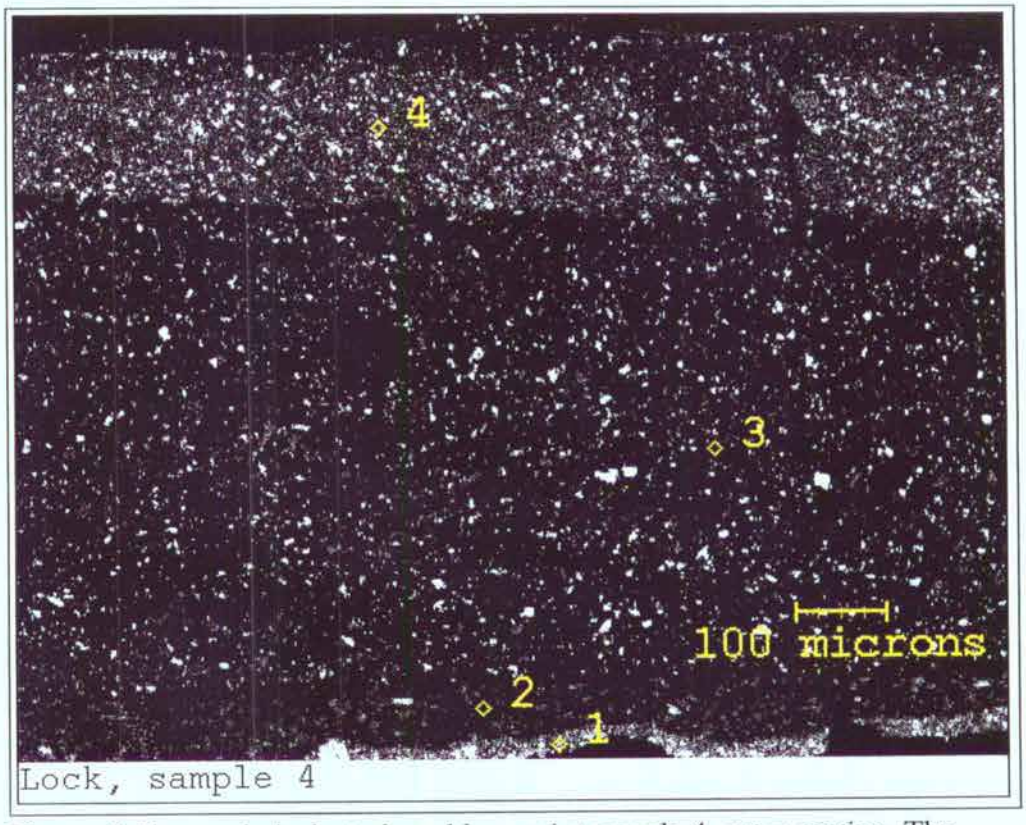

Figure 9. Forepeak deck starboard lug, paint sample 4, cross section. The layers and the analysis spots are numbered from 1 to 4.
Shades of the layers: 1-light brown, 2-grey; 3-medium blue; 4-blue. Black crevice between layers 3 and 4.

- Forepeak deck starboard lug, paint sample 5

Paint sample 5 was analysed for the white and red paint spots found on the paint surface. The results of the EDS-analyses are given in Appendix 5.
Stereomicroscope pictures of the paint splashes are presented in Appendix 6.

Visor lug (KTH 4511)

The BSE-image of the cross section of the paint system is given in figure 10. The layers found are marked from 1 to 9. Number 1 is the rust layer.

The paint system consisted of a multilayer coating with a very poorly adherent white top coat consisting of two layers (7 and 8 in Fig. 10).

The coating system under this loose paint layer had a red top coat (5 in Fig. 10). This red coating was built of two layers, some white paint (6 in Fig. 10) was seen here and there between these two red layers.

Some of the underlying layers where seen only here and there, for instance layer nr 9 was found only sporadically.

The EDS-analyses of the layers are given in Appendix 7.

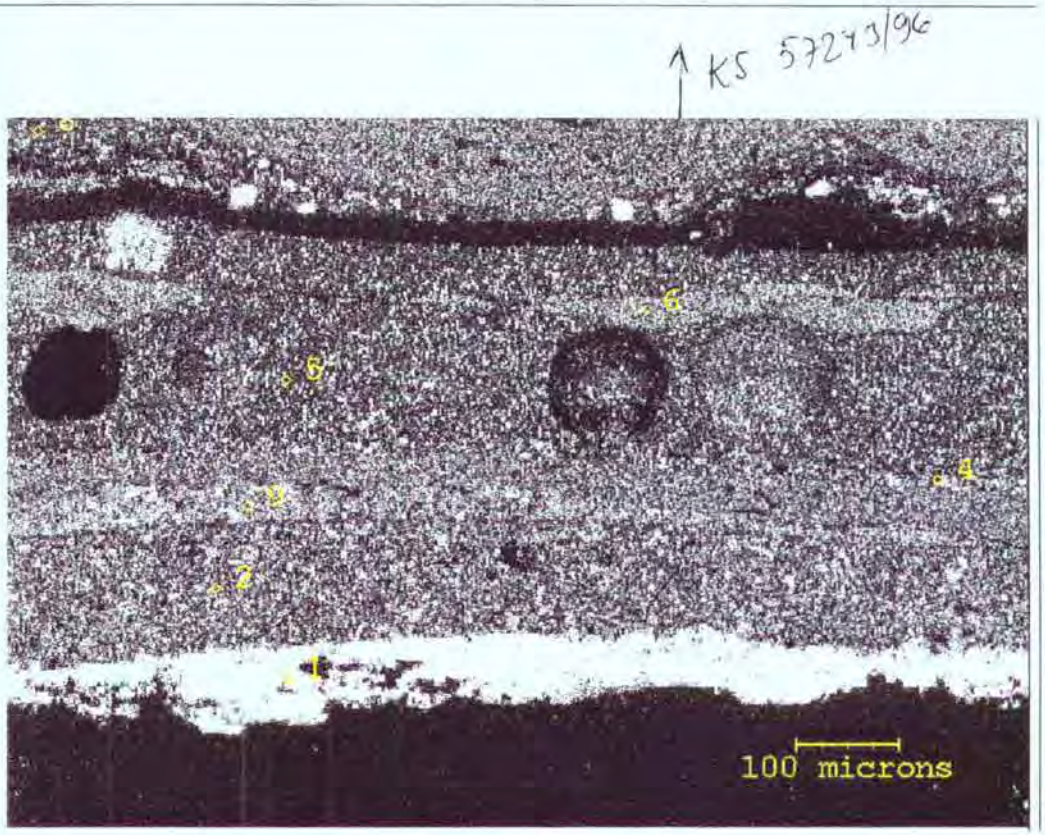

Figure 10 . Visor lug, paint system sample, cross section. Layer 1-rust; layer 2-yellowish; layer 3-white; layer 4-grey; layer 5-red; layer 6-white; layer 7-white; layer 8-grey; layer 9-light brown. Layers 8 and 7 were poorly adherent to the previous paint surface and rust was found underneath these layers.

Espoo 7.1.1997

Eva Häkkä-Rönnholm
Group Manager

Paula Raivio
Research Scientist

Appendices 7 pcs

Distribution

Accident Investigation Board	Original, copies 6 pcs
VTT	Original, copies 2 pcs

R6SU000172-167

SUPPLEMENT No. 510

Ingerma A. - Strizhak V.:

An Analysis of the Reasons of the Failure of the Locking Devices of MV Estonia.

Estonian Maritime Academy - Tallinn Technical University.

Tallinn 1996.

AN ANALYSIS OF THE REASONS OF THE FAILURE OF THE LOCKING DEVICES OF MV ESTONIA

A. INGERMA
V. STRIZHAK

ESTONIAN MARITIME ACADEMY
TALLINNN TECHNICAL UNIVERSITY

1996

Every technical expert study of an accident has the following main objectives:

1. To certify whether the design and calculations of the device/mechanism were correct;

2. To certify whether the construction of the device/mechanism was in accordance with the technical conditions (specifications);

3. To certify whether the regular technical inspections of the device/mechanism had been correctly arranged and carried out;

4. To present recommendations for the prevention of similar accidents.

The Technical Experts Group of the Joint Accident Investigation Commission of M/V Estonia consisted of the following experts at the Meeting of the Commission which took place in Stockholm on February 27-28 in 1996:

Estonia:

August Ingerma	Expert
Jaan Metsaveer	Expert

Finland:

Tuomo Karppinen	Member of the Commission
Klaus Rahka	Expert

Sweden:

Börje Stenström	Member of the Commission
Mikael Huss	Expert

Two opinions concerning the matter of strength and failure of the locking devices of MV Estonia were formed at the meeting of the Technical Experts Group:

Opinion No. 1 (Supported by J. Metsaveer, T. Karppinen, K. Rahka, B. Stenström, M. Huss):

The strength of the locking devices of the bow visor is estimated on the basis of static loads. The failure took place as a result of 2 - 5 overload, so it was a static failure. The fact that the ship had been in operation for 14 years is overlooked.

Opinion No. 2 (Supported by A. Ingerma, V. Strizhak):

The strength of the locking devices of the bow visor is estimated on the basis of alternating cyclic load. The failure took place as a result of cyclic load, i.e. it was a fatigue failure [1], hereby we also present the strength calculations of the side lock.

Arguments contradicting the concept of static failure:

1. The theoretical technical calculations [3, 4] and model simulations [5] and the measurements of the pressure of sea forces on the bow visor [6] contribute to the statement that there exists alternating cyclic load from sea forces to the bow visor. The greatest forces had the following range:

Horizontal force:	FX = 7.7 MN (770 Tons).
Side force:	FY = 2.7 MN (270 Tons).
Vertical force:	FZ = 7.7 MN (770 Tons).

The opening moment of the bow visor relative to the hinges was YM = 35.4 MNm.
During the 3 hours of experimentation conditions under which the opening moment induced by the sea load was sufficient to exceed the closing moment created by the gravity of the bow visor were observed approximately 50 times. This was at a significant wave height of 4.3 m and at the speed of 14.5 knots.

Conclusion:

THE LOCKING DEVICES WERE OPERATING AT AN ALTERNATING LOAD.

2. The failure of the locking devices and their components on MV DIANA II, the sister ship of MV ESTONIA on Jan. 16th, 1993. This failure is a classical example of fatigue failure, where the breaking originated from the weakest locking device -- the welds of the side locking devices.

Conclusion:

THE FAILURE OF THE LOCKING DEVICES WAS A FATIGUE FAILURE.

3. On the 3rd of January, 1994, an inspection of the locking devices on MV DIANA II was carried out [7].

During the inspection the following clearances were measured between the lockbolt and the eye:

'The Atlantic lock' -- 35 mm, aft direction;
stb side lock -- 20 mm, fwd direction;
portside side lock -- 40 mm, aft direction.

Such increases in clearances occur during operation only due to alternating loads.

Furthermore, the differences in the amounts and directions of the wear indicate that:

3.1. The distribution of load on the locking devices is not uniform. The distribution of the load cannot be determined as the entire locking installation is not statically determined.

3.2. Some of the welds of the locking devices are subject to pressure and some to traction as the expansion of the eye in the aft direction indicates the direction of the opening of the bow visor and the expansion in the forward direction indicates the closing direction of the bow visor.

Conclusion:

THE FORCES ACTING ON THE LOCKING DEVICES ARE OF INDETERMINATE VALUE AND DIRECTION I. E. A STATICALLY UNDETERMINED SYSTEM. INITIAL DAMAGE SUCH AS THE FORMATION OF A FATIGUE MICROCRACK AND ITS FURTHER DEVELOPMENT INTO A MACROCRACK IS POSSIBLE, WHEN THE SEALOAD IS DIRECTED TO CLOSE OR OPEN THE BOW VISOR, INDEPENDENT OF THE DIRECTION OF THE FORCE.

4. The edges of the lug of the Atlantic lock of the bow visor has clear traces of hammering (ledges caused by hammering) on both sides (3.7 and 4.3 mm) in fwd direction. Hammered ledges can only be caused by a great number of impacts between the bolt and the lug.

The expansion of the eye in the forward direction as much as 5 mm [8] and the existence of hammered ears indicates the existence of a numerous cyclic load in the closing direction of the bow visor. Cracks were discovered in the weld joint between the hinge beams of the bow visor and the support bushing.

In the expert opinion [11] the calculated failure load of the bow visor (given the failure stress σ_u = 400 N/mm^2) was 95 tons. It is also pointed out that the appearance of the fracture surfaces suggests that some welding repairs have been carried out and that the plate material of the lug of the side lock has a tendency of delamination due to the fabrication process. It is also pointed out in [11] that the actual load carrying capacity of the side locking device was therefore significantly less than the calculated value of the failure load of 95 tons.

The divers estimated the clearance between the lockbolt and the eye to be 10 mm [17].

Conclusion:

THE INCREASE OF THE CLEARANCES AND THE FORMATION HAMMERED LEDGES IS POSSIBLE ONLY IF THERE EXIST CYCLICAL IMPACT LOADS. THE SIDE LOCK HAS BEEN PREVIOUSLY REPAIRED BY WELDING AND THUS IT IS NOT POSSIBLE TO RULE OUT THE PRIOR EXISTENCE OF FATIGUE CRACKS.

5. The analogous failures of locking devices on RO-RO passenger ferries operating on the Baltic Sea indicate the existence of alternating cyclical loads and clearances between the lockbolts and the eyes. The clearances increase during operation accompanied by an increase in the lack of uniformity in the distribution of the load, causing the failure of the lock. The incomplete lists include 8 marine accidents involving Finnish and Swedish RO-RO ships (mainly passenger ferries) during the years 1973-1993 that were due to damage to the locking devices of their bow visors. Four accidents occurred within the year of the construction. The conclusion to be drawn from this is that the locking system with clearances used in Scandinavia (one bottom lock/Atlantic lock and two sidelocks) is too small and poorly designed due to the clearances, sooner or later resulting in damage or maritime accident.

Yet it has been pointed out that on 30% of the ships inspected the bow visor locking devices have cracks or deformations. We know that a crack is a tension concentrator with the factor 3÷50. This means that the further development of the crack (which is the load-carrying capacity of the detail) shall progress with force that is 3÷50 smaller. This proves once more that the attachment devices are operating under alternating loads and that the calculations should be made on fatigue strength. In the former Soviet Union (from 1975 onwards) the RO-RO type ships had a locking system without clearances - a forced locking system consisting of a screw and a nut - and the total number of locks was fourteen, of those ten bottom locks and four side locks. There is no information concerning damages to the locking devices. Estonian Shipping Company has four ships of this kind and they have all been in operation for 20 - 22 years.

Conclusion:

THE LOCKING DEVICE SHOULD BE A FORCED LOCKING SYSTEM WITHOUT CLEARANCES.

6. Neither the shipyard nor the Bureau Veritas have presented the strength calculations during design. Therefore the quality of the design can not be verified.

Conclusion:

EITHER THE STRENGTH CALCULATIONS WERE OMITTED OR, THE GENERAL LOW QUALITY OF CALCULATIONS MADE IT IMPOSSIBLE TO PRESENT THEM.

7. During the construction two vertical stiffeners were welded to the (back of the plating) of the lug of the side lock. Calculations are omitted.

The welding of such vertical stiffeners into the back plating of the eye of the side lock does not increase the load carrying capacity of the side lock neither practically nor theoretically, as the flow of force through the eye of the side lock and the plating of the eye goes through the weld joint. Thus the weld joint remains the weakest point of the flow of force.

The strength of a fillet weld joint is determined by the thickness of the thinner detail (t) determining the leg of the weld joint k (k = t). The thickness of the plating is the thinner part of the weld joint t = 8 mm. This is also the basis for strength calculations.

It can not be determined and is also irrelevant whether the failure takes place in the weld joint or in the plating metal.

Conclusion:

THE INSPECTOR EVALUATED THE WEAKNESS OF THE SIDE LOCK ACCORDING TO HIS OWN EXPERIENCE AND THE REINFORCEMENT WAS CARRIED OUT ESTIMATING BY EYE.

8. In expert studies [9, 10, 11, 12, 16] where the basis for evaluation is failure under static stress, the methods of classical strength calculation have been used. Thus the ultimate stress (σ_u) of materials was used as basis for calculations. Furthermore, the strength of weld joints as the weakest parts of a structure is calculated using the failure stress of the base material. The concentration factor K = 2.5...4.5 present in weld joints and the calculable failure cross-section (0.7 of the length of fillet leg) are not taken into account. Weld joints must be calculated at shear stress $\tau = 0.6\sigma$. The coefficient of safety for locking devices is not taken into account. The generally recognized foundations for engineering calculations are missing. The purpose of such calculations remains unclear. They should be included in the final report so that they can be applied and verified by everyone.

The expert studies [9, 16] is incomprehensible from an engineer's viewpoint.
The expert study [10] contains calculational errors.
The calculations in the expert study [11], where the remaining strength of the welds, with a prior crack, of the base of the attachment area of the hydraulic actuators, the concentration factor caused by the crack has not been taken into consideration.
Model simulations (mock-up) [12] of the side locks have been performed. The simulations were based on static traction and the obtained failure load is 870...2140 kN (87...214 tons). The strength calculations were not presented and can therefore not be evaluated.
These simulations result in comparative data on laboratory models. The results can not be transposed to reality as the mechanisms of static and fatigue failure are completely distinct and not comparable. It must also be taken into

consideration that the MV ESTONIA was in operation for 14 years before the shipwreck.

Conclusion:

THE THEORETICAL CALCULATIONS BASED ON THE SCIENCE OF THE STRENGTH OF MATERIALS DO NOT PROVIDE A BASIS FOR EVALUATING THE STRENGTH OF REAL LOCKING DEVICES.

9. The calculations of forces affecting the bow visor [3, 4] and experiments [5, 6] confirm their cyclical nature, causing the fatigue failure of the details of the locking devices.
The failure has the following phases:
I — the formation of a fatigue microcrack, the existence of which is not always possible to determine after the failure;
II — as the microcrack has a large concentration factor of K = 3...50 [13], further development of the crack will take place under lesser tensions/compressions;
III — final failure.

Weld joints are especially sensitive to alternating cyclical loads. In general practice the permitted shear stress of weld joints subject to cyclical alternating stress is τ = 50...90 N/mm^2 [14, 15]. Using the above values, we get the calculable [1] load bearing capacity of the side lock as the weakest locking device F = 88...159 MN (8.8...15.9 tons).

Conclusion:

THE SIDE LOCKS ARE UNDERSIZED (THE CALCULABLE FORCE BEING 100 TONS) BY A FACTOR OF 100/8.8...100/15.9 = 11.4...6.3.

10. As all of the above will give rise to a discussion with the proponents of static failure, it would be prudent to render a written critical evaluation on each of the points presented above.

Conclusion:

PLEASE SUBMIT A MOTIVATED EVALUATION IN WRITING.

11. FINAL CONCLUSIONS

Answers to the basic problems of the expert study.

1. Was the construction of the device/mechanism in accordance with the technical conditions (specifications).

As the locking system of the bow visor is a statically undetermined system, the distribution of forces on the locking devices is of indeterminate direction and magnitude.
The locking devices of the bow visor are subject to alternating cyclical load, thus the strength calculations should be made (to fatigue).
Strength calculations are absent from the design. The designed locking devices have clearances, the side locks are undersized.

Conclusion:

THE QUALITY OF THE DESIGN IS LOW, FAILURES ARE INEVITABLE.

2. Does the device/mechanism comply to technical specifications.

There is no data on weld joints. Actual dimensions are not in accordance with the drawings [2, p 23]. The gaps in the beams of the hinges were cut by welding.

Conclusion:

DURING CONSTRUCTION DRAWINGS WERE NOT ADHERED TO AND INEXACT TECHNOLOGY WAS USED.

3. Was the technical inspection correctly arranged and carried out.

There were no criteria or norms for the normal operation of the locking devices. The clearances in the locking devices on DIANA II were not paid attention to after Jan 16th, 1993 and after the incident with DIANA II the inspections were not extended to other vessels' locking devices. There was no information on analogous damages to other ships (7 incidents) on the Baltic Sea.

Conclusion:

THE IMPLEMENTATION OF TECHNICAL INSPECTIONS WAS INADEQUATE AND INCOMPETENT.

4. Recommendations for the prevention of similar accidents.

The use of locking devices without clearances, such as screw-mechanisms is recommended.

It is recommended to set forth criteria and norms for the normal operation of locking devices and to inform the IMO and the IACS of the failures of the locking devices and to carry out an analysis of the reasons of all the failures.

Tallinn, March 13th, 1996

August Ingerma

Professor, Ph.D
Head of the Chair of Port Management
in Estonian Maritime Academy

Viktor Strizhak

Professor, Ph.D
Mechanical Engineering Institute
Tallinn Technical University

SOURCES USED

1. A.INGERMA, V.STRIZAK. Expert Calculation of the Load-Carrying Capability of the Looking Devices of MV ESTONIA. Tallinn 1995
2. PART-REPORT, MV ESTONIA The Joint Accident Investigation Commission of Estonia, Finland and Sweden. April 1995
3. TUOMO KARPPINEN, ANTTI RANTANEN. MV ESTONIA ACCIDENT INVESTIGATION. Numerical predictions of wave-induced motions. Technical Report VALC53 VTT. Espoo, December 1995.
4. TUOMO KARPPINEN, SAKARI RINTALA, ANTTI RANTANEN. MV ESTONIA ACCIDENT INVESTIGATION. Numerical predictions of wave loads on the bow visor. Technical Report VALC106 VTT, Espoo, December 1995.
5. M.HUSS. Wave impact loads on visor of MS ESTONIA. 1995.
6. SAULI LIUKKONEN. The bow door wave pressure measurements of MS SILJA SYMPHONY Technical Report VALC138 VTT, Espoo, December 1995.
7. INSPECTION REPORT. TURBOTECHNIK Wilhelmshaven, 05.10.1994.
8. KLAUS RAHKA. Atlantic look visor lug measurements and analysis of MV ESTONIA. Working Report 1996-01-26 VTT.
9. JAAN METSAVEER. STRENGTH CALCULATION OF ATTACHMENTS OF THE BOW VISOR OF MV ESTONIA. Tallinn 1995.
10. KLAUS RAHKA. M/S ESTONIA STATUS REPORT ON "LOSS OF BOW-VISOR' FOR INTERNATIONAL COMMISSION per. 14.10.1994, 15.10.1994 VTT.
11. Strength Considerations Regarding the Locking Devices for the Ramp and the Visor. First Draft, Working Paper.
12. KLAUS RAHKA, KAJ KATAJAMÄKI, TUOMO KARPPINEN. STRENGTH ESTIMATION OF VISOR LOCKING DEVICES. VTT 1996-01-11 WR 9602.
13. R.E.PETERSON. Stress concentration factors. JOHN.WILEY AND SONS, N-Y 1974.
14. J.E.SHIGLEY, C.R.MISCHKE. Standard Handbook of Machine Design. NY Hebrew-Hill Book Company. 1986.
15. R.KRIIS, E.SOONVALD. Masinaelemendid IV. Keevisliited. Eesti Riiklik Kirjastus. Tallinn 1953. (Details of Machinery IV. Weld Joints)
16. JAAN METSAVEER. Calculation of Load-carrying Capacity of the Bow Visor Locks. Tallinn 1996

SUPPLEMENT No. 511

Rahka Klaus:

MV Estonia. Visor Damage and Visor Attachment Strenght Investigations at VTT.

Report VALB243.

VTT Manufacturing Technology.

Espoo 15.9.1997.

VTT MANUFACTURING TECHNOLOGY

MV Estonia Visor Damage and Visor Attachment Strength Investigations at VTT

Report VALB243

Klaus Rahka

Espoo, Finland
15.9.1997

A Work report	
B Public report	x
C Confidential report	

Title of report
MV Estonia Visor Damage and Visor Attachment Element Investigations at VTT

Client/sponsor of project and order The Joint Accident Investigation Commission of Estonia, Finland and Sweden/Board of Accident Investigation, Ministry of Justice - Finland	Report No. VALB243
Project STONE	Project No. VAL4354
Author(s) Klaus Rahka	No. of pages/appendices 43 p.

Keywords
MV Estonia, visor, attachments, strength, materials, damage

Summary
Fractures of the MV ESTONIA visor attachments have been investigated and the strengths of individual attachments were estimated based upon testing full and sub scale models. A simplistic system using rules of statics was defined to estimate load levels at individual attachments as caused by wave loading according to model test results obtained elsewhere (the SSPA-Gothenburg tests).

Date Espoo 15.9.1997

Kenneth Holmberg
Research Manager

Klaus Rahka
Chief Research Scientist

T.K.
Checked

Distribution:
Client, 2 + 30 copies
VTT Manufacturing Technology/VAL6, 4 + 6 copies

VTT Manufacturing Technology
Operational Reliability
P. O. Box 1704
FIN-02044 VTT
Finland

Phone: +358 9 4561
Telefax: +358 9 456 7002
E-mail: Klaus.Rahka@vtt.fi
WWW: http://www.vtt.fi/manu/

Foreword

The investigations reported in this paper have been performed as part of research carried out to clarify the causes of the sinking of MV ESTONIA in late September 1994. The hypothesis of the casualty to have been initiated primarily by failure of the bow visor attachments due to their structural weakness compared to wave loads to the bow has been investigated by observations and material identifications of authentic parts as well as modelling by calculations as supported by model testing.

The efforts reported have been defined in the course of work of the Joint Accident Investigation Commission of Estonia, Finland and Sweden to which the writer was assigned as an expert of material and structural integrity issues.

I want to thank all experts and Commission members for their contributions to quantify the level of load carrying capacity of the bow visor attachments of MV ESTONIA. It is hoped that some untraditional solutions presented in this report will meet interest and provide some contributions to discussion among experts and engineers in the trade and elsewhere.

Espoo, August 1997

Author

Table of contents

1 Introduction

The MV Estonia sank during the early hours of 28 September 1994 in heavy weather in the northern Baltic Sea. All visor attachments were found to have broken and separation of the visor from the ship had occurred. Opening of the second water barrier of the bow, i.e. the bow loading ramp had followed as caused by interference with the visor leading to water entry to the automobile deck leading to considerable list. Capsizing of the vessel had resulted when upper decks were also flooded when doors and windows higher up had allowed water to enter.

Here we report on observations of damage, structural features and strength investigations of locking and lifting cylinder visor attachments. Some investigations of hinges have also been carried out.

The investigations include an approach to assessing visor attachment loading levels when the visor is loaded as measured during model experiments. Characterisation of fractures and deformations of authentic visor locking element related parts from the MV ESTONIA and model tests. Some relevant visor locking related structural elements from the near sister ship MV Diana II have also been ivestigated. Calculations were formulated and some fitted parameters used to analyse test results regarding attachment strength in order to obtain realistic estimates of actual attachments slightly deviating from the models. Side lock visor lug sites and the hinge bushing installation were also modelled by FEM (Finite Element Method) in other part-projects (VTT Technical Report VALC-246, Kaj Katajamäki and VALC-312/8.4.1997, Jukka Airaksinen), the results of which are also used in the estimation of the actual side locking strength. Bottom lock mock-up test results obtained by the Technical University of Hamburg were used together with hardness measurements of the authentic pieces for assessing the structural strength of that lock.

2 General information about performed investigations

Fracture morphologies of the MV ESTONIA visor attachments suggest that static type of ultimate strength is the practically relevant characteristic according to which release of the visor had occurred. Therefore - but not excluding e.g. the closely related low cycle fatigue requiring loads exceeding cross section yield limits - the investigations reported here have focused on determination of a realistic upper bound strength of the visor attachment system. Individual strength estimates are all based upon testing either complete full or sub size models (lockings) or testing parts of authentic components (hinge weldments and platings). All strength experiments performed have been done under monotonically increasing load up to failure of respective test piece and calculation parameters have been introduced to "calibrate" the calculation models accordingly. Features of the fractures as found have been examined on a minimum principle not striving for an exhaustive investigation. Specimens have been stored for availability to further interests. Wave induced loads as measured at a single support of a model visor have been recalculated to identify load levels at five primary attachment locations. It is believed that the extent of the investigation is sufficient for the conclusions that

it has been fully possible for the visor to have broken loose while the ship's bow has submerged into a wave to a depth less than needed to immerse its weather deck into green water.

3 Geometrical features, visor attachment loading and visor detachment scenarios

To help assessing a realistic way that the visor could have been detached from the bow of MV ESTONIA, a summary of the geometry of the visor and its attachment locations is presented. Load distribution onto the various attachments was estimated using simplistic representations of moment and force equilibrium and experimental information on wave induced lifting, pushing and sideways translating loads positioned to cause the resulting and measured opening, yawing and twisting moments that act to rotate the visor around its horizontal transverse, vertical and horizontal longitudinal axes. The shape of the visor and its attachment configuration were not accurately accounted for. Instead this shape effect is included in the parametric study that an assumed variation of the wave load centre of action implies.

3.1 Visor geometry

With reference to Figure 1 - using coordinates adopted by e.g. SSPA for reporting the wave load model tests with the origin about 8.5 m above still water level in the centre between the visor hinges -

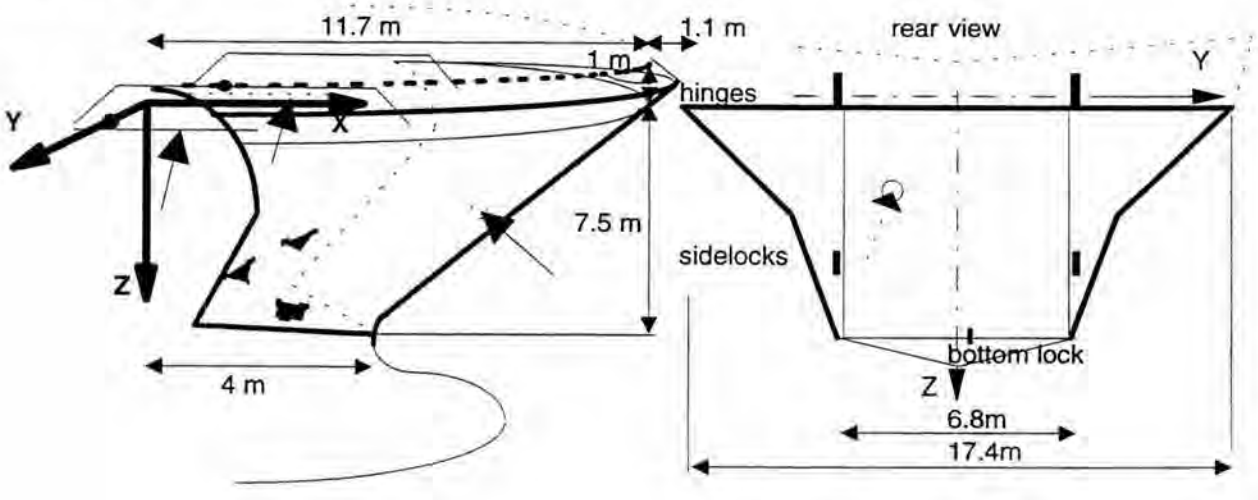

Figure 1. Bow of MV ESTONIA with visor and associated lockings.

the stem of the visor stretches approximately from X = 4 metres at Z=7.5 below the hinge axis or 1 metre above the still water level to X = 11 metres at -Z=1 metre above the hinge axis level. The largest width of the visor was Y = ±9 metres at X = 2.85 metres forward of the hinge axis at its upper aft edge at weather deck (Z = 0 metres at the hinge axis) and at the low end of the aft plating Y = ±3.4 metres at X = 1 metre and Z = 6.5 metres or 2 m from the still water level. At Z = -2 or 2 meters above the weather deck, a bulwark about +1,5 m high in its aft end and 1 m high further forward rose above the hinge level. The bulwark is more

vertical than the visor shell plating in its aft parts. In the plane normal to the stem and containing the hinge axis, the visor shell plating curvature is approximately a circle with a radius of 7 metres and leaning 45 degrees forwards. In this plane through the hinge axis the aft edges of the visor shell plating are at X = Z = 2.85 metres at their extreme at about Y = ±6 metres but the aft edges of the visor are drawn further back both below and above this location. The stem leans about 45° forwards. The flare of the visor shell plating is about 45°, except on the lower aft sides, where the side shell plating is somewhat steeper due to the passage to the car deck. Higher up the flare is 45° also here. The flare in the lower extreme is wider than 45 degrees Attachment coordinates are given in Table 1.

Table 1. Locations of visor attachments. Ref to Fig 1.

	X	Y	Z
Hinges	0	±3.4	0
Side locks	1.15	±3.4	4.3
Bottom lock	1.5	0.4	6.7
Lifting cylinder to hinge beam	1.3	±3.4	0

3.2 Forces and moments acting on the bow visor and their theoretical relationship

Forces and moments acting on the visor have been measured in straight head and oblique bow seas at the SSPA model test basins. Simulation for estimation of the lifting load for head seas has also been performed (work performed at VTT-Manufacturing technology). Measurement results were given as a set of force and moment components acting in a point centred between the hinges.

The force components are the longitudinal Fx (head load, positive forwards), transverse Fy (positive to starboard) and vertical Fz (positive down) of the resultant of the acting bow load. The components of the acting moment are the opening, yawing and twisting moments (My, Mz and Mx) about the horizontal transverse hinge axis (My about Y coordinate-axis) and vertical and horizontal longitudinal "axes" through the hinge centre (yawing Mz about Z-axis and twisting Mx about X-axis). These had been obtained in basin tests using a model of MV ESTONIA. The model visor had been supported on the model vessel by one single attachment composed by force and moment transducers.

The position of the line of the resultant of wave load action - giving one condition of the hydrodynamic centre of the visor - (X;Y;Z) is algebraically defined as follows:

Mx = Fz*Y - Fy*Z

My = Fz*X - Fx*Z

Mz = Fy*X - Fx*Y

From Mx: Z=Y*(Fz/Fy)-Mx/Fy,
From Mz: X=Y*(Fx/Fy)+Mz/Fy , which yield
My = (Fz/Fy)*Mz+Y*(Fx*Fz/Fy)-Y*(Fx*Fz/Fy)+(Fx/Fy)*Mx, that is

My*Fy = Mx*Fx + Mz*Fz

The three equations combine into the single condition as given in the box tying force and moment components together.

Measurements reported indicate that Fx is about as large as Fz. Fy is up to about 1/3 of Fx. Thus (Mz+Mx) is ≈ My/3. In (straight) head sea the load is symmetric at port and starboard causing Fy and Y to become 0. The twisting and yawing moments Mx and Mz and Fy thus occur only in oblique bow sea. With the above information the position of the load action line is unambiguously defined. However, the actual position of the wave centre of action on this line - the hydrodynamic centre of the visor or the value of (X;Y;Z) containing the information of visor shape - lacks accurate definition. Therefore, a parametric presentation of attachment reactions has been developed where the varied parameter is the X-coordinate of the wave centre of action, the origin (X = Y = Z = 0) being on the hinge axis midway between the hinges. Y and Z are defined by the measured ratios of force components and moments, i.e. the Fy/Fres-ratio and the ratio of Fx/Fz and also Mz/My. Mx follows from the others as accounted for above.

3.3 Measured values of force and moment components

Force and moment components obtained from model tests as performed by SSPA (Gothenburg, Sweden) are shown in Figure 2 together with a best estimate equation describing their relationship. Here the force is Fzx=Fx*1.414=Fz*1.414. The mean trend and its standard deviation are given in the graph. The fitted equation is by the present author for use only within the range of given data.

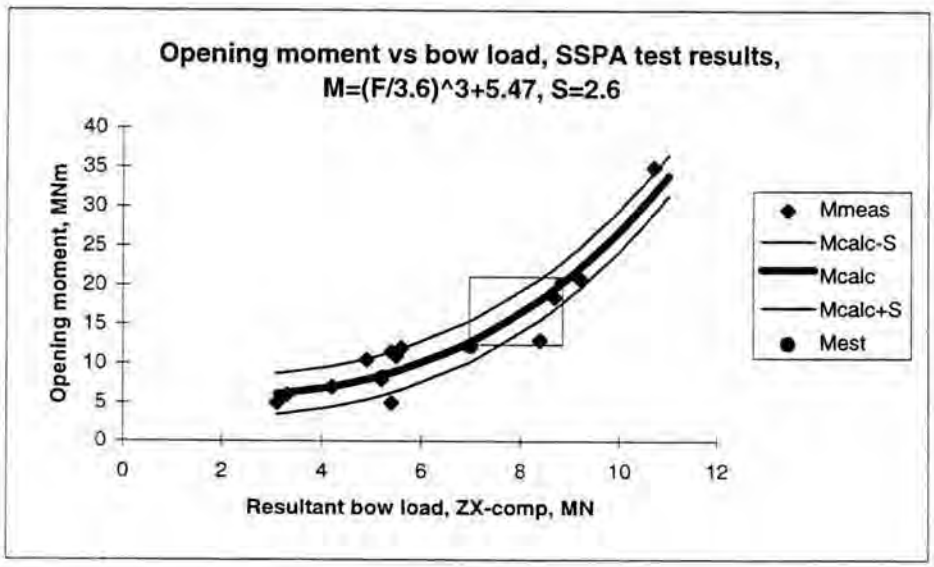

*Figure 2. The interrelation of the measured bow force and opening moment. Estimated critical range 7 to 9 MN indicated. Force is component Fzx in ship's longitudinal plane, Fzx=Fx*1.414=Fz*1.414.*

The experimental and sufficient (ch 3.2) independent relations regarding the basic force and moment components as used in the following are

Fz/Fx = 1 and Mz/My = 0.1 and Fy/Fres = 0.23.

3.4 Distribution of bow load onto visor lockings

There were five "engaged" attachments for the visor and additionally two lifting hydraulic cylinder systems connecting the visor to the hull. Two hinges supported the upper aft, two side locks the lower sides and one bottom lock was installed to secure the visor bottom in a location close to the aft centre of the visor lower extreme.

In calculating the reaction loads at the individual five actual attachment sites basic principles of statics have been employed. Thus the positions of the attachments and an assumed bow load action centre are input parameters in the analysis. A distance related part of structural stiffness of the visor is included in the reaction estimation. Due to the high number of attachment points the visor attachment system is statically undetermined and some load or moment sharing need to be taken as parameters. Here it turns out that only the opening moment needs to be shared by an assumed portion by the side locks and the bottom lock. The twisting flexibility may influence the relative reactions at the two side locks on the one hand and the hinges in carrying the net effect of the transverse component Fy of the bow load. Based upon visor and seal stiffness measurement results the stiffnesses of the individual attachment sites are taken to be much higher than the global stiffness of the visor, such that no evening of reactions (actually shift of load from side locks to hinges in order to maintain global balance) actually occurs between the two visor sides or upper and lower parts.

Load reactions were assigned to each attachment according to their relative distances from each other and the load action centre. This gave a system directly in balance both as to their direct sum as well as the reactive moments. The reactions are therefore determined only by the relative positions of the action centre with respect to the positions of the attachments. The calculations have been performed for a positive opening moment only, idealising the visor as a pivoting beam structure as illustrated in Figure 3.

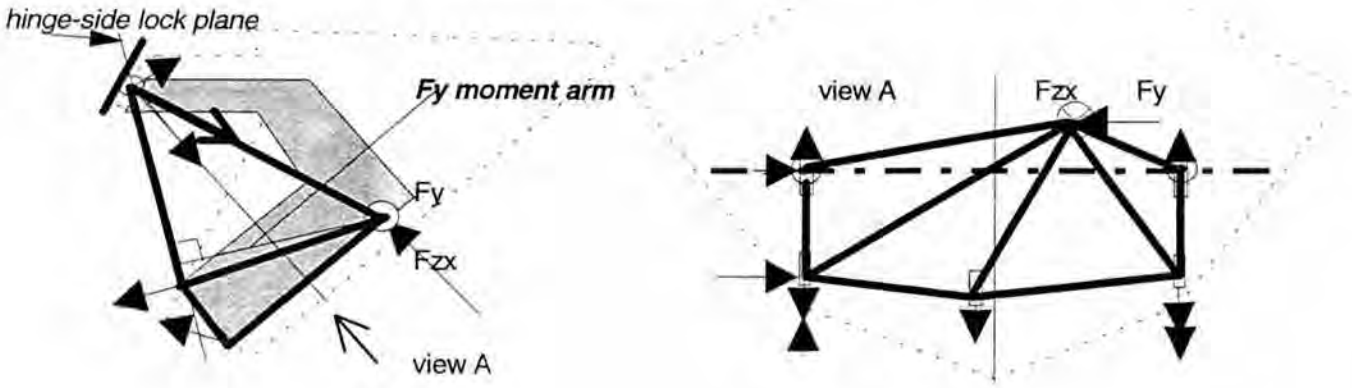

Figure 3. Side view of visor idealization as a rocking beam structure for attachment load calculation. Acting load components Fzx and Fy indicated by lettered arrows, some of the reactions by arrows only.

The position of the moment arm for the transverse force component Fy should be noted as this will bear upon how the attachment reactions depend on the position of resultant wave action. As this moment arm does not point to the hinge axis a load action centre independence is not obtained. No part of load is assumed to be taken to deform the visor.

In the force distribution scenario under an opening moment, direct load reaction is taken by the hinges only and opening moment is resisted by pull in the lockings. Push in a lock may be induced by sufficient effect of the sideways transverse load Fy. The total hinge reactions will include locking reactions also as the hinges are the centre of support of the visor structure - effectively a simply supported swing. Visor lock take no direct side reactions as locating horns are provided for this purpose. Reactions at locating horns at the side locking sites will also respond to the twisting and yawing moments and help the hinges to hold the visor from moving sideways. Here we assume that the lockings have some play and are flexible in the vertical direction so as to minimise vertical reaction, passing that onto the hinges. The solution may be an extreme value solution in so far as visor stiffness is not assumed to even out any reactions. The flexibility of the visor is high and suggests no effect of visor stiffness.

Sharing of opening moment reaction between the bottom and side locks is unknown. A base-line calculation has been done for 50/50 sharing of the opening moment by side locks vs bottom lock. The slight starboard location of the bottom lock may influence, and can – as one value shown in the equations – be allocated with 44% of the total according to its sideways location on starboard of the ship's keel ((3.4-0.4)/6.8 = 0.44) leaving 56% (0.56) to the side locks.

Sharing of the side lock reaction to the opening moment between port and starboard is obtained to be proportional to the sideways distance of the bow force action centre or the Y-coordinates of the lockings and the point of bow load action (X,Y,Z). For any oblique bow waves the action centre is obtained to be located Y metres from the ship's centre line to the wave encounter side, leading to sharing in proportions of (3.4-Y)/6.8 and (3.4+Y)/6.8 between starboard and port of the share of the total opening moment left over by reaction at the bottom lock. For port wave encounter pull will intensify on port. Y = Fy/Fx*(X-Xo) is obtained, where Xo = Mz/Fy.

In addition to pulling hold against the opening moment, any position of the action point forward of the hinge axis causes a yawing moment by the transverse Fy-load. The related reaction is a force couple pair acting in ensemble at the side locks and the hinges. The moment arm of Fy is the distance (length of normal) from the assumed action point to the hinge-sidelock plane. This induces an added pulling reaction at the port side lock and a tension relieving reaction at the starboard side lock (if the flexing of the visor and play in the lock admits, this could create even a pushing load at starboard) causing no change in the holding against the opening moment. The port side lock will experience severe pull compared to its strength and will break asking for least load to the bow (as the reader can deduce having noted the strength of the p-side lock reported later). This failure will cause relief of holding against the opening moment at the side locks and thus addition of some extra tensile reaction to the bottom lock will occur as demanded by hold requirement against the opening moment.

If the starboard side lock were not forced into a pushing reaction from the ship due to play in the lock, the opening moment reaction occurring at the bottom lock could also change, but this has not been assessed here. The total reaction in the port side lock may simply become as shown below, Figure 4. Transverse side support is provided by locating horns close to the side locks and by hinges in proportions of (a/(b-a)).

It may be found that wave action centre locations taken to be realistic seem to cause the port side lock to break at a load level lower than that needed to break the next attachment.

Pull in side locks (for stb replace +:s by - in F_{psl} eq):

$$M_y = ((Fzx/3.6)^3+5.47+s*2.6);$$

$$F_{psl} = My*0.56*((Y+3.4)/6.8)/4.45$$

$$+ 0.23Fzx* S (a/b)/6.8$$

$$-0.15$$

opening moment reaction share for port side lock

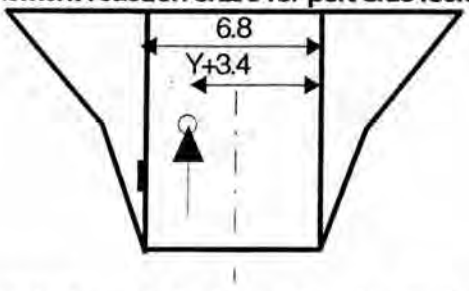

where -0.15 MN is approximately the side lock reaction due to the weight of the visor and the side lock force couple responding to the transverse force Fy = 0.23 Fzx is obtained through calculating:
The moment arm S for Fy is obtained according to the following:

a = Z*b/4.3 +
+(X-Z*1.15/4.3)*1.15/b

b = 4.45

S = (X-Z*1.15/4.3)*4.3/b

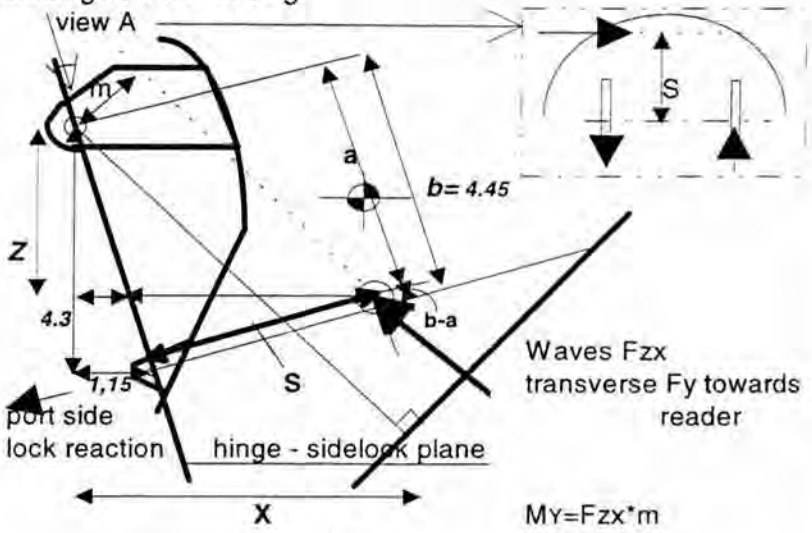

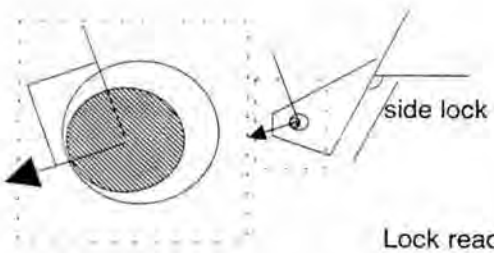

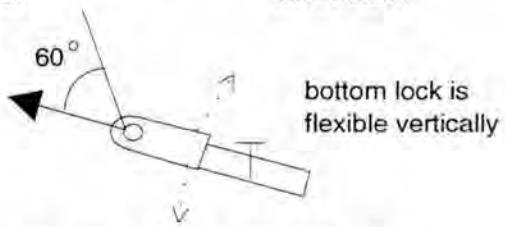

Lock reactions directed due to local play and local vertical flexibility

Figure 4. P-side lock load and visor dimensions in calculation of port side lock reaction to opening and yawing moments (transverse load component).

The following analysis given in Figure 5 deals with the load in the bottom lock also including this situation.

***The tensile load F_{bl} in the atlantic (bottom) lock** is estimated as:*

$M_y = (Fzx/3.6)^3 + 5.47 + s*2.6$

$F_{bl} = 0.44My/(6.82\sin 60) +$

-0.3

0.3 = visor weight support reaction

If port side lock breaks add: (0.23*Fzx*S*(a/b)/6.8)*4.45/6.82

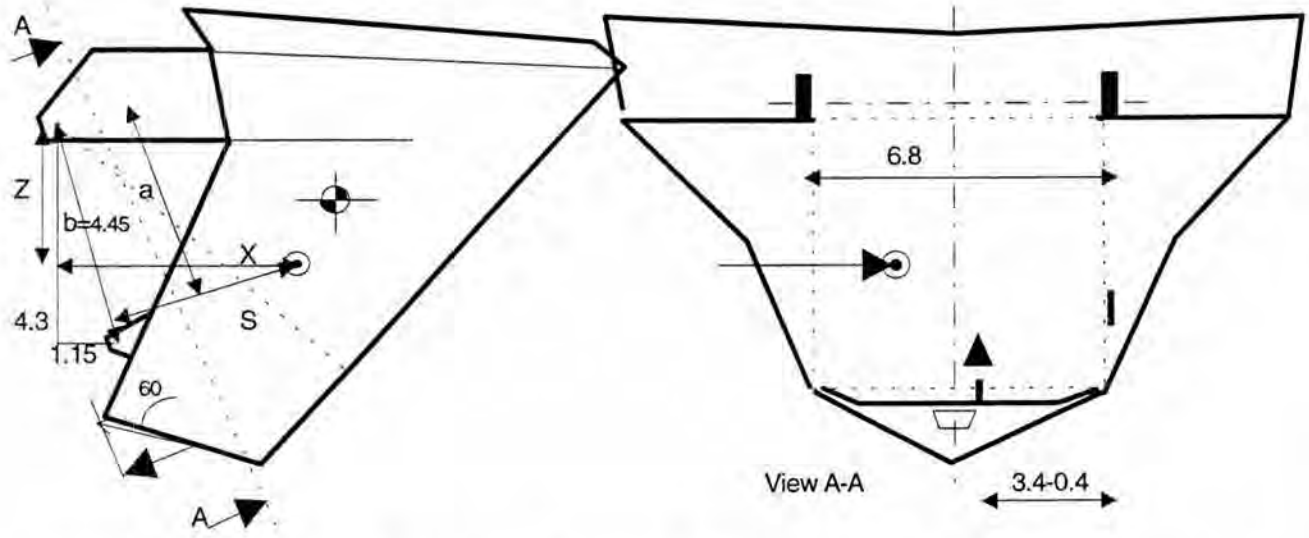

Figure 5. Bottom lock load and visor dimensions in calculation of bottom lock reaction to opening and yawing moments (transverse load component) after p-side lock failure.

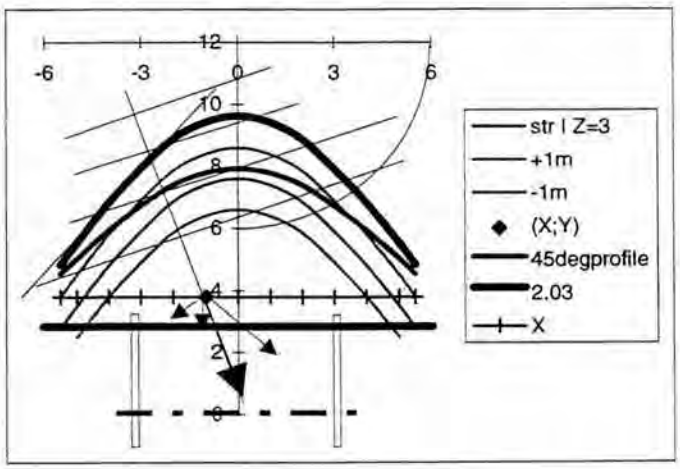

Figure 6. Horizontal sections of the visor in the vicinity of the wave load action centre (X;Y) indicating visor shapes through Z = 0.93 m below hinge axis and at stringer I (Z=3m) and str I ± 1m. Approximate actual visor shape in hinge plane perpendicular to stem also indicated showing also projection of line of wave load resultant for 30° oblique wave.

A schematic presentation of the visor profiles in the region of one assumed point of wave action centre for X = 3.8 metres is shown in Figure 6.

3.5 Loads on hinges

As the loads on the lockings react as aftwards tension to resist opening of the visor, the loads on the hinges will act as forwards and down directed support loads. The external and the lock reactions will thus be supported at the hinges. Thus the load components of the external load and the reactive tension in the bottom lock may be divided between the hinges in proportion to their transverse distances from the respective points of load action. The side lock reactions – as they occur at the same Y-coordinates as the respective hinges will add directly to the hinge on the same side as the respective side lock. In the asymmetric case of the port side lock having broken, some of the twisting and yawing moment will have to be balanced by small additional force couples at the hinges. These will be in the magnitude of 0.03 to 0.2 MN and will affect the hinge load levels only marginally.

3.6 Result examples

Results from visor attachment load calculations performed using the above methodology are presented in the following Figure 7a..

The bow load levels covered are 5, 7 and 9 MN and the mean value of opening moment was used. Calculation results are given for five positions of wave load action identified as "calc points" 1 to 5:

1. a point behind the visor encompassed volume or the only possible location of wave action on the ship's centreplane (Xo,0,Zo).

2. a point on the visor's aft plating (X = 2.85 m)

3. a point forwards of the visor's aft plating which yields the load on the sb side lock to become 0 from having been tension for the previous location of wave action centre

4. a point on a transverse line through the visor that bissects the horizontal cross section area of the visor

5. a point on the visor shell plating marking the forwardmost point where the line of load action enters the visor volume

The situation after p-side lock failure is displayed in the subsequent Figure 7b.

The calculation results indicate that the reactions at the visor side attachments obtain an increasing value as the point of wave action is assumed to lie more forwards. This sensitivity of the reactions to the position of the bow load action centre is essentially a result of the property of the geometrical layout of the attachment system which sets the condition for the choice of moment arm for the transverse Fy-load component. Had the visor been locked by a centrally positioned bottom lock only, sensitivity of reaction to bow load action centre would not have occurred. This is also evidenced by the b-lock load for the "all intact"-case. The side lock load is most sensitive to the assumed position when all attachments are holding. In port wave encounter the weakest of the locks – the p-side lock – is expected to break first leading to redistribution of reaction mainly to the bottom lock with some relief of load at the hinges.

All intact Fres=5.00 My=7.94 Xo=0.898 Fz=3.44 Fractions of Fres

calc point	X	Fphi-69	Fphi+21	Fshi-69	Fshi+21	X	Fpsl	Fssl	Fbl
5	6.150	0.65	0.43	0.19	0.18	6.150	-0.29	0.18	-0.08
4	4.890	0.59	0.40	0.24	0.21	4.890	-0.20	0.08	-0.08
3	3.300	0.52	0.36	0.32	0.25	3.300	-0.11	0.00	-0.08
2	2.850	0.50	0.35	0.33	0.26	2.850	-0.09	-0.02	-0.08
1	0.898	0.42	0.30	0.42	0.31	0.898	-0.05	-0.07	-0.08

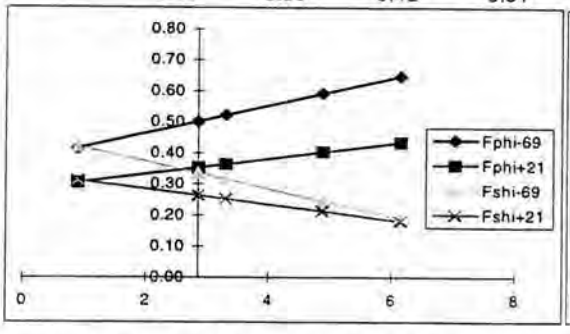

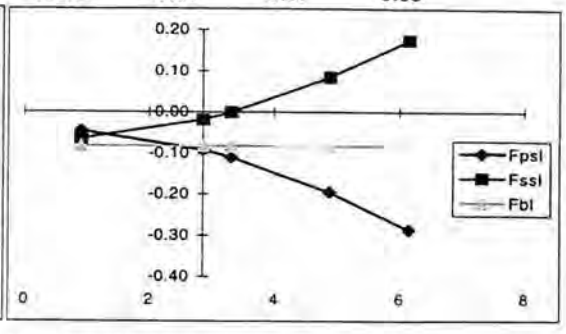

All intact Fres=7.00 My=12.25 Xo=0.989 Fz=4.82 Fractions of Fres

calc point	X	Fphi-69	Fphi+21	Fshi-69	Fshi+21	X	Fpsl	Fssl	Fbl
5	6.250	0.68	0.47	0.22	0.20	6.250	-0.32	0.17	-0.11
4	4.970	0.62	0.43	0.27	0.23	4.970	-0.22	0.07	-0.11
3	3.700	0.56	0.40	0.33	0.26	3.700	-0.15	0.00	-0.11
2	2.850	0.52	0.38	0.37	0.29	2.850	-0.11	-0.04	-0.11
1	0.989	0.44	0.33	0.45	0.34	0.989	-0.06	-0.09	-0.11

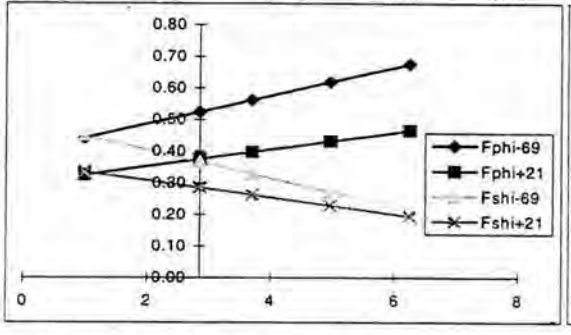

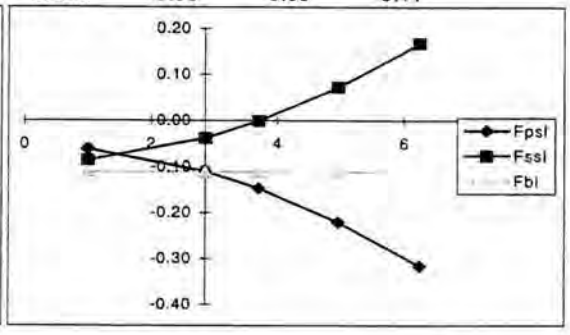

All intact Fres=9.00 My=19.87 Xo=1.248 Fz=6.19 Fractions of Fres

calc point	X	Fphi-69	Fphi+21	Fshi-69	Fshi+21	X	Fpsl	Fssl	Fbl
5	6.550	0.70	0.53	0.24	0.23	6.550	-0.37	0.16	-0.16
4	5.190	0.64	0.49	0.30	0.27	5.190	-0.26	0.05	-0.16
3	4.430	0.61	0.46	0.34	0.29	4.430	-0.21	0.00	-0.16
2	2.850	0.54	0.42	0.41	0.34	2.850	-0.13	-0.08	-0.16
1	1.248	0.47	0.37	0.48	0.38	1.248	-0.09	-0.12	-0.16

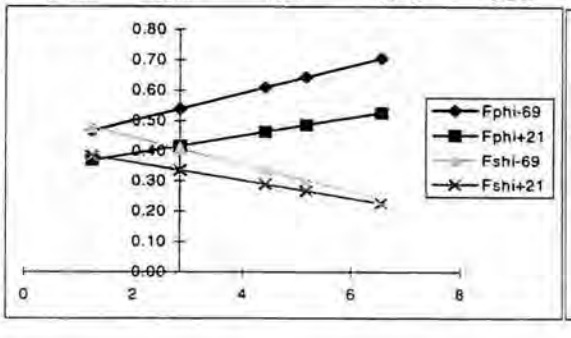

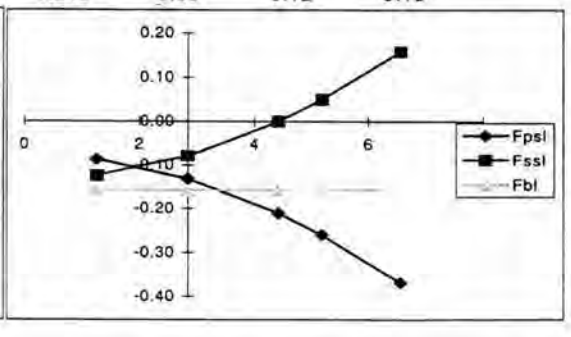

Figure 7a. Load reactions at visor attachments (left for hinges, right for locks) when all are holding for Fres 5, 7 and 9MN from top to bottom row. Pull from ship is negative, push positive. Fphi-69=load component in weak direction at port hinge, Fphi+21=load component in strong direction at port hinge asf (see also Ch 6.1), Fpsl=load at port side lock asf, Fbl=load at bottom lock. All values fractions of Fres. Horizontal axis is X for wave load centre, vertical axis is load fraction of Fres.

Port side lock broken Fres=5.00 My=7.94 Xo=0.898 Fz=3.44 Fractions of Fres

calc point	X	Fphpslb-69	Fphpslb+21	Fblpslb	criticality	X	Fphi-69	Fphi+21	Fphpslb-69	Fphpslb+21
5	6.150	0.67	0.25	-0.24	Hinge	6.150	0.65	0.43	0.67	0.25
4	4.890	0.61	0.23	-0.17	0.86	4.890	0.59	0.40	0.61	0.23
3	3.300	0.52	0.22	-0.11	BI	3.300	0.52	0.36	0.52	0.22
2	2.850	0.50	0.22	-0.10	0.30	2.850	0.50	0.35	0.50	0.22
1	0.898	0.40	0.23	-0.08		0.898	0.42	0.30	0.40	0.23

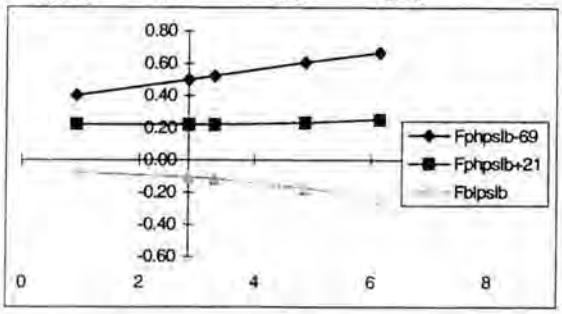

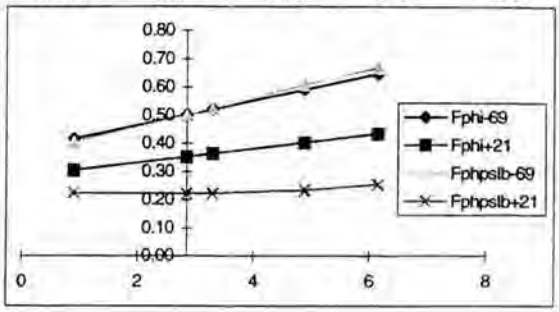

Port side lock broken Fres=7.00 My=12.25 Xo=0.989 Fz=4.82 Fractions of Fres

calc point	X	Fphpslb-69	Fphpslb+21	Fblpslb	criticality	X	Fphi-69	Fphi+21	Fphpslb-69	Fphpslb+21
5	6.250	0.70	0.25	-0.27	Hinge	6.250	0.68	0.47	0.70	0.25
4	4.970	0.64	0.23	-0.20	0.61	4.970	0.62	0.43	0.64	0.23
3	3.700	0.57	0.22	-0.15	BI	3.700	0.56	0.40	0.57	0.22
2	2.850	0.52	0.21	-0.13	0.21	2.850	0.52	0.38	0.52	0.21
1	0.989	0.43	0.22	-0.10		0.989	0.44	0.33	0.43	0.22

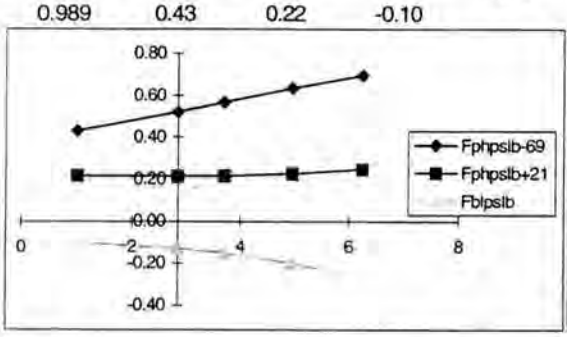

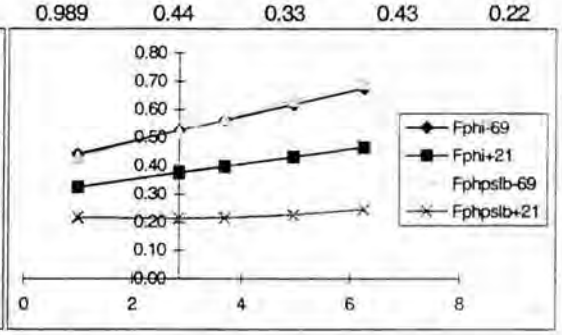

Port side lock broken Fres=9.00 My=19.87 Xo=1.248 Fz=6.19 Fractions of Fres

calc point	X	Fphpslb-69	Fphpslb+21	Fblpslb	criticality	X	Fphi-69	Fphi+21	Fphpslb-69	Fphpslb+21
5	6.550	0.73	0.24	-0.32	Hinge	6.550	0.70	0.53	0.73	0.24
4	5.190	0.66	0.22	-0.24	0.48	5.190	0.64	0.49	0.66	0.22
3	4.430	0.62	0.21	-0.21	BI	4.430	0.61	0.46	0.62	0.21
2	2.850	0.53	0.21	-0.17	0.17	2.850	0.54	0.42	0.53	0.21
1	1.248	0.45	0.21	-0.14		1.248	0.47	0.37	0.45	0.21

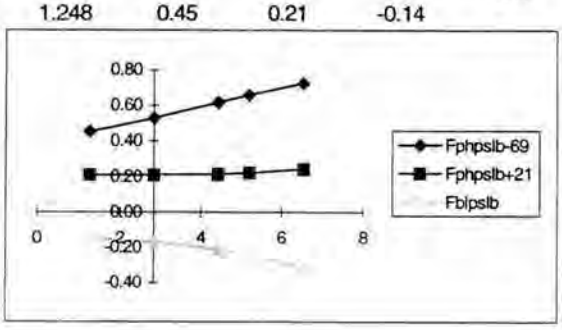

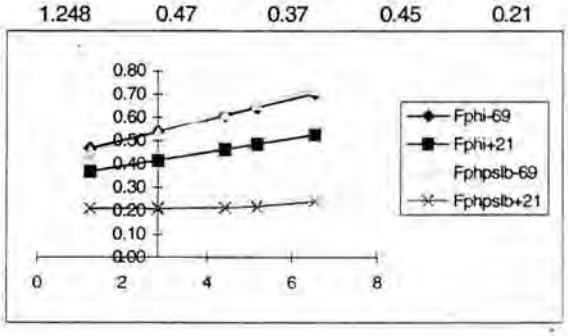

Figure 7b. Load reactions at visor attachments after port side lock failure. Note induced sensitivity of bottom lock reaction to choice of action location.

The bottom lock – according to the chosen logic of assigning reaction loads – was insensitive to the position of wave action centre as long as the wave encounter side lock was holding and the locking arrangement essentially symmetrical. The bottom lock reaction will become

sensitive to wave action centre assumption if the side lock breaks because the starboard side lock continues to be "unloaded" by the transverse Fy load being still sensitive to the position of the bow load action centre and holding lost by the p-side lock against the opening moment now has shifted to the bottom lock.

3.7 General conclusion

The above calculation indicates that breaking the side lock at 1.2 MN local reaction (equalling its strength as arrived at below) occurs at a wave load level which may be insufficient to break the next attachment. The side lock may thus break without another attachment failing. This would support the damage pattern that occurred to MV ESTONIA's sister ship DIANA II in January 1993 in the form of partial attachment failure. This involved side lock fracture and hinge damage. The shape of the bottom locking fore peak deck lugs of DIANA II was more robust indicating a stronger design (up to the limit of the visor lug of about 1.8 MN) than that of MV ESTONIA. A recurring judgement about an attachment breaking sequence of the MV ESTONIA accident is, however, not possible. For a direct head wave the bottom lock could reach its breakpoint of 1.5 MN at an estimated bow force of somewhat higher than the values given above before the side lockings became critically loaded.

The outcome of simplistic locking system load sharing analysis yields the possible effect of moving the bow load centre more forwards (an increasingly more forwards protruding bow design) implying an increasing effect of the transverse load to increase attachment reactions and thus to weaken the system strength. The load needed to overcome the strengths of the bow visor attachments is thus sensitive to the shape of the visor, which has not been investigated. This sensitivity intimately follows from the way the moment arm of the transverse load Fy is in position along the normal through the bow load centre to the attachment plane. This seems to be the effect of the visor´s shape and attachment configuration - particularly the aft positioned hinges in relation to the lockings.

3.8 Visor detachment scenarios

Visor detachment depends on the individual reactions in relations to the strength levels of the attachment sites. The above presented estimation has suggested that for 30° bow waves a minimum resultant bow force of 7 MN (lifting component around 5MN corresponding to design load level) may be sufficient to raise the pulling load on the port side lock up to 1.2 MN with some cautiously chosen wave action centre. According to work presented below this would be enough to break the side lock in the local load direction found to apply. The loads at the port hinge and the Atlantic lock are still below their breaking capacities. The weakness of the port side lock compared to the starboard side lock has been recognised. The least bow load seems to be needed to cause the port side lock to break first, followed by break of the next attachment – the hinge or the bottom lock – at a somewhat increased level of bow load. It has not been possible to define in great accuracy the strength of the hinges, but approximate evaluation indicates that a hinge may be at risk if the local transverse shearing load reaction component directed down and forwards reaches up to about 4.6 MN. Hinge failure may thus happen second if a total bow load higher than the values given above were combined with a lower (than average) opening moment, which would be insufficient to break the bottom lock

next. A combination of a higher bow load and a lower opening moment at a higher water pressure and less deep ingress of the ship (causing less opening moment) could raise the local load at the wave side hinge to the critical level before the lockings. In direct head sea a higher load is needed and then the bottom lock could be at risk first. A low bow load combined with a high opening moment would result in the port side lock becoming critical first, followed by. the bottom lock.

4 Structural features and damage to the visor

Some structural features on the visor were found to deviate from the drafted structures on drawings. Such features – which, however, were estimated not to affect the breaking of the visor lockings – were observed as follows:

- The vertical-longitudinal stiffener to which the bow end of the Atlantic lock visor lug was welded was lower than the drafted version. Since the weldments remained intact, this deviation had no effect on the casualty. (Visor bottom and stiffener edge plate failures on port side of lug stem appear to have come about at a later stage.)
- A couple of other stiffeners of the visor bottom plate were missing altogether. No effect on the events of the accident have been conceived.
- A structural reinforcement plate below the port side-locking lugs had been exchanged inside the visor as judged on the basis of weldment remnants from previous strengthening plate and the unpainted replacement plate's surface.
- Stiffener knee plates have been removed from the port side horizontal upper corner of the visor tying the visor deck to the aft bulkhead.
- About 100 mm of the 1000 mm long fractures on both sides of the visor bottom plate occurred in their fillet weldments, indicating some welding weakness, whereas the rest of the fractures were in the bottom plate. No effect has been conceived for the casualty of these weaknesses.
- An apparent crack indication in the lower port side outer shell plating, continuing into the stringer was observed to be a crack in the paint only.

It may be summarised that some minor features of damage and deviations from the as drafted structures have been observed. They may regarded to be unrelated to the visor or ramp attachment and none of these have been in a location or of the magnitude as having had any effect on the loss of the bow-visor. Other features related to the attachments are discussed in conjunction to the respective attachment.

5 Stiffness of the visor, visor seal and lifting cylinder reaction

Measurements of the stiffness of the visor were taken for purposes of judgement of the load distribution onto the various lockings under the action of the sea onto the visor shell plating. For this purpose one of the visor hinge arms (the portside) of the upside down stored visor

was lifted and the resulting changes of the diagonals of the visor central opening were measured. The visor was supported on four "feet", each approximately under the ends of the hinge beams. The result was obtained with a 37 ton lifting load - which needed a 20 ton counterweight at the other arm to hold the visor down. The diagonals changed by +6 and -5 mm's. This translates to +8.5 and -7 mm to the vertical deflections of the sides to the opening in the directions of load action with reference to the other side. The "shear compliance" of the visor is thus of the order of 25 mm/ 100 tons, which may be considered to be lower than the stiffnesses of the locking device regions. The conclusion is therefore that the visor is flexible enough that it may itself distort under load such that the loading distribution on the various lockings is not smoothed such as the design assumption of an even distribution of the sea loads onto the visor attachments would have meant. A more detailed study may be needed to clarify this issue however.

The flexibility of the seal was measured in order to facilitate comparison and quantification of reaction of visor support elements to wave-induced forces. The visor seal was found to have progressive stiffness, such that a 10 mm compression was reached with a 10 kN load per metre of seal length and the following 5 mm needed 15 kN more, see Figure 8.

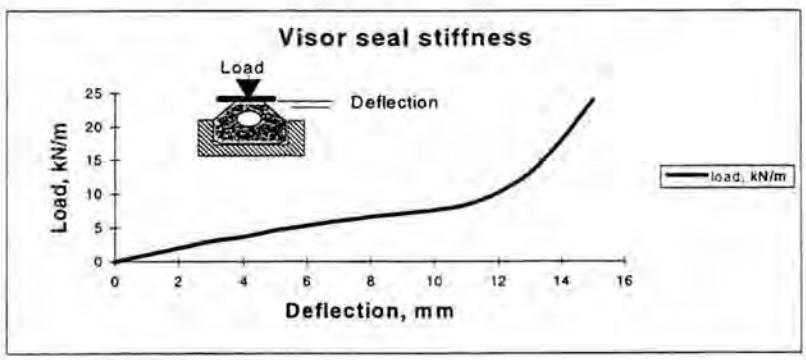

Figure 8. Visor seal stiffness as measured for 1 m length of seal.

Lifting cylinder reaction has been contemplated for whether they may have had an effect on the visor attachment reactions. Without considering oil flow inertia, the spring constant of the oil contained in the cylinder may be assessed based on the bulk modulus of oil. This is given as 1500 MPa in handbooks, translating to about 70 bars/% volume change. One percent volume change in one lifting cylinder will occur by about 13 mm compression and this would mean about 0.36 MN of load in the cylinder of id 280 mm and piston rod od 180 mm. 1 MN reaction at a cylinder would need then about 40 mm of piston displacement, translating to 4 times more at the side locks and up to six times more at the bottom lock. The lifting cylinders would therefore not cause a force reaction due to their spring reaction before the lockings had broken. Inertia effects of oil flow have not been considered as the wave load action is judged to develop more slowly than that causing oil flow inertial loads.

6 Strength of individual visor attachments

6.1 Hinges

The strength of the hinges is estimated in analogy with test results obtained at the Royal Institute of Technology using a slice of authentic hinge plate rim-bushings as recovered from the wreck.

Hinge strength assessed according to result by Royal Institute of Technology from testing authentic weldment

120000/(2x14x6.4) =717 N/mm^2

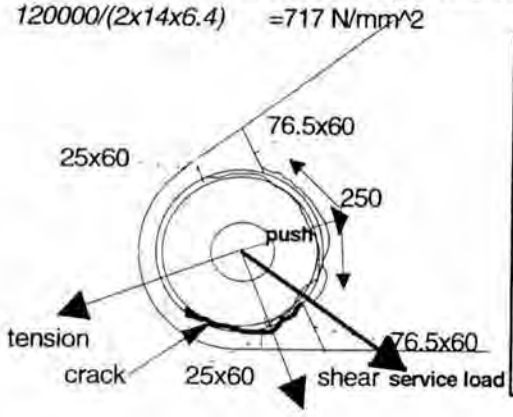

		area	strength	ultimate load	
Tension					
fillet weld	tension	6340	717	4.55	MN
	shear	1806.9	717	1.30	MN
weld total				**5.84**	MN
rims	tension	6000	250	1.50	MN
	TENSION TOTAL			**7.34**	MN
Shear					
weld tot	shear	6400	717	**4.59**	MN
rims	shear	18360	125	2.30	MN
	SHEAR TOTAL			**6.88**	MN

Figure 9. Hinge details and strength estimates for tension and shear. Effect of noted fatigue crack in the lower sector has been accounted for. Loads expected in service would cause push and shear components.

Accordingly, and referring to Figure 9, in loading vertically (called shear) and in aft directed tension (an irrelevant loading mode if locks are holding), the hinge is estimated to be able to carry load from 4.6 MN up to about 7 MN depending on hinge bushing to lug clearance, the weaker result applying to a larger clearance. Fatigue as noted in the lower sector of the bushing to lug weldment has been accounted for in the ultimate strength estimate but its effect is small. Progression of the fatigue damage, may, however, continue in cyclic load of lesser load amplitude. A large clearance between the bushing and the lug plate would increase the effect of fatigue and could lower the strength numbers from 4.6 MN.

6.2 Atlantic lock

Breaking of the Atlantic lock of MV Estonia occurred in the forepeak deck structure by fracture of weldments between locking bolt guiding and mating bushings and their holding lugs and bracket that held the bushings to the forepeak deck. Those fractures and the associated lug materials have been analysed and identified elsewhere. The mating lug on the visor had stretched and bent. The total lock is shown in Figure 10.

The strength of the fore peak assembly has been estimated (basic assessment also encompassed adapted EuroCode principles and methods for collapse strength communicated by Prof. E. Niemi, Lappeenranta University of Technology) to be twice the strength of the weaker or starboard side and is approximately then given by an equation as follows:

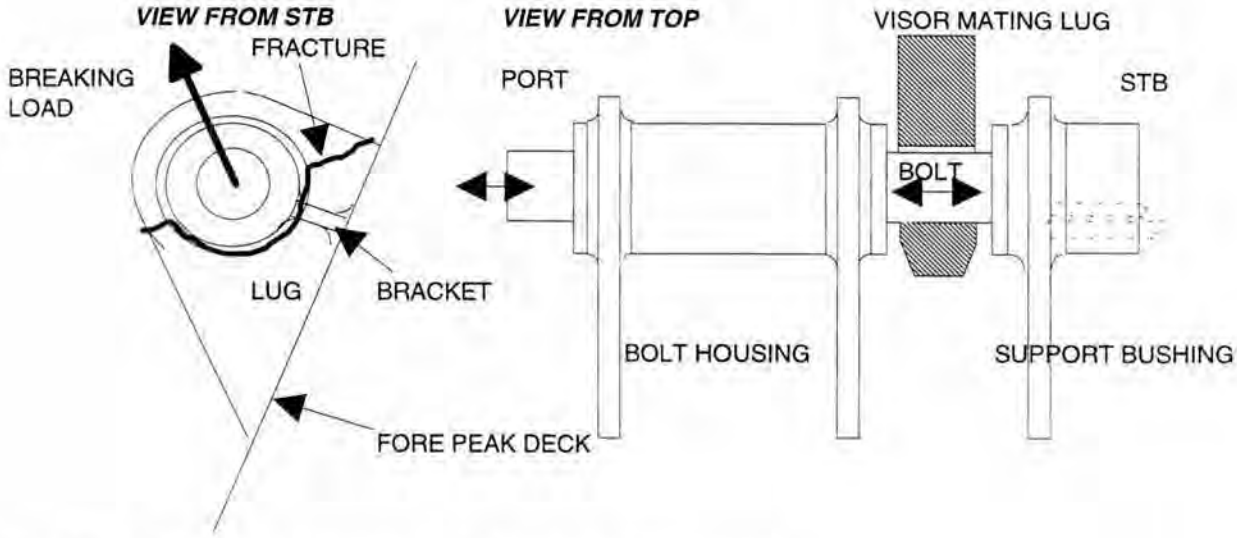

Figure 10. Atlantic lock fore peak deck structural components.

Strength of b-lock = 2 *	two sides
[f*UTS_w*a*(b(65+65)+128+128)/$\sqrt{2}$	weldment projections of bracket and lug at ultimate tension
+ f*0.57*UTS_w*a*(π/2*128-128)	lug weldment vertical sectors at ultimate shear
+2*g*YS_{pl}*15*36]	lug rims in tension at yield

Here the lug sections are loaded to a fraction g of the material's yield point (250 N/mm^2) and the weldments to a fraction f of their tensile strength (845 N/mm^2) on their projected cross section area, and corresponding fractions of their shear strength (0.57 of the tensile strength) on the parts of the weldments that are subjected to direct shear. To find values for f and g experimental results are used from welded and unwelded test pieces. An unwelded full scale model lock failing at 0.98MN yielded that g=0.89 applies to YS and a fully welded full scale test piece with nominally 3.9mm welds made of high strength steel St52 and tested at the Technical University of Hamburg (failure load 2.04 MN) that a factor f = 0.72 applies to the UTS. Such a value would not be far removed from a typical value frequently found for flow stress leading to fracture.

In the equation for the b-lock strength b is the bracket factor originating from the eccentricity of the loading mode of the starboard tie bracket. B = 0.125 = 0.5 * 16/64 from the assumption of bending of the bracket having a 16 mm internal moment arm and the local force couple being determined by tension on the projected area of a bracket fillet weld.

The narrowest range estimate of the strength of the bottom lock of 1.5 MN is based on analysing the deformation of the mating lug as presented below. For a loading capacity of 1.5 MN and a weld hardness of HV = 270 commensurate with UTS = 845 MPa as found on the actual weldment, a weld throat a = 3.5 mm is obtained. This compares well with spot checks of remnants of the authentic lock.

6.2.1 Authentic Atlantic lock visor-lug of MV Estonia

The mating lug on the visor had deformed both by stretching and bending. This study has found out how much the lug had stretched by tensile load alone (as part of the total stretch may have come about during excentric pulling after the maximum strength of the bottom assembly had been "consumed") and what tensile load has been necessary to cause that deformation. The material of the visor lug was identified to be mild steel by hardness testing.

A drawing of the visor lug is shown in Figure 11. A photograph of the Atlantic lock visor lug is shown in Figure 12 in its "in situ" upright position in the visor. The view is from aft port slightly from above the lowest horizontal stringer.

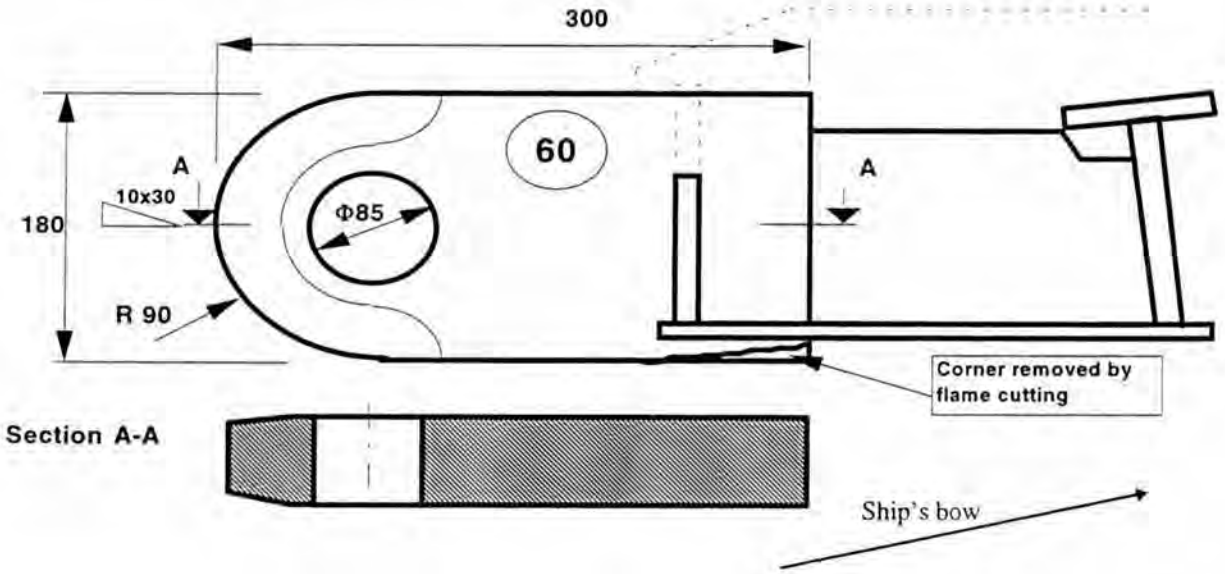

Figure 11. Atlantic lock visor lug as designed. The dashed part of the vertically positioned longitudinal stiffener to the visor bottom plate was missing in the actual visor above and to ship's bow from the lug.

The aft end of the lug is bent to starboard and the surrounding base plating of the visor has fractured on port and has buckled at starboard. This suggests that a fairly high starboard facing load in the bottom part of the visor has acted sometimes and apparently during the accident. Such a situation could have developed if a clockwise twisting rotation around the ship's longitudinal axis of the visor occurred due to a lifting action at the port side. Contact marks in the bottom locating horn recess on starboard suggest that the lower portion of the visor has been forced to port at some stage of the sequence of events. The resulting and remaining total sideways displacement of the aft end of the lug is on the order of 10 cm.

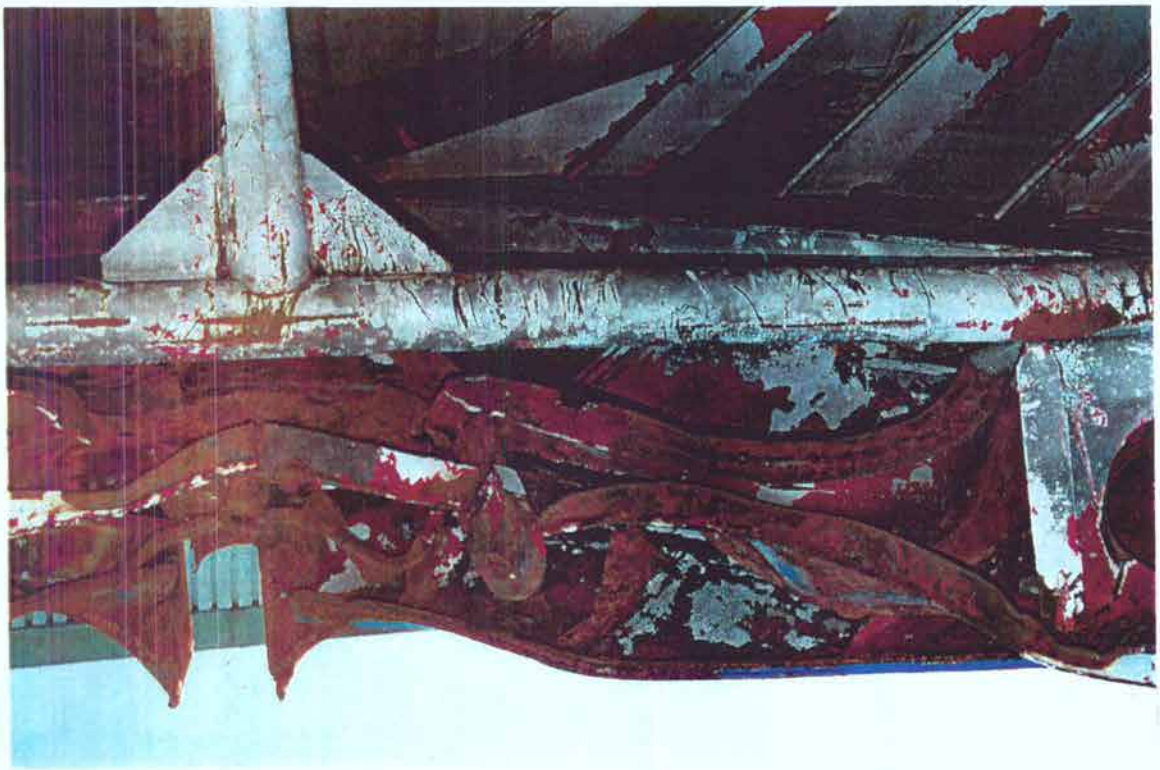

Figure 12. Atlantic lock lug site in the visor after visor recovery.

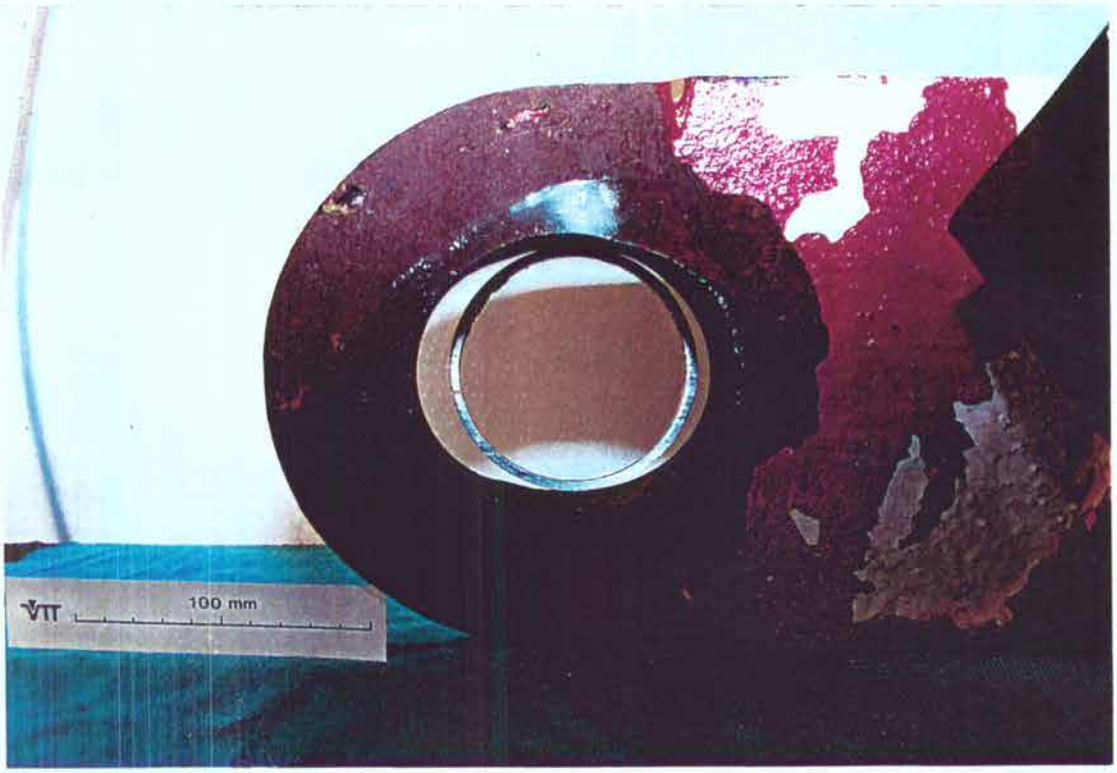

Figure 13. Side view from starboard of Atlantic lock visor lug after removal from visor. Ring insert in eye denotes the approximate apparent position of the eye in its original shape.

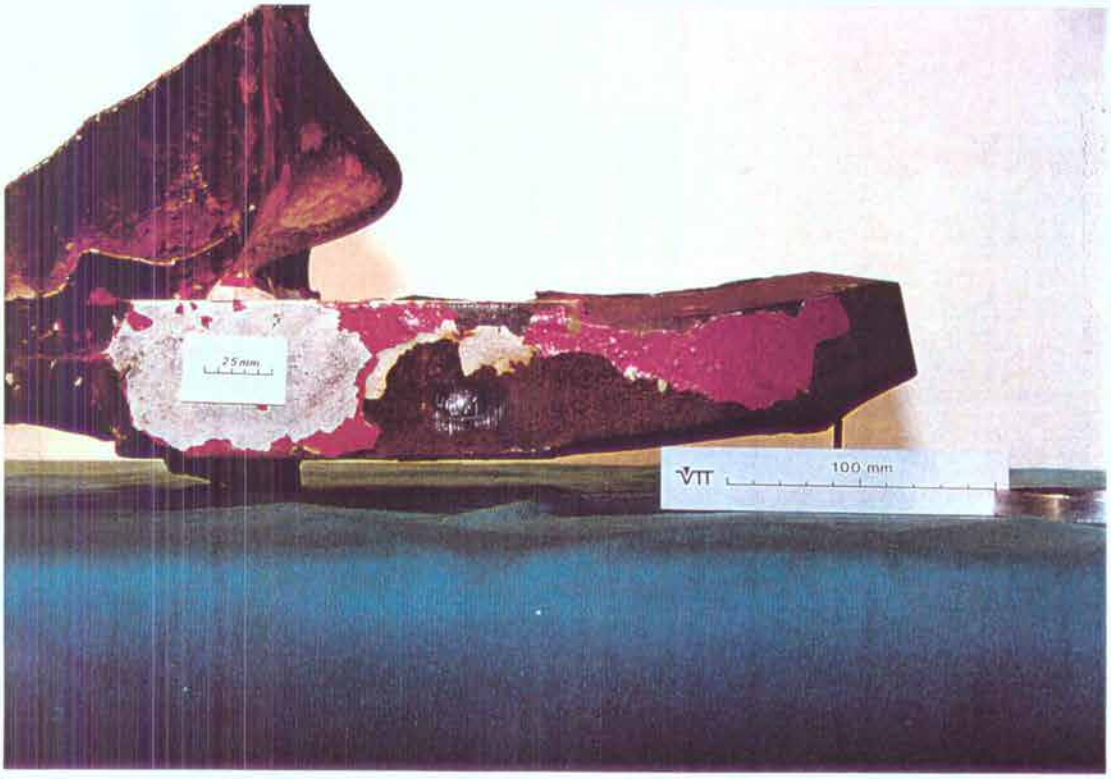

Figure 14. Top view of Atlantic lock visor lug after removal from visor. Lug aft end bent to starboard, bending of stem is very small and practically undetectable.

Photographs of the visor lug – as removed from the visor – are shown in Figures 13 and 14 from the side and from "top" respectively. Also here we may note deviation of the visor bottom plate stiffener dimensions from those marked on the drawing.

6.2.1.1 Visor lug material

The steel grade of the authentic visor lug was investigated by Brinell hardness number measurement using a 30kN (3000kp) indenting load and a 10 mm steel ball indenter. Three measurements gave HBS 10/3000 = 131, 136 and 137. This transforms into an ultimate tensile strength of around 450 MPa. It may be concluded that the steel grade is thus ordinary ship-building mild steel.

6.2.1.2 Visor lug deformations and maximum estimated load

In the following, the eye end is called the aft or stern end and the stem of the lug is located toward the bow end as the lug was in the ship. In the side view, a ring insert at about lug mid thickness is shown in the lug eye illustrating the apparent original position of the eye. At the upper pole of the eye the ring insert leans upon undamaged surface of the hole. The indication for this is that here we may discern machining marks from hole cutting potentially dating back to lug manufacture. In the long direction of the lug the original nominal diameter of the eye of 85 mm has elongated to the present deformed state of the lug such that at midthickness the hole is practically 95 mm "long". The transverse vertical diameter of the eye has reduced to about 83 mm. An analog transverse (vertical) contraction of the eye could be observed in

tensile testing of mock-up and model lugs, elaborated in later sections of this report. An additional deformation of the eye is observed at its end towards the ship's bow as indicated by the ring insert. Compression and/or wear of the stem - or bow - end of the lug appears to have occurred and stretch of the aft end of the lug is apparent. The aft ligament of the eye along the lug is 47.5 mm, which is as designed and indicates no wear of the aft end. The "pear" shape of the deformed eye with the narrow end facing aft, is noted. The narrow aft facing eye sector occurs through the thickness of the lug. At the (vertical)"waist" of the "pear" the eye is about 80 mm wide and it is possible to fit a Φ 78 mm disc into the "bottom" (or aft end) of this end of the elongated eye. Φ 78 mm corresponds approximately with the diameter of the locking bolt. Hence it is judged that the lug has stretched and that the tension action has been caused by the locking bolt (or the reacting load held by its attachments).

The full length of the eye is about 95 mm at midthickness and 93 mm at ¼ thickness from the concave (starboard) side. At the aft end of the hole the side bend is 10 mm or slightly less.

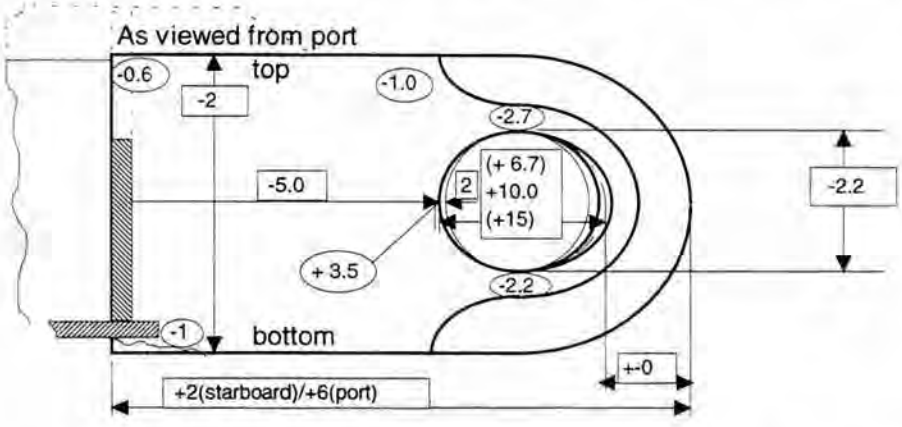

Figure 15. Lug dimensions as differences to nominal as drawn dimensions. Note also reduced thickness of eye ligaments above and below eye, which supports tensile stretch of lug.

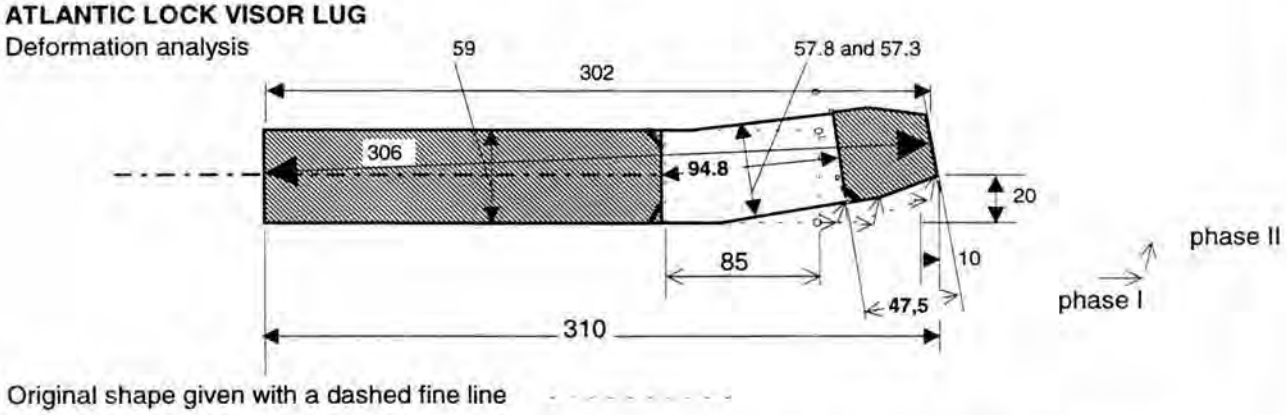

Figure 16. Longitudinal section of the deformed lug indicating also the path of assumed deformation. i.e. Phase I and Phase II. Crushed eye corners indicated.

Taken lug dimensions are given in Figure 15 as deviations from the nominal as drawn dimensions and in Figure 14 as actual millimetric dimensions of the lengthwise ("horizontal") through-thickness cross section of the lug.

An appraisal of the deformation of the lug end has been made. Here we observe that three of the eye hole corners (aft port and both bow corners) have been crushed leaving the stb aft corner unaffected. Apparently this crushing has occurred during later stages of the accident – i.e. the bending Phase II included – when the bending action by the locking bolt occurred after the forepeak deck side of the lock had broken. The bending has apparently occurred so that the locking bolt has been supported by the starboard bow end corner of the eye hole and the stern end port side corner has been pushed aft and to starboard by the bolt, the port end of the bolt having been held back by the hydraulic piston rod. The port bow corner crushing may have occurred during back and forth motions of the visor after all lockings and fastening sites had broken but with the locking bolt still in the lug eye and hanging on to the piston rod. This deformation can be produced with a comparatively low force and has been named Phase II. Analog crushing of eye corners at port aft and starboard bow corners of the eye were observed in all comparative mock-up tests.

Prior to this bending, stretching has occurred (Phase I) as evidenced most critically by the movement aft of the starboard aft corner of the lug. The shape of the eye prior to this bending, which also contributes some stretch, may be found drawing circles through the chosen stern midheight points of the eye ligament section using the supporting starboard bow corner of the eye hole as centre. The intersection of these circles with the corresponding profile lines of the unbent lug mark the locations of the eye hole ligament after phase I, i.e. at the end of the pulling phase, during which the critical forepeak deck lugs had broken. This "circular arc" deformation model was checked by back-calculating a 1/3-scale lug deformed by eccentric pulling at the Royal Institute of Technology". It was found that the elongation of the hole occurring due to this side bending is overestimated by the "circular arc"-model, and that a correction term equalling one tenth of the amount of side bending may be subtracted from the estimate of additional elongation for the side bending effect obtained by the circular-arc model to find the corrected elongated shape of the lug after phase I.

We may thus find the length of the hole prior to phase II bending by simple geometrical calculation. As illustrated below, by knowing the length of the eye at lug midthickness (l = 94.8 mm), thus having its measurement origin 30 mm sideways from the deformation circle centre C at the stb bow eye corner, and that the bending caused 10 mm movement of the stern end (the other end of the 94.8 measurement) to starboard we obtain for eye hole length after phase I

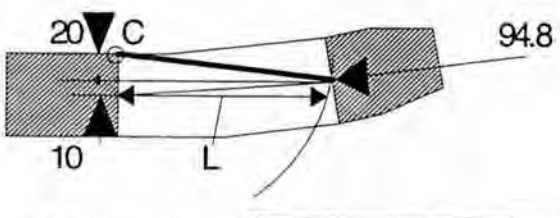

$$L(\textit{phase I}) = \sqrt{\left[94.8^2 - 10^2 + 20^2 - (20+10)^2\right]} + 10/10 = 92.8\ mm$$

The last term 10/10 is the empirical correction for the "error" of the circular arc model. This correction was deduced from a test using excentric tension performed at the Royal Institute of Technology, Stockholm.

For finding how much the eye had actually stretched during phase I, we need to identify the effect of wear on the shape of the eye. Here we get help from finding the original position of

the original eye hole, that is we need to find out whether the eye could have elongated due to other reasons than stretching, e.g. wear or crushing. For this purpose we note that the upper sector of the eye still bears machining marks and has therefore remained unharmed through the life of the lug. Also the aft end ligament was noted to be 47.5 mm which is as designed and therefore taken to be in its original shape. The only location bearing signs of a different lengthening effect than stretching could thus have occurred at the stem (ship's bow) end of the eye. For the purpose of identifying whether this eye sector has changed during use of the visor information on the behaviour of the position of the transverse ("pole to pole") midplane of the deformed hole during stretching is of help. We may find it so that the deformation of the hole may be divided up into deformations of the aft and bow halves of the eye. If the bow end deformation is subtracted from the total, the rest or the aft end deformation is taken to be due to loading.

To position the transverse ("pole to pole") midplane of the deformed eye the "radius" of the bow end of the hole was measured optically taking x-z coordinate readings of the hole edge at the aft and upper ("equatorial" and "polar") eye curvatures for both sides (port and starboard) of the lug (Note: By comparison to the original eye radius after finding of the "neutral" surface within the lug this measurement would also reveal the amount of wear on the bow side of the eye.). A second order curve fit was done to the measurement points. The position of its "lowest" or "polar" point was found by mathematical analysis and this point was taken as the position of the hole midplane as deformed. The position of the equatorial extreme bow end of the eye hole was read when the vertical hairline of the optical system was tangent to the eye hole profile. A second set of readings of the polar position was taken by fitting the tangent minimum to the hole or taking the midpoint between first "off-centre" grid intersections with the eye upper profile and taking the polar position as the midpoint of the former. Both methods were used for both sides of the authentic lug as well as both sides of the stretched only and the stretched and bent end of the full size mock-up lug reported below. Comparison measurement was used to test that method for one case using randomly chosen ten people to take measurements directly of the radius, i.e. everyone participating was asked to identify directly the position of the lowest point of the eye. Either method was found to give the position of the midplane to within 0.2 mm. This may be considered to be the objective accuracy of the determination of the original eye position (its "transverse" midplane) in the lug. Using the centric tensile only tested end of the full size lug mock-up it was found that the position of the vertical midplane of the eye stays at the distance of the original radius of the eye from the equatorial "bow" end through the tension loading. During eccentric pull the midplane rotates around an axle that is about 6 mm from the material midthickness towards starboard (the concave side), implying that some stretch of the stem end of the lug eye hole position occurs for phase II also at the lug midthickness.

From the full size mock-up tensile test explained in detail below the position of the midplane was found to remain unchanged during stretching. During the subsequent eccentric one sided tension - which caused mostly sideways bending and also some stretching - the mid transverse plane of the eye was observed to turn slightly such that the turning axis was around 6 mm displaced from the lug midthickness plane toward the concave side. At this position the radius of the deformed hole is 44 to 44.5 mm, which is 1.5 to 2 mm more than designed. It is logical to conclude that this difference is a result of wear or crushing.

We may summarise these measurements further as follows:

- The length of the bow end stem of the lug is up to 5 mm less than nominal. This has been assessed more closely by observing the probable position of the transverse midplane of the eye using measurements of the undeformed upper sector of the eye hole. This way wear or deformation on the bow face of the eye has apparently caused up to about 2 mm elongation of the hole leaving 3 mm of the missing length of the stem to be due to manufacturing.
- The outer length of the lug is 2 mm more than nominal on the concave side and 6 mm more than nominal on the convex side. The elongation on the concave side indicates also that the lug has elongated due to pulling. Both numbers match with the overall situation supporting the conclusion that the lug has been 3 mm shorter than designed and that the net elongation of the lug during phase I has been on the order of 92.8 - 85 - 2 ≈ 6 mm.
- The aft end eye ligament is 47.5 mm, which is exactly the nominal indicating no wear or observable thinning of the aft end of the lug. The elongation of the aft end of the eye is thus concluded to have resulted from tensile stretching.

The elongation due to tension of the authentic visor lug of the MV Estonia Atlantic lock has accordingly been found to be about 6 mm. Supported by results from centric and eccentric tensile testing of model lugs and the full size twin lug made of highstrength St52 steel (HBN 165) as explained below this elongation has been estimated for high strength steel St52 to have required a load of approximately 1.76 MN (180 tons). The authentic lug was found to be mild strength A-grade steel, which reduces the estimate for the authentic lug by a factor of about 1-((450+250)/2))/((520+350)/2)) = 0.195, that is by almost 20%. The Atlantic lock of MV Estonia is thus concluded to have carried a load of at most **1.50 MN (147 tons)**.

6.2.2 Ultimate strength of the visor lug

A cross check was performed of the lug fracture strength and design calculation. The result is as shown in Figure 17 and as follows.

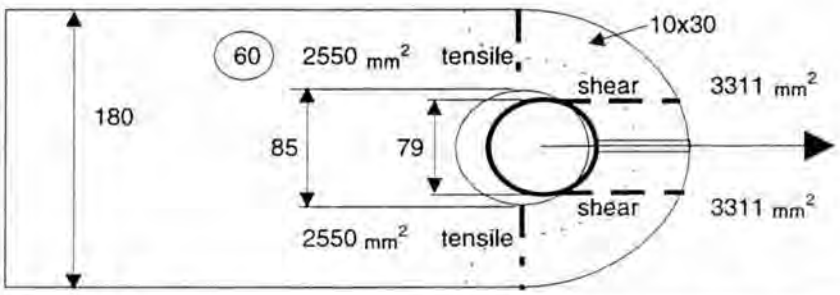

yieldonset MN	steel	GY/MN	tensile strength/MN	stress@1MN	shear strength/MN	stress@1MN
0.65	Fe 52	0.89	5100*520= 2.65	164 x 1.20	6622*286= 1.89	90 x 1.68
0.46	**A 42**	0.64	5100*450= **2.30**	125 x 1.57	6622*247= **1.64**	70 x 2.16
	STRESS AT 1 MN		196 MPa		151 MPa	

Figure 17. Ultimate strength and stresses at 1MN of visor lug.

The cross sections subjected to tensile stress are together 95 × 60 - 10 × 30= 5100 mm^2. Taking that these could determine the ultimate strength a breaking loading capacity of 2650 kN or nearly 300 tons would be obtained. At design load the tensile stress would be 1 MN/ 5100 mm^2 = 195 MPa, which is more than the used permitted design stress for high strength steel. The shear stress would be 1 MN/6622 mm^2 = 151 MPa, which would be more than the shear yield strength for high strength steel and exceed a moderate permitted design stresses for both high strength (90MPa) and mild (70MPa) steel. The calculated lower bound shear fracture load would be 1.65 MN for mild steel grade A 42 and 1.89 MN for high strength Fe 52, the latter also being slightly lower than the test result of 2.04 MN obtained at the Technical University of Hamburg.

6.2.3 Authentic Atlantic lock visor lug of MV Diana II

The visor lug and locking bolt of the former MV Diana II were recovered from the ship for purposes of comparing measurements with the ESTONIA-lug. This was necessitated because of earlier observations of this locking mechanism to have significant play (reported to be on the order of 30 mm by Turbotechnic after the January 1993 accident) after the MV Diana II had experienced heavy weather and damage to its visor locking devices in early 1993. It became of interest to find if the locking bolt was unbent or worn and if the visor lug had stretched and/or bent. Photographs of the lug and the bolt are shown in Figures 18 and 19.

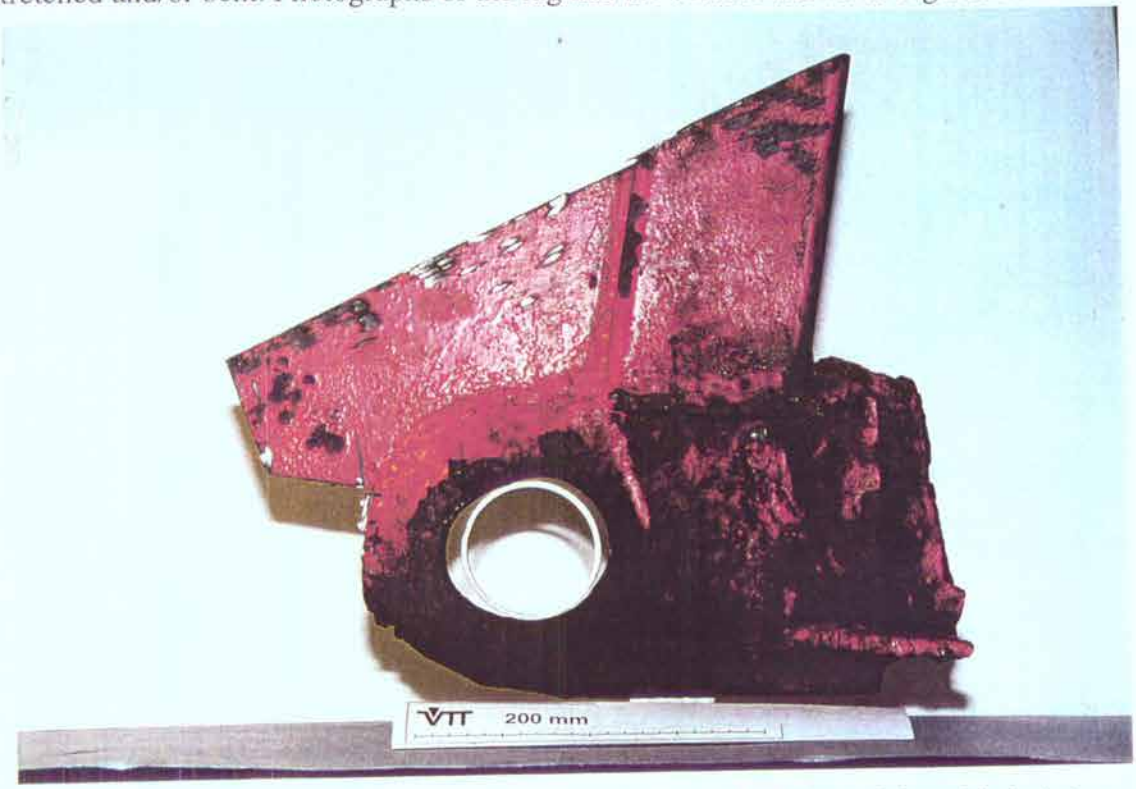

Figure 18. The Atlantic lock visor lug from the MV DIANA II. Part of the added plating surrounding the lug tip has been removed for measurement purposes.

The material of the visor lug of MV DIANA II was identified to be most probably mild steel. Brinell hardness was measured using 30kN (3000kp) load and a 10 mm steel ball indenter producing a 5.20/5.25 mm dent yielding HBS 10/3000 = 131/128, which corresponds with UTS = 430 MPa. The material is of similar strength as the MV ESTONIA lug.

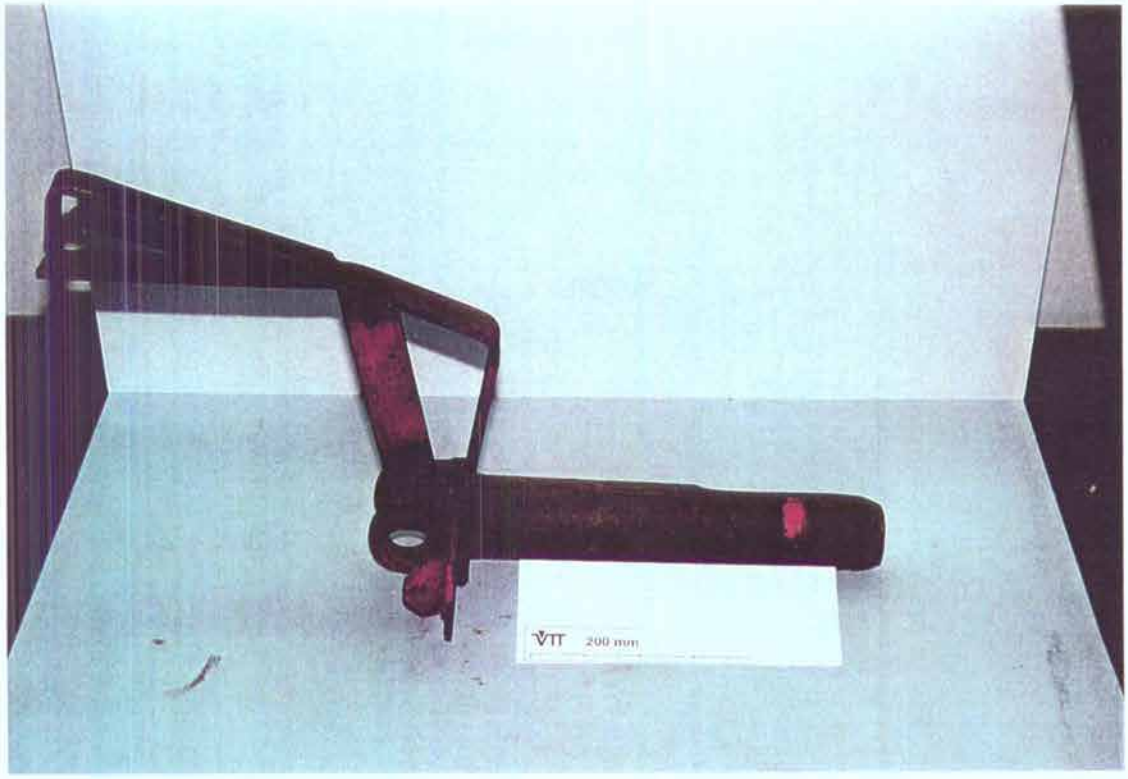

Figure 19. The Atlantic locking bolt from MV DIANA II. View from the upper aft sector.

The outer length of the lug is 305 mm, which is 5 mm more than the designed length. A ring insert measuring the designed eye diameter of 85 mm has been positioned into the lug eye. The ring demonstrates that the 5 mm increase in length appears to be due to stretching the aft or stern end of the lug. This is supported by noting the pear-shape of the eye, the stern end being close to the bolt diameter in close similarity with the eye of the MV ESTONIA lug. Significant wear is evident at the upper bow sector of the eye. Corresponding wear is evident on the bolt.

It is meaningful to note that the fore peak lugs of the MV DIANA II Atlantic lock have been more robust than those of MV ESTONIA, why it can be understood that the two ships can have met the same magnitude of bow forces as evidenced by equal magnitudes of lug lengthening, without the Atlantic lock having failed on DIANA II, however.

6.2.4 Full size mock-up tests performed by the Technical University of Hamburg

Of some interest is also to note the fullsize Atlantic lock mock-up test series performed by the Technical University of Hamburg on specimens manufactured by the Meyer Werft. The mock-ups had been manufactured of high strength steel (St 52) deviating from actual construction materials of the authentic lock found onboard of MV ESTONIA. The visor lug material of MV ESTONIA was identified only after the mock-up tests to be mild steel. Varying lug to bushing weldment lengths in the forepeak lug structure were applied. Because of unexpected breaking of the authentic sized visor lug in the initial test with "full" length weldments in the fore peak mock-up (3, numbers in order of strength of the mock-ups) leaving the forepeak

mock-up intact, an extra test (4) was performed using an "oversized" visor lug. Two tests (1 and 2) were performed later, one with intermittent weldments (2) and one with no weldments (1) in the forepeak lug assembly.

The test mock-ups that failed in the forepeak lugs and numbered here as 1, 2 and 4 had either no weldments as test 1, intermittent – nominally 3 mm – weldments, as test 2, and test 4 that had continuous, nominally 3mm weldments between the forepeak deck lugs and the boltholding bushings. Test 3 also had continuous, nominally 3mm weldments, but the failure occurred in the mating visor lug.

The mock-ups failed at 100 tons (1), 142 tons (2), and about 200 tons (3) and (4) by fracture of the forepeak structures in the tests numbered 1, 2 and 4 as listed whereas test no 3 failed in the pulling "visor" lug. Test 4 had an oversized "visor" lug. The conclusion is that about 200 tons seems to be the absolute theoretical maximum value of strength of the fore peak part of the Atlantic lock configuration as designed, if weldments were sufficient by "a" and continuous and had the lock been manufactured of high strength steel. Failure of the pulling/mating lug occurred by combined shear/tensile fracture of the tip of the lug and the failure load corresponds with simple shear failure criterion of 0.55 of the ultimate tensile strength being reached on both sides of the pulling bolt. 0.55 is slightly less than the theoretical for plane strain shear of 0.57 (or $\sqrt{3}/3$) indicating only slight deviation from simple theoretical and highest possible.

100 tons is the breaking capacity of the forepeak lug assembly if no weldments at all are made. While the minimum cross section of each lug was $36 \times 15 \times 2$ mm^2 = 1080 mm^2, giving about 520×1080 mm^2 = 57 tons for the capacity of each lug. The combined capacity of the system of three lugs is on the order of 1.8× the individual capacity. Information from spot checks of the weldment size was obtained indicating a = 3.9 mm. The hardness was HV10 = 330. Taking these values for the fillet weldment dimension and hardness and the weldments are obtained to break in direct tension at about 0.72 of their ultimate tensile strength on the normal projected cross section, which may be taken to suggest a simple ordinary flow stress criterion of a moderately tough weldment. The lug rims were assumed to be at a fraction of 1/1.8 of yield when the weldments break at the maximum capacity of the assembly. The weaker starboard side of the Atlantic locking may be taken to provide half of the loading capacity of the lock. This yields that the lug rims provide about 0.5 MN to the total loading capacity of the bottom lock and the rest will be provided by the weldments up to about 1.8 MN, which in turn is the maximum estimated capacity of the recovered authentic visor lug. Taking that the bottom assembly had broken at about 1.5 MN, the weldments can have had an average thickness of 3.5 mm had they been continuous. This is reasonable as the observed weldment dimensions have been on this order.

6.2.5 Model tests and load estimates of Atlantic lock visor lug

Five model test pieces were manufactured of the visor lug. All model lugs were double ended, meaning that they consisted of two lugs each lying "stem to stem". Two were in Fe 52 steel like the design intent of the authentic and three were made of extruded aluminium (AlSi1Mg). The steel model lugs were one in full scale and one in 1/3-scale (linear) and the aluminium lugs were in 1/6 scale. The two larger model lugs are shown with the authentic lugs in Figure 20.

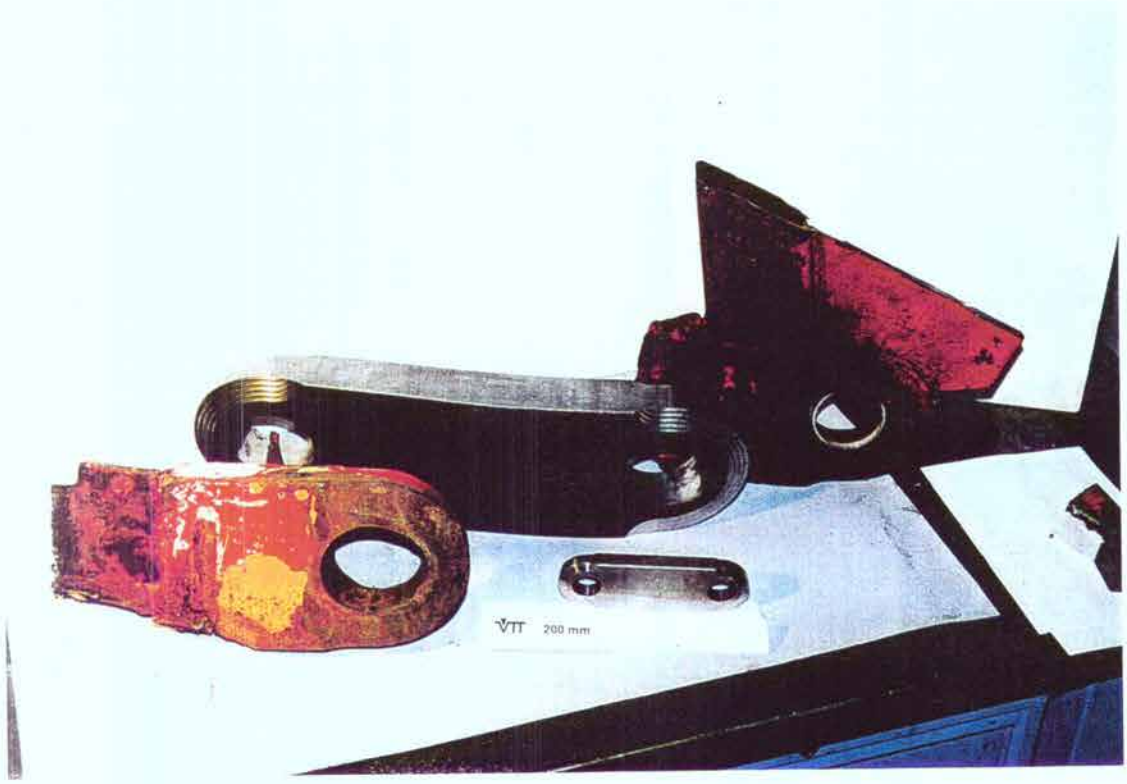

Figure 20. Full size and 1/3 scale model lugs together with authentic MV ESTONIA and MV DIANA II Atlantic lock visor lugs.

The tests were:

- **Centric full size Fe-52 tensile test**: The full size mock-up lug (both ends) was pulled to a total of 7.5 mm permanent elongation of each eye. The tensile eye elongation - load curve is shown in Figure 21. At final elongation of 7.8 mm for each hole the load was 1.92 MN. **In the range of deformation of interest for interpreting the authentic lug load, i.e. around 6mm eye elongation the curve is nearly linear according to load/tons = 172 + 8.5*(X-5) for Fe 52-grade steel, X being the permanent elongation in mm. A correcting term approximated by (50/350)*172 = 24 tons may be subtracted to obtain the number for A-grade steel (St42).**

- **Eccentric full size Fe-52 tensile test**: One end of the full size lug was subjected to loading by a bolt acting as a lever. The load was applied at one end of the bolt pulling along the length of the lug. The pulling force was applied in two phases, 350 kN and 115 kN at 0,2m and 0,6 m distance respectively to the lug, both excerting a maximum bending moment of 77 kNm plus a pulling stress of around 200 N/mm^2 on the side ligaments of the eye. The side bending thus achieved was 10 mm within the eye of the lug. Significant bending of the lug stem also occurred in addition to this. The position of the eye midplane transverse to the lug was subsequently found to have been unaffected by the bending at a distance of around 6 mm from the lug midthickness.

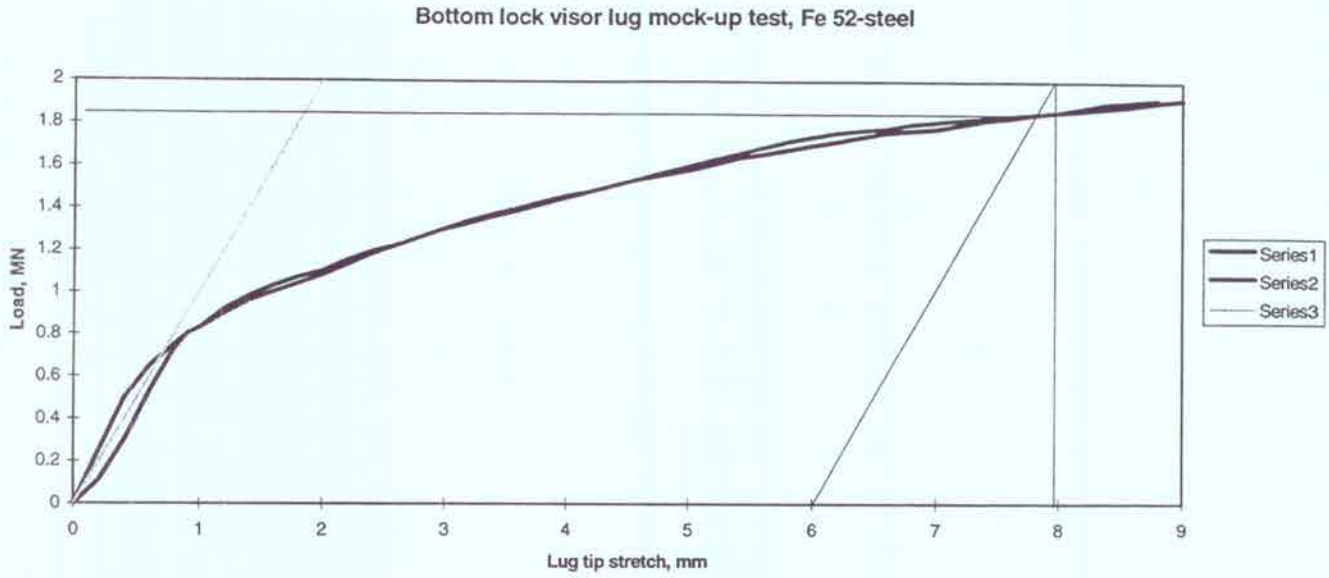

Figure 21. Load- eye elongation curve of full size Atlantic lock visor lug model of St 52 high strength steel.

- **Eccentric 1/3-scale Fe-52 tensile test with bolt end support**: This test was undertaken such that the bolt ends on one side of the lug were pulled with a supporting bracket inserted between bolt ends on the opposite side of the test lug to prevent them from taking support from the lug eye corners at the stem. The test was done because the deformation analysis of the authentic lock lug had indicated that some bending had evidently been combined with phase I pulling and it was unclear, whether such a combination of bending could reduce the pulling force needed to cause a certain nominal extension of the lug. It was confirmed that the lug deforms to closely resemble but slightly exceed the bending effect estimated for end of phase I of the authentic lug. The load required to stretch the lug midthickness location is not affected by this mode of applying the load.

- **Two eccentric 1/6-scale Aluminium tensile tests using pivoting C-clevises for bolt attachment**: Two tests were made. The purposes were to find the effect of the magnitude of eccentricity of pulling on the type of deformation that could be obtained. The magnitudes of eccentricity were $e > 5$ mm and $5 > e > 0$, i.e. the line of force being either outside of the lug dimensions or inside. In the first case the pulling started with the centre-line of the lug being 30 mm from the line of pulling. In the second test this distance was around 2 mm. The lug ends twisted in both cases, but only in the second case did the concave side of the lug stretch to a length larger than the original length of the lug. Bending was much less than for the case of the larger eccentricity and full contact between the bolt and the lug eye was obtained as in the authentic visor lug. Only eye hole corner contact with the bolt was obtained in the test with large eccentricity. A pear shape of the full thickness of the eye was only obtained in the test with small eccentricity. This test also supports the conclusion that the authentic lug was at some time pulled in a phase I-fashion with a force keeping the bolt in contact with the full thickness of the aft end of the lug.

6.3 Side locks

6.3.1 Fractures

Detailed observations of fracture morphologies were made on the side lock remnants on the visor on both sides. The corresponding locations of the visor are shown in Figures 22 and 23.

Figure 22. Side lock region on port side as found on visor after the casualty.

The general breaking mechanism had been by fracture of the horizontal stringer under the lug, vertical stiffener edge corner and tear (along the lug weld edge) of aft plating onto which the locking lug eye plate had been attached by welding. Apparently the lug to bulkhead-weldment had been stronger than the rest of the structure, judging from the fact that nothing of the lug related material had been left on the visor. The holes left in the visor aft bulkhead measured 390 mm * 85 mm, the foot print of the lug only being 380 mm * 60 mm. The width of the weldment along the plating outside of the lug plate footprint has thus been on the order of 12 to 13 mm.

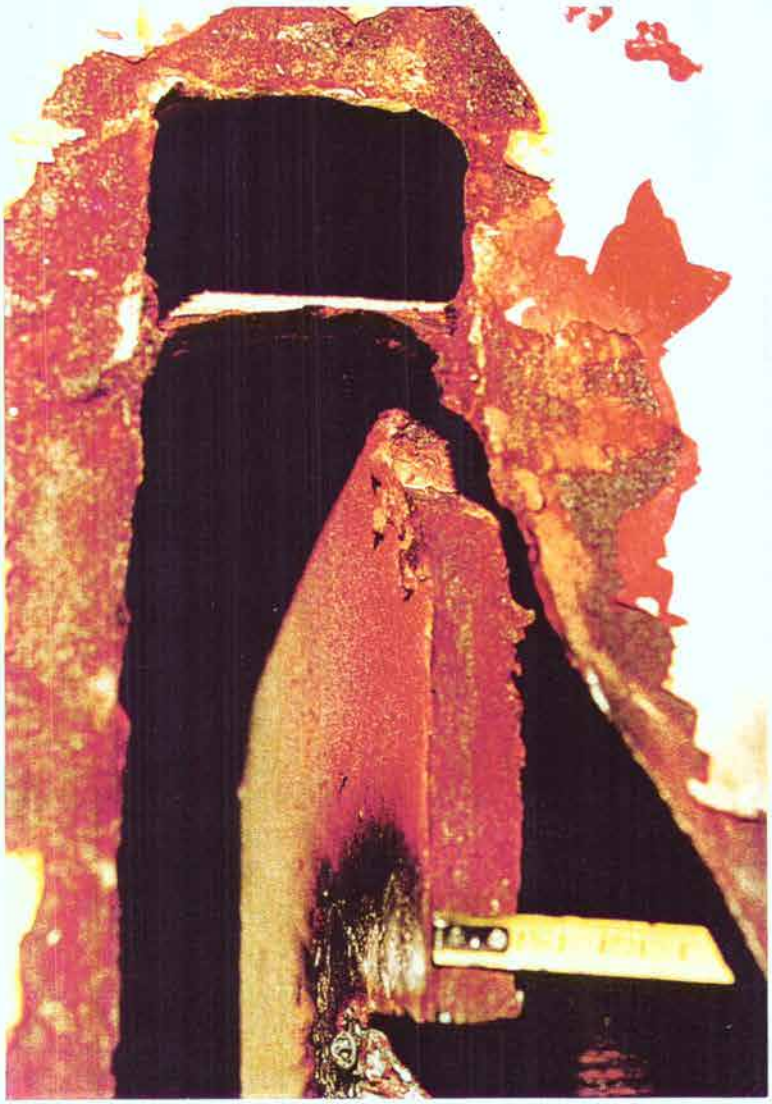

Figure 23. Starboard side lock site of the MV ESTONIA visor.

The strength estimation of the side locks presented a particular problem for numeric or analytic methods, because of their complex structure consisting of plate, stringer and stiffeners. Numerical modelling was done in a parallel project using finite shell elements and elastoplastic material constitutive laws for stress-strain interdependence, analytic calculations were done using "primitive" linear stress distribution assumptions. The static indeterminacy of the side-lock assembly called for an adjustment factor in the analytic calculation for structure member compliance differences. This factor was found by analysis of experimental data. Numerical modelling results were interpreted as such.

The testing program evolved into a series of tests because of new needs that uncovered consecutively after each test. Subsequent tests incorporating improved similarities with the authentic visor structures were then done. Four side lock mock-up tests were made altogether, the last of them corresponding best with the actual visor structure.

6.3.2 Material investigations related to visor side locks of MV Estonia

Photographs of the holes left in the visor at the sites of the side locks are shown in figures 22 and 23. The holes in the aft bulkhead measure 390 mm by 85 mm. Fracture had occurred by shear and tear through the bulkhead plate on both sides. The horizontal stringer fractures are different on port and starboard but the vertical stiffeners seem to have failed by shear and tear through the stiffener edge corners.

Basic mechanical material properties were determined by standard types of tensile tests for the bulkhead and horizontal stringer plates. Tests were done in the direction of the plating and one through thickness tensile test was performed to find out if the aft visor plate is weakened by lamellar tearing. The tests show that the plates are standard A-type high quality ship-building steel (Bulkhead: YS 306/311 MPa, UTS 454 MPa, A5 39%, RA 68%; Horizontal stringer YS 332/336 MPa, UTS 476 MPa, A5 33%, RA 58%). Through thickness strength is not reduced by bulkhead plate lamellarity (YS 335MPa, UTS 474 MPa). Chemical analyses were taken from the vertical stiffener, showing it to be good quality killed weldable structural steel plate (C 0.13, Mn 1.00, Si 0.19, P 0.025, S 0.027, Cu 0.01, Al 0.035 /%). The materials are thus of high quality as also evidenced by the ductile fracture morphologies.

From material investigations and fracture morphologies it may be summarised that side locking strength is not reduced by material or welding related factors on starboard, as fractures occur through the plates as shear and mixed shear and tear. On port side on the other hand attention is drawn by the horizontal stringer fracture, half of which is shear through the plate itself but the other half being a weldment related failure since the stringer plate edge can be seen. The lower corner of this edge has been sheared off but the upper surface of the plate seems almost untouched by welding and the corner of the edge is preserved.

An apparent small size of the fillet weld bead on the lower side has been well fused to the plate but failure occurred by the corner of the edge having torn off. The total width of the sheared fracture is on the order of the thickness of the plate. Having fractured due to almost simple shear, the weak half of the horizontal stringer to bulkhead joint has contributed to the strength of this joint by one half of its tensile strength. The other half being of full strength, a total of about 75% of the horizontal stringer strength has been assumed to contribute to the port side lock holding strength

The rest has apparently withheld as much force as was possible geometrically and materialwise, noting that the materials have good ductility and are therefore not sensitive to the sharp notches of the weldments in monotonically increasing load. Based on mock-up tests and strength calculations, the strength of the side locks has been estimated to be up to 1.59 MN for starboard and up to 1.19 MN for port using an assumption of load action at 38° to the aft plating plane of the visor and 3 mm width for the vertical stiffener weldment respectively. The height of the mating lug has then been taken as 214 mm from the eye centre to the visor aft plate midthickness. If the load had acted parallel to the aft plating, the readings would have been up to 1.35 and 1.02 MN for failure at the stringer at stb and port respectively. Only 1.2 MN would be relevant for starboard as the failure point would actually move to the bottom end of the lug as the shear limit strength of the aft plating would be reached first. The defected stringer would remain the critical location for port.

In order to check if lack of fusion can be suspected, a transverse cut sample was prepared by polishing and etching. It is shown in Figure 24, and displays apparent weakness of fusion on

the upper side. The weld on the lower side was apparently too slim. Together they were unable to move the failure into the stringer plate.

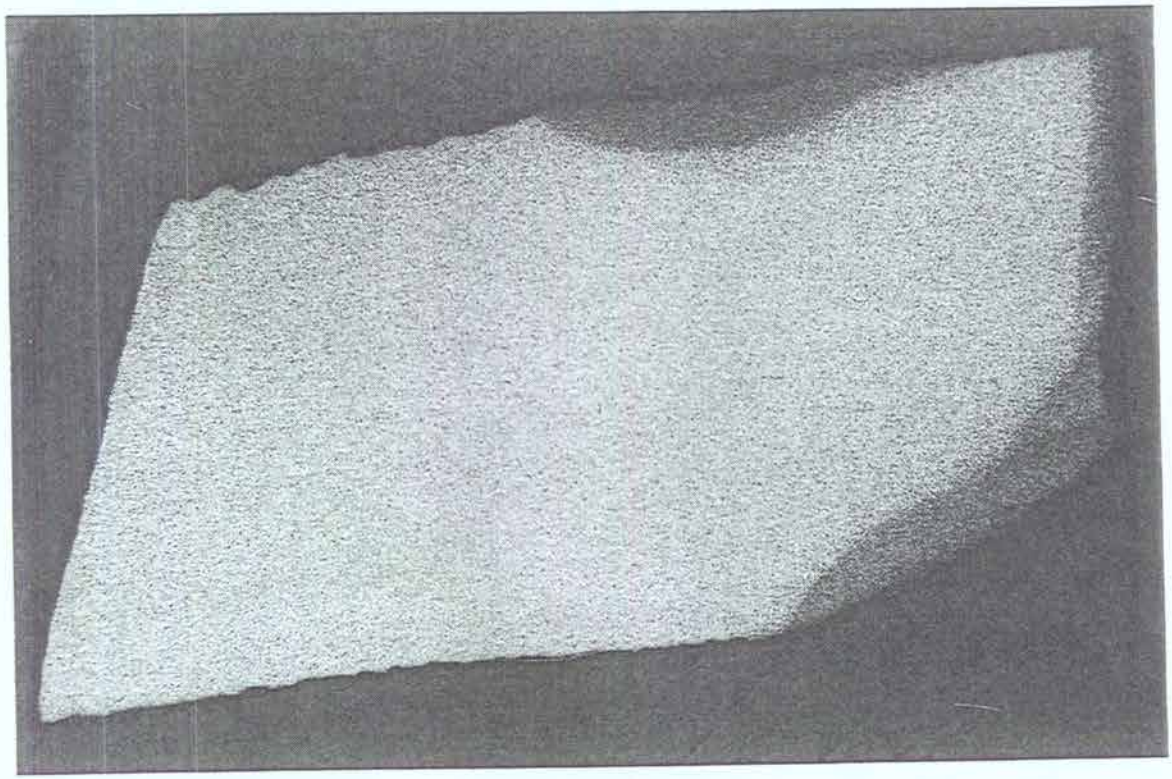

Figure 24. Etched section through the horizontal stringer aft edge on port at the side lock displaying about 4 mm shear width on the low side (shear through edge corner) and 4mm shear width along plate surface on the top side.

The vertical stiffener was assumed to be welded using a 3mm weldment projected width for the tensile cross section. In the yard-designed condition, i.e. without vertical stiffener, the load readings were estimated to be 1.10 MN for port and 1.45 MN for starboard at 38 degrees to the bulkhead and 0.96 MN and 1.29MN for port and starboard respectively with load parallel with the aft plating. In all calculations above the spring constant ratio of the aft plating and the stringer-stiffener structural elements has been taken to be equal to 0.315 as found by test 4/2 and being slightly less than the theoretical 0.36 for plane strain shear/plane strain tension (1-v^2)/(2(1+v)), v=0.285. For other ratios the load capacity estimates would be different and up to geometry/judgement. The theoretical shear/tension spring ratio would be a good guess slightly raising the capacity estimates and a categoric neglect of a ratio - taking the value as 1, would act to lower the calculated capacity a little because of the aft plating getting to be critical. Shear failure would be contemplated for aft plating failure and tensile failure would prevail for the stringer stiffener elements. If tensile failure were assumed for the aft plating then a close to double capacity would be obtained - obviously seriously in error compared to the strength against the relevant transverse loading mode. Of some interest is to note that a calculated capacity of 312 tons with load in the lug plane and at 38 degrees to the aft plating is obtained for the two added vertical stiffeners to work at their full capacity, i.e. that they should have been welded through and positioned both under the mating locking lugs. The mating lug joints should then have been welded to the same nominal weldment dimensions as the

stiffeners, i.e. with at least 20 mm penetrating weldments. The mock-up tests and estimation methods are elaborated below.

6.3.3 Side lock mock-up tests

The implemented mock-up test program for the side locks consisted of four tests altogether. A box measuring about 2000 * 600 * 200 mm was built such that side locking lug models were attached asymmetrically to the large faces of the box - simulating the visor aft plating. The lugs were positioned so that the load line of the assembly allowed pulling at 38° to the large face simulating tearing of the lug due either to visor opening or force couple reaction due to sideways loading causing the yawing moment. Tilting forward around the stempost would also cause the same local loading. A general view of the assumed load system of the visor and adopted asymmetric test arrangement is shown in Figure 25 (Other load directions were included in the calculations as explained below). A drawing of the last test mock-up is shown in Figure 26 and a picture of the test piece 4/2 in Figure 27.

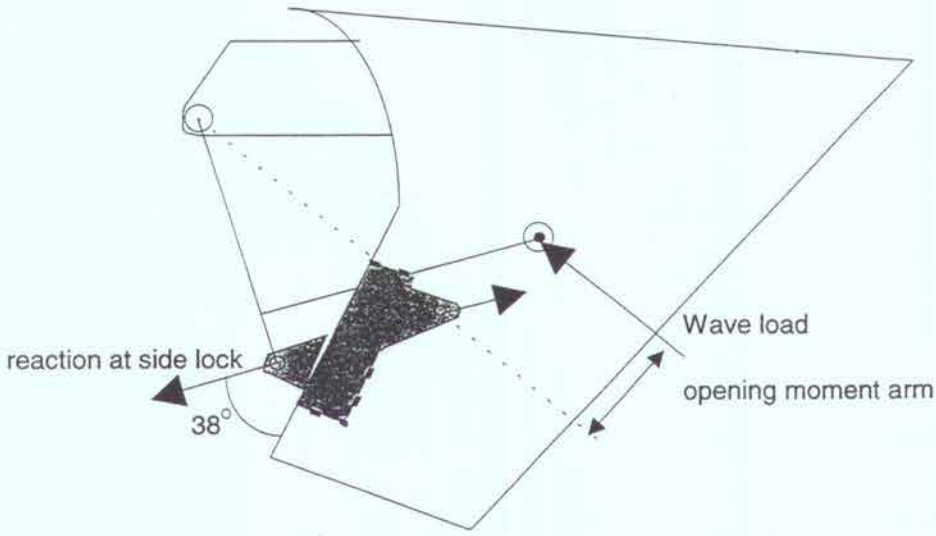

Figure 25. Antisymmetric structural arrangement and load system assumed for the side locking mock-up tests.

The four different tests differed from each other in the details of the stringer and stiffener arrangements. The fourth test mock-up box was further modified from the three first boxes by building the long side of the box to resemble the inner edge of the visor plating. The changes in structural arrangements from one test to the next had a very marked effect on the levels of failure loads, and it is summarised that only the fourth test result is relevant from the point of view of actual failure load reading.

The structural arrangements and failure details of the fourth test resembled the starboard side lock of the visor best of all tests. The second mock-up is also relevant in displaying the failure load level and stress value for only the aft plating of the visor after failure of the horizontal stringer but without vertical stiffeners, i.e. in yard "designed" condition. This failure occurred when the theoretical ultimate shear strength of the plate was reached at the point of maximum tensile resistance of the mock-up after holding by the horizontal stringer had been lost. This

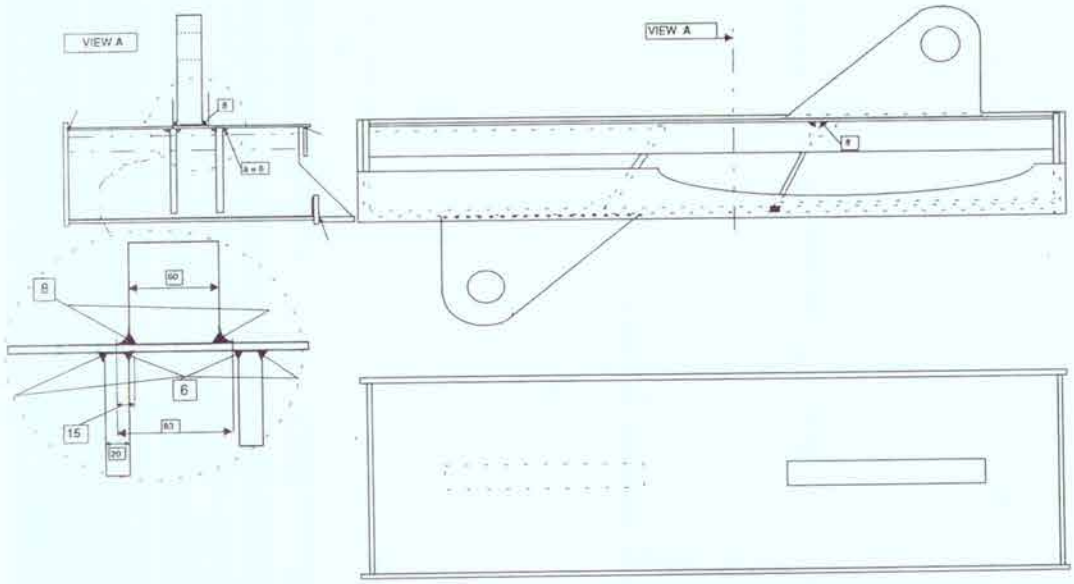

Figure 26. Drawing of side lock test mock-up No. 4.

Figure 27. Side lock test mock-up 4/2 after testing.

test also suggested that stiffness differences between the aft plating and the stiffeners may be assessed assuming plane strain - or out of plane shear - to dominate the stiffness of the bulkhead and plane strain tension to dominate for the stiffeners. The side lock site is statically

indeterminate and analytical strength modelling should therefore include such a stiffness ratio or spring constant effect for obtaining a realistic failure condition estimate and loading capacity number.

6.3.4 Strength calculations of side locks

For purposes of sensitivity analysis for structural and material deviations between the mock-ups and the actual structures a strength calculation macro of the side locks was programmed into EXCEL-worksheet assuming the linearized stress distributions (mechanically equivalent to real or the primary stress) around the bending neutral axis and linear stress-displacement interdependence. The geometry of the assembly and equations used are shown in Figure 28.

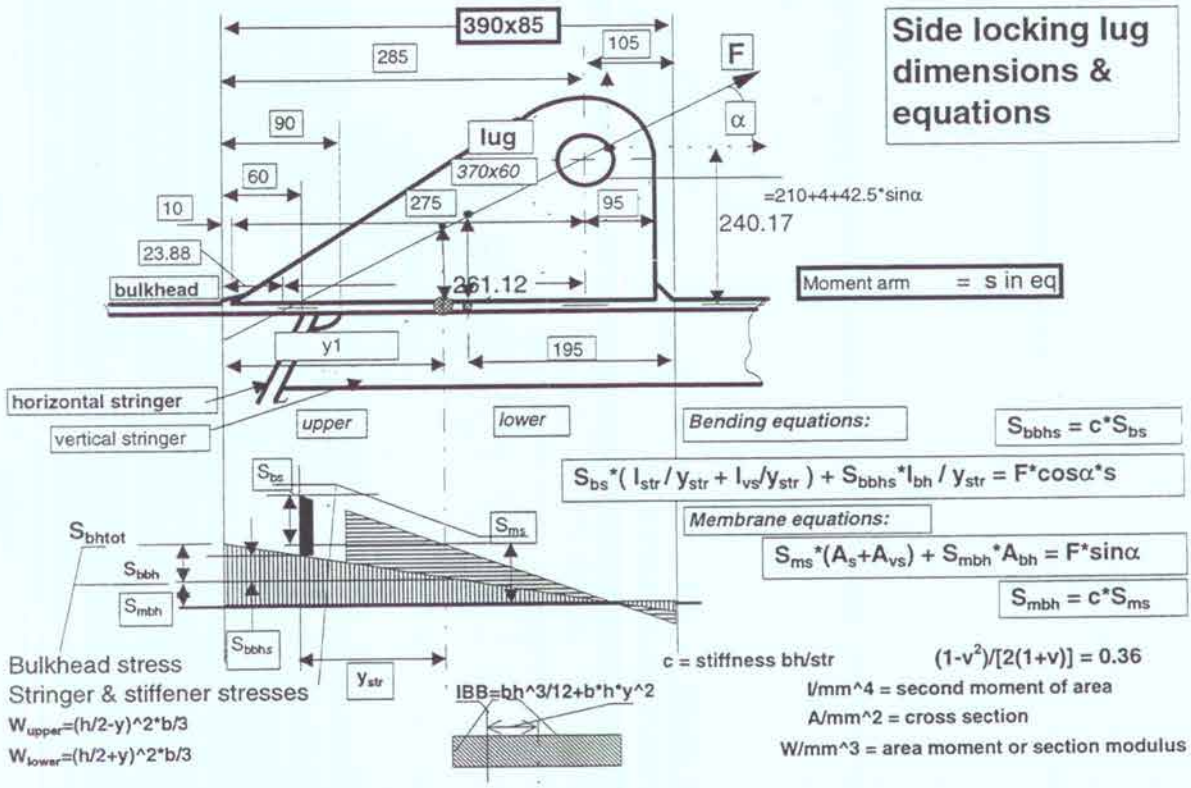

Figure 28. Configuration of side locks, structural details and equations used for strength sensitivity assessment.

The load capacities for starboard and port were thus possible to estimate. The procedure is the traditional, i.e. by seeking the neutral axis (NA) of bending (by setting the section moduli [mm^3] equal on both sides of NA) after which the moment arm for inclined pull is found asf.

Values for the breaking stresses of the various elements were as follows according to tensile testing of aft plating material:

Horizontal stringer and vertical stringer weldment in tension:	1.15*476 MPa = 547 MPa
Aft plating in shear:	0.57*476 MPa = 274 MPa

The effect of various directions of load action can be and was estimated. A load parallel to the visor aft plating was calculated, which would comply with a scenario of visor being raised without an opening movement as well as a load working through NA, i.e. a load with no bending effect. The former would correspond with e.g. an elastically "soft" direction of loading of the Atlantic lock and would include tension in the hinges. The pull only mode perpendicularly to the visor aft plating does not seem to be feasible but shear only parallel to the aft plating may be realistic. Supported by these test results, primarily test 4/2 (second loading of fourth mock-up after repair of its first irrelevant failure at 1.7MN) failing at 1.8MN, the estimated strength levels for the lock at starboard and port are given in Table 2. Plate dimension and material differences between mock-up and actual visor have been accounted for. The numbers represent those obtained for a 3 mm thickness of the broken vertical stiffener weldment.

Table 2. Side lock strength estimates for load acting in the plane of the lug.

	Port	Starboard
Load acting at 38°	1.19 MN	1.59 MN
Load acting at 0°	1.02 MN	~~1.35~~/1.22 MN
Load acting through NA(angle)	1.86 MN (62°)	2.43 MN (62°)

6.3.5 Side-lock mountings from MV Diana II

A side lock base left over from the bow modification for MV Mare Balticum was recovered for metallurgical survey of the remaining damages on the side locks of the January 1993 incident. Also the repair was observed, Figure 29.

The observation yielded remaining cracking in the original plating in several locations, one of them can be seen in the bulkhead plate starting at the toe of the fillet weldment of the vertical backing stiffener, Figure 29. Strengthening plate pieces had been added as part of the repair action, but the repair piece fit and welding quality of the repair appears poor. A strength estimate cannot be given.

6.4 Lifting cylinder lower platforms

Lifting cylinder lower platforms were torn from deck B, part of it accompanying the torn units. The principal strength element in this assembly is plate B and its circumference of the twin lug. It was found that on port slightly more than half of this circumference had cracked in a ductile manner displaying evidence also of fatigue. Part of older fatigue cracking was clearly evidenced by semielliptic black fracture surfaces, Figure 30.

The originally sharp-edged black colouring smoothed out as storage time elapsed, as shown in Figure 31. The black stain was quite evidently hydraulic oil and dirt.

Some of the rest of the remaining ligament was also due to fatigue and ductile tearing.

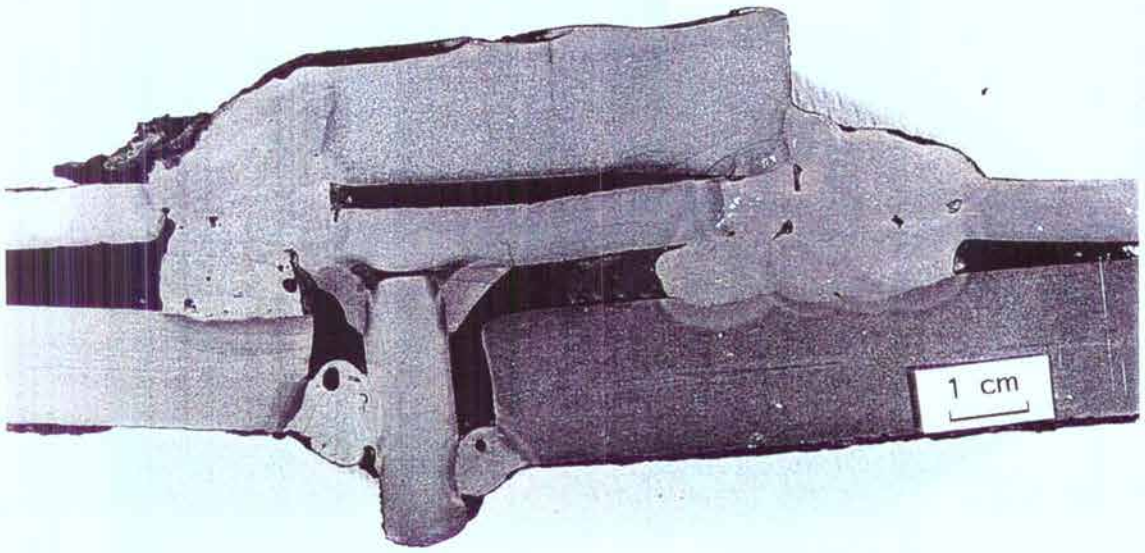

Figure 29. Metallurgical horizontal section through side locking lug, aft bulkhead, vertical stiffener and repair pieces of side lock site in MV DIANA II.

Figure 30. Port side lifting cylinder lower lug as recovered with visor.

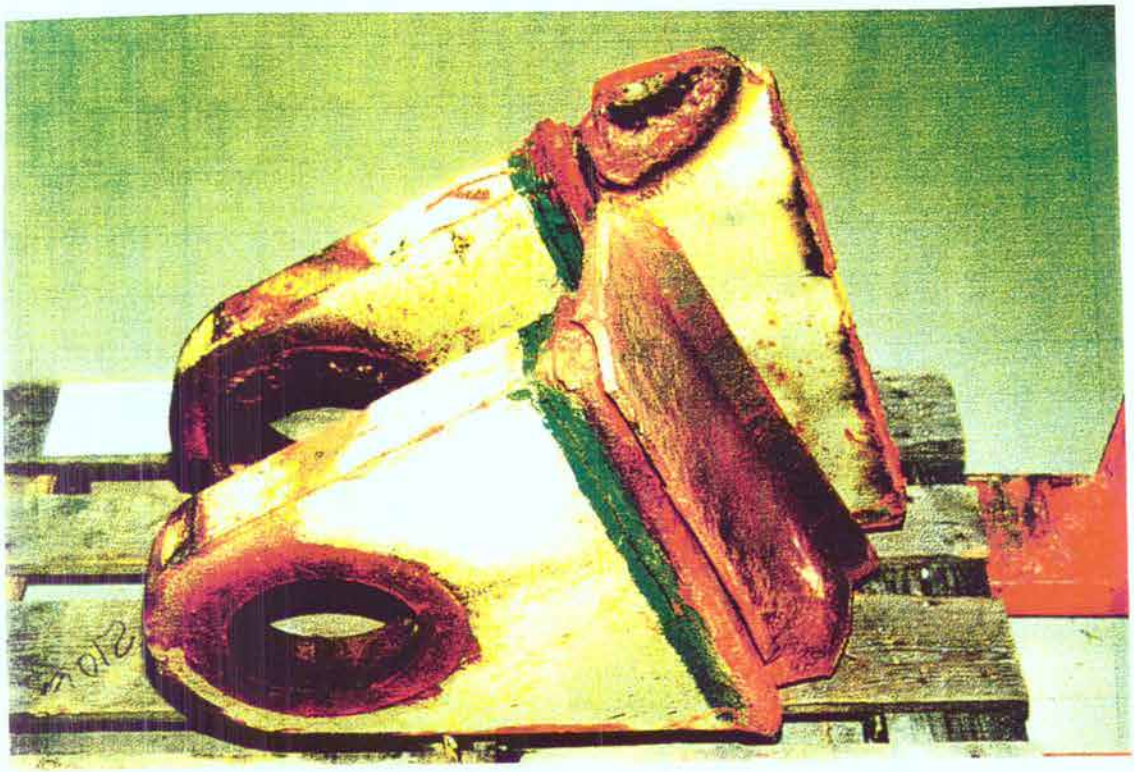

Figure 31 . Port lifting cylinder lower platform as seen from bow centre. Position tilted 120 degrees bow up. Bow end of lower port extreme stringer weld repaired. Centre stringer bent with broken fillet weld, nearest (centremost in ship) fillet weld missing.

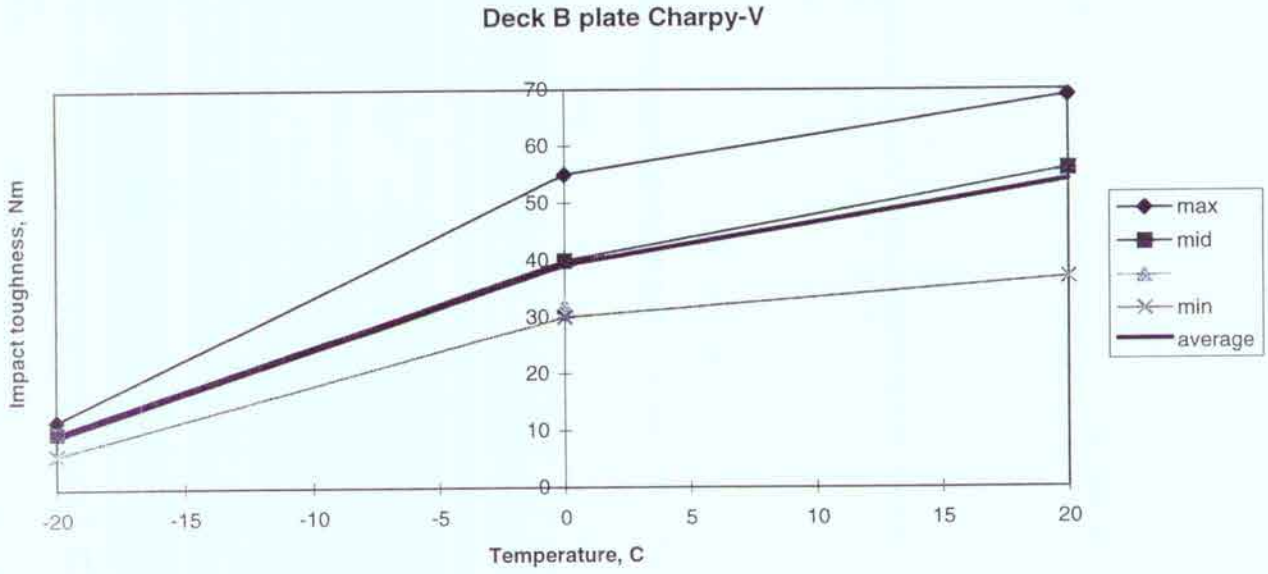

Figure 32. Deck B Charpy-V impact toughness values.

The extreme port side stringer under deck B had been weld repaired as evidenced in Figure 31. The centremost stringer had been welded with only one fillet weld - the other one missing. Twin fillets had been applied to all other stringers under port and starboard lifting cylinder lower lugs.

The remaining section had fractured by cleavage - a mechanism typical of cold brittleness. Deck B plate was also found by Charpy-V impact testing to have a tendency for cold brittleness, even at room temperature as indicated by impact toughness shown in Figure 32. The reduction of strength due to this possible source of weakness has not been assessed accurately, however.

The load to tear the lug platform from deck B may be estimated based on ultimate shear strength and the fraction of section left ahead of the fatigue cracked part of the plate. Taking that the platform perifery measures about 560+240+560+240 mm and the plate thickness is 20 mm, the total uncracked cross section = 0.032×10^6 mm^2 . Assuming an ultimate shear strength of 250 N/mm^2, the tearing strength without fatigue could have been 8 MN, excluding a supporting effect of the underlying stringers. With half of the section cracked, only half of this capacity was left on port, and somewhat more on starboard. Because of possible brittleness in deck B plate it could have been somewhat weaker, leaving a probable range of 4 to 2 MN.

7 Summary and Conclusions

Bow load division onto visor attachments and the strength of individual visor attachments of MV ESTONIA have been assessed.

In the assessment of local load levels at the individual visor attachments a three-dimensional "space frame" idealization was used to simplify the geometrical configuration of bow load action centre and its location with respect to the five primary attachments of the visor, these being the two hinges and three locks. Acting load information was taken from basin model test results obtained elsewhere (SSPA-Gothenburg) as theoretically further elucidated in this work concerning interrelationships of moment and force components. Due to the actual three-dimensional arrangement of visor attachments - in particular the far aft removed hinge points in relation to the longitudinal positions of the visor lockings, severe bow load accumulation onto the lockings was observed. In oblique head waves from port of the bow the wave encountering side lock was deduced to take most of the load of all locks - possibly twice the load taken by the bottom lock.

All strength assessments of individual lockings are upper bound numbers and the marginal possibility of fatigue induced further weakness has not been assessed except for the hinges, where cracking reported to the Commission has been accounted for. From the appearance of the fractures of authentic attachments the upper bound solutions are relevant.

Using full size model testing and direct observations on authentic fractures the port side lock was found to be only a little stronger than the design load assigned to each lock. It was apparently the weakest of all - partly weakened by welding related deficiency at its primary structural weldment within the visor and seems to have possibly broken or lost its holding rigidity first in the sea conditions prevailing during the accident night.

The strength assessment of the bottom lock was based upon analysis of the deformed visor lug. Using the result obtained the apparent weldment size of the broken fore peak deck assembly was calculated. The result - an average fillet weldment size of about 3.5 mm - conforms with direct observations on the authentic lock recovered from the wreck, which has been investigated elsewhere.

Materials used to build the authentic visor lockings have been identified complementing identification performed elsewhere. No indications of high strength steel of the St52 - type has been found in the structural elements checked either by hardness testing or by tensile tests (hardness tests of the b-lock bolt from the near-sister ship MV DIANA II indicate the bolt material to be of higher strength). All plate materials investigated as related to the primary five visor attachments have displayed high quality and ductility. Only the lifting cylinder bottom attachments -deck B - were found to display signs of cold brittleness, but the effect of it has not been quantified. Being a secondary attachment from the point of view of possibly retarding the sequence of the accident, further work was not performed on this element.

8 References

Prof. Matti Kleimola, Helsinki University of Technology: An Assessment of Bow Force Distribution onto Visor Attachments. Reports 1 and 2 (in Finnish), 6.4.1997 and 4.5.1997.

Prof. Erkki Niemi, Lappeenranta University of Technology: Upper bound estimation of the ultimate load capacity of the atlantic lock, 7.8.1997.

VTT Building Technology Research Report No RTE 57243/96, Eva Häkkä and Paula Raivio, Investigation of the Paint Systems from MV ESTONIA Bottom Lock,

VTT Working Notes, Pekka Pankakoski and Tuomo Karppinen: Flexibility measurements of the MV ESTONIA visor (in Finnish), 25.9.1996.

VTT Manufacturing Technology Research Report ValC-246, Kai Katajamäki: MV ESTONIA ACCIDENT INVESTIGATION, Strength investigation of the visor side locking device, numerical calculations, 27.6.1996.

VTT Research Report ValC 312, Jukka Airaksinen: MV ESTONIA Accident Investigation, Strength Investigation of the Visor Hinge, Numerical Calculations, 8.4.1997.

Prof. H. Petershagen & DI A. Krohn: Report of Systematic Fracture Tests with Atlantic Lock Mock-ups of MV ESTONIA, Institut für Schiffbau der Universität Hamburg, Hamburg September 1996.

VTT Research report Val72-7261, Klaus Rahka: M/V ESTONIA ACCIDENT INVESTIGATION - Mapping of Deck B Fractures of Lower Lug Attachments of Visor Port Side Lifting Cylinder, 19.11.1997

SUPPLEMENT No. 512

Airaksinen Jukka:

MV ESTONIA. Accident Investigation. Strength Investication of the Visor Hinge, Numerical Calculations.

Technical Report VALC312.

VTT Manufacturing Technology.

Espoo 1997.

VTT MANUFACTURING TECHNOLOGY

MV ESTONIA ACCIDENT INVESTICATION Strength Investication of the Visor Hinge, Numerical Calculations

TECHNICAL REPORT
VAL C 312/8.4.1997

Jukka Airaksinen

VTT MANUFACTURING TECHNOLOGY
P.O. Box 1705, VTT FINLAND
Tel.int.+358 9 4561, Telefax + 358 9 455 0619

Projekti/työ - Project identification	Sivuja - Pages	Päiväys - Date	Raportin nro - Report No.
VAL 4354	16 p. + app. 8 p.	8.4.1997	VAL C 312

Otsikko ja tekijä - Title and author

MV ESTONIA ACCIDENT INVESTIGATION
Strength Investigation of the Visor Hinge, Numerical Calculations

Jukka Airaksinen

Päivitys raporttiin nro - Update to report no.	Hyväksynyt - Approved by

Julkisuus - Availability statement — Määräpäivä - Until date

[] B (Julkinen - Public) [x] C (Luottamuksellinen - Confidential) [] C (Salainen - Secret)

Abstrakti, sisällysluettelo, tms. - Abstract, list of contents etc.

Abstract

The structural behaviour of the visor hinge of the ro-ro passenger ship MV Estonia was analysed using finite element method (FEM). Non-linear static analyses with linear material behaviour using solid elements and contact elements were performed. Contact elements allow sliding of the corresponding surfaces and these surfaces can not penetrate into each other. No friction was modelled between the contact surfaces. A 90° sector of the fillet weld joining the hinge plate and the sleeve was left open.

Two load cases were analysed representing possible cases which may have damaged the structure. In the first load case a total force of 2MN was applied to the hinge. In the second load case a total force of 4MN was applied to the hinge. Only one hinge plate was modelled with symmetric boundary conditions.

Contact elements were modelled between the hinge plate and the sleeve and also between the sleeve and the shaft, no friction was modelled. A 1mm gap was modelled between the hinge plate and the sleeve.

Stress results are presented as contour plots and also in tabulated form at selected nodes on hinge plates surface. Maximum stresses by von Mises criteria in load cases 1 and 2 are 736MPa and 872MPa respectively. Maximum displacements in load cases 1 and 2 are 0.36mm and 0.62mm.

Copies:
Klaus Rahka, VAL, 1
Jukka Airaksinen, VAL 1
VTT VAL3

1 INTRODUCTION

The objective of this study is to calculate the structural behaviour of the visor hinge of MV Estonia. Two load cases are analysed using finite element method (FEM). Non-linear static analyses with linear material behaviour were performed. The loading was assumed to be caused by wave pressure distribution acting on the visor side plating. A 90° degree sector of the fillet weld connecting the sleeve and the hinge plate was left open. The material used in calculations was linear isotropic steel.

2 STRUCTURE AND LOADING

The visor is supported by two hinges. The structure of one hinge is presented in Figure 1. The hinge consists of two hinge plates. Thickness of one hinge plate is 60mm. The diameter of the sleeve hole is 250mm. Both plates have a sleeve which is welded to the hinge plate by a filled weld. The effective throat thickness of the fillet weld is 7mm. The inner and outer diameters of the sleeve are 180mm and 248mm respectively, length of the sleeve is 150mm. Inside the sleeve there is a shaft which is supported to the ship structure. The outer diameter of the shaft is 180mm, length is 150mm. The hinge plate is supported to the visor structure. There is no gap between the shaft and the sleeve but there is a 1mm gap between the sleeve and the hinge plate surfaces.

Two separate load cases were analysed. In the first load case a vertical force of F_y=-2MN was applied to the hinge. In the second load case a total force of 4MN (components F_y=3.98MN and F_x=-0.398MN) was applied to the hinge. Positive co-ordinate directions are presented in Figure 2 where the geometry of one hinge plate with a welded sleeve is presented. In this picture the geometry of the weld is continuos, no 90° open sector is present. In both loads cases forces were applied into the same point. This point is at the shaft axis in that end cross-section which is not at the symmetry plane.

3 NUMERICAL MODELS

Only one hinge plate and one sleeve was modelled. Because of symmetry only half of the hinge plate and the sleeve were actually meshed. Also only this part of the shaft which is in the sleeve was modelled. Symmetric boundary conditions were applied to nodes which were on the symmetry plane. All nodes lying on edge of the hinge plate which is connected to the visor structure had all displacements fixed.

Parabolic solid elements were used. Because the shaft is not fixed to the sleeve special contact elements were used to model the interaction between those members. This allows sliding between the surfaces, no friction between the surfaces was modelled. Similar contact elements were also modelled between the sleeve and the hinge plate.

The fillet weld was modelled as a complete continuos weld then the corresponding elements lying on the 90° sector were deleted. This gives a representation of an open weld which can be seen in Figure 2.

Linear isotropic steel with Young's modulus of 206.8GPa and Poisson's ratio of 0.29 were used.

4 ANALYSIS METHODS AND PROGRAMS

Pre processing, analyses and post processing were done with I-DEAS /2/. Static analyses with contact elements were performed. Iteration is needed to obtain the equilibrium because contact elements are present. Contact elements are generated automatically during the solution process.

5 STRESS AND DISPLACEMENT RESULTS

Deformed geometry of the mesh in load case 1 is presented in Figure 6 as a hidden line plot. Maximum displacement is 0.36mm.

Von Mises criteria stresses on deformed geometry in load case 1 are presented in Figures 7 and 8. Only hinge plate elements are shown. Maximum stress is 734MPa at the location where the opening of the fillet welt starts.

Nodal stress components of selected nodes in tabulated form in load case 1 are presented in Appendix 1. These are nodal average stresses, nodal stresses of neighbouring elements are averaged. The locations of the corresponding nodes are presented in Figures 4 and 5.

Deformed geometry of the mesh in load case 2 is presented in Figure 9 as a hidden line plot. Maximum displacement is 0.62mm.

Von Mises criteria stresses on deformed geometry in load case 2 are presented in Figures 10, 11 and 12. Only hinge plate elements are shown. Maximum stresses are 872MPa.

Nodal stress components of selected nodes in tabulated form in load case 1 are presented in Appendix 2. These are nodal average stresses, nodal stresses of neighbouring elements are averaged. The locations of the corresponding nodes are presented in Figures 4 and 5.

6 REFERENCES

1. Part-report covering technical issues on the capsizing on 28 September in the Baltic Sea of the ro-ro passenger vessel MV Estonia. The Joint Accident Investigation Commission of Estonia, Finland and Sweden.

2 I-DEAS Master Series Release 4. Structural Dynamics Research Corporation.

FIGURES

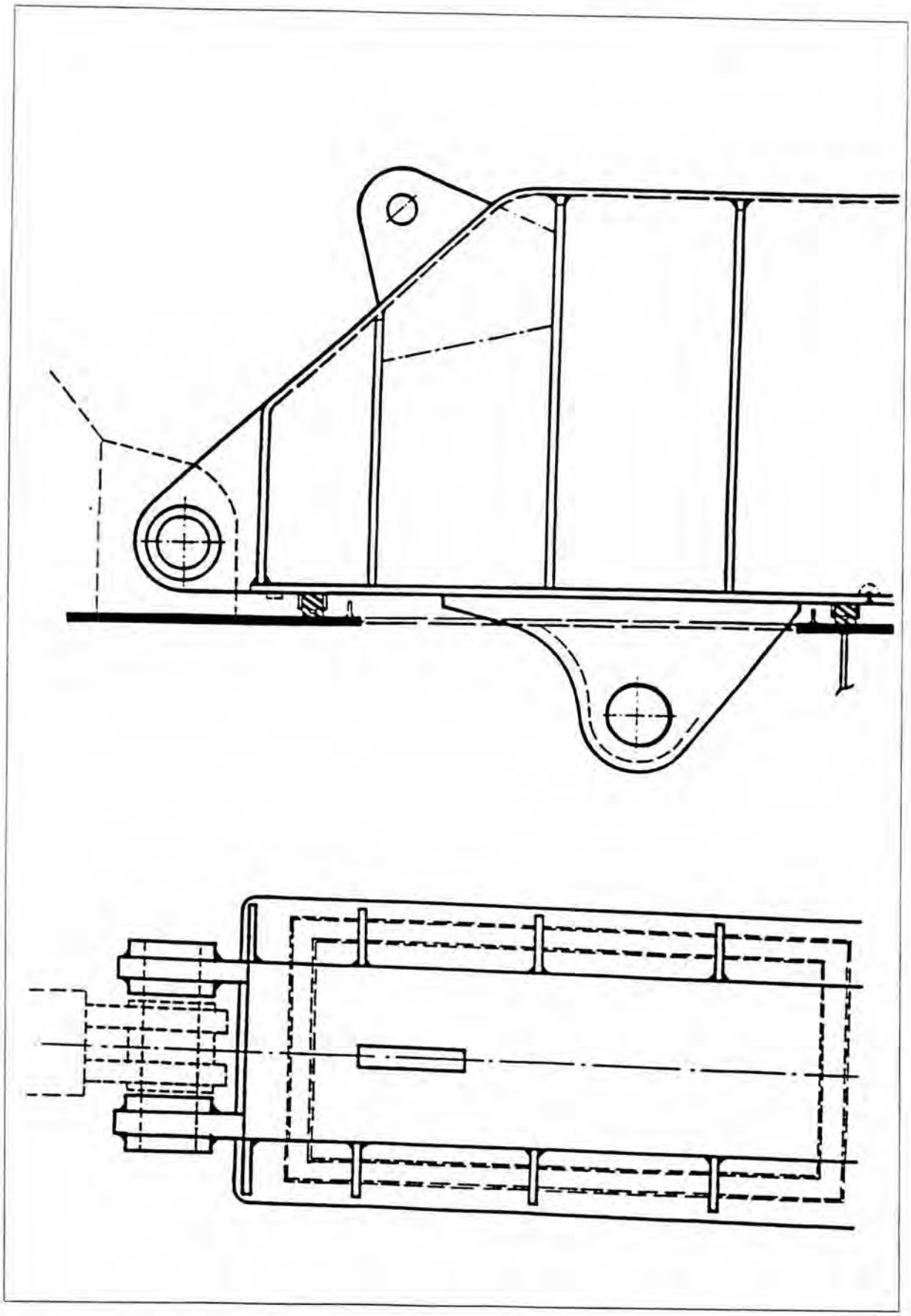

Figure 1. Hinge construction./1/

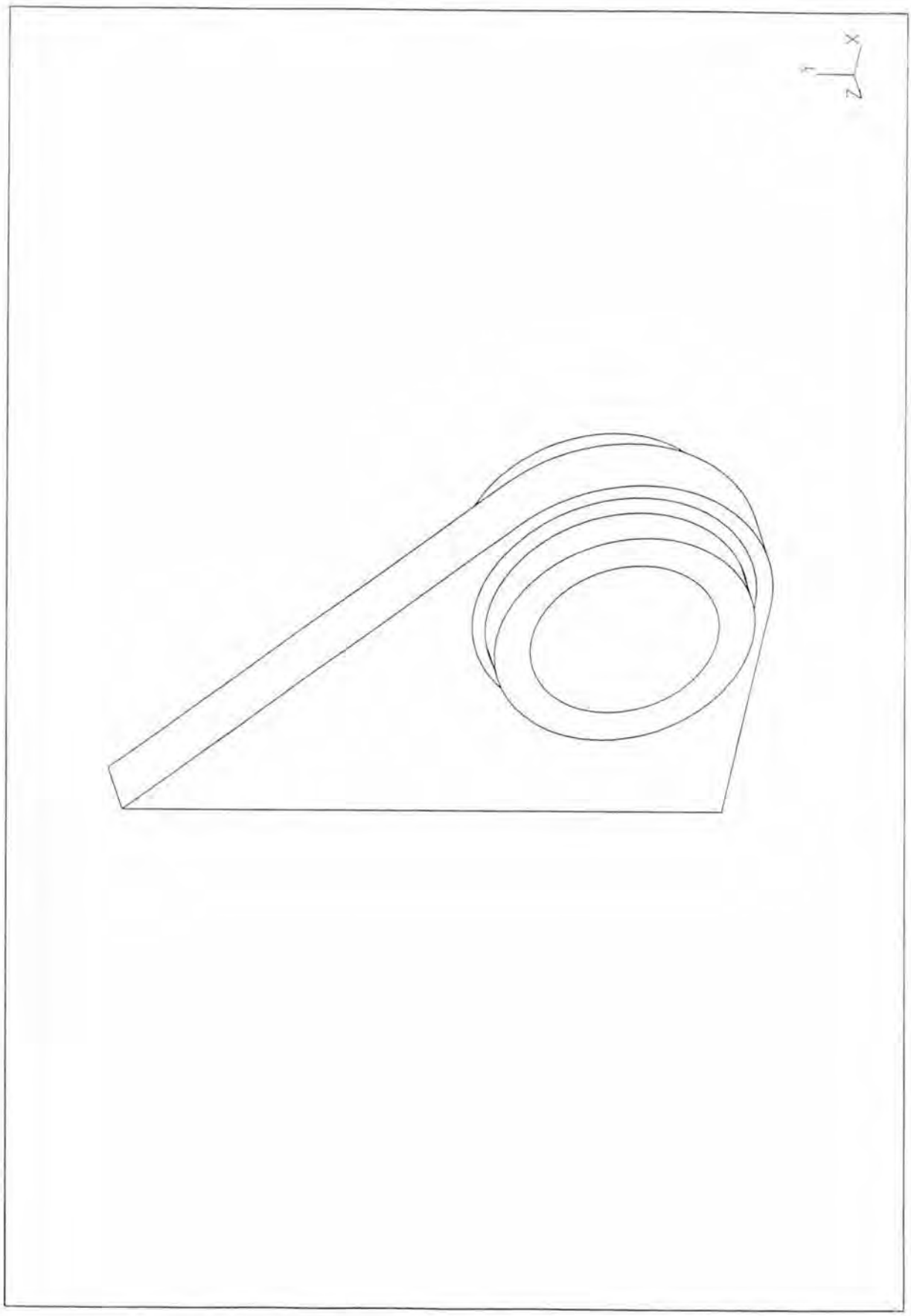

Figure 2. Geometry of the whole structure: hinge plate, sleeve with welds and shaft.

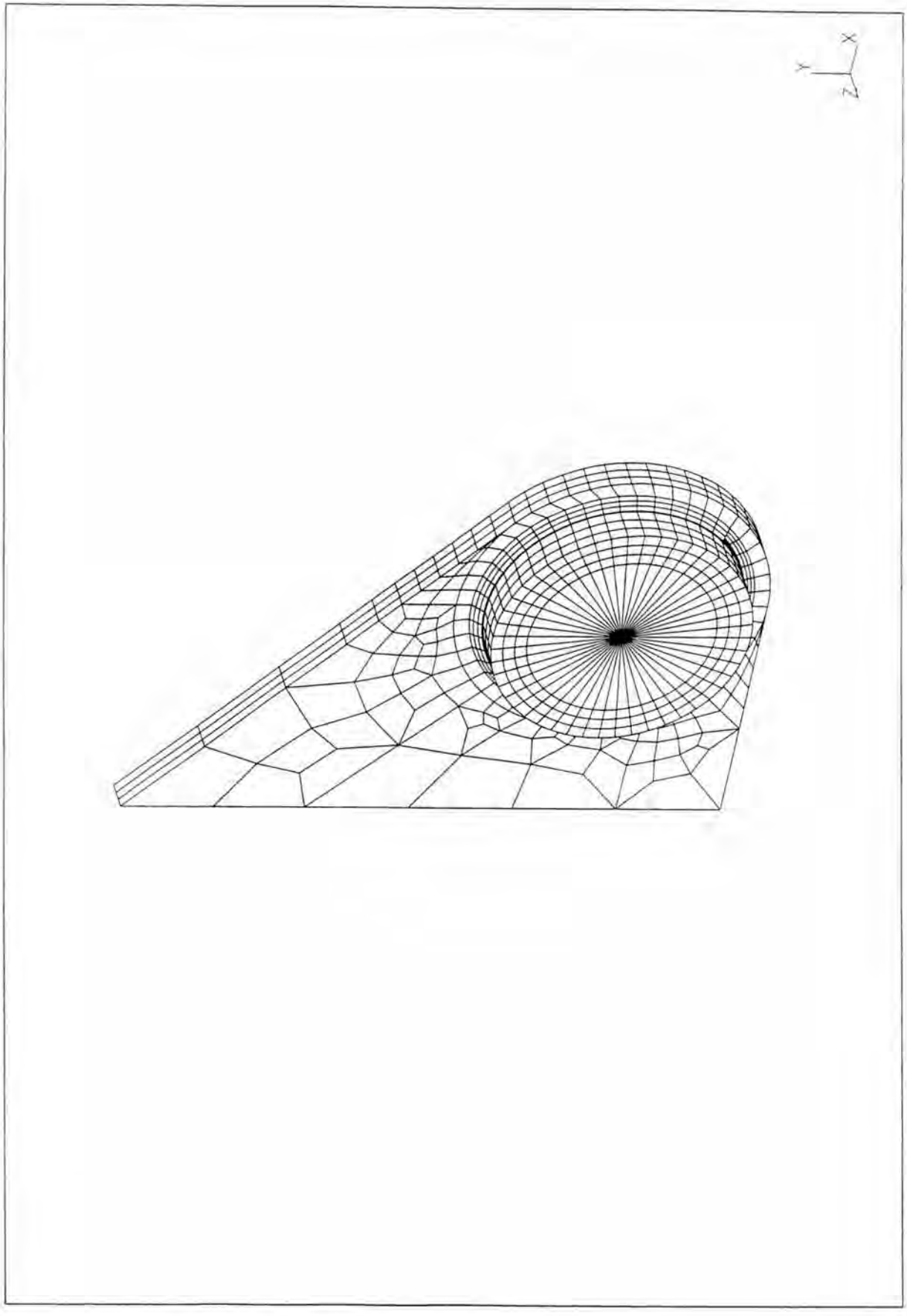

Figure 3. Finite element mesh of the model.

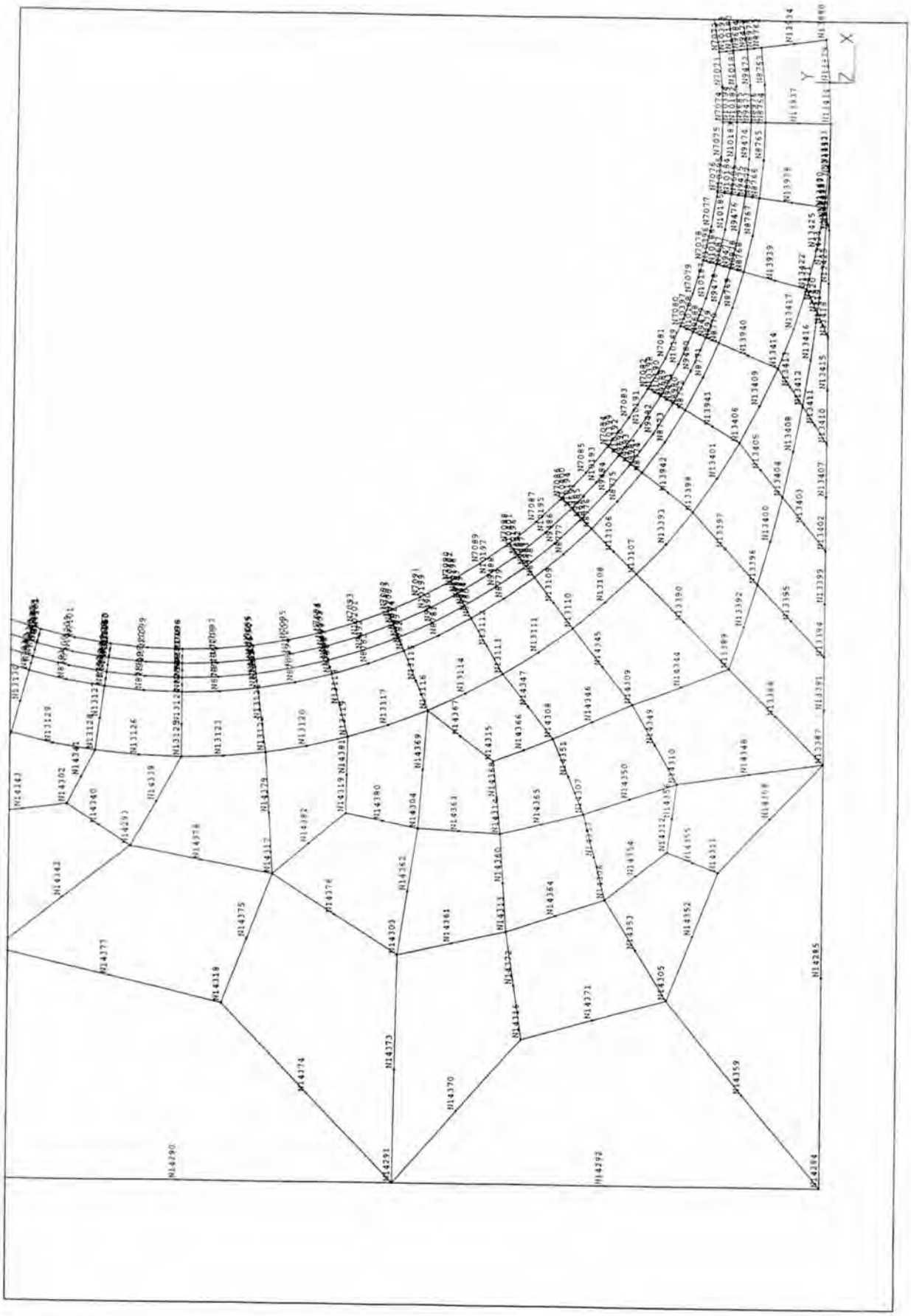

Figure 4. Nodes on the hinge plate.

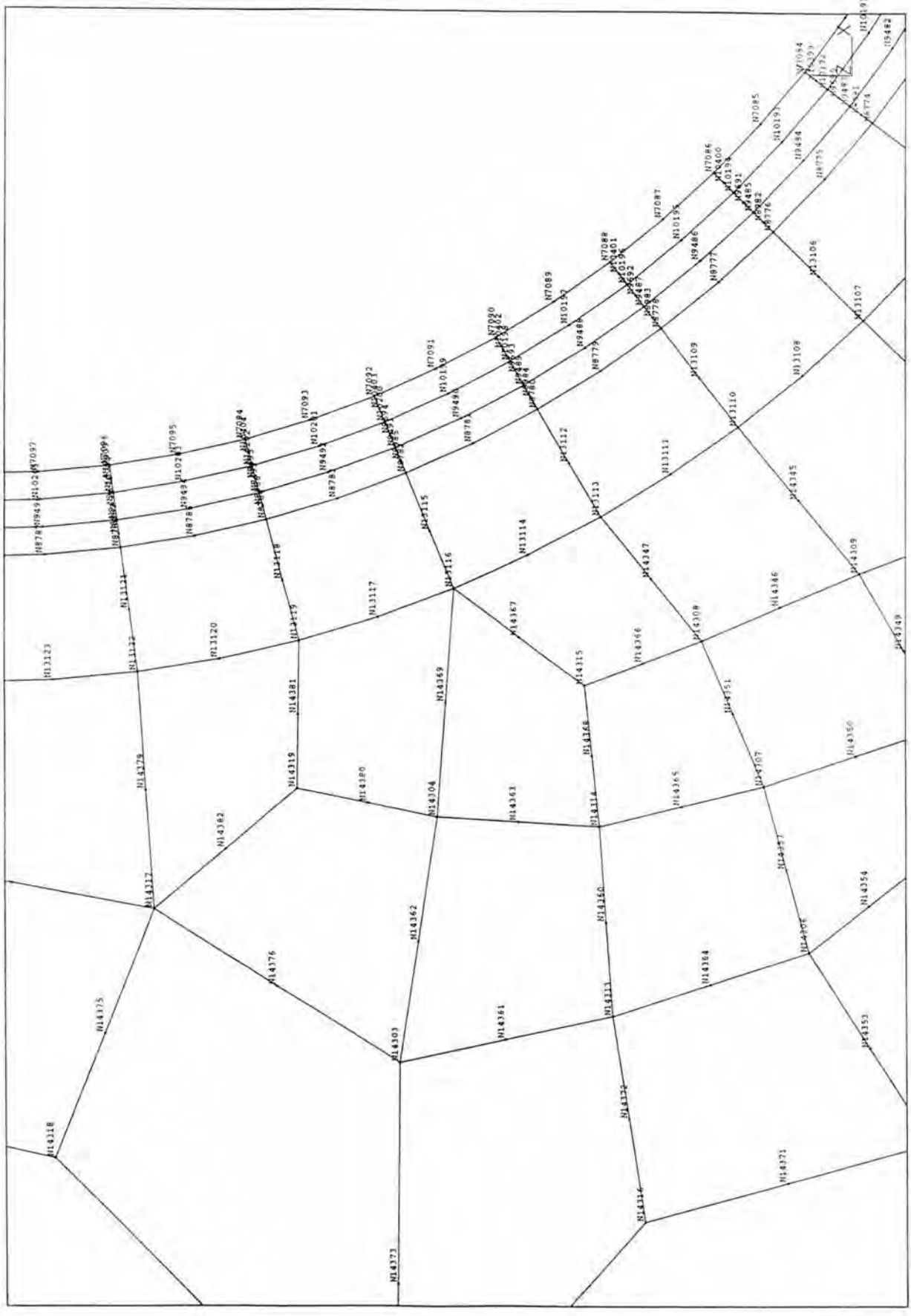

Figure 5. Nodes on the hinge plate, zoomed view.

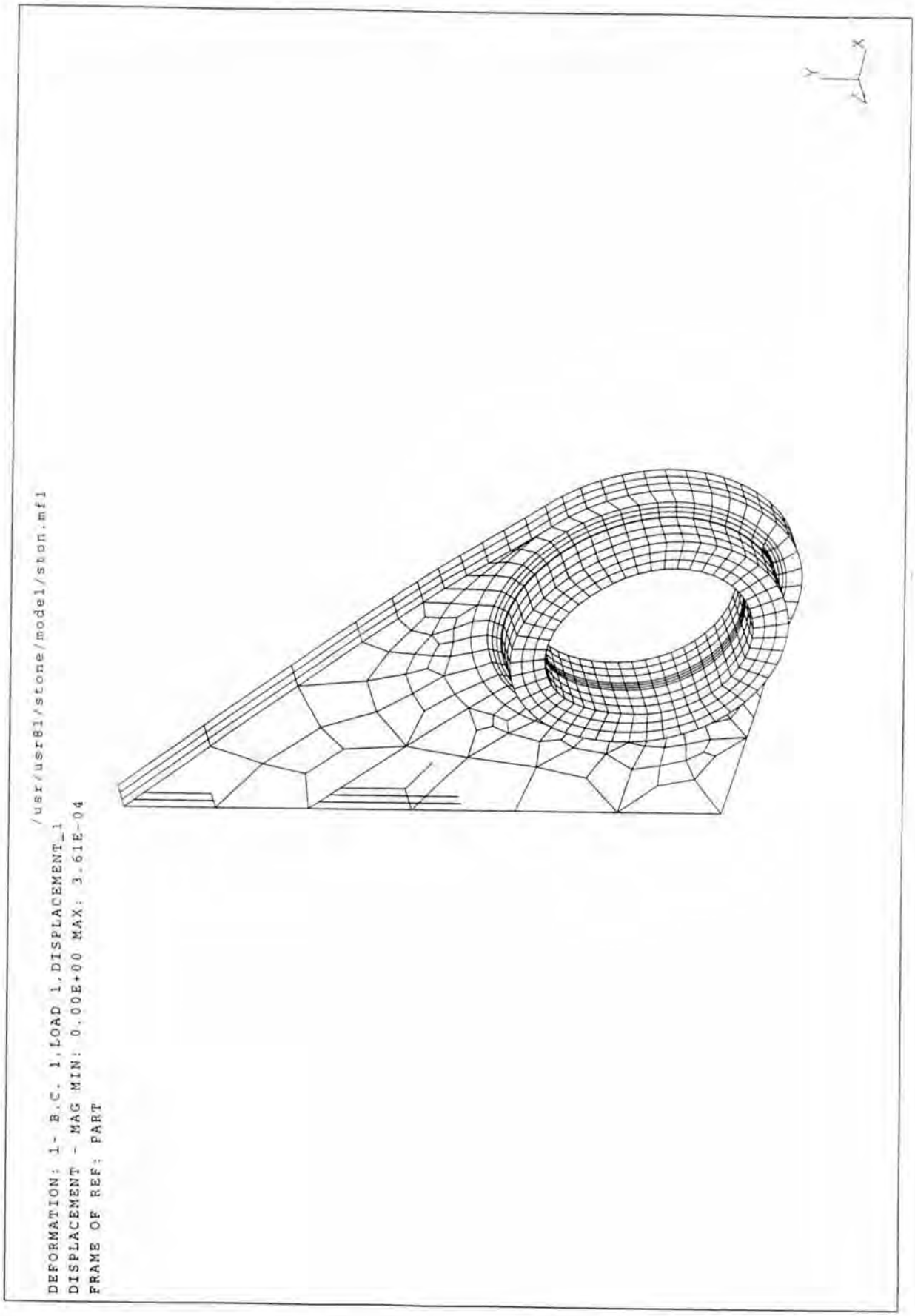

Figure 6. Load case 1, deformations.

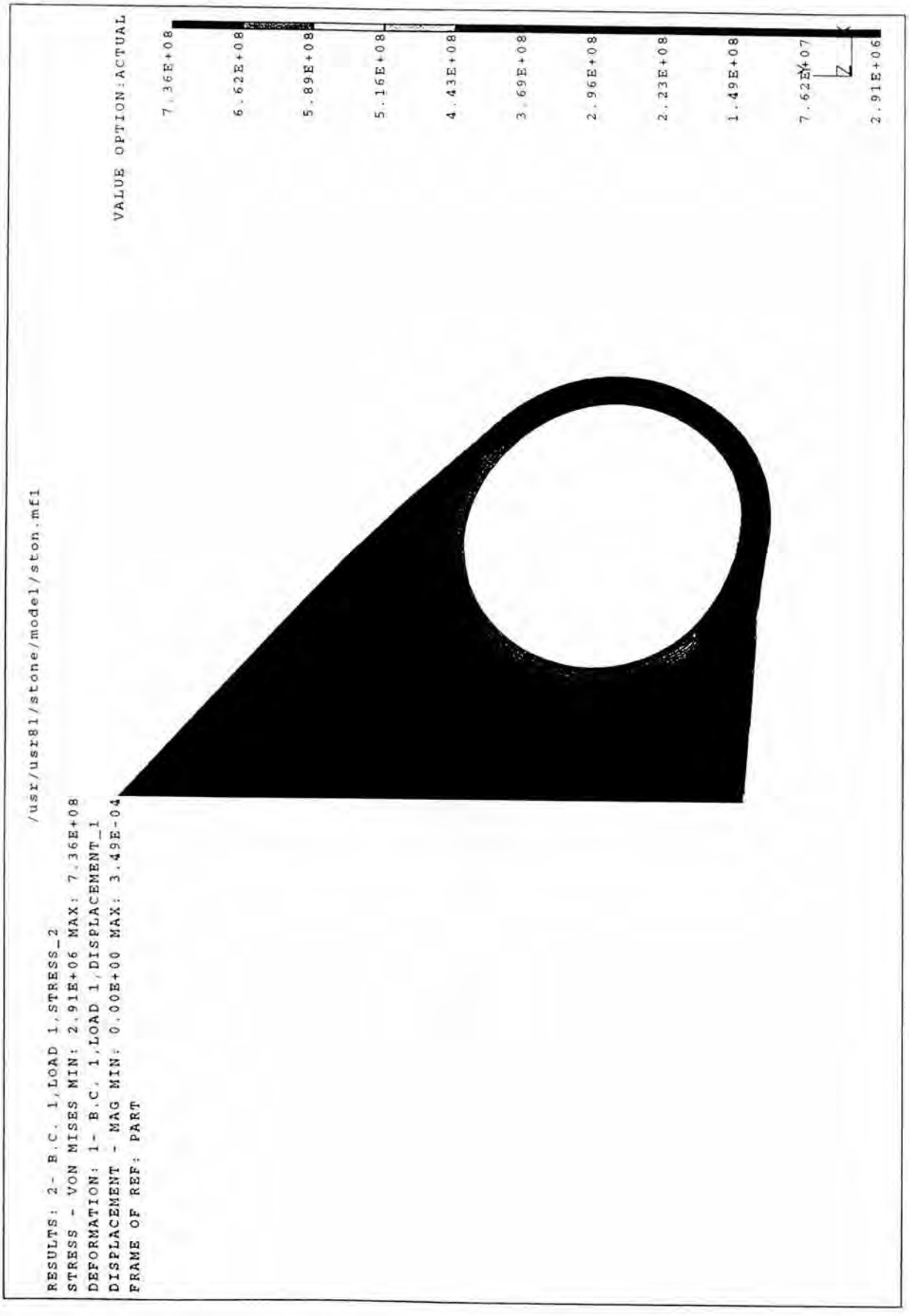

Figure 7. Load case 1, von Mises criteria stresses on deformed shape.

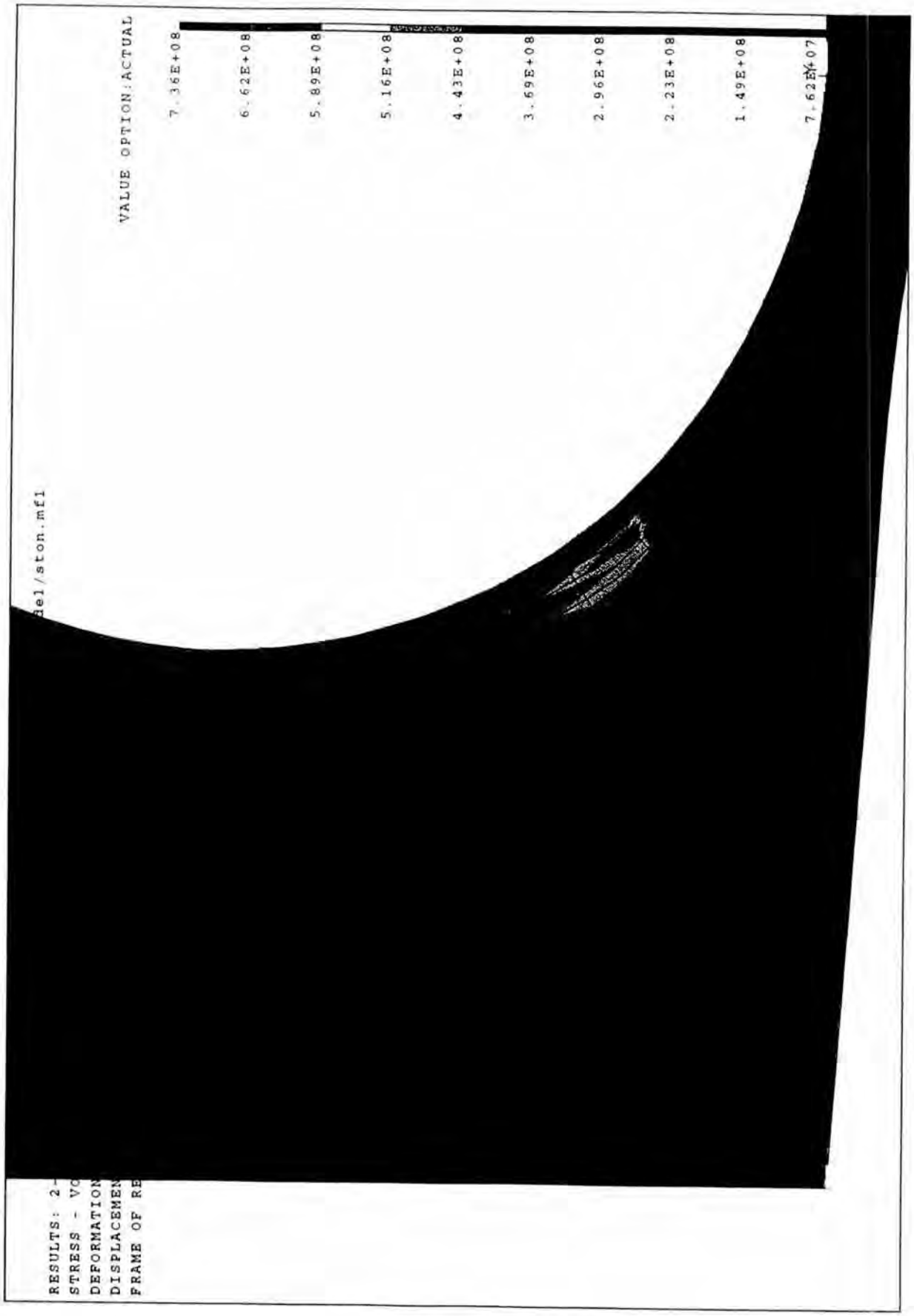

Figure 8. Load case 1, von Mises criteria stresses on deformed shape, zoomed view.

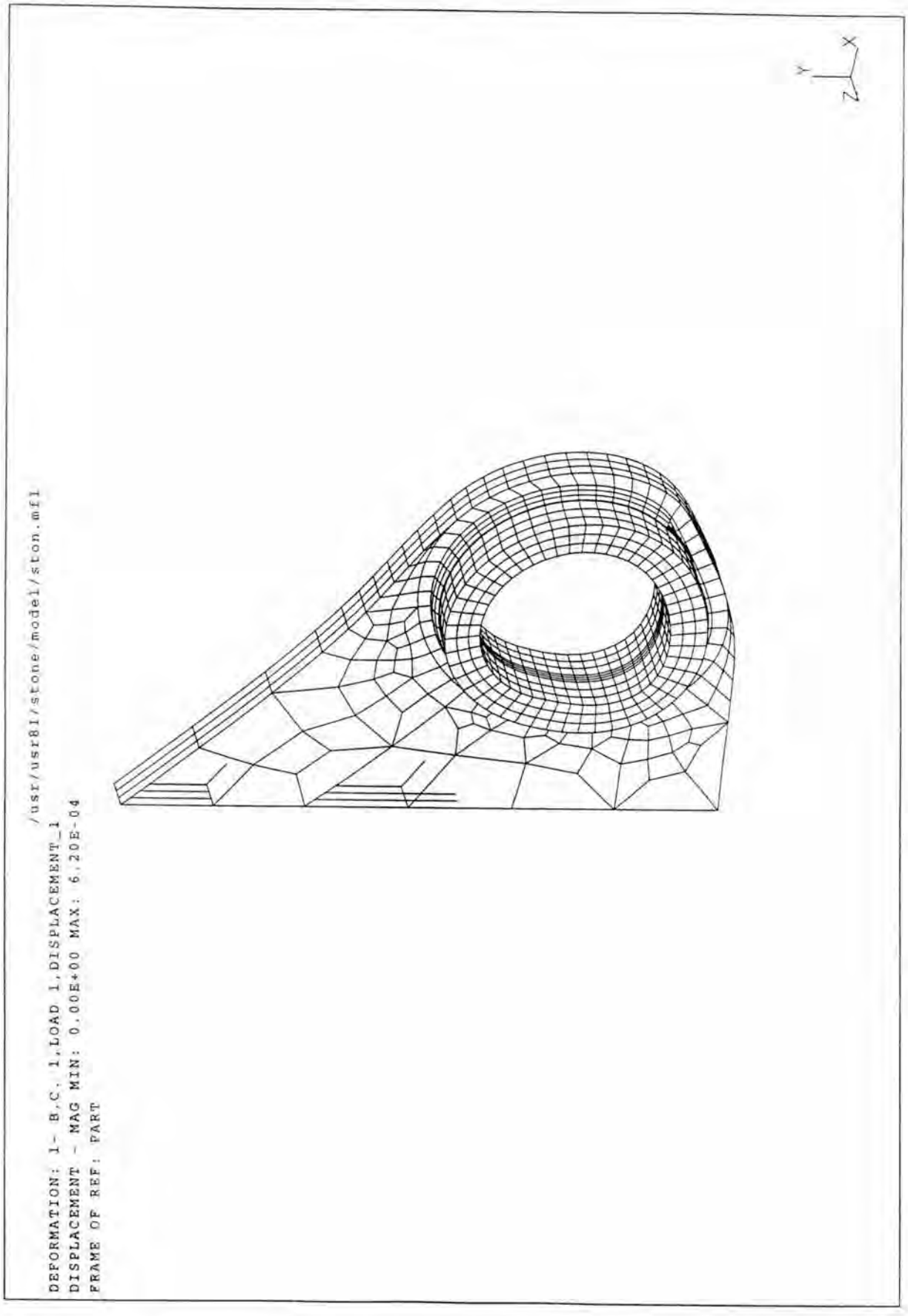

Figure 9. Load case 2, deformations.

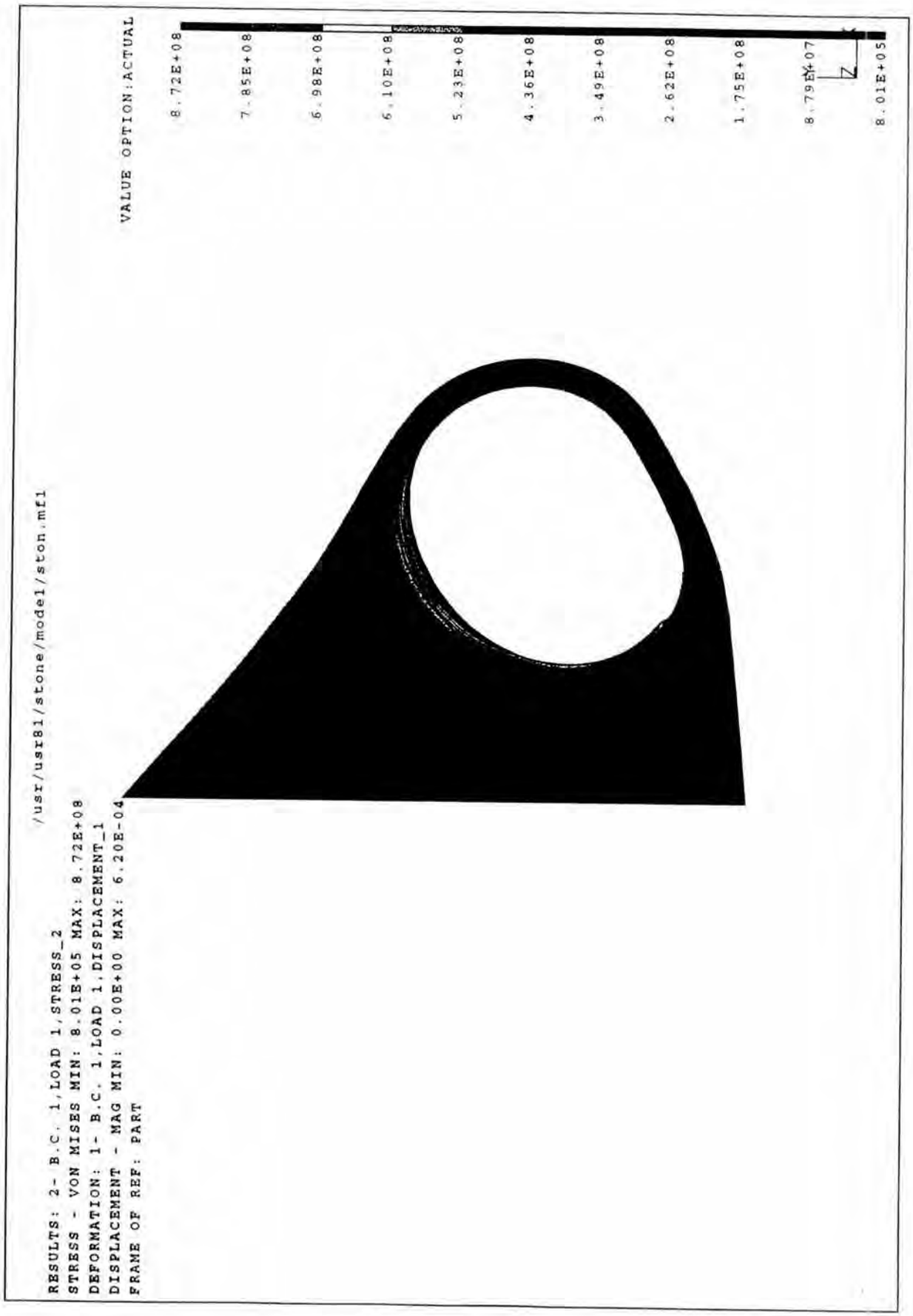

Figure 10. Load case 2, von Mises criteria stresses on deformed shape.

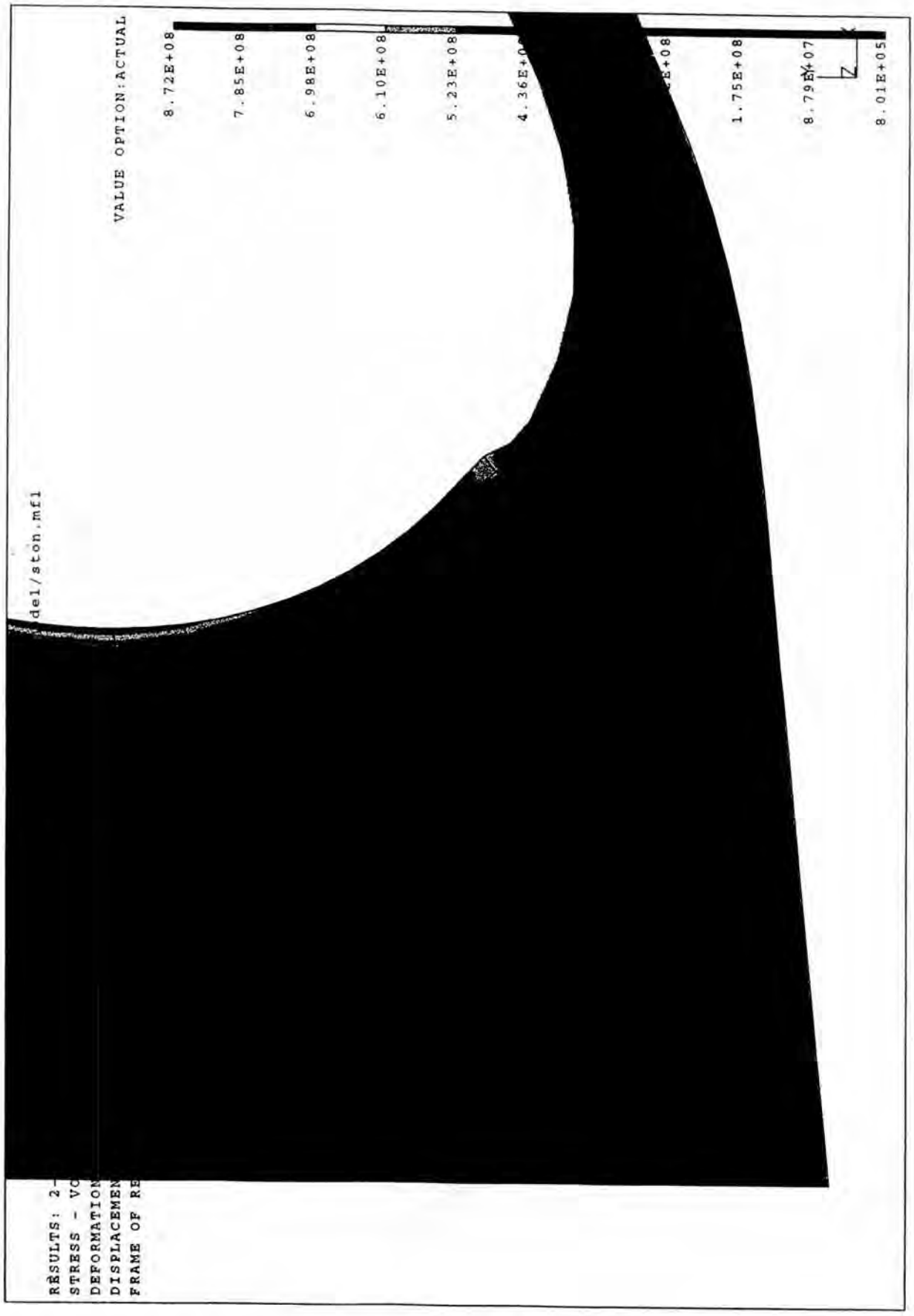

Figure 11. Load case 2, von Mises criteria stresses on deformed shape, zoomed view.

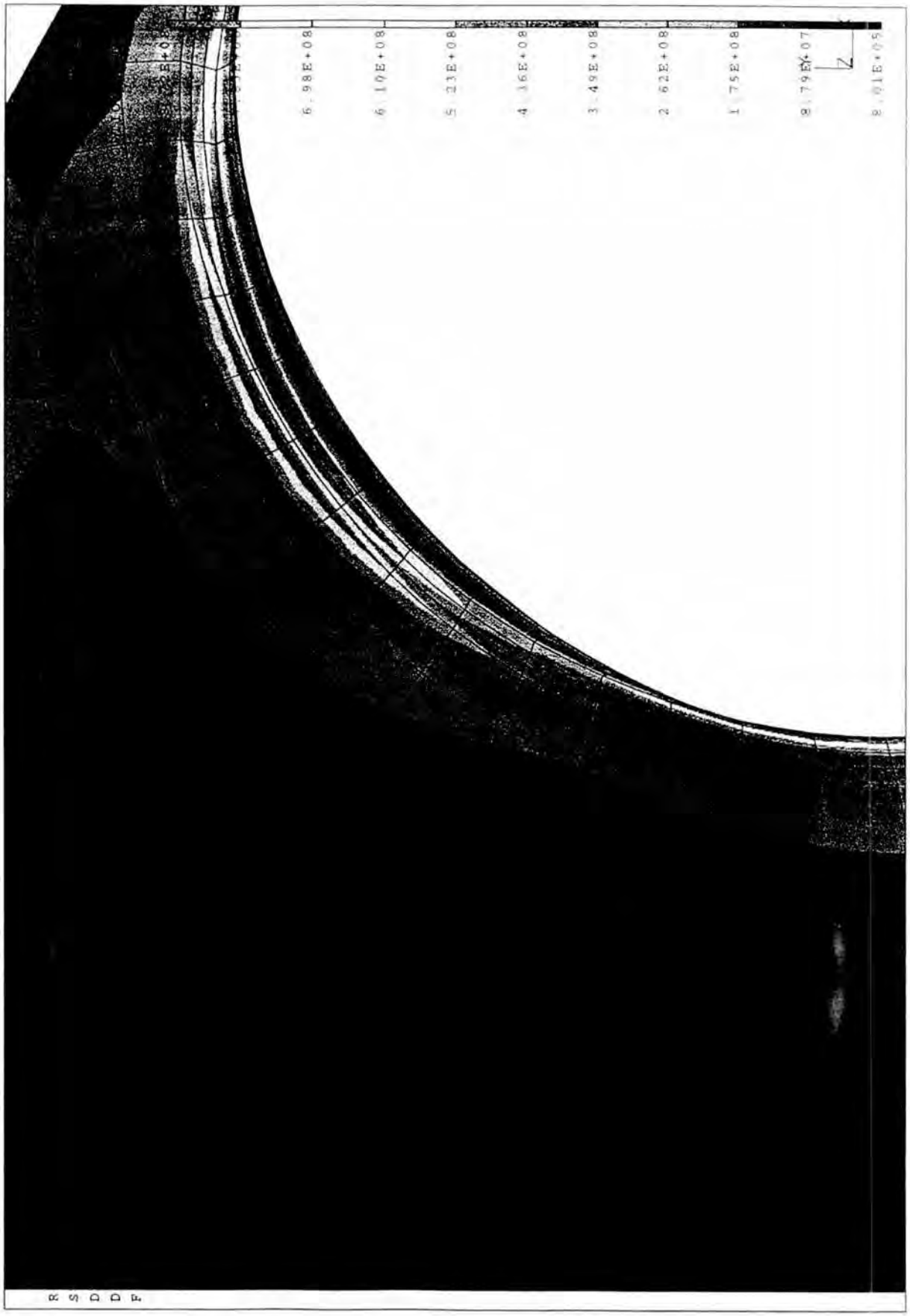

Figure 12. Load case 2, von Mises criteria stresses on deformed shape, zoomed view.

SUPPLEMENT No. 513

Kleimola Matti:

Laskelmat ESTONIAn keulavisiirin lukituslaitteiden kuormituksista.

Espoo 1997.

Kleimola Matti:

Calculations of the loadings on MV ESTONIA's
bow visor locking devices.

Espoo 1997

Prof. Matti Kleimola
Kaksoiskiventie 40
02760 Espoo

6.4.1997

LASKELMAT ESTONIAN KEULAVISIIRIN LUKITUSLAITTEIDEN KUORMITUKSISTA

1. Lähtöarvot

Estonian keulavisiirin kiinnityssaranoiden ja lukituslaitteiden kiinnityspisteet on esitetty alla olevassa kaaviossa. Kiinnityspisteitä on kaikkiaan 5; kaksi saranaa on ylhäällä ja kolme lukkoa alhaalla.

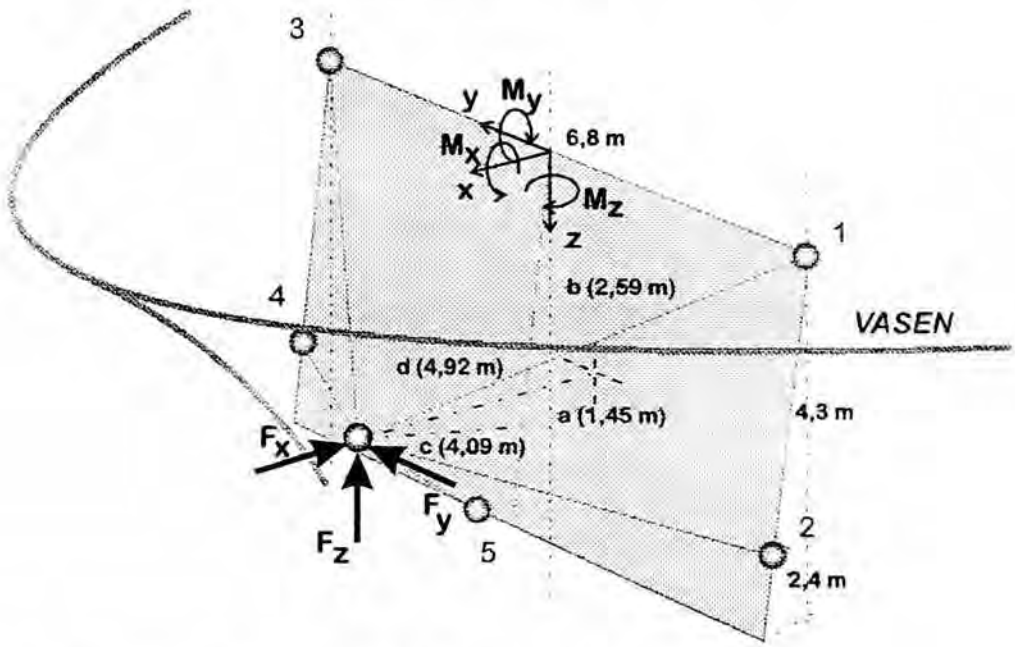

Visiiriä kuormittavan resultantin F_{res} koordinaatit ovat:

a = 1,45 m (y-aks.)	c = 4,09 m (res. et. tasosta 1,2,3,4)
b = 2,59 m (z-aks.)	d = 4,92 m (x-aks.)

Aaltokuormituksen suuruus on määritetty mallikokeiden pohjalta (SSPA) ja niiden mukaan visiiriin vaikuttavien momenttien ja voimien suhteet ovat: $M_x/M_y = 0,25$, $M_z/M_y = 0,08$ ja $F_x/F_z = 1$.

Kaikki visiiriin vaikuttavat voimat ja momentit voidaan esittää visiiriä avaavan momentin M_y avulla ratkaisemalla yhtälöryhmä (1).

$$\begin{cases} M_x = F_z \cdot y - F_y \cdot z \\ M_y = F_z \cdot x - F_x \cdot z \\ M_z = F_y \cdot x - F_x \cdot y \end{cases} \quad (1)$$

Kun yhtälöryhmään sijoitetaan edellä annetut momenttien suhteet sekä resultantin paikkakoordinaatit, saadaan

$$\begin{cases} F_x = 0{,}43 \cdot M_y = 0{,}69 \cdot F_{res} \\ F_z = 0{,}43 \cdot M_y = 0{,}69 \cdot F_{res} \\ F_y = 0{,}14 \cdot M_y = 0{,}23 \cdot F_{res} \\ F_{res} = 0{,}62 \cdot M_y \end{cases} \quad (2)$$

Visiirin omapaino G_v on 0,55 MN ja sen vaikutuspiste on aluksen keskiviivalla etäisyydellä 4,9 m yz-tasosta. Visiirin omapaino aikaansaa sekä suorat tukireaktiot kiinnityspisteihin että momentin y-akselin ympäri. Vaikutukset summataan aaltokuormituslaskelmien yhteydessä.

2. Kuormituksen jako kiinnityspisteisiin

Aaltokuormitusresultantin komponentit F_x, F_y ja F_z aikaansaavat tyypillisiä veto-puristusrasituksia ja leikkausvoimia visiirin kiinnityspisteisiin. Visiiri kiinnittyy laivaan kahdella saranalla, kahdella sivulukolla ja yhdellä pohjalukolla. Rakenne on staattisesti epämääräinen ts. analyyttisin menetelmin kiinnityskohtien kuormituksia ei voida laskea täysin eksaktisti, vaan on suoritettava likimääräistyksiä.

Visiiriä kuormittavien voimien tarkastelu

- F_x on visiiriä sulkeva voima ja se kuormittaa epäsymmetrisesti suoraan laivan pituusakselin suuntaisesti. Voima synnyttää kaikkiin kiinnityspisteisiin puristusjännityksen (epäsymmetrisyydestä johtuen vasemmalle puolelle hiukan suuremmat kuin oikealle puolelle).

- F_z synnyttää kaikkiin lukituspisteisiin leikkausvoiman z-akselin suunnassa ja tämä leikkausvoima ilmenee z-akselin suuntaisena vetona kaikissa kiinnityspisteissä. Suurin kuormitus on vasemmassa sivulukossa ja vasemmassa saranassa. F_z aikaansaa myös visiiriä avaavan momentin, jolloin sivulukkoihin ja pohjalukkoon syntyy vetokuormitus. Ylhäällä oleviin saranoihin kehittyy puristuskuormitus ja visiiriä sulkeva voima. Kokonaisvaikutus on epäsymmetrinen siten, että vasen sivulukko ja pohjalukko kuormittuvat eniten.

- F_y synnyttää leikkausvoimia saranoihin ja lukituslaitteisiin. F_y pyrkii myös avaamaan visiirin vasemman puoleiselta reunalta synnyttämällä

kiertomomentin z-akselin ympäri. Vetokuormitus on suurin vasemmassa sivulukossa ja -saranassa. Oikeanpuoleisiin saranoihin syntyy puristusjännitys. Pohjalukossa vetokuormitus jää vähäiseksi.

- Visiirin oma paino G_v siirtyy suoraan leikkausvoimana kiinnityspisteille. Lisäksi se aiheuttaa momentin y-akselin ympäri siten, että lukituslaitteisiin kohdistuu puristus- ja saranoihin vetorasitukset.

Kiinnityspisteiden kokonaisrasitus lasketaan yhdistämällä superpositioperiaatteen mukaan aaltokuormitusresultantin voimakomponentit ja resultantin synnyttämien momenttien tukireaktiot kussakin kiinnityspisteessä.

3. Voimien suora jako kiinnityspisteille

Jaetaan aluksi F_x , F_y , F_z ja G_v viidelle kiinnityspisteelle tasakuormina ja muodostetaan niille resultantit (epäsymmetria ja momenttivaikutukset otetaan huomioon myöhemmin). Laskelmissa käytetään aaltokuormitusresultantin jakoa $F_x=F_z= 0,69\ F_{res}$, $F_y= 0,23\ F_{res}$ ja visiirin suhteutettua painoa $G_v= 0,10\ F_{res}$.

Laivan keulaan vaikuttava aaltokuormitus F_x arvioidaan jakautuvan tasan kaikille kiinnityspisteille.

- $$F'_{1,2,3,4,5x} = -\tfrac{1}{5} \cdot F_x = -0,14 \cdot F_{res} \qquad (3)$$

Sivuaallokon vaikutuksesta syntyy visiiriin sivuttaisvoima F_y.

- $$F'_{1,2,3,4,5y} = \tfrac{1}{5} \cdot F_y = 0,045 \cdot F_{res} \qquad (4)$$

Pystyakselin suuntainen voima F_z synnyttää tukireaktion jokaiseen kiinnityspisteeseen. Voima jaetaan tasan kaikille kiinnityspisteille.

- $$F'_{1,2,3,4,5z} = -\tfrac{1}{5} \cdot F_z = -0,14 \cdot F_z \qquad (5)$$

Visiirin painosta syntyy kiinnityspisteisiin suora kuormitus.i

- $$G'_{1,2,3,4,5z} = \tfrac{1}{5} \cdot G_v = 0,02 \cdot F_{res} \qquad (6)$$

Saranoihin ja lukituslaitteisiin vaikuttavat resultanttivoimat lasketaan yhtälöistä (3), (4), (5) ja (6), jolloin voimien yhteisvaikutus määräytyy vektorisummana. Jokaisessa kiinnityspisteessä resultanttikuormitus on yhtäsuuri ja suunnaltaan sama.

- $F'_{1,2,3,4,6res} = 0{,}19\ F_{res}$

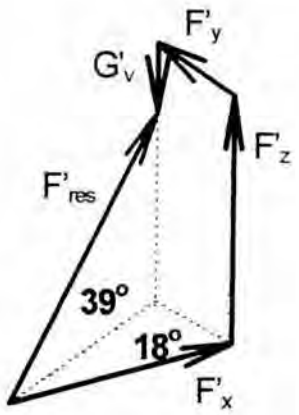

Jokaisen kiinnityspisteen resultantti suuntautuu taakse ja ylös. Kuormitus on visiiriä sulkeva.

4. Kuormituksen epäsymmetria ja momenttivaikutukset

Resultanttikuormituksen epäkeskeinen sijainti

Aaltokuormituksen epäsymmetria jaetaan saranoille ja lukituspisteille tasapainoehtojen perusteella siten, että ensin jaetaan visiiriin vaikuttavan voimakomponentin F_x kuormitus pelkästään saranoille (1,3) ja sivulukoille (2,4). Tasapainoehdosta seuraa, että saranat kantavat kuormasta yhteensä 40 % ja lukot 60 % ja että visiirin vasen reuna kuormittuu 70 % ja oikea reuna 30 %. Pohjalukon voidaan arvioida tasaavan sivulukkojen kuormitusta siten, että lukituslaitteet ottavat edelleen 60 % kuormituksesta F_x. Tasajaon asemesta saadaan kiinnityspisteiden kuormitusjako alla olevan kuvion mukaiseksi.

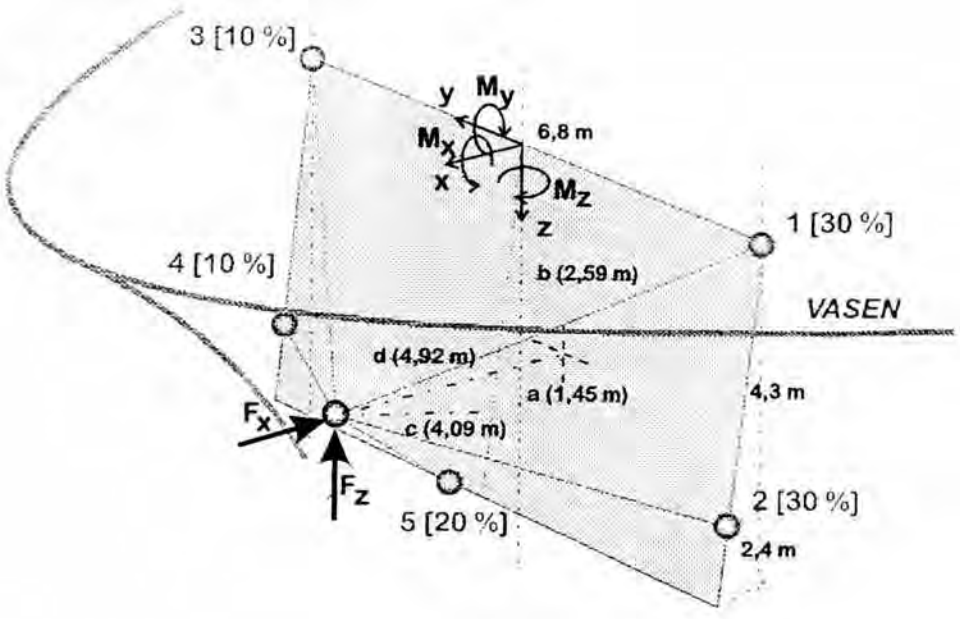

Pystysuuntainen voimakomponentti F_z on tasapainossa saman ehdon mukaan kuin x-akselin suuntainen resultantti F_x. Sivusuuntainen resultanttivoi-

ma F_y suuntautuu hyvällä tarkkuudella kiinnityspisteiden painopisteen kautta ja se voidaan jakaa kiinnityspisteille tasajaolla.

Kiinnityspisteiden resultanttikuormat voidaan nyt tarkentaa edellä kuvattujen tasapainoehtojen avulla, jolloin saadaan

- $\mathbf{F'_{1res} = 0{,}29\ F_{res}}$
- $\mathbf{F'_{2res} = 0{,}29\ F_{res}}$
- $\mathbf{F'_{3res} = 0{,}10\ F_{res}}$ (7)
- $\mathbf{F'_{4res} = 0{,}10\ F_{res}}$
- $\mathbf{F'_{5res} = 0{,}19\ F_{res}}$

Visiiriin vaikuttavien momenttien tarkastelu

Voimien F_y , F_z ja G_v momentit tasapainotetaan ja otetaan erikseen huomioon kiinnityspisteiden reaktiovoimina. Sivuaallokon synnyttämä ja visiiriä avaava momentti (F_y·c) välittyy nurkkapisteiden (1, 2) ja (3, 4) muodostamana momenttiparina saranoihin ja sivulukkoihin. Pohjalukkoon ei synny merkittäviä reaktiovoimia, koska se on laivan keskilinjan vieressä (0,4 m). Se voidaan jättää huomioon ottamatta.

Sivuttaisvoima F_y:

Lasketaan momenttitasapaino pystyakselin suhteen (suunta 15° z-akselin suunnasta):

$$F'_{1x}\cdot 3{,}4 + F'_{2x}\cdot 3{,}4 + F''_{3x}\cdot 3{,}4 + F'_{4x}\cdot 3{,}4 - F_y \cdot c = 0 \qquad (8)$$

missä F''_{1x} , F''_{2x} , F''_{3x} ja F''_{4x} merkitään yhtä suuriksi ja c on 4,09 m.

- $F''_{1,2,x} = 0{,}30 \cdot F_y = 0{,}07 \cdot F_{res} = -F''_{3,4x}$ (9)

Vertikaalikuorma F_z:

Voima muodostaa visiiriä avaavan kiertomomentin (F_z·d) sijaitessaan kiinnitystason edessä etäisyydellä d (4,92 m) y-akselista. Momentti välittyy pisteryhmien (1, 3) ja (2, 4, 5) voimaparina saranoihin ja lukituslaitteisiin.

Momenttitasapaino lasketaan y-akselin suhteen (ks. kuva sivulla 1):

$$F'''_{2x}\cdot 4{,}45 + F'''_{4x}\cdot 4{,}45 + F'''_{5x}\cdot (4{,}45 + 2{,}48) - F_z \cdot d = 0 \qquad (10)$$

missä F'''_{2x}, F'''_{4x} ja F'''_{5x} merkitään yhtä suuriksi ja d saa arvon 4,92 m

- $F'''_{2,4,5x} = 0{,}31 \cdot F_z = 0{,}21 \cdot F_{res}$ ja (11)
- $F'''_{1,3x} = -\tfrac{3}{2} \cdot F'''_{2,4,5x} = -0{,}32 \cdot F_{res}$ (12)

Visiirin paino G_v:

Visiirin omapainon (G_v) momenttivaikutus lasketaan y-akselin suhteen yhtälön (10) tapaisesti. Vaikutusetäisyys y-akselista on 4,9 m.

$$G''_{2x} \cdot 4{,}45 + G''_{4x} \cdot 4{,}45 + G''_{5x} \cdot (4{,}45 + 2{,}48) + G_v \cdot 4{,}9 = 0 \qquad (13)$$

missä G''_{2x}, G''_{4x} ja G''_{5x} merkitään yhtä suuriksi.

- $G''_{2,4,5x} = -0{,}31 \cdot G_v = -0{,}03 \cdot F_{res}$ ja (14)
- $G''_{1,3x} = \frac{3}{2} \cdot G''_{2,4,5x} = 0{,}05 \cdot F_{res}$ (15)

5. Kiinnityspisteiden resultanttikuormitukset

Seuraavaksi yhdistetään kiinnityspisteittäin vaikuttavat suorat reaktiovoimat ja aaltokuormitusresultantin momenttien tukireaktiot. Kiinnityspisteihin vaikuttava resultanttikuomitus muodostetaan neljän voimakomponentin yhteisvaikutuksena.

Vasen sarana (piste 1):

$F'_{1res} = 0{,}29 \cdot F_{res}$ (41° / 15° *taakse*)
$F''_{1x} = 0{,}07 \cdot F_{res}$ (15° *eteen*)
$F'''_{1x} = -0{,}32 \cdot F_{res}$ (−15° *taakse*)
$G''_{1x} = 0{,}05 \cdot F_{res}$ (15° *eteen*)

- ***F_{1res} = 0,43 F_{res}***
- ***(19° / 6° taakse - ylös - oikealle)***

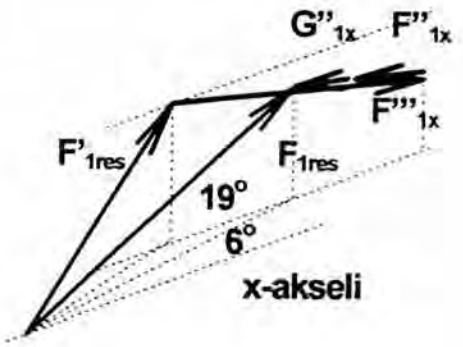

Vasen sivulukko (piste 2):

$F'_{2res} = 0{,}29 \cdot F_{res}$ (41° / 15° *taakse*)
$F''_{2x} = 0{,}07 \cdot F_{res}$ (15° *eteen*)
$F'''_{2x} = 0{,}21 \cdot F_{res}$ (15° *eteen*)
$G''_{2z} = -0{,}03 \cdot F_{res}$ (−15° *taakse*)

- ***F_{2res} = 0,26 F_{res}***
- ***(78° / 56° eteen - ylös - oikealle)***

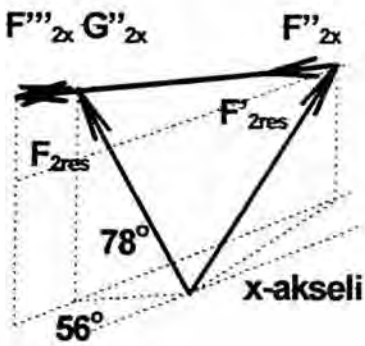

Oikea sarana (piste 3):

$F'_{3res} = -0{,}10 \cdot F_{res}(30° \,/\, 33° \, taakse)$

$F''_{3x} = -0{,}07 \cdot F_{res}(-15° \, taakse)$

$F'''_{3x} = -0{,}32 \cdot F_{res}(-15° \, taakse)$

$G''_{3x} = 0{,}05 \cdot F_{res}(15° \, eteen)$

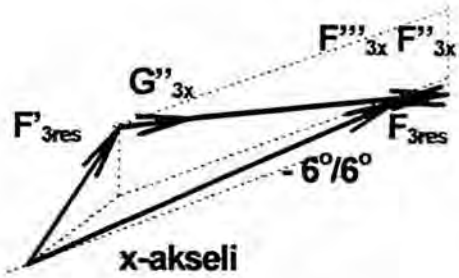

- ***F_{3res} = 0,40 F_{res}***
- ***(-6°/6° taakse - alas - oikealle)***

Oikea sivulukko (piste 4):

$F'_{4res} = 0{,}10 \cdot F_{res}(30° \,/\, 33° \, taakse)$

$F''_{4x} = -0{,}07 \cdot F_{res}(-15° \, taakse)$

$F'''_{4x} = 0{,}21 \cdot F_{res}(15° \, eteen)$

$G''_{4x} = -0{,}03 \cdot F_{res}(-15° \, taakse)$

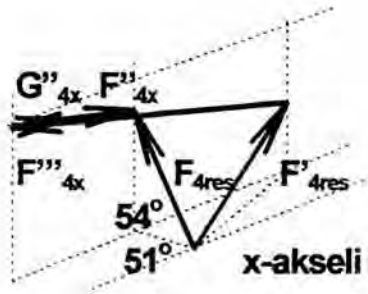

- ***F_{4res} = 0,10 F_{res}***
- ***(54°/51° eteen - ylös - oikealle)***

Pohjalukko (piste 5):

$F'_{5res} = 0{,}14 \cdot F_{res}(39° \,/\, 18° \, taakse)$

$F''_{5x} = 0 \cdot F_{res} = 0$

$F'''_{5x} = 0{,}21 \cdot F_{res}(15° \, eteen)$

$G''_{5x} = -0{,}03 \cdot F_{res}(-15° \, taakse)$

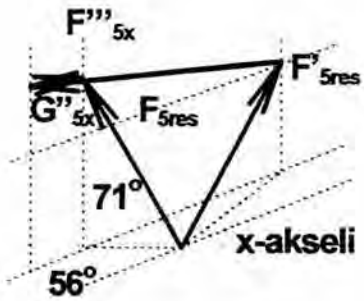

- ***F_{5res} = 0,18 F_{res}***
- ***(71°/56° eteen - ylös - oikealle)***

6. Laskentatulosten analysointi

Saranoille kohdistuu suurimmat kuormitukset. Esimerkiksi aaltokuormitusresultantti F_{res} = 5,55 MN (vastaten avaavaa momenttia M_y = 9,13 MNm) kehittää vasempaan saranaan 0,43 F_{res} = 2,39 MN:n suuruisen kokonaiskuormituksen. Kuormitustyyppi on puristava ja rakenteen kannalta suhteellisen vaaraton, vaikka onkin väsyttävä. Pystysuuntaisen komponentin suuruus on 0,14 F_{res} eli 0,78 MN.

Kaikissa lukituslaitteissa esiintyy visiiriä avaavien ja leikkaavien voimien yhdistelmä. Kuormituskuvio on siten oleellisesti erilainen kuin saranoissa. Vasemman sivulukon yhdistetty kuormitus 0,26 F_{res} on suurin vedon ja leikkausvoiman yhdistelmä. Jos käytetään edellä mainittua aaltokuormitusresultantin arvoa 5,55 MN, saadaan sivulukon kuormitukseksi 0,26 F_{res} = 1,44 MN. Vertailuna todettakoon, että pohjalukon kuormitus on yli 30 % pienempi. Oikea sivulukko kuormittuu vähiten. Sen kuormitus on 60 % pienempi kuin vasemman sivulukon kuormitus.

Jos arvioidaan visiirin liiketilaa resultanttivoimien valossa, voidaan tehdä seuraavia johtopäätöksiä:

- visiirin vasemmat kiinnityspisteet ja pohjalukko kuormittuvat voimakkaasti pystyakselin suuntaisesti,
- vasemmassa reunassa syntyy pystyakselin suuntaisia siirtymiä,
- vasempaan sivulukkoon kohdistuu vaarallisin vedon ja leikkausvoiman yhdistelmä ja se vaurioituu ensimmäisenä kiinnityspisteiden ollessa tasavahvoja vedon suhteen.

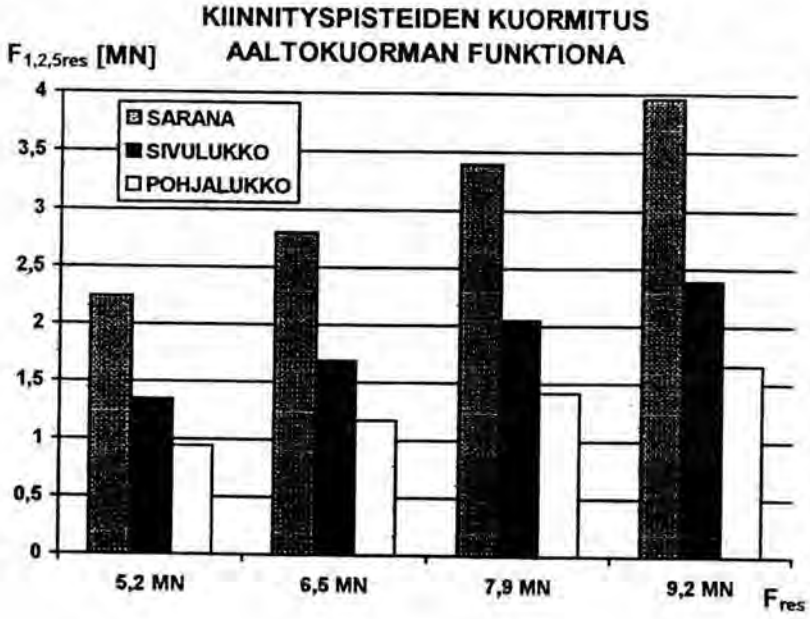

Laskentatulosten herkkyyttä voidaan tarkastella resultantin vaikutuspisteen siirrolla. Oletetaan että vaikutuspisteen z-koordinaatti saa arvon 2,79 m (+ 20 cm), jolloin x-koordinaatti saa arvon 5,12 m (+ 20 cm). Resultantin y-koordinaatti saa arvon 1,48 m (+ 3 cm). Vaikutukset ovat seuraavat:

- *Suorien x-akselin suuntaisten tukireaktioiden* muutos vaikutuspisteen z-koordinaatin kasvun seurauksena lisää vasemman sivulukon ja pohjalukon puristavaa kuormitusta noin 2 %.

- *Sivuttaisvoiman F_y ja nostavan voiman F_z* vaikutusetäisyyden kasvu (+ 20 cm) lisää avaavista momenteista johtuvia vetokuormituksia vasemmassa sivulukossa 7 % ja pohjalukossa 4 %.

- Sivulukon ja pohjalukon resultanttikuormitus ei oleellisesti muutu edellä kuvatun vaikutuspisteen muutoksen seurauksena..

Laskenta on suoritetty vektorilaskentaa hyväksi käyttäen. Koska kyseessä on avaruuskuormitustila, ei kiinnityspisteiden rasituksia voida esittää yhdellä lausekkeella. Likimääräismenettelyihin joudutaan siitä syystä, että rakenne on staattisesti epämääräinen.

7. Vaurion etenemisjärjestys

Laskettujen kuormitusten pohjalta voidaan ennakoida visiirin kuormituspisteiden irtoamisjärjestystä. Jos otaksutaan vasemman sivulukon murtuvan ensimmäisenä, jakautuu vasemman laidan kuormitukset pääosin pohjalukolle ja vasemmalle saranalle.

Vasen sarana (piste 1):

$F'_{1res} = 0{,}42 \cdot F_{res}$

$F''_{1x} = 0{,}14 \cdot F_{res}$

$F'''_{1x} = -0{,}32 \cdot F_{res}$

$G''_{1x} = 0{,}05 \cdot F_{res}$

- ***$F_{1res} = 0{,}50\ F_{res}$***
- ***(30^o/ 6^o taakse - ylös - oikealle)***

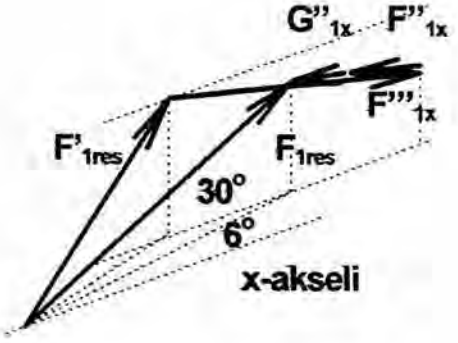

Pohjalukko (piste 5):

$F'_{5res} = 0{,}34 \cdot F_{res}$

$F''_{5x} = 0 \cdot F_{res} = 0$

$F'''_{5x} = 0{,}32 \cdot F_{res}$

$G''_{5x} = -0{,}045 \cdot F_{res}$

- ***F_{5res} = 0,31 F_{res}***
- ***(72°/70° eteen - ylös - oikealle)***

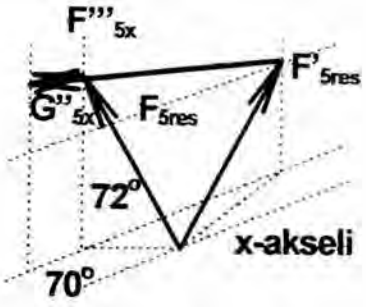

Vasemman saranan resultanttikuormitus kasvaa noin 0,07 F_{res} eli 16 %. Ylöspäin suuntautuvan komponentin suuruus on 0,25 F_{res}. Pohjalukon kuormitus lisääntyy 0,13 F_{res} eli 72 %.

Pohjalukon kuormituksen nousu vasemman sivulukon murtumisen jälkeen on progressiivinen.

Vaurion todennäköinen kulku on seuraava: ***sivulukko - pohjalukko - vasen sarana***.

KÄYTETYT LÄHTEET

Neuvottelut TkT Klaus Rahkan ja TkT Tuomo Karppisen kanssa
Teknillisiä kysymyksiä käsittelevä osaraportti ro-ro-matkustaja-alus mv Estonian kaatumisesta Itämerellä 28.9.1994
Laivan keulan konstruktiokuvat
Keskeneräiset tekniset raportit visiirin kuormituslaskelmista

SUPPLEMENT No. 514

Kleimola Matti:

Laskelmat ESTONIAn keulavisiirin lukituslaitteiden kuormituksista (2. raportti).

Espoo 1997.

Kleimola Matti:

Calculations of the loadings on MV ESTONIA's bow visor locking devices. 2nd Report.

Espoo 1997.

Prof. Matti Kleimola
Kaksoiskiventie 40
02760 Espoo

4.5.1997

LASKELMAT ESTONIAN KEULAVISIIRIN LUKITUSLAITTEIDEN KUORMITUKSISTA (2. raportti)

1. Lähtöarvot

Estonian keulavisiirin kiinnityssaranoiden ja lukituslaitteiden kiinnityspisteet on esitetty alla olevassa kaaviossa. Kiinnityspisteitä on kaikkiaan 5; kaksi saranaa on ylhäällä ja kolme lukkoa alhaalla.

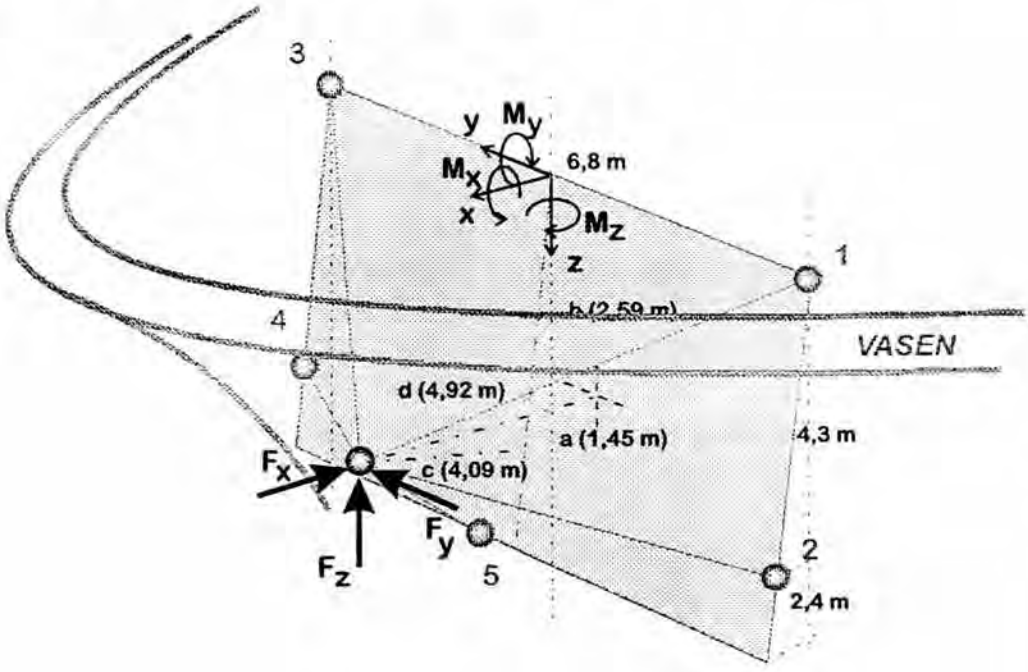

Kaikki visiiriin vaikuttavat voimat ja momentit voidaan esittää yhtälöryhmän (1) avulla.

$$\begin{cases} M_x = F_z \cdot y - F_y \cdot z \\ M_y = F_z \cdot x - F_x \cdot z \\ M_z = F_y \cdot x - F_x \cdot y \end{cases} \qquad (1)$$

Yhtälöryhmästä on ratkaistavissa visiiriin vaikuttavien voimakomponenttien ja momenttien keskinäiset suhteet eliminoimalla tuntemattomat suureet x, y ja z (resultantin vaikutuspisteen koordinaatit). Tällöin saadaan tulos

- $$F_x \cdot M_x - F_y \cdot M_y + F_z \cdot M_z = 0 \qquad (2)$$

Mallikokeiden pohjalta (SSPA) on osoitettu, että visiiriin kohdistuva vertikaalikuormitus ja laivan pituusakselin suuntainen aaltokuormitus ovat yhtäsuuret eli $F_x/F_z = 1$. Tästä seuraa edelleen

- $$\frac{F_y}{F_x} = \frac{F_y}{F_z} = \frac{M_x + M_z}{M_y} \qquad (3)$$

Mallikoetuloksia voidaan tarkastella ehtojen (2) ja (3) avulla.

KUORMITUS [MN/MNm]	A	B	C	D	E
F_r	3,9	5,2	6,5	7,9	9,2
F_x	-2,7	-3,6	-4,5	-5,4	-6,3
F_y	0,6	1,0	1,5	2,0	2,5
F_z	-2,7	-3,6	-4,5	-5,4	-6,3
M_x	0,6	1,7	3,1	5,0	7,4
M_y	4,0	7,5	11,3	15,5	20,0
M_z	0,5	1,0	1,5	2,0	2,5
F_y / F_x	0,22	0,28	0,33	0,37	0,40
F_x / F_r	0,69	0,69	0,69	0,69	0,69
F_y / F_r	0,15	0,19	0,23	0,25	0,27
M_x / M_y	0,15	0,23	0,27	0,32	0,37
M_z / M_y	0,13	0,13	0,13	0,13	0,13
$(M_x + M_z) / M_y$	0,27	0,36	0,41	0,45	0,49
* M_x / M_y	0,10	0,14	0,20	0,24	0,27
* M_x	0,39	1,08	2,27	3,74	5,44

Taulukosta voidaan havaita, että F_y / F_x on keskimäärin 20 % suurempi kuin $(M_x + M_z)/ M_y$. Ero voi johtua siitä, että M_x ja/tai M_z on määritetty liian suureksi tai M_y liian pieneksi. Laivan pituusakselin (x-akseli) ympäri kiertävä momentti M_x kasvaa lukuarvoltaan voimakkaasti. Jos momentin M_x suhteellinen arvo * M_x / M_y pienenee tasolle 0,10 - 0,27, toteutuu ehto kauttaaltaan. Käytännössä tällä erolla on varsin pieni merkitys visiirin kiinnityspisteiden rasitusten arvioinnissa.

Visiiriin vaikuttavan resultanttivoiman koordinaattiakselien suuntaiset voimakomponentit voidaan esittää niinikään momenttien ja vaikutuspisteen koordinaattien avulla yhtälöistä (1) ja (3).

$$\begin{cases} F_x = \dfrac{M_y}{x-z} = 0{,}69 \cdot F_{res} \\ F_z = \dfrac{M_y}{x-z} = 0{,}69 \cdot F_{res} \\ F_y = \dfrac{M_x + M_z}{x-z} = (0{,}15...0{,}27) \cdot F_{res} \end{cases} \quad (4)$$

Visiiriä kuormittavan resultantin F_{res} koordinaatit xz-tasossa voidaan hakea vaikutussuoralta $z = x - (M_y/F_x)$.

Visiirin omapaino G_v on 0,55 MN ja sen vaikutuspiste on aluksen keskiviivalla etäisyydellä 4,9 m yz-tasosta. Visiirin omapaino aikaansaa sekä suorat tukireaktiot kiinnityspisteihin että momentin y-akselin ympäri.

Lukituslaitteisiin syntyvät kuormitukset lasketaan em. taulukon kuormitusvaihtoehdolle C.

2. Momenttien ja voimien aiheuttamat tukireaktiot

Avaava momentti M_y:

Avaava momentti syntyy voimien F_x ja F_z vaikutuksesta ja välittyy kiinnityspisteiden (1, 3) ja (2, 4, 5) kautta aluksen runkoon. Saranaoihin (1, 3) muodostuu puristusrasitus ja lukituslaitteisiin (2, 4, 5) vetokuormitus.

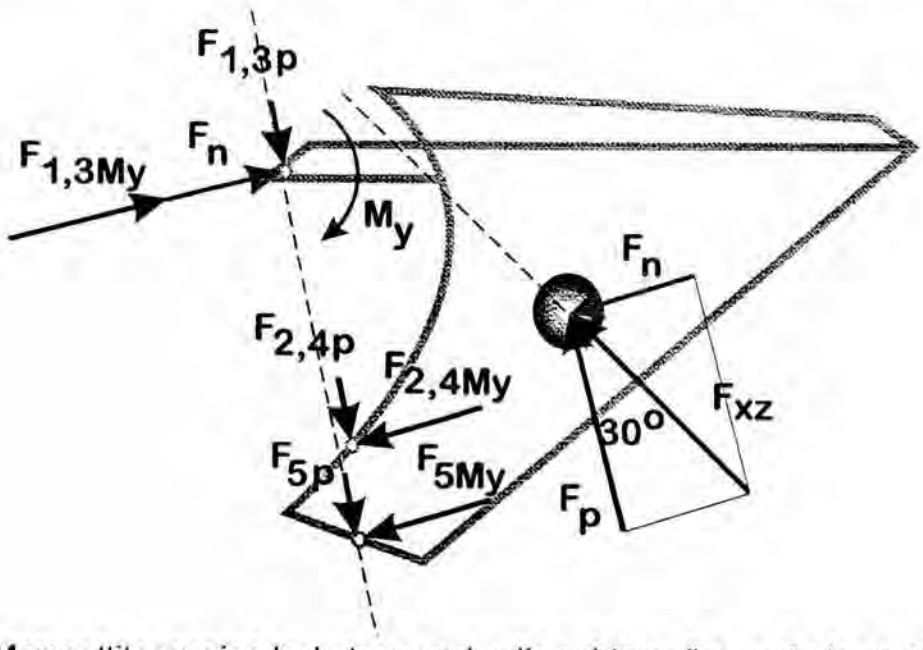

Momenttitasapaino lasketaan y-akselin suhteen (ks. myös kuva sivulla 1):

$$F_{2My} \cdot 4{,}45 + F_{4My} \cdot 4{,}45 + F_{5My} \cdot (4{,}45 + 2{,}48) - M_y = 0 \quad (5)$$

missä F_{2My}, F_{4My} ja F_{5My} merkitään yhtä suuriksi

- $F_{2,4,5My} = 0{,}063 \cdot M_y$ ja (6)
- $F_{1,3My} = -\frac{3}{2} \cdot F_{2,4,5My} = -0{,}095 \cdot M_y$ (7)

Voimien F_x ja F_z muodostama resultantti F_{xz} jaetaan kiinnityspisteiden muodostaman tason suuntaiseen komponenttiin F_p ja kohtisuoraan komponenttiin F_n. Tason suuntainen komponentti jaetaan tasan viidelle kiinnityspisteelle. Tasoa vastaan kohtisuora komponetti siirretään y-akselille.

- $F_{xz} = 0{,}69\sqrt{2} \cdot F_{res} = 0{,}98F_{res}$ (8)
- $F_n = \frac{1}{2}F_{xz} = 0{,}49F_{res}$ (9)
- $F_p = \frac{1}{2}\sqrt{3}F_{xz} = 0{,}85F_{res}$ (10)
- $F_{1,2,3,4,5p} = \frac{1}{5}F_p = 0{,}17F_{res}$ (11)

Kiertomomentti M_x:

Kiertomomentti välittyy kiinnityspisteiden (1, 2, 3, 4, 5) leikkausvoimien kautta aluksen runkoon. Jos oletetaan, että koko kiertomomentti välittyy tasan jokaiselle kiinnityspisteelle, saadaan seuraava tasapainoehto:

$$F_{2y} \cdot 4{,}3 + F_{4y} \cdot 4{,}3 + F_{5y} \cdot (4{,}3 + 2{,}4) - Mx = 0 \quad (12)$$

missä F_{2y}, F_{4y}ja F_{5y} merkitään yhtä suuriksi

- $F_{2,4,5y} = 0{,}065 \cdot M_x$ ja (13)
- $F_{1,3y} = \frac{3}{2} \cdot F_{2,4,5y} = 0{,}098 \cdot M_x$ (14)

Kiertomomentin synnyttämä kiinnityspisteiden leikkauskuormitus jää alhaiseksi. Kuormitusvaihtoehdossa C lukituslaitteiden kuormitus on noin 0,2 MN. Lisäksi visiirin sarvet ottavat ainakin osan leikkauskuormasta. Kiertomomentin vaikutus voidaan jättää huomioonottamatta.

Murtomomentti M_z:

Visiiriä pystyakselin ympäri avaava momentti tasapainottuu sivulukkojen ja kansisaranoiden kautta. Vasemmanpuolisiin kiinnityslaitteisiin syntyy vetorasitus ja oikanpuoleisiin puristusrasitus:

$$F_{1x} \cdot 3{,}4 + F_{2x} \cdot 3{,}4 + F_{3x} \cdot 3{,}4 + F_{4x} \cdot 3{,}4 - M_z = 0 \qquad (15)$$

missä $F_{1,2,3,4x}$ merkitään yhtä suureksi

- $F_{1,2x} = 0{,}048 \cdot M_z$ (16)

Murtomomentin vaikutus jää myös vähäiseksi. Kuormitusvaihtoehdossa C vasemmanpuoleisten lukituslaitteiden vetokuormituslisäksi saadaan 0,07 MN. Pohjalukkoon murtomomentti ei muodosta merkittävää lisäkuormitusta, koska se on kiertoakselin (z-akseli) vieressä.

Visiirin paino G_v:

Visiirin omapainon (G_v) reaktiovaikutus lasketaan y-akselin suhteen. Vaikutusetäisyys y-akselista on 4,9 m.

$$G_{2x} \cdot 4{,}45 + G_{4x} \cdot 4{,}45 + G_{5x} \cdot (4{,}45 + 2{,}48) - G_v \cdot 4{,}9 = 0 \qquad (17)$$

missä G_{2x}, G_{4x} ja G_{5x} merkitään yhtä suuriksi.

- $G_{2,4,5x} = -0{,}31 \cdot G_v = -0{,}17MN$ ja (18)
- $G_{1,3x} = \frac{3}{2} \cdot G_{2,4,5x} = 0{,}26MN$ (19)

Visiirin paino aikaansaa myös leikkausvoiman kiinnityspisteille ja se voidaan jakaa tasan. Leikkausvoimasta aiheutuu 0,11 MN vertikaalisuuntainen kuormitus jokaiseen kiinnityspisteeseen.

3. Kiinnityspisteiden resultanttikuormitukset

Lasketaan kiinnityspisteiden resultanttikuormitukset aaltokuormitustapaukselle C ja jätetään M_x, M_z ja G_v huomioonottamatta.

Vasen sarana (piste 1):

$F_{1n} = 0{,}25 \cdot F_{res} = 1{,}63MN$
$F_{1p} = 0{,}17 \cdot F_{res} = 1{,}11MN$
$F_{1My} = 0{,}095 \cdot M_y = 1{,}07MN$

- ***F_{1res} = 2,92 MN***
- ***(7° taakse - ylös)***

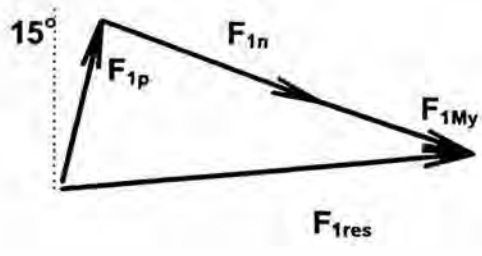

Vasen sivulukko (piste 2):

$F_{2p} = 0{,}17 \cdot F_{res} = 1{,}11 MN$

$F_{1My} = 0{,}063 \cdot M_y = 0{,}71 MN$

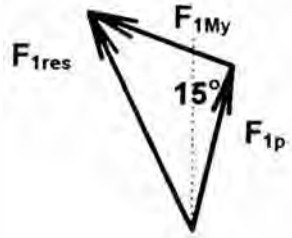

- ***F_{2res} = 1,33 MN***
- ***(72° eteen - ylös)***

4. Laskentatulosten analysointi

Kiinnityspisteiden kuormitukset laivan vasemmalla ja oikealla puolella ovat tässä laskentaesimerkissä yhtä suuret johtuen siitä, että momentit Mx ja Mz jätettiin huomioonottamatta. Erityisesti Mz aiheuttaa sen, että vasemman puolen kiinnityslaitteet kuormittuvat lisää vetojännityksistä ja oikean puolen sarana ja lukko puristusrasituksesta.

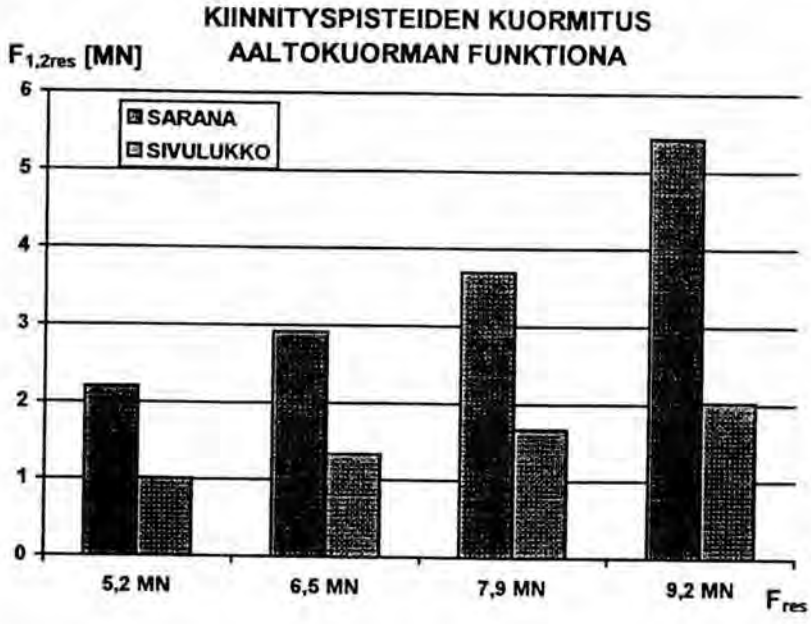

Tämänkin tarkastelutavan pohjalta voidaan todeta, että vasen sivulukko on rakenteen heikoin kohta

SUPPLEMENT No. 515

Niemi Erkki:

Upper Bound Estimation on the Ultimate Load Capacity of the Atlantic Lock.

Lappeenranta University of Technology.

Lappeenranta 1997.

Prof. Erkki Niemi
Lappeenranta University of Technology
P.O.Box 20
FIN-53851 Lappeenranta
FINLAND

UPPER BOUND ESTIMATION ON THE ULTIMATE LOAD CAPACITY OF THE ATLANTIC LOCK

Fig. 1 shows two alternative failure mechanisms. The ultimate load, F_R, is resolved based on principles of plastic theory. Each lug is assumed to resist the deformation developing a total resistance of $2R$. The resistance value R is formed by flow load of the rim cross-section, in addition to the ultimate fracture load of two 90° fillet welds. The fracture load of the two starboard bracket welds is denoted R_b.

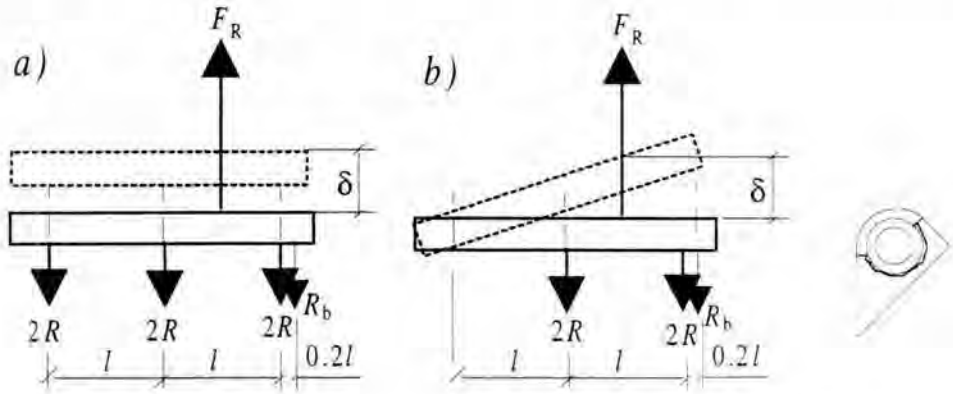

Fig. 1 *Two alternative mechanisms. In case a) all three lugs are assumed as load-bearing but the static equilibrium condition is violated. In case b) the static equilibrium is maintained.*

The plastic theory says that by setting the outer work and the inner work equal, an upper bound solution for load F_R is obtained. Of all possible mechanisms the lowest load capacity solution is the best one.

Case a) $$F_R \cdot \delta = 2R \cdot (\delta + \delta + \delta) + R_b \delta \Rightarrow F_R = 6R + R_b$$

Case b) $$F_R \cdot \delta = 2R \cdot \left(\frac{2}{3}\delta + \frac{4}{3}\delta\right) + R_b \cdot 1.47\delta \Rightarrow F_R = 4R + 1.47R_b$$

Prediction of the capacity of the test structures studied at the University of Hamburg

Rim capacity: $R_1 = 15 \cdot 36 \cdot \frac{250 + 417}{2} = 180000$ N (for one cross-section)

Lug weld capacity (a = 3.9 mm):

$$R_2 = a \cdot \pi \cdot r \cdot \frac{f_u}{\beta\sqrt{3}} = 3.9 \cdot \pi \cdot 64 \cdot \frac{450}{0.8 \cdot 1.73} = 255000 \text{ N}$$

Total capacity corresponding to one rim cross-section:

$$R = 180 + 255 = 435 \text{ kN}$$

Capacity bracket welds:

$$R_b = a \cdot l \cdot \frac{f_u}{\beta\sqrt{2}} = 3.9 \cdot 2 \cdot 65 \cdot \frac{450}{0.8 \cdot 1.41} = 202000 \text{ N}$$

Predicted ultimate capacity of the test structure:

$$F_R = 4 \cdot 435 + 1.47 \cdot 202 \text{ kN} = \underline{2037\text{kN}} \ (= 208 \text{ tons})$$

The calculation is based on following assumptions:

- The measured weld hardness of 330 HV corresponds to a flow stress of 450 N/mm^2 of the weld metal
- The weld throat a = 3.9 mm has been measured from the test structure
- The welds fracture at a deformation of about 1 - 2 mm
- The rim cross section developes a flow stress equal to average of yield and ultimate strengths at the moment of weld fracture
- The circular weld is mainly loaded in shear, hence square root 3
- The bracket weld is transversally loaded, hence square root 2.
- The rotation of the pin does not develop any bending stresses in the lugs and brackets due to the fact that they are already yielding.
- The rotation of the pin does not develop any moments in the mating lug because it is also yielding at the same loads.

The actual capacity of the tested lock structure was 2040 kN. Thus, the calculation model is shown to be valid.

Assessment of the average weld throat thickness of the Atlantic lock of Estonia

These calculations are based on the following assumptions:

- An actual capacity of 1500 kN of the Atlantic lock has been obtained based on the deformation of the mating lug.
- The rim has the same strength values as in the test structure.
- The flow stress of if the weld material is 368 N/mm^2 due to the lower hardness of 270 HV compared to the hadness of 330 HV of the test structure.

$$R = 180\ \text{kN} + \frac{a}{3.9} \cdot \frac{368}{450} \cdot 255\ \text{kN} = 180\ \text{kN} + 53.48a\ \text{kN}$$

$$R_b = \frac{a}{3.9} \cdot \frac{368}{450} \cdot 202\ \text{kN} = 42.38a\ \text{kN}$$

$$F_R = 4R + 1.47R_b = 1500\ \text{kN}$$

$$\Rightarrow \underline{a = 3.04\ \text{mm}}$$

Design capacity according to Eurocode 3

The design capacity according to Eurocode 3 of a properly welded structure is much lower than the predictions made using the above assumptions. The rims are assumed to develop a stress equal to yield stress over 1.1, and the welds must be calculated using the nominal ultimate strength of the base material over 1.25. This yields a design capacity of 1740 kN when the weld throat is a = 5 mm as it should have been.

SUPPLEMENT No. 516

Nilsson Fred - Öberg Hans:

Strength and failure assessments of parts from MV ESTONIA. Royal Institute of Technology.

Stockholm 1996.

KUNGL TEKNISKA HÖGSKOLAN

Solid Mechanics

Prof. Fred Nilsson
Direct phone +46-8-790 75 49
Sen. Research Eng. Hans Öberg
Direct phone +48-8-790 75 47

96-02-27

STRENGTH AND FAILURE ASSESSMENTS OF PARTS FROM MV ESTONIA

Fred Nilsson and Hans Öberg

1. BACKGROUND

An account is given in this report of studies performed at Kungliga Tekniska Högskolan at the Department of Solid Mechanics in order to determine the failure mechanisms and to estimate collapse loads of certain parts of the visor locking and pivoting devices.

a) Metallographic and fractographic investigation of different parts of the bow visor hinge and locking system. The parts examined were the three lugs of the bottom lock mounted on the hull, parts of the pivoting joint and parts of the side lock. In the following the three plates will be numbered 1, 2 and 3, respectively, where the number 1 designates the one located closest to the hydraulic actuator. The purpose of these investigations was to determine the failure mechanisms of the three plates. These investigations were performed at the Department of Materials Science and are reported separately in [1]-[2].

b) Tensile testing of material taken from plate 1 of the bottom lock mounted on the hull in order to determine the tensile properties of the material.

c) Estimate of failure load of the lock plates mounted on the hull.

d) Mechanical testing of material from the visor pivoting point.

e) Charpy impact testing of material from visor beam.

f) Estimate of collapse loads of the visor pivoting point.

A summary of the testing activities performed the Department of Solid Mechanics is given in Appendix A. In Appendix B an inventory of the parts presently stored at Kungliga Tekniska Högskolan is given.

2. FRACTOGRAPHIC INVESTIGATION OF BOTTOM LOCK PLATES

The findings of the metallographic and fractographic investigations are documented in separate reports [1]-[2]. The main result from examination of the material from the bottom lock plates is that

Postal address	Telephone	Telefax	e-mail
Royal Institute of Technology	Ex. +46-8-790 60 00	+46-8-411 24 18	fred@hallf.kth.se
Department of Solid Mechanics			
S-100 44 STOCKHOLM, SWEDEN			

the fractures surfaces exhibit a typical appearance of shear fracture due to an overload. Shallow cracks (1 mm) were detected along the weld between lugs and housings. The character of these cracks has not been determined. The same conclusions were arrived at for the material from the visor pivoting point. There is no basis for a conclusion that pre-existing defects at the hinges had a significant influence on the failure.

3. TENSILE TESTING OF BOTTOM LOCK MATERIAL

A tensile specimen (numbered 3037 in the internal test account of the department) was cut from plate 1 of *the bottom lock* (situated closest to the hydraulic actuator). The cross section was 14,0 mm x 30,3 mm, that is rather close to the broken ligaments that were roughly 15 mm x 35 mm. The specimen was loaded using the 500 kN MTS testing machine of the department.

The failure load was 177 kN which is proportional to a stress of 417 MPa which is then taken as the ultimate tensile strength σ_u. This value is in reasonable accordance with the expected behaviour of the material. A stress-displacement diagram is enclosed (Fig. 1). The displacement shown in the diagrams is the sum of the elongation of the specimen and of the fixtures and the testing rig. From Fig. 1 the yield stress can be estimated to 230 MPa.

The cross section after break was 9,3 mm x 22,5 mm. A 50 mm long gage length elongated to 68,3 mm during the test. This corresponds to an average strain of 36,6%.

Two standard tensile specimens with a circular cross section were also cut out from the lug and tested. The object of this part of the testing was to determine the yield and the ultimate strength of the material according to standard procedures. The two tests yielded virtually identical information and the stress versus strain behaviour is shown in Fig. 3. The yield strength was determined to 243 MPa and the ultimate tensile strength to 407 MPa. This is in reasonable accordance with the previously described testing on rectangular specimens.

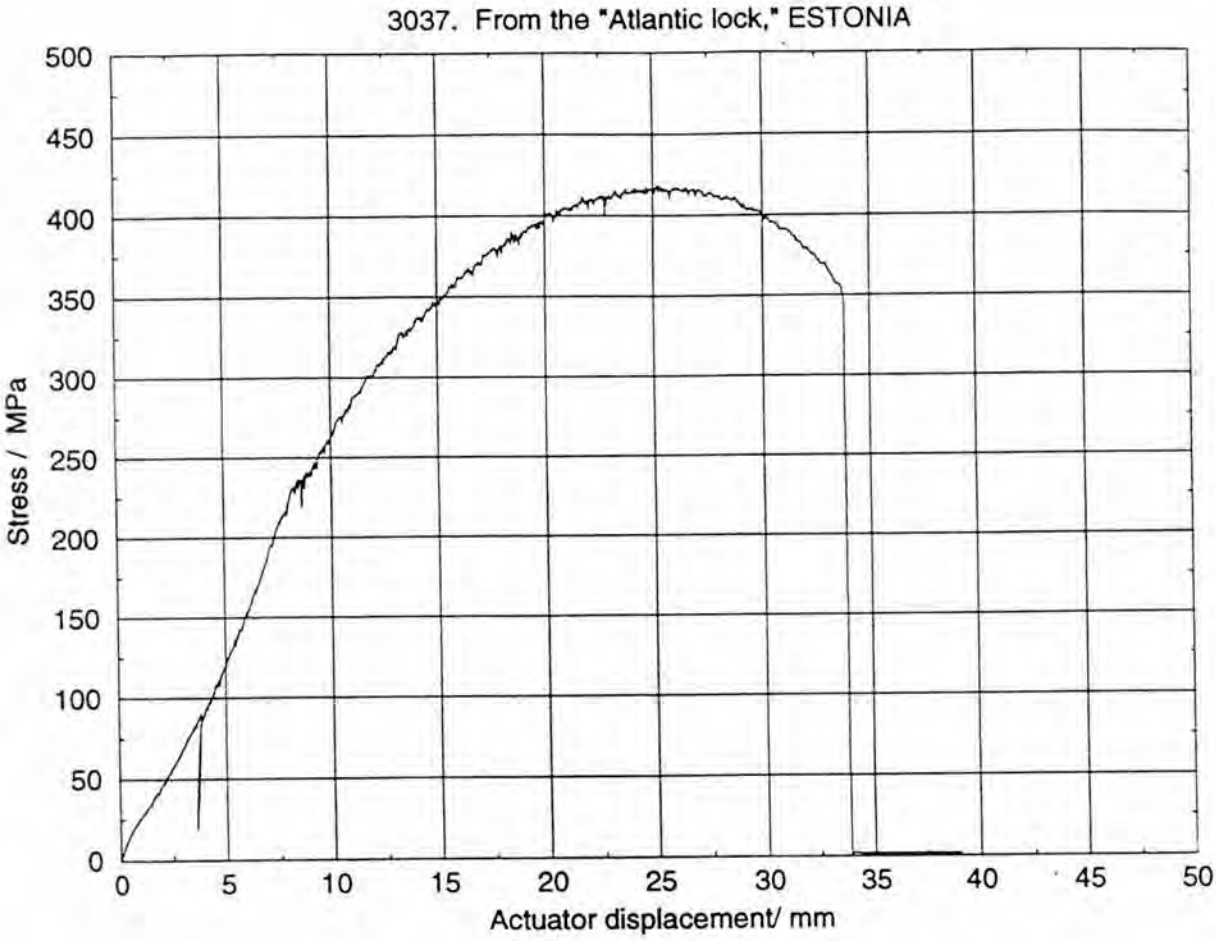

Fig. 1. Tensile testing of bottom lock material, rectangular specimen.

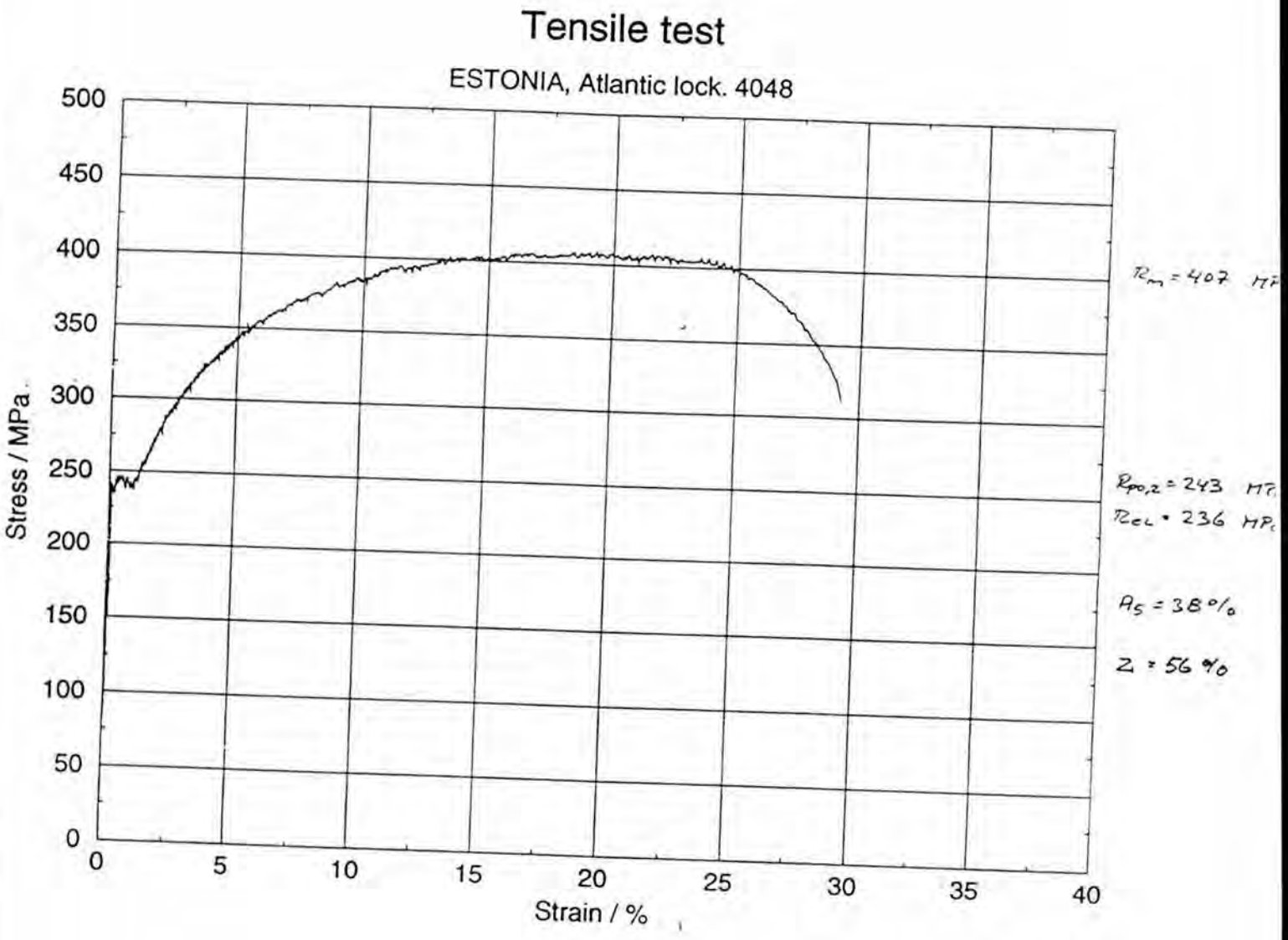

Fig. 2. Tensile testing of bottom lock material, standard cylindrical specimen.

4. ESTIMATE OF COLLAPSE LOADS OF BOTTOM LOCK PLATES

The collapse load for each plate is estimated in the following way. Each of the three plates exhibits two fracture surfaces having the overall appearance of tensile failure through a shearing mechanism similar to that of the performed tensile test. It is then simply assumed that at the point of failure the fracture surfaces resist by a purely normal load equal to the area of each fracture surface times the ultimate tensile strength σ_u. Possible in plane shearing forces will probably not be of any greater significance. Sketching the missing piece of a plate we then obtain the force geometry from Fig. 3.

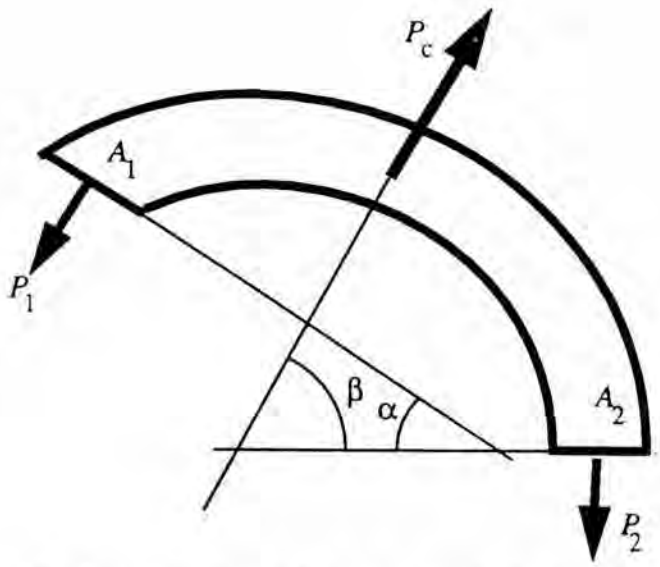

Fig. 3. Assumptions for calculation of the collapse load

The areas A_1 and A_2 and the angle α between the fracture surfaces are measured from the fractured parts. The loading angle β is assumed unknown and is determined by equilibrium considerations. Expressing equilibrium in the horizontal and vertical directions, respectively, we obtain

$$P_c \cos\beta = P_1 \sin\alpha \tag{1}$$

$$P_c \sin\beta = P_1 \cos\alpha + P_2 \tag{2}$$

With $P_1 = A_1\sigma_u$ and $P_2 = A_2\sigma_u$ we can solve for the critical load and the loading angle as

$$P_c = \sigma_u (A_1^2 + A_2^2 + 2A_1A_2\cos\alpha)^{1/2} \tag{3}$$

$$\beta = \arccos\left(\frac{A_1\sigma_u}{P_c}\sin\alpha\right) \tag{4}$$

The different measured quantities and the calculated results are given in Table 1. Two different values of the tensile strength have been used. The lower and more realistic one is formed by taking the average of the yield and the ultimate tensile strength, respectively, while the upper bound value in the table is obtained by using the ultimate tensile strength. In the last row the contribution from the different plates has been summed. The total load bearing capacity of the lock is not, however, necessarily equal to the sum of the limit loads in Table 1. This sum is rather an upper bound to the total capacity. The problem is statically indeterminate and if there is sufficient clearance for deformation, one of the plates may have failed before the others.

Table 1: Geometry data and estimated collapse loads

Plate	A_1/mm^2	A_2/mm^2	α/°	β/°	P_c/tons	P_c/tons upper bound	Upper bound of collapse together with weld
1	525	525	28	76	33	43	79
2	980	495	82	33	38	49	85
3	480	1050	25	82	49	63	99
Sum					120	155	263

In these calculations no account has been taken of the welds between the plates and the bushing. The load bearing capacity of these welds is very uncertain. The visual impression is that the welds were of poor quality and unfortunately no direct measurement of their load bearing capacity is possible. An estimate was, however, made in the following way. Assuming that these welds had the same strength properties are corresponding parts tested from the visor pivoting point as described in section 4 below. The load bearing thickness of the welds at the bottom lock plates was on average 4 mm (measured along the fusion line) in comparison with the 12 mm thickness of the welds from the visor pivoting point. A simple proportioning then gives that the load bearing capacity of the bottom lock welds should be 4/12 of the load bearing capacity per unit length of the welds subjected to testing. Calculating the total force on an area projected from a semi circle gives a force of 36 tons per plate. This contribution has been added in the right-most column of Table 1. It should be kept in mind that this is a very uncertain figure in view of the uneven quality of the welds.

5. MECHANICAL TESTING OF MATERIAL FROM THE VISOR PIVOTING POINT

Two slices, numbered 3042 and 3043, were cut from the *visor pivoting point*. The thicknesses of the slices were 14,0 mm and 13,9 (3043). The welded joints were loaded using equipment mentioned above. The results are shown in two diagrams enclosed (Fig. 4).

Welding defects could be seen in the broken welds. In spite of that, the load carrying capacity of the welds was good compared to that of the net section.

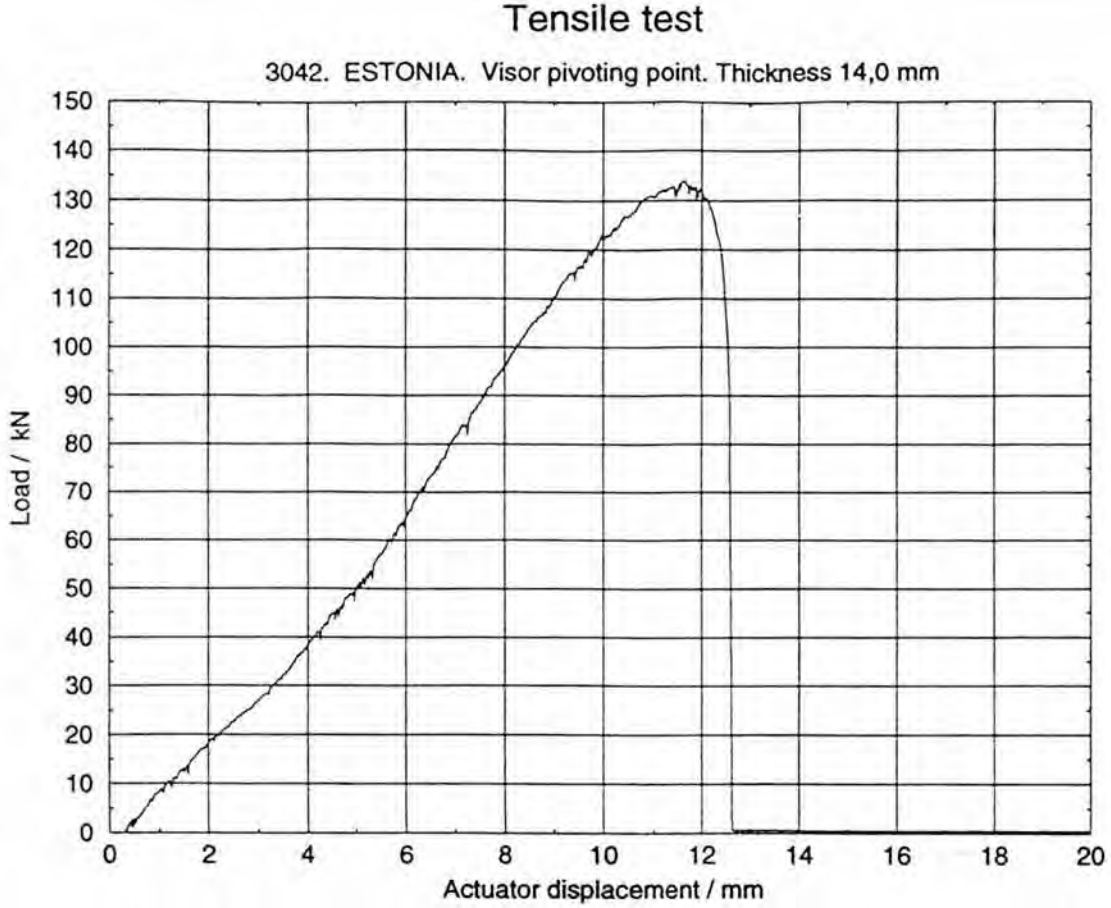

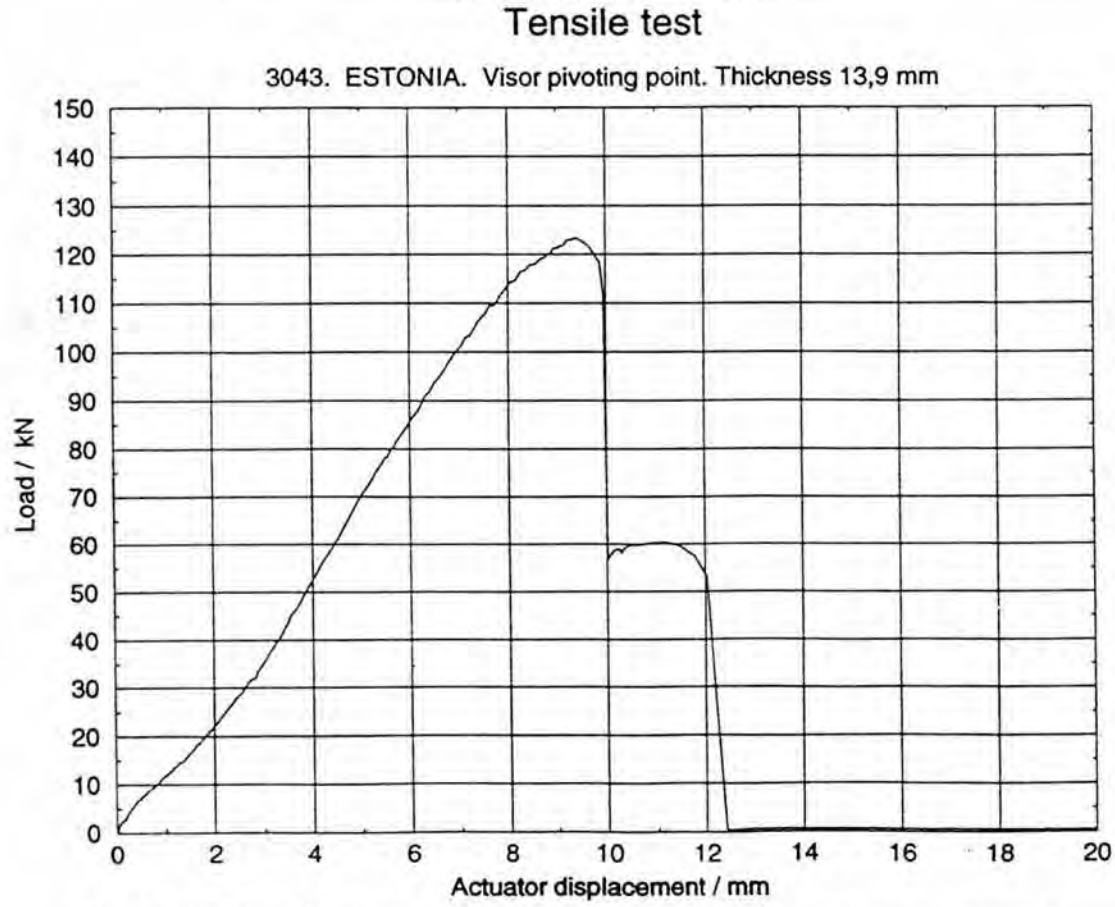

Fig. 4. Load vs displacement from testing of welds from visor pivoting point.

6. IMPACT TESTING OF VISOR BEAM MATERIAL

Impact testing using standard Charpy specimens machined from the visor beam was carried out in order to establish the toughness properties. The results from testing at different temperatures are shown in. The main conclusion is that the material possesses adequate toughness properties in the temperature interval considered.

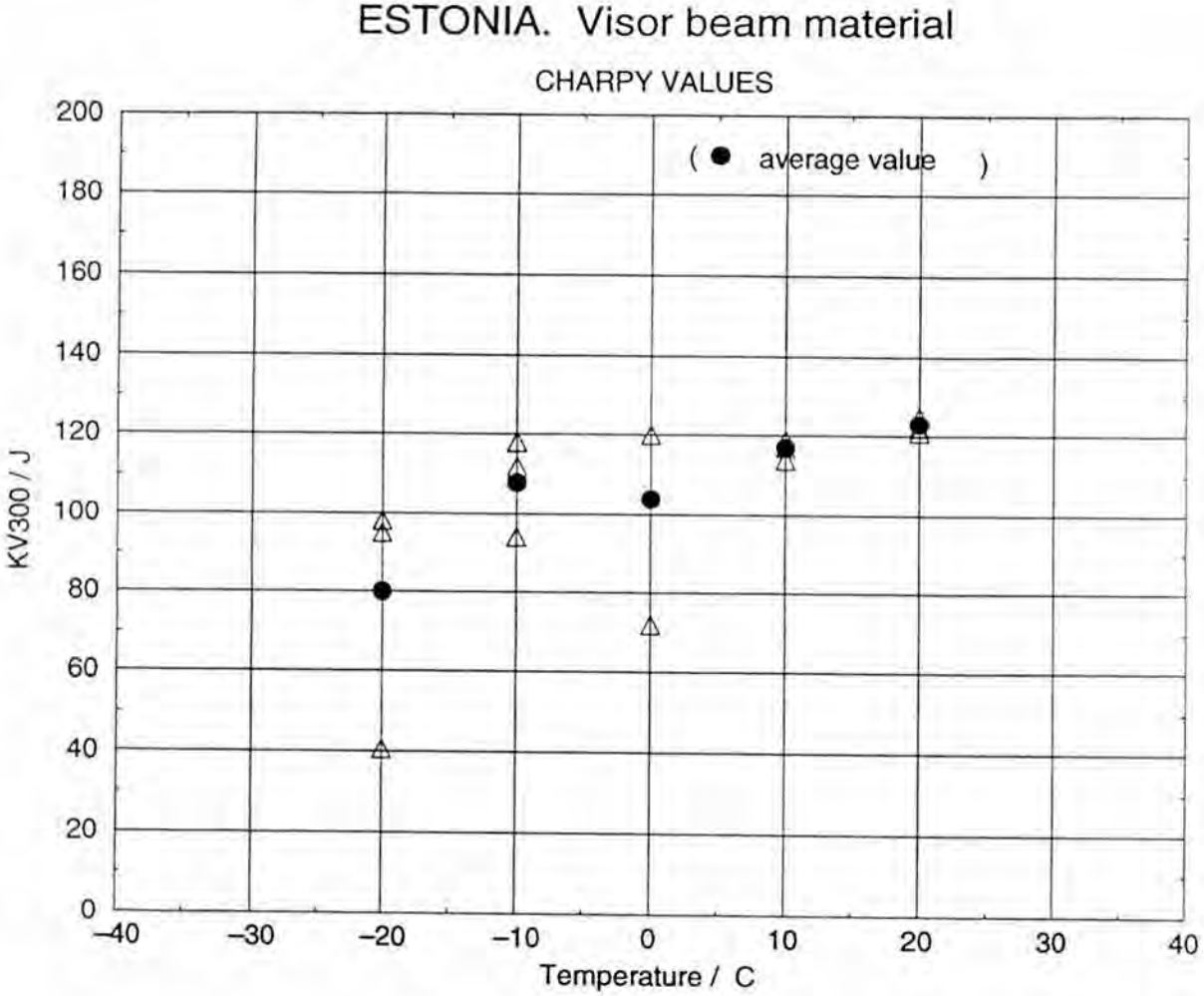

Fig. 5. Charpy impact toughness.

7. ESTIMATE OF COLLAPSE LOADS OF THE VISOR PIVOTING POINT

The same approach as for the bottom lock plates was used to calculate the collapse load of the visor pivoting point with the difference that the load bearing capacity of the welds this time was taken into account from the beginning. The experimental results from the testing described in sect. 5 were used for this assessment. The fracture modes of the four plates were so similar so that each plate is treated in the same way. This leads to a collapse load estimate 3 477 kN (the weld contribution is 2 143kN) which is 354 tons. In total the four plates are thus estimated to sustain at most 1 416 tons.

8. REFERENCES

1. K. Pettersson, P.-O. Söderholm and N. Lange, "Metallographic and fractographic examinations of samples from mv Estonia", Department of Materials Science and Engineering, Division of Mechanical Metallurgy, Royal Institute of Technology, 1994-04-12.

2. K. Pettersson, and P.-O. Söderholm, "Notes from metallographic and fractographic examinations of samples from mv Estonia", Department of Materials Science and Engineering, Division of Mechanical Metallurgy, Royal Institute of Technology, 1996-02-27.

APPENDIX A. Testing performed at the Department of Solid Mechanics, KTH

95-01-11

Tensile tests, plate specimens 3037, material from the bottom lock.

Tensile tests, slices of the visor hinge and bushing, 3042 and 3043. The weld between the visor lug material and the bushing was loaded.

Charpy testing of the visor lug plate (4525), portside hinge, starboard lug plate.

95-03-30

Tensile testing of material from the bottom lock, specimen number 4048 and 4049.

95-10-05

Production of fracture surfaces in the visor material. Two specimens were made of the visor material cut out near the hinge. Specimen 4331 was fatigued and specimen 4332 was broken by a static load. The purpose was to produce fracture surfaces in the material in a controlled way to enable a comparison with the real fracture surfaces.

APPENDIX B. Inventory of parts

MS indicates storage at the Department of Materials Science

SM indicates storage at the Department of Solid Mechanics

Number indicates marking on detail.

Number	*Part*
4525	The visor. Portside hinge. SM.
4526	The visor. Starboard hinge. SM
4527	The visor. Part of a bushing, unknown which. SM
4528	The visor. A minor art of the bushing. SM
4529	The visor. A thin part of the bushing including welds and visor lug material. SM
4530	The visor. Stempost. Portside shell plate. SM
4532	The visor. Stempost. Starboard shell plate. SM.
4533	The visor. Stempost. Thick part, folded into the hull. SM.
4534	The visor. As 4533 but from a lower position. SM.
4535	Visor shell plate, starboard. SM
4536	Visor bottom deck plate, portside. SM
4537	Bottom bracket. SM
4538	Bottom of visor / lower part of visor shell plate. Starboard. SM
4539	
4540	
4541	The portside plate (1) of the bottom lock close to the actuator. SM.
4542	The middle plate (2) of the bottom lock. SM.
4543	The starboard plate (3) of the bottom lock including a part of a supporting plate. SM
4544	Side lock? SM.
4545	The visor. The brass bushing. SM:
4546	The visor. part of the bushing. SM.
4547	The visor. Part of the bushing cut from detail 4546. SM.
4548	Starboard visor hinge, portside lug plate. Detail from fold at upper side of the hole. MS.
4549	Starboard visor hinge, portside lug plate, upper fracture surface. MS.
4550	The visor. Bushing covering plate. SM.
4551	Starboard side lock. MS 3a1.
4552	Part cut from 4551. MS 3a2.

4553 Part cut from 4551. MS 3a3.

4554 Portside side lock. MS 3b1.

4555 Stempost. Detail cut out between 4533 and 4534, divided into 6 parts. MS.

4556 Starboard visor hinge, starboard lug plate, upper fracture surface. MS.

Details from Mare Balticum

Hinge. Brass bushing. KP.

SUPPLEMENT No. 517

Pettersson Kjell - Söderholm P-O - Lange Nils:

Metallographic and fractographic examinations of samples from MV Estonia.

Royal Institute of Technology.

Stockholm 1995.

Metallographic and fractographic examinations of samples from MV Estonia

Kjell Pettersson, P-O Söderholm, and Nils Lange
Department of Materials Science and Engineering, Division of Mechanical Metallurgy, Royal Institute of Technology.

Background

A number of parts recovered from Estonia and its bow visor have been subjected to metallographic and fractographic examinations. The aim of the examinations have been to determine the mode of fracture for the different parts and also to see if there have been any abnormal occurrencies like pre-existing cracks, faulty material etc. The following parts have been examined:

- The remaining parts of three lugs of the bottom lock for the bow visor
- A tension test specimen prepared from one of the lugs.
- Parts of the pivoting joint of the bow visor found on the wreckage and its complement on the visor.
- Parts of the side lock for the bow visor.

Examination of the lugs and tension specimen from the bottom lock

Figure 1 shows one of the lugs. The slightly ondulated lower edge is a result of the cutting under water. The edge to the right and the sloping edge are parts of the original shape of the lug. The lug has failed in the ligaments between the hole and the external edges. Around the hole there is the remains of a fillet weld which has served to keep a housing insert in place. The weld is apparently of low quality and has not had any significant load carrying capacity. The weld has a triangular cross section with a leg size of 4 – 6 mm. The superficial impression of the weld is that in parts of it there is insufficient penetration and lack of fusion. A cross section of the weld is shown in Figure 2. In figure 3 is illustrated the lamellar microstucture of the plate material used for the lugs. It is characterized by elongated slag inclusion with a typical interlamellar distance of 0.06 – 0.09 mm. In some of the specimens examined slag inclusions with a length of over 1 mm have been observed, the largest one being over 6 mm in length..

The fracture surfaces have been examined in an optical stereo microscope and in a scanning electron microscope (SEM). The examination in the optical microscope showed that the surfaces were covered by a layer of rust. Two methods were used for removing the rust. The first method employs a mixture of relatively weak organic acids, which removed most of the rust. Examination of the fracture surfaces in the SEM showed that non-conductive oxides were still present on the fracture surface so a more effective method for removing oxides had to be used. In this method the specimen surface is connected as a cathode in an electrolytic bath of fused lithium nitrate. The current used is 6 A. This treatment is very effective and can be applied until the surface is clean. In order to determine if the metal surface is attacked during the treatment an initially clean fracture surface (from the tension specimen) was first examined in SEM, then treated and again examined in SEM. This experiment showed that some parts of the fracture surface were completely unchanged by the treatment while others showed signs of having been slightly oxidized. We interprete this as a result of the high temperature of the treatment and that the surface is oxidized by the air when it comes out of the electrolyte. However the main character of the fracture surface does not change by the treatment.

All fracture surfaces from the lugs were of a ductile character. There were two features which might suggest an influence of fatigue. One of the fracture surfaces was perpendicular to the plane of the lug while an overload failure normally results in a fracture surface where parts of the surface make an approximately 45° angle with the stress direction. However the detailed SEM examination of the surface showed that it had a completely ductile character.

The other feature was a coarse striation pattern, so coarse that normal ductile dimples can be seen on the striations, figure 4. The striation spacing is aboout 0.05 – 0.01 mm, which is about the same as the spacing between the elongated slag inclusions in the material. It thus seemed reasonable to suspect that these striations were a consequence of the slag inclusions rather than of a fatigue process. In order to confirm this hypothesis the fracture surface from the tension specimen was examined. As can be seen in Figure 5 it is also possible to see striation-like features on the fracture surface from the tension specimen. The most reasonable conclusion thus is that the lugs have failed by a single overload. It should also be added that there were no features on any of the lugs which indicated any pre-existing defects apart from the poor fillet welds for attachment of the housing inserts.

Material from the pivoting joint (hinge)

The piece received was a 5° sector of the pipe insert of the hinge of the bow visor with the attached part of the hinge beam which had fractured. This fracture surface was compared to the four fracture surfaces on the bow visor part of the hinge. The fracture surface from the bow visor which seemed most likely to be the mate of the surface on the pipe section was cut off and the two pieces can be seen in Figure 6. The bearing section is in the top and the hinge beam part below. The conclusion that the two pieces belong together is based on the appearance of the upper edge of the two pieces. The fit between the edges was not perfect but it is conceivable that minor pieces of material at the edges may have disappeared in connection with a relatively fast fracture.

Figure 7 shows the two pieces from another angle. It is now possible to see that the hinge beam piece has become thinned (or necked) somewhat in connection with the failure. From this angle the fit between the surfaces is not particularly good, but that could conceivably be a result of the plastic deformation of the hinge beam part. Figure 8 shows the two pieces from yet another perspective. The most interesting feature from this angle is perhaps the crack in the weld. This is again a sign of the questionable quality of the welds of the bearing inserts. In the gap between the plate and bearing a black stuff identified as an iron oxide is present. The oxide was also magnetic which is a strong indication that it is magnetite. The magnetite is also present in the crack in the weld. Since magnetite forms under conditions of low oxygen partial pressure the most reasonable conclusion is that it has formed under a long period of time when moisture has leaked in through the narrow crack in the weld. This crack is thus a pre-existing weld defect which has been present for a long time. It looks as if the corrosion has reduced the load carrying area of the plate around the hole, see Figure 8. The corrosive attack on the plate around the crevice can also be seen in other samples not included in the present report.

The general impression of the fracture surfaces was that they were more heavily corroded than those on the lock lugs. This led to inital thoughts that this crack might have been present before the shipwreck. However the extensive plastic deformation of the bow visor piece makes this an unlikely possibility since it seems inconceivable that such a crack could have passed unobserved when a significant part of the housing insert weld must in that case also have been failed.

The fracture surface of the plate material welded to the housing insert piece was cleaned with the organic rust remover which in this case removed almost all of the rust. Examination in an optical stereo microscope showed a striation pattern which can also be seen in the SEM picture shown as Figure 9. We again believe that this striation pattern is related to the microstructure of the material which contains elongated inclusions oriented in the same direction as the striation pattern. The material also has a banded perlite-ferrite structure where the perlite and ferrite bands may corrode at different rates and thus give a striated appearance on the cleaned fracture surface. The spacing of the striations, 0.05 mm, matches almost exactly the spacing of the ferrite-perlite bands. Apart form the striations the general character ot the fracture surface was of a ductile dimpled type as can be seen in Figure 10. It also gives the impression that the features of the dimples are not as sharp as on the fracture surfaces on the lock lugs which again suggests that this surface has corroded more than the surfaces of the lugs. However this could have been caused by a difference in corrosion properties between the plates used for the different parts.

Two other fracture surfaces from the hinge were examined later with the aim of determining whether or not any cleavage fracture had ocurred. This examination was decided at a meeting by the committee of investigators of the shipwreck in February 1995. The two fracture surfaces were more heavily corroded than any of the other fracture surfaces we had previously looked at. It was thus more difficult to characterize the type of fracture after removal of the rust. We do however conclude that the mode of fracture is ductile with no indications of any cleavage. We believe that the thick rust layer is a result of the exposure to air during the time to beginning of March 1995. This has apparetly happened despite the fact that the surfaces were sprayed with a protective liquid by one of the investigators fairly early after they came out of the water. It is perhaps conceivable that salt water trapped in an initially formed rust may have contributed to the relatively rapid corrosion.

The side lock

The material from the attachment of the side lock to the ship was a piece of 8 mm thick plate from which a semi-elliptic flap of material had been teared. The flap was still attached to the plate along a length a 30 mm where the material had bent nearly 180°. This demonstrates the high ductility of the 8 mm plate material. The actual fracture surface was as expected of a typically ductile character. The microstructure was completely normal for the type of steel used.

The lugs of the side locks were attached to the 8 mm thick plate. On the other side of the plate was a 20 mm thick support plate. According to the information given to us the support plate was not attached directly under the lug plate but rather a few cm to the side. Sections were made through the 8 mm plate and the two support plates in order to see if these had ever been repaired. One of the sections, from a piece marked SL1, can be seen in Figure 11. It is obvious from the Figure that there has been some deformation of the weld but there is no indication of any repair work having been done to the weld. Apart from a few minor defects the weld looks perfectly sound. There is also some indication of corrosive attack in the crevice between the two weld beads but not so much that there has been any significant threat to the integrity of the weld. It can be that the thickness of the 8 mm plate in this section is only about 4–5 mm. We interprete this as a result of a delamination failure of the plate when the lug was pulled away, a failure mode not unlikely for a plate with an abundance of elongated slag inclusions in the plane of the plate. The triangular gap between the 20 mm plate and 8 mm plate may have been caused by a slight bending of the 20 mm plate relative to the 8 mm plate.

The other cross section, from a piece marked SL2, is shown in Figure 12. Here we note that the etchant has attacked the weld material differently, a difference which suggests that two different electrode materials have been used. The weld is however perfectly sound and there is no indication of any repair work, at least not any work which has impaired the integrity of the weld. The odd feature in Figure 12 is the small apparently loose piece of material just under the support plate. On inspection of the whole piece of 8 mm plate with attached support plate it became clear that the apparently loose piece of material is part of a tongue of material from the 8 mm plate just under the support plate which appears to have been hammered away from the rest of the plate by one or several severe blows to the plate. Such a conclusion is supported by several markings on the 8 mm plate. From the appearance of these markings it seems reasonable to conclude that the markings come from the lug plate which first have been pulled loose from the 8 mm plate and then as a result of movement of the bow visor has struck and slid against the 8 mm plate several times.

In order to confirm the hammering against the 8 mm plate a new metallographic section was prepared a few cm below the section of Figure 12. This cross section clearly showed that where there were markings on the surface it is also possible to see severe cold work on the surface. This tends to confirm a hammering action as the cause of the

surface markings. It is alternatively possible that a similar structure could be caused by chiselling. However the visual appearance of the surface gives more the impression of hammering with some lateral sliding than chiselling. The metallographic cross section is shown in Figure 13.

A piece of the fractured weld between the lug plate and the 8 m plate was inspected in SEM. Despite the flat appearance of the fracture surface the micro character of the fracture was that of a dimple fracture with no signs of cleavage.

Discussion

All observations on the fracture surfaces are consistent with failures caused by overloading of the structures. The question mark is that we do not have any experience with the effect of salt water corrosion on the present type of fracture surfaces. Therefore we can not say with absolute certainty that the striations observed are actually a result of the banded structure of the material with subsequent corrosion. It may thus be interesting to do some control experiment where fracture surfaces of the present materials are exposed to salt water, the rust removed, and the appearance of the fracture surfaces before and after corrosion with rust removal, is compared. Such an experiment might also throw some light on the question about the age of the fracture surface on the hinge.

Figure 1. One of the lugs

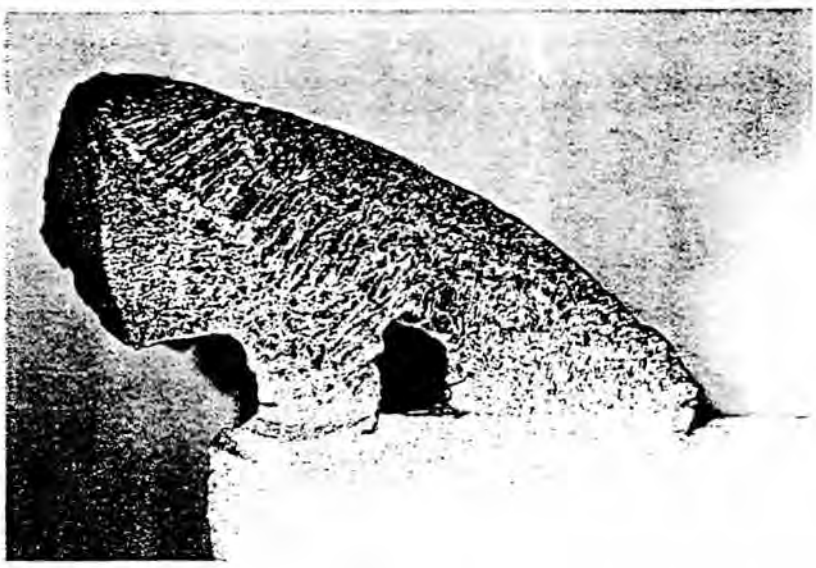

Figure 2. Cross section of fillet weld Note the large pore, the undercut and poor penetration. 10x.

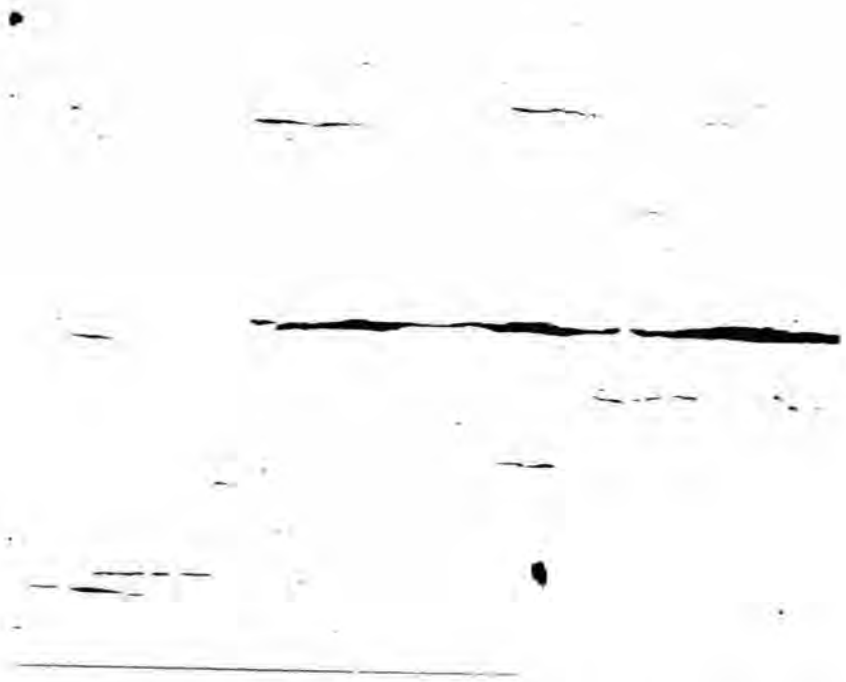

Figure 3. Metallographic cross section of the base metal. Note the elongated slag inclusions. Unetched. 66x.

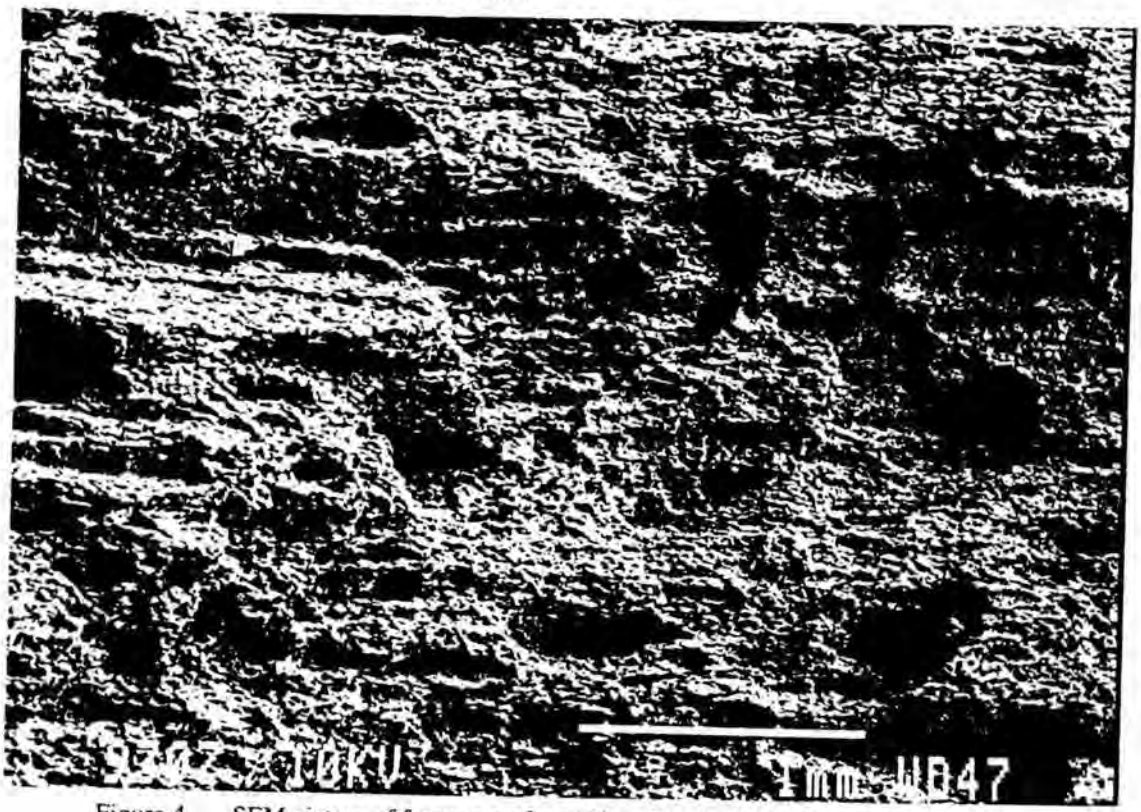

Figure 4. SEM picture of fracture surface of lug. The "striations" are oriented parallell with the slag inclusions. 38x.

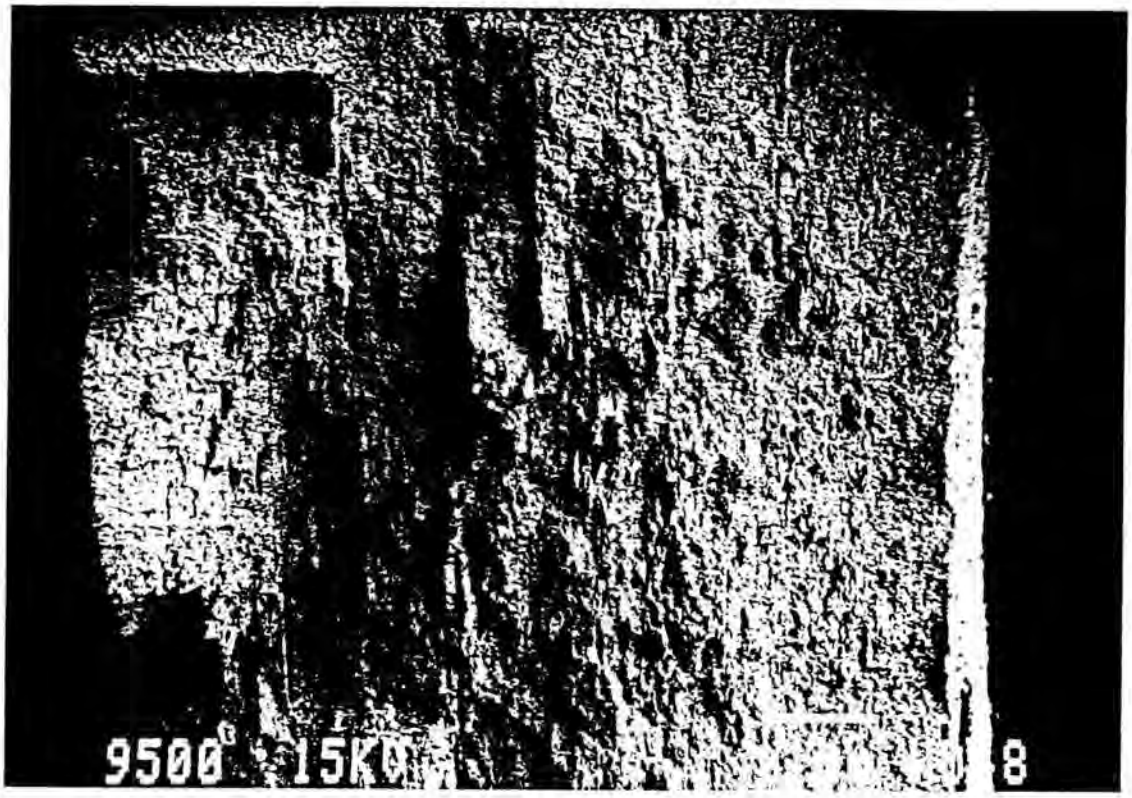

Figure 5. Fracture surface of tension specimen. 13x.

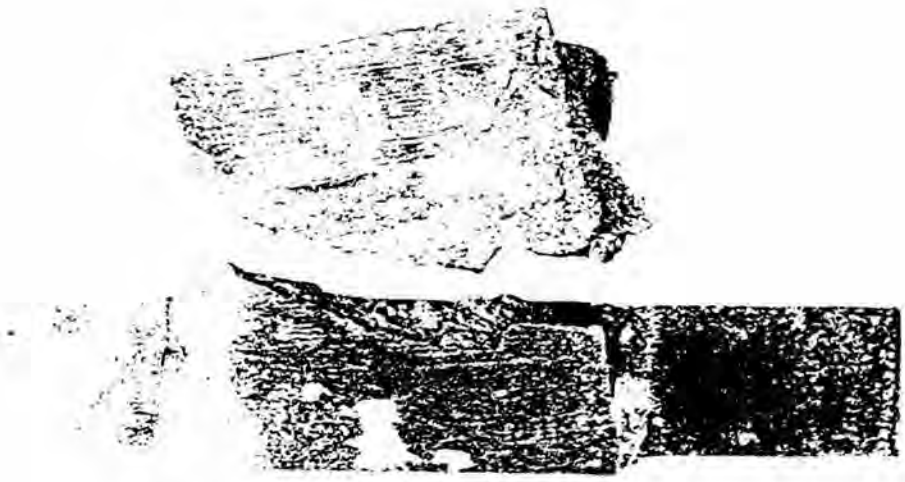

Figure 6. Mating fracture surfaces at the hinge. (ca 1x)

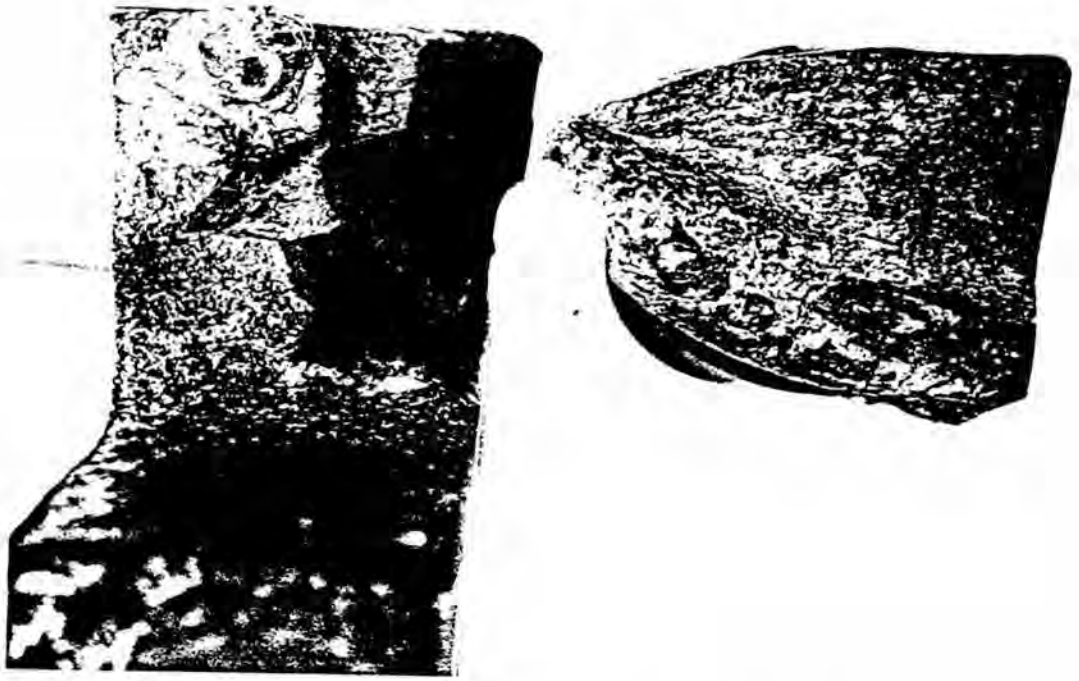

Figure 7. The two pieces from the hinge seen from the side. (ca 2x)

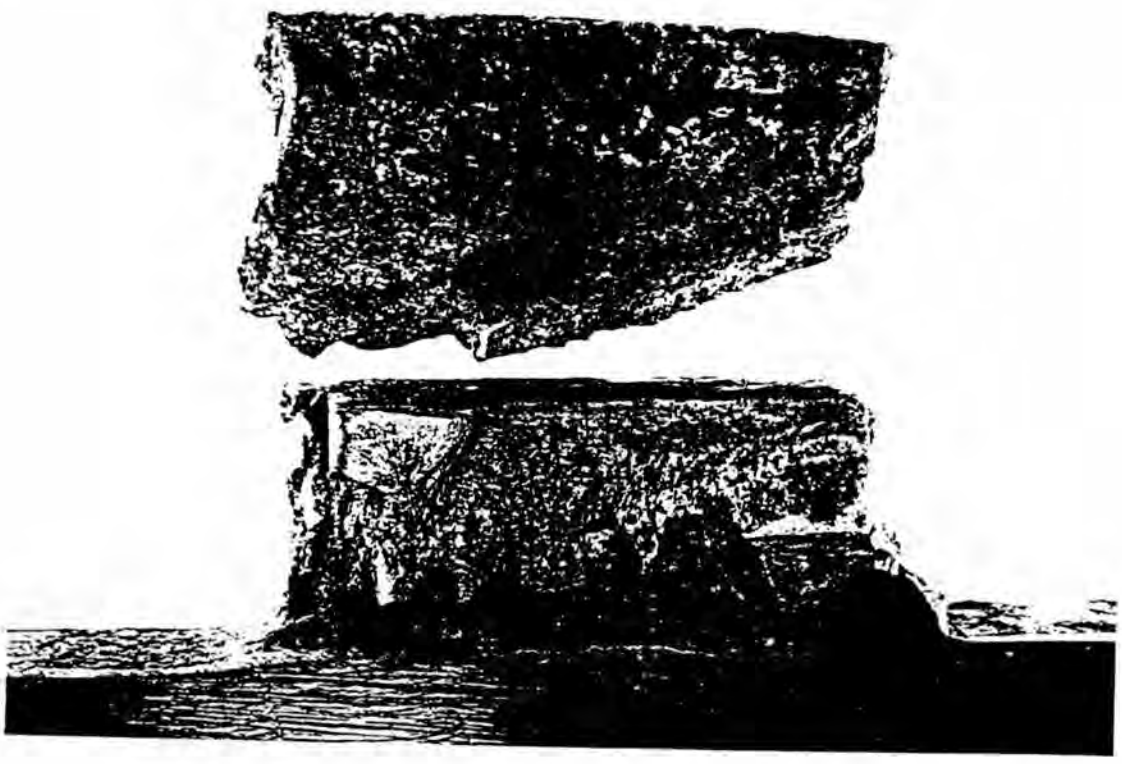

Figure 8. The two pieces of the hinge seen from a third angle. Note the crack in the weld. (ca 2x)

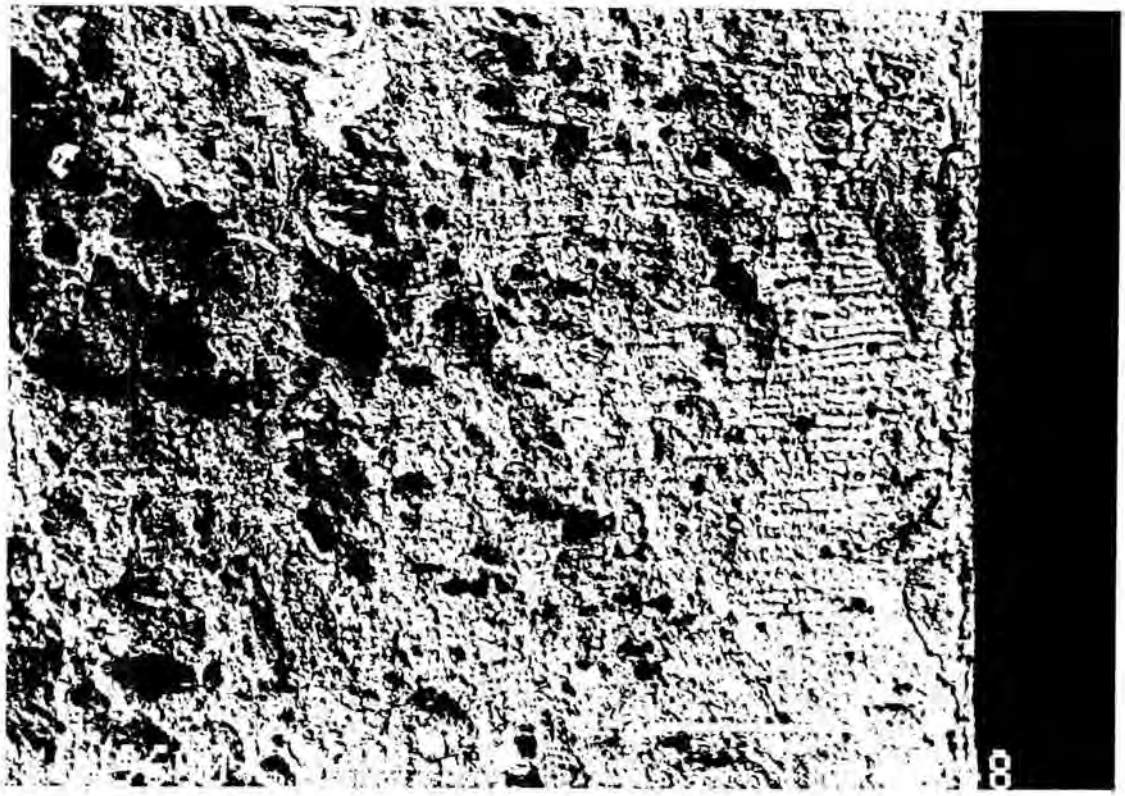

Figure 9. Fracture surface of hinge. SEM 29x.

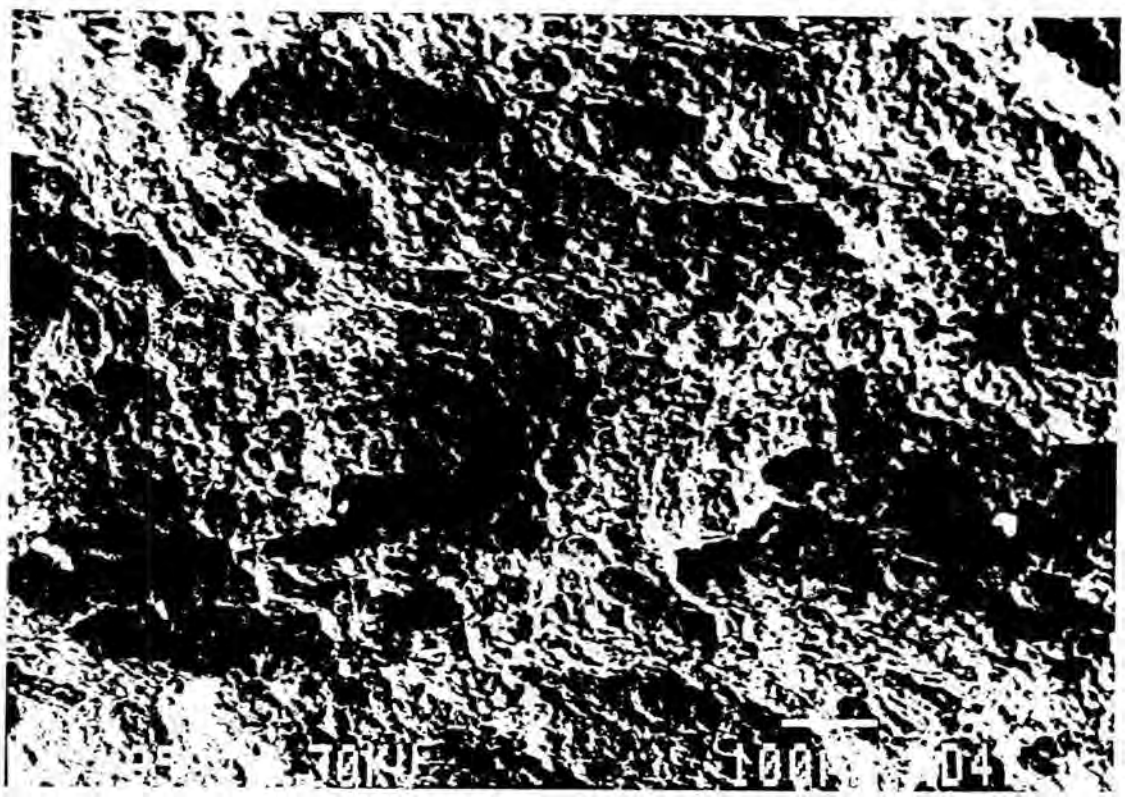

Figure 10. Fracture surface of hinge. SEM 130x.

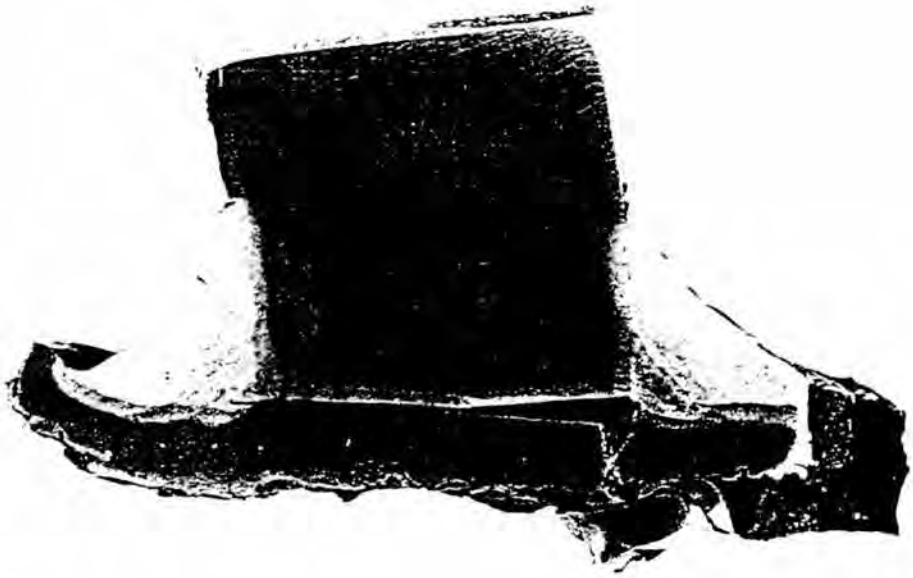

Figure 11 Cross section of side lock specimen marked SL1 (ca 2.5x)

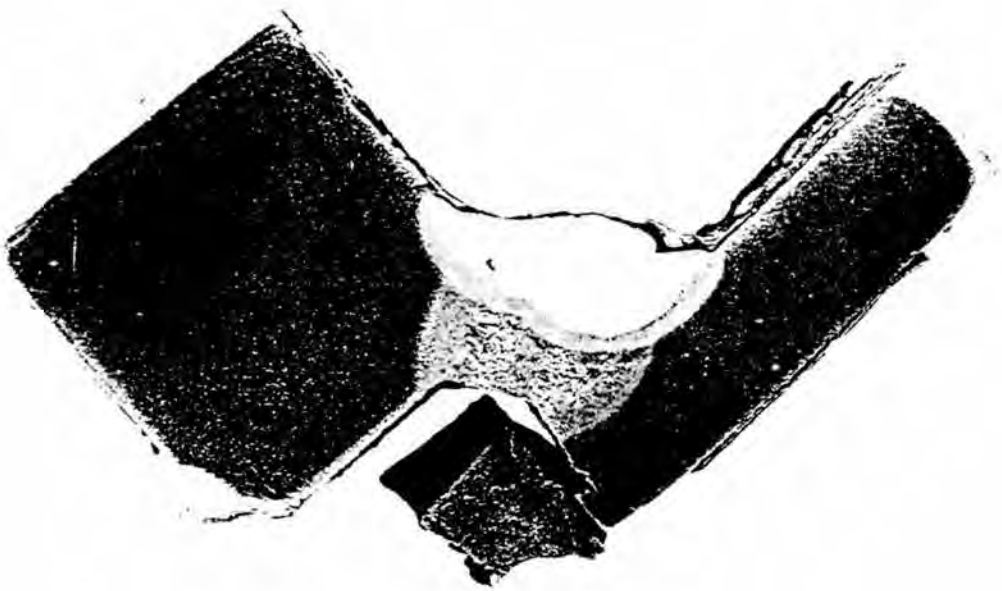

Figure 12 Cross section of side lock specimen marked SL2 (ca 2.5x)

SUPPLEMENT No. 518

Pettersson Kjell - Söderholm P-O: Notes from metallographic and fractographic examinations of samples from MV Estonia.

Royal Institute of Technology.

Stockholm 1996.

Notes from metallographic and fractographic examinations of samples from MV Estonia

Kjell Pettersson and P-O Söderholm
Department of Materials Science and Engineering, Division of Mechanical Metallurgy, Royal Institute of Technology.

Background

In a previous report dated 1995-04-12 [1] we discussed the results of examinations of the following parts from MV Estonia:

- The remaining parts of three lugs of the bottom lock for the bow visor
- A tension test specimen prepared from one of the lugs.
- Parts of the hinge of the bow visor found on the wreckage and its complement on the visor.
- Parts of the side lock for the bow visor.

The main conclusion in that report was that there were no indications of any pre-existing cracks which might have played a role in the failure of the bow visor. It was noted however that the welds joining the housings to the bottom lock lug plates were of very poor quality which meant that the main load carrying area of the bottom lock were the remaining ligaments of the lug plates. It was also noted that there were defects in the welds between the bushing and hinge plates of the hinge. The corrosive attack in the gap between bushing and hinge plate showed that these defects had been present for a long time before the shipwreck.

Since then we have been assigned by the Swedish Board of Accident Investigation to do a few additional examinations of the pieces previously stored at KTH and also on some new pieces of material both from Estonia and the sister ship Mare Balticum. The present report which documents our observations and interpretations of these observations has been written on the request of the Swedish Board of Accident Investigation. We would like to stress that we did not at any time have any assignment to make a full investigation of the extent and causes of any cracking prior to the shipwreck. Such an investigation would have required a considerably larger effort than spent on the present

examinations. In particular, as suggested in our previous report, such an investigation would have required an investigation into the effects of salt water corrosion on the appearance of fracture surfaces and the time dependence of such effects.

Observations on hinges.

We noted in our previous report that there were defects in the welds between the hinge plates and the bushing. This had resulted in the formation of a corrosion layer in the gap between plate and bushing. This corrosion layer was identified as magnetite and must have been formed before the failure. Figure 1 shows an overview of the two visor hinges after removal from the visor. There is a difference in the fracture character between the ligaments A1–A4 and those marked A5–A8. The latter ligaments have failed in pure tension as evidenced by a plastic contraction over the the whole ligament in connection with the failure. The orientation of the fracture surfaces is such that large portions of them make an angle of approximately 45°with the tensile direction. The examination of A7 showed a typical ductile failure [1]. (Note that these comments refer to A5 and A7 since A6 and A8 have been severely damaged due to impact on or from other objects). The ligaments A1–A4 have another character. The fracture surfaces are more perpendicular to the direction of the ligaments. These are contracted on the inside and expanded on the outside, suggesting a failure by bending. Evidence of this bending can still be seen on ligament A3, Figure 1, which has bent at a secondary crack. A fractographic examination of A4 was conducted with the object of finding evidence of cleavage fracture [1]. However that examination only revealed ductile dimpled fracture. Some features on the surface which in low magnification in an optical stereo microscope looked like striations were identified to be a result of the banded microstructure of the material.

It can be noted that the inside surface of the holes in the visor plates for the bushings has been formed by flame cutting with fairly deep cut markings. This flame cutting can also be noted by the presence of a heat affected zone layer in metallographic cross sections of the hinge lugs. The secondary cracks on ligament A3 have initiated in the cut markings. This is also true of the primary fracture of A3. There are a few indications in connection with the cracking of A3 and A4 which suggest that they may have formed by a process of corrosion assisted fatigue. This evidence is crack branching and the presence of corrosion products in the cracks. We have examined one of the primary fracture surfaces, A4, without seeing any evidence of fatigue. This was done on a surface which had been cleaned of rust by an electrochemical process

described in the previous report [1]. We have no reason to believe that the cleaning process leads to any false structure on the surface or that it would remove any striations if they had been present on the surface. It is interesting to compare the observations on A4 with the examinations of fracture surfaces of two bend test specimens prepared of material from the hinge plate. In one of the tests the notched specimen was bent to complete failure. Macroscopically the fracture surface is nearly perpendicular to the specimen surface with shear lips only at the edges. This demonstrates that fracture surfaces with a similar macroscopic appearance to those of the ligaments A1–A4 can be produced by bending. In the SEM the general appearance is similar to that observed on A4. On the other bend specimen the crack was grown by fatigue. Figure 2 shows an example of the fracture surface at a location where the crack growth has been about 0.6 µm per cycle. It does not seem very likely that any of those striations would be visible after a corrosive attack and the general appearance of this surface is totally different from that of A4.

Another indication of a fatigue process can be seen on one side of one of the pieces from the ligament A4 used for examination of the fracture surface. On that side there is a surface where the fillet weld has separated from the plate. If that surface is viewed in an optical stereo microscope with oblique illumination striation like features can be seen. We do not however conclude that these features necessarily are a result of a fatigue process. We feel that they can equally well be the result of the banded microstructure of the material. The bands are parallel with the plate surface. The fracture surface between the plate and fillet weld makes a slight angle with the plate surface so it cuts through several bands of the microstructure which then show up as striations.

As noted above there is some inconclusive evidence of pre-existing fatigue cracking. However the noticeable expansion of the cross section on one side and reduction on the other of ligaments A1–A4 clearly suggests a bending type of failure. It is difficult to envisage that this could have occurred prior to the clearly tensile failure of the ligaments A5–A8. It is clear that the fillet welds must have contained cracks for a significant period of time as evidenced by the thick magnetite layer. However we would not like to speculate on the cause of these weld defects.

In summary we feel that the available information does not support a conclusion that pre-existing fatigue cracks have played a significant role in the failure of the hinges.

The stempost

We have made a visual examination of a crack surface on the stempost. This crack is one of many cracks in the stempost and goes right through the cross section of the piece. Macroscopically we see so called chevron markings, a feature typical of a fast cleavage failure. The orientation and location of the markings are such that they indicate that the fast fracture has started at a weld defect on one of the sides of the stempost. This type of crack is typically formed at a fast impact at low temperature. In the present case it may have formed if the bow visor fell down on the bulb as indicated in the preliminary accident investigation report [2]. Whether or not that is a probable scenario is dependent on the brittle to ductile transition temperature of the material in the stempost. It should be noted that if we regard the stempost as a large impact specimen it can be expected to have a noticeably higher transition temperature than the standard Charpy-V specimen normally used for measuring the transition temperature since specimen size can have a significant effect on impact properties [3].

The bottom lock lugs.

A closer examination of the bottom lock lugs has shown the presence of cracks at several locations along the weld between lug and housing. Figure 3 shows a metallographic cross section of one of these cracks. As can be seen in the picture the crack is about 1 mm deep. None of the other cross sections of similar cracks examined contained a deeper crack. The cause of the cracking has not been determined. The crack faces are corroded and it will be impossible to see for instance any fatigue striations since these will have corroded away. As evidenced by the opening of the crack, 20–60 µm, seen on Figure 4 the corrosion on the faces have removed at least 10 µm of metal. The crack branching might be taken as evidence of a corrosion assisted crack growth. On the other hand the branches are parallel to the band structure of the material so they may be the result of a localized corrosive attack on elongated slag inclusions. Such inclusions can be seen in higher magnification than that used in Figure 4. It should be noted that the elongated features in Figure 4 are colonies of pearlite which actually have dissolved and reprecipitated as rounded colonies in the heat affected zone where the crack is located.

A comparison between the hinge materials on Estonia and Mare Balticum.

The bow visor hinges on Estonia and the sister ship Mare Balticum are of similar design. They consist of a cylindrical bushing welded to the hinge plate. Inside the

bushing is a bronze cylinder functioning as a bearing. A piece of a hinge on Mare Balticum was cut out in order to provide a comparison with the Estonia hinges. Figure 5 shows a metallographic cross section of the weld between hinge plate and bushing of Mare Balticum. To the left in the figure it is possible to see the heat affected zone after flame cutting of the hole in the hinge plate. Several cavities and a crack can be seen in the weld. In connection with the crack there was a grey-black deposit which we believe is magnetite because it looks like magnetite and is magnetic. This indicates that somewhere along the weld there must be a penetrating defect.

The crack is shown in higher magnification in Figure 6. The wide part marked with an arrow is not actually part of the crack but a cavity formed during welding which just happened to be located in the cross section. The main part of the crack is the branch extending to the right in the figure. It is interesting to note however that a very fine crack has initiated in the bottom of the cavity as shown in Figure 7. This indicates that the hinge is subjected to fatigue loadings which can initiate and grow cracks.

The compositions of the materials in the hinges from Estonia and Mare Balticum were also determined. The compositions of the bronze bearings were deterimined by wet chemical analysis after that it had been determined by EDS analysis in SEM that the only significant elements were Cu, Sn, and Pb. The following results were obtained:

	Estonia	Mare Balticum
Cu	85±2	88±1.5
Sn	11±0.5	9.5±0.4
Pb	0.56	0.46

The fact that the amounts do not sum up to 100% is just a reflection of the imperfections of the analysis.

The compositions of the bushings were determined by X-ray fluorescence for most of the elements. For carbon IR measurement on gases released in connection with combustion of the material in oxygen was used. For sulphur both methods were used. The following results were obtained:

	Estonia	Mare Balticum
C	0.22	0.35

Si	0.29	0.41
Mn	0.61	0.62
P	0.008	0.025
S	0.031(0.029)	0.047(0.05) (=combustion method)
Cr	0.02	0.23
Cu	0.025	0.27

Results were also obtained for Al, Ni, V, Mo, W, and Ti but these were all below 0.1% for both samples. The carbon content of the sample from Mare Balticum was considered surprisingly high. Therefore an additional sample was analysed as a check on the previous analysis. None of the values for that sample deviated from the values in the table by more than 0.03% and for C the value was identical.

Discussion

The additional observations reported here do not change the main conclusions of the previous report. The load carrying area at the bottom lock lugs was limited to the ligaments in the lug plates. The weld was of poor quality and as noted in the present report it contained pre-existing cracks. For the hinge there is clear evidence of pre-existing defects in the weld between plate and bushing. It is possible that these defects have grown by a process of corrosion assisted fatigue. The importance of these defected welds is the same as for the bottom lock lugs: the load carrying area is reduced to the ligaments around the hole in the hinge plate. It should however in this context not be forgotten that tensile samples of the weld between bushing and plate were prepared and tested by the department of Solid Mechanics at KTH. Those tests showed that intact welds had an adequate strength. The problem is that we do not know the extent of the weld defects and therefore we can not be certain to what extent the weld has contributed to the load carrying capacity of the hinges.

Other evidence of fatigue is the secondary cracks seen on the inside of the hole in the hinge plates. These cracks have initiated in the grooves formed by the flame cutting of the holes. To us it is conceivable that these cracks might equally well have formed in connection with the final failure of the hinge. The material in the zone heat affected by flame cutting is brittle so it is quite possible that cracks may form in connection with a temporary overload.

References

1. Pettersson, K., Söderholm, P-O., and Lange, N.
Metallographic and fractographic examinations of samples from MV Estonia.
Materials Science and Engineering, KTH, 1995-04-12

2. The Joint Accident Investigation Commission
Part-Report on the Estonia disaster of 28 September 1994.
April 1995

3. Alexander, D. J. and Klueh, R. L.
Specimen size effects in Charpy impact testing.
Charpy Impact Test: Factors and Variables, ASTM STP 1072, John M. Holt, Editor, American Society for Testing and Materials, Philadelphia, 1990, pp. 179–191.

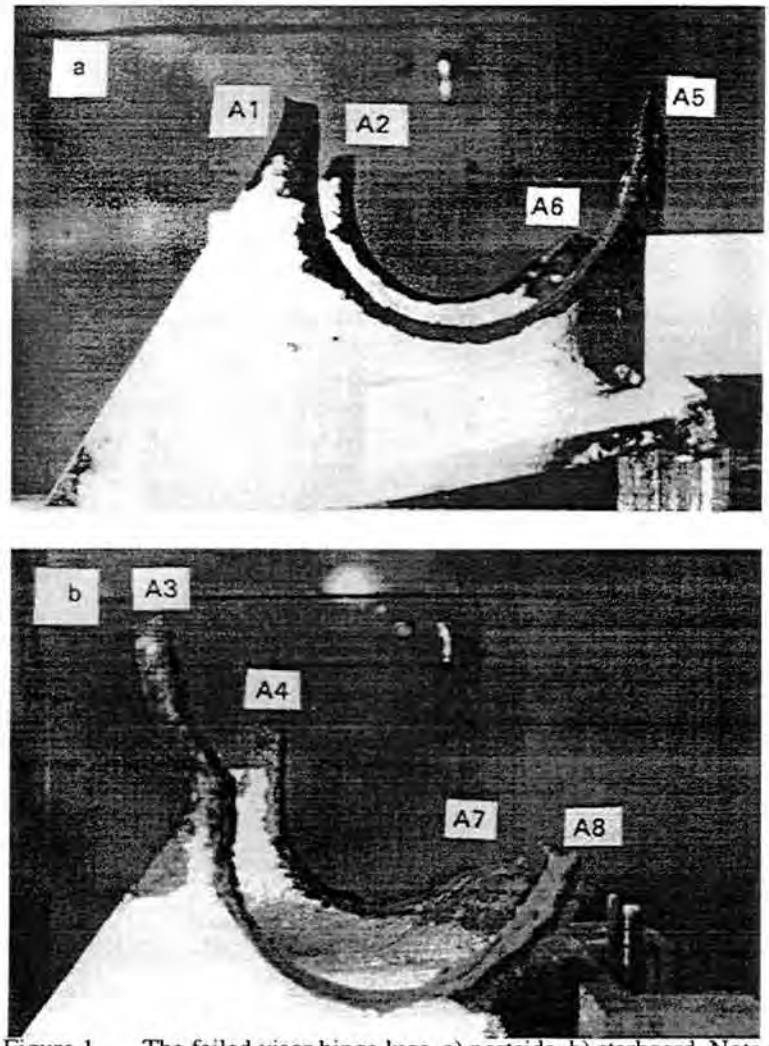

Figure 1. The failed visor hinge lugs. a) portside, b) starboard. Note that A7 is on the near side of the lug and A8 on the far side.

Figure 2. Fatigue fracture surface on laboratory specimen from visor hinge plate. 5000x.

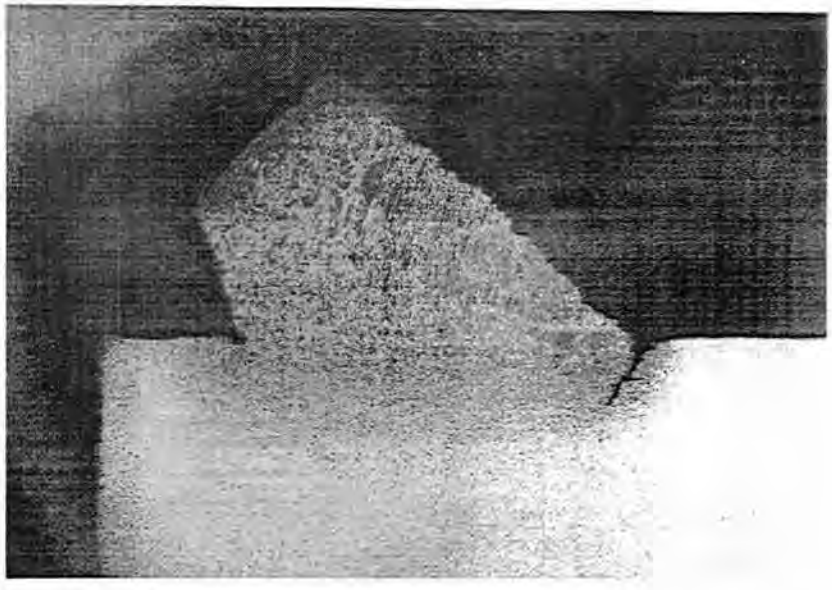

Figure 3. Metallographic cross section of crack in bottom lock weld. 8x.

Figure 4. Metallographics cross section of crack in bottom lock weld. 100x.

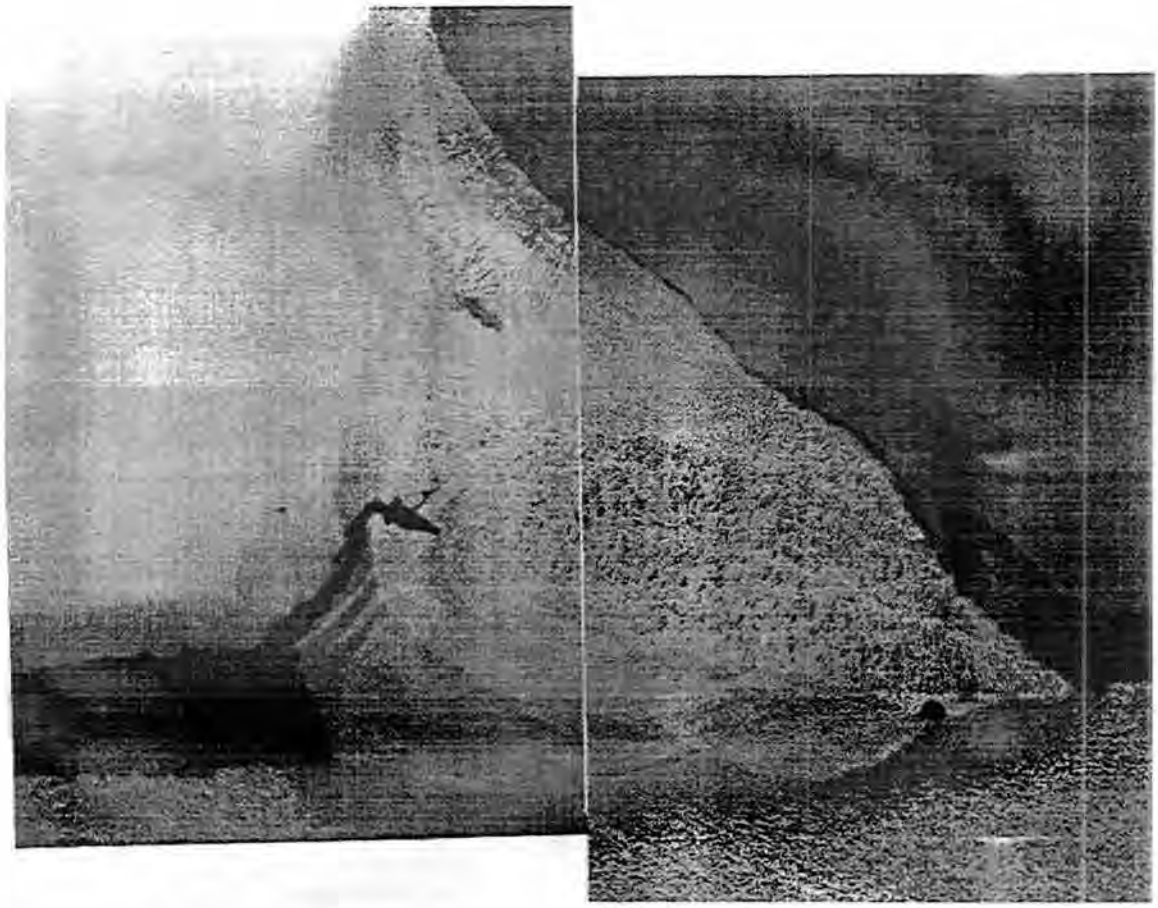

Figure 5. Cross section of weld between hinge plate and bushing on Mare Balticum. 7x.

Figure 6. Cross section of weld in higher magnification. The wide part of the crack is actually a pre-existing cavity formed during welding. 50x

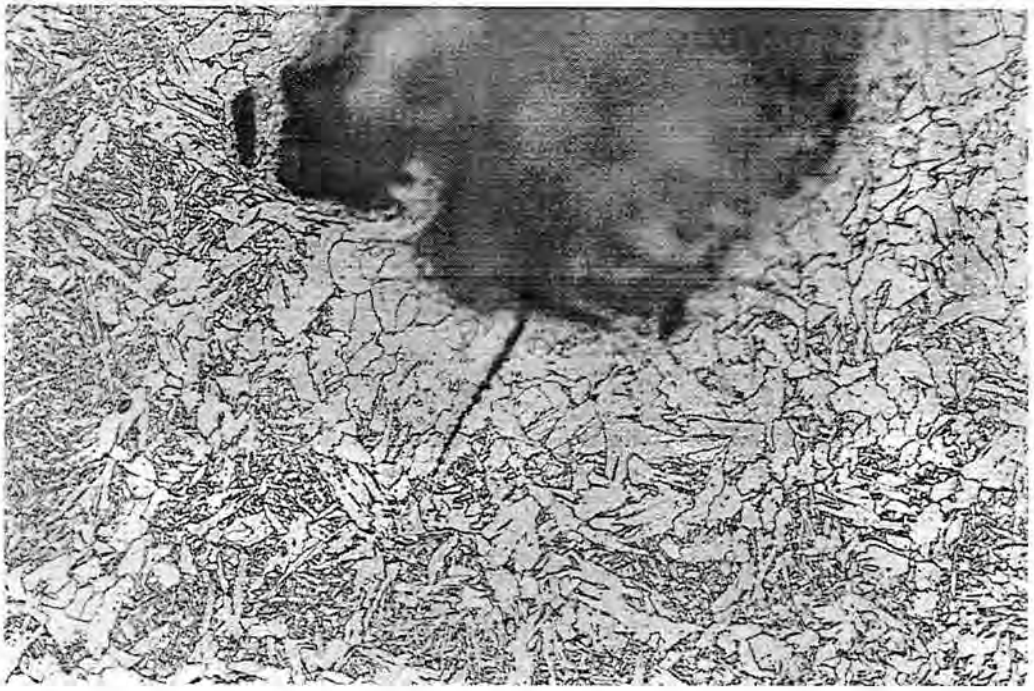

Figure 7. A sharp crack initiated in bottom of cavity, presumably by fatigue. 500x.

SUPPLEMENT No. 519

Öberg Hans:

Investigation of deformations and related loads, applied to the lug of the visor bottom lock of MV ESTONIA.

Royal Institute of Technology.

Stockholm 1996.

KUNGL
TEKNISKA
HÖGSKOLAN

Hållfasthetslära
Hans Öberg
tel 08-790 7547

REPORT
96-03-26

The Accident Investigation Commission

Börje Stenström

Investigation of deformations and related loads, applied to the lug of the visor bottom lock of MV Estonia

An investigation was commissioned by SHK to be carried out by the Department of Solid Mechanics at KTH (the Royal Institute of Technology) in Stockholm in order to show the behaviour of the lug of the bottom lock when subjected to a combined bending and pulling force. The test was carried out by Hans Öberg, Senior Research Engineer at the Department and was witnessed by Dr. Tech. Mikael Huss and Mr. Börje Stenström on behalf of the Accident Investigation Commission.

Test specimen and loading set up

A test specimen was made in one third scale compared to the original. See **Figure 1**. It was manufactured in steel to the Swedish specification SS 2172, being approximately equivalent to the earlier St52. The specimen contained two test sections, arranged back to back. The holes for the locking bolt of diameter 28,0 mm was elongated in the longitudinal direction of the lug by machining to the length of 31.5 mm in one hole (1.) and 30.0 mm in the other (2.) in order to illustrate two different conditions of original wear of the hole. The elongations were located symmetrically around the centre of the original hole.

The loading of the specimen was made at the ends of two bolts of diameter 26.3 mm with dimensions to give an arm of momentum of 80 mm to the centre of the lug. It should however be observed that the arm of momentum decreased substantially during the test due to deformation of the holes and bending of the bolts.

Test equipment

The servohydraulic material testing machine MTS 160 kN was used. Load versus loadpoint displacement was stored in a connected PC.

Photos of the test piece were taken at different load levels, using a camera with f=50 mm at a distance of about 400 mm.

Postadress
KTH, Inst. för Hållfasthetslära
Osquars Backe 1
100 44 STOCKHOLM

Telefon
Vx 08-790 60 00
Direkt 08-790 7547

Telefax
08-411 24 18

The bending and elongation of the test piece were measured during the loading using a calliper. After testing the symmetry section of the test piece was uncovered by sawing and milling. The section geometry was measured using a coordinate measuring equipment. See **Figure 2**.

Testing

The test specimen was loaded in increments of 10 kN. It was photographed at each load level. The length of the lug and the deflection in way of the centre of the hole were measured at each step. Plastic deformation started to develop at the edges of the holes at 10 kN. Loading was continued until the deformation as measured as the angle between the stem of the lug and the bolt was about 30 degrees. This could not be determined accurately during the test as the bolts themselves showed significant bending. The testing was suspended at a load of 50 kN. Load versus loadpoint displacement is shown in **Figure 4**.

The test specimen was cut apart along its centre line in order to better show the deformation and the contours of the holes. The section of the deformed specimen is shown in **Figure 2**.

Observations

It was observed that considerable elongation had taken place in the bolt holes, being close to 1.5 mm in the test scale at mid thickness of the lug. Detailed dimensions are shown in **Figure 2**. Considerable plastic deformation had taken place at the contacting points between the bolts and the edges of the holes. Some plastic deformation was also noted on the bolts, resulting in a smoothening of the contact pressure distribution. The elongation was not accompanied by any increase of the length of the entire specimen in the bent condition.

Photos of the test set up at 0.1 kN and 50 kN respectively in **Figure 3** demonstrates the decrease of the arm of momentum due to deformations.

Hans Öberg

Postadress
Kungl. Tekniska Högskolan
Inst. för Hållfasthetslära

Telefon
Vx 08-790 60 00
Direkt 08-790 7547

Telefax
08-411 24 18

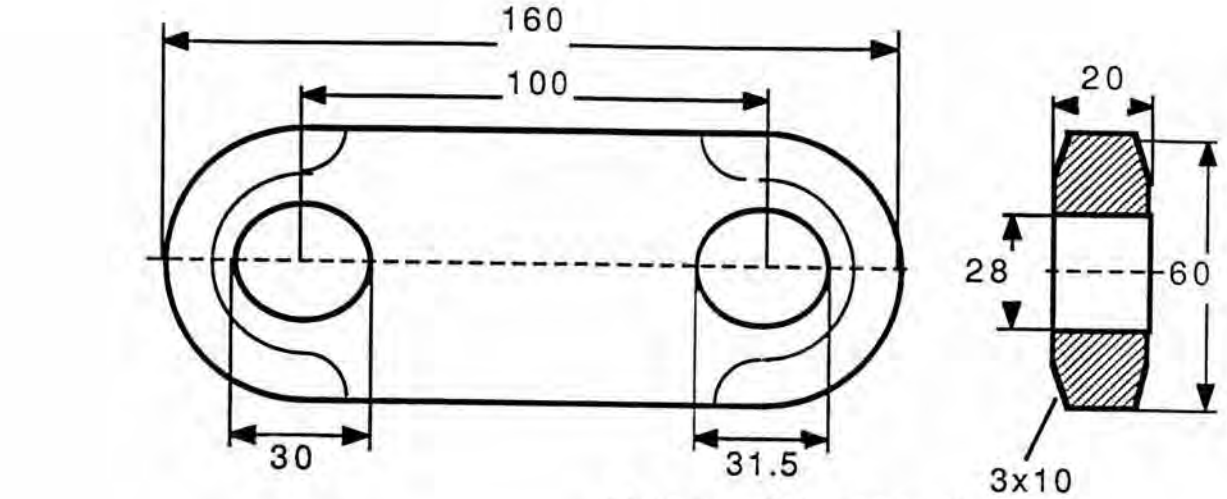

Material: SIS 2114 (St 52)

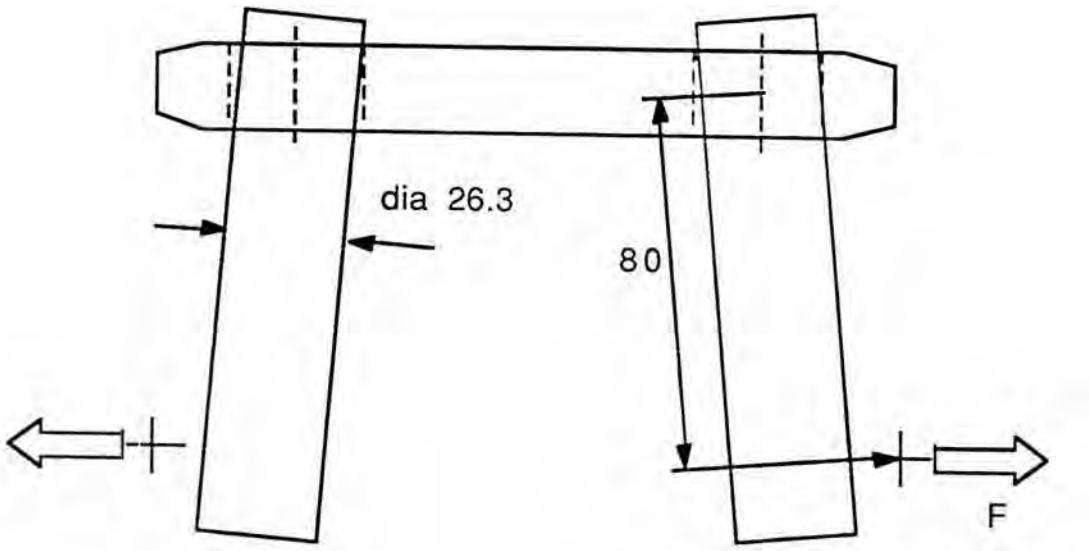

F = 10, 20, 30, 40, 50 kN

FIGURE 1 TEST SPECIMEN AND TEST ARRANGEMENT

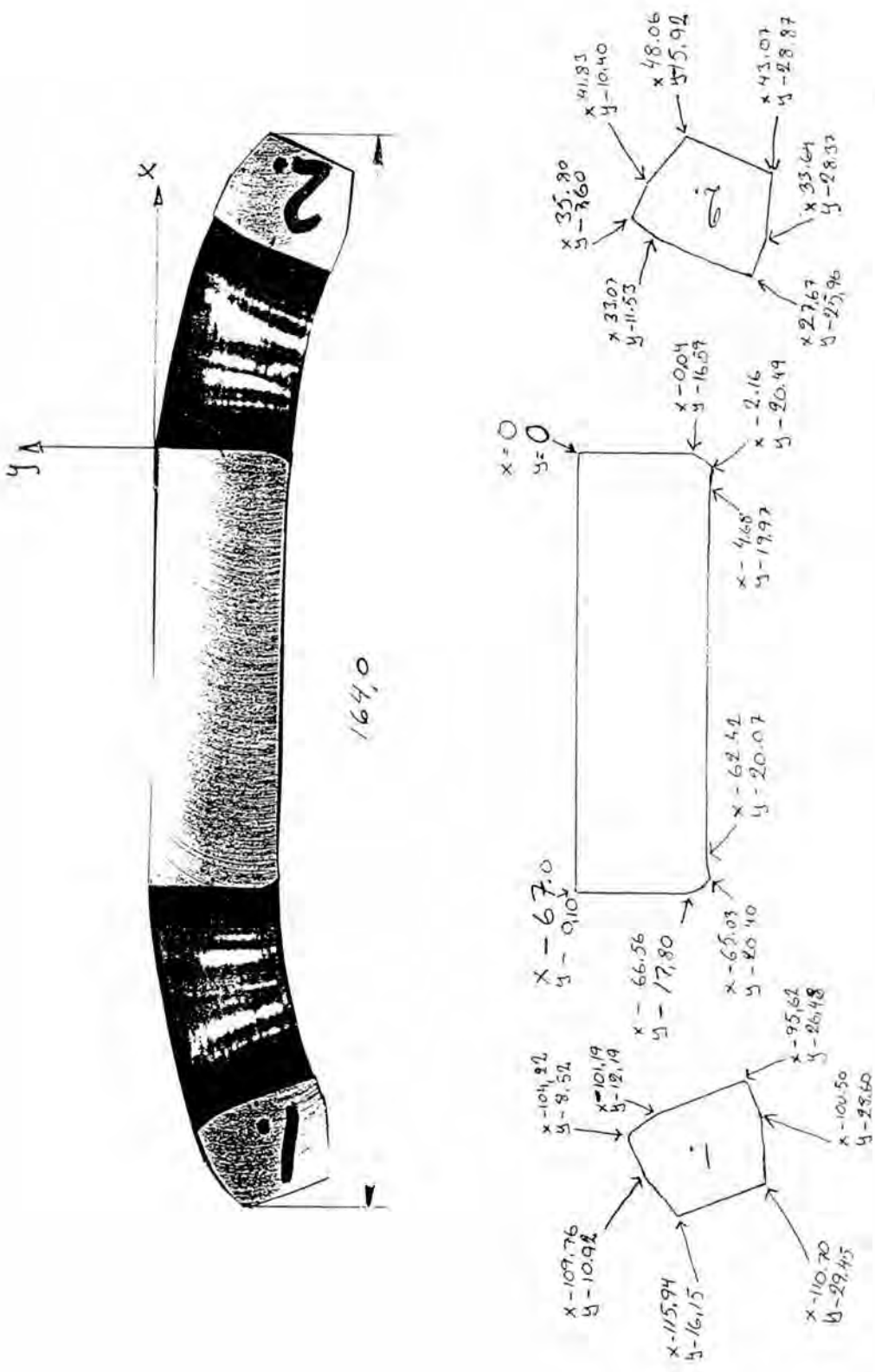

FIGURE 2 SYMMETRY SECTION AFTER TEST

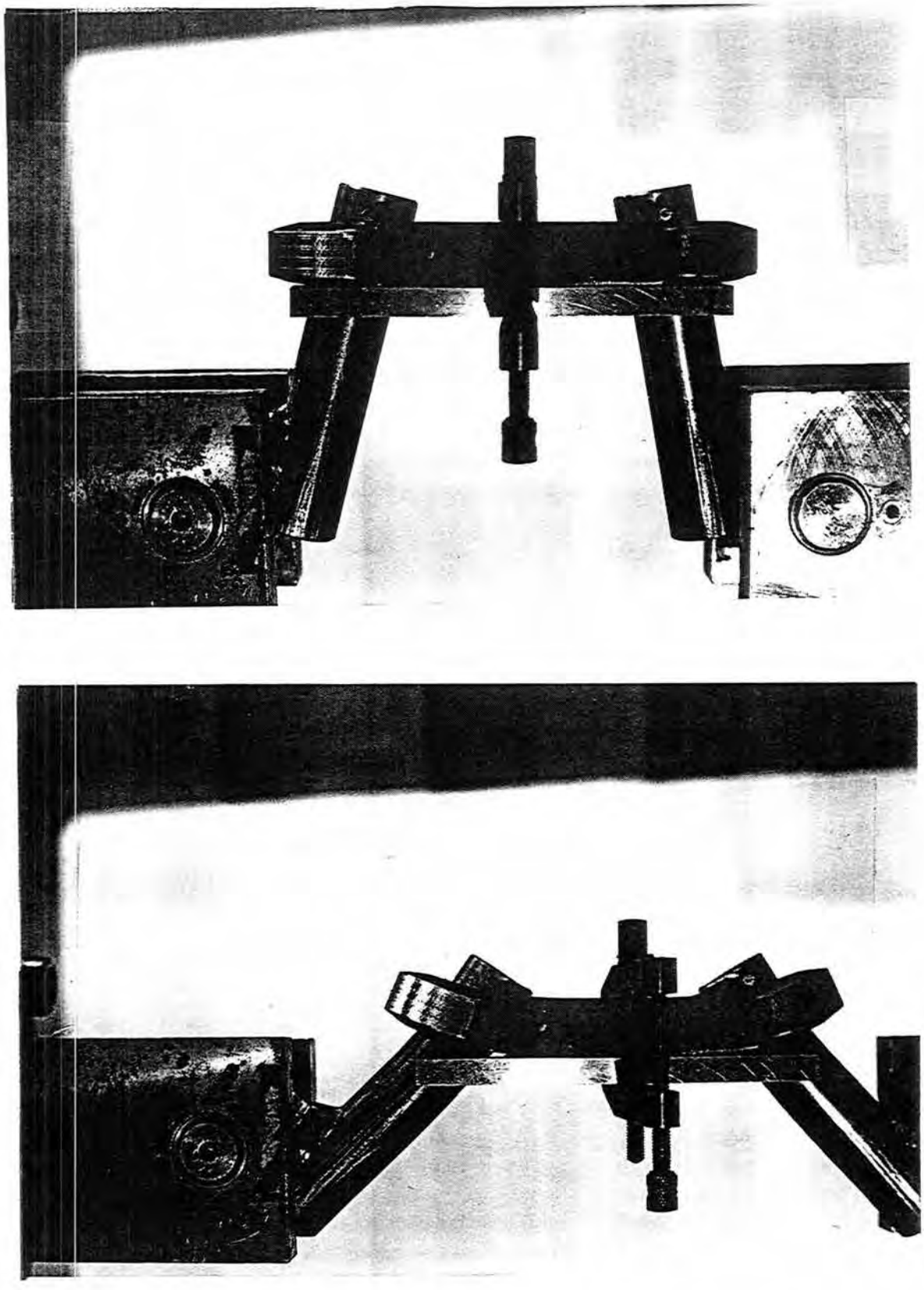

FIGURE 3 TEST SET UP AT 0.1 kN AND 50 kN

FIGURE 4

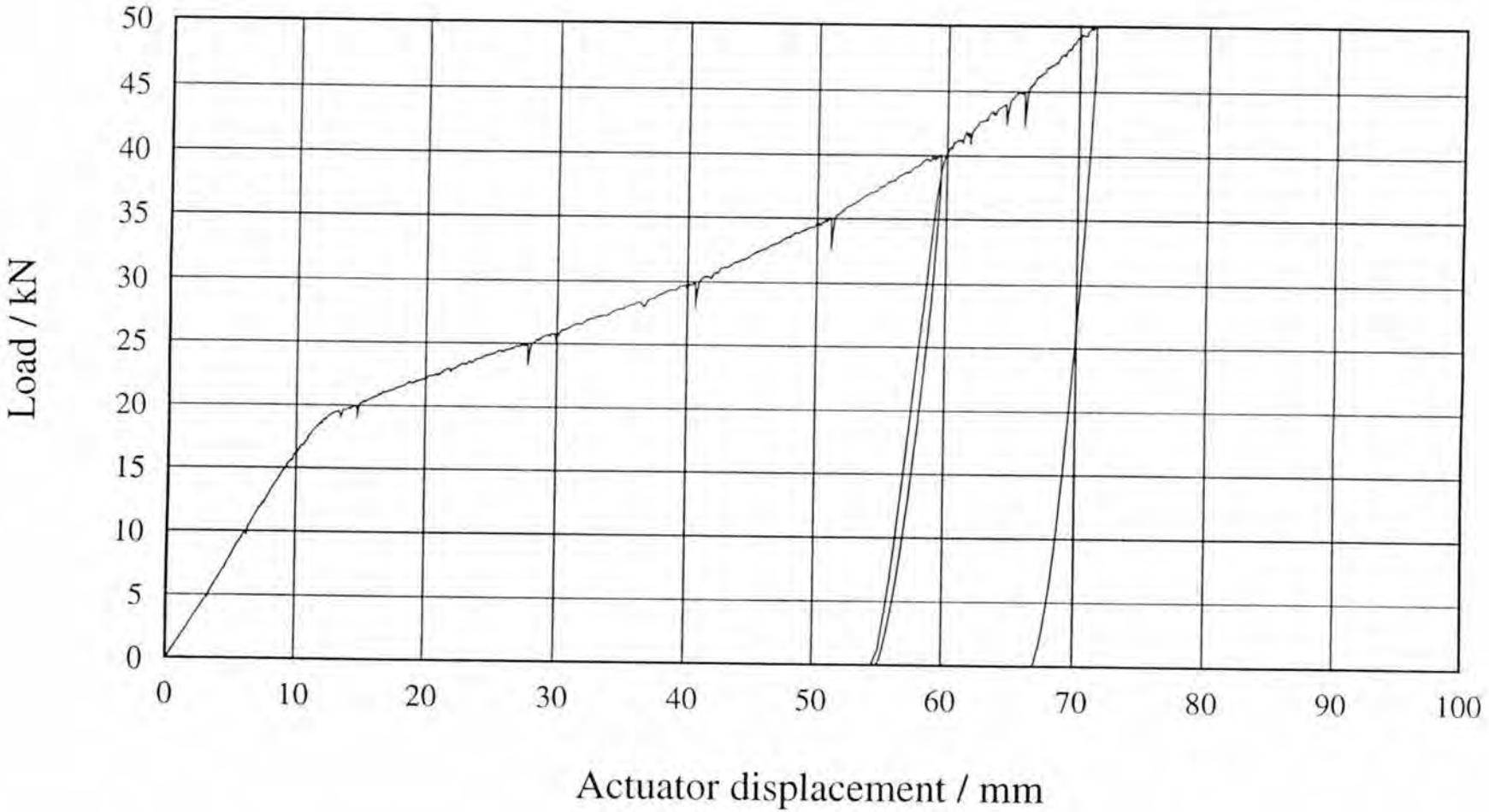

96-03-20

SUPPLEMENT No. 520

MS ESTONIA Bow Visor. Inspection Report of PS-side Hydr. Lifting Cylinder.

MacGREGOR (FIN) Oy.

Piikkiö 1995.

MacGREGOR
MEMBER OF THE INCENTIVE GROUP

East Europe Division

MacGREGOR (FIN) OY

21500 Piikkiö

T.Mäki

February 1, 1995

MS ESTONIA BOW VISOR

INSPECTION REPORT OF PS-SIDE HYDR. LIFTING CYLINDER

Type of the cylinder: CD9-38725-6 250
Main dimensions:

Outer diameter of the cyl.tube:	355mm
Inner diameter of the cyl.tube:	280mm
Diameter of the piston rod:	180mm
Diameter of the cylinder eyes:	160mm
Stroke of the cylinder:	1800mm

On the cylinder tube was stamped: 21.3.1980 TP 350 bar

Before opening the cylinder it was pressure tested on both sides and it was noted that there was no leakage on lifting side, but the oil went thorough the piston seals from piston rod side to lifting side. The piston rod was after this pressed completely out to inspect the piston rod condition and it was noticed that there was heavy damages on at the distance when the piston rod is about 400mm open.

The damages were on side SB-side of the piston rod. it was also noticed damages on piston cover's fixing screws. The ends of these hexagon screws were like hammered.

When the am. cylinder was opened the only damage inside was that the support ring and pressure seal which keep the pressure on the piston rod side was damaged which is most probably caused by very high pressure on piston rod side.

By the a.m. report we can see that the lifting cylinder has been opened at least about 400mm and there has been very high pressure on the piston rod side.

Kind regards,

MacGREGOR (FIN) OY
Marine Services
Tarmo Mäki

encl. photos

MacGREGOR (FIN) OY
VAT No FI01133200
ALV rek. No 0113320-0

Address
Hadvalantie 10,
FIN-21500 Piikkiö,
Finland

Telephone
358-21-892 111

Telex
62382 macgr fi

Telefax
358-21-892 517

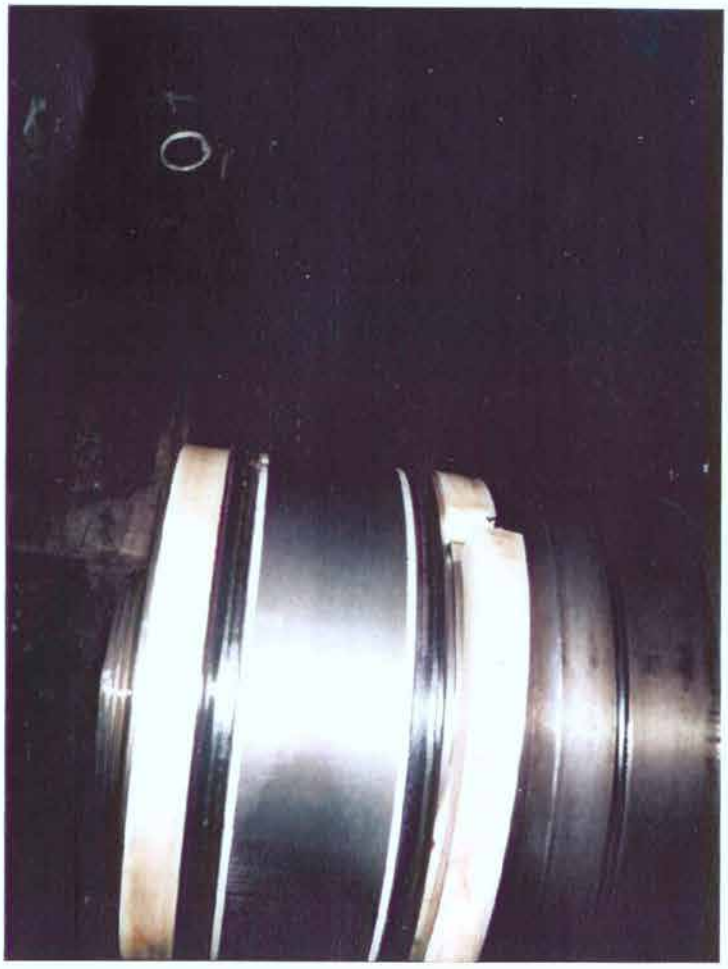


MT38

SUPPLEMENT No. 521

Larjo Kari:

ESTONIA's shedule, ETA-PILOT and NaviSailor 2100.

15.10.1996.

The International Accident Investigation Commission of

MV ESTONIA.

Kari Larjo
15 October 1996.

ESTONIA's shedule,

ETA-PILOT and NaviSailor 2100.

ESTONIA's master notified the officer of the watch a few minutes after 01.00 that ESTONIA was one hour late. The automatic speed control ETA-Pilot and the navigation computer NaviSailor 2000 were able to give this information with ease. Master's statement is an important hint about the last discussions on the bridge.

Testimonies about being late.

The trainee second officer was on the bridge before the midnight and the master was there also. The master remarked that the vessel was late but he did not mention any specific time for it (Turku 29.09.94).

The AB seaman of the watch testified in Gothenburg the 31th march 1995 that captain stated prior the accident that the ship was one hour late. The hearing was documented by Kari Lehtola (in finnish) as follows:

* The AB seaman left the car deck for the bridge at 00.50 where he arrived about 01.00.
* The AB seaman was present when the captain arrived to the bridge. The captain asked how many main engines were on. He noted also that the vessel was about on hour late. The discussion was between the captain and the mate.

The information was in fact very precise and not 'about one hour' as the AB seaman heard it.

Background.

ETA-Pilot is an automatic propulsion control device. It was installed on m/s Viking Sally after her delivery from the shipyard in Papenburg. The installation took place between the years 1981-1984 when the vessel was sailing between Turku and Stockholm.

NaviSailor 2000 (Trans Marine, UK) is a navigation computer with electronic chart, route planning facility and an online GPS function. The system was delivered to Estline 26.01.93.

The ETA-Pilot speed control.

The ETA-Pilot has three operating modes.

1. **The Consumption mode** is utilized in tanker and bulk carrier traffic. This mode is unsuitable for passenger traffic tied to tight schedules.

2. **The Speed mode** adjusts the propeller pitch automatically to maintain the selected speed.

3. **The Estimated Time of Arrival (ETA) mode** employs a user defined speed profile. The speed is programmed between the Way Points and they are restricted for legal speed limits, for squat in shallow water and for fairway bends. The speed is free on the open sea passage and the computer uses vessel's maximum speed as an upper limit. Required time of arrival is fed in the computer and the Eta-Pilot will answer if it will be achieved or how much the vessel be late.

Captain **Anders Andersson** employed by the Hornet company told the commission (07.08.1995) that 'the ETA Pilot was normally used' ('Man kör normalt med ETA-Pilot'). He did not define the operating mode.

Captain **Bengt Skogberg** the master of m/s Mariella told Kari Larjo (12.09.1996) that the ETA-Pilot speed mode was used even in heavy wether. ETA-Pilot worked safely in heavy seas when the speed command was low enough. Captain Skogberg stressed that the ETA mode should newer be used in heavy sea because the automatic control would use too much power to keep the vessel on the schedule.

Technician **Leif Hagner** from Vaasa revealed (30.09.96) that the Raytheon Doppler speed information was unreliable. Mr Hagner connected the GPS speed to the ETA-Pilot when Estonia sailed for Silja Line between Vaasa and Umeå as Wasa King. With reliable speed information ETA-Pilot operated satisfactory.

The NaviSailor 2000 navigation computer.

ETA is always visible to the next the WayPoint. The default speed is zero for the open sea passage and for the archipelago the speed limits and the allowance for the shallow water are programmed into the WayPoint database. NaviSailor utilises the GPS Speed Over Ground to calculate the time to the next WayPoint.

The reconstruction of the time schedule at 01.00hrs.

Time schedule at 01.00hrs in normal conditions.
Normal condition means low sea state and average speed 17.0 knots from Naissaar to the Swedish archipelago. Estonia was 7 minutes late at 01.00hrs compared to her normal schedule. This means that captain Andresson did not compare the situation at 01.00hrs to the normal condition.

Time schedule check with the chart work.
To solve the time schedule problem on the chart the master had to measure the distance from the position at 01.00hrs to the entrance of the Swedish archipelago. He estimated most likely that the distance to Armbågen could be covered with the speed at the moment 14.5 knots. After Armbågen the sea state should have decreased and the appropriate speed should have been 17.0 knots to Söderarm. From Söderarm to Marö the fairway is sheltered and there are no speed limits an maximum speed 19.0 knots should have been safe. This graphical solution should have revealed that the vessel was 34 minutes late. The graphical method was too cumbersome. It is doubtful if the master had time to use this graphical method during the short time the AB seaman and the master were simultaneously on the bridge.

Time schedule check with the ETA-Pilot.
One can use ETA mode as a calculator. The ETA-Pilot should have utilised the actual speed 14.5 knots as maximum speed for the remaining distance to the Way Point where the speed limit of 12.0 knots begins at 01.00hrs. The ETA mode would have informed the master that the vessel was 1 hour and 3 minutes late. His comment that Estonia was one hour late was very accurate.

Time schedule check with the NaviSailor 2000.
The easiest way to find the ETA to Stockholm was to enter the Stockholm WayPoint number and the present Speed Over Ground (SOG) as set speed in the computer. The NaviSailor should have informed at 01.00hrs that the vessel was 1_{hr} 3_{min} late. According to the NaviSailor operation manual (version 09/93) it takes only few keystrokes to get the data:

- <F2>
- ETA/Calc
- WayPoint number
- Speed (in this case 14.5 knots)
- <Enter>

Conclusion.

The master noted about 01.00hrs that the vessel was one hour late from her schedule. His comment is very accurate and relates to the method the automatic speed control ETA-Pilot and the navigation computer NaviSailor 2000

calculate the schedule. According to the reconstruction she was one hour and three minutes late at 0100. It is likely that the master got the information from the navigation computer which was online to the GPS position fixing system. Master's concern about the schedule reveals that he was not aware of the state of the bow visor at the moment.

SUPPLEMENT No. 522

Huss Mikael:

Simulation of the capsize. MV ESTONIA Accident Investigation.

Internal report 1995 - 1997.

MV ESTONIA Accident Investigation
Internal Report
1995-1997

Simulation of the capsize

by
Mikael Huss

1 Summary

This report has been made in order to verify if the capsize scenario, as described by witnesses on board MV ESTONIA, can be reasonably explained by the loss of the bow visor, the opening of the forward ramp and the subsequent flooding of car deck.

The analysis concerns only the first phase of the capsize, before water started to enter the upper decks of the vessel. It is made in three different stages described in the separate sections of the report:

Floating condition and stability
The floating condition and quasi-static residual stability have been calculated for the first phase of the capsize when water was accumulating on the A-deck (car deck).
The calculations give input to the simulation of water inflow rate.

As is well known, a ship like the ESTONIA with a fully open vehicle deck is extremely sensitive to ingress of water. A relative small amount of water like 1000 ton (0.3 m water on the deck) will result in a heel angle of over 20°. Such a large heel will cause severe damage to the interior of the public areas, significant shift of vehicles and cargo, and presumably panic among the passengers. However, the water on the car deck is in itself not sufficient to make the ship capsize as long as the hull is intact below and above the open deck. The capsize is fulfilled only when water starts entering other areas of the ship. According to the hydrostatic calculations, this condition appears when 1500-2000 ton has entered the A-deck and the heel angle is in the range of 35°-40°. Apparently there have also been some water leaking down through the centre casing doors before the flooding of upper decks. However, this is believed to have had no significant effect on the stability or heeling of the vessel.

Relative motions at the bow
The vertical relative motions between the bow and the waves have been calculated with linear strip theory for the intact ship. Approximate calculations have also been made for two heeled conditions. The result show that the motions are very sensitive to the mean period of the wave spectrum and to the relative heading of the ship towards the waves. The influence of speed is less significant in the present condition. The relative motions for heeled conditions are generally smaller than for the intact ship in head and bow sea but similar or larger in beam sea.

Simulation of water inflow
The rate and time sequence of water inflow have been simulated from the frequency distribution of relative vertical motion amplitudes. The simulation takes into account the changed floating condition, heading and speed as estimated from manoeuvring simulations and witnesses statements. The results show that the assumed probable time sequence well can be verified by the simulations. However, the uncertainty in estimates is large and the time sequence is shown to be very sensitive to small changes in the condition.

2 Floating condition and stability

The hydrostatics characteristic of ESTONIA has been calculated with the program HYSS developed by the author. The calculation method has been verified in several independent comparisons with other well known commercial program systems. The ship geometry is modelled with a number of transverse sections, to which can be added or subtracted external or internal compartments.

Figure 2.1 shows the base model of the ESTONIA hull. A separate geometry model has been used for the car deck in the calculations of flooded conditions.

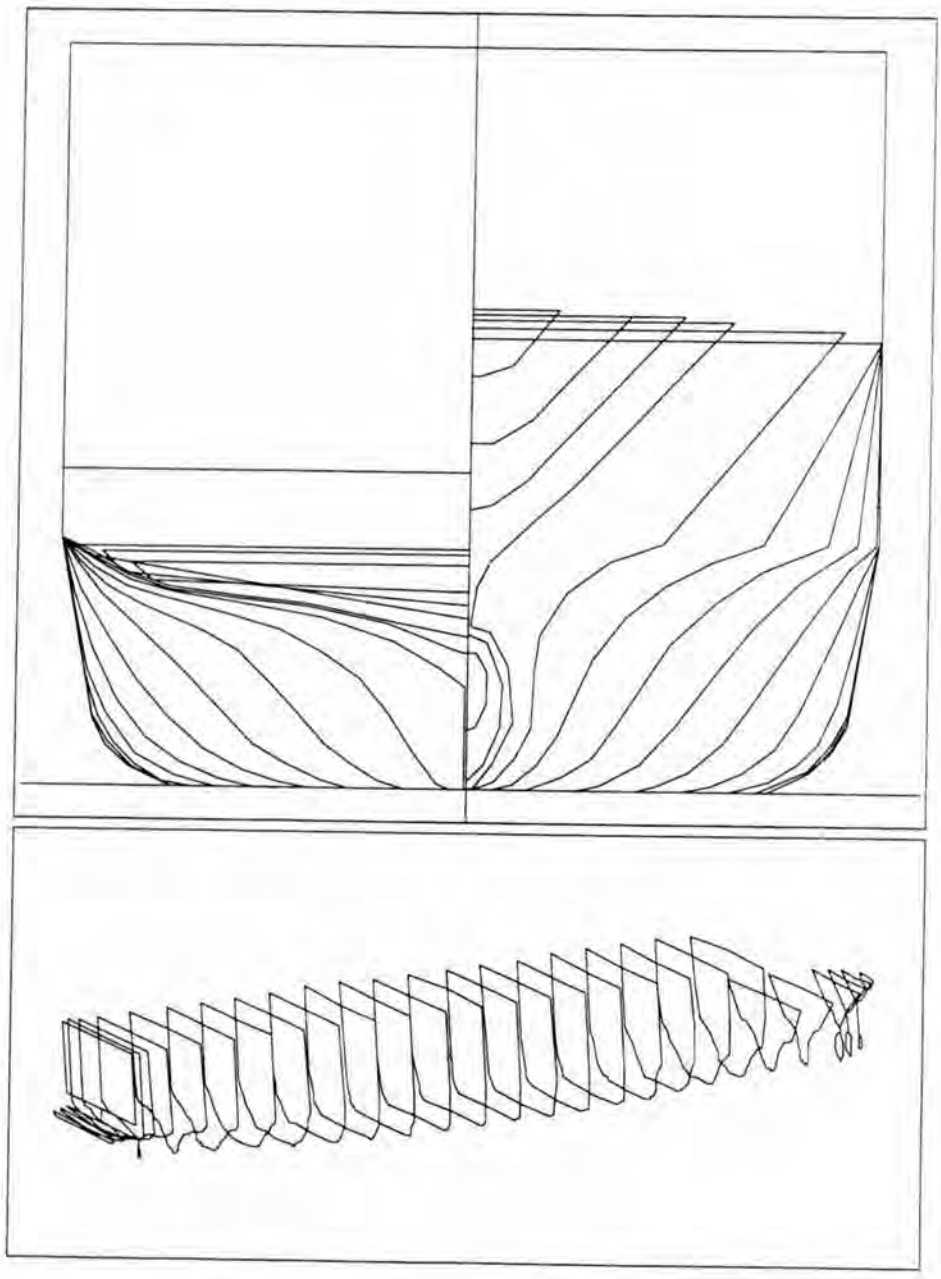

Figure 2.1 Hull geometry model of the ESTONIA used for hydrostatic calculations

2.1 Condition before flooding of car deck

The intact condition is taken from previous calculations with the NAPA program reported in [1].

Intact Condition

Displacement	12050 ton (11931 m^3 with an assumed density of 1.010 ton/m^3)
LCG	63.85 m fwd AP
KG	10.62 m

All calculations in this report refer to the conditions after the stem visor had left the ship. The weight of the visor is here assumed to be approximately 60 ton.

Damaged condition (before flooding)

Displacement	11990 ton
LCG	63.47 m fwd AP
KG	10.61 m

It is further assumed that no significant free surfaces were present except for the flooded car deck. This assumption gives a little over estimation of the initial stability (GM') but it is considered to be of no importance for the purpose of this study.

Main hydrostatic data for the intact and damaged condition is given in Table 2.1 below. A comparison with the intact floating condition calculated by HYSS and by NAPA [1], shows a difference of 0.020 m in draught and 0.013 m in trim. This difference is small and well within the uncertainty margin of the actual loading condition.

Dens SW = 1.010 ton/m^3		*Intact*	*Damaged*
Displacement SW	(ton):	12 050.00	11 990.00
LCG fw AP	(m):	63.850	63.470
TCG ps CL	(m):	0.000	0.000
KG	(m):	10.620	10.610
Equilibrium at:			
Draught mld at L/2	(m):	5.370	5.336
Trim (pos aft)	(m):	0.448	0.633
Heel a (pos ps)	(deg):	0.00	0.00
Displacement vol	(m^3):	11 930.66	11 871.30
LCB fw AP	(m):	63.828	63.434
TCB ps CL	(m):	0.000	0.000
KB	(m):	2.902	2.891
Waterplane Area	(m^2):	2 798.067	2 807.91
LCF fw AP	(m):	59.479	58.960
TCF ps CL	(m):	0.000	0.000
KF	(m):	5.400	5.380
BM - transv	(m):	8.958	9.047
KN - transv	(m):	0.000	0.000
BM - longit	(m):	306.988	311.77
Wetted Surface	(m^2):	3 687.457	3 691.06
GZ	(m):	0.000	0.000
dGZ/da	(m/rad):	1.240	1.328

Table 2.1 Main hydrostatic data before flooding for intact and damaged condition.

2.2 Effect of water inflow on A-deck

Floating conditions as function of the amount of water on A-deck have been calculated for the ship with C-deck intact and with C-deck and above open to flooding respectively. The later condition simulates the final part of the capsize when water has been reported entering accommodation decks by windows and aft doors.

In all calculations, the water on A-deck is allowed to flow freely to static equilibrium within the defined deck volume. The final equilibrium floating condition of the ship and the water distribution on A deck is solved by iteration. The A-deck has been modelled with the non-symmetric centre casing assumed to be intact. The permeability of car deck is assumed to be 90%. The influence from the permeability on the floating condition is however found to be rather small.

Figures 2.2-2.3 show examples of static stability curves (GZ) for different amount of water on A-deck. Figure 2.4 shows the stability curve for the condition of free flooding of all decks above A-deck. The results are close to the results presented in ref [1]. Floating equilibrium conditions in terms of heel, initial stability, draught and trim for different amount of water on A-deck is presented in Figures 2.5 - 2.8.

There has not been any attempt to model the flooded condition in the later stage of the capsize. When water starts entering the C-deck (i.e. the passenger deck above car decks), the ship is predestined to sink. The stability curves show that if the decks above car deck would have been water tight, the ship would probably have continued to float with a heel angle less then 50° at least for a significant period of time.

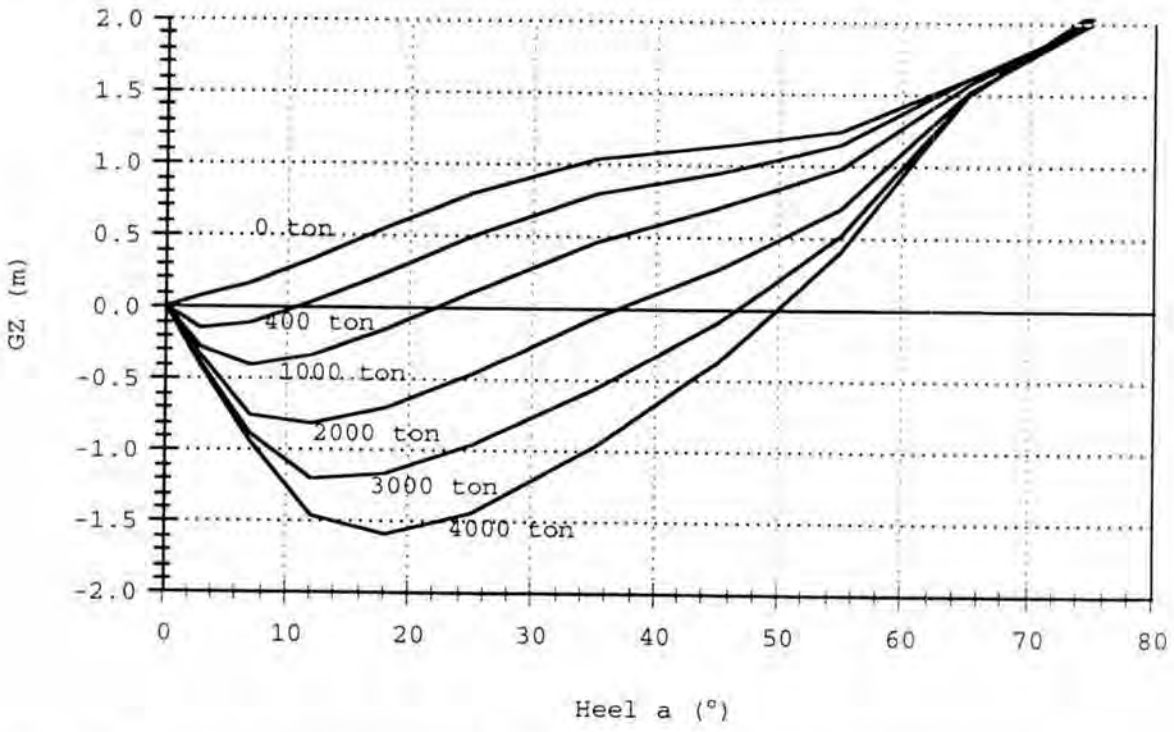

Figure 2.2 Static stability curves for different amount of water on A-deck. Volume permeability of A deck 0.90. C-deck and above intact.

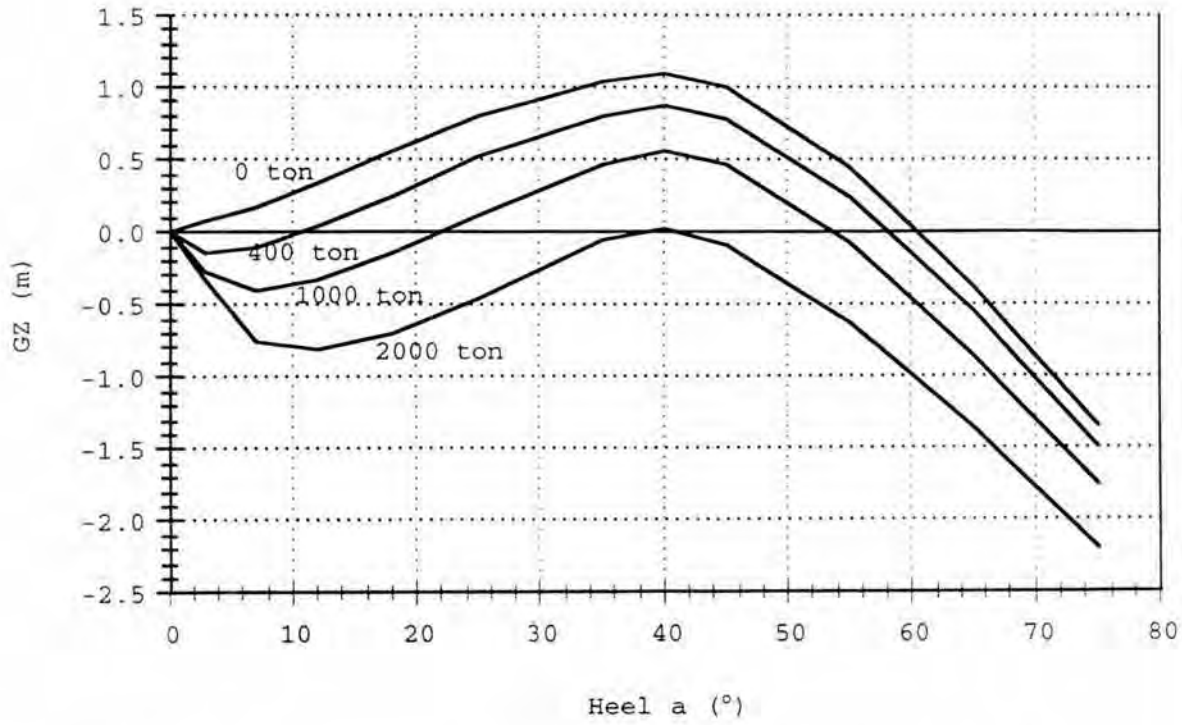

Figure 2.3 Static stability curves for different amount of water on A-deck.
Volume permeability of A deck 0.9.
C-deck and above open to free flooding (permeability 1.0).

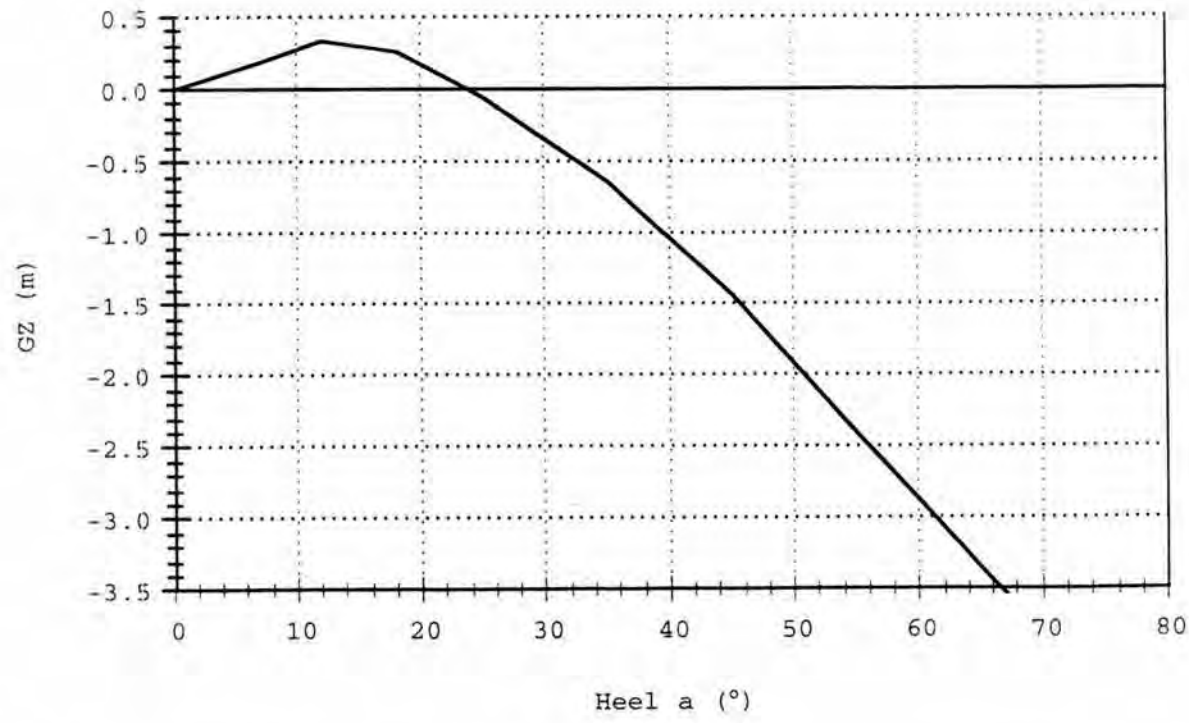

Figure 2.4 Static stability curves for A-deck and above open to free flooding.

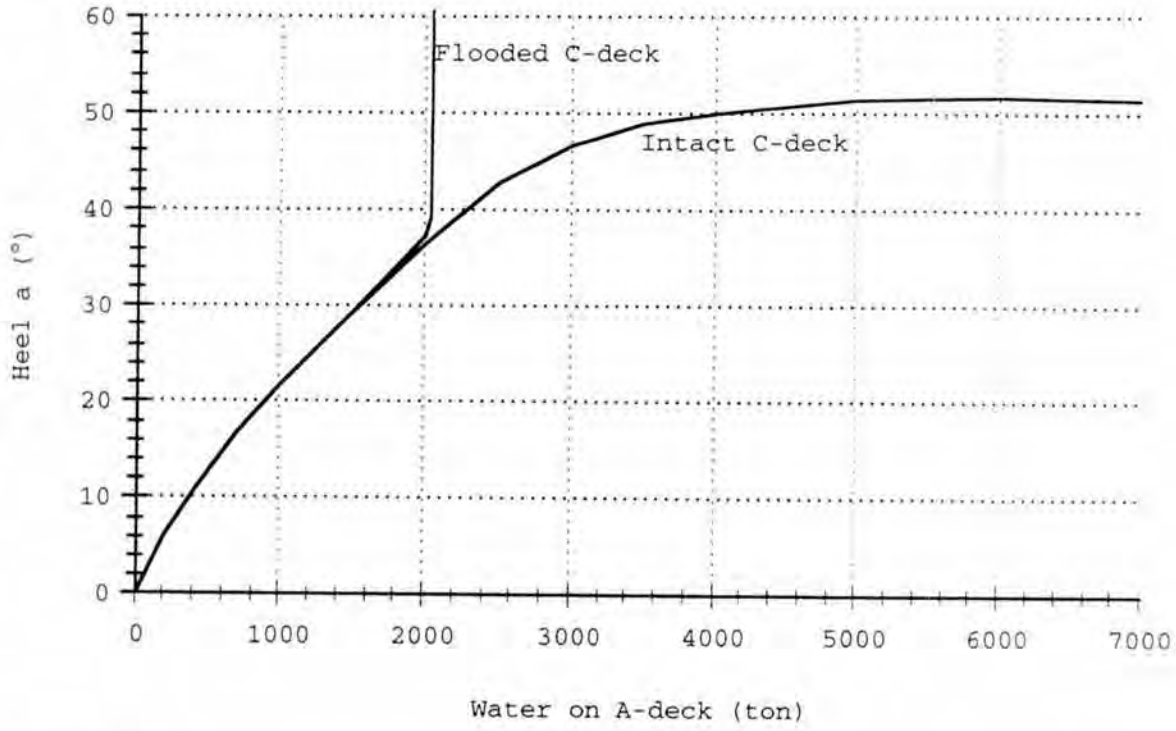

Figure 2.5 Heel angle at static equilibrium as function of water on A-deck

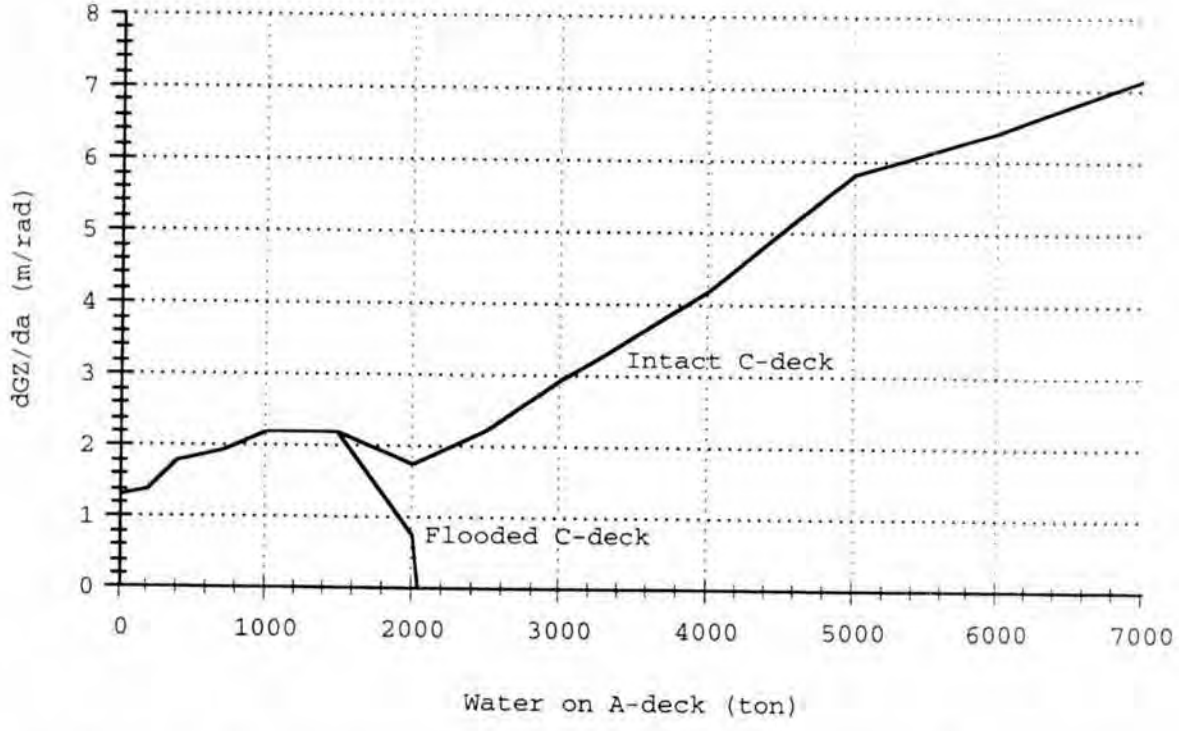

Figure 2.6 Stability derivate (initial stability) at heeled equilibrium condition as function of water on A-deck

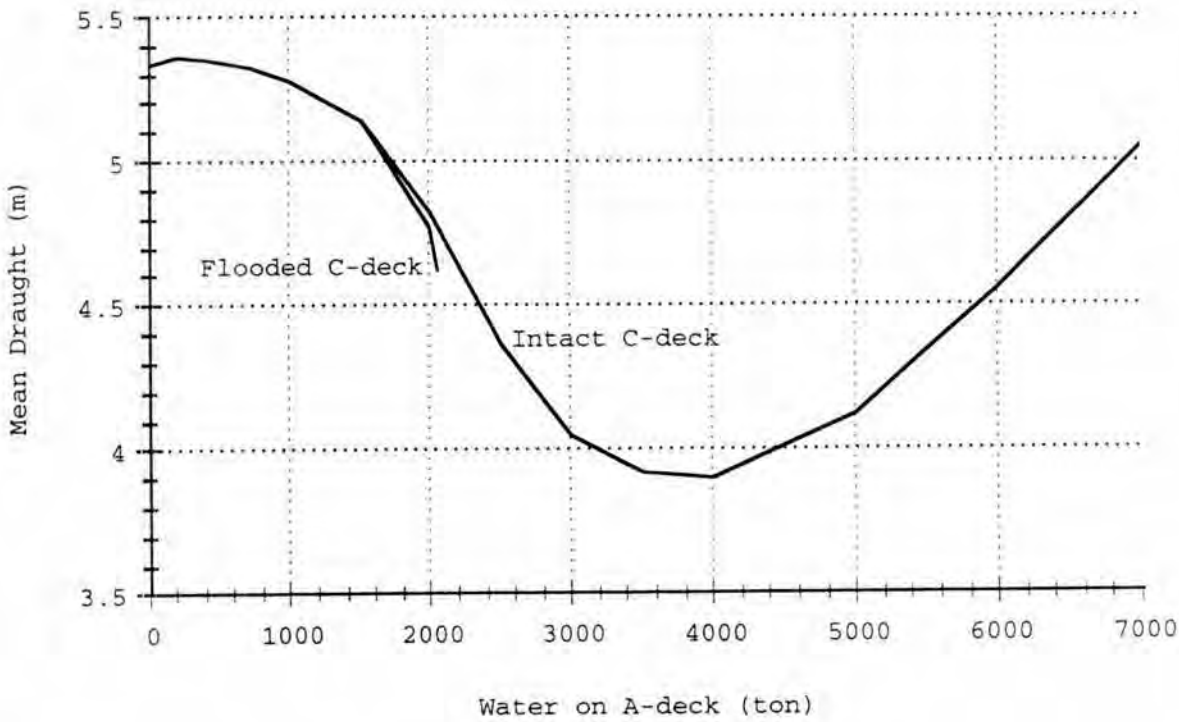

Figure 2.7 Mean draught (amidships at CL) at static equilibrium as function of water on A-deck

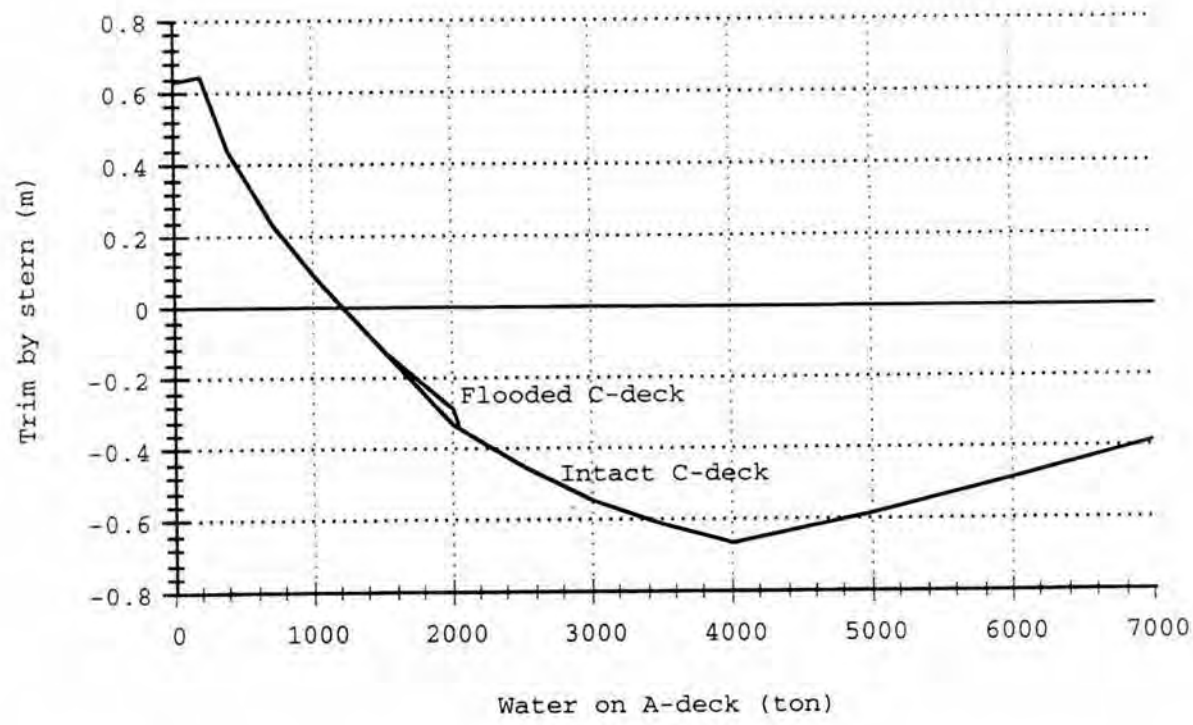

Figure 2.8 Trim by stern (at CL) at static equilibrium as function of water on A-deck

2.3 Influence of permeability and cargo shifting on A-deck

The filling rate or permeability of the cargo space will also have some effect on the stability characteristics during flooding. An assumed low permeability will result in lower heeling moments but at the same time in higher centre of gravity of the water. These two effects works contradictory, and the combined effect is very small. Figure 2.9 shows the effect of permeability on the static equilibrium heel angle. In all the previous figures, the permeability of car deck is assumed to be 0.9 and of the accommodation area 1.0.

It is very difficult to ascertain how shifting of vehicles and cargo on car deck developed during the water inflow. The weight of all vehicles have been estimated to about 1070 ton in total. The maximum transverse shift is of the order of one or a few meter. Every 1.1 m of cargo shift would have the effect of 0.1 m shift of the ships total centre of gravity. The resulting effect on the static stability curves is illustrated in Figures 2.10 and 2.11 for intact C-deck and open C-deck respectively.

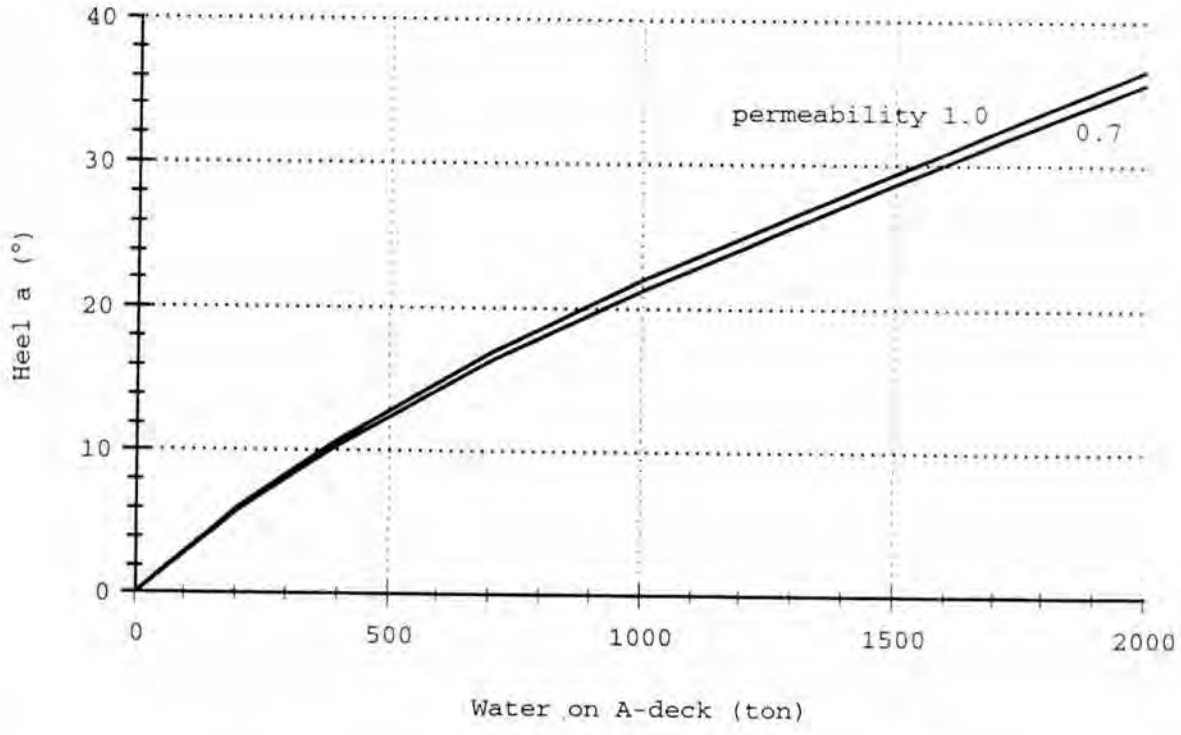

Figure 2.9 Heel angle at static equilibrium as function of water on A-deck. Effect of different assumptions of volume permeability

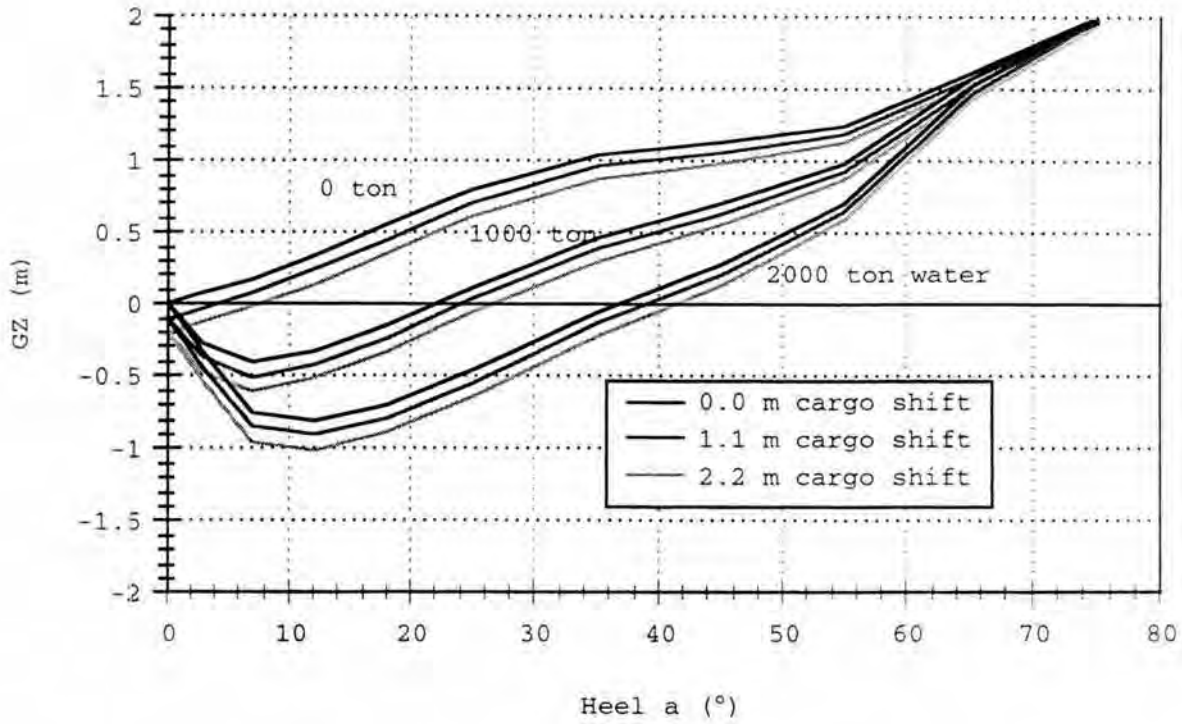

Figure 2.10 Effect of cargo shifting on static stability curves. C-deck and above intact.

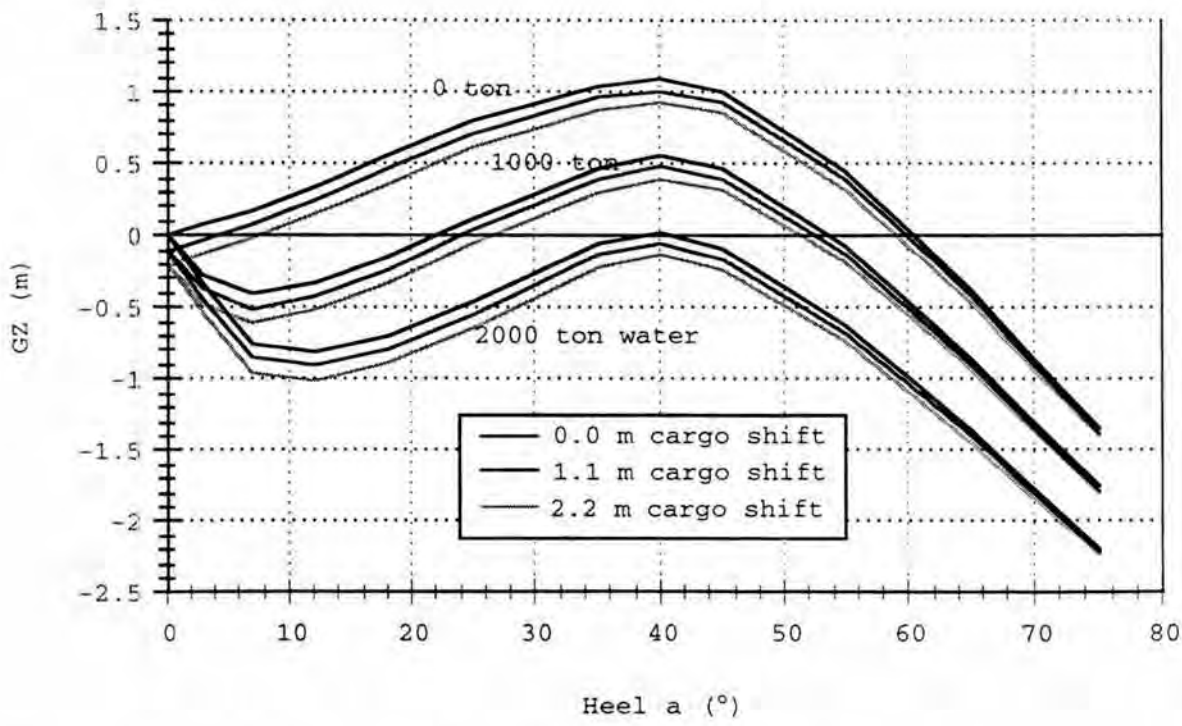

Figure 2.11 Effect of cargo shifting on static stability curves.
C-deck and above open to free flooding.

3 Relative motions at the bow

The statistical distribution of relative vertical motions between the ship bow and waves has been calculated with linear strip theory (Salvesen et al 1979). The sectional geometries were represented by 3-parameter Lewis transformations. For ordinary ship hull forms in upright/symmetric condition, this is a well established method that has been shown to give accurate results.

In an attempt to study the influence of water ingress on the relative motions, the same method has here also been used for heeled conditions. The transformation is in this case based on the heeled waterline breadth, the sectional area and the maximum draught measured perpendicular to the undisturbed waterline at each section. The non-symmetric geometry of the heeled sections is not taken into account, neither is the influence of the dynamics of the water entered into the ship. The results must therefore bee seen as rough estimates, but are believed to be reasonable accurate for the purpose of this study.

All calculations were performed with a general Naval Architecture program system 'MacSkepps' developed at KTH.

Figures 3.1-3.3 show the transformed geometry of the intact ship, and of the ship in equilibrium heeled condition with 1000 ton and 2000 ton water on A-deck respectively.

All calculations have been made for irregular seas using the JONSWAP wave spectrum with a peak magnifying factor of 3.3 to represent the frequency distribution.

Examples of calculated relative motion at the bow of the intact ship as function of speed and spectrum peak period, Tp, is shown in Figure 3.4. The results are very close to the results obtained from calculations with the linear strip theory according to Raff presented in reference [2], Fig. A.7, Fig. A.13.

A comparison of the response in long-crested and short-crested sea is shown in Figure 3.5. For the purpose of water inflow simulations as described in the next section, the motion response in short-crested waves have been used. The directional spreading is modelled with a $\cos^4$ -spreading function which is rather narrow and gives results in between the more broader $\cos^2$ - spreading function and long-crested waves.

Examples of calculated relative vertical motions at the bow for different speed, wave heading and amount of water on A-deck is given in Figures 3.6-3.9.

The influence of speed is not very significant. The flooded and heeled conditions in bow and head sea result in a reduction of the relative motions. The lowest relative motions appear in beam seas where the motion amplitudes approaches the wave amplitudes, i.e. the ratio rs/Hs is close to 0.5. Here rs is significant single amplitude relative vertical motion and Hs is significant wave height (double amplitude).

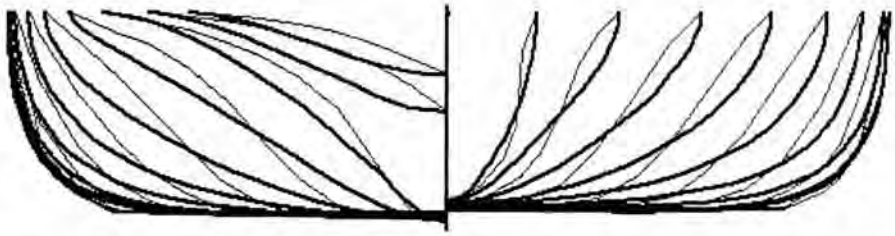

Figure 3.1 Comparison between transformed geometry and actual hull geometry, intact condition. (Bold lines show transformed geometry)

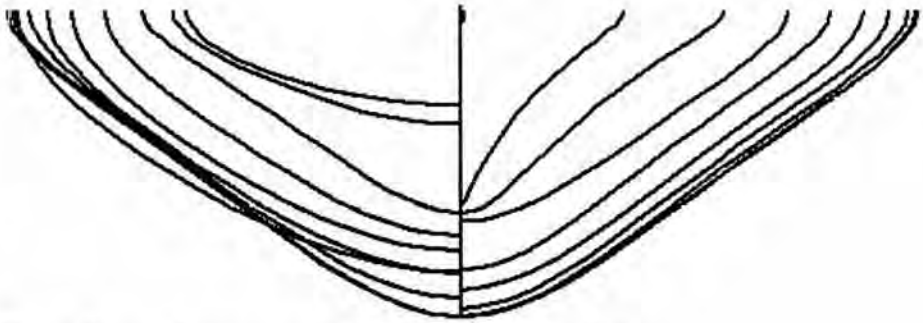

Figure 3.2 Transformed geometry for flooded condition
1000 ton water on A-deck, 22° heel

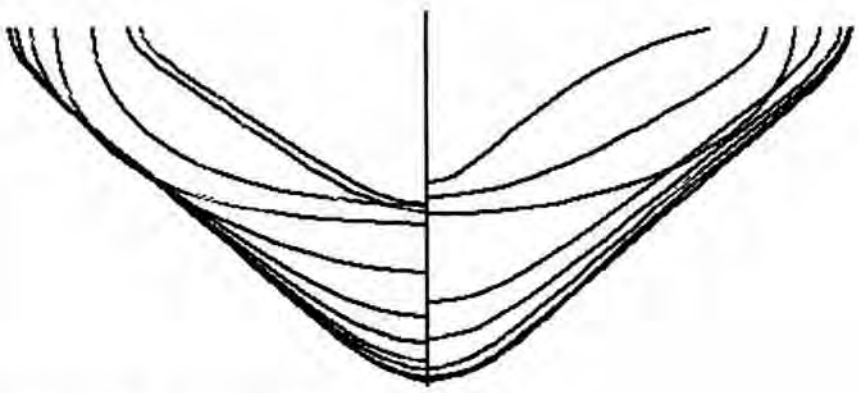

Figure 3.3 Transformed geometry for flooded condition
2000 ton water on A-deck, 37° heel

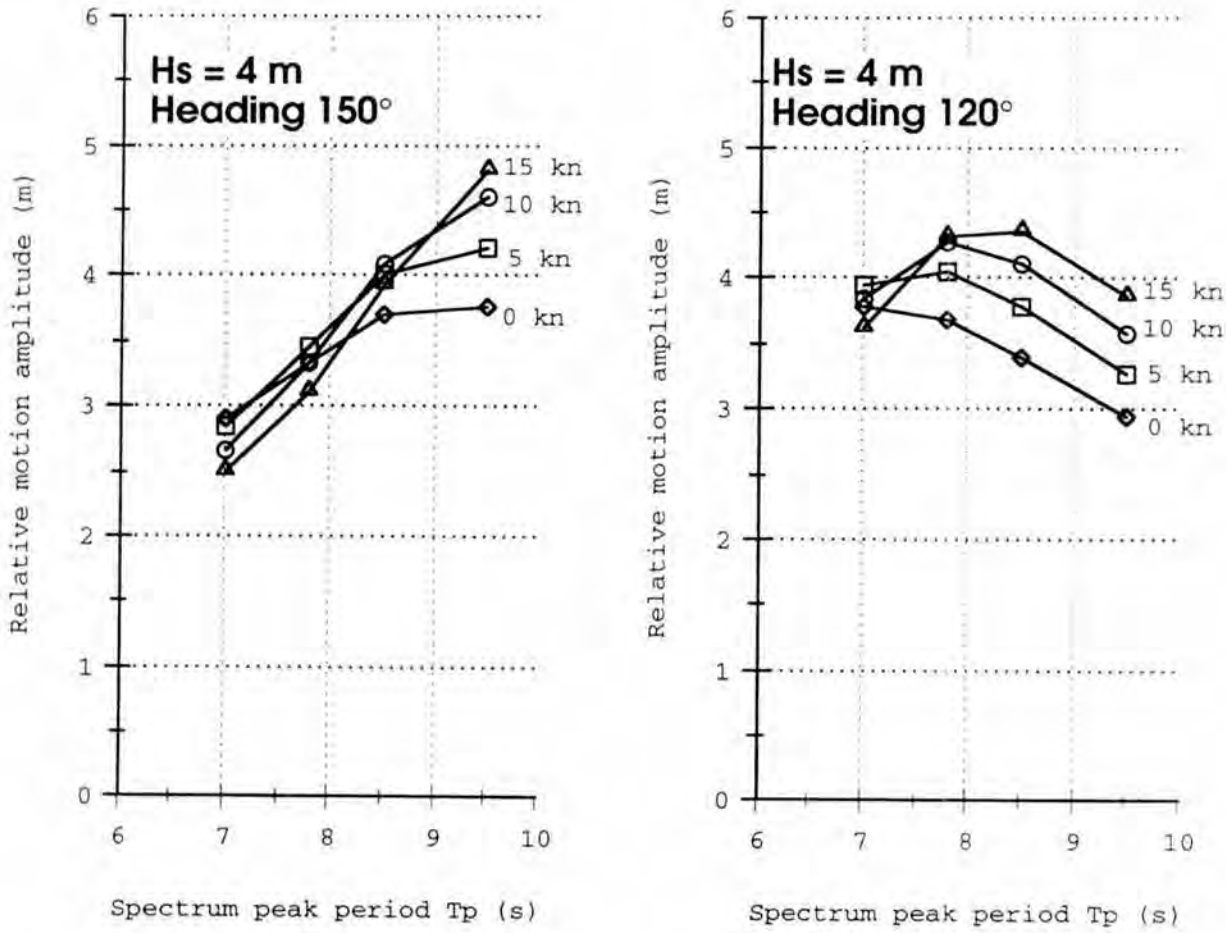

Figure 3.4 Relative vertical motion at bow in bow seas, long-crested waves

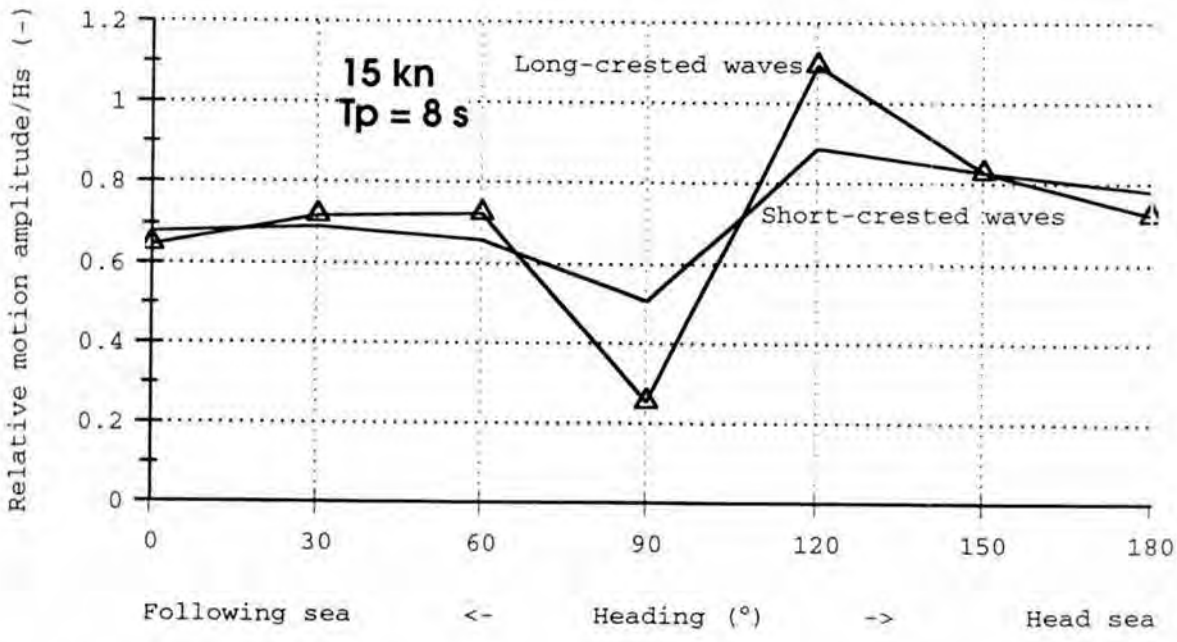

Figure 3.5 Comparison between long-crested and short-crested wave representation

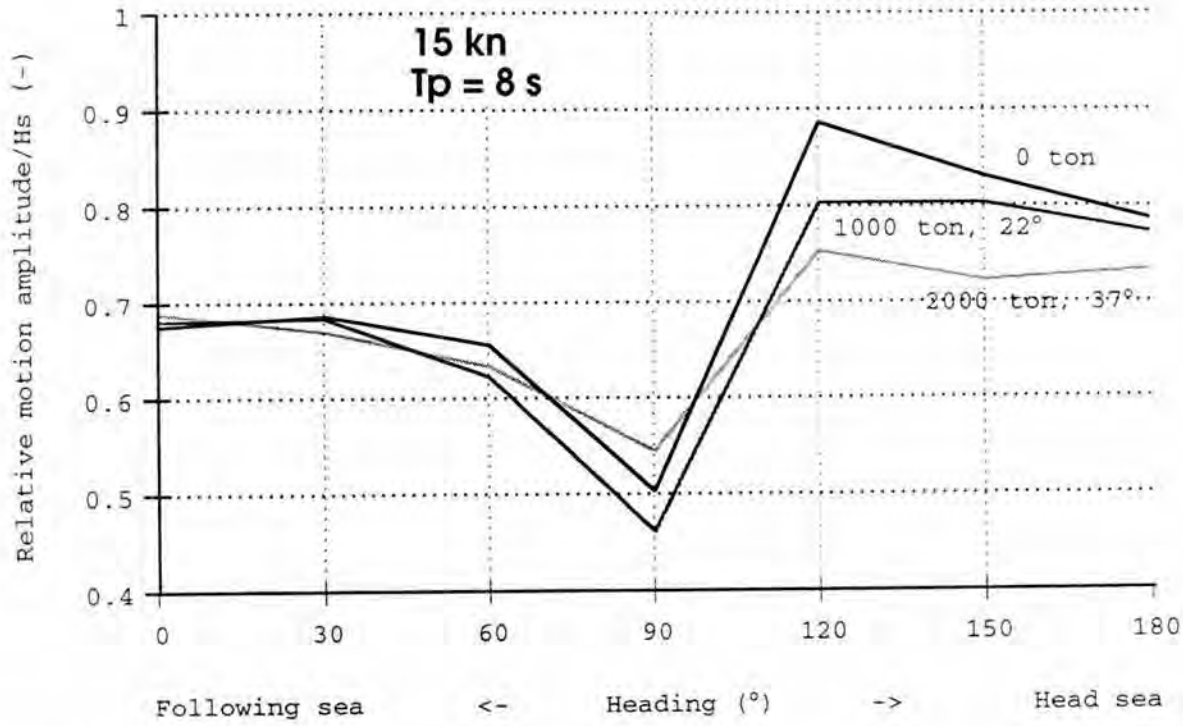

Figure 3.6 Non-dimensional relative vertical motion at bow as function of heading and amount of water on A-deck. 15 knots, Tp 8.0 s, short-crested waves.

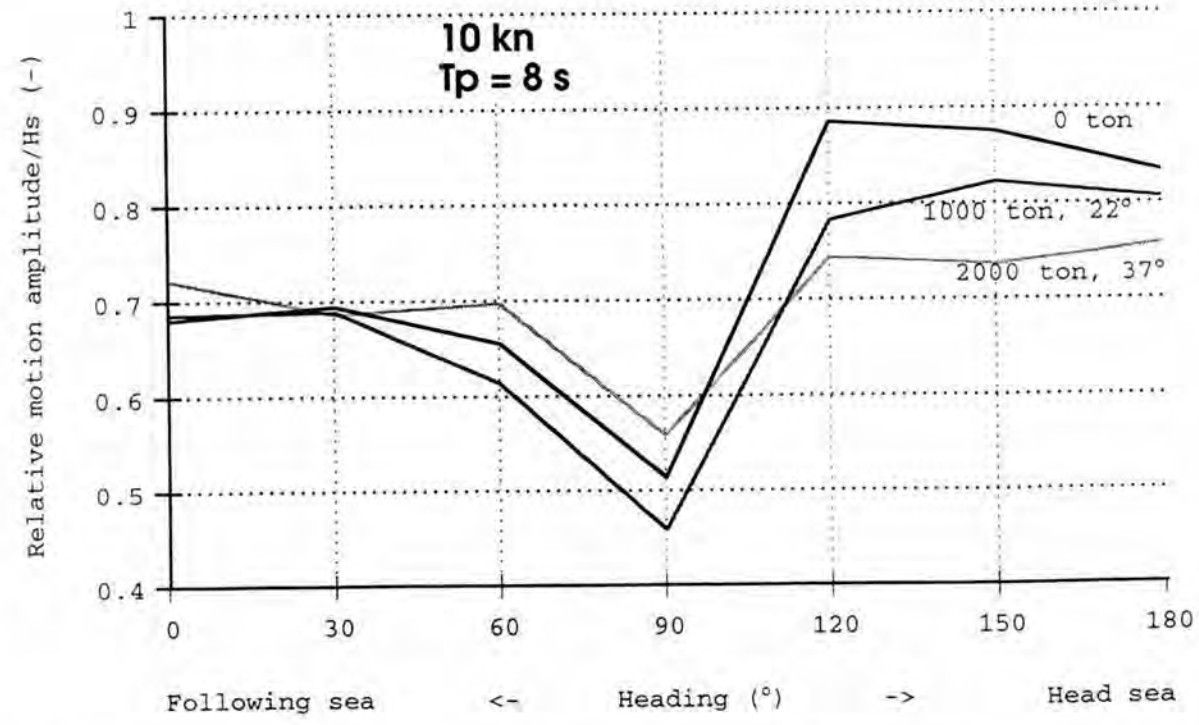

Figure 3.7 Non-dimensional relative vertical motion at bow as function of heading and amount of water on A-deck. 10 knots, Tp 8.0 s, short-crested waves.

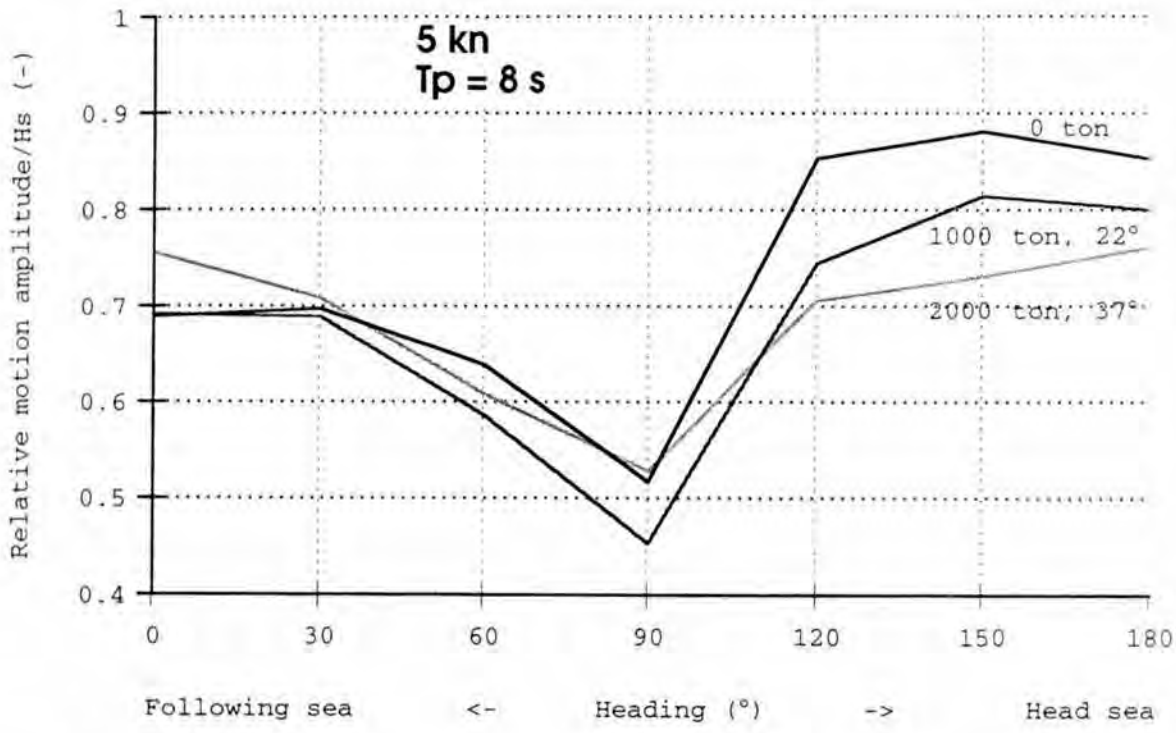

Figure 3.8 Non-dimensional relative vertical motion at bow as function of heading and amount of water on A-deck. 5 knots, Tp 8.0 s, short-crested waves.

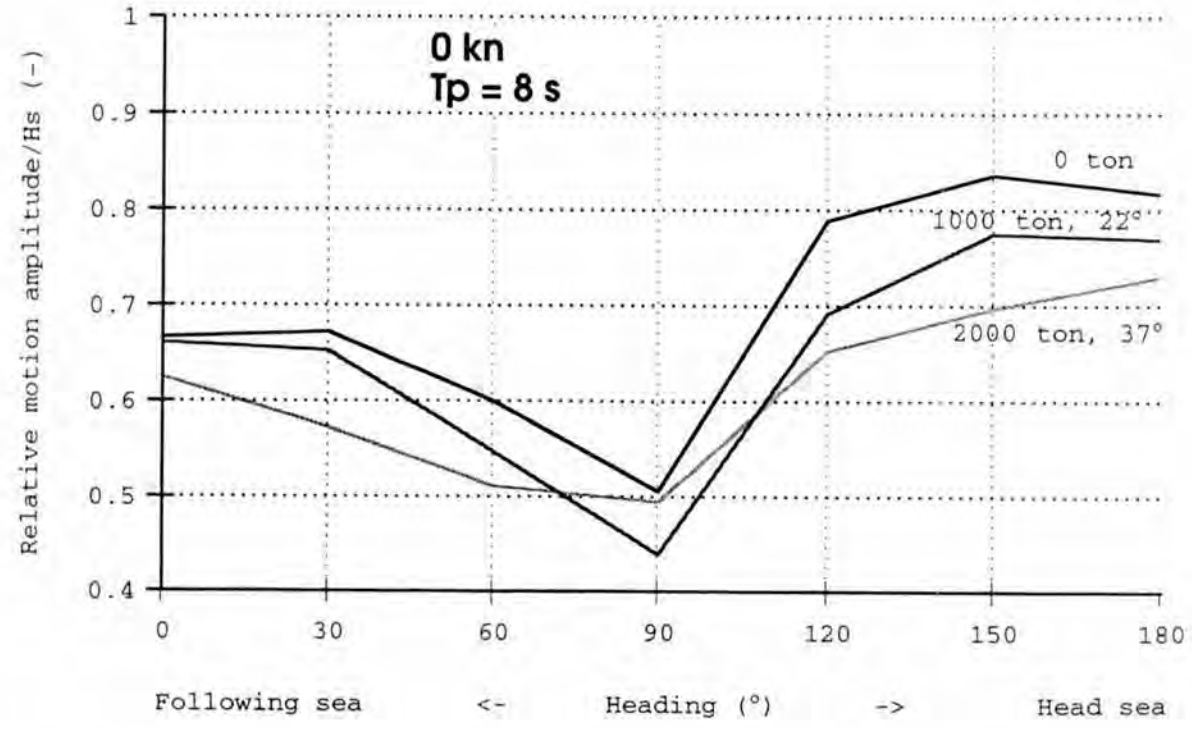

Figure 3.9 Non-dimensional relative vertical motion at bow as function of heading and amount of water on A-deck. 0 knots, Tp 8.0 s, short-crested waves.

4 Simulation of water inflow

The water inflow through the ramp opening when the visor was lost and the ramp torn open, has been estimated from the frequency distribution of the relative motion. The simulation was made on the basis of the previous described calculations of static equilibrium floating conditions and significant relative motions.

The results obtained from the simulations are very sensitive to small changes in the initial parameters and the inherent uncertainty in the random nature of waves and ship motions during short periods of time is very large. Therefore, this simulation (or any other) cannot be used to independently prove a certain time sequence. On the contrary, one important input to the simulation was actually a presumed time sequence. So the purpose of the simulation is mainly to verify whether an assumed capsizing scenario is likely to have happened or not.

4.1 Methods and assumptions

The general equation describing the water inflow in this simulation is formulated as:

$$Q_W(W,V_s,\beta,rs) = \int_{F(W)}^{\infty} \int_{F(W)}^{H(W)} V_W(z,r,W,V_s,\beta) \cdot b(z,W) \cdot f_r(r,rs)\, dzdr$$

with the following definitions:

$Q_W(W,V_s,\beta,rs)$	Mean volume of water inflow per second, (m^3/s)
W	Amount of accumulated water on A-deck, (ton) (Decisive for the heel and the draught at the bow)
V_S	Ship speed (m/s)
β	Ships heading relative to the waves, (°), (180° for head waves)
rs	Significant relative vertical motion at the bow opening, (m) (rs is a function of both the sea condition and the ship condition)
$F(W)$	Distance from the mean water level to the lowest corner of the ramp opening, (m)
$H(W)$	Height of the ramp opening measured perpendicular from the mean water surface, (m)
$V_W(z,r,W,V_s,\beta)$	Velocity of water inflow, (m/s)

z	Vertical ship coordinate defined from the still water line, (m)
r	Relative motion between wave surface and ship bow, (m) defined from the still water line
b(z,W)	Breadth of ramp opening at position z, (m)
$f_r(r,rs)$	Frequency distribution of relative motion, (1/m)

Definitions of z, F(W), H(W) and b(z,W) is shown in Figure 4.1.

The inflow velocity at a certain position z is approximated with the following expression:

when $r \geq z$

$$V_W(z,r,W,V_s,\beta) = C \cdot \sqrt{V_{rel}^2 + 2g(r-z)}$$

else

$$V_W(z,r,W,V_s,\beta) = 0$$

where

C	Inflow coefficient, taken as 1.0 in the presented results, (-)
V_{rel}	Relative velocity between water particles and ship, (m/s) $V_{rel} = V_s - V_{we} \cdot \cos(\beta)$
V_{we}	Horizontal velocity of the water particles, (m/s) (in the presented simulations, V_{we} is taken as a constant, 1.6 m/s representing an approximate average horizontal velocity).
g	acceleration of gravity, 9.8 m/s^2

The inflow coefficient C is difficult to estimate. In general it should be less then 1.0, but the open ramp may also have the effect of increasing the inflow rate. However, the presented results can be linearly scaled to any other estimated coefficient

Finally the frequency distribution of relative vertical motion is given by the Gauss- or Normal-distribution, here expressed as function of the significant relative motion rs equal to 2.0 times the standard deviation of the relative motion.

$$f_r(r,rs) = \frac{1}{(\frac{rs}{2})\sqrt{2\pi}} e^{-2\frac{r^2}{rs^2}}$$

The significant relative motion, rs, is a function of the ships speed, heading and amount of water, as well as of the mean wave period and the significant wave height

Since only the ramp opening was modelled, the water inflow simulation was stopped at the level when water started entering the C-deck. The final sequence of water ingress is deemed to be impossible to simulate with any accuracy.

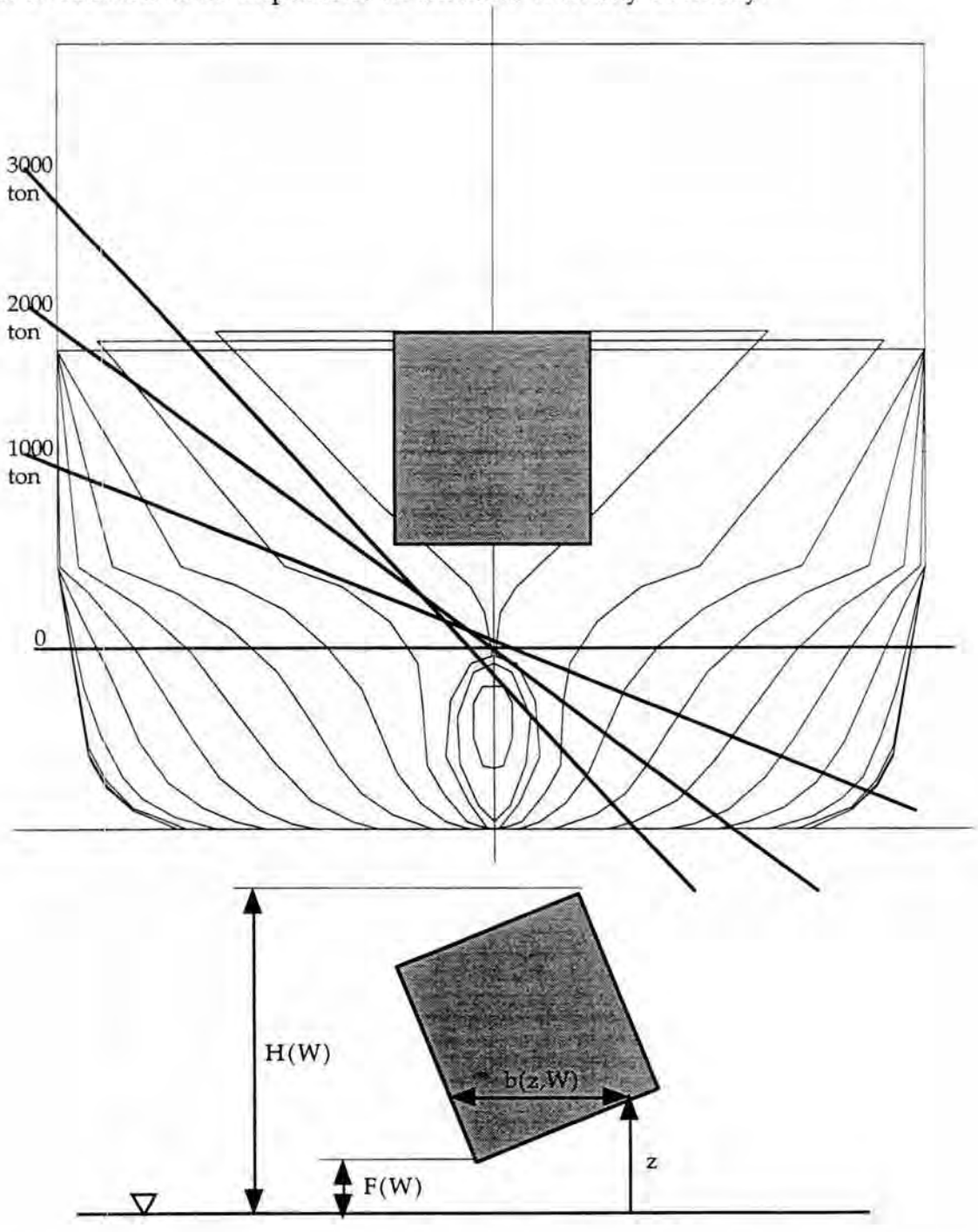

Figure 4.1 Examples of equilibrium water level for different amount of water on A-deck.Below is shown definition of geometry variables used in the general equation for calculation of water inflow.

4.2 Mean water inflow, example results

Calculated mean water inflow is given in Figures 4.2 - 4.8 as function of heading, speed and water on deck A. The three most important factors for the inflow is in decreasing order: the 'freeboard' distance F(W) from water level up to the opening, the significant relative vertical motion between ship and waves, rs, and the speed of the ship, V_s. They are however difficult to separate since the relative motion varies with the ship speed, and also the distance F(W) is affected by speed through the bow wave generated by the ship. The presented results include a bow wave correction on the mean water level estimated from the SHIPFLOW-calculations of the ESTONIA as given in Fig.3.7 of ref.[3]. Similar to the assumptions made in [4] this correction is taken as 1.0 m at 15 knots, 0.4 m at 10 knots and 0.2 m at 5 knots

In order to show more clearly and explicit the influence of different conditional parameters, Table 4.1 below has been prepared. However, it must be stressed that it is only a theoretical illustration. In the physical reality, all these parameters are coupled and will change in a much more complex way. For instance, at a constant displacement, an increased angle of heel will result in a decreased freeboard to the ramp opening. In the heel angle variation below, the F(W) has been kept constant and the inflow variation is only an effect of the rectangular geometry of the ramp opening.

Variation in speed (excl effect on bow wave and rs)

Vs (knots)	0	5	10	15	20
Qw (ton/min)	72	105	148	194	242

Variation in heading (excl effect on rs)

β (°)	60	90	120	150	180
Qw (ton/min)	112	125	138	148	151

Variation in 'freeboard'

F(W) (m)	1.5	2.0	2.5	3.0	3.5
Qw (ton/min)	475	273	148	75	36

Variation in heel angle (excl effect on freeboard and rs)

α (°)	0	10	20	30	40
Qw (ton/min)	148	84	55	42	38

Variation in relative vertical motion

rs (m)	2.5	3.0	3.5	4.0	4.5
Qw (ton/min)	25	71	148	254	387

Variation in water on C-deck,
(freeboard and heel variation included, rs constant)

W (ton)	0	200	400	700	1000
Qw (ton/min)	148	155	201	256	324

Table 4.1 Separate effect of different parameters on the calculated water inflow
The basic condition is: V_s = 10 knots, β = 150°, F(W) = 2.5 m, heel = 0°, rs = 3.5 m, W = 0 ton

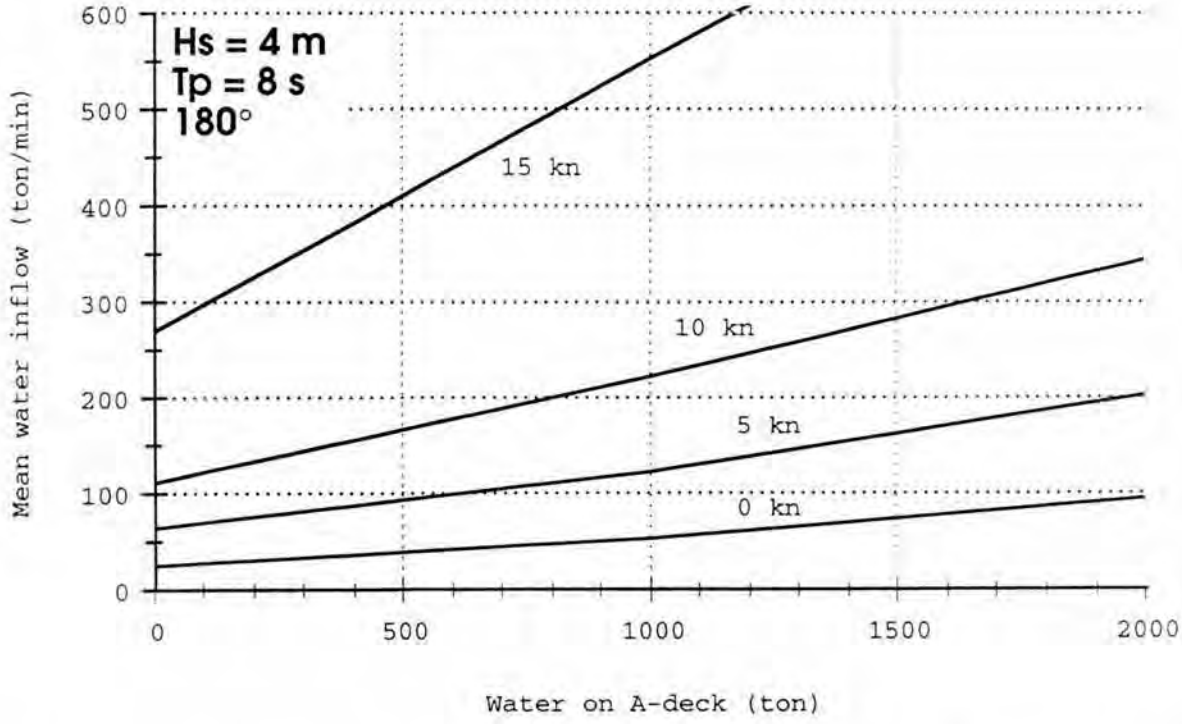

Figure 4.2 Mean water inflow as function of speed and amount of water on A-deck. Head sea 180°

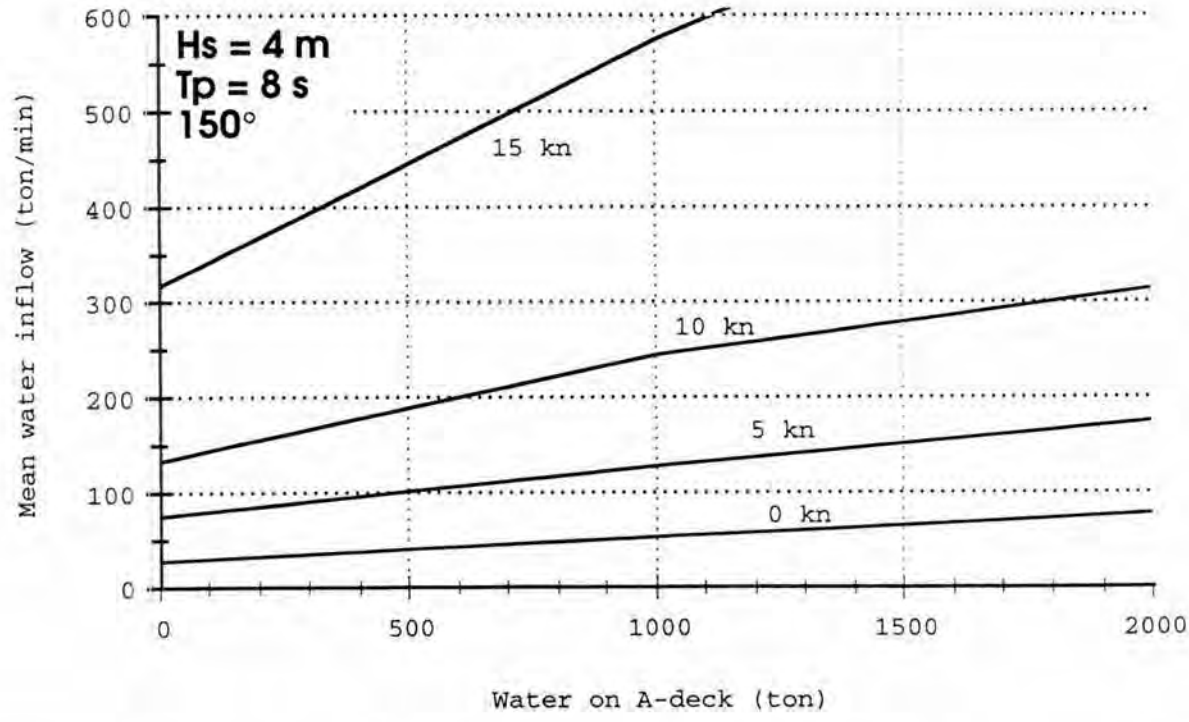

Figure 4.3 Mean water inflow as function of speed and amount of water on A-deck. Bow sea 150°

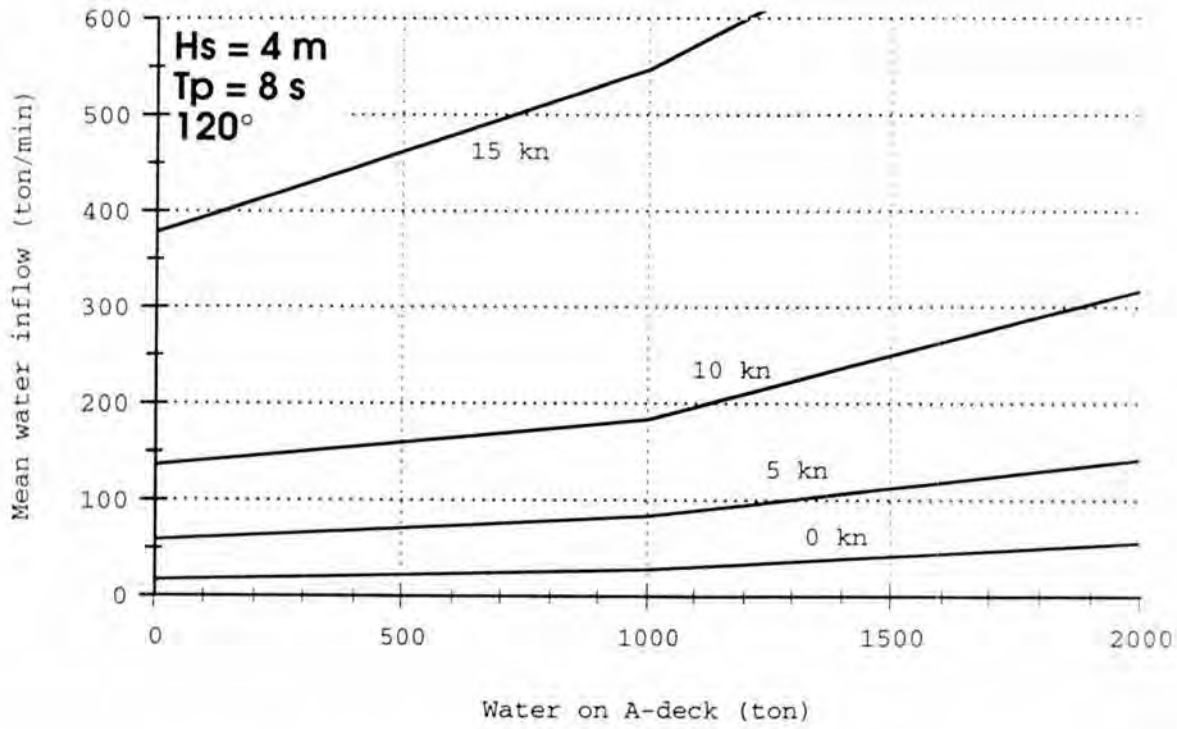

Figure 4.4 Mean water inflow as function of speed and amount of water on A-deck. Bow sea 120°

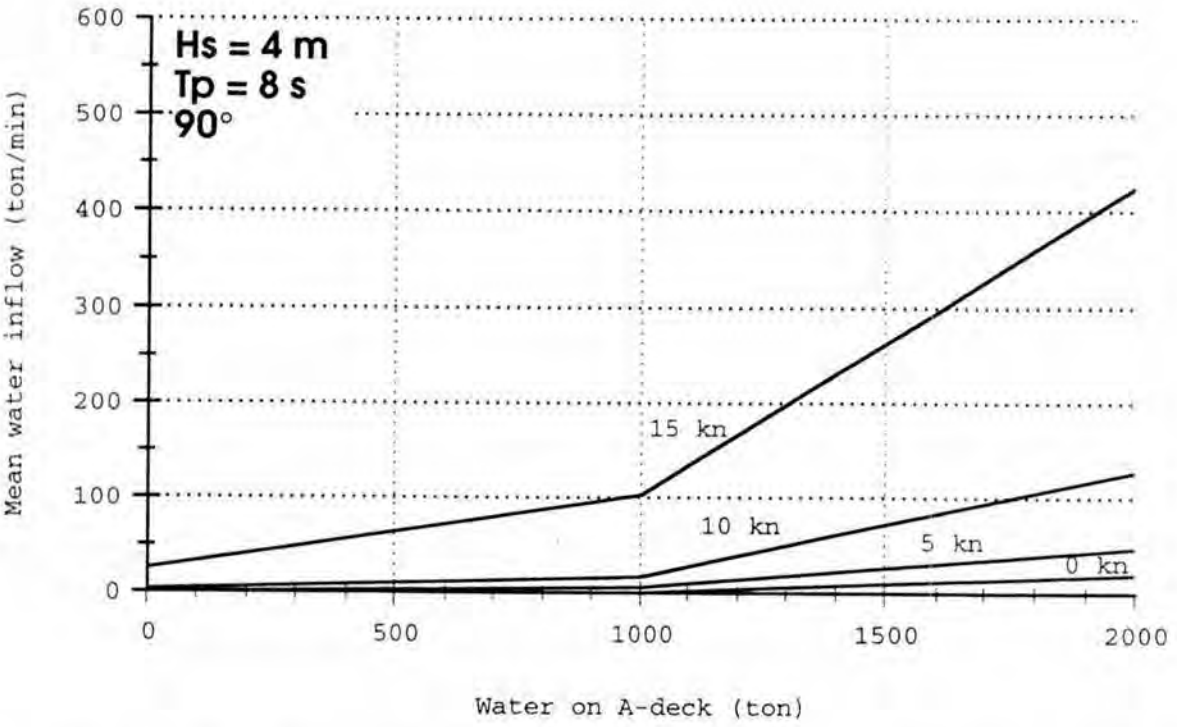

Figure 4.5 Mean water inflow as function of speed and amount of water on A-deck. Beam sea 90°

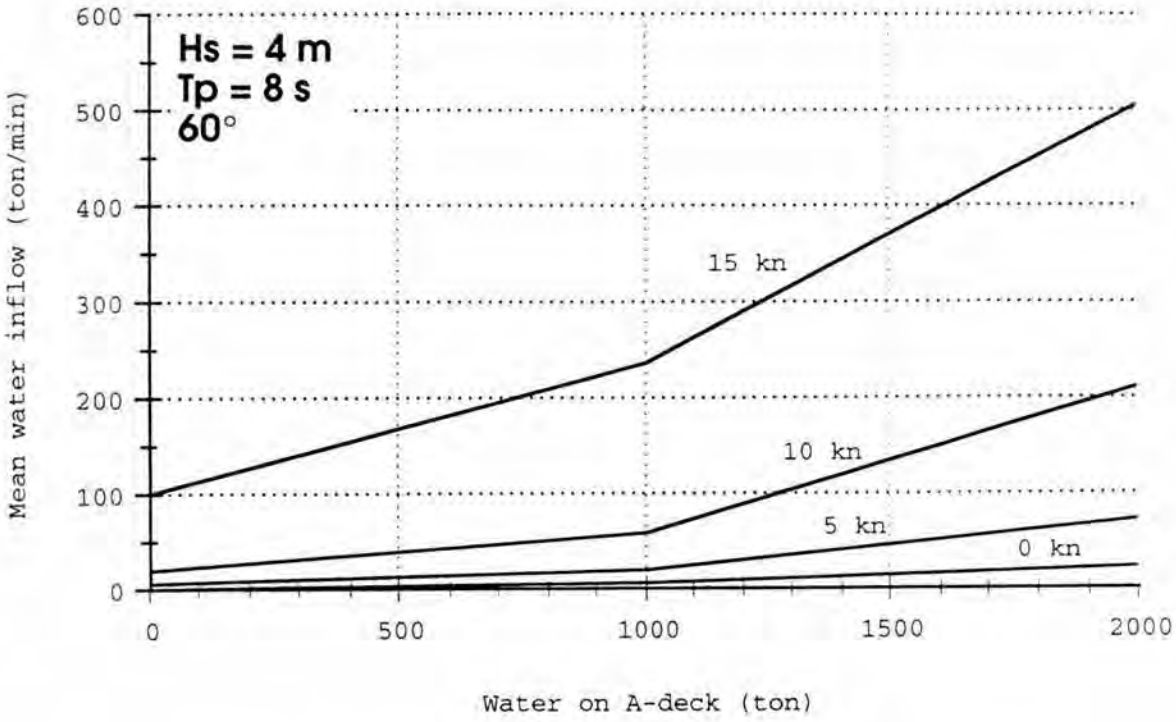

Figure 4.6 Mean water inflow as function of speed and amount of water on A-deck. Quarter sea 60°

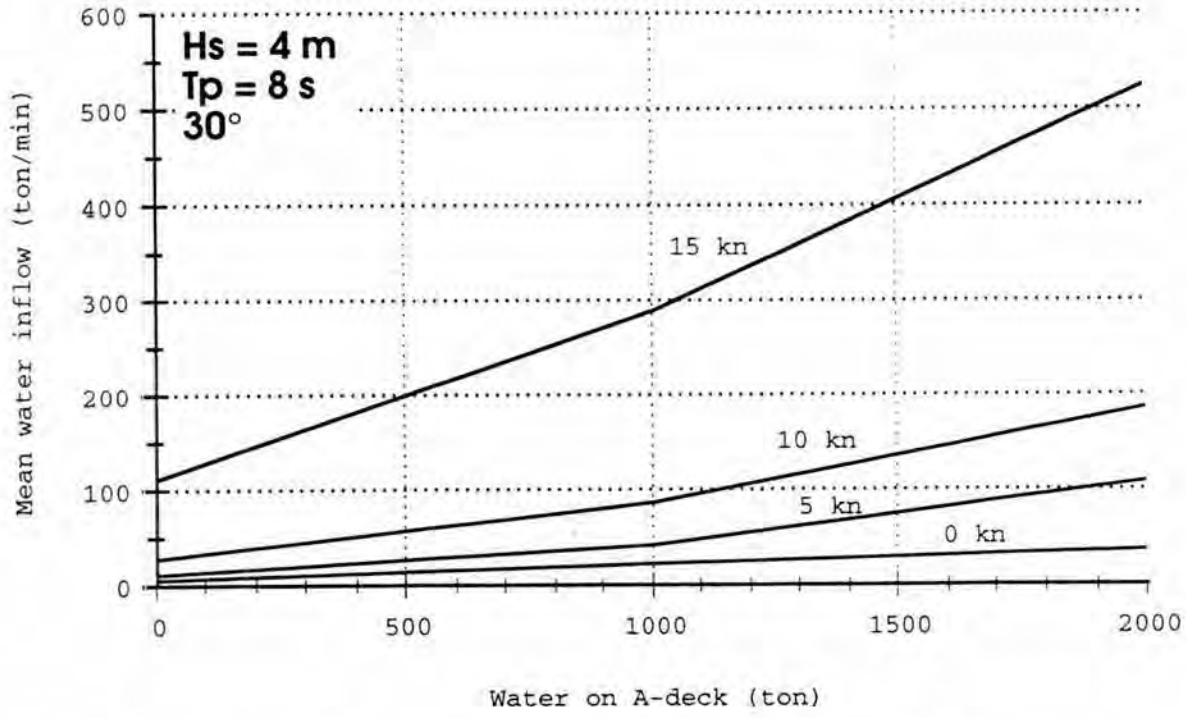

Figure 4.7 Mean water inflow as function of speed and amount of water on A-deck. Quarter sea 30°

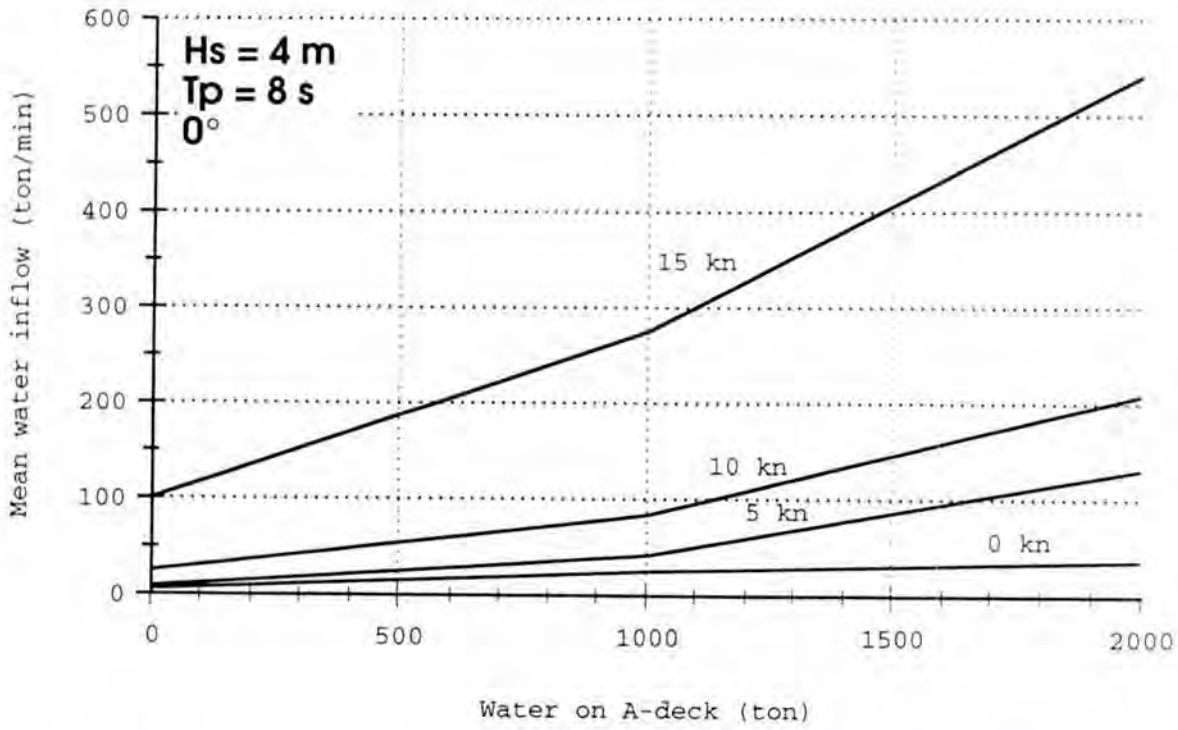

Figure 4.8 Mean water inflow as function of speed and amount of water on A-deck. Following sea 0°

4.3 Time sequence of water inflow

The amount of water on A-deck as function of time is obtained by integration. In principle the governing equation can be expressed as:

$$W(t) = \int_0^t Q_W(W(t), V_s(t), \beta(t), rs(t))\, dt$$

Since W(t) is recursive in the expression, it has been solved with iterations in which the conditional parameters are adjusted to fit the time sequence results. The solution is therefore linked to an assumed general sequence of events with regard to the speed and heading of the ship. As a consequence there exist an infinite number of different possible solutions. In this report, only a few examples are given.

Example 1 A time sequence according to track simulations at Kalmar 1995

The first example is coupled to an early manoeuvring simulations of the ESTONIA during the last hour. This simulation was carried out at Kalmar Maritime Academy in order to find a possible track that could fit with the different positions of the bow visor and the wreck at the seabed. The simulation included the general manoeuvring characteristics of the ship and the effect of current and wind, but not directly the effect of heeling and wave motions. However, in an attempt to get as realistic conditions as possible, the projected area of the superstructure was continuously adjusted to account for the effect of heel on the wind drifting force.

The ship heading before the visor was lost was assumed to be 290° and the wave direction was assumed to be 245° which equals an initial relative heading to the waves of 135°.

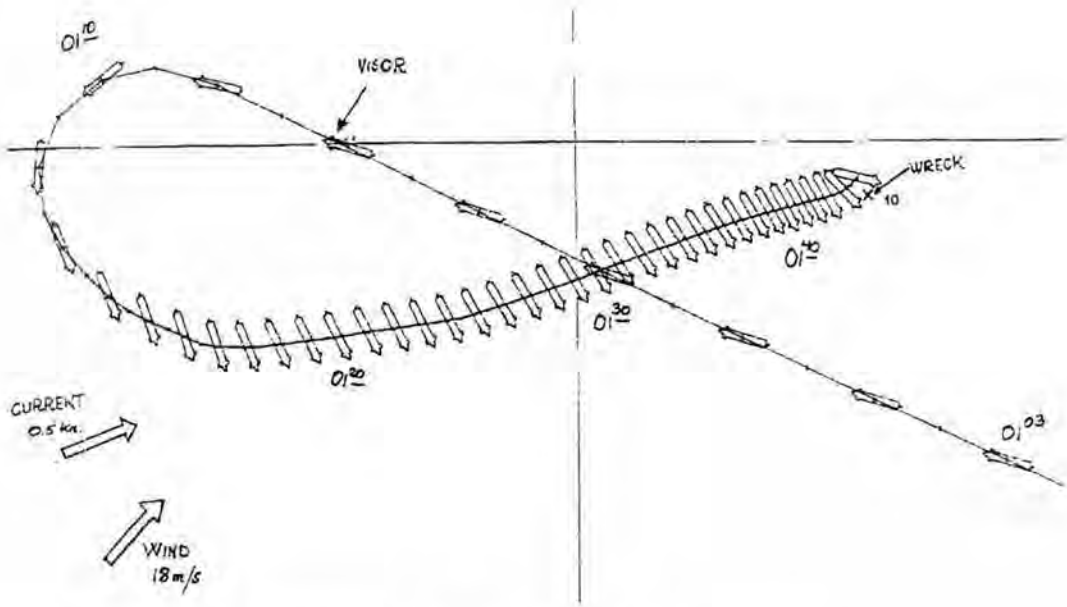

Figure 4.9 Plot of simulated track of the ESTONIA, Example 1.

Table 4.2 shows the different conditions used as base for the inflow simulation. The time, speed and heading fits approximately the sequence shown in Figure 4.9.

The result in terms of mean water inflow rate, accumulated water on A-deck and time is shown in Figures 4.10-4.11. According to this simulation it would have taken about a quarter of an hour from the first water ingress until larger amount of water started to enter the decks above car deck.

Time t (min)	Water W (ton)	Heel α (°)	Ship speed Vs (knots)	Rel Heading β (°)	Rel motion rs (m)	Sign Wave H Hs (m)	Wave period Tp (s)
0.0	0	0	14.5	135	3.5	4.1	8.0
0.6	200	6	14.5	135	3.5	4.1	8.0
1.4	400	11	11.5	150	3.5	4.1	8.0
2.7	700	17	9.0	-150	3.4	4.1	8.0
5.6	1000	22	3.0	-115	3.0	4.1	8.0
16.0	1500	29	0.0	-115	2.7	4.2	8.0
26.0	2000	37	0.0	-115	2.6	4.2	8.0

Table 4.2 Sequence of conditions in simulation example 1

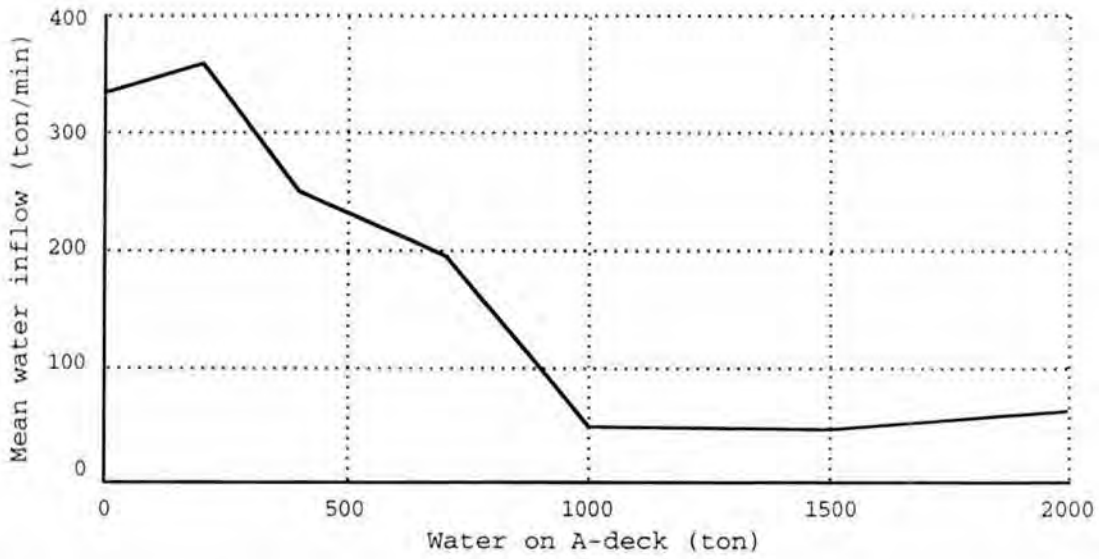

Figure 4.10 Mean water inflow per minute in simulation example 1.

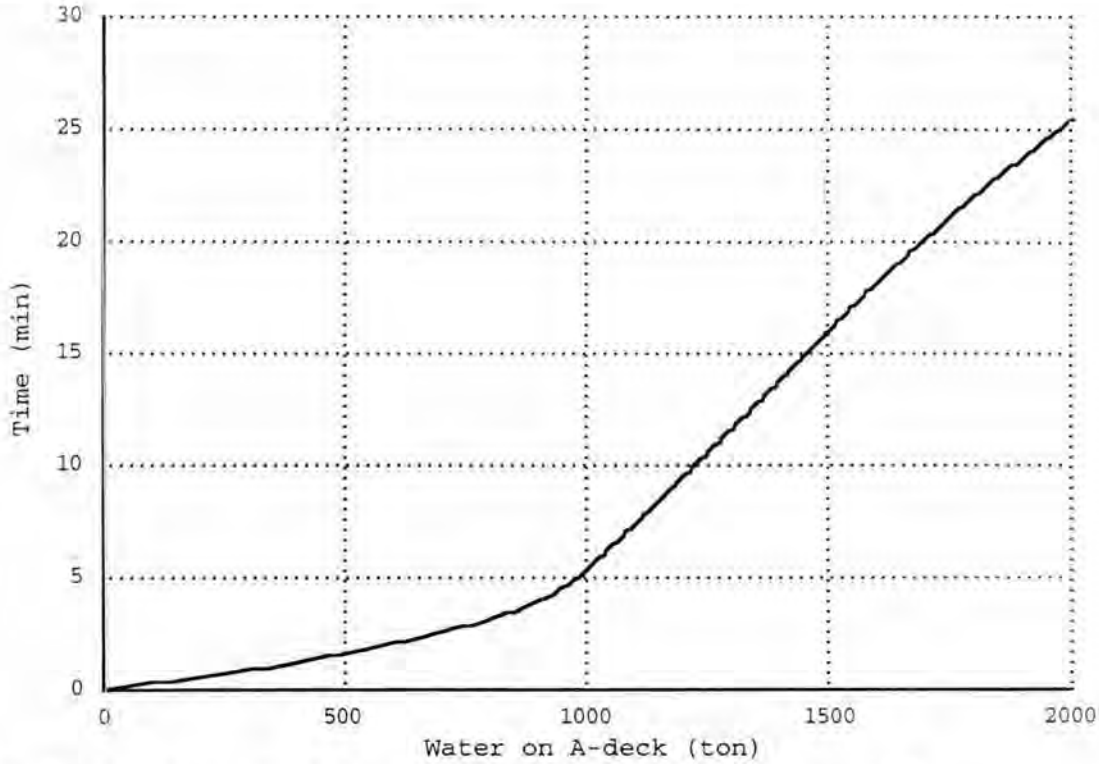

Figure 4.11 Time sequence of water inflow in simulation example 1.

Example 2 A time sequence according to track simulations at Kalmar 1996

This example is related to a later manoeuvring simulations of the track of ESTONIA. In this simulation the ship is assumed to have continued its course for about a minute after the ramp was opened. The speed was then reduced and a hard port turn was initiated. To fit the positions of the wreck and the visor on the seabed, the ship must have been running at low speed a few minutes on contra-course before the engines tripped and the ship started to drift with the sea on starboard beam. The simulated track is shown in Figure 4.12 and the assumed conditions in Table 4.3. The rate of inflow, and the accumulated water on deck is shown in Figures 4.13-4.14.

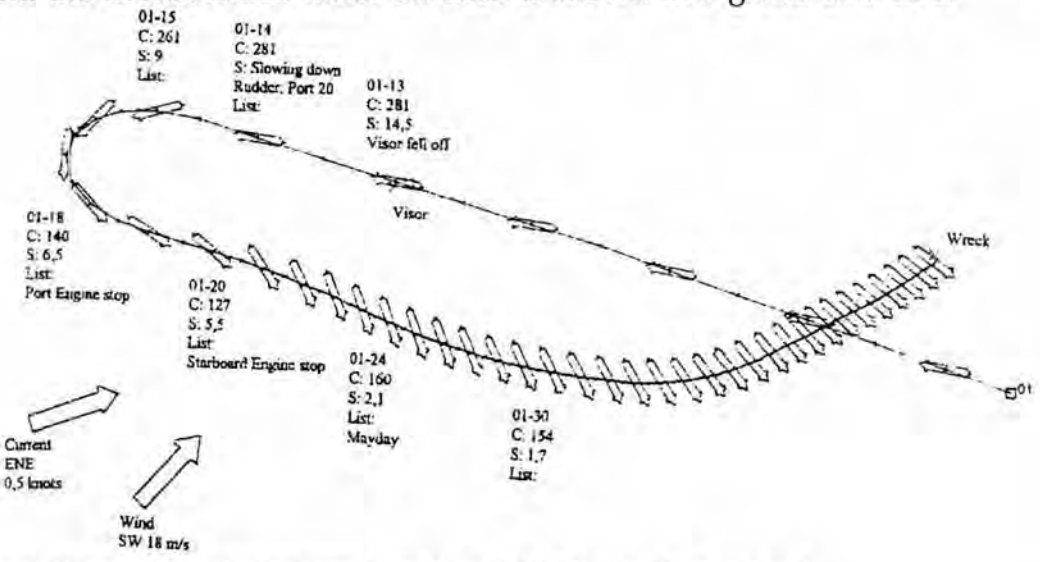

Figure 4.12 Plot of simulated track of the ESTONIA, Example 2.

Time t (min)	Water W (ton)	Heel α (°)	Ship speed Vs (knots)	Rel Heading β (°)	Rel motion rs (m)	Sign Wave H Hs (m)	Wave period Tp (s)
0.0	0	0	14.5	135	3.5	4.1	8.0
0.5	200	6	14.5	135	3.5	4.1	8.0
1.2	400	11	13.0	150	3.4	4.1	8.0
2.4	700	17	8.5	180	3.4	4.1	8.0
6.0	1000	22	5.5	-75	2.3	4.1	8.0
19.0	1500	29	0.0	-115	2.8	4.2	8.0
28.0	2000	37	0.0	-115	2.6	4.2	8.0

Table 4.3 Sequence of conditions in simulation example 2

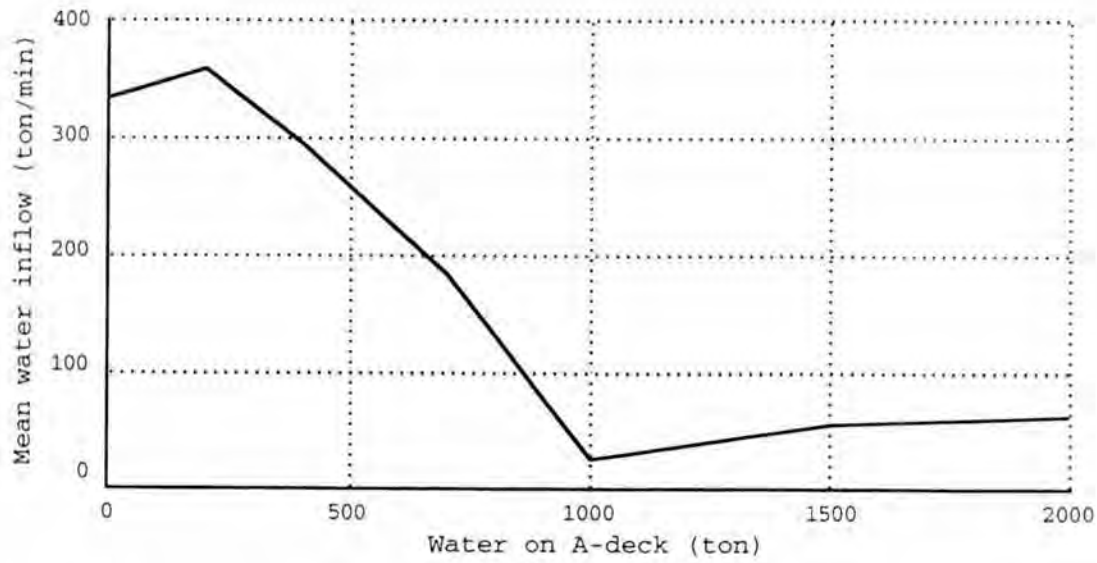

Figure 4.13 Mean water inflow per minute in simulation example 2.

Figure 4.14 shows that in this simulation the water inflow is slightly larger in the beginning of the sequence but significantly less 6-9 min after the ramp is opened. During this period the ship has completed the port turn and is running at 6 knots with close to beam seas. Such a plateau in the development of the list is also reported by witnesses but is stated to have occurred at a list of about 30°. If the ship in this simulation example had continued for about one more minute in bow or head sea, then the results would have fit these statements quite well, both with regard to the timing and to the development of the list.

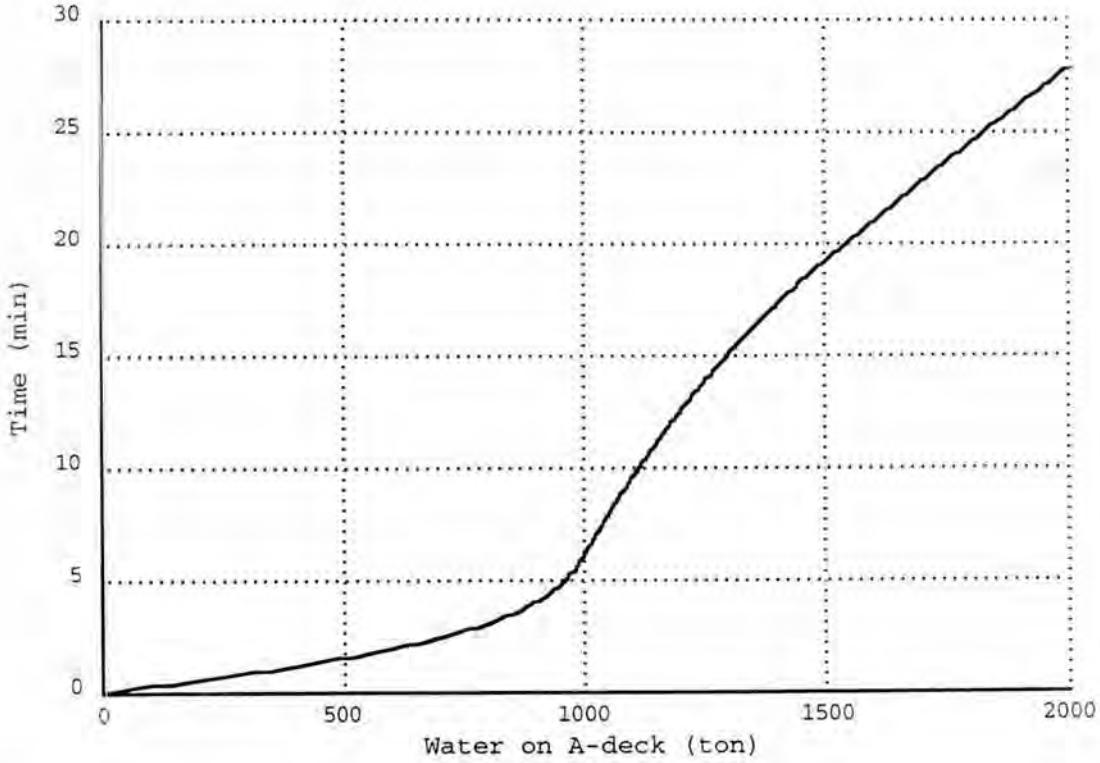

Figure 4.14 Time sequence of water inflow in simulation example 2.

Example 3 A hypothetic time sequence

Finally a hypothetical case has been simulated in order to illustrate what could have been the effect if the officers on bridge had been aware of the situation and had taken immediate actions in order to decrease the water inflow by decreasing speed and steering the ship to beam sea. The results indicate that there might have been a fair chance to save the ship if the heading was changed off the waves during the first critical minute. The simulation is however not very reliable since the random nature of seas and ship motions makes mean value estimates over just a few minutes very uncertain.

Time t (min)	Water W (ton)	Heel α (°)	Ship speed Vs (knots)	Rel Heading β (°)	Rel motion rs (m)	Sign Wave H Hs (m)	Wave period Tp (s)
0.0	0	0	14.5	135	3.5	4.1	8.0
0.7	200	6	13.0	120	3.5	4.1	8.0
2.0	400	11	5.0	90	2.2	4.1	8.0
70.0	700	17	0.0	90	2.2	4.4	8.0

Table 4.4 Sequence of conditions in hypothetic simulation example 3

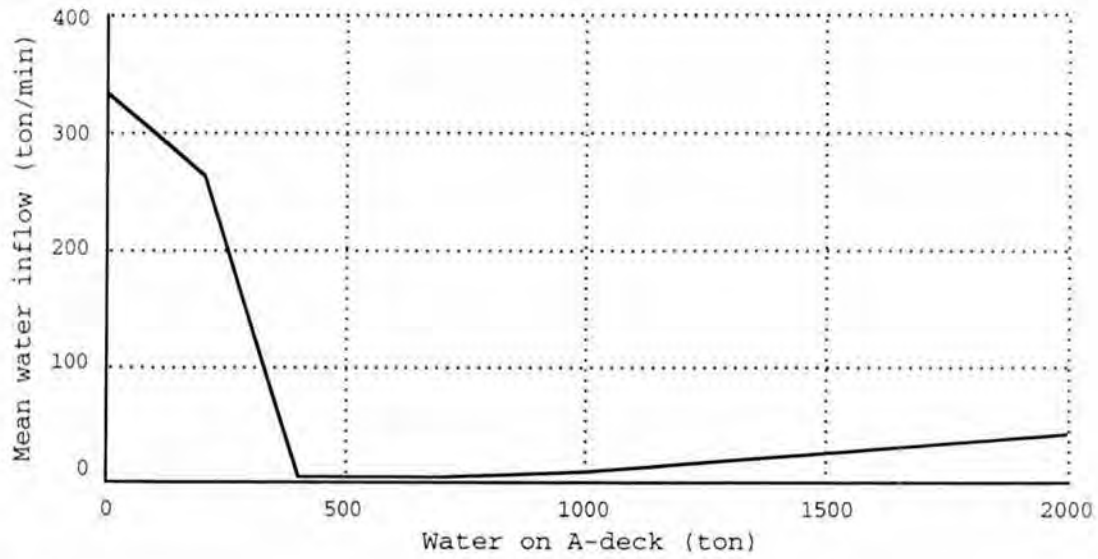

Figure 4.15 Mean water inflow per minute in hypothetic simulation example 3.

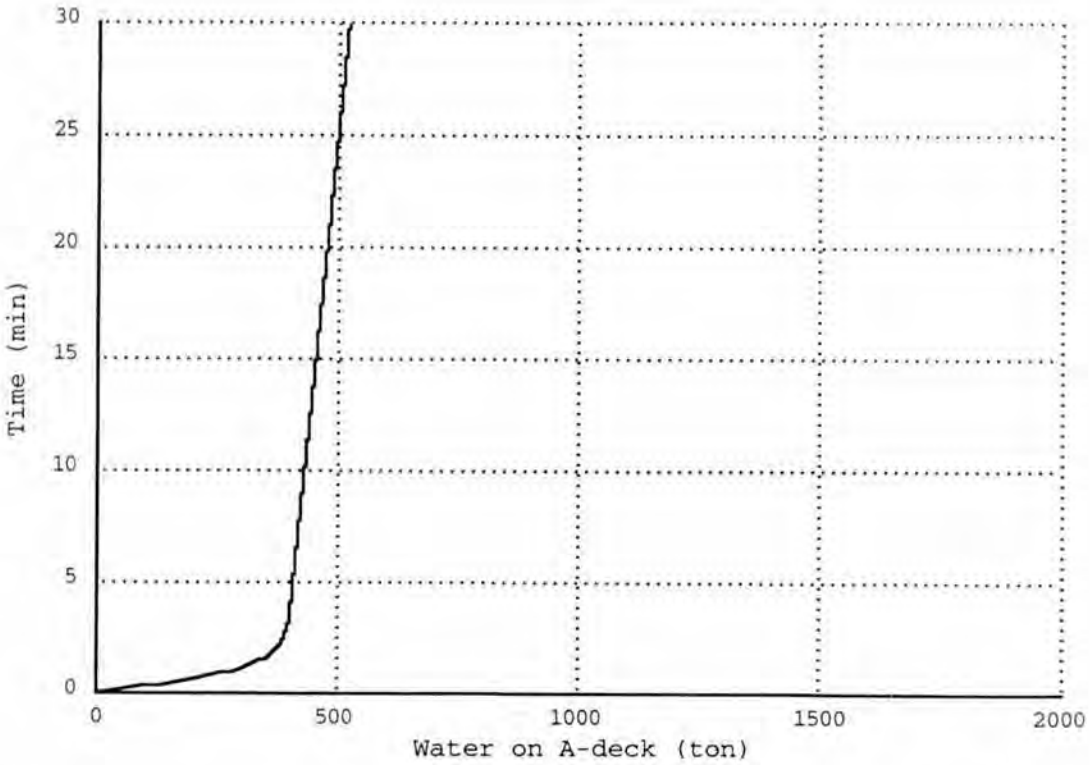

Figure 4.16 Time sequence of water inflow in hypothetic simulation example 3.

4.4 Comparison with time domain simulations at VTT, (4)

In ref [4] the water inflow has been predicted by using time series simulation instead of using the frequency distribution of relative motions as presented in this report. The principal differences between the two approaches are:

- The simulation in the time domain can take into account the actual velocity of water particles in each time step, while an average water velocity must be used in the frequency distribution approach presented in this report.

- The direct simulation makes it possible to predict the probability of exceedance of water inflow while the present simulation only can predict mean values of inflow.

Besides these principal differences there are also a number of other modelling differences between the two simulations.

- The relative motions in heeled condition has in [4] been calculated using the MOT35-program which is able to handle asymmetric hull shapes. In the present study, an ordinary strip-theory has been used with the submerged hull in heeled condition approximated as symmetrical, (Figures 3.2-3.3).

- In the time domain simulation, the irregular waves were assumed to be long-crested while the present study use relative motions calculated for a short-crested wave representation.

- The relative horizontal velocity and the inflow velocity due to hydrostatic pressure are treated separately and additive in [4], while in this study the two velocities are treated together according to the classical Bernoulli's equation (see e.g. Massey, Mechanics of Fluids, 3rd ed. eq (3.25)). In both simulations an inflow coefficient equal to unity has been used.

- Finally, the most important difference is that the still water freeboard at ramp opening in the VTT simulations were assumed to be 2.4 m while in this study it was calculated to be 2.97 m. This difference makes in general the calculated mean inflow in this report only half of what have been presented in [4] !

A comparison of results between the two approaches for mean values of water inflow is shown in the following Table 4.5. The table also includes results from the present approach but with separated horizontal velocities according to the VTT simulations. The same bow wave corrections on the freeboard, 1.0 m at 15 kn, 0.4 m at 10 kn, 0.2 m at 5 kn, 0.0 m at 0 kn, have been used in the comparison. The large difference is almost entirely caused by different assumptions of freeboard. The only exception to this are the values for 22° heel for which the MOT35 program gives much lower relative motions than for 0° or 35° heel and also much lower than those calculated approximately for 22° heel in this report.

If exactly the same condition is used, both approaches give also the same result of mean inflow, with differences of only a few percent, but it must once again be stressed that the simulations include many simplifications and uncertainties and the quantitative results should not be used uncritically.

If the higher inflow rates as given by the results from VTT would be used in simulation example 1 or 2, more than 1500 ton of water would enter the ship in two minutes. Such a rapid development of the list is not in accordance with witnesses statements.

				Mean water inflow [ton/min]		
Hs [m]	Vs knots	Heading [°]	Heel [°]	VTT approach ref [4]	Present appr.	Pres. appr. but sep. hor. veloc.
4	15	180	0	666	270	338
4	15	180	22	775	552	703
4	15	180	35/37	2078	829	1063
4	10	180	0	285	111	144
4	10	180	22	324	222	293
4	10	180	35/37	805	346	459
4	5	180	0	157	66	89
4	5	180	22	171	123	168
4	5	180	35/37	437	203	279
4	15	150	0	954	316	398
4	10	110/120	0	219	138	183
4	10	110/120	22	125	185	248
4	10	110/120	35/37	553	316	424
4	5	110/120	0	86	59	80
4	5	110/120	22	39	85	116
4	5	110/120	35/37	228	142	196
4	0	110/120	0	19	19	23
4	0	110/120	22	6	29	35
4	0	110/120	35/37	56	58	69
4	5	0	0	53	11	13
4	0	0	0	12	6	2

Table 4.5 Comparison of calculated mean water inflow by different methods and assumptions

5 References

[1] Karppinen T., Rantanen A., MV ESTONIA, Stability calculations, Technical Report VALC110, VTT, 1995

[2] Karppinen T., Rantanen A., MV ESTONIA, Numerical predictions of wave-induced motions, Technical Report VALC53, VTT, 1995

[3] Karppinen T., Rintala S., Rantanen A., MV ESTONIA, Numerical predictions of wave loads on the bow visor, Technical Report VALC106, VTT, 1995

[4] Rintala S., Karppinen T., MV ESTONIA, Numerical prediction of the water inflow to the car deck, Technical Report VALC174, VTT, 1996

SUPPLEMENT No. 523

Rintala Sakari - Karppinen Tuomo:

MV ESTONIA Accident Investigation. Numerical predictions of the water inflow to the car deck.

Technical Report VALC174.

VTT Manufacturing Technology.

Espoo 1996.

MV ESTONIA ACCIDENT INVESTIGATION

Numerical prediction of the water inflow to the car deck

CONFIDENTAL

TECHNICAL REPORT VALC174

Sakari Rintala & Tuomo Karppinen

Espoo, February 1996

VTT MANUFACTURING TECHNOLOGY
Tekniikantie 12, Espoo, P.O.Box 1705
FIN-02044 VTT, Finland
Tel. + 358 0 4561, Fax + 358 0 4550619, Telex 122972 vttha fi

Projekti/työ - Project identification	Sivuja - Pages	Päiväys - Date	Raportin nro - Report No.
VAL435401	20	12.02.1996	VALC174

Otsikko ja tekijä - Title and author

MV ESTONIA ACCIDENT INVESTIGATION

Numerical prediction of the water inflow to the car deck

Sakari Rintala & Tuomo Karppinen

Päivitys raporttiin nro - Update to report no.	Hyväksynyt - Approved by

Julkisuus - Availability statement

[] B (Julkinen - Public) [x] C (Luottamuksellinen - Confidential) [] C (Salainen - Secret)

Määräpäivä - Until date

Abstrakti, sisällysluettelo, tms. - Abstract, list of contents etc.

ABSTRACT

Water inflow to the car deck of MV Estonia have been simulated in irregular seas at different headings and different forward speeds by applying a non-linear numerical method. Conclusions are based on the present estimate of the sea state, speed and heading at the time of the accident. The numerical predictions indicate that the amount of the water inflow was so great that MV Estonia could not run the ramp slightly open very long without anybody noticing it. It is also clear that the ship could not run the ramp fully open very long in head or oblique seas. Otherwise the turn to the opposite heading would not have been possible. The evaluation of water inflow during the turn is very difficult, because several disturbances may take place. Moreover, the wave-induced motions of the ship near beam seas depend on the heel of the ship and the water inflow is very sensitive for the freeboard.

CONTENTS

VTT VALMISTUSTEKNIIKKA
Laiva- ja meritekniikka

VTT MANUFACTURING TECHNOLOGY
Maritime Technology

P.O. Box 1705
FIN-02044 VTT
FINLAND

Tel.int.+358 0 4561
Telefax +358 0 455 0619
Telex 122972 vtiha sf

1.INTRODUCTION

As a part of the accident investigation water inflow to the car deck of MV Estonia on her accident voyage have been estimated by a numerical method. The method and the results of the predictions are presented in this report. The water inflow simulation is based on the simulation of the wave-induced motions of the vessel in irregular seas. However, seakeeping characteristics of MV Estonia from the point-of-view of wave-induced motions and calculation of the relative motion are discussed in other technical reports VTT VALC53 and VTT VALC106, respectively. An estimate of the sea condition used in the calculations are the same as reported in VTT VALC106.

2. SIMULATION METHOD

The target of the simulation was to determine the velocity of water inflow to the car deck at different time steps and then to integrate the velocity of water inflow with respect to time. The simulation method of water inflow is based on the method presented in a technical report VTT VALC106. In the present method, it is important to know the values of the relative motion at the ramp opening during the simulation. All the other quantities can be calculated, when the variables such as forward speed, heel and bow wave height of the ship together with the dimensions of the ramp opening are known. Only heave and pitch motions of the ship are considered. Thus, the effect of roll on the vertical relative motion at the ramp has been ignored. When determining the motions of the ship, the heel was taken into account by calculating the transfer functions and their phases for the inclined ship. This was done using MOT35-program (McCreight,1976), which is able to handle asymmetric hull shapes.

2.1. THE FORMULAE OF THE WATER INFLOW

Irregular waves and ship motions were simulated as reported in VTT VALC106. The formulae of the elevation of a long-crested wave surface, the wave-induced motions of the ship and the relative motion of the ship are presented by Formulae 1, 4 and 5 of VTT VALC106, respectively. The formula of the water inflow can be divided into three separate parts i.e. water inflow due to wave particles, water inflow due to the static pressure and water inflow due to the ship speed. In the following, these components of the water inflow will be treated more detailed.

The water inflow due to wave particles

Velocity potential of the plane waves for deep water, when the situation is considered with respect to the steady moving ship, can be written in the form:

$$\phi = \sum \frac{g a_i}{\omega_i} e^{k_i z} \sin(k_i x \cos\mu + k_i y \sin\mu - \omega_{ei} t + \varepsilon_i) \ , \quad (1)$$

where

a_i = Amplitude of the ith harmonic wave component
ω_i = Circular frequency of the ith harmonic wave component
ω_{ei} = Encounter frequency of the ith harmonic wave component
g = Acceleration due to gravity
k_i = Wave number of the ith wave component
xyz = Cartesian co-ordinate system moving at the mean forward speed of the vessel with origin on the mean free surface defined by z=0. The positive direction of z points upwards and the centre of gravity of the ship is on the z-axis and x-axis points in the direction of the moving ship
μ = Heading of the ship
ε_i = Random phase angle of the ith wave component

The velocity of the wave particles in the direction of the x-axis can be derived by differentiating the velocity potential with respect to x. Thus the velocity of water particles gets the form

$$V_{wp}(t) = \frac{\partial \phi}{\partial x} = \sum \omega_i a_i \cos\mu e^{k_i z} \cos(k_i x \cos\mu + k_i y \sin\mu - \omega_{ei} t + \varepsilon_i) \qquad (2)$$

In the linearized wave theory, the free surface is defined as the plane z=0. Using this approximation in (2) and by assuming that the y-coordinate is small, the velocity of water particles gets the form

$$V_{wp}(t) = \sum \omega_i a_i \cos\mu \cos(k_i x \cos\mu - \omega_{ei} t + \varepsilon_i), \qquad (3)$$

Mass inflow of water particles can be calculated from the formula

$$\dot{M}_{wp}(t) = -\rho V_{wp}(t) A(t), \qquad (4)$$

where

ρ = Density of water
$A(t)$ = Area of the opening.

A(t) can be calculated using the definitions of Fig. 1 from the formula

$$A(t) = \int_0^{Z_r(t)-C} b(\bar{z})d\bar{z}. \qquad (5)$$

Thus, the vertical variation of the fluid particle velocity in the wave is disregarded. Formula (5) is valid only when the relative motion $Z_r(t)$ is greater than C, which is the freeboard to the lowest corner of the opening.

The water inflow due to the static pressure

Water velocity due to static pressure can be written in the area of the opening in the form

$$V_{st}(t) = \sqrt{2g(Z_r(t) - \bar{z} - C)} \qquad (6)$$

and the corresponding water inflow in the form

$$\dot{M}_{st}(t) = \rho \int_0^{Z_r(t)-C} b(\bar{z})V_{st}(t)d\bar{z} = \rho \int_0^{Z_r(t)-C} b(\bar{z})\sqrt{2g(Z_r(t) - \bar{z} - C)}d\bar{z} \qquad (7)$$

The water inflow due to the ship speed

Mass inflow of water due to the ship speed can be written in the form

$$\dot{M}_{sp}(t) = \rho \bar{V} A(t), \qquad (8)$$

where

$\bar{V}$ = Ship speed

Total mass of water on the car deck

Total mass of water on the car deck can be obtained by integrating the components of water inflow with respect to time

$$M_A = \int_0^t (\dot{M}_{wp}(t) + \dot{M}_{st}(t) + \dot{M}_{sp}(t))dt \qquad (9)$$

Besides above mentioned variable dependencies, also heading and heel of the ship are time dependent, if the total sequence of events is considered. Moreover the water inflow is of great deal probabilistic in nature because of irregular waves. Therefore the whole inflow phenomenon is factorized so that the certain variables are considered as constants and the so obtained subphenomena are simulated in the time domain and treated in the probabilistic way. In this way, it is easier to judge the importance of each variable on the calculated result.

3. THE TURNING CIRCLE OF MV ESTONIA

Turning circles of different car and passenger ferries built in the beginning of 80's are reported in Table 1. The length of the ship L, the velocity of the ship during the turn V, the diameter of the turning circle D and the ratio of D/L are shown in the table. Common for these ships is that they have the propulsion system with two propellers and the rudders are situated behind the propellers.

Table 1. Diameters of the turning circle for different car and passenger ferries

	L/[m]	V/[knots]	D/[m]	D/L
Ship 1	127.4	19.5	374	2.9
		18.2	341	2.6
		10.6	416	3.3
Ship 2	166.0	20.0	515	3.1
		20.0	560	3.4
		15.0	480	2.8
		15.0	560	3.4
Ship 3	166.0	20.0	533	3.2
		22.0	557	3.3
Ship 4	121.2	20.6	339	2.8
		21.0	338	2.8
Ship 5	157.3	20.0	481	3.1
		20.0	491	3.1
		15.0	482	3.1
		15.0	505	3.2

As can be seen in Table 1 the diameter of the turning circle D is proportional to the ship length and the ratio of D/L is almost constant for all ships. It is remarkable to notice that the diameter of the turning circle for each ship seems to be independent on the ship speed.

When the average value of D/L is used, the diameter of the turning circle for MV Estonia D=3.1*L=3.1*155 m=480 m and the length of the circle arc during the turn P=π *240 m =754 m. The duration times of the turn at different speeds are shown in Table 2.

Table 2. The duration times of the turn at different speeds

V/[knots]	T/[min.]
15	1.6
10	2.5
5	4.9
3	8.2

The duration times of the turn in Table 2 can be considered to represent quite rough estimates, because several disturbances may take place during the turn. Such factors of the disturbance are high wind speed, rough sea and heel of the ship, which may slow the turn or help the turning vessel depending on the phase of the turn. It is also probable that the ship speed was not constant during the turn. The duration times of the turn in Table 2 are, however, quite short. Thus, due to the short turning time it seems not possible that very large quantities of water came to the car deck during the turn.

4. RESULTS

Main results of the simulations are curves presenting probabilities at which water inflow exceeds different levels in terms of water in tons per one minute. Figures 2-10 show curves of exceedance probabilities. The exceedance probabilities are plotted on a logarithmic scale while water inflow is on a linear scale.

Water inflow is non-linear with regard to the relative motion at the visor and the statistical distribution of water inflow is not known. Therefore the simulated sequences have been one hour in which time the vessel encountered about 800 waves. Thus all together 60 one minute long samples were obtained during the simulation time and the highest value of

water inflow represents an exceedance probability level of about 0.017. The time step of 0.1 s and the significant wave height of 4.0 m were used in each simulation sequence.

The transfer functions of the vessel at different headings and speeds were determined for the heel values of 0°, 22° and 35° which correspond to the cases of 0 ton, 950 tons and 1800 tons water on the car deck, respectively. Effects of these transfer functions on the water inflow are shown in the figures, too.

5. DISCUSSION

Figure 2 shows an exceedance probability of water inflow when the breadth of the opening changes and the other variables are as follows: the significant wave height Hs=4.0 m, the heading of the ship HEAD=150°, the heel of the ship HEEL=0°, the velocity of the ship V=15 knots, the distance from the mean free surface of the water to the lowest corner of the opening C=1.4 m and the bow wave BW=1.0 m. The purpose of the different opening breadths is to simulate the different clearances between the ramp and ship hull. Thus the values of the opening breadth B of 0.5 and 0.1 m correspond to the clearance values of 0.25 m and 0.05 m between the ramp and the ship hull, respectively. As can be seen in Fig. 2 the mass inflow of water is directly proportional to the value of the clearance. At the exceedance probability level of 0.5 the water inflow values of 18 tons/minute and 90 tons/minute are obtained, when the breadth of the opening B is 0.1 and 0.5, respectively.

Figure 3 presents results of the calculations for the speed of 15 knots when the heading and the heel of the ship are changing. The change in the heel has also an effect on the variable C so that for the heel value of 35° the variable C gets even a negative value i.e. the lowest corner of the opening is below the mean free surface of water. Here the freeboard C has been reduced by 1 m due to the bow wave. The effect of the bow wave on the freeboard in this dynamic case is difficult to estimate. This is unfortunate since the freeboard has a very significant effect on the water inflow. The bow wave height has been estimated by numerical predictions of the SHIPFLOW-program. The effect of the open ramp laying on the forepeak deck on the water inflow has not been considered. The mass inflow of water seems to be larger in the bow seas (HEAD=150°) than in the head seas (HEAD=180°). This is probably due to the larger wave-induced motions of the ship in bow seas. The mass inflow of water with the heel value of 22° is only slightly greater than in the case the ship floating upright although the freeboard C is considerable smaller in the former case. The mass inflow of water is largest in the case where the heel angle of the ship is 35°. This case is perhaps irrelevant, because the main engines of the ship were hardly functioning with so great value of the heel.

The effects of the transfer functions on water inflow with different values of the heel are investigated in Figure 4. The water inflow was calculated in head seas when the velocity of

the ship V=15 knots and the effect of the heel on the freeboard C was not taken into account i.e. it is constant. Only the transfer functions and their phases were changed and in this way the influence of the wave-induced motions on the mass inflow of water was obtained. C=1.4 m was used in the predictions. The slowest inflow of water was obtained with the transfer functions corresponding to the heel value of 22° while the wave-induced motions at the opening are largest when the transfer functions of the heel value 35° are used. An exceedance probability curve of water inflow is between these two cases when transfer functions of the upright ship are employed. The exceedance probability curves for the upright ship are almost identical in the cases when the transfer functions obtained from SCORES- and MOT35-programs are used. The general trend of the wave-induced motions can be noticed in Fig. 4: the wave-induced motions decrease when the ship begins to incline and after a certain value of the heel the wave-induced motions of the ship begin dramatically to increase. The water plane area of the ship seems to behave vice versa: it firstly increases and secondly after a certain value of the heel it decreases when the ship is gradually inclining.

Figure 5 shows the results of the calculations in head seas when the significant wave height is 4.0 m and the velocity of the ship 10 knots. The exceedance probability curves are plotted for three different values of the heel angle. The curves for the two lowest values of heel are almost one on the other. The greatest values of water inflow were obtained for the heel angle of 35°. Effects of the ship velocity on water inflow can be seen when Figures 3 and 5 are compared. The trends of the probability curves are quite similar although amounts of water inflow are smaller when the ship speed is 10 knots. This is partly due to the smaller bow wave. The similar conclusions can be made when Figures 5 and 6 are compared with each other. Figure 6 shows the case where the ship is moving in head seas at the velocity of 5 knots.

Figures 7, 8 and 9 represent the results of the calculations when the heading of the ship is 110° and speeds of the ship are 10 knots, 5 knots and 0 knot, respectively. Because of the symmetry the curves in the figures correspond to the case of the 250° heading, too. The effect of roll motion on the vertical relative motion at the ramp opening has not been considered. When the vessel had forward speed the roll damping fins reduced roll motion and later it seems on the basis of witness accounts that the roll motion was not very significant. Due to the relatively small width of the ramp opening the vertical motion of the ramp corner due to roll is not very large. The heel value of 22° gives the smallest and the heel value of 35° the greatest values of the water inflow. The exceedance probability curve for the ship without heel is located between the above mentioned cases. The ship speed seems to have a very significant effect on the water inflow.

Figure 9 shows also results of a comparison when the ship speed is 0 knot, the heel angle is 35° and the freeboard C is changing. The freeboard C has really a significant effect on the

water inflow. The changes of the water inflow in this case are only due to the water inflow caused by the static pressure.

Figure 10 shows the exceedance probability curves in the following seas for two speed values of the ship upright.

The numerical predictions show that if the ramp is fully open the water flow into the car deck at 15 knots speed in head or oblique seas with the significant wave height of 4 m is rapid. The water inflow easily exceeds 500 tons in one minute and flow rates of about 2000 ton per minute seem possible if the ship has a heel angle of 35°. Forward speed has a strong effect on the water inflow which drops to about 300 tons/minute in head seas at 10 knots speed when the heel angle is less than 22°. In this case there is a chance of 1 to 10 that the flow rate exceeds 400 tons/minute, i.e. once in ten minutes. At a heel angle of 35°, the inflow may exceed 800 tons/minute at a probability of 50 % in head seas at 10 knots speed. In the following seas with 4 m significant wave height for the ship upright at 5 knots speed the inflow of water exceeds 50 tons/minute at a probability of about 30 % and 100 tons/minute at a probability of 20 %.

Because the phenomenon of the water inflow is so complicated and unstable, it is impossible to exactly simulate the sequence of the events on the basis of the water inflow calculations only. Also stability calculations (Report VTT VALC110) and interpretations of the witness accounts are needed when the sequence of the events is considered.

6. CONCLUSIONS

The water inflow to the car deck of MV Estonia has been simulated for different headings, heel angles and speeds of the vessel by a numerical method. Each simulation sequence took one hour and an exceedance probability curve of the water inflow rate was determined for each case. Only heave and pitch motions of the ship were considered when the relative motion at the ramp opening was defined in different time steps of the simulation.

Because the phenomenon of the water inflow is so complicated and unstable, it is impossible to exactly simulate the sequence of the events on the basis of the water inflow calculations only. Also stability calculations of the ship and interpretations of the witness accounts are needed when the sequence of the events is considered. However, some conclusions can be made on the basis of the water inflow calculations.

MV Estonia run some time in oblique seas at about 15 knots speed so that the visor pressed the ramp which was slightly open and water flowed to the car deck through the narrow gaps at the sides of the ramp. If the width of the openings on both sides in total was 0.1 m or 0.5 m, the inflow of water to the car deck may have been near 20 tons/minute or about 80

tons/minute, respectively. The amount of the water inflow was so great that MV Estonia could not run the ramp slightly open very long without anybody noticing it.

The numerical predictions show that if the ramp is fully open the flow of water to the car deck at 15 knots speed in head or oblique seas with the significant wave height of 4 m is rapid. The water inflow easily exceeds 500 tons or even more in one minute. The ship could not run the ramp fully open very long in head and oblique seas. Otherwise the turn to the opposite heading would not have been possible.

The turn to the opposite heading at the speed of 10 knots takes about 2.5 minutes. The evaluation of the water inflow during the turn is very difficult, because several disturbances may take place. Such factors of the disturbance are high wind speed, rough sea and heel of the ship. It is also probable that the ship speed was not constant during the turn. Moreover, the wave induced motions of the ship (i.e. the water inflow) near beam seas depend on the heel of the ship and the water inflow is very sensitive for the freeboard.

For the ship floating upright, the water inflow may exceed 30 tons/minute at a probability of 10 % in the following seas at 0 knot speed. Forward speed of the ship has a strong effect on the water inflow.

7. REFERENCES

McCreight, K. K. 1976. Manual for mono-hull or twin-hull ship motion prediction computer program. David W. Taylor Naval Ship Research and Development Centre. Bethesda, Maryland.

Karppinen, T. & Rantanen, A. 1995. MV Estonia accident investigation. Stability calculations, VTT Manufacturing Technology, Report VALC53, Espoo, December.

Karppinen, T., Rintala, S. & Rantanen, A. 1995. MV Estonia accident investigation. Numerical predictions of wave loads on the bow visor. VTT Manufacturing Technology, Report VALC106, Espoo, December.

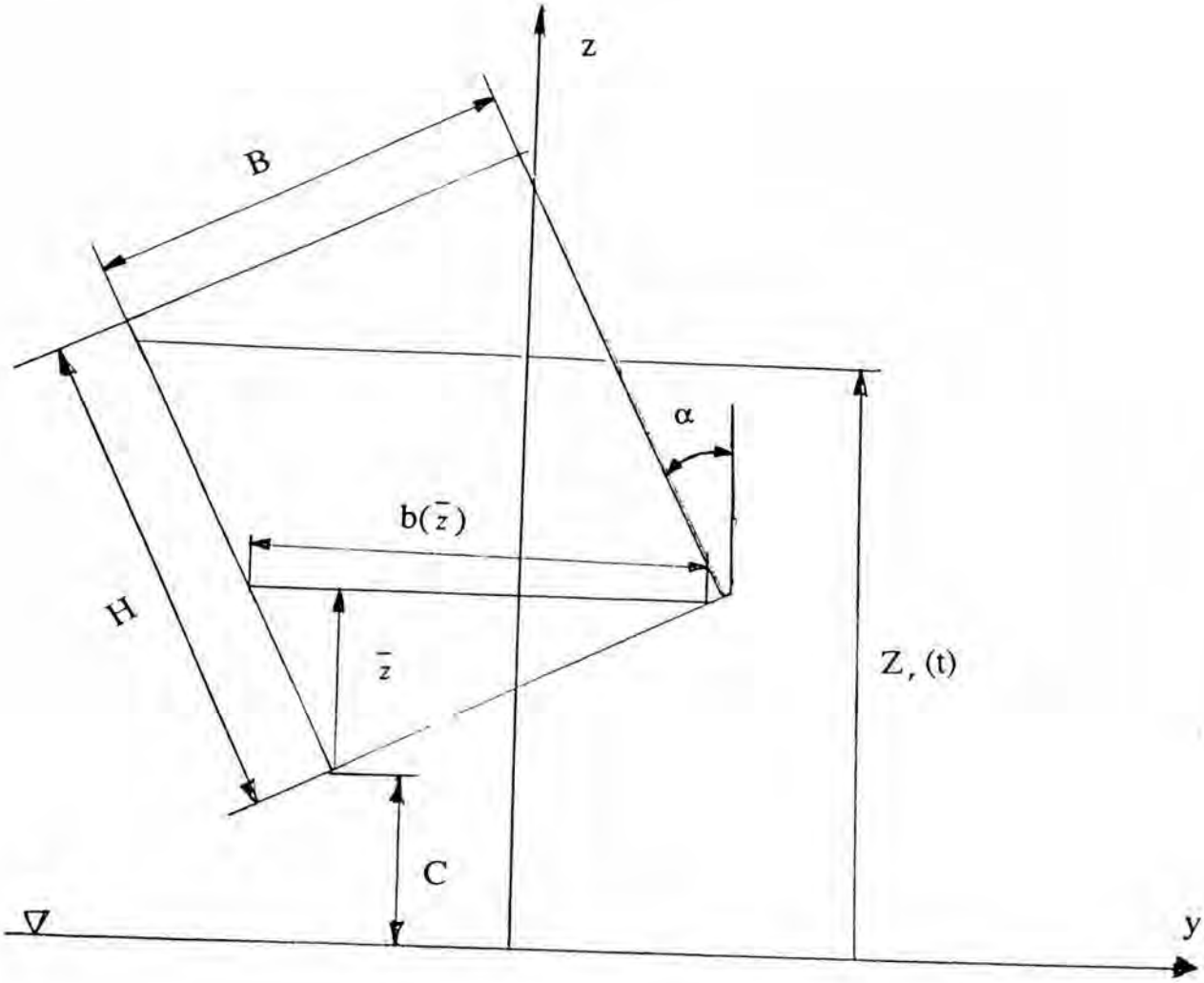

B = Breadth of the ramp opening
H = Height of the ramp opening
C = Distance from the free surface of water to the lowest corner of the opening
$\bar{z}$ = Coordinate from the lowest corner of the opening
$b(\bar{z})$ = Local breadth of the opening parallel to the free surface of water
$Z_r(t)$ = Relative motion of the ship at the opening
α = Heel of the ship

Fig. 1. Geometric definitions of the ramp opening used in the calculations

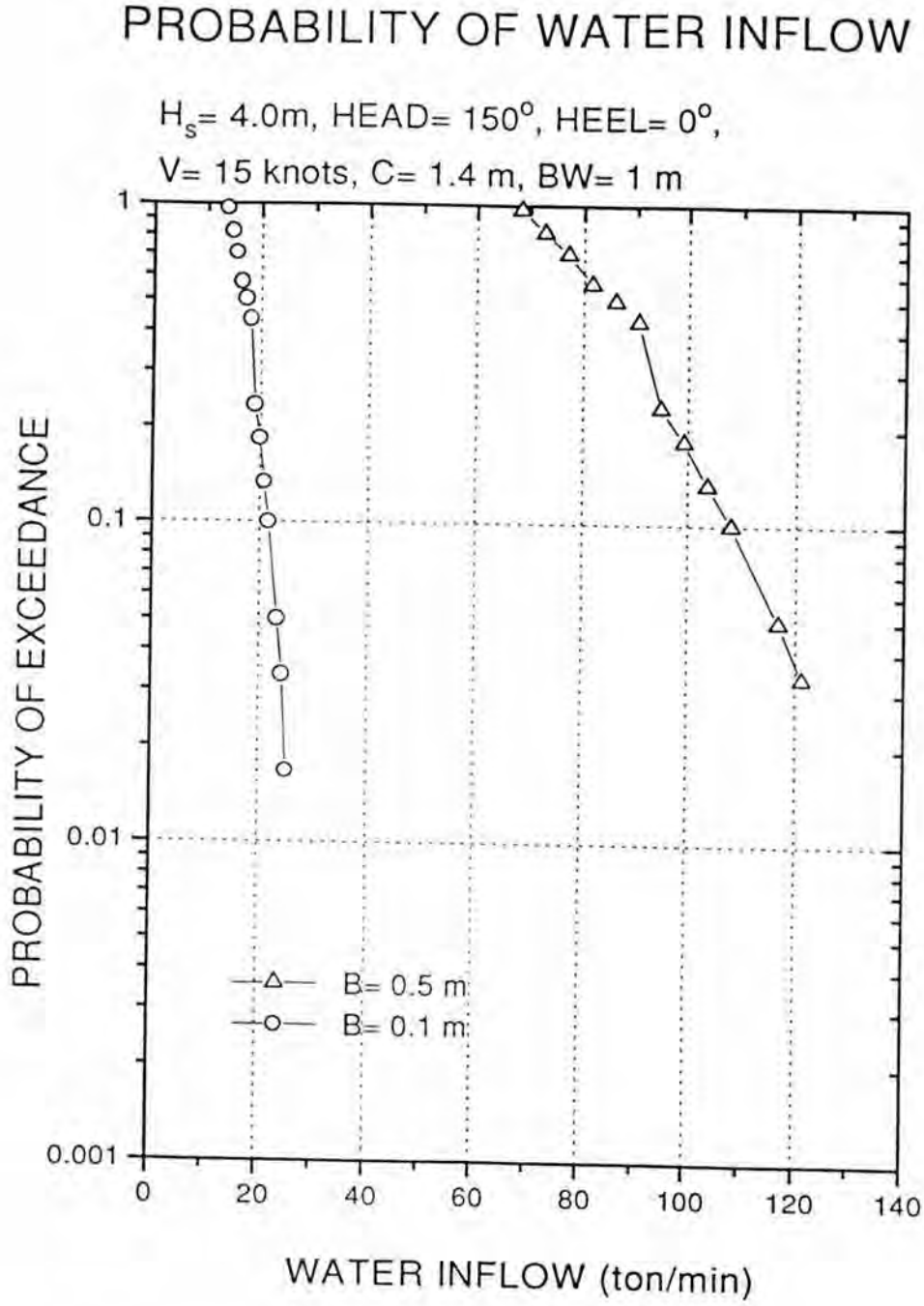

Fig. 2. Water inflow to the car deck in the bow oblique seas with Hs = 4.0 m

VTT VALMISTUSTEKNIIKKA
Laiva- ja meritekniikka

VTT MANUFACTURING TECHNOLOGY
Maritime Technology

P.O. Box 1705
FIN-02044 VTT
FINLAND

Tel.int.+358 0 4561
Telefax +358 0 455 0619
Telex 122972 vtiha sf

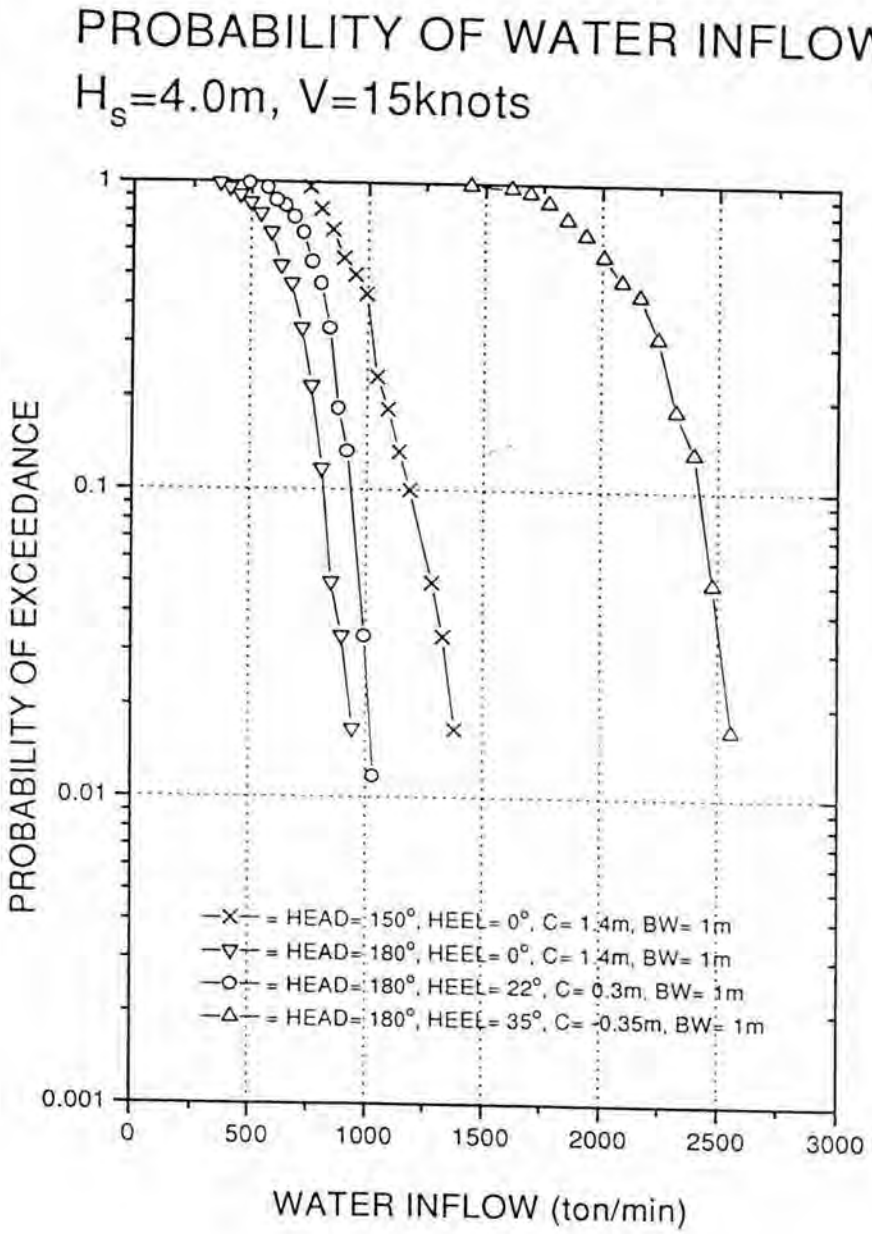

Fig. 3. Water inflow to the car deck in the oblique and head seas

VTT VALMISTUSTEKNIIKKA
Laiva- ja meritekniikka

VTT MANUFACTURING TECHNOLOGY
Maritime Technology

P.O. Box 1705
FIN-02044 VTT
FINLAND

Tel.int.+358 0 4561
Telefax +358 0 455 0619
Telex 122972 vtiha sf

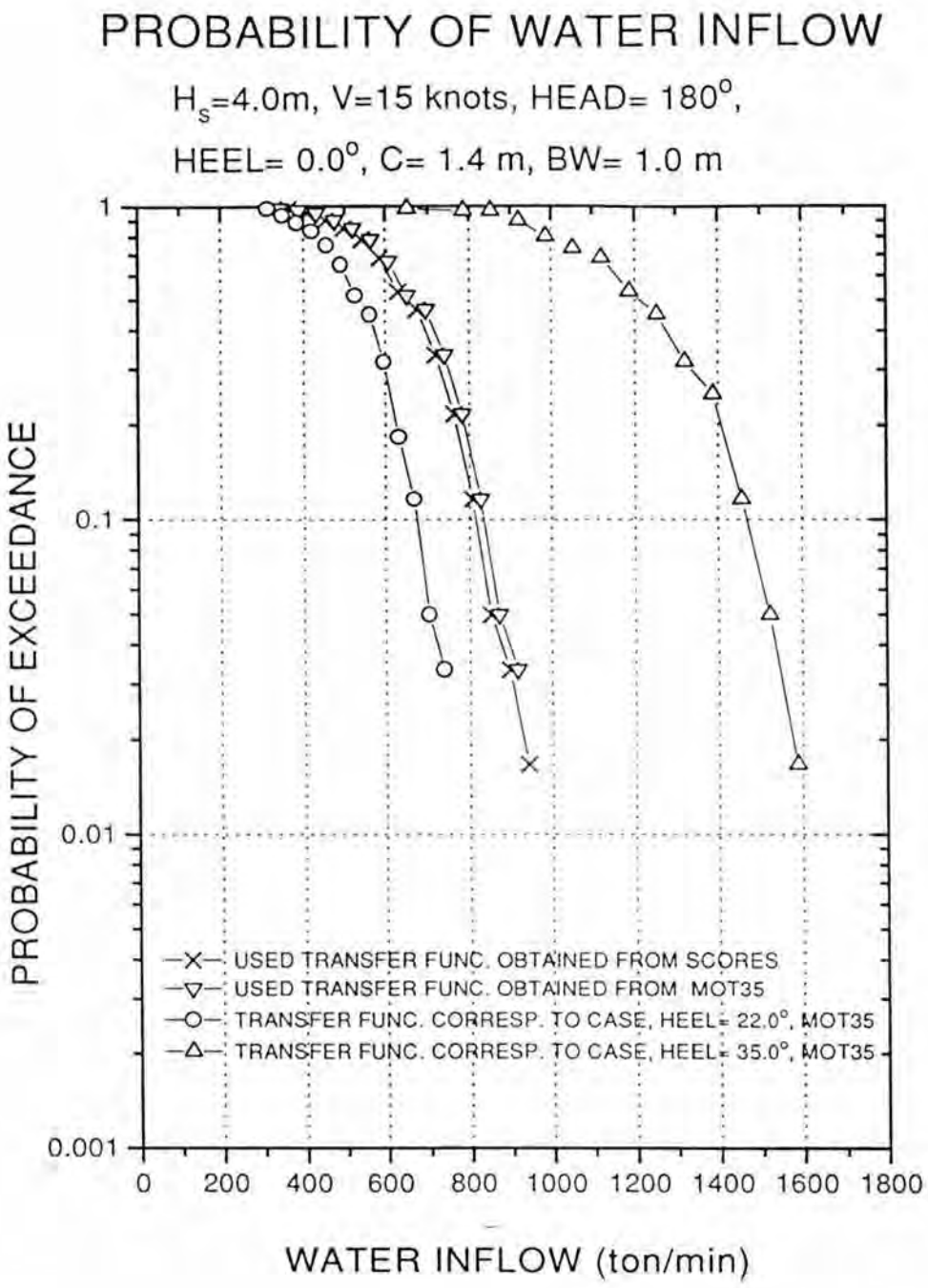

Fig. 4. Water inflow to the car deck calculated with different kinds of the transfer functions.

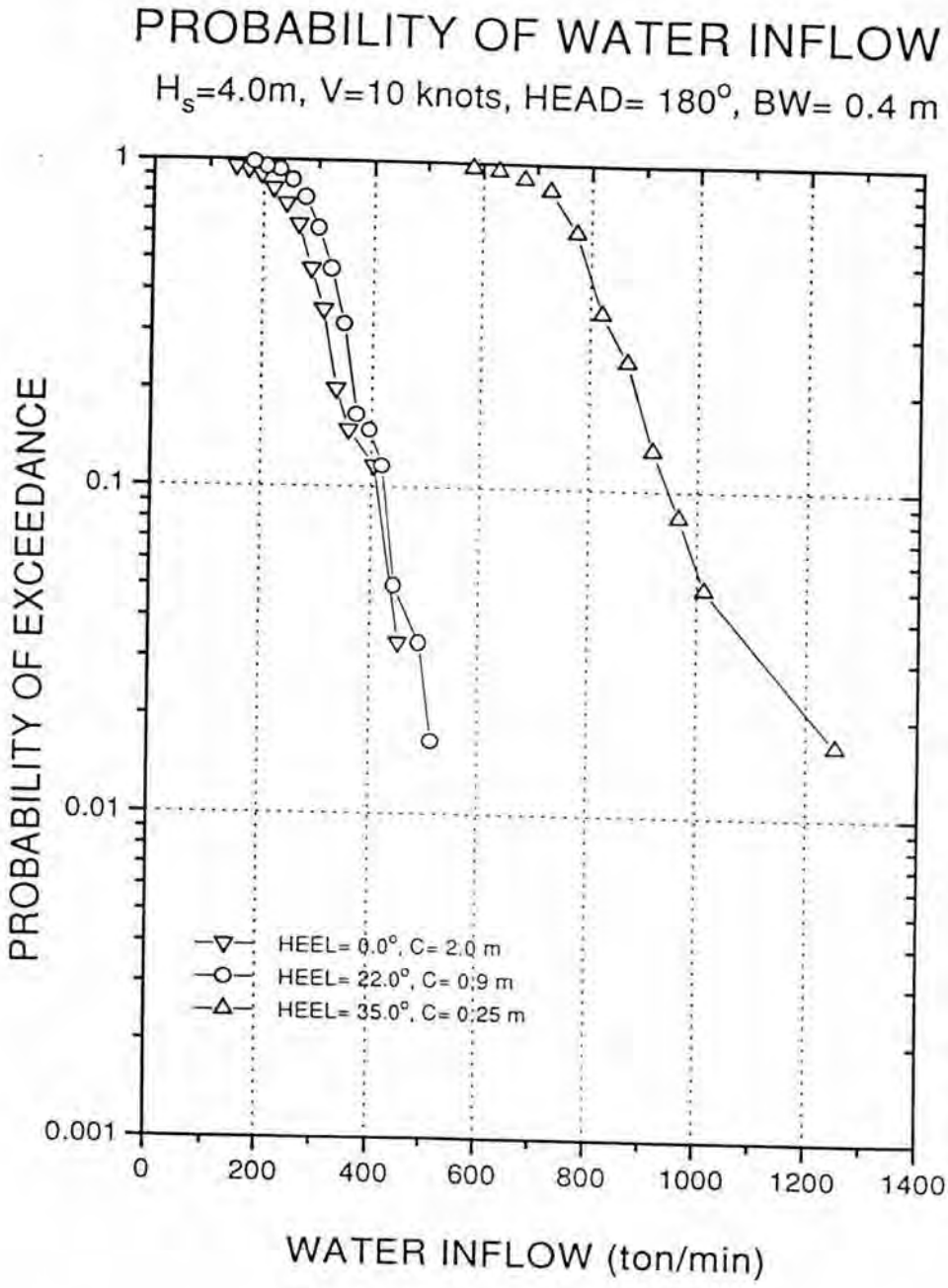

Fig. 5. Water inflow to the car deck in the head seas

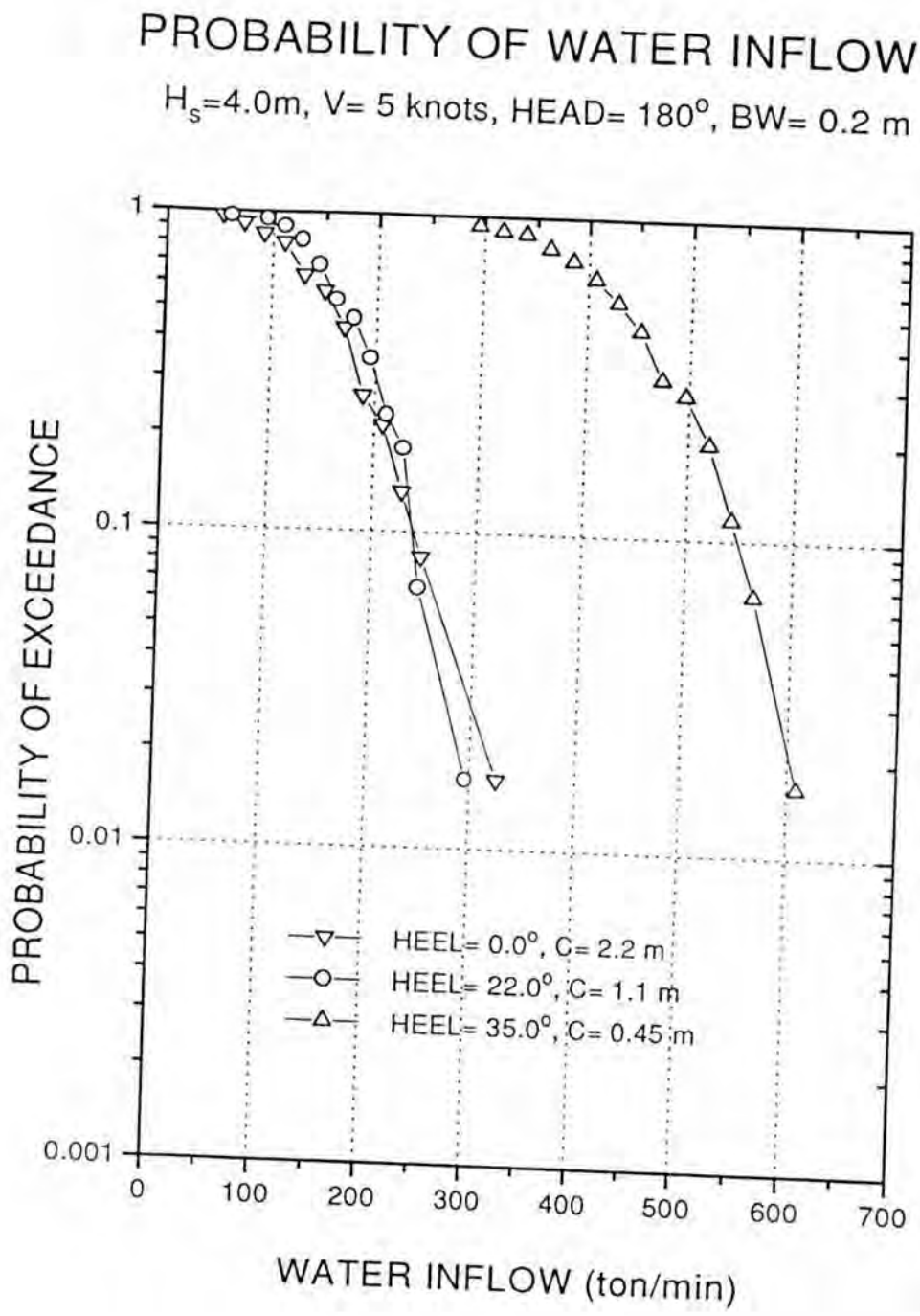

Fig. 6. Water inflow to the car deck in the head seas

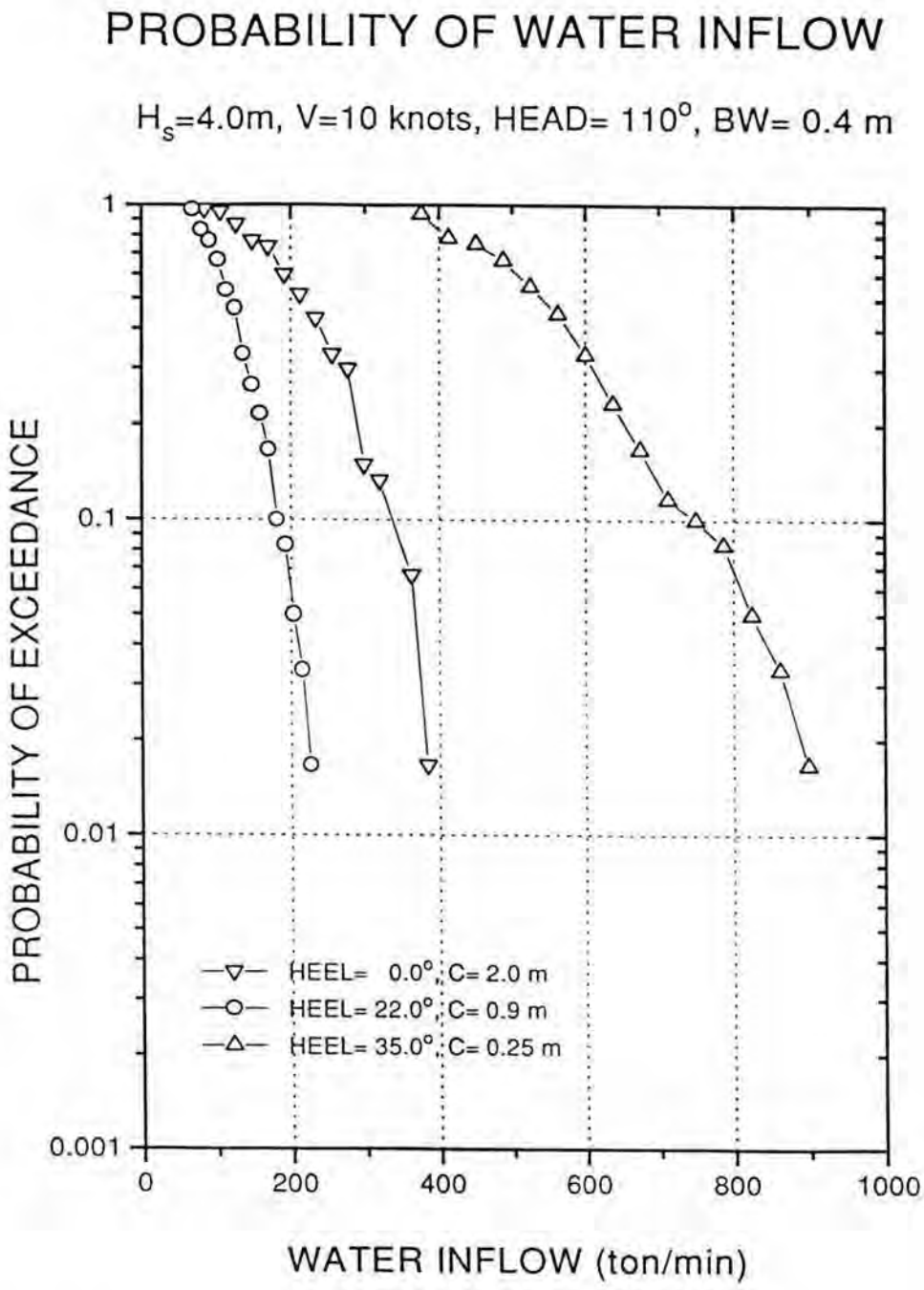

Fig. 7. Water inflow to the car deck in the beam seas

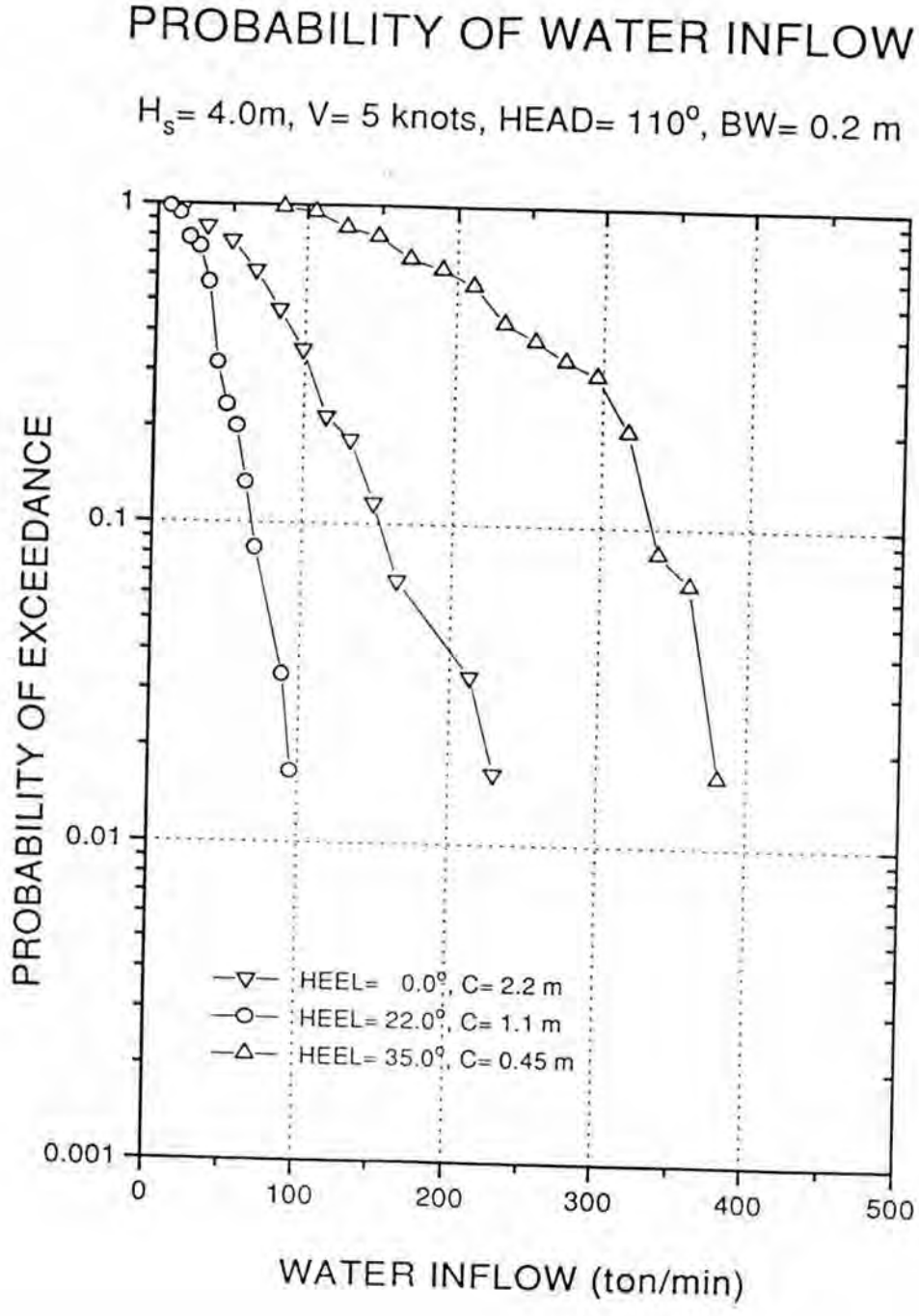

Fig. 8. Water inflow to the car deck in the beam seas

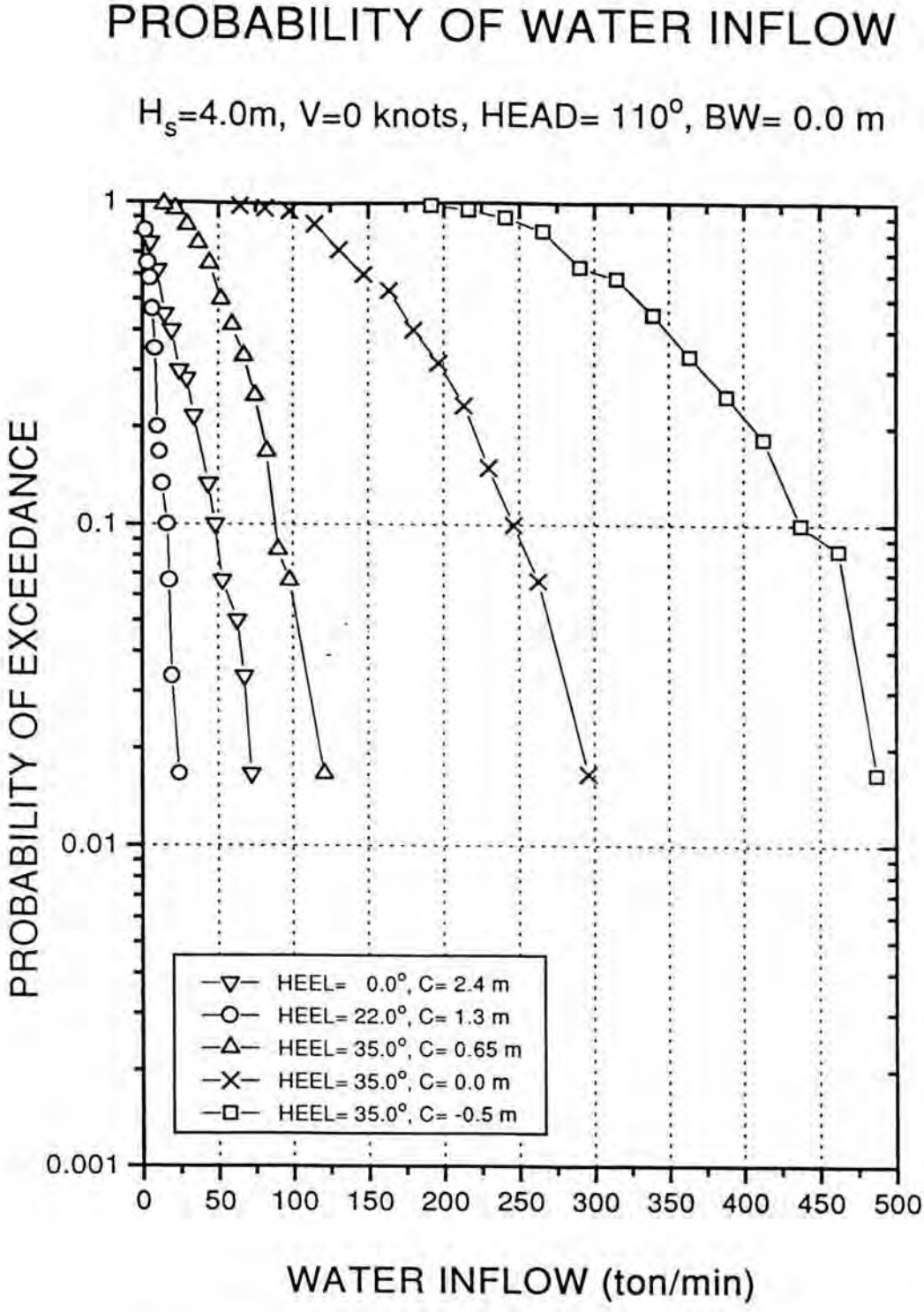

Fig. 9. Water inflow to the car deck in the beam seas

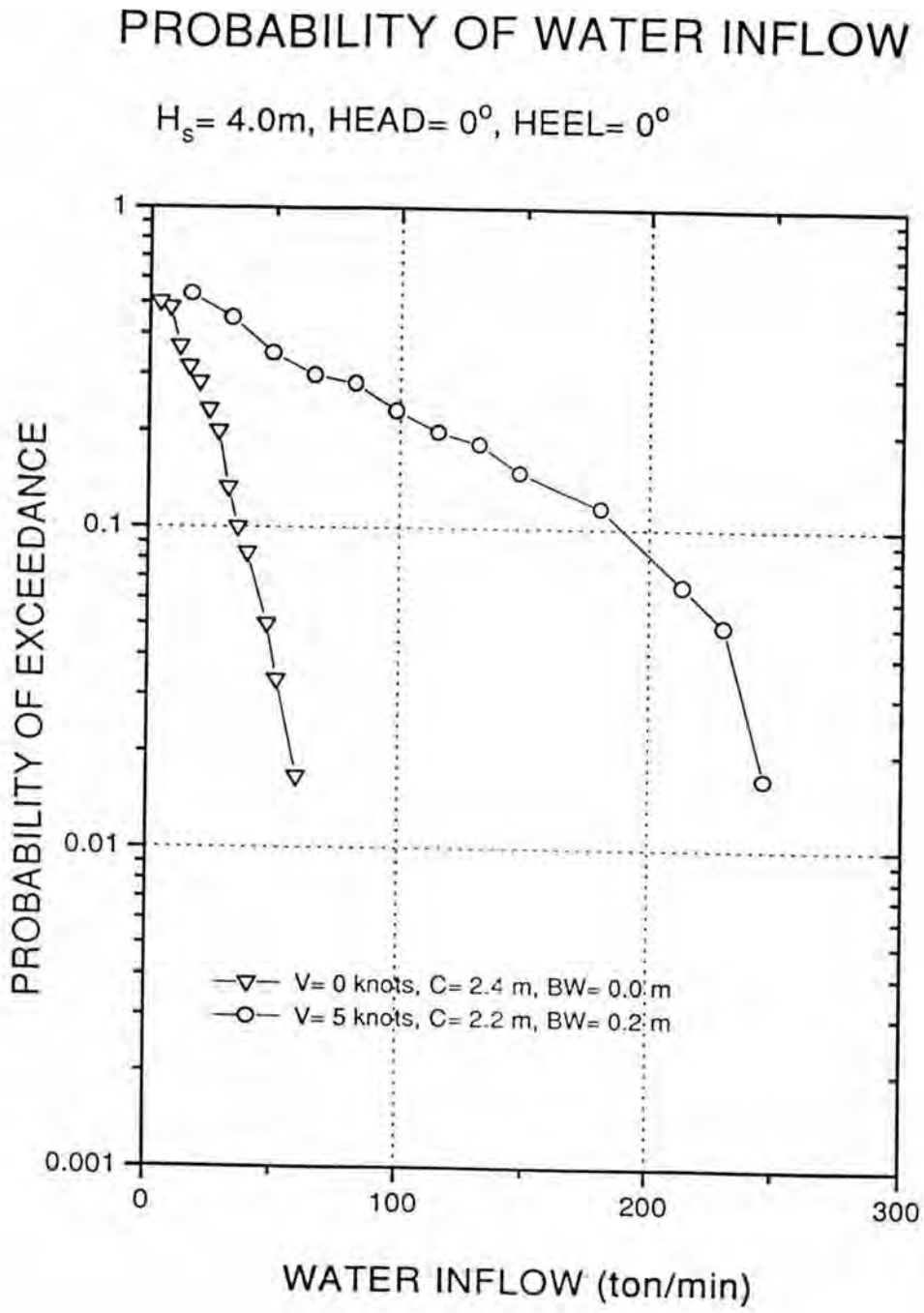

Fig. 10. Water inflow to the car deck in the following seas

SUPPLEMENT No. 524

Wermelin Hans: M/S Estonia, a ship emanating from The Baltic Phenomenon.

An historical overwiev made by *ADC Support AB*.

Stockholm 1995.

M/S Estonia

a ship emanating from The Baltic Phenomenon

An historical overview
made by

ADC SUPPORT AB

Box 100 75, S-100 55 Stockholm Sweden
Tel. +46 (0)8 664 08 00 · Fax +46 (0)8 664 13 50

for

The Joint Accident Investigation Commission of Estonia, Finland and Sweden

Content

INTRODUCTION - M/S ESTONIA

M/S Estonia belonged to the type of ships noted *as Passenger/RoRo Cargo/Ferry* in ship registers. The ship was delivered in June 1980 by the shipyard Jos L. Mayer for Rederi ab Sally in Mariehamn situated on the island of Åland (part of the archipelago of Finland). The ship was designed and built according the rules of the classification society, Bureau Veritas. Bureau Veritas and the Finnish Board of Shipping and Navigation surveyed the design and the construction of the ship. Finally The Finnish Board of Shipping and Navigation issued a *Passenger Ship Safety Certificate,* certifying that the newbuilding fulfilled the international safety standard *Safety of Life at Sea*, SOLAS, for short international voyages

The ship was named *M/S Viking Sally* and commenced her service in Viking Line on July 5 1980 on the route Kapellskär (a small terminal Viking Line used about 90 km north of Stockholm) - Mariehamn - Naantali (about 20 km north of Turku, Finland). For eight months she belonged to the group of biggest ships ever seen in the ferry service between Finland and Sweden. In March 1981 Silja Line introduced the even bigger ship M/S Finlandia on the Stockholm - Helsinki route. M/S Viking Sally was after some time moved to the Stockholm - Mariehamn - Turku route.

The passenger- and general cargo trade between Sweden and Finland has since 1960 been dominated by two groups, the Silja Line and the Viking Line. The EffJohn group owned by the Swedish company Johnson Line and the Finnish company EFFOA, was the parent company of the Silja Line. In 1987 EffJohn acquired Rederi ab Sally with ships and interests in Viking Line included. The other owners of the marketing company Viking Line, Rederi AB Slite and SF Line then bought the shares of Rederi ab Sally in Viking Line from EffJohn. Rederi AB Slite chartered M/S Viking Sally back and the ship continued the service Stockholm - Mariehamn - Turku until Mars 1989. In February 1989 however, EFFOA bought the ship from EffJohn and chartered her to Rederi AB Slite. The ship continued the same service until April 1990. Then she operated under the name *M/S Silja Star* for Silja Line on the Stockholm - Turku route until she was transferred to the Vaasa-Umeå-traffic also belonging to the EffJohn group. The ship was renamed to *M/S Wasa King*. On 15 January 1993 the ship was sold to Estline Marine Co Ltd in Cyprus. The ship was renamed to *M/S Estonia* and bareboat chartered to E-Line Ltd and was put into the service of Estline on the route Stockholm - Tallinn. These companies were equally owned and controlled by the Swedish company Nordström & Thulin and Estonian Shipping Company in Estonia.

Although the history of M/S Estonia is more confusing than for most ships in the ferry service between Sweden and Finland it reflects the dynamic in this trade. This paper shall describe some of the circumstances behind the remarkable development of the ferry services between Sweden and Finland. In the worldwide shipping communities this is mentioned as *The Baltic Phenomenon*. Many questions have been raised; how can such an expansion of a ferry service occur so rapidly, how can the adoption and the development of new technic and concepts be so rapid, how can the high service level be maintained under the tough conditions in the Baltic Sea (confined waters, ice etc), how can the top class service concepts remain profitable.

The design of a ship is the final outcome of considerations and compromises in many different areas. Laws of nature, traditions/know-how, material & equipment, rules & regulations, ambient conditions etc. These are tools and/or limitations for the physical ship design. Software aspects i.e. atmosphere in the shipping industry when the ship is ordered is another important factor. The Owners purpose, vision, perspective etc. etc. are more dominating factors for the final result than the actual design and construction process. It should not be forgotten that the process is run by humans.

Hopefully it will be easier to understand the case of M/S Estonia when knowing the background to the Baltic Phenomenon from which M/S Estonia emanates.

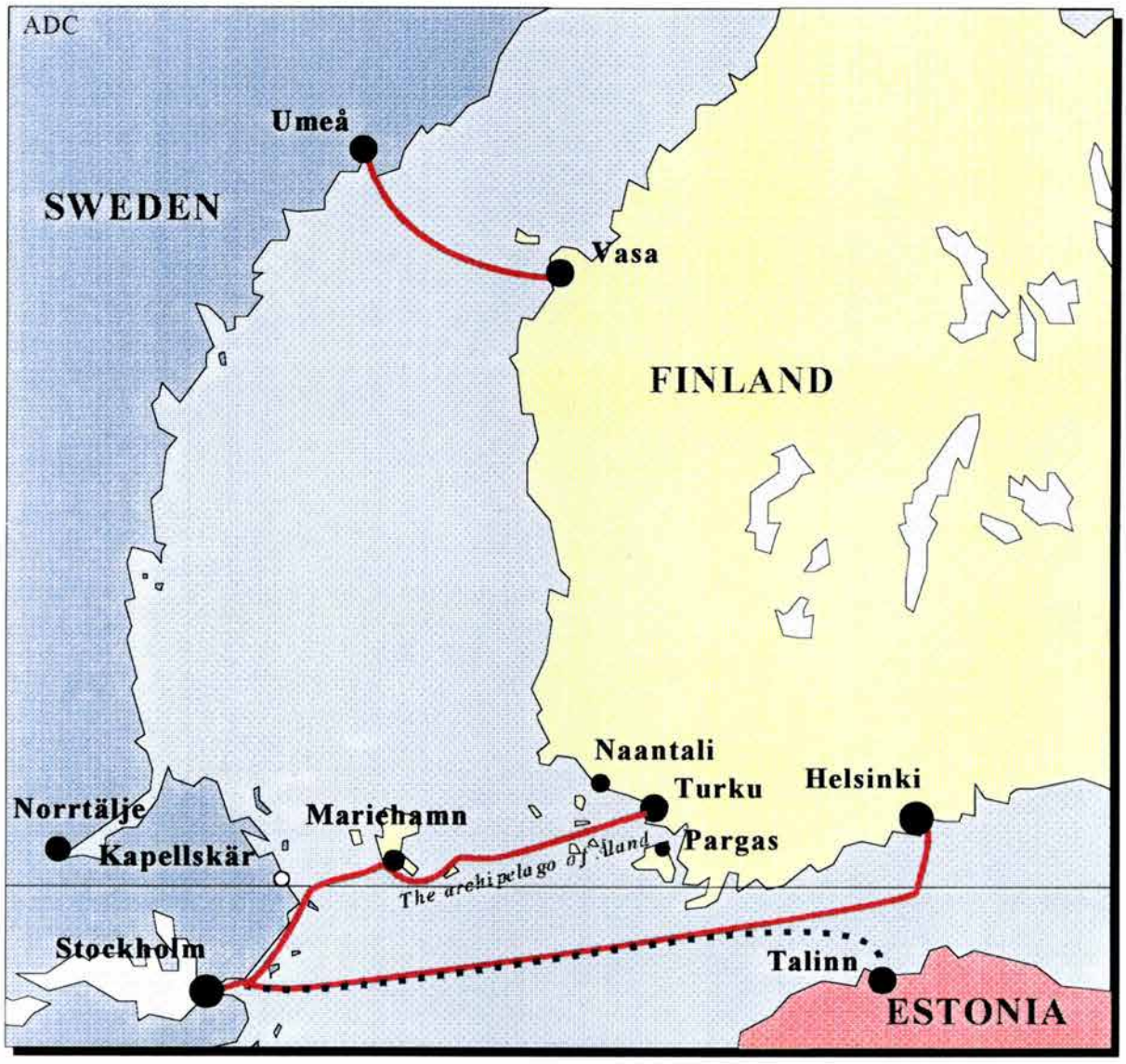

THE PASSENGER/RORO CARGO/FERRY - M/S ESTONIA

M/S Estonia was built for satisfying the increasing demand for transportation capacity on the route Sweden through the Åland archipelago to the mainland of Finland. On this route the ships are making a round trip every 24 hours.

The ship was built to operate as a *day and night ferry* for *passengers and rolling cargo*. There were cabins of different categories. The Passenger Safety Certificate permitted the ship to carry 2 000 passengers. When the ship was introduced some passengers preferred to save money by just buying a "deck ticket" on the night trip, therefore the ship had just 1 223 beds arranged in 529 cabins and the deck passengers were offered to relax in comfortable chairs during the night hours.

The ship had dual purposes. Equally important with the transportation of the passengers was the transportation of cargo. To manage a round trip of about 250 nautical miles in 24 hours including port-calls, exchange of passengers and cargo, bunkering and handling of stores, only cargo rolling on wheels could be considered. On a *RoRo Cargo Ferry* the cargo is driven onboard and ashore either self-propelled or towed by so called tug-masters (a kind of tractor) e.g. trailers and containers on flat wagons (Mafis) are handled by tugmasters. Since on this route there was no time to turn or reverse the cargo flow, a drive-though concept with openings in both ends of the ship was the only solution.
Finally, with *ferry(service)* is meant a ship operating on a regular basis with fixed arrival- and departure times in defined ports. Normally this is associated to road-ferries. In this trade however, the ships are constructed for unrestricted service.

THE BALTIC PHENOMENON

The expression "The Baltic Phenomenon" alludes in shipping circles on the development of the ferry-services between Stockholm in Sweden and Turku and Helsinki in Finland. In the following explanations will be given to the amazing development of the ferry services in this region.

The tradition

To begin with, some characteristic factors of shipping will be discussed. The shipping industry is more complex than many other industrial activities. Experience and know-how are key factors tying progress of shipping to continuity. Shipping is a capital intensive industry, but also very flexible. There are many examples of steps in the development of shipping activities. In many such cases new technical solutions have been introduced enabling new superior commercial concepts. However, most new concepts in shipping fail due to underestimation of the complexity and/or lack of know-how.

Some aspects of shipping :

- Merchant ships should be regarded as individuals. In general just one or a few sister ships are built according to the same specification. Thus merchant ships are not standardised like cars, aircrafts or series of navy ships.

- The shipping industry can develop new technical concepts in shorter time than most other industries.

- Standard solutions in shipping are rare. Like all other transport services shipping has to adopt to varying conditions e.g. treatment of cargo, geography, infra-structures, customs of the trade etc.

- A ship is not just an autonomous movable production plant, but also a separated society.

- The production capacity of an established service (number-, performance- and size of ships in a fleet) can be changed in a short time through sale, purchase or various charter arrangements.

- In shipping rapid changes can be made; change of owners, flag, operator, crew, trade etc.

- The competition is normally unlimited, global.

- Supply of sea transport services adopt normally quickly to demand.

- Due to the complexity of shipping, tradition, experience, information and know-how takes more time to build up than in many other industries.

The story of the Baltic Phenomenon includes many of these factors. The introduction of the RoRo-technique was the initiation to the Baltic Phenomenon. Though the development was very fast it followed the traditions of the trade. The new technique just opened new business opportunities. There were several factors synchronously promoting the development of the traffic.

Influencing factors on traffic growth:

- Geographical conditions
- Cultural and historical background in Finland and Sweden
- Economical development in Finland and in Sweden
- Taxation in Finland and Sweden
- Ship-owners tradition in the region.
- The infrastructure of the shipping industry in the area, know-how, research, subcontractors, ship-yards etc.
- Etc. etc.

This traffic is entirely commercial. The competition and the profits have motivated the main operators Silja Line and Viking Line to develop new commercial concepts. Although the competition has always been intense it has been understood that safety- and environmental questions are of common interests for the traffic. Crew members from both lines has always maintained the good seaman tradition to exchange navigational experiences of the trade. The extensive newbuilding program kept the organisations updated with the development. The level of the discussions when ordering new ships was accordingly high. Thus the collected bank of technical navigational experiences from this trade is rich.

Before the Phenomenon

Some historical facts

In 1809 Sweden lost Finland and the archipelago of Åland to Russia. In Turku, which used to be the administrative centre, Swedish was the official language. The Finnish speaking Helsinki became capital in the Russian province. First in 1917, Finland became an independent country. In a cease-fire with Russia 1944 Finland was forced to pay war indemnity to the Soviet Union. Peace with the Soviet Union was settled three years later. Unlike most other countries in similar situations, Finland paid the indemnity in full. The last payment was done in 1986. Following that, trade pacts were signed between Finland and USSR which occupied large parts of the Finnish industrial capacity. The trade pact ended in 1986, initiating a need for expanding the Finnish trade with Western Countries From 1960 the development of the ferry traffic to/from Sweden has been an important contributing factor for the development of the Finnish industry. Since then the Finnish trade has developed towards more refined industrial products to/from the western countries.

Sea traffic Finland - Sweden

The sea traffic can be separated into two main activities, full shiploads (e.g. forest-, oil products, etc.) and combined shiploads (e.g. general cargo, passengers & trucks, etc).

The ferry service handles mixed cargo and is performed on fixed published schedules. Except for dangerous cargo the service is offered on a general basis, a common transport service open to everyone.

The cargo is normally standing on its own wheels and represents in general a high value per ton. Ships carrying such cargo e.g. a truck-load of TV-sets, require a lot of space. This type of transport services have become increasingly time sensitive, until todays just-in-time (J-I-T) logistic systems. Today J-I-T services are important elements for the competitiveness of modern industry.

Late 1800 steamers were introduced on the trade to transport mail and passengers. The steamers were during the 60's replaced by diesel motor driven RoRo-ferries. In 1918 FÅA (the Finnish steamship company, later changed to the phonetic abbreviation EFFOA), the Finnish owner Bore and the Swedish owner Svea founded *De Samseglande Rederierna* (the jointly operating shipping companies). In the beginning they coordinated their services on the line Turku - Stockholm and in 1919 the line Helsinki - Stockholm was also included. These services were commonly called *The White Ships*. In 1957 the same owners founded Ab Siljarederiet. In 1970 the liner services were reorganised and the marketing company *Silja Line* was founded i.e. at that time Passenger/ RoRo Cargo/ Ferries had been used for about a decade in this trade.

The initiation

In the autumn 1957 the sea captain Gunnar Eklund returned home to Åland from sea service for vacation. Mr. Eklund got however unhealthy and the verdict of the doctors involved was that he must not go back to sea again. On the Åland island there are few alternatives to earn living than from the sea. At the hospital there was plenty of time for Mr. Eklund to find solutions on how he should fulfill his economical obligations to his family. He realised that car traffic had increased a lot and the way around the Baltic Sea between population centres in Sweden and Finland was very long.

The concept of the liner services between Sweden and Finland remained at this time about the same as in the beginning of the century. The ships had got a few private car positions on deck and the cars were hoisted onboard.

Mr. Eklund told his friend sea captian Henning Rudberg that he had the idea to use a carferry between Åland and Sweden. Mr. Eklund had noticed the rapid increase of private cars in Sweden. As Mr. Rudberg had similar thoughts he supported the idea and wanted to join an potential investment. In February 1959 a British steam ferry laid up in Dover, England was found. It was the train- passenger ferry S/S Dinard, built 1924 in Dumbarton, England. The ship was bought with brokerage assistance from a good friend in England.

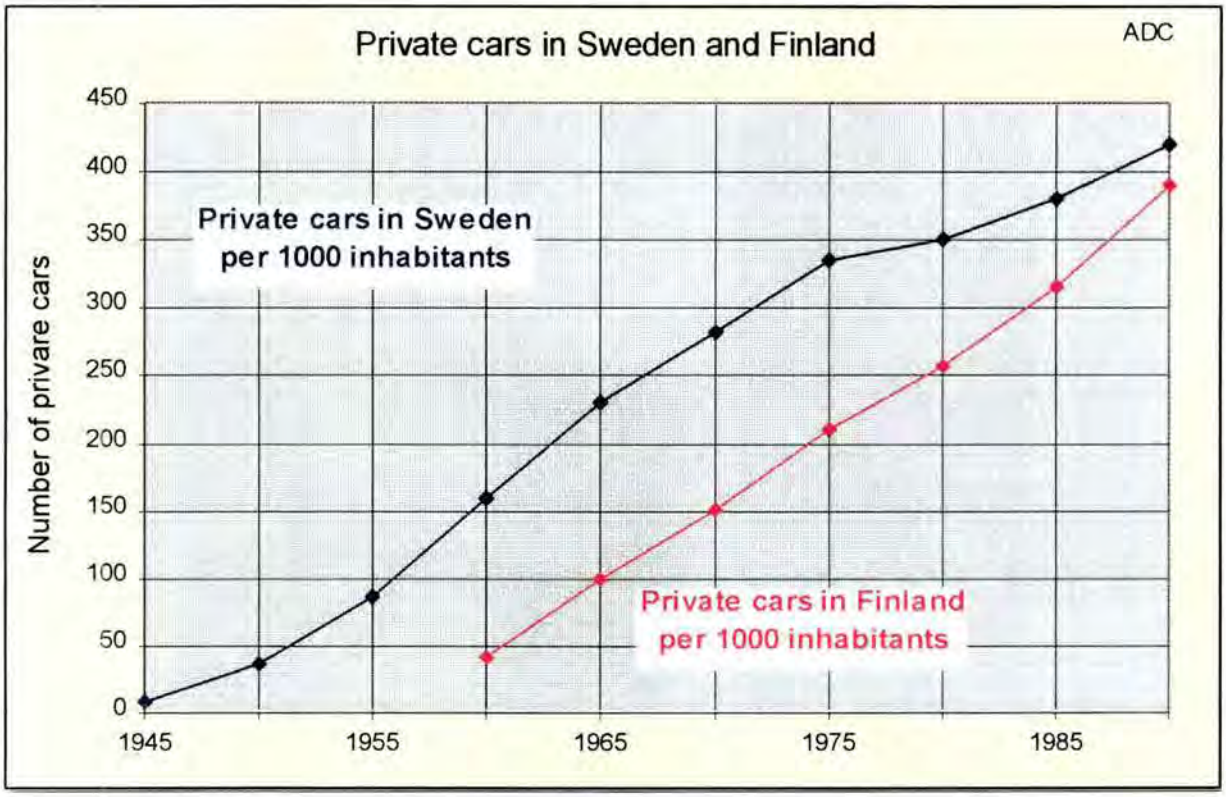

In April the ship was taken to Aalborg Værft, Denmark, for refurbishment and necessary rebuilding. The ship was renamed as *S/S Viking* and the line was inaugurated in *June 1 1959*. The route was Gräddö (Sweden), over the Åland Sea - Mariehamn (Åland), through the Åland and Turku archipelago - Korpo (an island close to Turku with road-connection to mainland Finland). About the time for the introduction Mr. Algot Johansson, managing director and founder of Rederi Ab Sally, Mariehamn also joined the project. He had a strong belief in the new connection over the Åland Sea.

The monopoly they had created lasted 5 days. The shipowner Carl Bertil Myrsten, Rederi AB Slite from the Swedish island Gotland then introduced M/S Slite on the route Simpnäs, Sweden - Mariehamn, Åland. Instead of using the ship on the intended line Klintehamn, Gotland - Grankullavik, mainland Sweden, M/S Slite started to compete with S/S Viking.

M/S Slite was originally a dry cargo coaster of 950 tdw, built 1955 at the Sölvesborg Yard in Sweden. The ship was converted to a Passenger/ RoRo Car/Ferry . The arrangement was simple, a side ramp for cars on deck, and reclining seats and a bar for the passengers in the cargo hold.

The above competitors formed later on the joint marketing company Viking Line, for the three shipowners, Rederi Ab Sally (Algot Johansson, Henning Rudberg), SF-Line (Gunnar Eklund) and Rederi AB Slite (Carl Bertil Myrsten). A duopoly situation developed soon between this formation and what later on should be The Silja Line. The competitor Silja Line was formed by Bore Line (Turku), EFFOA (Helsinki), Rederi AB Svea (Stockholm) and the jointly owned Silja Rederiet (Turku) i.e. "The White Ships".

In this overview we will not go into the internal formations of the groups and to simplify, the groups will in the following just be called Silja and Viking Line.

In comparison with The White Ships, S/S Viking and M/S Slite were not impressing. Although the very introduction of the new service was a bit shaky the traffic very soon generated growing and stable profits. Already the second year in service (1960) the Viking Line transported 30% of the passengers, 60% of private cars and 100% of the trucks.

Silja Line couldn't deny that the new conceptual solution was a threat. Their philosophy that passenger and cargo traffic should be separated had to be revised. It wasn't a pleasant prospect that their passengers should be forced to go with "the newcomers" if they wanted to bring their car. It was however considered as a comfort that the loss of passengers market share was caused by a lot of new passengers that later on should hopefully realise that it would be worth while to spend some more money on the journey for the standard that Silja Line offered. The owners within Silja Line had previous long experience of project development. The technical departments had already for some time been studying RoRo-ferry concepts. Now they were assigned to develop a concept that should restore Silja Line's market position. In May 1961 M/S Skandia was delivered from Wärtsilä Ship-Yard and in May the following year the sister ship M/S Nordia was delivered to Silja Rederiet. These ships were the first purposely built Passenger/ RoRo Cargo/ Ferris for the trade between Sweden and Finland.

The development of the traffic

The diagrams below describes the development of the traffic between Sweden and the mainland of Finland from 1960 to 1994. During the following 30 years from 1960, the number of:

- passengers grew from about 500.000 per year to about 7.500.000 +1.400%
- number of private cars from about 30.000 to about 600.000 +1.900%
- trucks from about 900 to about 140.000 +15.500%

During the same period, in addition to above figures, passenger cruise traffic in the area and traffic to/from Åland has grown substantially.

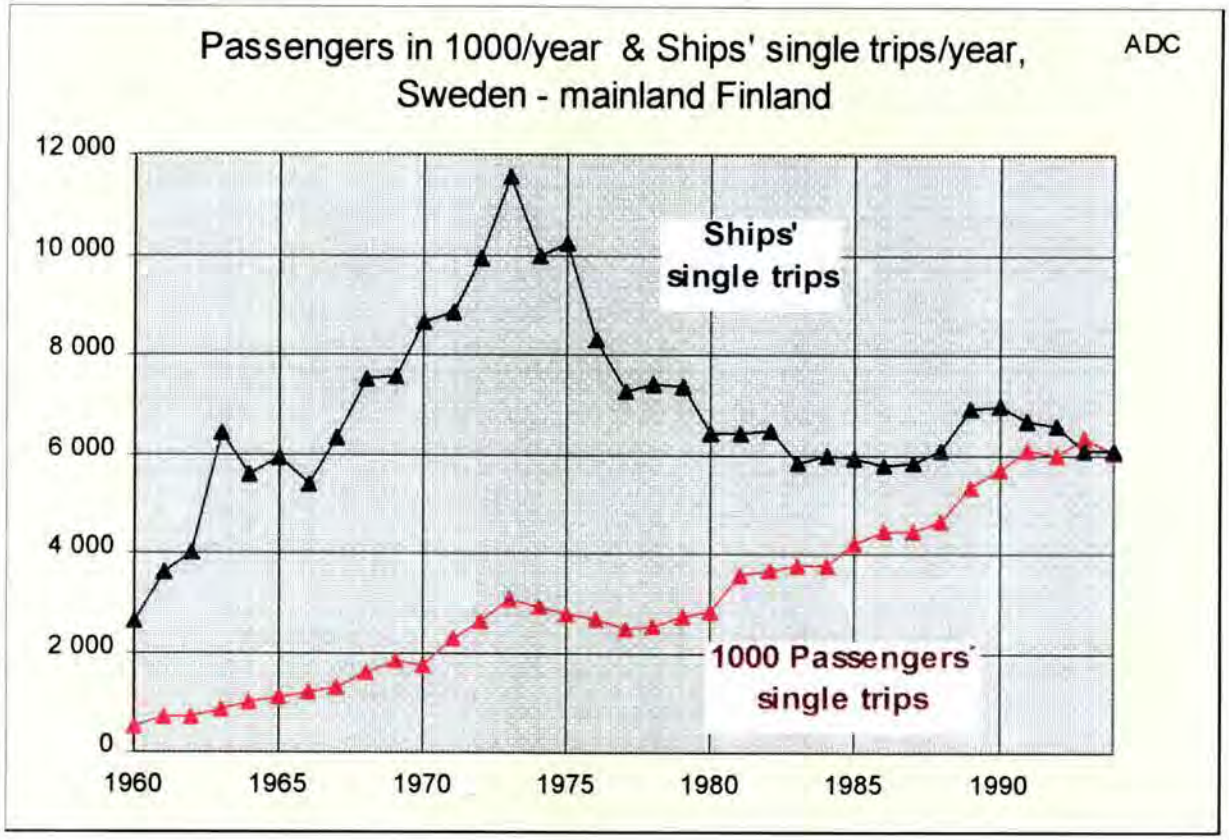

The number of passenger single trips exceeds today the entire population of Finland. The population in Finland is about 5,0 million people. The portion of passengers from Sweden, Finland and other countries varies with time and route. Today however the Finnish passengers are in majority.

The diagram also shows that the number of ships' voyages culminates in 1973. Although the number of passengers grew, from that year the number of ships voyages have decreased and is now stabilising.

The reason is, competition has forced the traffic to be rationalised. Fewer and bigger ships made more transport work. This is not just an effect of economy of scale. The operators have also expanded their market by introducing new commercial concepts.

When this traffic began in about 1960 nobody could foresee the development. Required transport capacity had until about 1970 been covered by employing more ships in the trade. The ferry service began to play an increasingly important role for transportation of industrial goods and merchandises to/from Finland. The exp./imp. between Finland and Sweden (+transit W.Europe) was increasing. On the same time the way of transporting changed. Trucktransportation became increasingly frequent also for long distance transportation, rail-roads had difficulties to offer the required service quality. The different track width in Finland and Sweden discriminated also, at that time, the development of rail-road transportation. (Today there are two lines with rail-road services in the trade.)

The demand for improved service quality of the ferry transports also constantly increased. In the winter 1965/66 M/S Apollo maintained winter traffic on Kapellskär - Pargas. Earlier the traffic had been interrupted when the ice had been too difficult. In 1971/72 Silja Line continued the traffic during the winter on the Stockholm- Helsinki route. This was a test made with S/S Svea Jarl. The following winter 1973/74 Silja Line could offer the market a substantially improved service on the Stockholm- Helsinki Line by introducing the newbuildings M/S Aallotar and M/S Svea Regina. These ships, as well as M/S Apollo, were ice-strengthened to Swedish/Finnish ice class 1A. The ships had for that time, the impressive engine power of almost 12.000 kW (Maximum Continuous Rating) for forcing the ice. M/S Apollo had 5.880 kW. The ships were Passenger/RoRo Cargo/Ferries. The logistic transport infrastructure between Finland - Sweden (W.Europe) had improved a lot also on the Helsinki Line. The trucker could now offer door-to-door transports around the year.

It was important that the trucker could control the whole transport chain by having the same truck and the same driver all the way. When the ship carried the truck over the Baltic the driver got a proper rest.

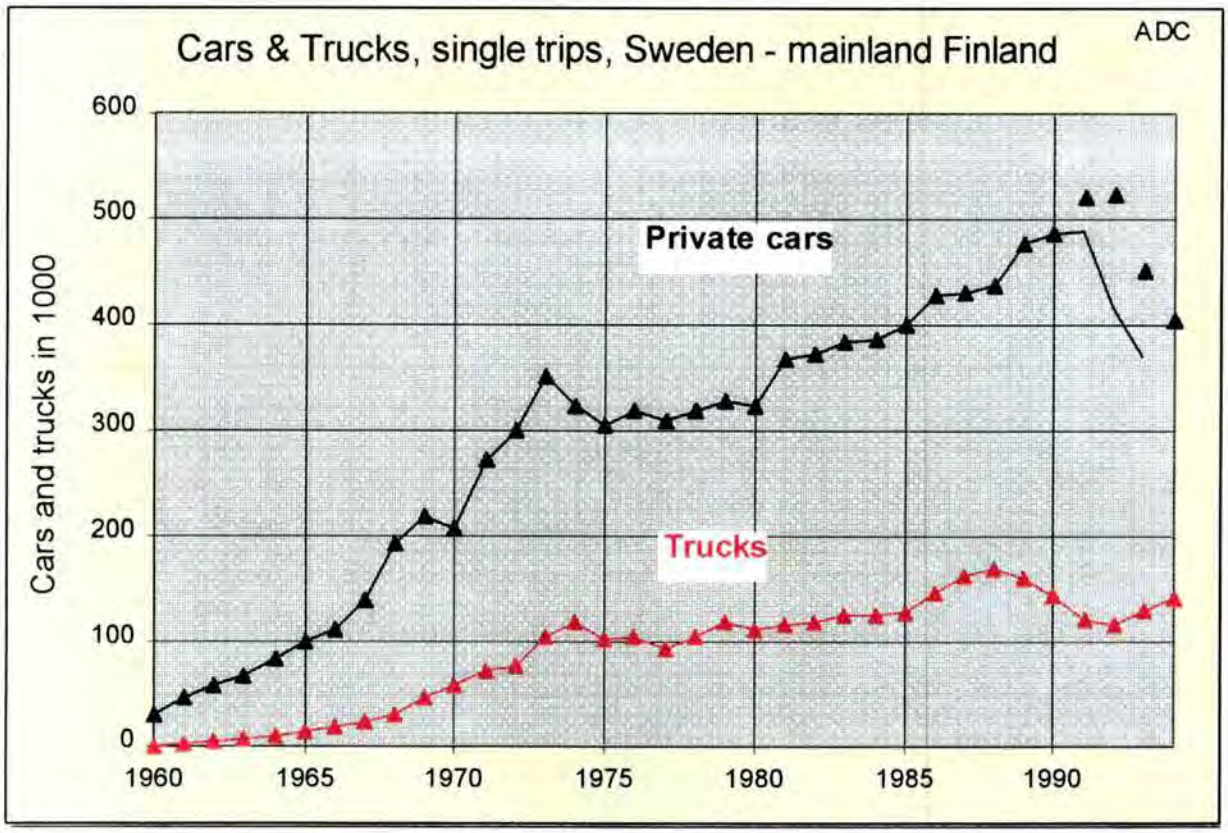

The diagram also shows a substantial increase of private cars. The combination of private cars and rolling cargo showed to work. In vacation periods when the trucking activities were low, space was available on RoRo-deck for private cars.

The increased number of ships in the trade was also the result of an escalating competition. In June 20 1973 Viking Line started a service Stockholm - Mariehamn - Turku i.e. in direct competition with Silja Line. In 1974 Viking Line also started to compete on the Stockholm - Helsinki route.

The fight for market shares

The two competitors approached the market in different ways. Silja Line followed their tradition to develop quality concepts. More and more specially designed newbuildings were delivered. Encouraged by what seemed to be the never ending success, Viking Line ran for capacity. Regarding the cargo Viking Line also aimed for quality. The different approaches reflected the dissimilar structures of the competitors. Viking Line was built on equal effort from the participating owners. This encouraged capacity grow, if one owner introduced a ship the others should also respond with the corresponding capacity. Silja Line on the other hand had a pool arrangement with economic compensation for efforts and profit charing.

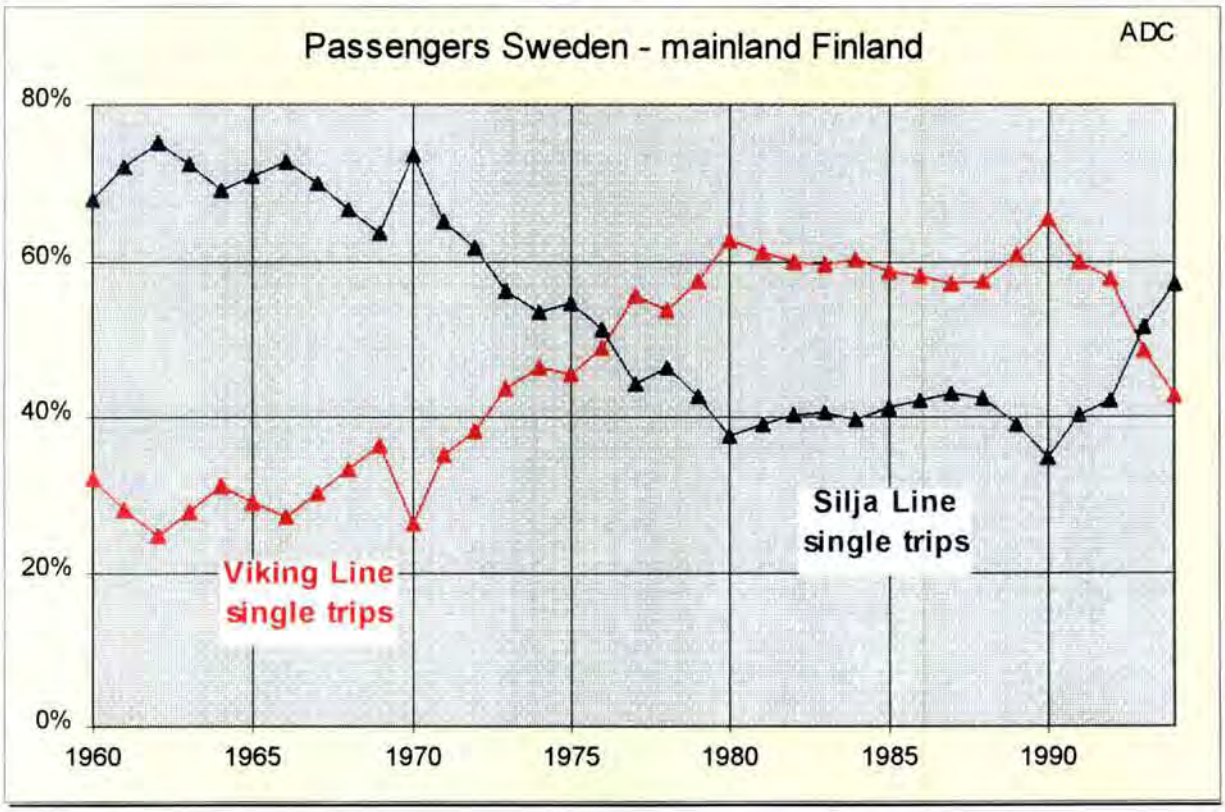

Although Viking Line almost immediately succeeded in gaining 30% of the passengers, Silja Line could defend their majority position until 1975. By chartering ships and an extensive new building-program Viking Line then took a bigger share than Silja Line. On the other hand it was some comfort to Silja Line that they could maintain somewhat higher prices for their services.

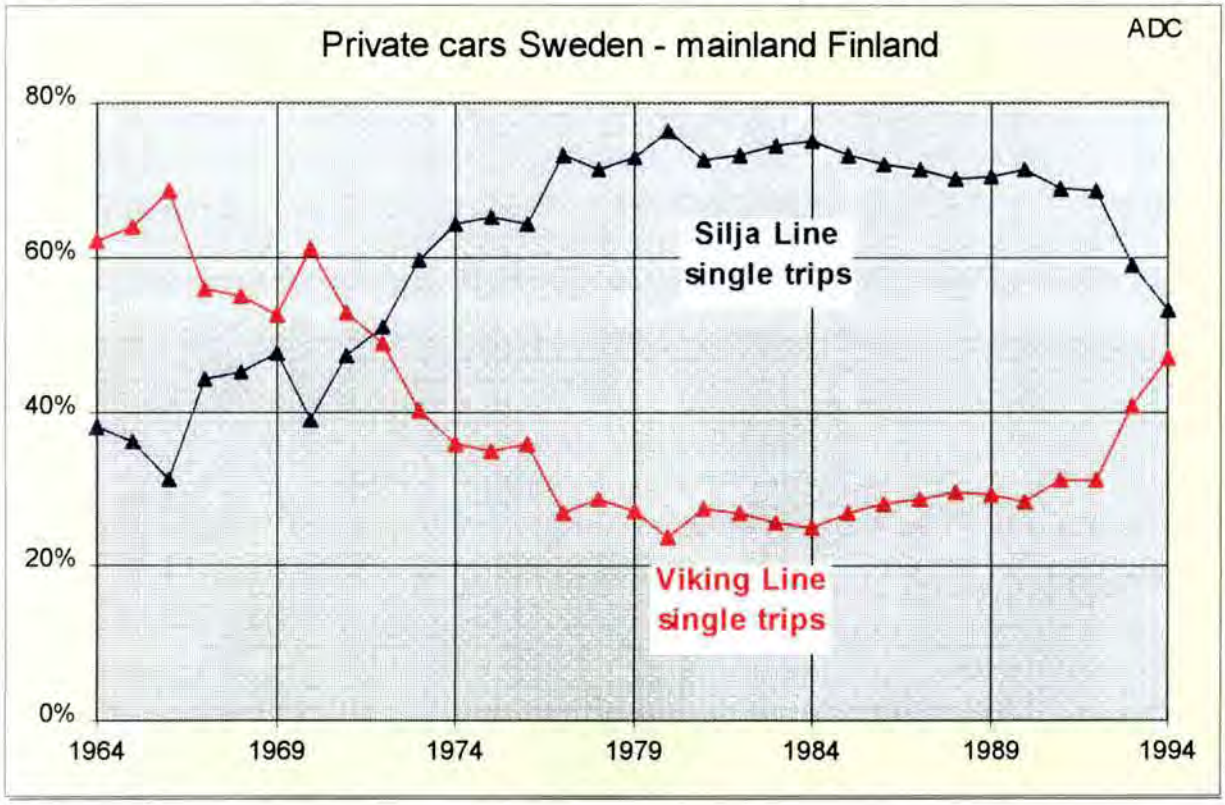

Viking Line got the initiative in the market of private cars. As seen in the diagram it took some time until the Silja Line passengers brought their cars over the Baltic. An explanation is that in the beginning the passenger with car selected the most affordable alternative for the transport. Later on the price for the car became less important for the customers choice of transport alternative. If the car was needed it was neither complicated nor expensive to bring it with on the ships.

When Viking Line started their traffic they surprised Silja Line with their cargo carrying capacity. The statistics in the enclosed figure doesn't reflect the substantial cargo carrying activity going on by pure cargo ships managed within the sphere of Silja Line. Silja Line however, regained soon a leading role as carrier of cargo also in the passenger ferry service. This was accomplished by introducing the purposely built Passenger/ RoRo Cargo/ Ferry M/S Skandia in 1961. Thus taking back the initiative for some years. The owners of Silja Line were in the beginning running RoRo cargo ferry services in parallel with the passenger service, since they considered that they complied better with the requirements of the market in that way. A reason was the difficulties to arrange a time table that was attractable for both passengers and cargo. It was also an inertia built in as the transport systems for cargo was there and had so far worked satisfactory. From mid 70's until late 80's Viking Line was however a bigger cargo carrier than Silja Line. A reason to that was their higher cargo carrying capacity over the Åland Sea.

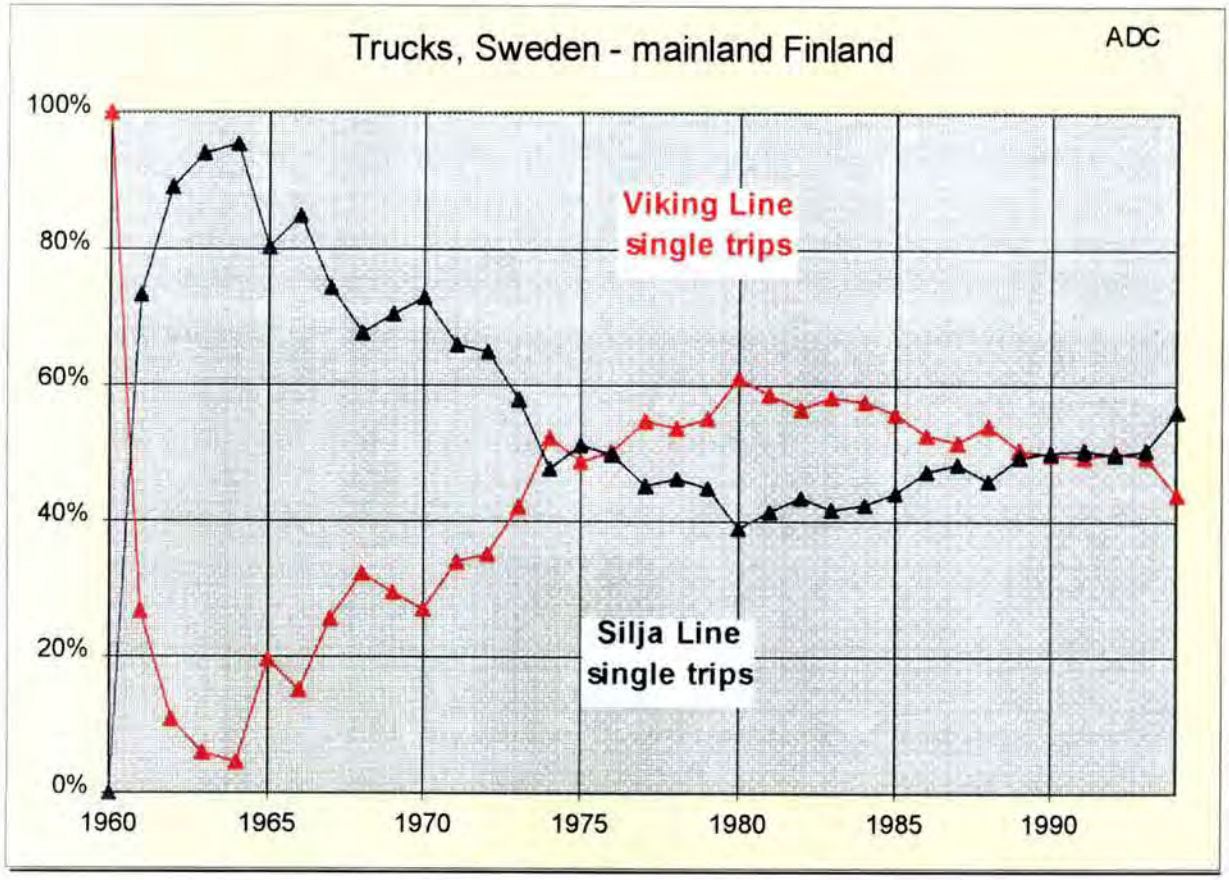

Today all the diagrams of market shares converge momentarily to a 50/50 relation. The differences in capacity and product have diminished by the introduction of the so called Super Ferries. In 1992 the trend of growing passenger market was broken by the recession in Sweden and Finland. In addition to that the Estonia catastrophe suddenly changed the passengers attitude to the traffic. The instant loss of passengers caused by those two factors acting simultaneously, had never been experienced before in this traffic. By reducing ticket fairs the number of passengers has been restored, but still the economic result is not what it used to be.

Economic factors

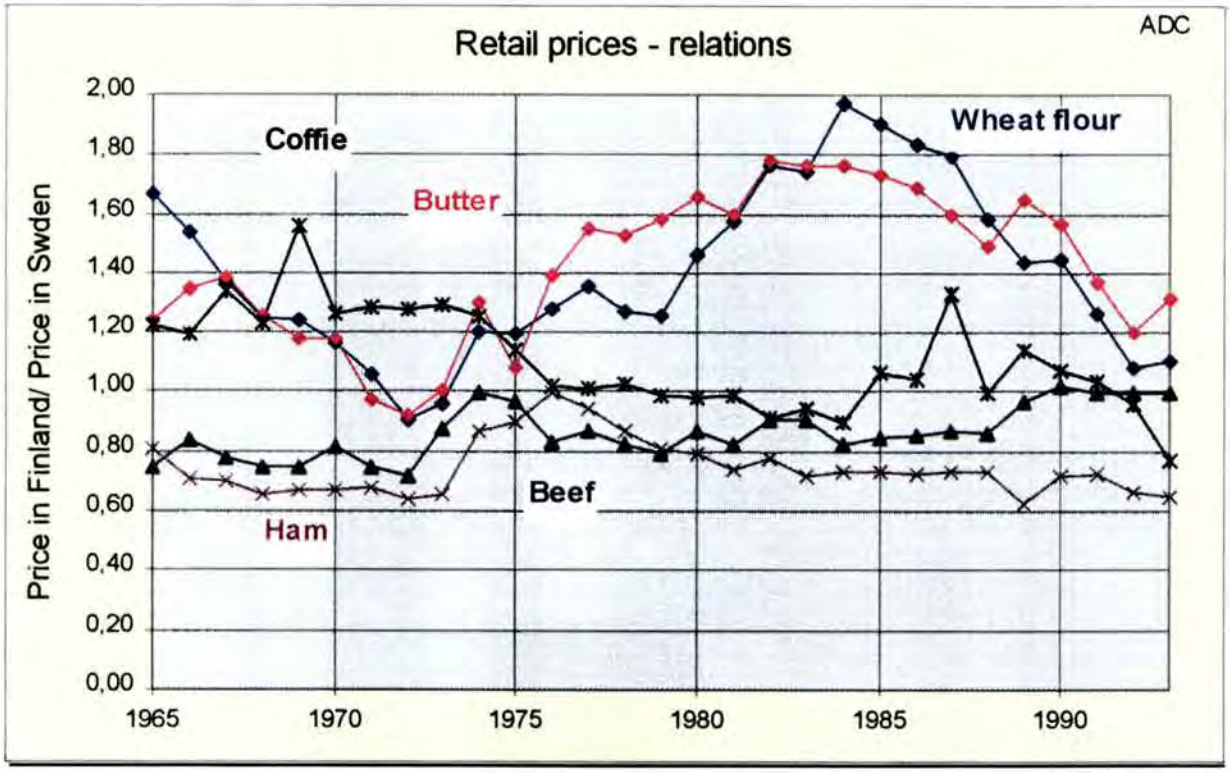

Explanations to the development are primary found in Finland and not so much in Sweden. Although this RoRo/Passenger traffic was started in the Åland Sea, the driving force in the traffic has been the development of the Finnish economy.

The traffic over Åland Sea between Sweden and Åland was elementary. The business idea was to make it easier to bring private cars between Sweden and Finland and to explore border trade. Border trade, meat and tax-free, soon made the traffic popular in Sweden. The Finnish people on the other hand were attracted by the low price of coffee and fruit-syrup in Sweden.

Fluctuations in currency exchange rates stimulates travelling in one or the other direction all the time.

When the traffic grew other economic factors got increasingly important. One was the "the big neighbour in East", Russia, that always had influenced the conditions in Finland.

When this traffic started, Finland was from transport point of view blocked Eastward by the Soviet union. Conventional ships' services connected Finland with the rest of the world, including Sweden. The constantly increased integration of Western industry and trade made rational transports an important factor in the competition. Rail-roads and conventional shipping services had difficulties in offering the quality standard required by high valued cargo (merchandises, semi-manufactored products etc.). On short and medium distances door-to-door truck transportation in combination with the RoRo ferries could offer the required service quality. In this case quality was expressed in terms of reliability, flexibility and short transit times.

Thus a major infrastructural obstacle for the development of the Finnish trade and industry was solved by the frequent RoRo services over the Baltic Sea. Finland got by time a very reliable connection with Sweden and N.Europe.

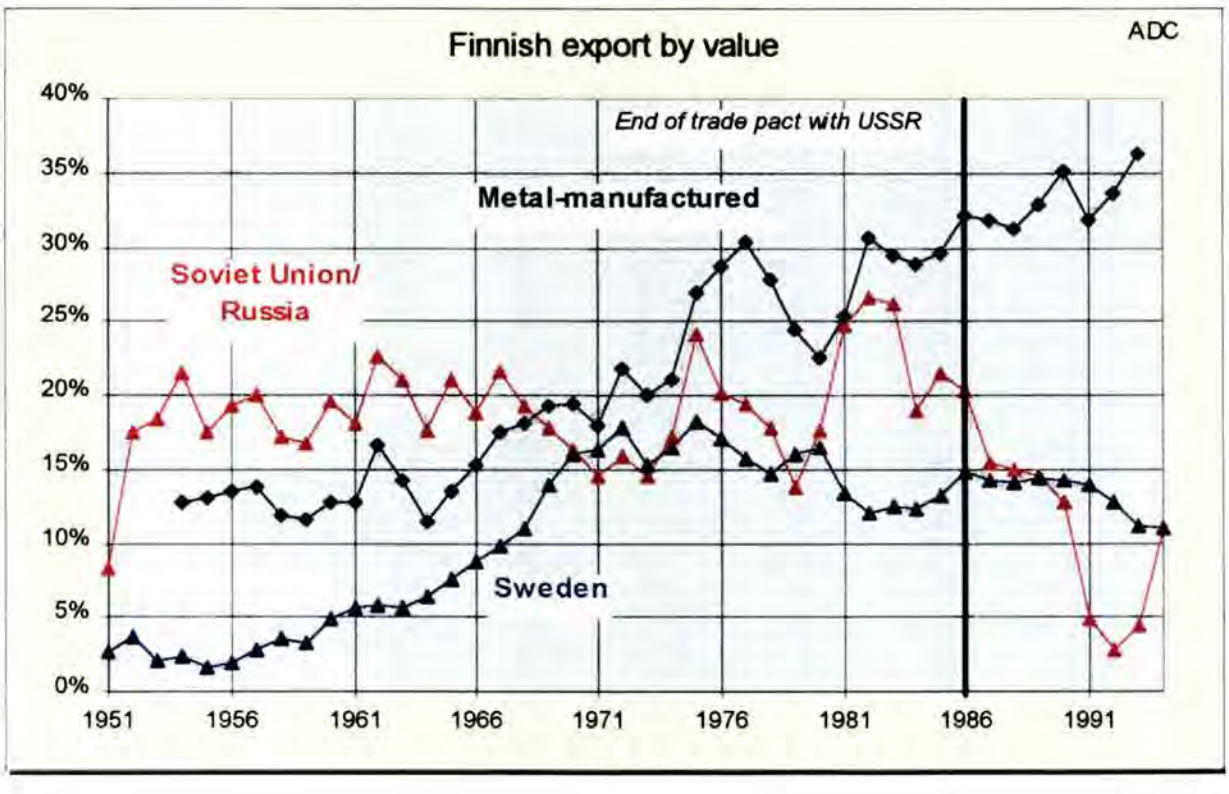

The diagram "Finnish export", shows how the trade grew with Sweden during the 60's. Then the industrial activity of Finland continued to increase. The Swedish share in % of the total volume declined however somewhat when other markets grew faster.

The diagram "Finnish export Soviet Union and Sweden excluded" on page 20 shows that Finland has an extensive trade with other countries than their close neighbours (60- 80%), still though most high valued cargo pass to/from N.Europe via the ferry services between Finland and Sweden. In the last decades export from the Finnish forest industry represents increasing values.

The increase of the truck fleet reflects to some extent the increased demand for flexible transports, but also the increased transport work that the highly specialised industries required.

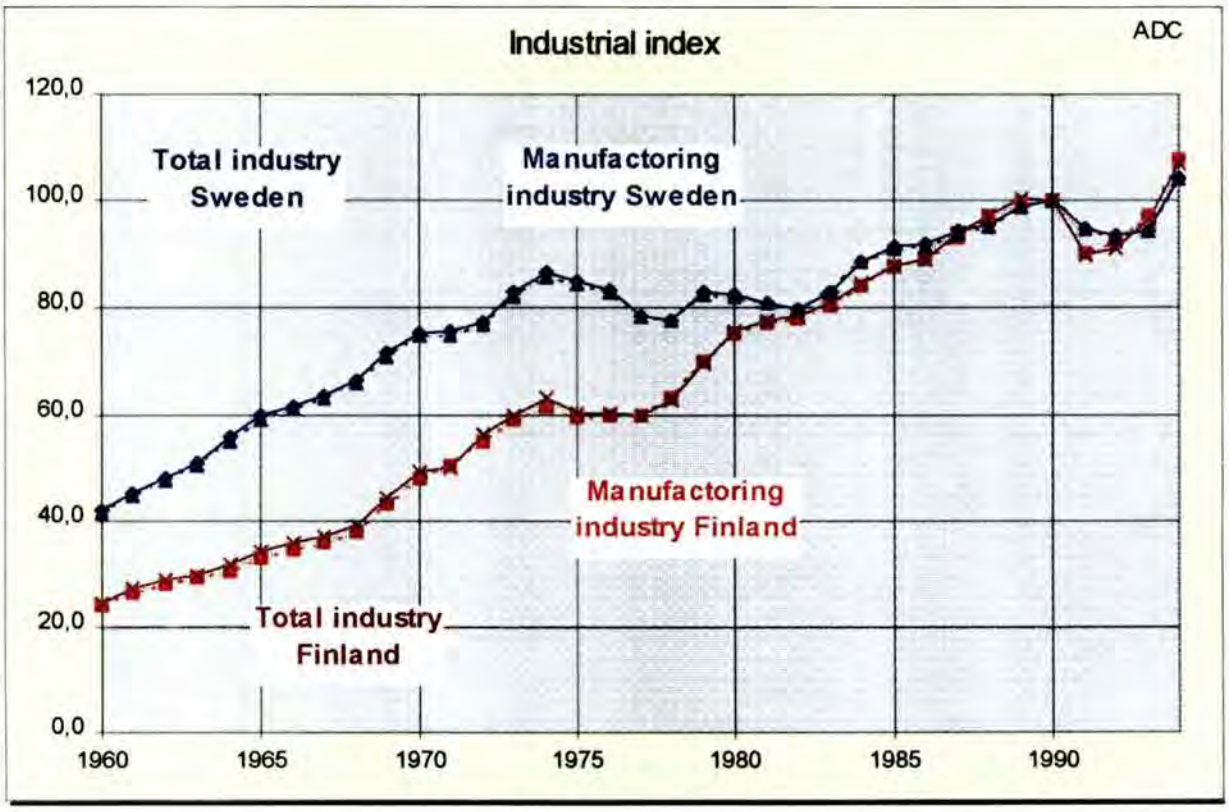

Industrial index (100% 1990) shows that industry in Finland had a faster expansion of the industrial sector than Sweden during the period 1978 to -82. During this time the quality of the transport service also improved a lot. In 1981 the reliability was close to what it is today.

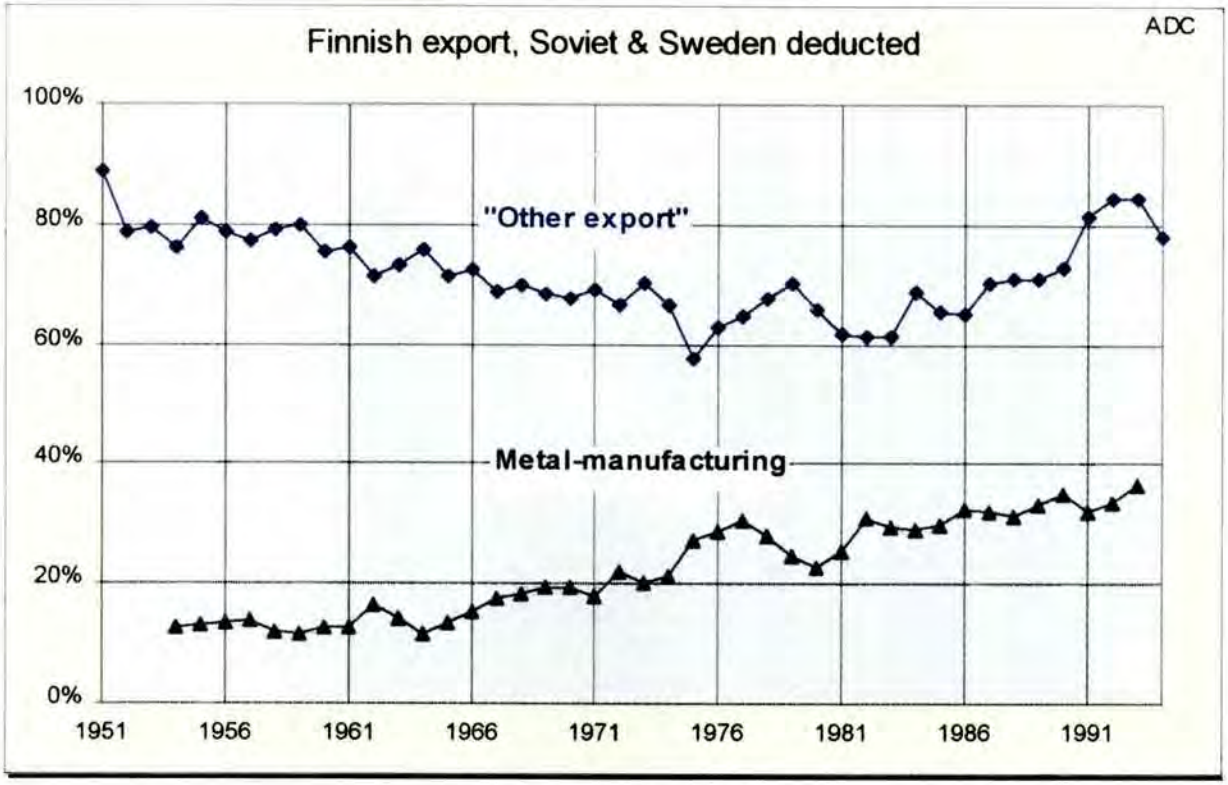

With the expansion of industry followed increased GDP. Sweden used to be ahead of Finland until today when GDP/person is practically the same for the two countries.

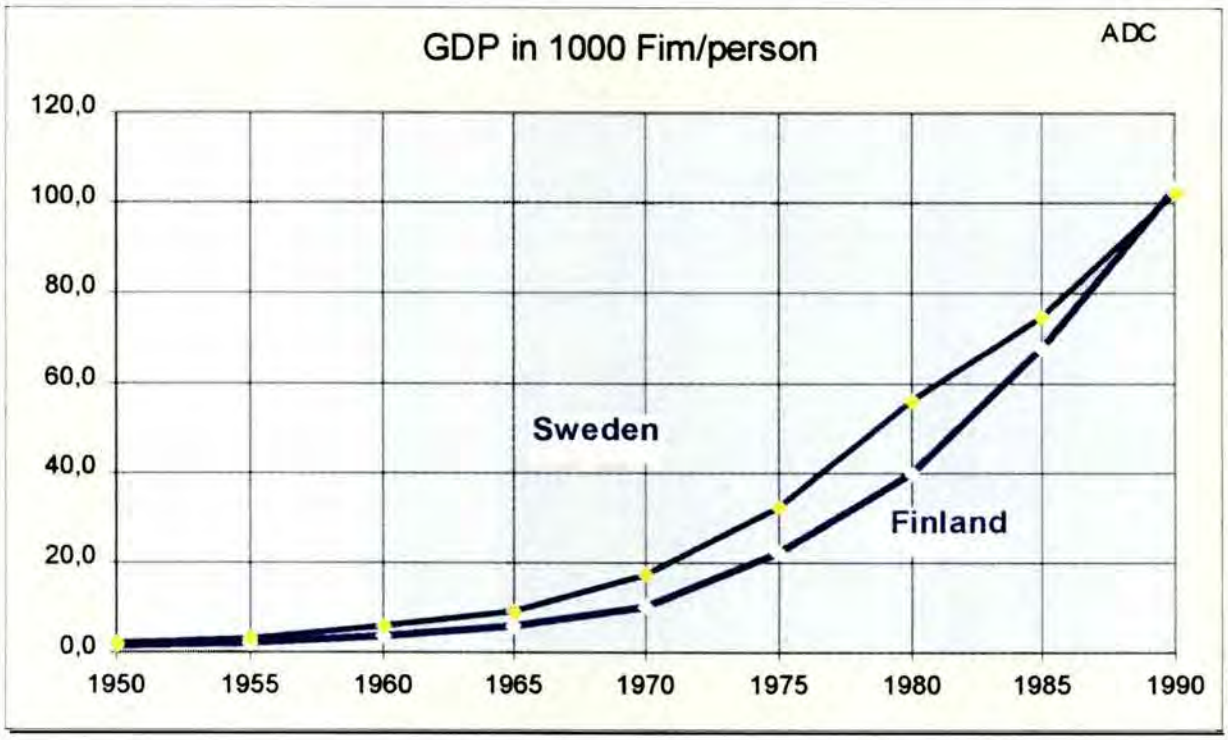

Private consumption expenditure /person shows a synchronised development curve.

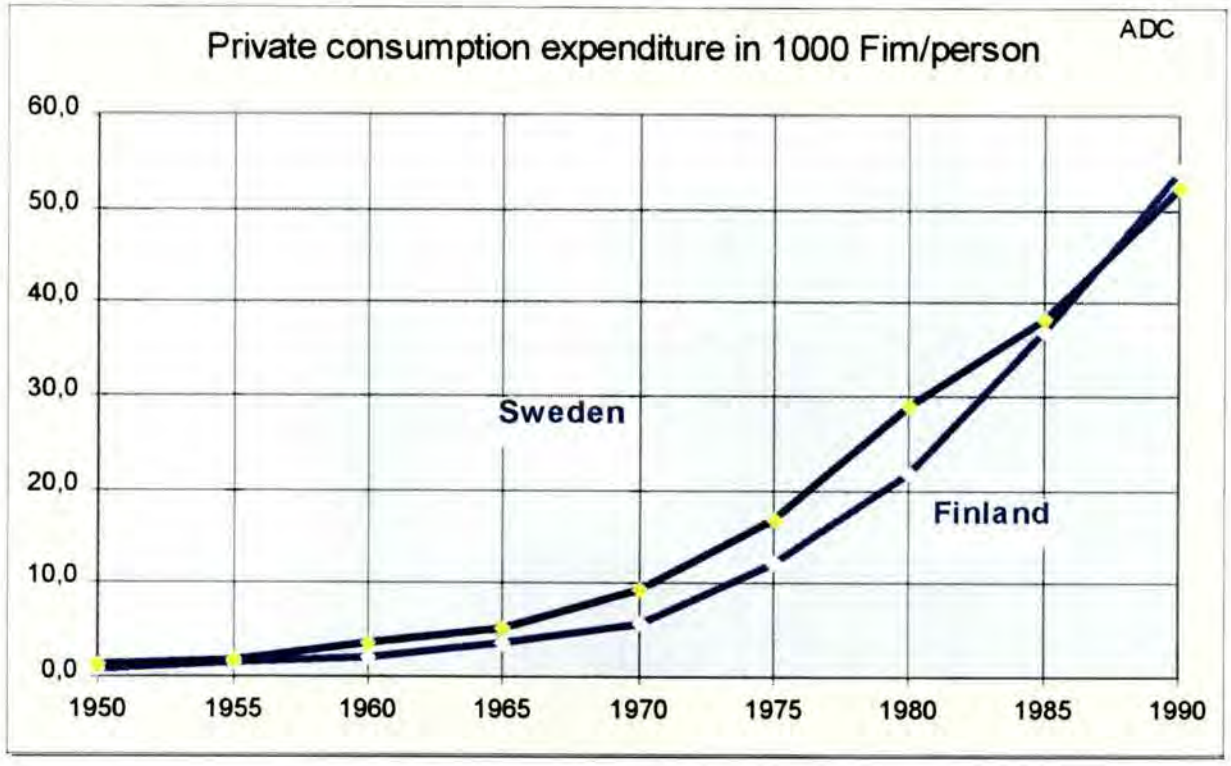

Improved standard of living in Sweden and Finland in combination with prices within reach encouraged travelling. The lower price offered by Viking Line was a good supplement to the more expensive Silja Line standard. Though competition was hard there was a market for both lines.

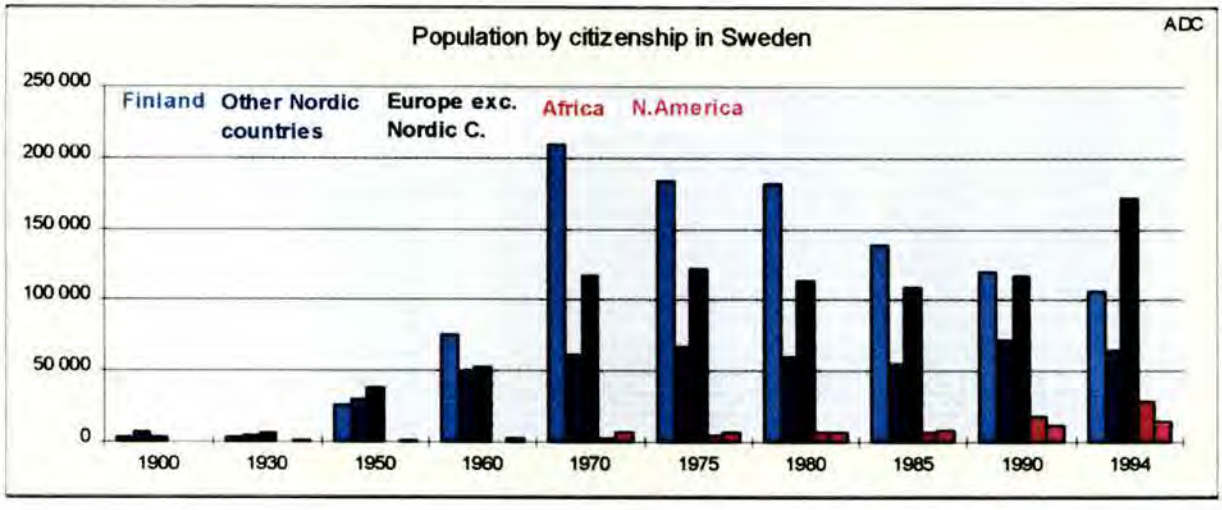

The Finnish colony in Sweden has always been big. Today the first and second generation of people originating from Finland living in Sweden is 443.000 persons. The improved ferry services made it much easier to see relatives and friends in the other country. Despite the big capacity the journeys before and after big holidays have to be booked long time in advance. Travelling to see relatives is however going on all the days of the whole year.

With the increased living standard, leisure trips for one or a couple of days to the other country became more frequent. The scheduling made it also possible to arrange attractive programs for tourist trips.

Taxation of tobacco- and alcoholic products in the Nordic Countries is high. To attract passengers by the low onboard tax-free prices was a part of the original business idea of Viking Line. Though tax-free still is important for the traffic, this argument has weakened by time and due to both countries membership in EU. Tax-free may be enjoyed in the future by including calls in Åland or Estonia. In Finland Estonia appears to be the new destination for tax-free travelling. Thus the Lines have for some time tried to focus on other attractions in order to maintain passenger volumes in the future.

Since 1960, almost every family has access to a private car, diagram page 9. When visiting the other country it was very convenient to bring the car onboard the ships. If the start and/or the end of the trip was not close to the ferry terminals this was a competitive alternative.

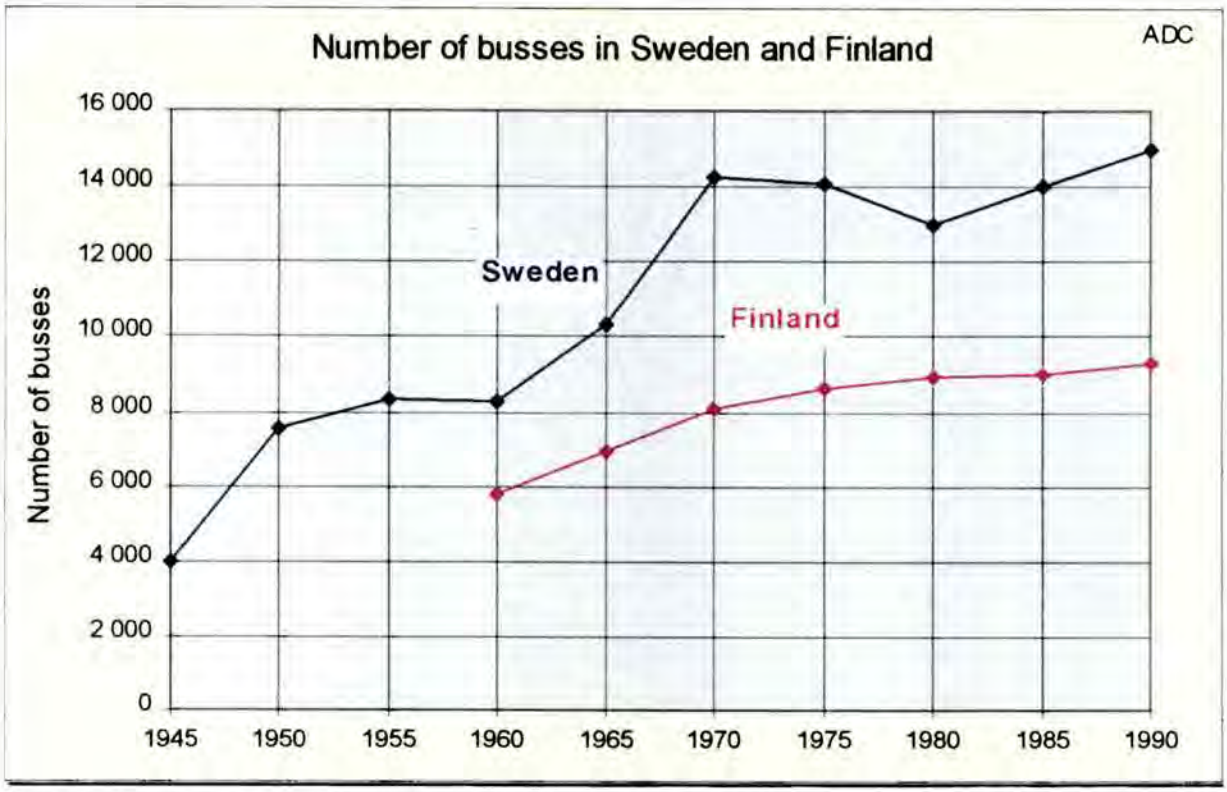

To travel by car became thus a common alternative. To bring the car on a ferry to Sweden and go further south in Europe became also an attractive alternative for the people living in Finland.

For those who didn't use a car various bus-trips were arranged in the neighbouring country.

Conceptual development

Almost all curves in the above diagrams show an upward trend from 1960 until today. The introduction of further developed passenger/ RoRo-cargo concepts has had good timing. Keeping in mind the difficulties to foresee the future, many great initiatives have been taken by the ship owners when building up this traffic.

An important factor for reducing the economical risks have been the circumstance that these ships have been attractive on the second hand market. The average life time of a ship in this trade used to be about seven years. After service in this trade the ships could in general be sold for the purchase prise. Thus the costs for the huge investment finally were relatively small. For many years the ships worked like gigantic saving boxes. Today many claim, that this rule is no longer valid with the huge capacity of a Super Ferry. This has been said before and it remains to be seen if the second hand market, once again, has grown to also receive the Super Ferries.

The competition between the two lines made it important to react quickly on market signals. The owners were also motivated and able to adopt new conceptual ideas. Thus the tonnage was replaced frequently, ships were often rebuilt even when still in service. By that more or less constant modernisation took place. New functions and conceptual ideas were tried out and refined in a high tempo.

The owners tradition and competence and the advantage of easy access to a supporting infrastructure of marine expertise in the region were important key elements for the development. The Lines developed the concepts they believed attracted their targeted market. Silja Line defended by tradition the upper segment of the market and had the initiative in conceptual development in that sector, while Viking Line concentrated on concept that could attract ordinary people.

Silja Line aspired to a quality profile and Viking Line focused on ordinary people's value for money. This was also reflected in the organisations of the lines. Silja Line made more internal development work than Viking Line. Although Viking Line introduced new concepts for the trade they could in general enjoy a more relaxed position by monitoring the outcome of Silja Line's novelties before they made up their mind.

The shipping industry, shipyards and subcontractors, realised soon that this traffic represented a big and quality conscious market. Thus the lines were offered developing resources, in general free of charge. Even if several first class shipyards in the region closed down in the early 80's, the network of first class makers still remained in the area and N.Europe still is the centre in the world for building high class cruise ships and passenger ferries.

In the beginning of the competition the activities of Silja and Viking Line were quite different. Silja Line was the traditional carrier in the trade. Viking Line focused on developing an economical and uncomplicated transport alternative by rolling cars on and off the ships and transport deck-passengers. It wasn't considered necessary to offer the passengers cabins during the trip. Soon however, due to competition it became necessary to arrange cabins for truck drivers.

Silja Line's idea was that the RoRo concept had to be combined with cabins of high standard and first class service for the passengers. By time the differences in prices and concepts of the two lines have diminished and today many have difficulties to see the differences.

Commercial concepts

The requirements have changed over the years and so also the response from the Lines market's. From the beginning the new-buildings have been purposely built in order to fit the particular market profiles of the Lines. Even though the ships accommodated several different commercial functions simultaneously, this shall not be associated with the *multi purpose philosophy* sometimes practised by ship owners who want to have the option to use a ship in alternative trades.

Passenger transport over The Åland Sea and the possibility to facilitate the transport of a car between Sweden and Åland/Finland were the primary objectives when Viking Line started. In the beginning border trade was important and e.g. the low coffee price in Sweden (see diagram page 17) generated numerous Finnish passengers for Viking Line. The main purpose was however to offer an uncomplicated transport alternative between the countries which could also be used by ordinary people for leisure travelling. Consequently the commercial concept was simplified.

In about 1970 Viking Line offered the same bed capacity as Silja Line, "calendar" page 27.
To improve the passengers appreciation of the trip high qus a superior alternative compared with the li

market response on the new transport alternative introduced by Viking Line showed clearly that the market was elastic i.e. the right transport product generated more traffic. With more traffic the lines could use bigger ships and get benefits from economy of scale and then offer more competitive products to the market, and so on in a happy spiral.

The development in the countries created new demands on transports and the supply of transport services in the trade grew synchronously with the demand.

Silja Line was traditionally the main provider of sea transports between the countries. The option to bring a car on the passenger ship was for them in the beginning more a service than a sales point. Their passenger concept had then similarities with what was offered to travellers on the Atlantic Liners between Europe and USA; good cabin standard, excellent food- and service concepts and sometimes passengers were even divided into different classes.

Silja Line responded rapidly to Viking Line's introduction of the RoRo concept. In May 1961 Silja line introduced the first purposely built Passenger/ RoRo cargo/ Ferry in this trade, M/S Skandia. The next year the sister ship M/S Nordia came. Silja Line had noted the "newcomers" almost immediate success during the summer. On December 23 the same year (1959) the order of M/S Skandia was signed with Wärtsilä shipyard in Helsinki. The entire freeboard deck was reserved for truck- and car transportation. With hoistable car decks the cargo deck got two functions, increased deck area for private cars in high season and enough height for trucks in low season. In summertime the ships made so called double trips, a round trip in 24 hours, calling the ports of Norrtälje - Mariehamn - Turku. The service speed 18 knots made the time in port short. Consequently a drive trough solution with stern- and bow ramps was arranged for the cargo handling. This was also a convenient solution for the drivers, the frequency of damages to vehicles also showed to be low.

The number of passengers, 1000 persons, was impressing and still is when comparing with todays some 2500 passengers of a Super Ferry. There is however a big difference in standard. The reclinable seats for resting was at that time an appreciated standard for passengers travelling with M/S Skandia. Today most passengers have a private cabin on night trips. In the mid 80's Silja Line took the decision to not accept deck passengers any longer on night trips.

"Silja- and Viking Line" Calendar

	Birger Jarl	1959	(Viking (0), Slite (0))	
	SS Bore	1960		
	Skandia (106)	1961	(Boge (0))	
	Nordia (209), Svea Jarl (250)	1962		
	Ilmatar, Floria (cargo only)	1963	(Ålandsfärjan (0))	Kapellskär
		1964	Apollo (0) (Drotten (72))	
	(Holmia)	1965	(Visby)	Winter traffic Kapellsk. Pargas
Silja to Värtan	Fennia (296)	1966		
	Botnia (162)	1967	Kapella (120), (Visby (245), Stena Baltica)	
		1968	(Viking 2 (0))	
		1969		
New name: Silja Line	Floria (186)	1970	Apollo (222), Viking I (206), Marella (172)	
		1971		
Winter traffic Stockholm-Helsinki	Aallotar (412), Svea Regina (412)	1972	Viking 3 (226), Diana (240)	
	Bore I (377) *The 1:st Oil Crisis*	1973	Viking 4 (198), Aurella (328)	New route for Viking Line '73 Stockholm - Mariehamn-Turku
		1974		New route for Viking Line Stockholm-Helsinki '74
	Svea Corona, Wellamo, Bore Star (810) (1175) (650)	1975	Viking 5 (410), (Viking 6 (432))	
		1976	(Apollo III (500))	
		1977	(Ålandsfärjan)	
	The 2:nd Oil Crisis	1978		
		1979	Diana II (828), Turella (750)	
		1980	Rosella, Viking Song, Viking Sally, Viking Saga (740) (1223) (1190) (1452)	
	Finlandia (1544), Silvia Regina (1544)	1981		
		1982	(Aurella (328), Ålandsfärjan (0))	
		1983	(Ålandsfärjan(0))	
		1984	(Ålandsfärjan(0))	New name: Viking Line
	Svea (1625)	1985	Mariella (2447), (Ålandsfärjan (0))	
	Wellamo (1937)	1986	Olympia (2333)	
		1987	(Ålandsfärjan (0))	
		1988	Amorella (2112)	
		1989	Athena (1712), Cinderella (2766), Isabella (2004)	
	Silja Serenade (2626) (Silja Star)	1990	Kalypso (2165)	
	Silja Symphony (2626)	1991		
	(3700) (2188)	1992		
	(Silja Europa, Silja Scandinavia)	1993		

Notes: Ships within brackets are not purpous built for the trade. Figures in brackets are passenger bed capacity

ADC Support AB
Stockholm 1993

The easiest way to travel by sea between the region of Stockholm in Sweden, and Southern Finland has always been via the region of Turku in Finland. On the alternative route Helsinki - Stockholm, due to the distance, the ships can make just one single trip in 24 hours. The Turku route therefore has a character of transportation, whereas the Stockholm - Helsinki route has more of the glamour of connecting the two capitals.

The ships following after Skandia and Nordia had in principal the same basic arrangement. The difference was the increased space requirement, improved comfort, more service and entertainment i.e. cabins, more private cars, more restaurants, shops and bars etc.

The key to the development of the traffic has been ability to offer attractive services in low-season. In high season for passenger traffic, about three months a year, the market is less sensitive to commercial concepts. In the beginning and the end of vacation periods some trips are peaking then the matter is concentrated to transport capacity. Due to this unbalance in demand during the year it has been economically necessary to make the ships more attractive in low season. The option to charter ships in high season has always been there but then supply of suitable ships to acceptable prices is very restricted.

In 1964 Viking Line got the first purpose built ship M/S Apollo. That was the first ship with ice breaking capacity in the fleet of Viking Line. Thus in the winter 1965 -66 Viking Line also opened winter traffic, Kapellskär (Sw) - Pargas (Fi). At that time the traffic had pure transport character, as late as in the early 70's both Silja- and Viking Line gave discount on weekend trips.

During the 70's serious competition between Silja- and Viking Line started. Then both lines received a lot of new-buildings and Viking Line opened new services on Stockholm - Turku, Stockholm - Helsinki in direct competition with Silja Line. In order to feed the growing fleets, both lines also started to build up relatively extensive marketing organisations. At that time weekend trips became attractive, consequently the prices on weekend trips increased and discount was instead given on weekday trips.

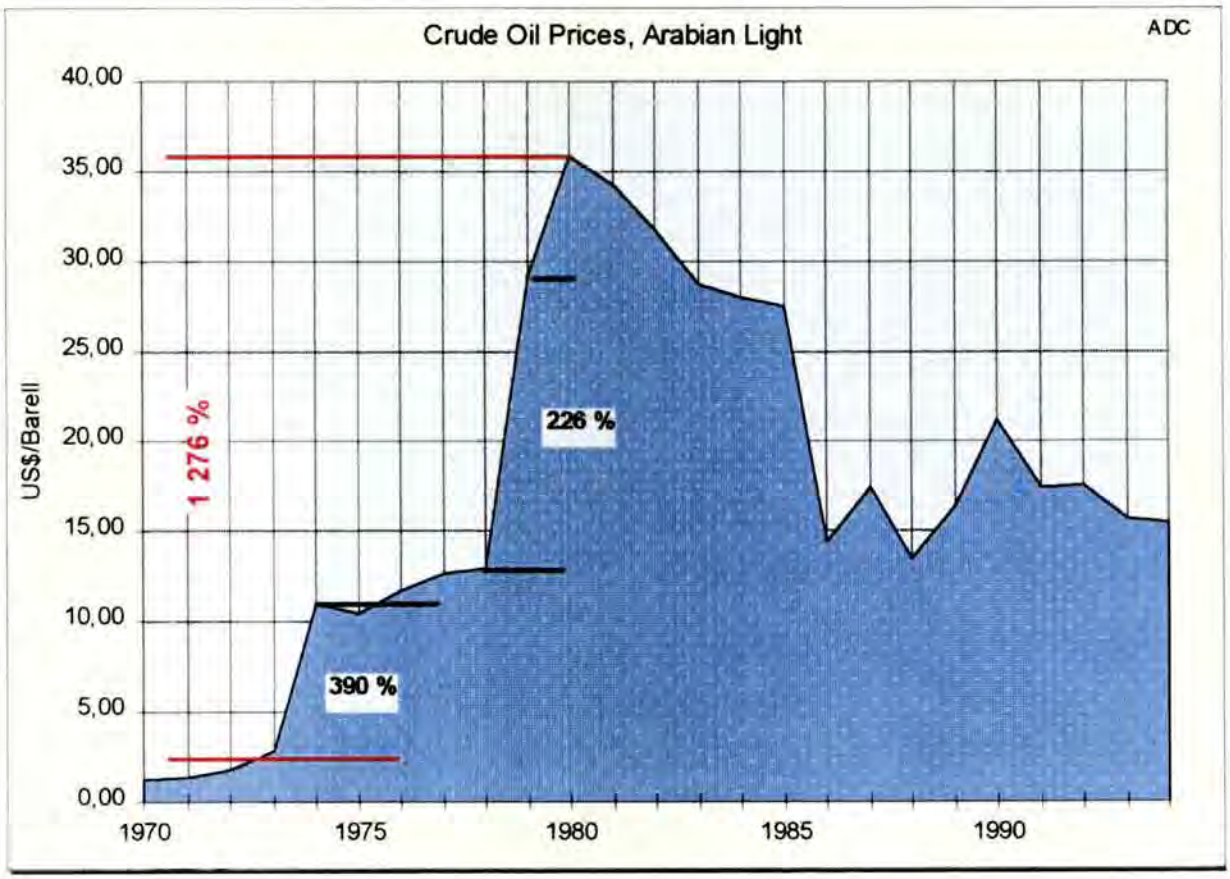

During the 70's oil crises chocked the shipping world, so also the ferry traffic. The first chock came in 1973 and the second in 1978. Cost for bunker was suddenly a strategic important factor in shipping. From 1973 to 1974 price of bunker increased with almost 400% and from 1978 to -79 with about 200%. All together bunker prices increased from 1973 to 1980 with about 1.300%.

Late in the 70's, discussions in Sweden started about "the right of participation in decision-making". Employees should be informed and give their views on important decisions for the company/ organisation. That created a lot of meetings. The discussion had roots in the unique Swedish tradition of educating adults. Federal support for adult education had existed for decades. A similar system was now built up to finance employees education in joint decision making.

These ideas were after some time combined with similar ideas from management schools, learning that management and employees should come closer and develop coordinated and motivated acting. The human resources should be developed. To implement such philosophies it was no longer sufficient with meetings in the offices, conferences had to be held. Such conferences required thorough preparations and in many cases the social off duty, get-to-gather, was the most important object of the conference.

Conference trips shall not be mixed up with group travelling. Such travelling has been going on all the time and there is no significant traditional difference between the countries with regard to group travellers.

Although occupancy rates of the ships were stable and high, the drastic increase of the oil price eroded the profits of the lines. There was however no serious sign of weakening markets for the traffic. The possibilities to increase prices were limited. In this situation there were two options, one was to go for economy of scale and the other was to improve occupancy rates in low seasons by making the ships more attractive.

Silja Line tried to combine that with the ships they received in 1975, two years after the first oil crisis, "The French Sisters". The three newbuildings were considerably bigger and such a high standard had never been seen before in this RoRo trade. With these ships conference centre was for the first time in the trade arranged onboard, 143 seats distributed on 4 conference rooms. Certainly meeting rooms had been arranged onboard before but then it had just been a service item. Now conferences with hostess service and conference facilities were tested as a business concept. Two years later in 1977, the second oil crisis came. This time Viking Line was active, six new ships were ordered. In the design, economy of scale were applied. Two ships were delivered in 1979 and four in 1980. Among these were **M/S Diana II**, delivered 1979 nowadays **M/S Mare Balticum** in the Tallinn - Stockholm trade, and **M/S Viking Sally**, delivered 1980, she should later on become **M/S Estonia**. Both ships had extremely short delivery time, less than one year. This can be compared with the two years that is normal. M/S Viking Sally was an enlarged version of M/S Diana II. M/S Viking Sally was about 15 meter longer and had a different superstructure that gave the ship a gross tonnage of 15.566 m^3, to be compared with M/S Diana II's 11.537 m^3. The engine installation and the hull form except for the bulbous bow was the same.

This massive introduction of new buildings aimed also to strengthen the market position of Viking Line against the competitor Silja Line.

Viking Line introduced conference facilities with the ships M/S Viking Song, -Sally and -Saga. This time however, the conference centre was a multipurpose area, in the evenings it was transformed to a night club.

Silja Line had three still relatively modern ships delivered in 1975. They took a cautious position and spent more time on developing their concept for the future. Two new ships for the Helsinki Line was ordered, M/S Finlandia and M/S Silvia Regina. With these ships the conference concept has further developed. The ships had a big "dining & dancing" saloon that should show to be a very good compliment to the conference centre.

The positive response from the Swedish conference market surprised most people in the trade. As a spill over effect conference groups also begun to fill up the meeting rooms that had always existed on the ships in the trade. The key to the Super Ferries was found.

Then the conference capacity was increased by retrofits on existing ships. In 1985 both lines received their first "conference" ships. Silja Line got M/S Svea for the Turku line and Viking Line got M/S Mariella for the Helsinki line.

The conference concept offered to the Swedish market was very competitive. Thus conference groups evened out fluctuations in occupancy rates over the year. The conference concepts was further developed to include exhibitions and even sometimes advancing to close to congress dimensions. At the same time cruise ferry concepts were developed. Some shares from the leisure market should also even out occupancy rates. This time also the market in Finland was addressed. This development resulted in the Super Ferries of today. Still though the ships provide a basic transport service between the countries. The various passenger concepts for low seasons made cost effective just-in-time transports possible. Thus this traffic has got the record of being the most reliable transport system in the region.

The Estonia catastrophe resulted in an immense loss of passengers on these routes. Conference groups disappeared almost instantly and still one year after, the big conference groups have not returned. Until recently conferences have been a typical Swedish activity but now the Finnish conference market is picking up and starts to use the ships.

Finally some about the cargo transport concept. Conventional RoRo ferries have served this trade all the time, thus balancing the flow of cargo. The economy of the RoRo Cargo/ Passenger Ferries is a symbiotic combination of three components 1/3 passenger tickets, 1/3 tax free and 1/3 cargo. The transportation of cargo has been "subsidised" by the two other activities. The concept for cargo once introduced by M/S Skandia is principally unchanged. The lines have found a compromise in the scheduling that truckers adopt to. Today the traffic is a high quality link in the industrial network of just-in-time door-to-door transports.

This transport service for high valued products is an important factor for the effectiveness of the economy in the region. The drivers also appreciate their own specially designed spaces onboard.

The cargo carrying capacity of the ships have not increased as much as the passenger capacity. Supplementary RoRo services offers good transport alternatives, and so the requirements from the market are balanced.

The stagnation of cargo carrying capacity has to do with the planning of such ships and the requirements of efficient cargo handling. As passenger service always has had a high priority in this trade, a second deck for cargo above or below the freeboard deck have not been motivated. Sometimes such space has been arranged for private cars. A private car deck is however, much easier to arrange as the strength requirements of decks and ramps as well as the requirements of turning radius for cars are much less than for trucks. Compromises between different commercial functions and technical solutions have up to today resulted in the freeboard deck still being the cargo deck. For the latest generation of ships, the freeboard deck is not even fully utilised for cargo. Cabins are arranged along the outside on both sides. When these ships were designed the experiences from the catastrophe of The Herald of The Free Enterprise was discussed. The motive for such an arrangement to reduce the ships sensitivity for water on RoRo deck was important for the decision to reduce the width of cargo deck. This is an example of how a safety aspect has influenced the design.

Technical concepts

Design philosophies

The two lines had different backgrounds for their technical development. Within the Silja sphere there was a long tradition in the trade. They had accepted and aspired to fulfill the responsibility of being the main provider of sea transports between the two countries.

Behind Viking Line there were also experienced ship owners. But their experiences mainly came from other trades. Even though Viking Line started as a entrepreneurship over the Åland Sea they soon learned the trade by exchanging professional experiences with colleagues from the competitor . From a technical point of view, the design philosophy of Viking Line has been to apply good ship building standard. There were some reluctance to apply solutions exceeding existing rules and regulations. But if there were good reasons such solutions were adopted. Thus both Lines contributed to the technical development.

Silja Line's design philosophy was to focus on functions more than rules and regulations. They concentrated on what they believed was required in their traffic in order to maintain their own unwritten quality standard. It happened that such solutions didn't cope with the existing rules and regulations. This was in general solved when reasons and solutions had been presented to the Administration and approval within the scope of IMO was given as "equivalent or better solution". Silja Line has in this way had impact on e.g. the Finnish/Swedish Ice Class, IMO's rules for fire protection, structural strength of fore ships with bow opening etc.

Viking Line however, was more receptive for new technical solutions developed in the shipping industry e.g. in spite of the ice conditions in this traffic they took the initiative to use barge typed aft body lines, high lift rudders, resiliently mounted main engines etc.

The turn around of ships (see the above "Calendar") indicates the two Lines different philosophy. Viking Line had a quicker turn around and got more opportunities for testing whereas Silja Line relied more on their development inhouse.

The cargo deck and -accesses

Ever since M/S Skandia the design of cargo decks is generally the same only detail design has developed, thus improving cargo handling and safety and environmental conditions on cargo deck.

Stern ramps and stern openings have been improved but the design principal remain the same, i.e. in lowered position the ramp is a driving way and in the upper position the ramp seals the stern opening to cargo deck. This ramp is located in the aft most position of the ship with the aft collision bulkhead located forward of the stern ramp. The Joint Accident Commission will report about position of the forward collision bulkhead and the arrangement in the bow area of M/S Estonia. This overview will be limited to cargo deck accesses in fore ships.

On page 34 these is a scheme of the ships in the trade. There is indicated type of opening in the forward part of cargo deck. Bow openings can either be arranged by using a pair of doors or a so called visor.

- **Bow doors** are normally hinged on heavy arms. The doors are opened by hydraulic cylinders moving the doors outside along the ship's sides. There are also some old designs where the doors are swinging. In closed position, pressure forces acting on the doors are transferred to the ship's hull via reinforced supports. Though the framework along the contours of the doors absorb some forces, the primary function is to keep the sea away from the space between the ramp and the doors. The primary function of locking devices is to prevent the doors from falling out from the ship.

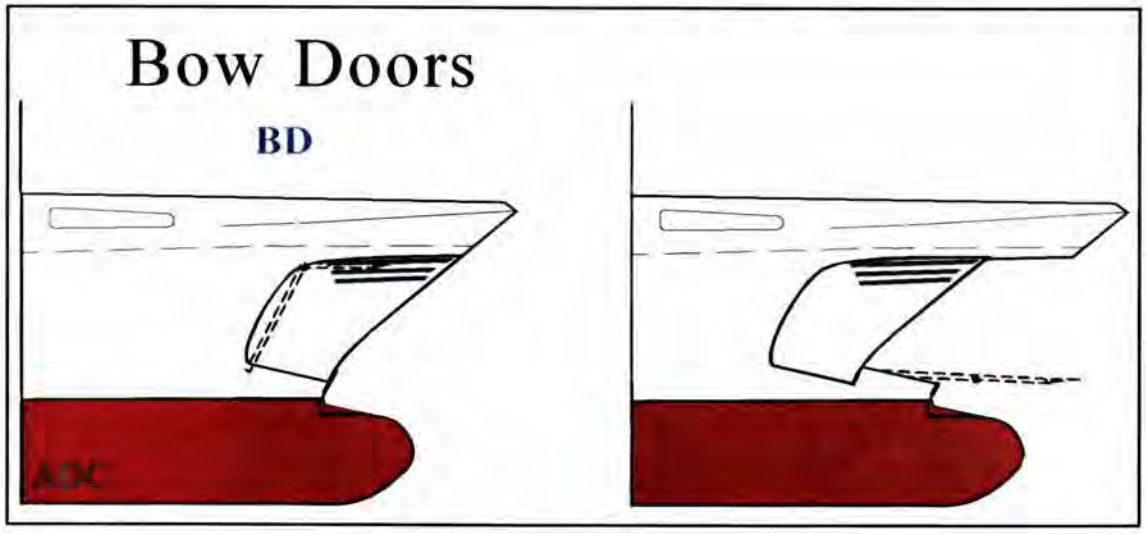

- **A bow visor** forms the bow on a ship. The visor is normally hinged on the forecastle deck and is opened upwards by hydraulic cylinders. The visor's supporting structures in the hull doesn't prevent the visor from opening. Only the locking devices have that function. The space between the visor and the ramp is sealed to the sea along the visors contouring frame. Depending on the geometry of that frame and the elasticity of the visor the frame may absorb some of the forces acting on the visor.

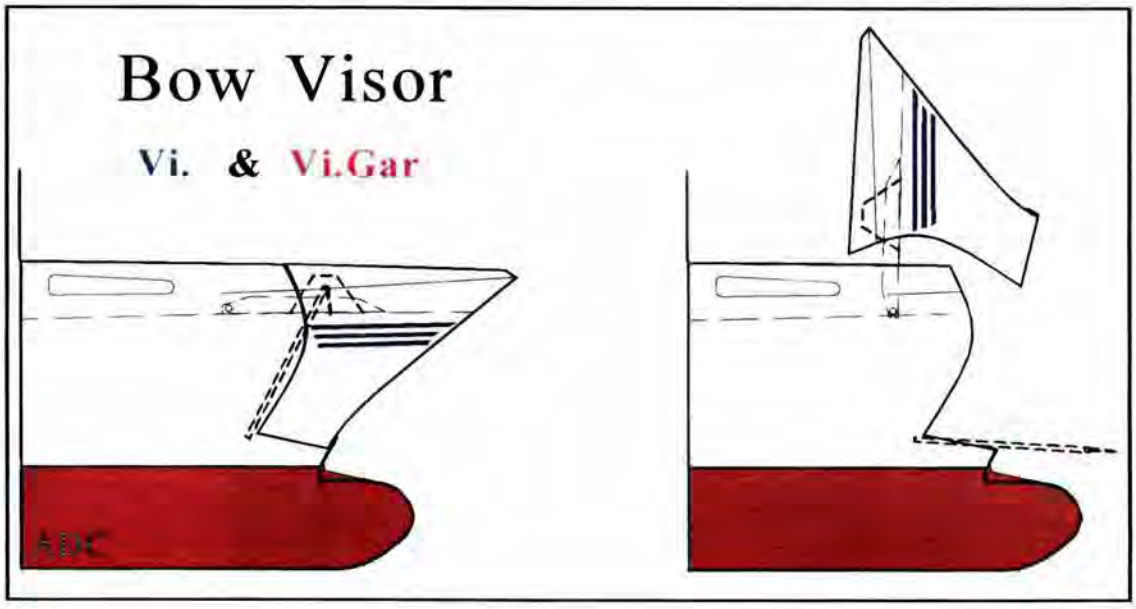

- **Side door(-s)** are used for many purposes on ships. Side doors in closed position rest on a supporting and sealing framework in the hull. The doors are opened by hydraulic cylinders moving the doors horizontally or sometimes vertically to the outside of the ship.

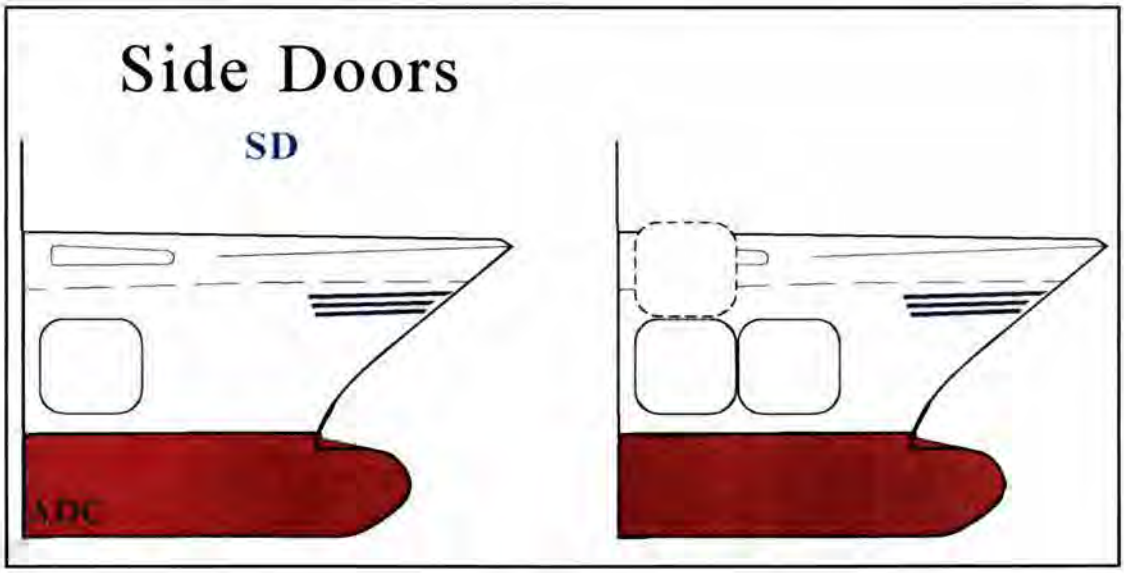

In the scheme below **Vi** marked ships have a bow visor that from safety point of view is independent of the ramp. To get access to cargo deck, two barriers has to be passed.

Vi.Gar marked ships have a bow visor design including a garage for stowing the ramp. From safety point of view the visor and the ramp can be regarded as a single barrier, the design is integrated.

BD indicates bow doors, two independent barriers has to be passed to open the ship, the doors and the ramp.

SD indicates side door, one barrier has to be passed to open the ship. The strength of the side door arrangement should be equal with the ship's side.

On the sketches of the openings the ship is shown with a bulbous bow. In the trade Apollo from 1970 was the first ship with a bulb. Without having specially designed landing ramps it was, for the ships with bulb necessary to arrange a longer bow ramp. Generally the hight in the fore-ship was not sufficient to accommodate the full length of the ramp when raised.

"Silja- and Viking Line" Bow Arrangements

	Birger Jarl, Lo/Lo	1959	(Viking, Slite)	
	SS Bore SD	1960		
	Skandia Vi.	1961	(Boge SD)	
	Nordia Vi., Svea Jarl SD	1962		
	Floria Lo/Lo	1963	(Ålandsfärjan)	Kapellskär
	Ilmatar SD	1964	Apollo Vi. (Drotten)	
	(Holmia Vi.)	1965	(Visby Vi.)	Wincer traffic Kapellsk.-Pargas
Silja to Värtan	Fennia Vi.	1966		
	Botnia Vi.	1967	Kapella Vi., (Visby Vi., Stena Baltica Vi.)	
		1968	(Viking 2 Vi.)	
		1969		
New name; Silja Line	Floria Vi.Gar	1970	Apollo Vi.Gar, Viking 1 Vi.Gar, Marella Vi.	
		1971		
Winter traffic Stockholm-Helsinki	Aallotar BD, Svea Regina BD	1972	Viking 3 Vi.Gar, Diana Vi.Gar	
	Bore I Vi.Gar *The 1.st Oil Crisis*	1973	Viking 4 Vi.Gar, Aurella Vi.Gar	New route for Viking Line -73 Stockholm- Mariehamn-Turku
		1974		New route for Viking Line Stockholm-Helsinki -74
	Svea Corona, Wellamo, Bore Star Vi. Vi. Vi.	1975	Viking 5 Vi.Gar, (Viking 6 Vi.)	
		1976	(Apollo III SD)	
		1977	(Ålandsfärjan Vi.)	
	The 2.nd Oil Crisis	1978		
		1979	Diana II Vi.Gar, Turella Vi.Gar	
		1980	Rosella, Viking Song, Viking Sally, Viking Saga	
	Finlandia Vi.Gar, Silvia Regina Vi.Gar	1981	Vi.Gar Vi. Vi.Gar Vi.	
		1982	(Aurella Vi., Ålandsfärjan Vi.Gar)	
		1983	(Ålandsfärjan Vi.Gar)	
		1984	(Ålandsfärjan Vi.Gar)	New name; Viking Line
	Svea BD	1985	Mariella Vi.Gar, (Ålandsfärjan Vi.)	
	Wellamo BD	1986	Olympia Vi.Gar	
		1987	(Ålandsfärjan Vi.)	
		1988	Amorella BD	
		1989	Athena BD, Cinderella BD, Isabella BD	
	Silja Serenade BD, (Silja Star)	1990	Kalypso BD	
	Silja Symphony BD	1991	*Notes:* SD = *Side Doors*, BD = *Bow Doors*	
	BD BD	1992	Vi.Gar = *Visir & Ramp-garage* Vi = *Indipendant Visir*	
ADC Support AB Stockholm 1995	(Silja Europa, Silja Scandinavia)	1993	Vi.Gar = *Visir & Ramp-garage and barrier*	

There were two possibilities to accommodate a long ramp, either to make the forward part of the ramp foldable or simply to increase the hight by arranging a garage on the above deck in which the ramp could be stowed.

In order to make the design simple and the operation uncomplicated the solution with the garage used to be more frequent. Then the garage was built on the deck of the visor. Consequently the two construction elements was integrated. Accordingly the ship had then in practice just one protecting barrier against the sea.

The other solution was to make the uppermost part of the ramp foldable forward under the mooring deck. The shapening of the bow limited the length of the folded part. This was also in practice an "integration" of the visor and the ramp. Thus if the visor for some reason was moved outside its normal track it could effect the folded part of the ramp.

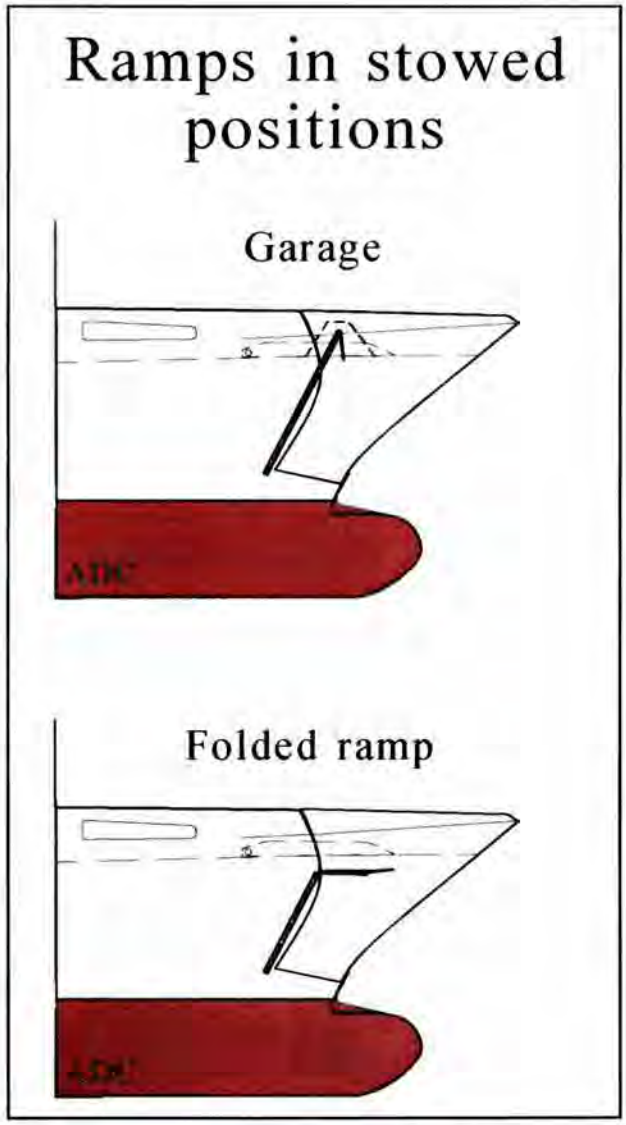

There was also a solution aiming to reduce the required length of the ramp. The pivoting point of the ramp was simply forward and thus could the ramp be made shorter. Often this was not sufficient so this was often combined with the above described arrangements. When the ramp was moved forward the ramp couldn't in general fulfill the requirements as an extension of the forward collision bulkhead as specified in SOLAS. That had to be compensated. To arrange a 2,3 m high extra barrier behind the ramp was then considered as an equivalent solution to the rules in SOLAS.

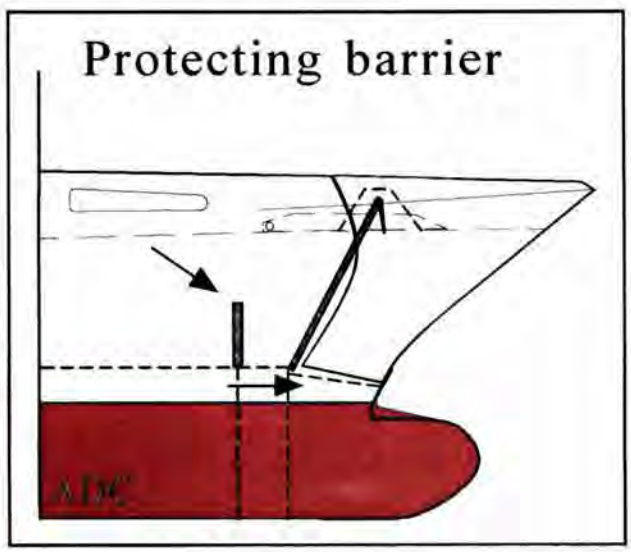

M/S Estonia had a garage built on the visor to accommodate the upper part of the ramp. The ramp was moved forward and therefore did not fulfill the rules as an extension of the collision bulkhead. The arrangement could have complied with the rules of SOLAS if an additional barrier had been arranged.

The "French Sisters" Svea Corona, Wellamo and Bore Star had an interesting solution. Instead of the garage a store was arranged on the fore castle deck. The ramp was stowed towards the forward bulkhead of that store. The foremost part of the forecastle deck belonging to the visor was then raised to the same level as the roof of that store. Thus the ramp and the visor was no longer an integrated design.

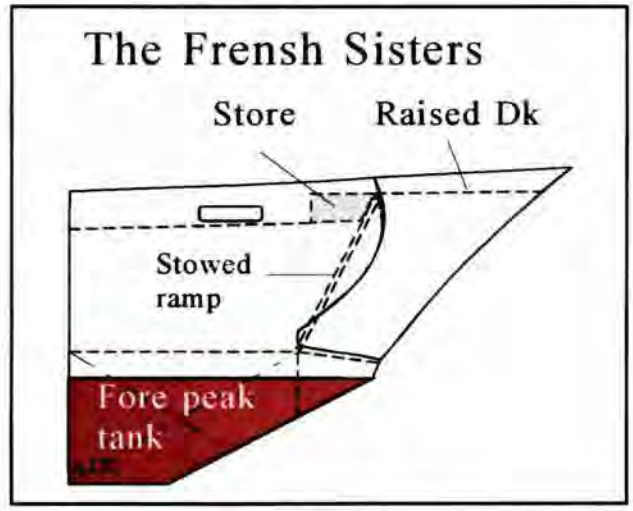

From design point of view, visors and bow doors is shapening the bow of the ship. Properly designed the bow shape would contribute to good sea keeping performance. Although it is the ambition, it is practically impossible, to keep the space forward of the ramp completely dry, but the construction shall prevent rough sea from penetrating the space between the bow and the ramp. The ramp on the contrary, has to tighten against the frame. When under way it is normal that some water in certain sailing conditions is sloshing on the fore peak tank top in front of the ramp. If the sealing of the ramp does not work properly, an early warning will be given by a wet cargo deck. Then this is normally corrected by operational reasons as soon as possible, far before that water will be a safety issue.

From a safety point of view bow doors are a better design than a bow visor. The external forces on a visor are acting in an opening direction. That means that a failure can result in an unsafe situation. On a bow door design the heavy forces from the sea on the contrary are closing the doors. Thus a failure doesn't result in an unsafe situation.

Most bigger relatively new Passenger/ RoRo cargo/ Ferries have bow doors. In some cases the impact forces from sea have been underestimated and the supporting structures have not been strong enough. Consequently when such doors have been overloaded the construction has jammed making the doors difficult to open. This is an example of how a failure didn't result in an unsafe situation.

The consequence of a properly designed supporting structure for a bow door arrangement is often that the forward mooring deck is covered. Thus a stiff box construction provides the foundation of the supports absorbing vertical forces. It has not been difficult to get acceptance for such arrangements in this traffic as this reduce the problem with ice and snow on mooring deck wintertime. An other advantage is that the risk to ship "green water" on fore castle deck is avoided. The forces acting on the bow door's locking devices are not just the mass forces of the doors. Under some circumstances the water flow in the bow region can cause suction forces on the surface of the door. These forces, are however much less than the pressure caused by sea impacts on the bow.

Safety and redundancy

After the second oil crisis the size of ships in the trade grew considerably . Also some of the tradition regarding suitable bow shapes for the Baltic Sea was lost. The challenging bow flare of M/S Estonia is an example of that. Another example is a small local knuckled flare some meter above the water line that M/S Finlandia/ Silvia Regina had when delivered. This was a cavity that captured waves. Very high pressure was built up in the cavity and when the energy was released water was shot far away from the ship. Even during normal sea conditions passenger experienced that as explosions and many had difficulties to sleep. This was quickly redesigned by Silja Line. That incident showed the importance passenger comfort. Ever since passenger comfort is a very important aspect when the route is planned. Silja Line also made efforts to soften bow shapes on the following ships.

During the 60's and 70's the conceptual development of deep sea shipping was very fast. In ship design the laws of nature was often violated when struggling for maximising transport productivity. Also the ship yards wanted to offer high productive ships in terms of cargo carrying capacity and high trial speeds. Cost for bunker had at that time low priority an the marine engines available could deliver the required power. Ship engines were turbo charged already in the 50's, the car industry begun with that in the 80's. The design philosophy many times was to build a ship like a wrapping around the cargo with easy accesses for cargo handling. Thereafter the necessary power was installed. To improve productivity on the ship yards flat panels were used as much as possible. The result of all this was boxed shaped ships with low hydrodynamic efficiency and bad sea keeping performance.

Consequently most Owners in the West also learnt that the engine power of "modern" ships could endanger the ship if the power resource was not handled gently. The diagram below shows the ratio of ship power to breadth over the years, in this traffic.
The ratio just mirrors the potential a ship has to maintain speed through rough sea. Since also other factors are influencing on the ships performance in rough sea the plotting in the diagrams shall just be regarded as indications.

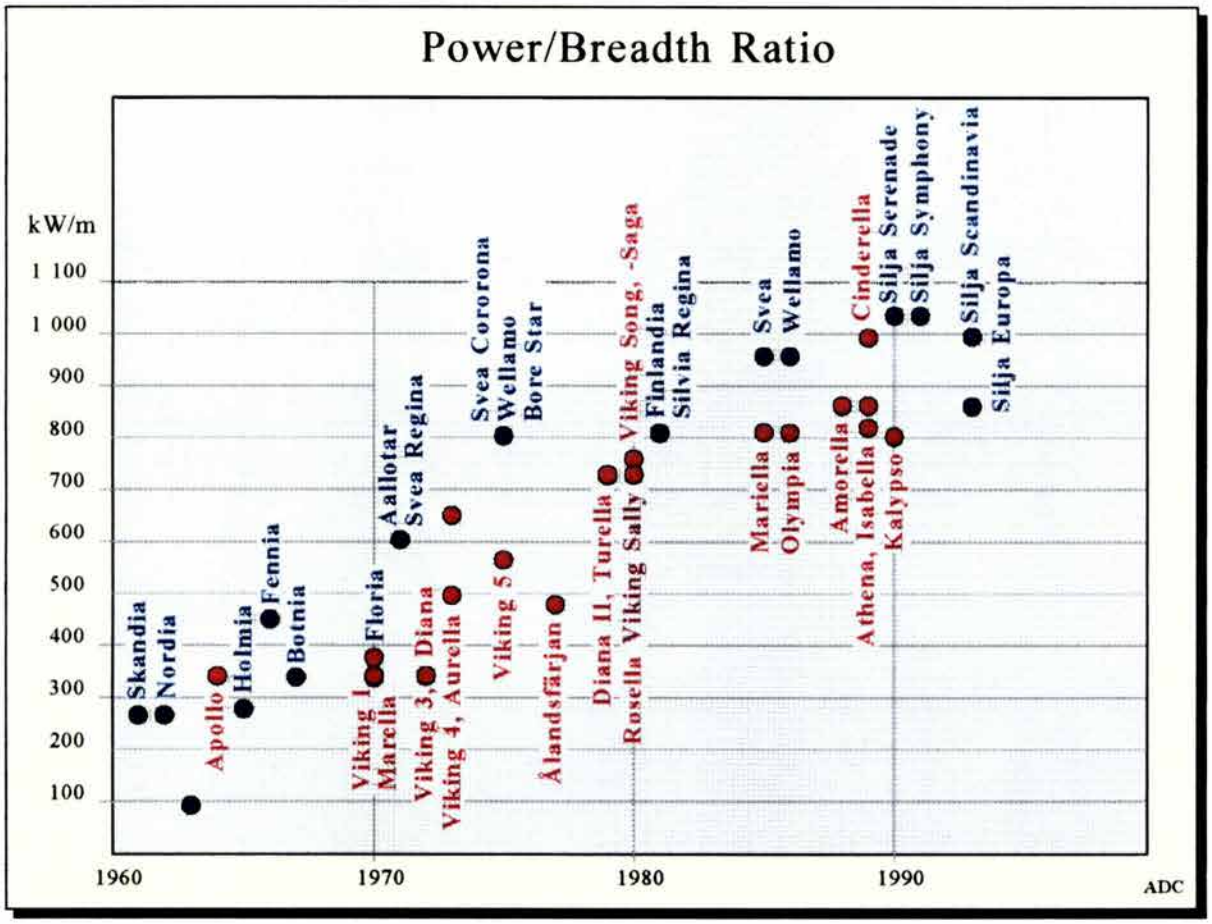
Power/Breadth Ratio
kW/m
1 100
1 000
900
800
700
600
500
400
300
200
100
1960
1970
1980
1990
ADC
Skandia
Nordia
Apollo
Holmia
Fennia
Botnia
Viking 1
Marella
Floria
Aallotar
Svea Regina
Viking 3,
Viking 4, Aurella
Diana
Svea Cororona
Wellamo
Bore Star
Viking 5
Ålandsfärjan
Diana II, Turella
Rosella
Viking Song, -Saga
Viking Sally
Finlandia
Silvia Regina
Svea
Wellamo
Mariella
Olympia
Amorella
Athena, Isabella
Cinderella
Kalypso
Silja Serenade
Silja Symphony
Silja Scandinavia
Silja Europa

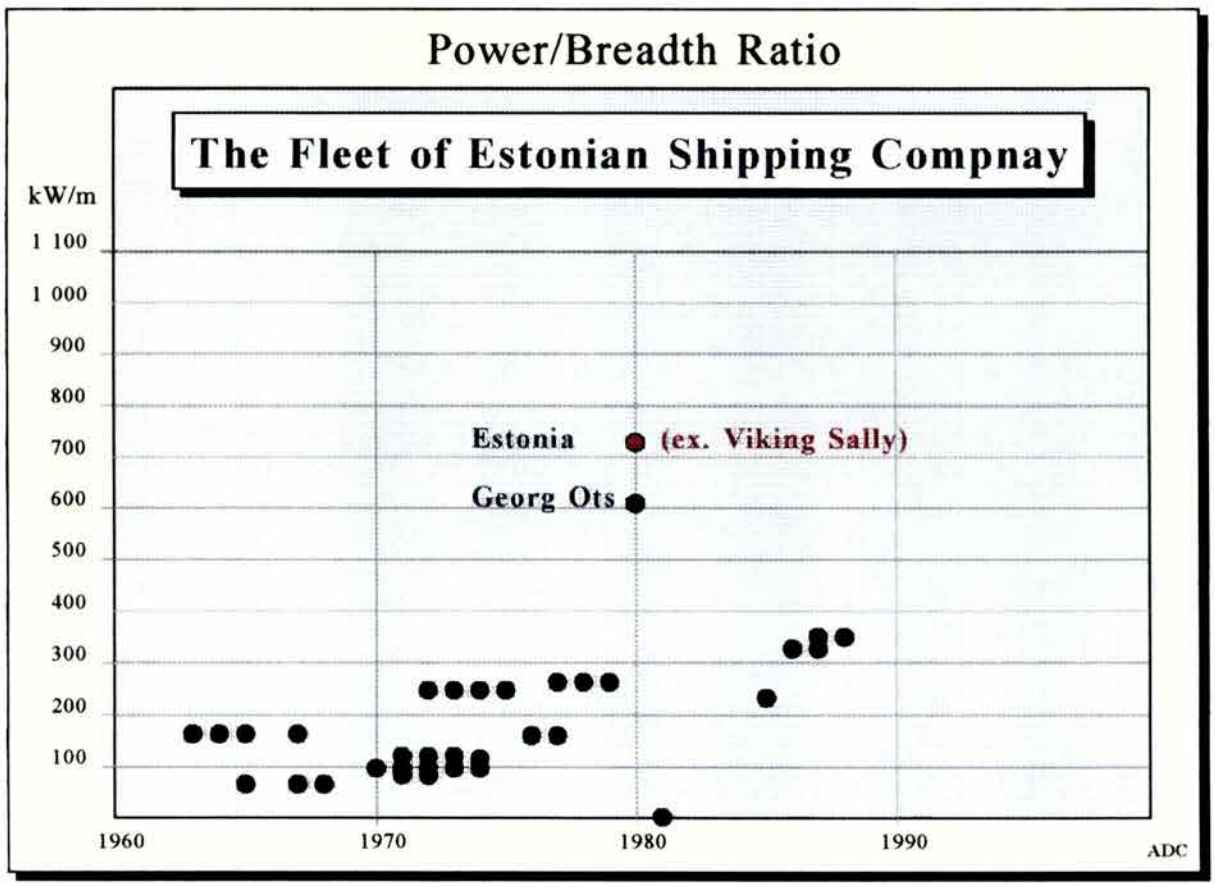
Power/Breadth Ratio
The Fleet of Estonian Shipping Compnay
kW/m
1 100
1 000
900
800
700
600
500
400
300
200
100
Estonia
(ex. Viking Sally)
Georg Ots
1960
1970
1980
1990
ADC

The crew of M/S Estonia (M/S Viking Sally) was recruited from Estonian Shipping Company (ESCO). The diagram shows the corresponding power/breadth ratio of the ESCO fleet in early 1993.

Ships navigation and operation at sea was before The Estonia catastrophe not considered as a main risk factor. The routines were well proven and it was no doubt the ships should be seaworthy. Safety was focused on all the time. Checking lists for operation of the ships were made and followed as far as practical. The two competitors agreed on how the ships should cooperate in confined waters. A near accident report system was introduced but at the time it was no success due to that the integrity of individual persons could not be safely guaranteed. The seagoing personnel exchanged however a of lot vital information of how to handle the ships safely.

Until the mid 80's the technical development dominated the owners' efforts to make the ships safer. Redundancy and single point failure i.e. multi engine arrangements and back up solutions had been applied from the beginning. Techniques and routines to minimise risks for black out (powerless ship) were developed. In case of a black out there was a lot of technical systems available and prepared routines to assure safe handling of the ship. For the first time in commercial shipping computer aided navigation systems were introduced etc. etc.

Although safety against fire was improved for shipping in general, these operators took fire risks even more serious. The local fire brigade onboard the ships solved many fire incidences on the ships with minimal consequences. Serious fires occurred but in these cases the ships were out of traffic, docking etc. Thus the Lines had a leading position in preventing and fighting fires, both from hardware (structural and equipment) and software (routines and handling) point of view. To ensure safe handling of the ship in a damage condition extensive training programs were run onboard.

Cooperating accident training with land forces was routine both on the Swedish and the Finnish side. Some exercises were made in full scale e.g. including Swedish and Finnish helicopters, fire brigades from shore on road ferries etc. For example, the experiences from an exercise at Korpo in the Åland Archipelago contributed to the decision in Finland to renew the helicopter fleet.

In fact some of these exercises emanated from discussions from mid 80's about how the impossible accident should be handled. "The accident that couldn't happen", that happened M/S Estonia. This was concluded by stating; if it is hard weather it doesn't matter how many the ships are in the area. The only assistance they can give is to serve as On Scene Commander, and to receive and treat distressed people from helicopters. The ships had already at that time developed routines for sending sick passengers from the ships with helicopter to hospitals. A result of that discussion was however that it was decided to make the electrical motors for hoisting lifeboats stronger. Before, these motors were just able to lift the lifeboats onboard when exercising, now the motors should be able to lift a lifeboat filled with rescued people.

The list of safety measures can be made longer. In the end of the 80's both lines formalised the safety work by establishing permanent functions in the organisations.

Some major accidents as e.g. M/S Herald of the Free Enterprise, M/S Scandinavian Star put passenger safety into focus and the public pressure on authorities to do something increased. Thus a lot of the rules and regulations for ships were revised and for the first time requirements on ship owners organisation were formulated in the so called ISM-Code, the International Ship Management Code for safe ship operation.

The collective record of Silja- and Viking Line from 1960 to 1995 is five killed passengers on 107 million passenger single trips i.e. one casualty per almost 18 million single trips. This can be compared with the risk to be struck by the lighting when living in UK, that has been calculated to be 1 in 10 million. These five causalities was caused in one accident, it was one ship running into a cabin of another ship. The reason was that the captains had misunderstood how the ships should pass each other in a narrow section of a fairway.

EPILOGUE

The purpose with the description of The Baltic Phenomenon, from which M/S Estonia emanates, has been to mirror the atmosphere in which the ship were designed and operated. It is also an history of how competition force the two rivals to adopt to the market situation in the trade and thereby discovering new market segments.

The economical situation and the extensive know-how of the trade, formal and informal network of contacts between specialists in the region have contributed to give this ferry services a leading position in the world. This is not just concerning the commercial concept development but also from a safety and ship design point of view. The traffic has been pioneer in many safety areas e.g. navigation systems, fire systems, redundancy of vital technical systems, ships construction, onboard safety routines and training etc. Many of these ideas have later on been adopted by authorities as rules and regulations.

This overview with the explanations of the work with safety is contrasting to the Estonia catastrophe. The reason is that until this happened the design philosophy was that big volumes of water should not enter into cargo deck when the ship was properly closed at sea. When the catastrophe showed this was a false philosophy an intensive work started to make these ships safe regardless of water on cargo deck. In fact this work was already started after the catastrophe with the Herald of The Free Enterprise. Thus the latest purposely built ships in the trade manage to carry a lot of water on the cargo deck: M/S Silja Symphony and M/S Silja Serenade manage one meter and M/S Silja Europa has to sink before she capsizes.

Sea transportation is almost as important for the development of Estonia as it has been and still is for Finland. The Baltic Phenomenon is however not expected to be repeated in the Estonian trade. The different geographical situation of Estonia, is reason to expect a different development. The commercial development irrespectively, such traffic will be included in the discussions and the development of safety- and environmental standards for the region.

Stockholm in December 1995

Hans Wermelin
Naval Architect M.Sc.

SOURCES

The Swedish Central Bureau of Statistics	National statistics
Statistics Finland Library	National statistics
Cruise & Ferry Info	Traffic statistics
Lloyds Register of Ships	Ships particulars
Club Maritime	Ships history

SUPPLEMENT No. 525

Laur Uno:

Report. Damage to bow visor locking devices of passenger car ferry "DIANA II" in January, 1993, and preliminary conclusion i.r.o. the loss of the bow visor of m.v. "ESTONIA" on September 28th, 1994.

Tallinn 1994.

FOR COMMISSION USE ONLY

To the members of the Joint Accident Investigation Comission

REPORT

Damage to bow visor locking devices of passenger car ferry "DIANA II" in January, 1993. and preliminary conclusion i.r.o. the loss of the bow visor of m.v. "ESTONIA" on September 28th, 1994

Referring to the ***Detailed Report of Survey No. HBG/93/7-A*** made by a surveyor of ***Bureau Veritas*** and appropriate photos it should be noted that a casualty similar to "Estonia" disaster was going to take place with m.v. "Diana II" in January 1993.

According to the above mentioned Report and photos a damage survey together with damage repairs of locking devices of m.v. "Diana II" was carried out on January 16 - 17, 1993.

Extract from the Report
...following damages were found on the bow door.

The lug for SB lock plunges was lost.
The lug in center line (the "Atlantic lock") was bent and the weld cracked.
The lug for Port side plunges was bent and the weld cracked.
A minor crack at the hinge on SB side.
The girder in center line and two webs on SB side cracked.

Following repairs carried out:

The lug SB side renewed with doubling plate on the back side.
The lug in center line faired and rewelded. The stay above the lug renewed.
The lug Port side faired and the crack chiselled and welded.
The crack at SB hinge chiselled and welded.
The cracks at the girder and the webs chiselled and welded.

Function test of the bow door carried out and found to be in order.

According to information available the "Diana II" was in January, 1993, trading on regular passenger/cargo line between Trelleborg and Rostock with a distance between those ports about 95 n.m. A weather report of *Estonian Meteorological and Hydrological Institute* says that South, South Westerly and Westerly winds up to 20 metres per second were prevailing in this area on January 15 - 16, 1993.

Taking into account that the above mentioned area is exposed to South Westerly winds the damage to the locking devices of m.v. "Diana II" was presumably caused when proceeding from Trelleborg to Rostock on January 15th and/or 16th, 1993.

Since the bow construction of m.v "Estonia and m.v. "Diana II" was identical it would be considered highly regrettable that *Bureau Veritas* had not taken any preventive measures in respect of the bow visors of all vessels of this type classed by the same classification society.

If they had the tragic loss of the "Estonia" could have been avoided. Unfortunately resolute measures were taken and appropriate instructions given only after the disaster.

Please find attached:

1. Copy of the *Detailed Report of Survey No. HBG/93/7-A* of *Bureau Veritas*.
2. Copy of the *Weather Report of Estonian Meteorological and Hydrological Institute*.
3. Copy of a fax message of *Bureau Veritas No. 1463, of 1.10.1994*.
4. **"DIANA II"** picture of the damaged bow visor's SB side lock.
5. **"DIANA II"** picture of the damaged bow visor's Port side lock.
6. **"ESTONIA"** picture of the damaged bow visor's SB side lock.
7. **"ESTONIA"** picture of the damaged bow visor's Port side lock.

I suppose comparing the above pictures of very similar damages of the both ships together with other details available it would be possible to find out the real sequence of separating the bow visor of m.v. "Estonia" on the tragic night of September 28th, 1994.

Kindly

Uno Laur
Master Mariner
Member of the Joint Accident Investigation Commission

10. December 1994
Tallinn

Encls.

Bureau Veritas

MARINE BRANCH

DETAILED REPORT OF SURVEY

Annex No [B] to Report No [HBG/93/7-A] Page No [1] Total Pages [1]

Register Number [35 V 002] Name of Ship ["DIANA II" .]

Cert. concerned | PROV | HULL X | MACH | AUT | MB | AB | RMC1 | | (one square only to be ticked off)

Visa No endorsed [7] or survey of C.S. ☐ or D.S. ☐ Items (continuation to AdE 2528)

Survey carried out from [16/01/93] to [17/01/93]

REPORT OF SURVEY

On request by the Chief Engineer survey of the closing devices for the bow door carried out and following damages were found on the bow door.

The lug for SB lock plunges was lost.

The lug in center line (the "Atlantic lock") was bent and the weld cracked.

The lug for Port side lock plunges was bent and the weld cracked.

A minor crack at the hinge on SB side.

The girder in center line and two webs on SB side cracked.

Following repairs carried out:
The lug SB side renewed.with a doubling plate on the back side.

The lug in center line faired and rewelded. The stay above the lug renewed.

The lug Port side faired and the crack chiselled and welded.

The crack at SB hinge chiselled and welded.

The cracks at the girder and the webs chiselled and welded.

Function test of the bow door carried out and found to be in order.

BUREAU VERITAS EXPERT de GÖTEBORG PARIS 1828 REGISTRE INTERNATIONAL

FROM

DEC-01-94 1:53P P.001

EMHI EESTI METEOROLOOGIA JA HÜDROLOOGIA INSTITUUT
ESTONIAN METEOROLOGICAL AND HYDROLOGICAL INSTITUTE

METEOROLOOGIAKESKUS
METEOROLOGICAL CENTRE

Hr.KALLE PEDAK
VEETEEDE AMET

Teie Your 01.12.1994.a. No

Meie Our 01.12.1994.a. nr. MP/-199

ILMAANDMED. WEATHER REPORT

Teatame ilmatingimused marsruudil Rostock-Trelleborg ajavahemikus 12.-16.jaanuar 1993.a.

Kuupäev	Kellaaeg UTC	Tuule suund, kiirus m/s		Sademed	Ohutemperatuur °C
12.01	00.00-15.00	edela, lääne	10-15	hoovihm, äike	+2, +5
	15.00-24.00	lääne	15-20	kohati äike	+2, +4
13.01.	00.00-09.00	lääne	15-20	sademeteta	+3, +4
	09.00-18.00	edela, lõuna	10-15	sademeteta	+4
	18.00-21.00	lõuna	12-17	vihm	+6, +8
14.01.	00.00	lõuna, edela	20-25	hoovihm	+6, +8
	03.00	lääne	25-30	hoovihm	+3, +5
	06.00	lääne	15-20	sademeteta	+3, +5
	09.00	} lääne	15-20	} hoovihmad	} +3, +5
	12.00				
	15.00	lääne	10-15	hoovihm	+3, +4
	18.00	lääne	10-15	kohati hoovihm, äike	+2, +4
	21.00	lääne	10-15	sademeteta	+3, +4
15.01.	00.00-03.00	lääne	10-12	sademeteta	+3, +4
	03.00-06.00	lääne, edela	7-10	sademeteta	+2, +4
	06.00-15.00	lõuna	12-17 S	vihm	+4
	15.00-18.00	lõuna, edela	15-20 S, SW	vihm	+4, +6
	18.00-24.00	edela	10-15 SW	hoovihm, äike	+6, +8
16.01.	00.00-18.00	lääne	15-20 W	vihm	+4, +6
	18.00-24.00	lääne	12-17 W	vihm	+8, +10

Ene Linno
Meteoroloogiliste prognooside
osakonna juhataja

Lõvalaia 9
EE0108 Tallinn
Estonia

Tel. (372 2) 44 40 59
44 08 33
Fax (372 2) 44 94 84

Telex
808 259 EMHI EE

A/arve 120 068/500 168 151
A/S Eesti Sotsiaalpank
kood 420 101 551

BUREAU VERITAS

MARINE DIVISION
SHIPS IN SERVICE MANAGEMENT (DNS)

DIVISION MARINE
DIRECTION NAVIRES EN SERVICE (DNS)

ESTONIA NATIONAL MARITIME BOARD
9, VIRU STREET
200100 TALLINN
ESTONIA

365 DNS

Paris la Défense, 5th October 1994

SUBJECT : PASSENGER FERRY - ROLL ON-ROLL OFF - PROVIDED WITH BOW VISOR AND FORWARD RAMP

Following to the tragic loss of the passenger-ferry "ESTONIA", BUREAU VERITAS has decided, as a prevention measure and without waiting for the official inquiry, the inspection of the bow visor and the forward ramp of all vessels of this type currently in class.

For your information, please find annexed our fax No. 1463 dated 1 October 1994 sent to our survey centres all over the world. In addition, owners have been required to carry themselves the same inspection pending our own attendance (Model of letter annexed).

All these inspections shall be completed by the 17 October 1994. BV is ready to fully cooperate with all the Administrations and, if deemed necessary, to conduct these specific surveys in collaboration with Administration representatives.

Yours faithfully,

Gilberto CHAVES
DIRECTOR SHIPS IN SERVICE

encl.

BUREAU VERITAS

FAX

Paris-La-Défense,
Date :

1st October 1994

BRANCHE MARINE
MARINE BRANCH
DNS / 33 (1) 42.91.52.93

Ref. : 1463
Nbre de pages : 1
Nb of pages : 2 1

A / *To* ALL DISTRICTS
De / *From* DNS

Objet / *Subject* SHIPS WITH SERVICE NOTATION - PASSENGER FERRY - ROLL ON ROLL OFF PROVIDED WITH BOW VISOR AND FORWARD RAMP

1. Head Office has decided to submit for inspection the bow visor and forward ramp arrangements of ships in caption at the next call at the home port.

2. Your are kindly requested to contact the managers of such ships by Monday 3rd October 1994 in order to plan the immediate inspection as soon as the ships are in the home port.

3. You must establish a list of such ships belonging to your district and to communicate the same to your MO and CM by Tuesday PM, 4th October 1994, at the latest.

4. All ships covered by this scheme of inspections must be inspected prior to 17th October 1994.

5. The extent of the inspection to be conducted is as follows:

5.1 BOW VISOR

To verify the condition of:

- plating and internal structure
- packing and the fastening devices
- manual or remote closing and securing devices

Note: All parts of the locking devices, irrespective of their type, including their attachments to the hull or visor are to be carefully inspected.

- bow visor deck hinges and their supporting devices, including the attachments on the deck and to the bow visor.
- bow visor closing indicators (locally and on bridge) where applicable. They should indicate that the door is properly closed and secured.
- test operation of bow visor and power pack system to be carried out, to the verification that the locking devices are fully engaged.

5.2 FOREWARD RAMP

To verify the condition of:

- plating and internal structure.
- packing and the fastening devices
- hinges and their attachments to hull and ramp.
- locking and securing devices.
- ramp door closing indicators(locally, if any, and on bridge). They should indicate that the ramp is properly closed and secured.
- operation of the video camera, checking its efficiency, if no video camera is provided the checking of the leak detection system.
- operation of all ramp doors, including verification that all locking and securing devices are fully engaged, and the efficiency of the power pack.
- hose test to be carried out.

6. Further to the above inspections the surveyor will have to request immediate repairs in case defects are found or mal functioning of the equipment. In case repairs cannot be undertaken immediately, the MO must be informed by the fastest means of communication for instructions. In all cases the MO, copy to CM, must be informed immediately of any damages or defects.

7. On completion of the inspections, the surveyor must endorse the hull certificate with the following visa:

"Occasional survey of hull for inspection of Bow Visor and Forward Ramp Door"

8. The survey will be at Owner's cost.

9. The usual procedure for invoicing and reporting is to be applied.

Regards

G. Chaves

BUREAU
VERITAS

FAX

MARINE DIVISION
DNS / 33(1)42.91.52.93

Ref.:
Page No.: 1/2

TO:

FROM:

SUBJECT : SHIPS WITH SERVICE NOTATION

PASSENGER FERRY
ROLL ON - ROLL OFF

Dear Sirs,

- Bureau Veritas has decided to carry out inspections of ships' types "PASSENGER FERRIES" and "ROLL ON - ROLL OFF" provided with bow visor and forward ramp at the next call to their home port.

- We have instructed our local representative to contact you in order to make the necessary arrangements for this intervention which we shall endeavour to be completed by the 17th October 1994.

- The scope of these inspections will be as follows :

BOW VISOR

To verify the condition of :

- plating and internal structure,
- packing and the fastening devices,
- manual or remote closing and securing devices.

Note : All parts of the locking devices, irrespective of their type, including their attachments to the hull or visor are to be carefully inspected.

- Bow visor deck hinges and their supporting devices, including the attachments on the deck and to the bow visor.

- Bow visor closing indicators (locally and on bridge) were applicable. They should indicate that the door is properly closed and secured.

- Test operation of bow visor and power pack system to be carried out [illegible] verification that the locking devices are fully engaged.

BUREAU VERITAS FAX

Ref. :
Page N° 2 / 2

FOREWARD RAMP

To verify the condition of :

- plating and internal structure,
- packing and the fastening devices,
- hinges and their attachments to hull and ramp,
- locking and securing devices,
- ramp door closing incidators (locally, if any, and or bridge). They should indicate that the ramp is properly closed and secured.
- Operation of the video camera, checking its efficiency, if no video camera is provided the checking of the leak detection system.
- Operation of all ramp doors, including verification that all locking and securing devices are fully engaged, and the efficiency of the power pack.
- Hose test to be carried out.

- In the meantime, you are kindly requested to instruct your staff to conduct an immediate examination of the above items. In the event of any defects being found would you kindly notify us and we shall arrange our Surveyor to attend.

We would be grateful for your full cooperation to expedite these inspections.

Best regards,

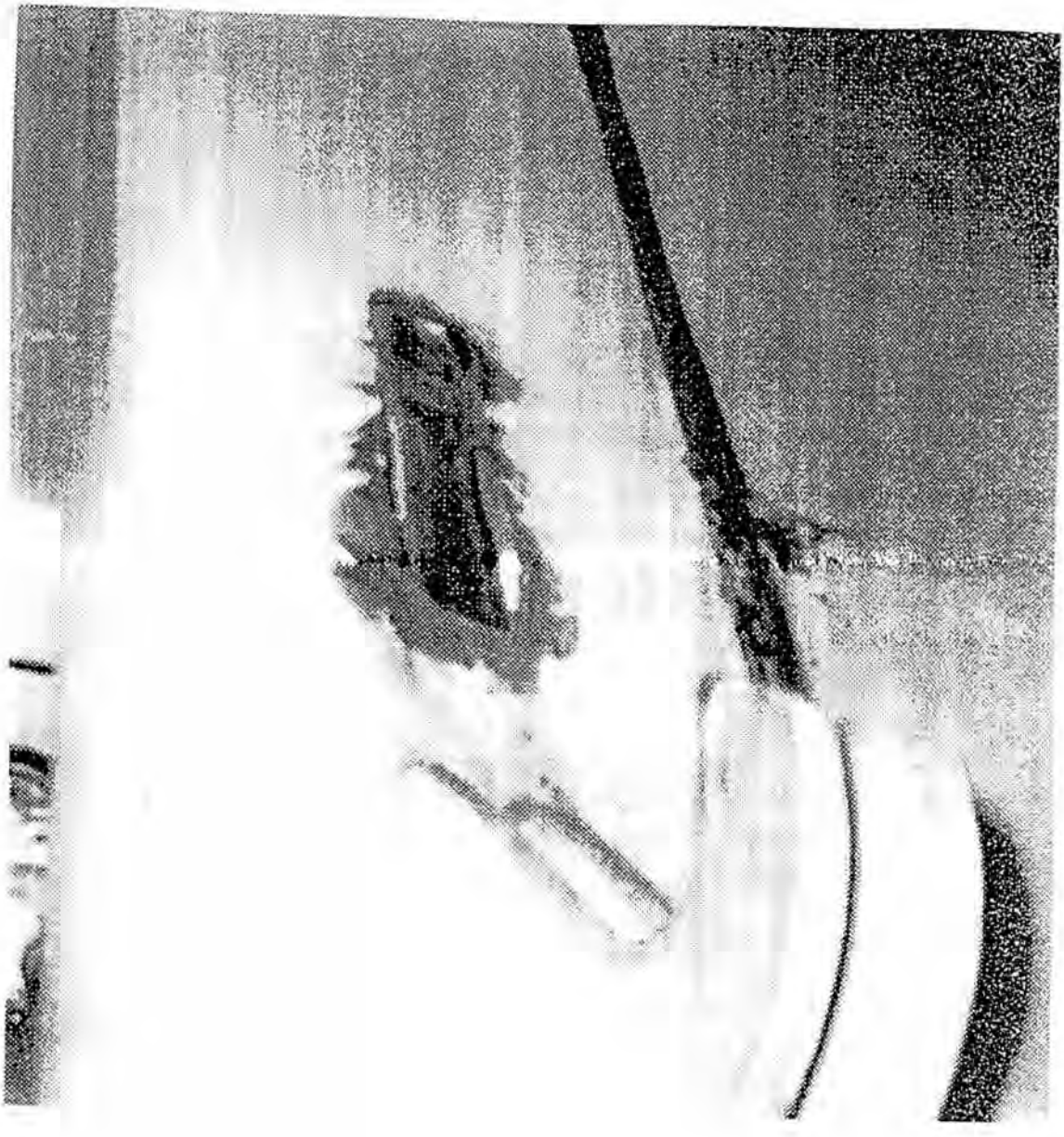

"DIANA II"

PICTURE OF THE DAMAGED BOW VISOR S SB SIDE LOCK

"DIANA II"

PICTURE OF THE DAMAGED BOW VISOR S PORT SIDE LOCK

"ESTONIA"

PICTURE OF THE DAMAGED BOW VISOR`S SB SIDE LOCK

"ESTONIA"

PICTURE OF THE DAMAGED BOW VISOR`S PORT SIDE LOCK

SUPPLEMENT No. 526

Lehtola Kari:

Damage to the Bow of the SILJA EUROPA at the Time of the Accident Involving the ESTONIA 28.9.1994.

THE JOINT ACCIDENT INVESTIGATION COMMISSION FOR THE MV ESTONIA

PROMEMORIA
20.8.1995/FIN

DAMAGE TO THE BOW OF THE SILJA EUROPA AT THE TIME OF THE ACCIDENT INVOLVING THE MS ESTONIA

1. The events

The Silja Europa departed from Helsinki for Stockholm on 27 September 1994 at 18.00. The following night she received the mayday message from the Estonia and proceeded immediately to the scene of the accident. Soon after the accident the captain of the Silja Europa, captain Esa Mäkelä was appointed the on-scene commander (OSC). The Silja Europa remained at the scene of the accident engaged in the rescue until 18.30 on 28 September 1994, at which time she was allowed to continue her voyage to Stockholm. The Silja Europa arrived at Stockholm on 29 September 1994 at 05.30.

Immediately upon arrival at Stockholm, it was noted that the door on the BB side of the bow of the vessel opened only about 40 cm. The vessel is equipped with so-called butterfly doors. The vessel was turned around and the vehicles were unloaded through the stern doors.

A Bureau Veritas inspector noted the following damage to the bow (the numbering refers to the numbers noted in the photograph and the drawings):

1. buckling of the side and bottom plates of the shaft of the door hinge
2. buckling of rib no. 218 (reinforced after the sea trial)
3. crack in the fastening of the guide roller on the top of the door
4. buckling of rib no. 219 (may be related to an earlier incident)
5. this illustrates how the sides of the door meet
6. buckling of the longitudinal web (also this is probably related to an earlier incident)

In addition to the above, several smaller deformations were noted.

The vessel was found to be seaworthy although the door could not be used before it was repaired.

The damage was repaired within a few days, without taking the vessel out of traffic.

It has not been possible to give an exact time for when the damage occurred.

2. The speed of the Silja Europa on 27-28 September 1995

The track recorder, which is part of the electronic navigation system of the Silja Europa, has data on the speed of the vessel on the night of the accident involving the Mv Estonia. During the evening, the vessel proceeded at a greater speed than normal since it was known that the wind would grow stronger and the sea become rougher during the night, when the speed would have to be decreased. Accordingly, the speed was gradually decreased, as shown by the following:

Time	*Speed*
00.25	14,8
00.47	13,8
00.58	12,4
01.02	12,0
01.09	11,5
01.14	11,5
01.20	10,9

At the time she received the mayday message from the Estonia, the Silja Europa was proceeding at a speed of about 9,5 knots. On turning towards the reported location of the Estonia, she used an "emergency" speed that was at most 12,5 knots and at the least 8,7 knots.

3. Pitching of the Silja Europa

When the drafter of this memorandum interviewed sea captain Mäkelä on 2 August 1995, he stated that on her voyage from Helsinki to the scene of the accident involving the Ms Estonia,

the Silja Europa pitched unusually strongly. Waves washed over the forecastle. Mr. Harry Holmberg, a Finnish rescue instructor, has taken a video of the events at sea immediately at dawn of 28 September 1994. This clearly shows the waves hitting against the bow of the Silja Europa.

APPENDICES

No.	*Language*	*Document*
1	FIN	Damage to the bow door, 29 September 1994. The report of the chief engineer of the Silja Europa to the shipping company
2		Six photographs
3	FIN, ENG, GER	Three drawings
4	ENG	Printout from the track recorder on the Silja Europa regarding the speed of the vessel on the night of the accident involving the Estonia
5		Printout from the track recorder on the Silja Europa regarding the position of the vessel on the night of the accident involving the Estonia
6	FIN	Graphic speed diagram regarding the Silja Europa, prepared by captain Esa Mäkelä on the basis of the printouts from the track recorder

Keulaportin vauriot 29.09.1994

Yritettäessä avata keulaporttia aamulla Tukholmaan tulon jälkeen, havaittiin että portin SB puoli aukeni normaalisti mutta BB puoli liikkui ainoastaan n. 40 cm.

Tarkoitus oli ensin avata puolikas väkisin, mutta onneksi emme tehneet sitä. Emme olisi saaneet portin puolikasta enää tämän jälkeen kiinni.

Kun portti yritettiin avata, se otti kiinni kohtiin 7 ja 8 niin kovasti ettei hydrauliikka jaksanut.

Alus käännettiin ja lastin purku tapahtui peräportin kautta.

Portti suljettiin ja taljoilla portin yläpäästä auttamalla saatiin lukitukset kiinni.

Ilmoitettu asiasta Harri Kulovaaralle n. klo 5 sekä Erik Schalinille n. klo 5.30.

Bureau Veritaksen tarkastaja Lars Olof Ålander tuli paikalle n. klo 6, tutki vauriot ja antoi luvan lähteä merelle. Porttia ei saa kuitenkaan käyttää ennen korjausta. Visa N:o 7.

Löydetyt vauriot:

Kuva ja kohta 1:	Saranavarren sivu– sekä pohjalevyjen lommahtamiset.
Kuva ja kohta 2:	Tukikaaren # 218 lommahdus. (Vahvistettu merikoeajon jälkeen.)
Kuva ja kohta 3:	Portin yläpään ohjausrullan kiinnityksen murtuminen.
Kuva ja kohta 4.	Tukikaaren ~~#209~~ 219 lommahtaminen. (Saattaa olla vanhempi juttu.)
Kuva ja kohta 5.	Osoittaa vain miten portin puolikkaat ovat vastakkain.
Kuva ja kohta 6.	Lommahdus pitkittäisjäykkääjässä. (Tämäkin on vermasti vanha.)
	Näiden lisäksi joukko pienempiä muodonmuutoksi.

(Alus oli merikoejallo erittäin pahassa ilmassa ja tällöin tuli vaurioita samalle alueelle melko paljon. Tällöin tehtiin vahvistuksia ja korjauksia.)

Oltu yhteydessä MacGregor Naviren Tarmo Mäkeen sekä Pyökäriin. He toimittavat 3 korjausmiestä alukselle illalla 29.9 n. klo 22.30.

Samalla tulevat paikalle Bureau Veritaksen edusta Curt–Olof Eklund sekä käyttötarkastaja Erik Schalin.

SEPPO MATTILA
Chief Engineer
m/s SILJA EUROPA

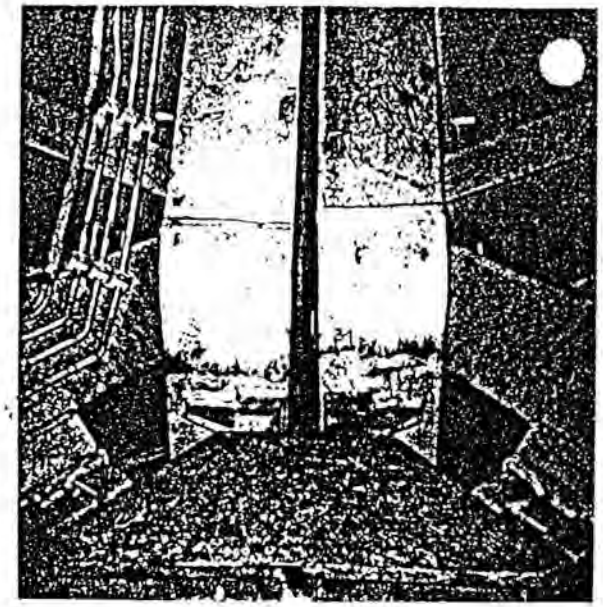

29.9-94

5.

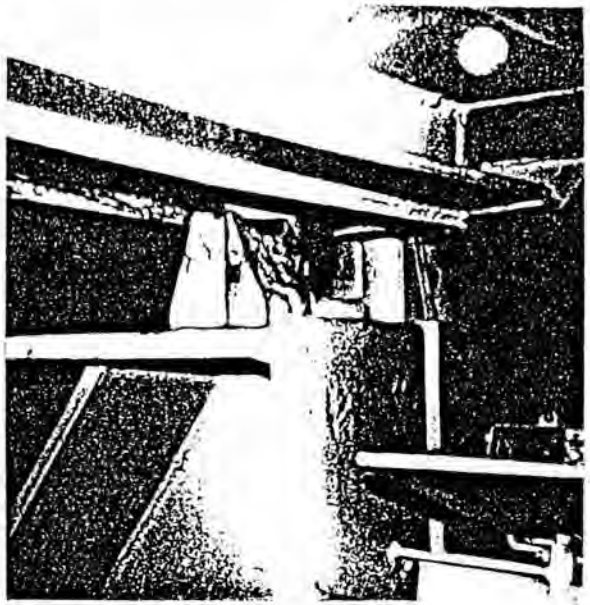

BB ohjaustrissa
29.9-94

3.

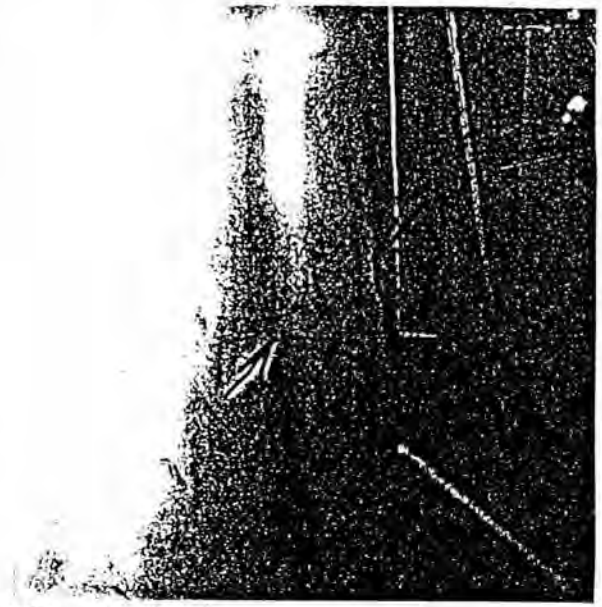

BB tukikaari #218
29.9-94

2.

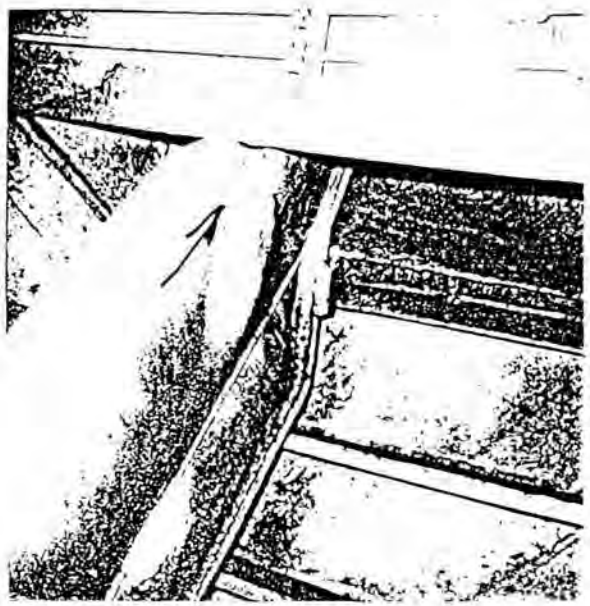

6.

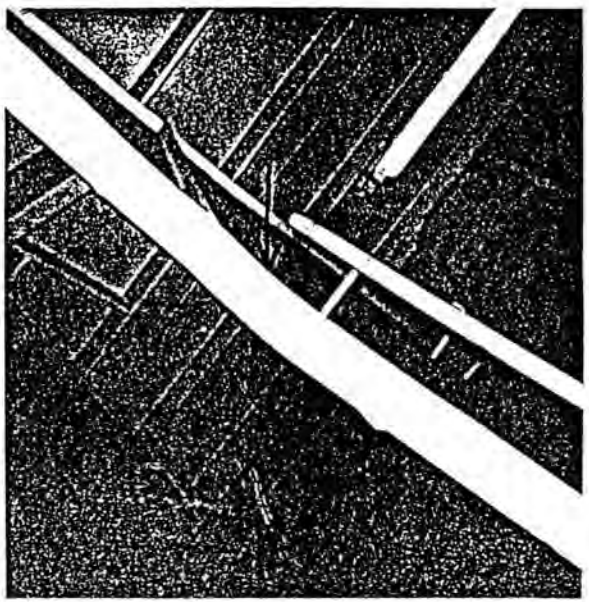

#209212

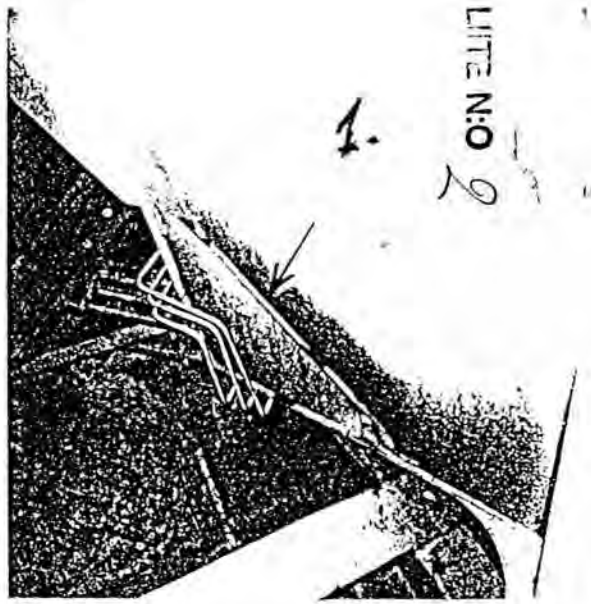

BB sacanaracs.

1.

LIITE N:O 2

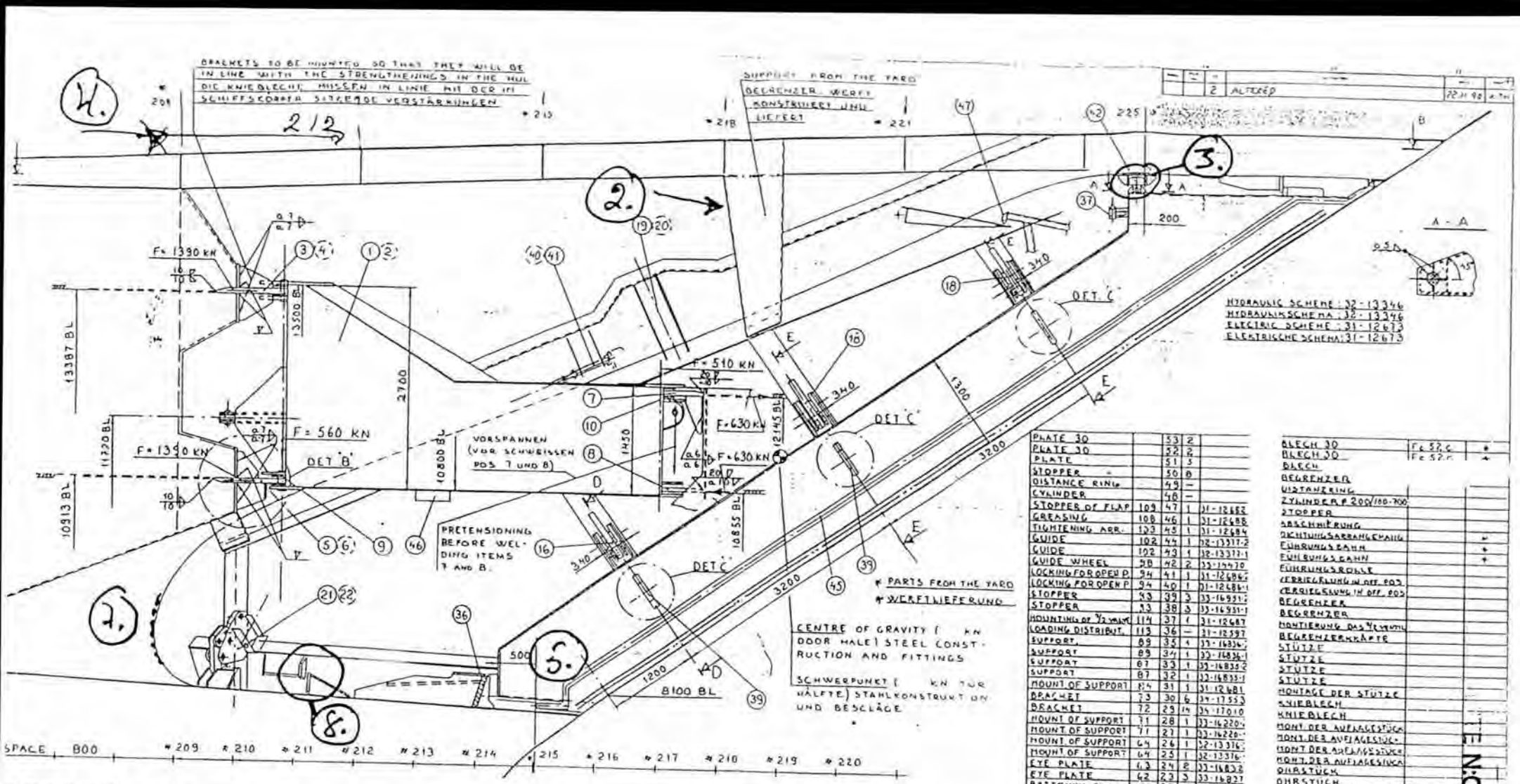

PLATE 30		53	2		
PLATE 30		52	2		
PLATE		51	5		
STOPPER		50	8		
DISTANCE RING		49	–		
CYLINDER		48	–		
STOPPER OF FLAP	109	47	1	31-12652	
GREASING	108	46	1	31-12688	
TIGHTENING ARR.	103	45	1	31-12684	
GUIDE	102	44	1	32-13317-2	
GUIDE	102	43	1	32-13317-1	
GUIDE WHEEL	98	42	2	33-17470	
LOCKING FOR OPEN D.	94	41	1	31-12686	
LOCKING FOR OPEN P.	94	40	1	31-12686-1	
STOPPER	93	39	3	33-16931	
STOPPER	93	38	3	33-16931-1	
MOUNTING OF ½ VALVE	114	37	1	31-12687	
LOADING DISTRIBUT.	113	36	–	31-12597	
SUPPORT	89	35	1	33-16836	
SUPPORT	89	34	1	33-16836-1	
SUPPORT	87	33	1	33-16833-2	
SUPPORT	87	32	1	33-16833-1	
MOUNT OF SUPPORT	84	31	1	31-12681	
BRACKET	73	30	6	34-17553	
BRACKET	72	29	14	34-17010	
MOUNT OF SUPPORT	71	28	1	33-16220	
MOUNT OF SUPPORT	71	27	1	33-16220-1	
MOUNT OF SUPPORT	64	26	1	32-13316	
MOUNT OF SUPPORT	64	25	1	32-13316-1	
EYE PLATE	43	24	8	33-16838	
EYE PLATE	42	23	3	33-16827	
BATTENING DEVICE	55	22	1	31-12645	
BATTENING DEVICE	55	21	1	31-12693-1	
BATTENING DEVICE	51	20	1	31-12685	
BATTENING DEVICE	51	19	1	31-12693	
BATTENING DEVICE	45	18	6	32-12630	
BATTENING DEVICE	43	17	2	31-12638	
BATTENING DEVICE	31	16	1	31-12957	
EYE PLATE	30	15	2	34-13053	
HEXAGON SCREW		14	8		
LOCKING PLATE	9	13	4	34-10931	
PIN	29	12	4	34-12784	
PLATE		11	12		
RING	28	10	2	34-11851	
RING	28	9	2	34-11893	
EYE PLATE	27	8	2	32-13382	
EYE PLATE	24	7	2	32-13383	
EYE PLATE	23	6	1	32-13381	
EYE PLATE	21	5	1	32-13380	
EYE PLATE	20	4	1	32-13377	
EYE PLATE	20	3	1	32-13376	
HINGE ARM ASS	4	2	1	32-13360	
HINGE ARM ASS	4	1	1	32-13280	

BLECH 30	Fe 52 C	*	
BLECH 30	Fe 52 C	*	
BLECH			
BEGRENZER			
DISTANZRING			
ZYLINDER Ø 200/180-700			
STOPPER			
ABSCHNITTRUNG			
DICHTUNGSSARRANGEMENT		*	
FÜHRUNGSZAHN		*	
FÜHRUNGSZAHN		*	
FÜHRUNGSROLLE			
VERRIEGELUNG IN OFF. POS			
VERRIEGELUNG IN OFF. POS			
BEGRENZER			
BEGRENZER			
MONTIERUNG DES ½ VENTILS			
BEGRENZERANKÄPFE			
STÜTZE			
STÜTZE			
STÜTZE			
STÜTZE			
MONTAGE DER STÜTZE			
KNIEBLECH			
KNIEBLECH			
MONT. DER AUFLAGESTÜCK			
MONT. DER AUFLAGESTÜCK			
MONT DER AUFLAGESTÜCK			
MONT. DER AUFLAGESTÜCK			
OHRSTUCK			
OHRSTUCK			
VERSCHLUSSANORDNUNG			
VERSCHLUSSANORDNUNG			
VERSCHLUSSANORDNUNG			
VERSCHLUSSANORDNUNG			
VERSCHLUSSANORDNUNG			
VERSCHLUSSANORDNUNG			
OHRSTUCK			
SECHSKANTSCH.			
ACHSENHALTER			
ZAPFEN			
BLECH			
RING			
RING			
OHRSTUCK			
OHRSTUCK			
OHRSTUCK			
OHRSTUCK			
OHRSTUCK			
OHRSTUCK			
MONTAGE DER SCHARNIERARM			
MONTAGE DES SCHARNIERARM			

DE MOUNTING OF THE HINGE ARM

- BEFORE CUTTING THE BOW DOOR SHELLS APART FROM THE HULL THE STOPPERS LOCKING DEVICES, HINGE ARMS AND GUIDE ROLLERS WITH GUIDES TO BE ADJUSTED AND MOUNTED TO THEIR PLACES USING TACK WELDS.
- THE STEEL STRUCTURE OF THE BOW MUST BE READY WELDED BEFORE CUTTING.
- THE BRACKETS OF HINGE ARM IN HULL SIDE TO BE MOUNTED SO THAT WHEN THE ADJUSTMENT RESERVE IS ACCORDING TO THE DRAWING 32-13379 THE OUTER END OF THE HINGE ARM IS ABOUT 18 MM ABOVE THE HORIZONTAL LEVEL. THE HINGE ARM IS THEN UNLOADED.
- THE PRELOADING (PRESSING DOWN) OF OUTER END OF HINGE ARM TO BE DONE WITH FORCE WHICH CORRESPONDS TO THE WHOLE WEIGHT +10 % OF DOOR HALF. THE BRACKETS OF HINGE ARM IN DOOR SIDE ARE TO BE MOUNTED TO THAT THE ADJUSTMENT RESERVE IS IN THE MIDDLE ACCORDING TO THE DRAWING 32-13378. ALL WELDINGS TO BE DONE BEFORE ENDING THE PRELOADING.
- AT HINGES WITH THRUST BEARING 2 SHEAVES THE SLIDING SURFACES TO BE PARALLEL.
- THE ADJUSTMENT WEDGES AT HINGES ARE TO BE FIRMLY TIGHTENED AND TO BE LOCKED WITH SCREWS.
- HYDR. PIPING IN HULL IN WAY OF BOW DOOR TO BE READY IN GOOD TIME SO THAT IT COULD BE USED FOR MOVING OF OPENING AND LOCKING CYLINDERS WITH CONTEMPORARY POWER PACK WHEN THE COMPRESSION OF RUBBER PACKING WILL BE ADJUSTED.

NOTE !

- STRENGTH OF FIXING POINTS OF PARTS TO BE CHECKED AND DESIGNED BY THE YARD. SPECIAL ATTENTION TO BE PUT ON FIXATION POINTS OF STOPPERS, HINGES AND LOCKING DEVICES.
- YARD DESIGNS AND FABRICATES LADDERS TO PROVIDE ACCESS TO BATTENING CLEATS.
- YARD ARRANGES ACCESS TO THE SPACE BETWEEN THE CLOSED BOW DOOR AND THE HULL.

MONTAGE DER SCHARNIERARM

1- DIE ANSCHLUSSFUGE DES BUGTÜRSEGMENTES VOM SCHIFFSKÖRPER MÜSSEN DIE BEGRENZER, VERSCHLUSSANORDNUNGEN UND FÜHRUNGSROLLEN MIT FUGUNGEN ANGEPASST UND MIT UNTERBROCHENE SCHWEISSNAHT MONTIERT WERDEN.

2- DIE GANZE STAHLKONSTRUKTION IN BUG MUSS FERTIG GESCHWEISST SEIN VOR DEM AUSSCHNEIDEN.

3- DIE SCHIFFSBODENSEITIGE KNIEBLECHE VON SCHARNIERARM MÜSSEN SO MONTIERT WERDEN DASS WENN DER EINSTELLBEREICH IST WIE IN ZEICHNUNG 32-13379 DARGESTELLT IST DER ÄUSSERE ENDE VON SCHARNIERARM ETWA 18 MM ÜBER HORIZONTALLAGE DER SCHARNIERARM IST UNBELASTET.

4- DIE VORSPANNUNG (NACH UNTEN) AUF DER ÄUSSERE ENDE VON SCHARNIERARM SOLL MIT EIN KRAFT, DEN DAS GEWICHT VON EIN TÜRSEKTION +10 % ENTSPRICHT, GEMACHT WERDEN. DIE TÜRSEITIGE KNIEBLECHE MÜSSEN IN DER MITTE DER IN ZEICHNUNG 32-13378 GEFORDERTE EINSTELLBEREICH MONTIERT WERDEN. VORSPANNUNG ERST DANN ENTFERNEN WENN DER SCHARNIERARM FERTIG GESCHWEISST IST.

5- DIE GLEITFLÄCHEN FÜR DIE AXIALLAGERSCHEIBEN MÜSSEN PARALLEL SEIN

6- DIE VERSTELLKEILE FÜR DIE SCHARNIERE MÜSSEN FEST MONTIERT WERDEN UND MIT SICHERUNG GESICHERT WERDEN.

7- DIE VERRIEGELUNG IN TÜRENBEREICH 2025 FESTSETZUNG GEMACHT WERDEN SO DASS DIE TÜREN UND VERSCHLÜSSE MIT EIN HILFSAGGREGAT GESCHLOSSEN WERDEN KÖNNEN BEIM EINSTELLEN DER GUMMIEINDRUCK.

ACHTUNG !

- FESTIGKEIT VON HINTERBAUTEN WERDEN WERFSEITIG BERECHNET UND KONSTRUIERT BESONDERE AUFMERKSAMKEIT AUF HINTERBAUTEN VON AUFLAGEN, SCHARNIERE UND VERSCHLUSSANORDNUNGEN

BOW DOOR MOUNTING - DRAWING

NEVESBUREF NB 627
BUGPFORTE
MONTIERENZEICHNUNG

NO

MARK	PLAN NO	ITEM	ALTERATION	DATE	SIGN
		2	POS. 5, 34-18863 → 34-18863	21.1.91	JU
		3	POS 14 ADDED	29.04.91	KTM
		4	ITEM 15 ADDED	07.11.91	KTM

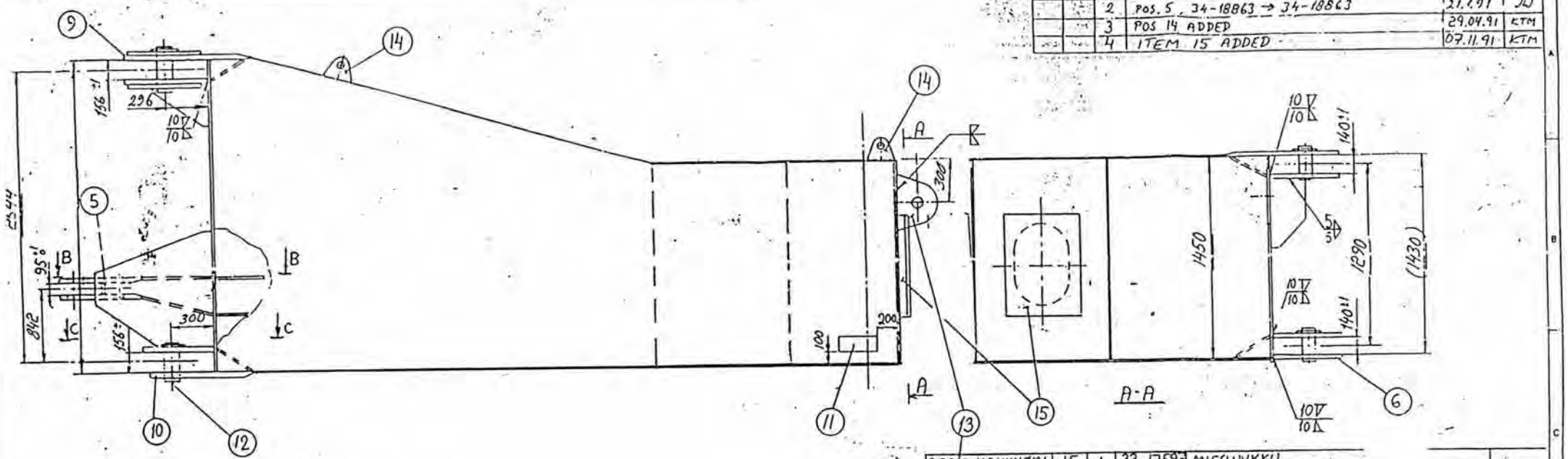

SURFACE MANHOLE	M6	15	1	33-17597	MIESLUUKKU	
LIFTING EAR	19a	14	2	TS 4-131	NOSTOKORVA.	POS 2
LIFTING EAR	19a	13	1	TS 4-131	NOSTOKORVA	POS. 6
GREASE NIPPLE		12	1		RASVANIPPA	
VAME PLATE	19	11	1	HGN 10900	NIMIKILPI	
EYE PLATE	17	10	1	33-15083	SARANA KORVA	
EYE PLATE	14	9	1	32-13379	SARANA KORVA	
EYE PLATE	12	8	(1)	33-16833-2	SARANAKORVA	LEFT
EYE PLATE	12	7	1	33-16833-1	SARANAKORVA	RIGHT
EYE PLATE	7	6	1	32-13378	SARANAKORVA	
EYE PLATE	6	5	1	34-18863	KORVA	
STEELPLAN	5	4	(1)	31-12697-2	TERÄSPIIRUSTUS	LEFT
STEELPLAN	5	3	1	31-12697-1	TERÄSPIIRUSTUS	RIGHT
HINGE ARM ASSY	4	2	(1)	32-13380-2	SARANVARREN VAR. OS	LEFT
HINGE ARM ASSY	4	1	1	32-13380-1	SARANAVARREN VAR. OS.	RIGHT

ITEM NO	NO OFF	DRAW NO	DENOMINATION	MATERIAL	REMARKS

HINGE ARM ASSEMBLY

SARANAVARREN VARUSTEIDEN ASENNUS

S.No. IN DRAW LIST

ITEM MASS	MATERIAL	REMARKS
MASS —	SYSTEM OF TOLERANCE ISO 10135	NO DRG LIST 4
SCALE ~	MATERIAL	
PROJ METHOD	DRAWN KTM	
	DATE 08.08.90	
EDITION	DRAWING NO 32 13280	SHEET
REG NO		

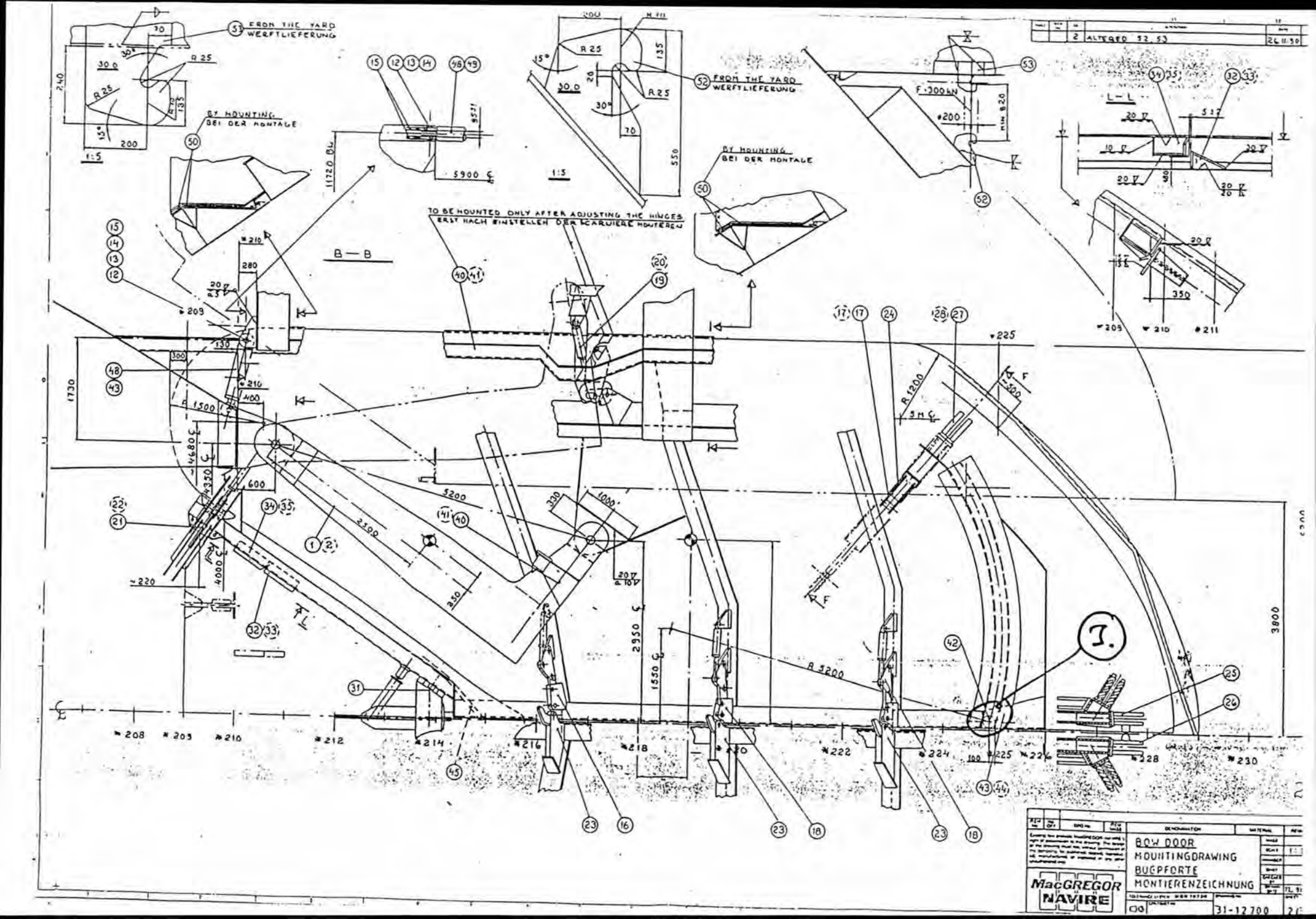
FROM THE YARD
WERFTLIEFERUNG
BY MOUNTING
BEI DER MONTAGE
TO BE MOUNTED ONLY AFTER ADJUSTING THE HINGES
ERST NACH EINSTELLEN DER SCHARNIERE MONTIEREN
B — B
L — L
1:5
2 ALTERED 32, 53
26.11.90
BOW DOOR
MOUNTINGDRAWING
BUGPFORTE
MONTIERENZEICHNUNG
MacGREGOR
NAVIRE
31-12700

LIITE N:O 4

M/S Silja Europa Track Recording: 01270994.GPS 20.10.1994
Ship relative to track history

Nr	Time UTC hh:mm:ss	Nav Mde	Latitude	Longitude	SOG kn	COG deg	HDG deg	Drift deg
T01	20:14:56	2D DGPS	N 59:39.428	E 23: 9.557	19.0	260.0	254.5	< 5.5
T02	20:23:52	2D DGPS	N 59:38.876	E 23: 4.149	19.0	257.0	253.3	< 3.7
T03	20:43:18	2D DGPS	N 59:37.642	E 22:52.582	18.1	258.2	256.2	< 2.0
T04	20:54:16	2D DGPS	N 59:36.955	E 22:46.270	18.2	258.9	257.3	< 1.6
T05	21:04:02	2D DGPS	N 59:36.342	E 22:40.703	17.5	257.2	255.2	< 2.0
T06	21:13:46	2D DGPS	N 59:35.732	E 22:35.238	17.5	257.2	255.0	< 2.2
T07	21:21:44	2D DGPS	N 59:35.280	E 22:30.802	16.8	258.7	256.6	< 2.1
T08	21:28:58	2D DGPS	N 59:34.898	E 22:26.855	16.3	261.1	257.3	< 3.8
T09	21:36:08	2D DGPS	N 59:34.536	E 22:23.050	16.3	258.3	255.3	< 3.0
T10	21:47:34	2D DGPS	N 59:33.945	E 22:16.957	16.0	258.8	255.9	< 2.9
T11	21:54:46	2D DGPS	N 59:33.585	E 22:13.197	15.7	258.6	255.8	< 2.8
T12	21:59:16	2D DGPS	N 59:33.353	E 22:10.846	15.7	258.6	253.6	< 5.0
T13	22:12:32	2D DGPS	N 59:32.671	E 22: 4.070	15.0	255.8	255.3	< .5
T14	22:25:10	2D DGPS	N 59:32.023	E 21:57.674	14.8	259.4	255.3	< 4.1
T15	22:31:54	2D DGPS	N 59:31.687	E 21:54.393	14.6	260.8	254.4	< 6.4
T16	22:44:28	2D DGPS	N 59:31.266	E 21:48.051	14.8	274.5	272.6	< 1.9
T17	22:47:28	2D DGPS	N 59:31.351	E 21:46.579	13.8	274.0	273.0	< 1.0
T18	22:58:50	2D DGPS	N 59:31.683	E 21:41.077	12.4	279.9	275.4	< 4.5
T19	23:02:16	2D DGPS	N 59:31.771	E 21:39.635	12.0	277.5	272.5	< 5.0
T20	23:09:48	2D DGPS	N 59:31.974	E 21:36.473	11.5	275.8	271.5	< 4.3
T21	23:14:04	2D DGPS	N 59:32.061	E 21:34.790	11.5	273.9	268.9	< 5.0
T22	23:20:46	2D DGPS	N 59:32.196	E 21:32.120	10.9	273.1	272.3	< .8
T23	23:26:30	2D DGPS	N 59:32.346	E 21:29.817	9.4	277.1	267.4	< 9.7
T24	23:30:10	2D DGPS	N 59:32.417	E 21:28.626	9.7	273.4	265.7	< 7.7
T25	23:36:38	2D DGPS	N 59:32.521	E 21:26.487	8.7	271.3	263.1	< 8.2
T26	23:45:48	2D DGPS	N 59:31.870	E 21:23.985	12.5	187.1	197.7	> 10.6
T27	0:06:18	2D DGPS	N 59:29.227	E 21:28.560	9.5	149.2	165.9	> 16.7
T28	0:20:40	2D DGPS	N 59:27.244	E 21:31.196	10.8	118.0	141.9	> 23.9
T29	0:45:48	2D DGPS	N 59:24.789	E 21:36.732	7.4	109.9	135.8	> 25.9
T30	1:01:20	2D DGPS	N 59:24.227	E 21:39.427	2.7	69.0	146.1	> 77.1

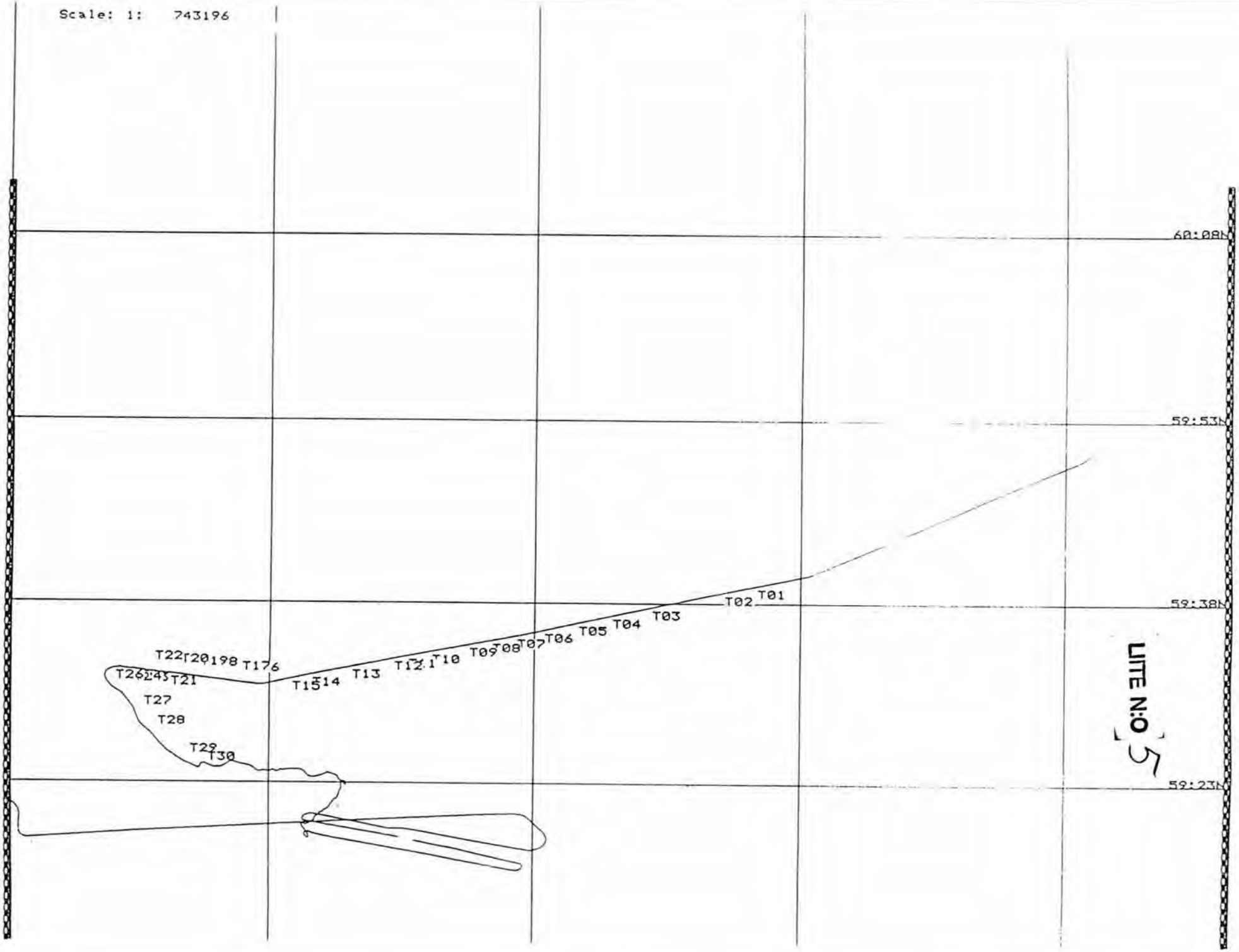
Scale: 1: 743196
60:08N
59:53N
59:38N
59:23N
T01
T02
T03
T04
T05
T06
T07
T08
T09
T10
T11
T12
T13
T14
T15
T16
T17
T18
T19
T20
T21
T22
T26
T27
T28
T29
T30
LITE NO. 5

Vauhtikäyrät Estonia/normaali

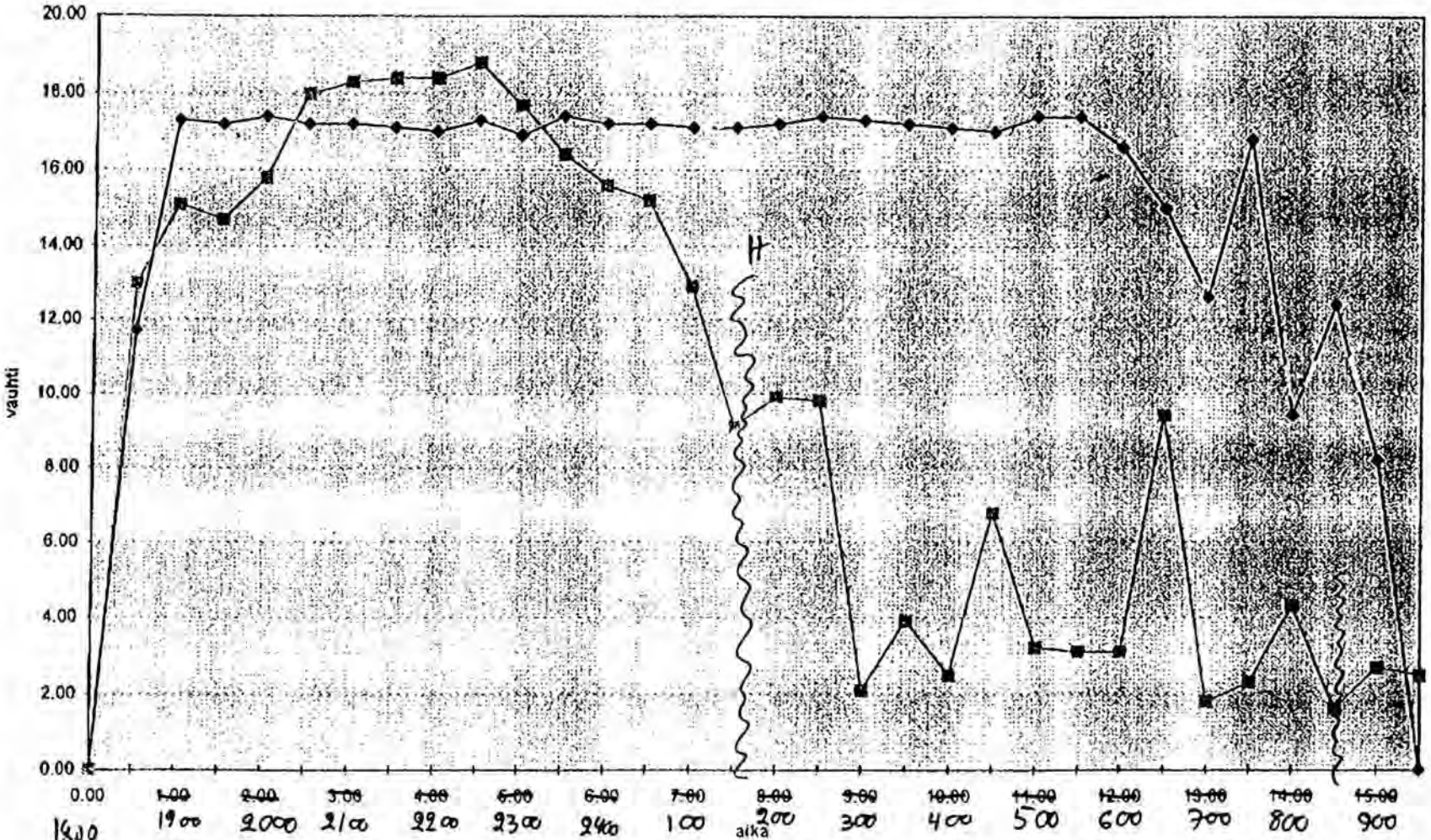

SUPPLEMENT No. 602

Suuronnettomuuden pelastussuunnitelma Saaristomeren meripelastusalueella. 18.6.1991.

Rescue Plan for Major Maritime Accident in the Archipelago Sea Maritime SRR. 18.6.1991.

SAARISTOMEREN MERIVARTIOSTO
Esikunta
Meritoimisto
Turku

SUUNNITELMA

18.6.1991

SUURONNETTOMUUDEN PELASTUSSUUNNITELMA SAARISTOMEREN MERIPELASTUSALUEELLA

SISÄLLYSLUETTELO

SUURONNETTOMUUDEN PELASTUSSUUNNITELMA SAARISTOMEREN MERIPELASTUSALUEELLA

1. YLEISTÄ

Suuronnettomuudella merialueella tarkoitetaan meripelastuspalvelun vaaratilannetta,

- jossa samanaikaisesti on kymmeniä ihmisiä hengenvaarassa taikka lukuisia ihmisiä samanaikaisesti menehtyy tai vammautuu ja,
- jonka pelastustoiminta edellyttää meri-, lento- ja yleisen pelastuspalvelun tavanomaista laajamittaisempaa yhteistoimintaa kotimaassa ja mahdollisesti myös muiden maiden meripelastuspalvelujen kanssa ja,
- joka herättää julkisuudessa tavanomaista suurempaa kiinnostusta.

Tämä suunnitelma perustuu Saaristomeren meripelastusalueen meripelastussuunnitelmaan ja on sitä täydentävä, erikoisesti suuronnettomuustilannetta varten laadittu.

2. SUURONNETTOMUUDEN UHKA-ARVIO

2.1. Yleistä

Suuronnettomuuden riskikohteita ovat säännöllisessä linjaliikenteessä olevat matkustaja-alukset, risteilyalukset ja vesibussit sekä lastialukset. Ilma-alusliikenteessä riskikohteina ovat merialueella lentävät matkustajakoneet.

Pahimpana onnettomuustyyppinä pidetään alusten yhteentörmäystä ja sen seurauksena tai muuten aiheutuvaa tulipaloa tai räjähdystä.

Saaristoisella ja karikkoisella rannikkoalueella ovat karilleajot todennäköisiä sumussa, lumi- tai räntäsateessa sekä myöhäissyksyn pimeinä ja myrskyisinä aikoina. Karilleajossa alukset saavat usein pahoja vuotoja, jolloin uppoamisen ja erilaisten päästöjen vaara on suuri.

Matkustaja-alusten riskialueina voidaan pitää Turku/Naantali - Tukholma ja Helsinki-Tukholma autolauttareiteillä niitä paikkoja, joissa reitit risteävät pohjois-etelä suuntaisiin laivaväyliin Utö - Isokari väylällä ja Ahvenanmerellä sekä karikkoisia ja ahtaita saaristokapeikoita.

Suurin kemikalio-onnettomuuden vaara on Uuteenkaupunkiin ja Naantaliin kulkevilla väylillä.

Suurin yhteentörmäyksen vaara on sisäsaaristossa ja Ahvenanmerellä.

2.2. Yhteentörmäys, vuoto, uppoaminen

Vakavin suuronnettomuus on laivojen yhteentörmäys, jossa ainakin toisena osapuolena on matkustaja-alus. Yhteentörmäyksen seurauksena voi olla tulipalo, räjähdyksiä, kemikalioiden tai kaasujen päästöjä, loukkaantumisia ja kuolemantapauksia. Pelastustoimien kannalta on merkityksellistä se onko uppoamisvaaraa vai ei.

Vuoto aluksessa tai uppoaminen on usein seurauksena yhteentörmäyksestä, karilleajosta tai räjähdyksestä. Tällöin matkustajien ja miehistön on jätettävä tai ainakin varauduttava jättämään laiva.

2.3. Räjähdys ja tulipalo

Räjähdyksen tai tulipalon sattuessa aluksella, on ensisijaisena tehtävänä rajoittaa palo niin, että pelastustoimet ovat mahdollisia. Tässä tehtävässä aluksen oma sammutusjärjestelmä on avainasemassa, mutta ulkopuolisen avun tarve on välttämätöntä, mikäli palo riistäytyy laivaväen hallinnasta.

2.4. Karilleajo

Matkustaja-alusten reitit kulkevat läpi saariston, jossa on olemassa karilleajomahdollisuus. Karilleajossa alukseen kohdistuva isku ja vauriot tulevat laivan alarakenteisiin eivätkä seuraukset ole yleensä niin pahoja kuin yhteentörmäyksissä.
Karilleajon seurauksena alus saattaa joutua uppoamisvaaraan, jolloin on varauduttava evakuoimaan miehistö ja matkustajat sekä rajoittamaan enempien vaurioiden syntyminen ympäristötuhon estämiseksi.

2.5. Kemikalio-onnettomuus

Kemikalio-onnettomuuden uhka kohdistuu ensisijaisesti erilaisiin kemikaliotankkereihin. Vaarallisia aineita kuljetetaan myös ro-ro-laivoilla ja autolautoilla rekka-autoilla sekä kontteihin pakattuina. Kemikalio-onnettomuudessa valmistaudutaan kuljettamaan myrkytyksen saaneet henkilöt evakuointikeskuksiin sekä erikoisvarusteiset torjuntaryhmät onnettomuusalukselle.

3. PELASTUSTOIMINNAN PERUSTEET

Meripelastuspalvelun kansalliset perusteet on säädetty laissa meripelastuspalvelusta (628/82) ja sen perusteella annetussa asetuksessa (661/82). Laki määrittelee meripelastuspalvelun koskemaan ihmishenkien pelastamista merihädässätai uhkaavasta vaaratilanteesta merialueella.

Rajavartiolaitoksen tehtävänä on etsintä- ja pelastustoiminnan lisäksi suunnitella, valvoa, johtaa ja koordinoida meripelastuspalvelua. Asetuksessa meripelastuspalvelusta määrätään rajavartiolaitoksen lisäksi meripelastuspalveluun osallistuvien muiden viranomaisten ja laitosten tehtävät sekä annetaan perusteet meripelastuspalvelujärjestelmän suunnittelulle ja toiminnalle.

Sisäasiainministeriön julkaisema MERIPELASTUSOHJE edellyttää, että meripelastus- ja lohkokeskuksilla on käytettävissään ajan tasalla olevat meripelastuspalvelusuunnitelmat. Tämä suunnitelma täydentää Saaristomeren meripelastusalueen meripelastussuunnitelmaa ja sen päämääränä on mahdollistaa oikea-aikaisten pelastustoimien käynnistäminen suuronnettomuustilanteissa.

4. PELASTUSSUUNNITELMA

4.1. Toiminnan perusajatus

Suuronnettomuustilanteessa tai sen uhatessa

- hälytetään meripelastuspalvelun ja yleisen pelastuspalvelun johto-organisaatiot, henkilöstö ja yksiköt hälytyskaavion mukaisesti toimi- tai kokoontumispaikoilleen tai suoraan toiminta-alueilleen,

- kuljetetaan onnettomuusalueelle lähtevillä ilmaalus ja / tai pintayksiköillä johtamis- ja yhteistoimintahenkilöstöä sekä tilanteen vaatimaa erikoishenkilöstöä ja -materiaalia tilanteen edellyttämille toimipaikoilleen,

- aloitetaan pelastus-, evakuointi- ja etsintätoimenpiteet onnettomuusalueella paikalle saapuvilla yksiköillä sekä avustetaan pelastustoimintaa onnettomuusaluksella paikalle tuodulla erikoishenkilöstöllä ja -materiaalilla,

- evakuoidaan paluukuljetuksina vaikeimmin loukkaantuneet ja kiireimmin apua tarvitsevat haaksirikkoiset suoraan sairaalaan tai hoidon jatkoyhteyspaikkaan,

- perustetaan yleisen pelastuspalvelun toimesta tilanteen vaatiessa evakuointikeskus, johon pääosa haaksirikkoisia evakuoidaan,

- jatketaan pelastus- ja etsintätoimintaa sekä evakuointia tilanteen asettamien vaatimusten mukaisesti luodun suuronnettomuusjohto-organisaation ja vartioston johtoryhmän johtamana ja koordinoimana sekä

- laaditaan onnettomuuden pelastustoiminnasta alkutiedote ja järjestetään tiedotustilaisuuksia tilanteen kehittymisen mukaan joukkotiedotusvälineille.

4.2. Pelastusyksiköt ja niiden valmius

Meripelastuskeskuksessa pidetään jatkuvasti tilannekuvaa merivartiostojen aluskaluston ja vartiolentueen ilma-aluskaluston sekä muiden meripelastusviranomaisten ja vapaaehtoisten järjestöjen meripelastusresursseista ja niiden valmiudesta.

Edellä mainittujen lisäksi pelastustehtäviin käytetään niihin soveltuvia kulussa olevia kauppalaivoja sekä kuntien ja yksityisten omistamia aluksia. Tarvittaessa pyydetään lisäapua lentopelastuskeskukselta ja muiden maiden meripelastuspalveluilta.

Yleisen pelastuspalvelun yksiköiden valmius ja tilannekuva saadaan yhteistoiminta-alueen palopäälliköltä.

4.3. Johtosuhteet

Meripelastuskeskuksen toimintaa johtaa vartioston komentaja tai hänen määräämänsä upseeri.

Komentajan (valmiuspäivystäjän) harkinnan mukaan hälytetään meripelastuskeskukseen yhteistoimintaviranomaisista koostuva meripelastusalueen johtoryhmä kokonaan tai tarvittavilta osiltaan.

Johtoryhmä kokoontuu vartioston esikuntaan sille varattuihin tiloihin. Johtoryhmän kokoonpano ja hälytysnumerot ovat meripelastusalueen meripelastussuunnitelmassa.
Suuronnettomuuden johtosuhteet liite n:o 1.

4.3.1. Johtaminen

Meripelastuskeskus johtaa ja koordinoi vastuualueellaan etsintä- ja pelastustoimintaan osallistuvien alajohtoportaiden toimintaa määräämällä niiden tehtävät ja antamalla niiden suorittamiseen liittyviä käskyjä, ohjeita ja tietoja sekä pitämällä yllä niiden toimintaedellytyksiä ja hankkimalla lisää tilanteen edellyttämiä resursseja.

4.3.2. Toiminta merivartiostojen sauma-alueella

Sauma-alueiden johtosuhteiden järjestelyistä, jotka poikkeavat normaalijärjestelyistä, meripelastuskeskukset sopivat keskenään.

4.3.3. Yhteistoiminta toisen valtion kanssa

Kukin valtio suorittaa itsenäisesti etsintä- ja pelastustoimenpiteet oman valtionsa aluevesillä. Jos toisesta valtiosta tarvitaan lisäresursseja, sopivat maiden meripelastuskeskukset keskenään avun saamisesta. Kansainvälisellä merialueella toimitaan osallistujamaiden välisten meripelastussopimusten mukaisesti tai meripelastuskeskukset sopivat keskenään johtosuhteista ja vastuualuejaosta.

4.3.4. Yhteydet ulkomaille

Meripelastuskeskus ottaa tarvittavat yhteydet ulkomaille sekä ylläpitää niitä maiden välisten kahdenkeskisten sopimusten mukaisesti.

4.4. Hälytyssuunnitelma

Suuronnettomuuden hälytyssuunnitelma on liitteenä n:o 2. Kaavioon sijoitetut yksiköt hälytetään tärkeysjärjestyksessä tilanteeseen soveltuvin osin ja laajuudessa.

Suuronnettomuustilanteessa meripelastuskeskuksen henkilöstöä vahvennetaan hälyttämällä esikunnan henkilöstöä työpaikalle hälytyskaavion mukaisesti.

4.5. Alajohtoportaiden tehtävät

4.5.1. Meripelastuskeskus

Meripelastuskeskuksen päivystäjä:

- pitää yllä tilannekuvaa meripelastusvalmiudesta,
- kirjaa onnettomuudesta saamansa tiedot ja merkitsee ne tasolle,
- käskee nopeimmin toimintakykyiset meripelastusyksiköt onnettomuuspaikalle pelastustoimintaan ja yksityiskohtaisen tilannekuvan saamiseksi,
- hälyttää tehtäväpäivystäjän ja valmiuspäivystäjän,
- aloittaa hälytysten toimeenpanon hälytyskaavion mukaisesti.
- selvittää vallitsevan sään ja sääennusteen sekä tilaa tarvittaessa ajelehtimislaskelmat.

Tehtäväpäivystäjä:

- hälyttää tarvittavat lisäresurssit,
- hälyttää komentajan ja tarvittavan lisähenkilöstön,
- informoi rajavartiolaitoksen esikunnan, naapurivartioston, ympäristöministeriön ja varustamon,
- alustavan tiedotteen laadinta ja jakelu.

Valmiuspäivystäjä:

- johtaa toimintaa komentajan apuna tai sijaisena,
- organisoi meripelastusalueen johtoryhmän työn,
- informoi naapurivaltiot,

Meripelastuskeskus:

- selvittää tilanteen ja avun tarpeen onnettomuuspaikalla,
- hankkii tiedot hälytettyjen yksiköiden lähtöajasta, arvioidusta saapumisajasta ja varustuksesta,
- antaa tehtävät ja ohjeet alayksiköille ja tarvittavalle erikoishenkilöstölle sekä yleiselle pelastuspalvelulle,
- määrää onnettomuuspaikan johtajan (OSC), joka koordinoi pelastusyksiköiden toimintaa onnettomuusalueella,
- määrää pintaetsinnän johtajan (CSS), joka koordinoi alus- ja venekalustolla suoritettavaa etsintää ja huolehtii yleisestä järjestyksestä ja turvallisuudesta onnettomuusalueella,
- määrää ilma-alustoiminnalle johtajan (CATS), joka koordinoi ilma-alusten käyttöä,
- määrää evakuointikeskuksen (keskusten) perustamisen ja yhteysupseeri(t),
- tiedottaa hädässä olevalle pelastustoimenpiteiden käynnistymisestä ja edistymisestä,
- ylläpitää pelastusorganisaation toimintaedellytyksiä tilanteen mukaan sekä hankkii tarvittavia lisäresursseja,
- huolehtii pelastustoiminnan tiedottamisesta ja koordinoi sitä sekä
- päättää pelastustoiminnan lopettamisesta.

Kun kuva onnettomuuden laadusta ja avun tarpeesta on sel-

vinnyt, meripelastuskeskus saattaa sen meripelastusyksiköiden ja muiden johtoportaiden tietoon.

4.5.2. Onnettomuuspaikan johtaja (OSC)

Meripelastuskeskus määrää onnettomuuspaikan johtajan. Onnettomuuspaikan johtajan tehtävänä on pelastustoiminnan johtaminen onnettomuusalueella meripelastuskeskuksen määrittämien tehtävien ja ohjeiden mukaisesti;

- tilannekuva
- johtosuhteet
- tehtävät alayksiköille,

- yhteistoiminta onnettomuusaluksen kanssa,
- yhteistoiminta evakuointikeskuksen kanssa,
- yhteistoiminta pintaetsinnän johtajan kanssa,
- yhteistoiminta lentotoiminnan johtajan kanssa,
- yleisen järjestyksen ja turvallisuuden ylläpito onnettomuusalueella ja
- tilannekuvan välittäminen meripelastuskeskukseen.

4.5.3. Pintaetsinnän johtaja (CSS)

Meripelastuskeskus määrää pintaetsinnän johtajan. Pintaetsinnän johtajan tehtävänä on yhteistoiminnassa onnettomuuspaikan johtajan, lentotoiminnan johtajan, evakuointikeskuksen johtajan ja lennonjohdon kanssa johtaa onnettomuusalueella pelastuslauttojen ja veneiden sekä veteen joutuneiden ihmisten etsintä- ja pelastustoimintaa sekä ylläpitää ja johtaa yleistä järjestystä ja turvallisuutta meripelastuskeskuksen määrittämien tehtävien mukaisesti;

- pitämällä tilannekuvaa
- järjestämällä johtosuhteet
- antamalla tehtävät alayksiköille ja
- välittämällä tilannekuva meripelastuskeskukseen.

4.5.4. Lentotoiminnan johtaja (CATS)

Meripelastuskeskus määrää lentotoiminnan johtajan. Lentotoiminnan johtajan tehtävänä on yhteistoiminnassa onnettomuusaluksen, onnettomuuspaikan johtajan, pintaetsinnän johtajan, evakuointikeskuksen ja lennonjohdon kanssa johtaa lentopelastusyksiköiden toimintaa meripelastuskeskuksen määrittämien tehtävien mukaisesti;

- pitämällä tilannekuvaa
- antamalla tehtävät alayksiköille ja
- välittämällä tilannekuva meripelastuskeskukseen.

4.5.5. Evakuointikeskus

Meripelastuspalvelun ja yleisen pelastuspalvelun yhteistoiminnan varmistamiseksi onnettomuusalueelta evakuoitujen haaksirikkoisten ja menehtyneiden vastaanottamiseksi, rekisteröimiseksi ja huoltamiseksi perustetaan onnettomuuspaikan läheisyyteen edullisten maantie- ja vesitieyhteyksien kohtaamisalueelle, jossa haaksirikkoisten huoltoedellytykset ovat olemassa, e v a k u i o n t i k e s k u s.

Evakuiontikeskuksen perustaa yleinen pelastuspalvelu yhteistoiminnassa meripelastuskeskuksen kanssa. Meripelastuskeskus asettaa evakuiontikeskukseen tarvittaessa yhteysupseerin, jonka tehtävänä on avustaa evakuointikeskuksen johtajaa yleisen pelastuspalvelun ja meripelastuspalvelun koordinoimisessa evakuointikeskuksessa.

Evakuointikeskukset Saaristomeren merivartioston pelastusalueella on esitetty liitteessä n:o 3 olevana karttapiirroksena.

Evakuointikeskuksen tehtävät ovat:

- haaksirikkoisten vastaanotto, rekisteröinti, majoitus, ensiavun anto, jatkohoitoon saattaminen sekä jatkoyhteyksien järjestäminen,
- menehtyneiden vastaanotto, rekisteröinti, kokoaminen ja jatkokuljetuksen järjestäminen,
- yleisen järjestyksen ja turvallisuuden ylläpitäminen evakuointikeskuksessa,
- toiminta onnettomuusalueen henkilöstön, materiaalin ja kuljetusten huoltoetappina ja välivarastointipaikkana,
- järjestää elueelle ilmakuljetuksia varten helikopterien laskeutumis- ja odotusalueet ja polttoainetäydennysmahdollisuuden sekä
- tiedottaminen pelastustoimista evakuointikeskuksen ja yleisen pelastuspalvelun kannalta.

4.5.6. Yhteysupseerit

Meripelastuskeskus asettaa tarvittaessa yhteysupseerit
- onnettomuusalukselle ja
- evakuointikeskukseen

Yhteysupseerien tehtävänä on avustaa sijoitusyksikköään asiantuntijana meripelastuspalvelun toimintaan ja hyväksikäyttöön liittyvissä kysymyksissä ja välittää sijoitusyksikkönsä tilannekuvaa ja erityistarpeita meripelastuskeskukseen ja onnettomuuspaikan johtajalle.

5. VIESTIYHTEYDET

Viestiyhteydet toteutetaan maissa olevien toimintapisteiden välillä pääasiassa puhelin-, telex- ja telefax-yhteyksinä.

Viestiyhteyskaavio on liitteenä n:o 4.

Operatiivinen johtoverkko toteutetaan VHF:n kanavilla 16 ja 14. Operatiivisessa johtoverkossa ovat mukana:

- onnettomuusalus
- meripelastuskeskus

- meripelastuslohkokeskus
- onnettomuuspaikan johtaja
- pintaetsinnän johtaja
- lentotoiminnan johtaja
- evakuointikeskuksen johtaja.

Kunkin alijohtajan käyttöön perustetaan seuraavan kanavajaon mukaiset erillisverkot:

- onnettomuusalus VHF-kanavat 15 ja 17
- onnettomuuspaikan johtaja VHF-kanava 10
- pintaetsinnän johtaja VHF-kanava 73
- lentotoiminnan johtaja VHF-kanava 67 sekä ilmailuradion taajuus 123,1 MHz
- evakuointikeskuksen johtaja, palo- ja pelastustoimen sekä poliisin radiokalusto.

6. TIEDOTTAMINEN

Onnettomuuden pelastuspalvelun kokonaistilanteen ja meripelastuspalvelun tiedottamisesta ja sen koordinoimisesta huolehtii keskitetysti merivartioston nimeämä tiedotusupseeri vartioston komentajan (vast) tai pelastustoimintaa johtavan upseerin antamien ohjeiden mukaisesti, mikäli rajavartiolaitoksen esikunta tai valtioneuvosto ei ole ottanut tiedotusvastuuta.

Onnettomuusalusta, sen miehistöä ja matkustajia sekä pelastustoiminnasta itse aluksella koskevasta tiedottamisesta huolehtii aluksen omistava varustamo ja aluksen päällikkö.

Yleistä pelastuspalvelua ja evakuointikeskusta koskevasta tiedottamisesta huolehtii läänin pelastustarkastaja ja / tai evakuointikeskuksen johtaja.

Meripelastuskeskus antaa onnettomuudesta alkutiedotteen mahdollisimman nopeasti. Tiedote koostuu ainakin seuraavista asioista:

- mitä on tapahtunut ?
- kenelle/mille on tapahtunut ?
- missä on tapahtunut ?
- milloin on tapahtunut ?
- milloin ja missä järjestetään ensimmäinen tiedotustilaisuus.

Tiedote luetaan vartioston tiedotusnauhuriin ja lähetetään telefaxilla STT:lle välitettäväksi edelleen muille tiedotusvälineille.

Tilanteeseen soveltuvin väliajoin järjestetään tiedotustilaisuuksia ja niistä tiedotetaan tiedotusvälineille erikseen.

Merivartiosto kuljettaa mahdollisuuksien mukaan tiedottajia

onnettomuuspaikalle. Pyrkimyksenä on saada onnettomuusalueelle vähintään tiedottajaryhmä, jonka aineisto on muiden tiedottajien vapaasti käytettävissä. Ryhmä koostuu TV:n kuvausryhmästä sekä lehdistön ja radion edustajista.

Tiedottamista varten varataan operatiivisista yhteyksistä riippumattomat erilliset viestiyhteydet.

Saaristomeren merivartioston komentaja

Kommodori

R Tiilikainen

Meritoimiston toimistopäällikkö

Komentajakapteeni

T Eckstein

LIITE N:O 1

MERIPELASTUSPALVELUN JOHTOSUHTEET

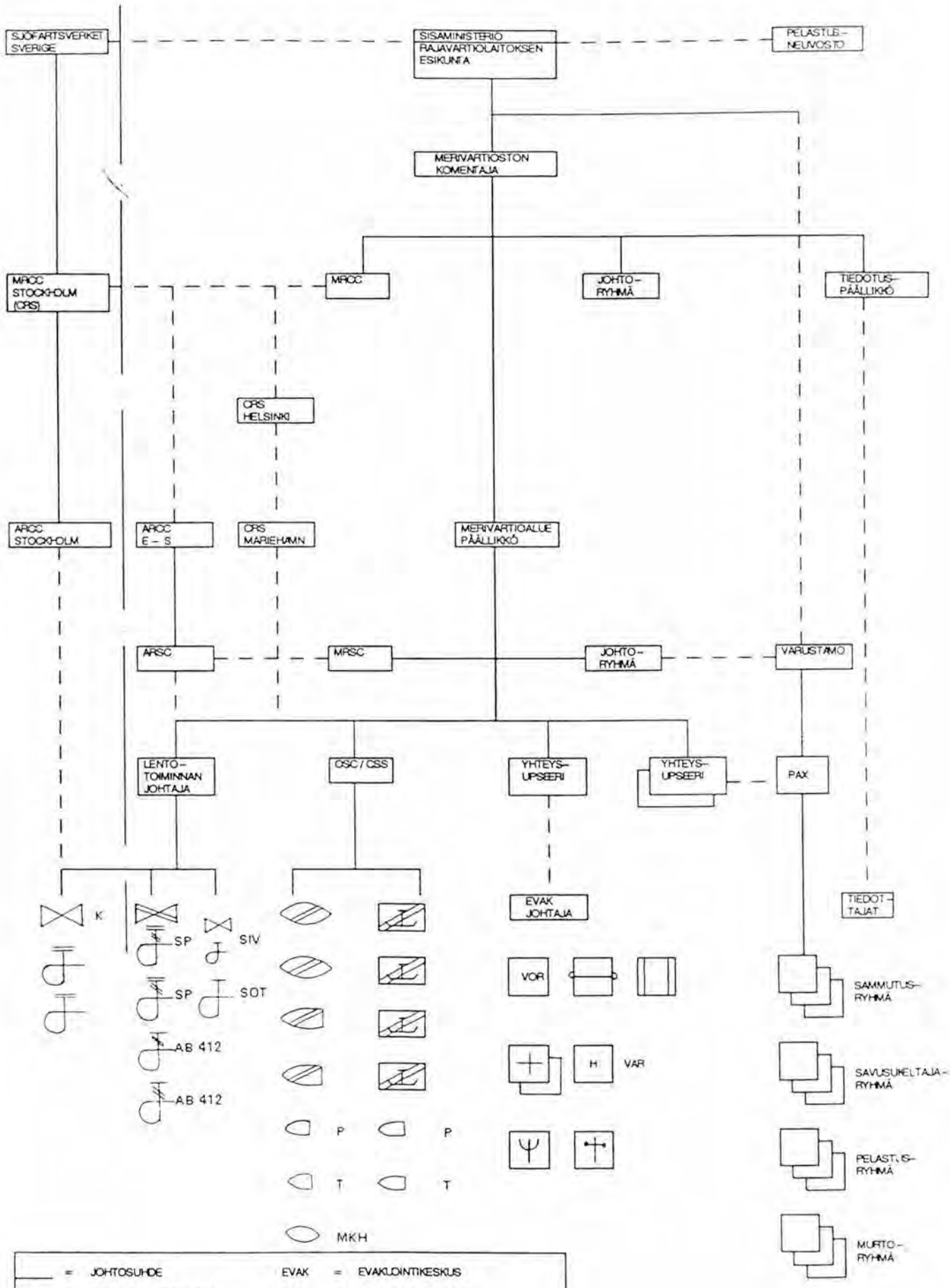

———	=	JOHTOSUHDE	EVAK	=	EVAKUOINTIKESKUS
– – –	=	YHTEISTOIMINTASUHDE	VOR	=	VASTAANOTTORYHMÄ
MRCC	=	MERIPELASTUSKESKUS	P, T	=	POUISI, TULLI
MRSC	=	MERIPELASTUSLOHKOKESKUS	PAX	=	MATKUSTAJA-ALUS
ARCC	=	LENTOPELASTUSKESKUS	OSC	=	ONNETTOMUUSPAIKANJOHTAJA
CRS	=	RANNIKKORADIOASEMA	CSS	=	PINTAETSINNÄN JOHTAJA

LIITE N:O 2

HÄLYTYSKAAVIO

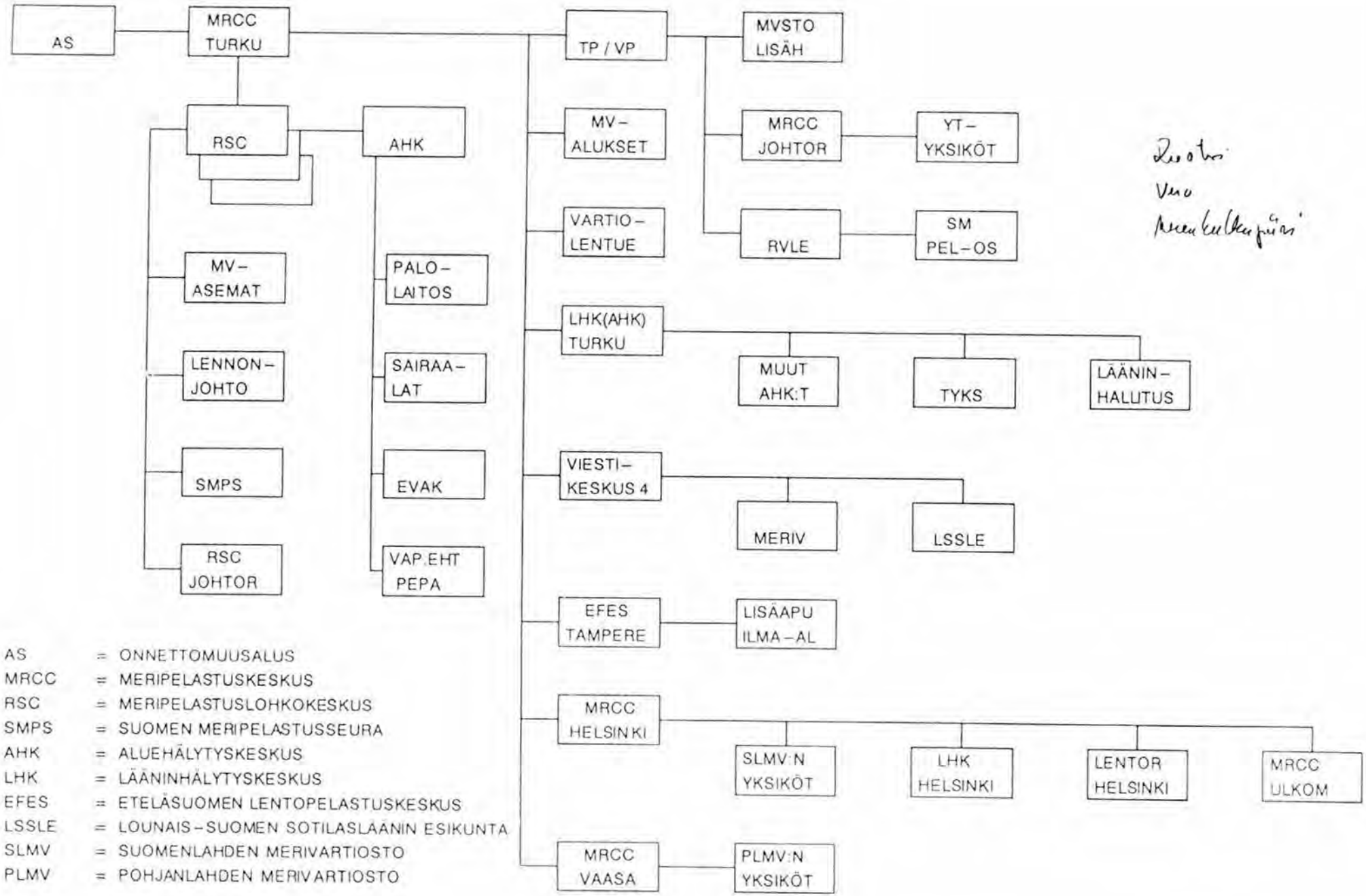

AS = ONNETTOMUUSALUS
MRCC = MERIPELASTUSKESKUS
RSC = MERIPELASTUSLOHKOKESKUS
SMPS = SUOMEN MERIPELASTUSSEURA
AHK = ALUEHÄLYTYSKESKUS
LHK = LÄÄNINHÄLYTYSKESKUS
EFES = ETELÄSUOMEN LENTOPELASTUSKESKUS
LSSLE = LOUNAIS-SUOMEN SOTILASLÄÄNIN ESIKUNTA
SLMV = SUOMENLAHDEN MERIVARTIOSTO
PLMV = POHJANLAHDEN MERIVARTIOSTO

LIITE N:O 3 EVAKUOINTIKESKUKSET

TURUN MERIVARTIOALUEEN EVAKUOINTIKESKUKSET

- Viking Line terminaali, Turku	921 - 63311
- Viking Line terminaali, Naantali	921 - 852111
- Silja Line terminaali, Turku	921 - 652211
- Airiston matkailuhotelli, Parainen	921 - 889114
- Gyltön linnake, Korppoo	926 - 31540
- Utön linnake, Utö	925 - 47111
- Örön linnake, Örö	925 - 673111

Satamaterminaalien hälyttämisen voi suorittaa myös poliisitalon lyhytvalintanumeroilla sekä
VHF -radiolla:
Turun satama kanava 12
Naantalin satama kanava 11

AHVENANMAAN MERIVARTIOALUEEN EVAKUOINTIKESKUKSET

- Viking Line terminaali, Maarianhamina
- Långnäsin lauttalaituri, Långnäs
- Eckerön postitalo, Eckerö

Näiden hälyttämisen hoitaa Ahvenanmaan AHK
928-000 tai 928-11000

RAUMAN MERIVARTIOALUEEN EVAKUOINTIKESKUKSET

- Merikarvian urheilutalo, Merikarvia	939 - 511512
- Reposaaren koulu, Reposaari	939 - 344037
- Mäntyluodon koulu, Mäntyluoto	939 - 343217
- Luvian seurojentalo, Tasala	939 - 581064
- Linnainmaan koulu, Eurajoki	938 - 82067
- Kuuskajaskarin linnake, Kuuskajaskari	938 - 221566

- Rauman merenkulkuoppilaitos, Rauma	938 - 223400
- Kammelan koulu, Pyhäranta	922 - 42136
- Pohitullin koulu, Uusikaupunki	922 - 1551
- Katanpään linnake, Kustavi	922 - 77815
- Kivimaan koulu, Kustavi	922 - 17101
- Trappulan koulu, Taivassalo	922 - 18202

EVAKUIONTIKESKUKSET

1. Merikarvian urheilutalo, Merikarvia
2. Reposaaren koulu, Reposaari
3. Mäntyluodon koulu, Mäntyluoto
4. Luvian seurojentalo, Luvia
5. Linnainmaan koulu, Eurajoki
6. Kuuskajaskarin linnake, Kuuskajaskari
7. Rauman merenkulkuoppilaitos, Rauma
8. Kammelan koulu, Pyhäranta
9. Pohitullin koulu, Uusikaupunki
10. Katanpään linnake, Kustavi
11. Kivimaan koulu, Kustavi
12. Trappulan koulu, Taivassalo
13. Viking Line terminaali, Turku
14. Viking Line terminaali, Naantali
15. Silja Line terminaali, Turku
16. Airiston matkailuhotelli, Parainen
17. Gyltön linnake, Korppoo
18. Utön linnake, Utö
19. Örön linnake, Örö
20. Viking Line terminaali, Maarianhamina
21. Långnäsin lauttalaituri, Långnäs
22. Eckerön postitalo, Eckerö

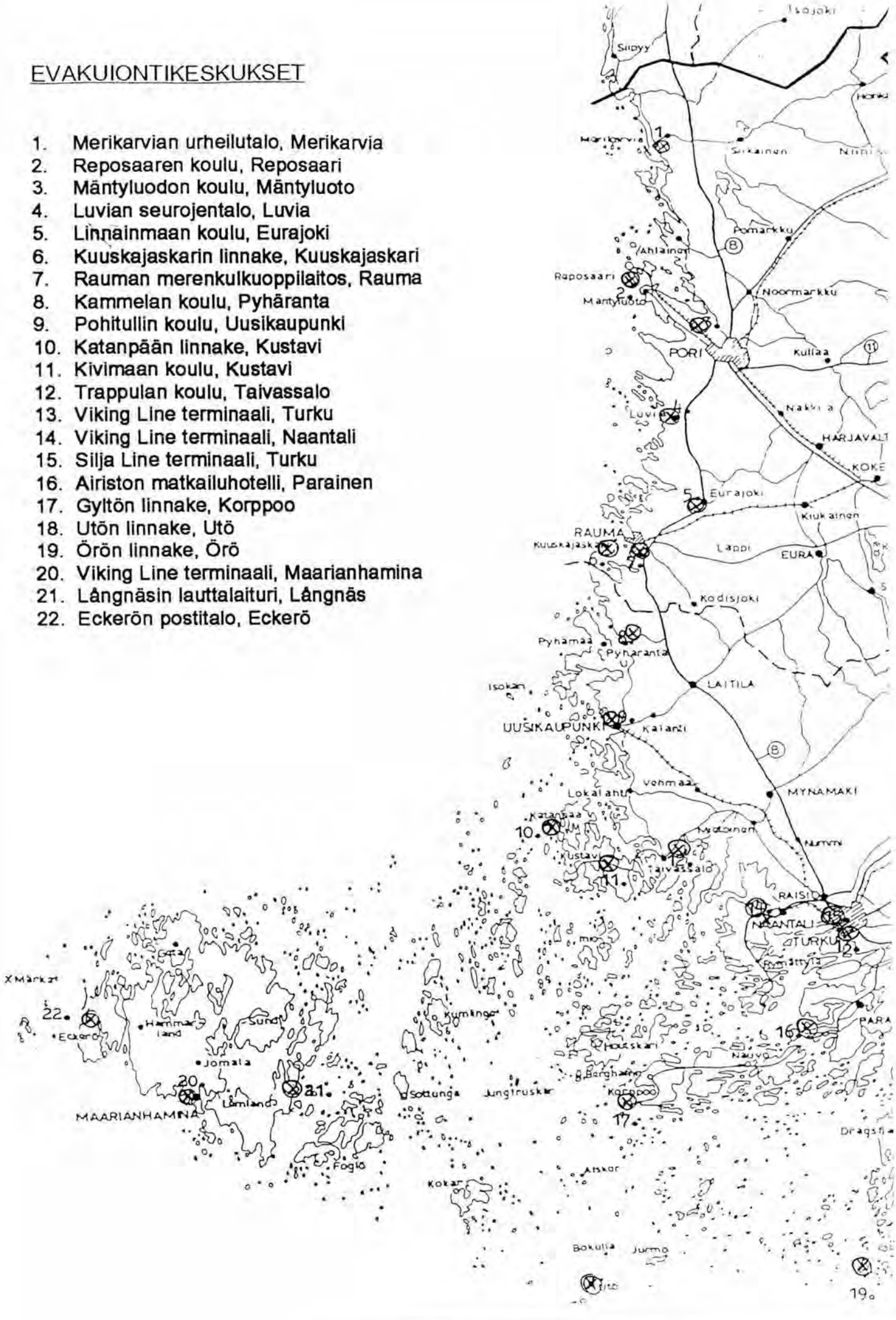

LIITE N:O 4

SUURONNETTOMUUDEN RADIOYHTEYSKAAVIO

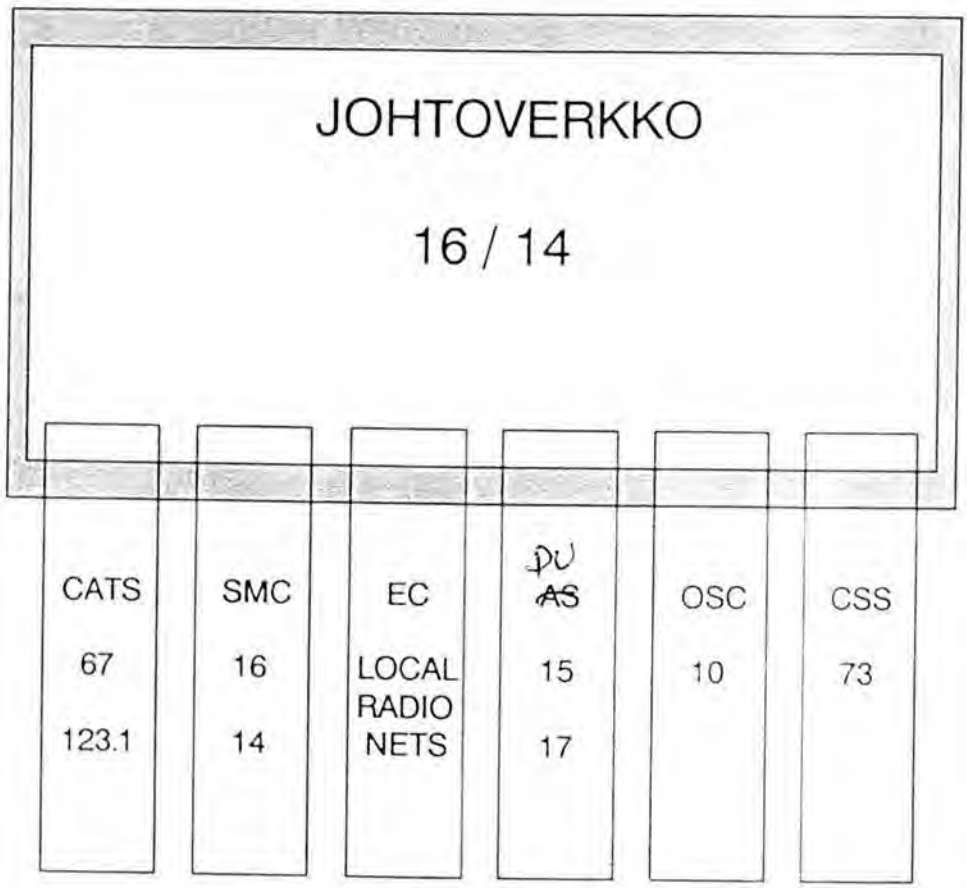

ERILLISVERKOT

CATS = CO-ORDINATOR AIR TRAFFIC SERVICE
SMC = SEARCH AND RESCUE MISSION CO-ORDINATOR
EC = EVACUATION CENTER
~~AS = ACCIDENT SHIP~~ DU = DISTRESSED UNIT
OSC = ON-SCENE COMMANDER
CSS = CO-CORDINATOR SURFACE SEARCH

SUPPLEMENT No. 603

ARCC Arlanda:

Bakgrund avtal enl Räddningstjänstlagen, larmtider och erfarenheter.

Flygräddningstjänst "Estonia" 1994-09-28--29.

3
ESTONIA
G 19

Bakgrund - avtal

ARCC ansvarsområde är enligt Räddningstjänstlagen av 1986:1102 § 26:

" Vid flyghaveri inom Sveriges sjöterritorium med undantag för vattendrag, kanaler och hamnar samt andra insjöar än Vänern, Vättern och Mälaren samt Sveriges ekonomiska zon, skall Luftfartsverket svara för räddningstjänsten. Luftfartsverket skall svara för förebyggande räddningsinsatser mot skador när ett luftfartyg är nödställt eller när fara hotar lufttrafiken. Verket skall också svara för efterforskning av luftfartyg som saknas." Utöver svensk lag har Sverige i enlighet med ICAO Annex 12 åtagit sig att svara för flygräddningstjänst inom svensk flyginformationsregion.

Detta innebär att vid flyghaveri inom svensk räddningsregion ansvarar Luftfartsverket/Flygräddningscentralen för "Efterforskning" över svenskt territorium och ut till flyginformationsgräns samt även "Undsättning" över hav ut till flyginformationsgränsen och över Vänern, Vättern och Mälaren.

1994-03-20 slöts avtal på regeringsnivå mellan Sverige och Finland om samarbete vid sjö och flygräddning. 1994-02-01 undertecknades ett "Protokoll" på myndighetsnivå avseende räddningstjänst. I dessa avtal förtecknas principer för samarbete vilket följer rekommendationer från ICAO i Annex 12. Principen är att den central inom vars räddningsregion en olycka inträffar är ledande central och övriga centraler bistår med begärda resurser.

I biavtal till huvudavtalet mellan Luftfartsverket och Försvarsmakten anges i "Särskilda uppgifter för ARCC/CEFYL avseende försvarsmakten" bl a att:

- ARCC/CEFYL beslutar, med avseende på flygräddningstjänst och på uppdrag av försvarsmakten, om insats och ledning av de flygräddningsresurser som beskrivs i Mil AIP.

- ARCC/CEFYL fattar också beslut om insats för och ledning av försvarsmaktens övriga räddningsresurser, som på avrop ställts till ARCC/CEFYL förfogande för räddningstjänst.

- ARCC/CEFYL får därutöver, på begäran av annan statlig eller kommunal räddningstjänst, besluta om insats och ledning av försvarsmaktens resurser angivna i Mil AIP eller som i övrigt ställts till ARCC/CEFYL förfogande för ändamålet. Detsamma gäller insatser inom ramen för träffade avtal med Sveriges grannländer om bistånd med räddningsresurser. Beslutade räddningsinsatser rapporteras till försvarsmakten.

Detta har senare förtydligats till att gälla all räddningsverksamhet och alla insatser med flygande enheter.

- ARCC/CEFYL skall reglera och leda sådan särskild verksamhet som påverkar flygräddningsresursernas beredskap och tillgänglighet. Exempel på sådan verksamhet är; sjuk- och personaltransporter. Detta innebär att ARCC/CEFYL ansvarar för att flygräddningsresurser finns tillgängliga. I förekommande fall efter ombaseringar.

Sjöfartsverket ansvarar för sjöräddning inom motsvarande områden genom de räddningscentraler MRCC som finns upprättade. F n en central i Göteborg och en i Stockholm. Centralen i Stockholm skall enligt beslut läggas ned och ansvaret överflyttas till centralen i Göteborg från ca -98.

Vid ett flygräddningsfall inom svensk räddningsregion är ARCC/CEFYL ledande central och begär hjälp från andra centraler och vid sjöräddningsfall begär MRCC hjälp med flyginsats. Respektive central leder alltid "egna" resurser. Detta förutsätter dock en klar återrapporteringsrutin.

Beredskap

Under natten 27 september larmade MRCC S om hjälp med helikopterinsats för sjöräddningsfall söder Öland. En helikopter från Ronnneby var därför i luften när begäran om hjälp kom från MRCC Åbo via MRCC S. Grundberedskap i övrigt under "icke militär flygövningstid" är:

- 1 helikopter Puma ur flygvapnet, basering Visby, 1 tim beredskap.

- 1 helikopter Puma ur flygvapnet, basering Ronneby, 1 tim beredskap.

- 1 helikopter Vertol ur marinen, basering Berga, 2 tim beredskap. I praktiken 1 tim beredskap.

- 1 helikopter Vertol ur marinen, basering Säve, 1 tim beredskap.

På flygräddningscentralen finns två st flygräddningsledare. Normalt i jour i sovrum vid räddningscentralen. Vid aktuell tid fanns en ansvarig flygräddningsledare i centralen p g a sjöräddningsuppdraget söder Öland. Normal insatstid från jour är omedelbar. Larmning m m kan ske från jourrum.

Larmning

Kl 0103 kom larm från MRCC S. "Färjan Estonia pos 5922/2140 har 30° slagsida och begär assistans". Larmet kom från MRCC Åbo via MRCC S.

0107 Larm till hkp Visby.
0109 Larm till hkp Berga.
0125 Larm till besch i hemmet i Ronneby (ej beredskap).
0136 "Estonia har ev slagit runt. Inget eko".
0137 Ronneby hkp i luften. Order gå mot Visby för tankning och sedan mot färjan.
0142 Larm i bostad till besch i Söderhamn (ej beredskap).
0146 Larm till berhkp på Säve.
0147 Begär ytterligare resurser på Berga.
0150 Larm i bostad till marinhkp Ronneby (ej beredskap).
0225 CARCC, på tjänsteresa, orienteras.
0315 Karup erbjuder två hkp SeaKing.
0324 MRCC S inget svar från MRCC Åbo.
0330 Info till VB Hkv.
1020 Startorder till berhkp Kallax.

Flygvapnets räddningshelikoptrar används primärt för militär flygräddning och har hög beredskap under militär flygövningstid (må-to 0730-1600, fre 0730-1200). Övrig tid beredskap enligt ovan. Marinens hkp används primärt för incidentberedskap och i övrigt för räddningstjänst med beredskap enligt ovan.

Sammanfattning:
Första hkp på plats 0240. Därefter kontinuerlig tillförsel så att kl 0700 fanns:
4 st Puma ur flygvapnet
5 st Vertol ur marinen
2 st SeaKing ur danska flygvapnet i eller på väg mot området.
Detta antal bibehölls sedan hela dagen genom att helikoptrar med tekniska fel ersattes av andra. MRCC Åbo avböjde ytterligare hkpinsatser m h t väder och svårt att leda hkp.
Kvar i Sverige fanns:
1 Puma på Såtenäs.
1 Puma på Kallax.
1 Puma på Söderhamn.
1 Vertol på Säve.

Insatser

Flygtiden från närmaste baser Berga och Visby är ca 1 tim. Första hkp var på plats ca 0240 - i stort 1 1/2 tim efter första larm. Inledande larmet var inte av typen haveri utan som i flygräddning kallas "fara för haveri". Trots detta reagerade och agerade flygräddningsledaren som om allvarlig fara förelåg. Detta torde ha påskyndat räddningsförloppet och har därigenom bidragit till att många kunde räddas. Insatserna hade kunnat ökas efter gryningen men MRCC Åbo ansåg sig inte kunna ta emot fler helikoptrar.

Ledning

Enligt grunddokument och avtal var det i detta fall MRCC Åbo som var ansvarig och ledande central då förlisningen ägde rum inom finsk räddningsregion. Begäran om hjälp ställdes till MRCC S då det är naturligt att arbeta sjöräddning till sjöräddning och flygräddning till flygräddning. Enligt tidigare nämnt "Protokoll" kunde MRCC Åbo ha vänt sig direkt till ARCC med begäran om hkphjälp. Att så inte skedde bedöms inte ha påverkat tider eller insatser.

Enligt svenska helikoptrar fanns ingen direktledning från MRCC Åbo. Samordning mellan helikoptrarna och insatsområden ägde rum på plats. Detta torde ha medfört "dubbelarbete" genom att ex vis samma livflotte undersöktes flera gånger. Någon samordning av flygsäkerhetsskäl förekom inte heller.

Var och en arbetade för sig och det är möjligt att en samordnad insats under ledning av en flygräddningsledare hade medfört större antal räddade.

Kaptenen på Silja Europa i området fungerade som OSC, On Scene Commander, för ytenheter. Denne hade dock ingen utbildning i motsvarande funktion för flygande enheter. Senare tillfördes två st flygledare till "Europa" dock troligen först då räddningsförloppet avslutats och inga ytterligare överlevande fanns. Samarbetet med ACC Tammerfors för tillstånd för inpassage i finskt område fungerade snabbt och bra.

Återmatning

En mycket viktig del i räddningstjänst för den central som har att bistå med resurser är återmatning av information om vad som händer på olycksplatsen och om fler resurser behövs.

Det förefaller som om denna information inte har funnits ens vid MRCC Åbo. Därför kunde tillräcklig information inte erhållas varken vid MRCC S eller ARCC. En besättning ringde via NMT till ARCC och avrapporterade. Då normalt samband via kortvåg, HF, inte fungerade under natten (normalt) och p g a tekniskt fel inte heller under förmiddagen fanns inga möjligheter att få aktuellt läge. En återmatning och kontinuerligt samband måste säkerställas, av flygsäkerhetsskäl t ex uppföljning av flygande enheter.

Bedömningar

Viss kritik har riktats mot ARCC för att inte sätta in samtliga tillgängliga helikopterresurser. Som framförts tidigare finns endast 4 hkp i 1 tim beredskap. Flygräddningsledarens tidiga bedömning att detta kunde bli något stort säkerställde en så tidig och omfattande insats som var möjlig. En högre beredskap kunde möjligen ha tidigarelagt insatsen men då endast marginellt. Dimensionerande för insatstiden är flygtiden till området.

För att ersätta hkp som fått tekniska fel fanns en viss beredskap på bl a Berga. Hkp från Kallax som till en början

fått order att gå mot Åbo fick, då MRCC Åbo inte kunde ta hand om flera hkp, i stället landa Söderhamn för att snabbt kunna ersätta annan hkp i räddningsområdet. Denna hkp drabbades också av omfattande tekniskt fel. Flygräddningsledarens bedömning att tidigt "ligga på förhand" har medfört en så snabb insats som är möjlig m h t avståndet och så omfattande som beredskapsläget medger. Samtidigt upprätthölls en viss beredskap över landet för andra insatser. Vindstyrka över Västerhavet ex 27 m/s.

Materielfunktion

Livlinan mellan ARCC och helikoptrarna är kortvågen, HF. Denna är normalt av låg kvalitet under dygnets mörka timmar på använd frekv 5680. Nattfrekvensen 3023 fungerade inte heller under den tid då initialinsatserna gjordes. Tekniskt fel under morgonen och förmiddagen försvårade ytterligare situationen.

Den kryptoutrustning som ARCC föreslagit skall tillföras ARCC och samtliga räddningshkp, -kryapp 302-, i skr 1994-03-29 till Flygvapenledningen har ännu inte besvarats. Det bedöms att en sådan utrustning säkerställt erforderligt samband.

Annan sambandsmöjlighet finns inte då räddningsområdet p g a avståndet inte gick att nå med VHF. En möjlighet kunde ha varit att beordra försvarets radar- och radiostationer för aktuellt området och att via rrjal sända till och mottaga meddelanden från hkp.

Erfarenheter och förslag

För en framgångsrik insats är det betydelsefullt att tidigt få all tänkbar information. Lika betydelsefullt är att fortlöpande få information om utvecklingen på olycksplatsen. I fallet "Estonia" fanns varken tidig information eller information om utvecklingen.

Den ledande centralen bör föra dialog med den central som ställer resurser till förfogande för att säkerställa att all tillgänglig information presenteras. Om deltagande enheter inte har gemensamt språk skall engelska användas. Alternativa sambandsmöjligheter måste skapas.

Beredskapen är för normala händelser tillräcklig. Det är tveksamt om det är kostnadseffektivt att höja denna. Genom att anflygningstiderna i vissa fall blir oacceptabelt långa bör beredskap införas även för Söderhamn/Kallax. Kostnaden för detta bör bestridas av samhället.

Vid omfattande olyckor kan ytterligare resurser relativt snabbt kallas in. Detta visas av resurstillväxten vid "Estonia".

I detta fall hände en stor olycka på finskt område. Beredskap och planering måste finnas i Sverige för att kunna leda stora insatser med ledning från svensk central. Särskilt gäller detta flygräddning där Luftfartsverket har ett undsättnings-ansvar ut till FIR-gränsen. Vid en olycka öster och sydost om

Gotland kan föutsättas att de baltiska länderna saknar resurser och att Sverige då måste ta på sig rollen av räddningsledare.

Utan att hålla beredskap har helikopterförbanden mycket snabbt samlat besättning och kunnat starta mot området. P g a dettas läge var anflygningarna långa och insatserna på plats kunde ske först efter relativt lång tid.

Larmningen har fungerat mycket bra. Möjligen kan förbanden se över larmrutiner och tilldela besättningar ex p-sök för snabb larmning. Meteorolog måste mycket snabbt vara på plats i Rväd C för att inom ca 15 min kunna leverera kartor till hkpförb och Cefyl.

Centralerna bör "för säkerhets skull" larmas tidigt för att kunna ligga "på förhand". Ledningsproblematiken har debatterats och har haft uppenbara brister. Helikoptrarna har fått ta egna initiativ för sökområden och egna beslut i stor omfattning. En förutsättning för en konkret ledning är att fullgott samband kan upprättas, så var inte fallet nu.

Vid en så omfattande insats måste det finnas OSC för resp ytenheter och flygande enheter. OSC flyg bestående av två man vid omfattande operationer - en för flygledning och en flygräddningsledare. Lokalisering till Arlanda är från denna synpunkt ovärderlig genom att insatser kan ske över hela ansvarsområdet relativt snabbt.

Baser måste förberedas och förtecknas med ex tanknings-möjligheter i samtliga angränsande länder. Baserna bör m h t samband och ex landnings- och tankningsmöjligheter vara flygplatser.

Under hela operationen var sikten i området bra. Försvårande var dock stark vind och mycket kraftig sjögång. Om vädret och sikten varit nedsatt hade räddningsinsatserna försvårats avsevärt och en OSC flyg varit helt nödvändig. Troligen hade dessutom inte samma antal hkp kunnat sättas in samtidigt.

Dessa fall där extraordinära resurser måste kallas in bör VB i centrala och regionala staber instrueras att på avrop från flygräddningsledare ställa begärda resurser till förfogande. Beslut angående utnyttjande av försvarets radar- och radiostationer är ett exempel.

Materielens funktion har inte varit utan anmärkning. Vinschar, spånvarning m m har medfört att periodvis färre antal helikoptrar kunnat verka inom området.

Återigen, om fungerande samband funnits kunde ersättare snabbt ha satts in. Sambandet är inte bara livlinan mellan Cefyl och hkp utan är också nödvändig som informationslänk. Kryapp 302, satellittelefon - alla möjligheter måste beaktas.

Den central som blir räddningscentral för en operation av denna omfattning kan inte klara uppgifterna med ordinarie bemanning. Ytterligare personal måste mycket snabbt förstärka för att inte centralen skall bli blockerad. F n med ARCC på Arlanda finns denna möjlighet genom att personalen bor nära. Tre räddningsledare kan vara på plats inom ca 15 min. Efter flytten till Göteborg saknas denna möjlighet under åtskilliga år.

Förslag i sammandrag

- Dialog direkt mellan ledande central och stödjande central (Distaff).
- Höjd beredskap för hkp i Norrland m h t anflygningstider.
- Beredskap och planering för en insats där ARCC är ledande central måste finnas.
- Funktioner för larmning av besättningar som inte är i beredskap överses.
- Meteorolog i hög beredskap.
- Översyn av sambandsmöjligheter.
- On Scene Commander flyg förbereds från ARCC Tp med hkp. Transportabel radioutrustning för VHF anskaffas.
- Lämpliga baser i angränsande länder förtecknas. Motsvarande underlag för Sverige tillställs övriga länder.
- Central och regional beslutsnivå förbereds för extraordinära insatser.
- Personalförstärkning måste säkerställas.
- Hkp bör utrustas med ex färgspray för att markera att livflotte undersökts.

SUPPLEMENT No. 604

Penttilä Antti - Ranta Helena: Medicolegal Examination and Identification of Victims of M/S Estonia Mass Disaster.

Department of Forensic Medicine, University of Helsinki - The Finnish DVI Team - Ministry of Justice.

Helsinki 1996.

For official use only

MEDICOLEGAL EXAMINATION AND IDENTIFICATION OF VICTIMS OF M/S ESTONIA MASS DISASTER

Antti Penttilä Professor MD,PhD
Helena Ranta Chief Dental Officer DDS,PhD

Department of Forensic Medicine, University of Helsinki
The Finnish DVI Team
Ministry of Justice

Helsinki 16.1.1996

MEDICOLEGAL EXAMINATION AND IDENTIFICATION OF VICTIMS OF M/S ESTONIA MASS DISASTER

Manpower in Forensic Medicine and Forensic Odontology in Finland

Finnish Disaster Victim Identification Team (DVI-team) was established in 1989. In addition to 16 policemen of the Finnish National Bureau of Investigation, a psychologist and a priest, two forensic pathologists and two forensic odontologists belonged to the team in September, 1994 (Table 1).

In 1994, there were altogether 25 specialists in forensic medicine in Finland working as medical examiners in the provinces, teachers at the universities and medical officers in the National Board of Medicolegal Affairs.

In addition, there are 20 dentists in Finland with experience in forensic odontology and practising on the field.

Facilities of the Department of Forensic Medicine, University of Helsinki

Preliminary plans for the medicolegal examination of victims in mass disasters had been drafted in advance at the Department of Forensic Medicine since 1988. The staff had been trained in advance in two small-scaled aircraft accidents with few victims in 1988 and 1992.

Considering the medicolegal autopsies in mass disasters in the future in Finland, it is reasonable to conclude that they should be performed at the Department of Forensic Medicine of the Helsinki University because the department has the best resources in Finland to perform examinations in major accidents and disasters.

A summary of facilities, staff and public services of the Department of Forensic Medicine of the Helsinki University in 1994 are presented in Table 2.

Preliminary Medicolegal Measures in Estonia Disaster

Shortly before 2 a.m. on Wednesday morning, 28 September, 1994 the Estonian ro-ro passenger vessel M/S Estonia capsized and sank in the international waters in the Baltic Sea about 35 kilometers south-east from the most southern Finnish island.

The Estonian police requested legal assistance from the Finnish police to examine the cause of death of the victims as well as to identify them. After the Swedish authorities had accepted this procedure, the identification process was officially started.

The Finnish DVI-team assembled for a meeting in Helsinki by noon, 28 September, 1994 and transferred with the rolling stock to Turku. At the meeting in Turku at 6.20 p.m., 28 September, 1994 the police investigator in charge of the investigation of the disaster requested the Finnish DVI-team to proceed with the examination of the cause of death and identification of victims.

At the morning meeting, 29 September, 1994 in Turku it was decided that the medicolegal examination of victims will be performed at the Department of Forensic Medicine, University of Helsinki. Medicolegal autopsy of all victims was to be performed by the order of the police investigator in charge.

After this meeting all the involved employees at the Department of the Forensic Medicine, University of Helsinki were informed and asked to prepare for the work by checking facilities, equipment and material necessary in the examination. An information session was arranged for the whole staff in the afternoon, 29 October, 1994. Due to the prevailing information the staff was informed about the possibility of identification of several hundreds of victims.

Medicolegal autopsies of Estonia victims

A demonstration autopsy was performed in the morning, 30 September, 1994. All the policemen, medical doctors, dentists and technicians working at the autopsy section attended the demonstration autopsy. The procedures to be followed in the examination of victims were described in detail to standardize the working routines.

All 92 victims found shortly after the disaster were examined in 6 days (Table 3). One victim was found and examined on 17 October.

One victim died in Stockholm, Sweden and was examined there.

A policeman, a forensic pathologist and a forensic odontologist belonging to the executive group of the Finnish DVI-team were in charge of the autopsy section.

The staff working full time at the autopsy section comprised 5 forensic pathologists, 8 autopsy technicians, 5 secreteries and 2 cleaners from the Department of Forensic Medicine, 2 medical examiners from the province of Häme, 11 consulting forensic odontologists and about 15 policemen. The whole staff of the department was involved part time in the examination.

The autopsy group comprised of a forensic pathologist, an autopsy technician and 3 technical investigators of the police. On day 3 the number of groups was raised from 3 to 4.

The maximum number of autopsies per team was 5 per day. The teams worked from 08 a.m. to 06 p.m. Routine medicolegal autopsies were performed either before or after office hours.

The storage of victims and working order at medicolegal autopsies are presented in Table 4. In all cases a complete medicolegal autopsy was performed with a careful external and internal examination and documentation of findings. All necessary samples were taken at autopsy. The autopsy protocol was completed and the Interpol form for victim identification filled at autopsy. Later final autopsy reports and death certificates were given.

After autopsy odontological examination was made by a team comprising 2 dentists and 1 technician. The total number of teams was 5 of which 2 were working at a time.

The autopsy reports and Interpol forms were delivered to the identification center at the National Bureau of Investigation on the same or the following day after autopsy. The final autopsy reports were delivered in one to two weeks after autopsies and death certificates on the day when the victims were identified.

Two uniformed policemen guarded the entrance of the department during office hours and the Finnish Defence Forces the morgue 24 hours a day.

Autopsy Findings

The number of medicolegal autopsies was 93 of which 52 were males and 41 females.

Of males 35 (67 %) died from drowning, 16 (31 %) from hypothermia and 1 (2%) from injuries. The respective rates for females were 34 (83 %), 6 (15 %) and 1 (2 %) (Table 5).

In all cases of drowning, hypothermia was regarded to be a contributing factor to death (Table 5). One fourth (25/27 %) of the victims were naked or almost naked, 18 (19 %) had very insufficient and 40 (43 %) insufficient clothing for the weather condition at the time of the accident. Only 10 (11 %) victims had extra clothing. 74 victims (80%) were not wearing shoes and 3 (3 %) had only one shoe.

Severe injuries were regarded to be contributing factors to death in 14 cases (6 males and 8 females) and heart disease in 2 males (Table 5).

Fractures and/or injuries to inner organs were found in 28 (30%) cases and all victims had suffered minor or more extensive superficial excoriationes, bruises, etc.

Presence of glucose in urine was quite common (58 cases, 62 % of those tested) obviously due to the strenuous stress situation. Only two victims suffered from diabetes on the basis of AM information.

Alcohol and/or medicaments did not play any significant role. Classical narcotics were not found, either (Tables 6 and 7).

Gender and age distribution of the people on board

1. Passengers and members of the crew

Based on the latest passenger and crew lists on 4 January, 1996 it is assumed that there were 989 people from 17 countries on board, of which 504 were males, and 485 females (Table 8). More than half (56 %) of them were Swedish and one third (35%) from Estonia.

The distribution of all people on board by gender and age is presented as follows:

Table 9	Number of passengers and crew members
Table 10	Rescued persons
Table 11	All victims
Table 12	Missing victims
Table 13	Identified victims

More than half of the males (52 %) and females (56%) were middle-aged (25-54 years). The number of children (<15 years) or elderly people (≥ 75 years) was small (Table 9).

Only 26 (5 %) of the women, opposite to males (111/22%), were rescued (Table 10). The majority belonged to the age group of 15-44 years. Only 3 % of the males but none of the females over 45 years were rescued.

2. Passengers

The distribution of passengers by gender and age is presented as follows:

Table 14 All passengers
Table 15 Rescued passengers
Table 16 Killed passengers
Table 17 Missing passengers
Table 18 Identified passengers

3. Members of the crew

The distribution of the members of the crew by gender and age is presented as follows:

Table 19 All crew members
Table 20 Rescued crew members
Table 21 Killed crew members
Table 22 Missing crew members
Table 23 Identified crew members

Ante-mortem (AM) and post-mortem (PM) data

INTERPOL's victim identification forms were used in collecting AM and PM data. The Finnish DVI-team translated AM forms into Estonian and printed 500 copies. AM information was collected in different countries with the help of the local police. In Estonia, members of the Finnish DVI-team and other Finnish police officers were active in collecting information.

There were 6 PCs for processing AM data and 3 PCs for processing PM data in the identification center. The secreterial staff comprised 10 employees.

PM data were transferred to data base the same day and AM data the same or the following day after being received at the identification center.

Computerized IDENT^{R} program for dental and HUID^{R} program for other comparisons were applied.

In general, the AM forms were properly filled, e.g.in 98 % of the victims examined and identified in Helsinki. In some cases there were two or more AM forms available. More than half (50/54%) of the victims had a family doctor and more than two thirds (65/70%) a family dentist.

No AM data was available at the time of medicolegal autopsies.

Time schedule of arrival of AM and PM data to the identification center was as follows:

28 September, 1994	Disaster.
30 September, 1994	First AM forms from Finland and the Netherlands.
30 September, 1994	First PM forms.
05 October, 1994	Last PM forms.
07 October, 1994	Training seminar on completing of AM forms for Estonian police officers in Tallinn by Finnish authorities.
09 October, 1994	Putative identity of about half of the victims. Collecting information of these cases was speeded up both in Sweden and Estonia.
17 October, 1994	One victim found in Jussarö, Finland.
31 October, 1994	All victims identified. AM form missing in 172 cases.
January, 1995	47 AM forms from Estonia. Information collected by a member of the Finnish DVI-team.
17 May, 1995	The last AM form from Estonia.
04 January, 1996	No AM information available in 2 cases and very insufficient in 1 case.
	AM dental data missing in 211 cases (21%). Most of these victims are from Estonia (Table 24).
	After 17 October, 1994 no further Estonia-victims have been found.

Identification

In the identification the procedure presented in Interpol's Manual for Disaster Victim Identification was used as a starting point. The identification document was produced at the identification sessions. The executive group of the DVI-team (head, police officer, forensic pathologist and forensic dentist), one or two

presenters (police officers), the police officer responsible for collecting post-mortem information, a session secretary and a secretary preparing the identification document were present. The identification document was signed by the members of the executive group.

The first identification session was a demonstration where the strategy of the procedure was agreed.

At the following ten identification sessions all 93 victims were identified by 31 October, 1994, i.e. within 33 days of the disaster (Table 25).

Gender, age (+/- 5-10 years), heigth (+/- 5 cm), body build and hair colour in addition to specified characteristics were the main characteristics applied in searching the putative identification.

Identification of all Estonia victims was concluded on the basis of one or in many cases several specified and the above mentioned general characteristics.

From specified methods dental identification was most powerful (Table 26). With one exception, all victims of Sweden (97%) were identified by teeth, whereas only 27 % of those from Estonia.

The results of identification by other specified methods are preseneted as follows:

Table 27	Visual identification by legal documents by members of the DVI-team
Table 28	Visual identification by PM photographs by next to kin
Table 29	Visual identification of crew members by PM photographs by company physician
Table 30	Identification based on specified personal items
Table 31	Identification based on physical characteristics
Table 32	Identification based on characteristics of medical treatment

In Table 33 is summarized identification by visual and dental methods in various combinations. 90 victims (97%) could be identified by combining visual and dental identifications.

ABO/Rh blood group information was obtained in 21 cases (23 %). In 18 of these victims the results matched whereas in 3 cases discrepancy existed.

Table 1. The Finnish DVI-team in 1994

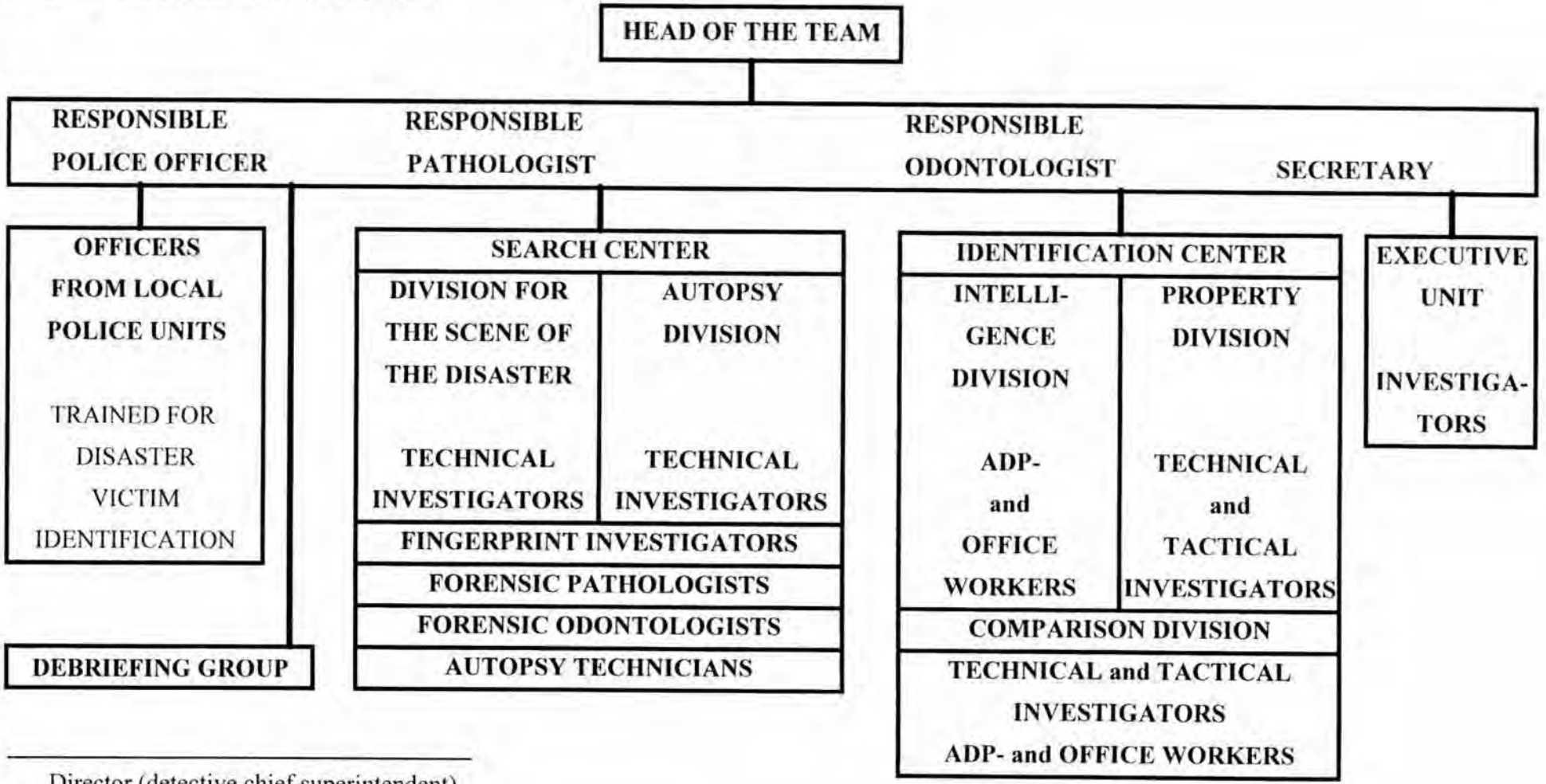

	Director (detective chief superintendent)
15	Police officers
2	Forensic pathologists
2	Forensic odontologists
	Priest
	Psychologist
22	Total

Table 2. Department of Forensic Medicine, University of Helsinki (1994)

1. Facilities

Building
built 1974
volume 23500 m^3
floor space 6413 m^2

Autopsy division
floor space 464 m^2
3 autopsy rooms with three autopsy tables
1 autopsy room with one autopsy table
1 orthopanthomograph
5 x-ray apparatures

Morque division
floor space 486 m^2
refrigerated space (0°C) for 200 cadavers
2 refrigerated mobile containers (0°C) for 100 cadavers (after autopsy)

2. Staff

Pathology section
7 medical doctors
2 medical examiners (province of Uusimaa)
8 autopsy technicians
4 laboratory technicians
7 secreteries

Odontology section
3 odontologists (consultants)

Toxicology section
1 medical doctor
8 chemists
7 laboratory technicians
1 secretary

Biochemistry section
1 chemist
2 laboratory technicians

DNA laboratory
1 laboratory technician

Diverse
13 employees

Total 61 employees

3. Public services

Medicolegal autopsies	2276
Toxicological analyses (number of cases)	4406
Biochemical analyses (number of cases)	326
Histological slides	20483
DNA analyses (number of cases)	4
Clinical forensic examinations	3288
Forensic odontological examinations	113

Table 3. M/S Estonia medicolegal autopsy schedule

Time		Estonia[a] autopsies	Routine[b] autopsies
Disaster Wed 28 Sep 1994			
Fri	30 Sep 1994	1[c] + 6	7
Sat	01 Oct	15	
Sun	02 Oct	20	
Mon	03 Oct	20	8
Tue	04 Oct	20	4
Wed	05 Oct	10	14
Mon	17 Oct	1[d]	9
Total		93	42

[a]performed between 08 a.m. and 06 p.m.
[b]performed before 08 a.m. or after 06 p.m.
[c]demonstration autopsy
[d]the victim was found on 17 October

Table 4. Storage of corpses and working order of medicolegal autopsies

Storage in cardboard coffins at 0°C

External examination

Clothes, property
Finger prints
Medical examination
Photography

Internal examination

Medicolegal autopsy
Photography
Samples

Toxicology	blood, vitreous humor, urine, liver, stomach content
	other after consideration
Microscopy	4 samples of lungs
	other after consideration
Biochemistry	vitreous humor, urine
Serology	blood
DNA	blood

Radiology after consideration

Autopsy protocol
Interpol form

Final autopsy report
Death certificate

Odontological examination

Photography
Orthopanthomography
Clinical examination

Interpol form

Embalming

Storage in refrigerated containers at 0°C at the Department of Forensic Medicine

Long-term storage in wooden coffins at an installed morque at 0°C

Re-examination (5 cases)

Repatriation of victims to authorities of respective countries

Table 5. Cause of death

Underlying cause	Males n	Females n	Total n
Drowning	**35**	**34**	**69**
Contributing factor			
Hypothermia	35	34	69
Injuries	6	8	14
Heart disease	2	-	2
Hypothermia	**16**	**6**	**22**
Contributing factor			
Heart disease	2	-	2
Injuries	**1**	**1**	**2**
Contributing factor			
Hypothermia	1	-	1
Total	**52**	**41**	**93**

Table 6. Blood alcohol concentration (o/oo) of victims

Concentration	Males		Females		Total	
	n	%	n	%	n	%
0	40	77	40	98	80	86
0.35 - 0.5	9	17	1	2	10	11
0.5 - 0.99	3	6	-		3	3
Total	52	100	41	100	93	100

Table 7. Medicaments and narcotica

Medicament	Males n	Females n	Total n
Cardiovascular	6	2	8
Psychotropic	-	3	3
Analgetic	1	1	2
Cough and COCD preparations	-	2	2
Narcotica	-	-	-
Total	7	8	15

Table 8. Nationality

Country	Total	Rescued	Missing victims	Identified victims
	n	n	n	n
Belarus	1		1	
Canada	1		1	
Denmark	6	1	5	
Estonia	348	63	237	48
Finland	13	3	9	1
France	1		1	
Germany	8	3	4	1
Latvia	23	6	13	4
Lithuania	4	1	3	
Morocco	2		2	
Netherlands	2	1	1	
Nigeria	1		1	
Norway	9	3	6	
Russia	13	2	10	1
Sweden	553	52	462	39
Ukraine	2	1	1	
United Kingdom	2	1	1	
Total n	989	137	758	94
%	100	14	77	10

Table 9. Number of passengers + crew members

Age (yrs)	Males n	Males %	Females n	Females %	Total n	Total %
< 15	9	2	6	1	15	2
15-19	20	4	20	4	40	4
20-24	60	12	40	8	100	10
25-34	85	17	77	16	162	16
35-44	98	19	85	18	183	19
45-54	82	16	106	22	188	19
55-64	61	12	73	15	134	14
65-74	76	15	69	14	145	15
≥ 75	13	3	9	2	22	2
Total	504	100	485	100	989	101

Table 10. Distribution of rescued people at different age groups

Age	Males		Females		Total	
(yrs)	n	%	n	%	n	%
< 15	1	11	0		1	7
15-19	7	35	2	10	9	23
20-24	26	43	4	10	30	30
25-34	25	29	10	13	35	22
35-44	30	31	6	7	36	20
45-54	16	20	3	3	19	10
55-64	4	7	1	1	5	4
65-74	2	3	0		2	1
≥ 75	0		0		0	
Total	111	22	26	5	137	14

Table 11. Missing and identified victims at different age groups

Age	Males		Females		Total	
(yrs)	n	%	n	%	n	%
< 15	8	89	6	100	14	93
15-19	13	65	18	90	31	78
20-24	34	57	36	90	70	70
25-34	60	71	67	87	127	78
35-44	68	69	79	93	147	80
45-54	66	80	103	97	169	90
55-64	57	93	72	99	129	96
65-74	74	97	69	100	143	99
≥ 75	13	100	9	100	22	100
Total	393	78	459	95	852	86

Table 12. Missing victims at different age groups

Age	Males		Females		Total	
(yrs)	n	%	n	%	n	%
< 15	8	89	6	100	14	93
15-19	13	65	16	80	29	73
20-24	26	43	33	83	59	59
25-34	49	58	59	77	108	67
35-44	56	57	63	74	119	65
45-54	56	68	95	90	151	80
55-64	50	82	68	93	118	88
65-74	70	92	69	100	139	96
≥ 75	13	100	9	100	22	100
Total	341	67	418	86	759	77

Table 13. Identified victims at different age groups

Age	Males		Females		Total	
(yrs)	n	%	n	%	n	%
15-19	0		2	10	2	5
20-24	8	13	3	8	11	11
25-34	11	13	8	10	19	12
35-44	12	12	16	19	28	15
45-54	10	12	8	8	18	10
55-64	7	11	4	5	11	8
65-74	4	5	0		4	3
Total	52 +1[a)]	11	41	8	93 +1[a)]	10

[a)]One victim examined and identified in Stockholm, Sweden

Table 14. Assumed number of passengers

Age (yrs)	Males		Females		Total	
	n	%	n	%	n	%
< 15	9	2	6	2	15	2
15-19	18	4	13	3	31	4
20-24	40	10	18	5	58	7
25-34	57	14	52	14	109	14
35-44	77	18	53	14	130	16
45-54	68	16	92	24	160	20
55-64	60	14	73	19	133	17
65-74	76	18	69	18	145	18
≥ 75	13	3	9	2	22	3
Total	418	99	385	101	803	101

Table 15. Rescued passengers at different age groups

Age (yrs)	Males		Females		Total	
	n	%	n	%	n	%
< 15	1	11	0		1	7
15-19	6	33	1	8	7	23
20-24	18	45	1	6	19	33
25-34	16	28	6	12	22	20
35-44	21	27	3	6	24	18
45-54	12	18	2	2	14	9
55-64	4	7	1	1	5	4
65-74	2	3			2	1
≥ 75	0		0		0	
Total	80	19	14	4	94	12

Table 16. Missing and identified passengers at different age groups

Age	Males		Females		Total	
(yrs)	n	%	n	%	n	%
< 15	8	89	6	100	14	93
15-19	12	67	12	92	24	77
20-24	22	55	17	94	39	67
25-34	41	72	46	88	87	80
35-44	56	73	50	94	106	82
45-54	56	82	90	98	146	91
55-64	56	93	72	99	128	96
65-74	74	97	69	100	143	99
≥ 75	13	100	9	100	22	100
Total	338	81	371	96	709	88

Table 17. Missing passengers at different age groups

Age	Males		Females		Total	
(yrs)	n	%	n	%	n	%
< 15	8	89	6	100	14	93
15-19	12	67	11	85	23	74
20-24	19	48	17	94	36	62
25-34	38	67	44	85	82	75
35-44	45	58	41	77	86	66
45-54	50	74	84	91	134	84
55-64	49	82	68	93	117	88
65-74	70	92	69	100	139	96
≥ 75	13	100	9	100	22	100
Total	304	73	349	91	653	93

Table 18. Identified passengers at different age groups

Age	Males		Females		Total	
(yrs)	n	%	n	%	n	%
15-19	0		1	8	1	3
20-24	3	8	0		3	5
25-34	3	5	2	4	5	5
35-44	11	14	9	17	20	15
45-54	6	9	6	7	12	8
55-64	7	12	4	5	11	8
65-74	4	5	0		4	3
Total	34 +1[a)]	8	22	6	56	7

[a)]One victim examined and identified in Stockholm, Sweden

Table 19. Members of the crew

Age (yrs)	Males		Females		Total	
	n	%	n	%	n	%
15-19	2	2	7	7	9	5
20-24	20	23	22	22	42	23
25-34	28	33	25	25	53	28
35-44	21	24	32	32	53	28
45-54	14	16	14	14	28	15
55-64	1	1	0		1	1
Total	86	99	100	100	186	100

Table 20. Rescued members of the crew at different age groups

Age (yrs)	Males		Females		Total	
	n	%	n	%	n	%
15-19	1	50	1	14	2	22
20-24	8	40	3	14	11	26
25-34	9	32	4	16	13	25
35-44	9	43	3	9	12	23
45-54	4	29	1	7	5	18
55-64	0				0	
Total	31	36	12	12	43	23

Table 21. Missing and identified members of the crew at different age groups

Age	Males		Females		Total	
(yrs)	n	%	n	%	n	%
15-19	1	50	6	86	7	78
20-24	12	60	19	86	31	74
25-34	19	68	21	84	40	75
35-44	12	57	29	91	41	77
45-54	10	71	13	93	23	82
55-64	1	100			1	100
Total	55	64	88	88	143	77

Table 22. Missing members of the crew at different age groups

Age	Males		Females		Total	
(yrs)	n	%	n	%	n	%
15-19	1	50	5	71	6	67
20-24	7	35	16	73	23	55
25-34	11	39	15	60	26	49
35-44	11	52	22	69	33	62
45-54	6	43	11	79	17	61
55-64	1	100			1	100
Total	37	43	69	69	106	57

Table 23. Identified members of the crew at different age groups

Age	Males		Females		Total	
(yrs)	n	%	n	%	n	%
15-19	0		1	14	1	11
20-24	5	25	3	14	8	19
25-34	8	29	6	24	14	26
35-44	1	5	7	22	8	15
45-54	4	29	2	14	6	21
55-64	0				0	
Total	18	21	19	19	37	20

Table 24. Missing ante-mortem dental data by 4 January 1996

Country	Missing AM dental data	
	n	%
Belarus	1	100
Canada	-	
Denmark	3	50
Estonia	148	43
Finland	1	8
France	-	
Germany	-	
Latvia	10	43
Lithuania	3	75
Morocco	1	50
Netherlands	-	
Nigeria	1	100
Norway	-	
Russia	7	54
Sweden	34	6
Ukraine	1	50
United Kingdom	1	50
Total	211	21

Table 25. Identification schedule

Time			Cumulative	
		n	n	%
Disaster Wed 28 Sep 1994				
Mon	10 Oct 1994	10	10	11
Tue	11 Oct	14	24	26
Thu	13 Oct	24	48	52
Fri	14 Oct	5	53	57
Mon	17 Oct	7	60	65
Tue	18 Oct	10	70	75
Fri	21 Oct	7	77	83
Tue	25 Oct	6	83	89
Thu	27 Oct	8	91	98
Mon	31 Oct	2	93	100
10 sessions		93	93	100

Table 26. Dental identification

Country	Victims	Dental identification		Dental comparison	
	n	n	%	n	%
Estonia	48	13	27	12	25
Sweden	38	37	97	1	3
Latvia	4	3	75	1	25
Finland	1	1	100	-	
Germany	1	1	100	-	
Russia	1	1	100	-	
Total	93	56	60	14	15

Table 27. Visual identification (various legal documents)

Identification	Males n	Females n	Total n
Yes	13	9[a)]	22
No documents	39	32	71
Total	52	41	93

[a)]One victim originally incorrectly identified

Table 28. Visual identification by next to kin (PM photograph)

Country	Identification n	%
Estonia	45	94
Sweden	5	13
Germany	1	100
Russia	1	100
Total	52	56

Table 29. Visual identification of crew members by company physician (PM photograph)

Identification	n
Definitive	10
Highly probable	5
Probable crew member	2
Incorrect	2
No identification	18
Total	37

Table 30. Identification based on personal items

Item	n
Specified ring	13
Several specified rings	11
Specified watch	2
Specified necklaces	1
Clothing + shoes	1
Specified jewellery	1
Watch + keys	1
Buckle of belt	1
Belt	1
Combinations	4
Total	36

Table 31. Identification based on physical characteristics

Characteristic	n
Specified tattoo	6
Birthmark (face)	5
Birthmark (other)	3
Freckles	1
Specified body build	1
Moustache	1
Face + moustache + height	1
Exceptional anatomy of mandible	1
Posttraumatic status (fingertip)	1
Total	20

Table 32. Identification based on characteristics of medical treatment

Characteristic	n
Operations/scars	15
Pace maker	2
Orthodontic appliance	1
Total	18

Table 33. Identification by visual and dental methods

Method	n	Cumulative n	Cumulative %
Visual			
company physician	15		
legal document	22		
next to kin	52		
company physician/legal document		32	34
company physician/legal document/next to kin		59	63
Dental	56		
dental/visual (company physician)		65	70
dental/visual (legal document)		69	74
dental/visual (company physician/legal document)		75	81
dental/visual (next to kin)		89	96
dental/visual (company physician/legal document/next to kin)		90	97
Other methods		93	100
Total of victims	93	93	100